

Novel Resorcinol Platforms with Pharmaceutical Applications

Marco Maurizio Daniele Cominetti

School of Pharmacy

University of East Anglia



A thesis submitted for the degree of Doctor of Philosophy

June 2015

© This copy of the thesis has been supplied on condition that anyone who consults it is understood to recognize that its copyright rests with the author and that use of any information derived there from must be in accordance with current UK Copyright Law. In addition, any quotation or extract must include full attribution.

Declaration

This thesis is submitted to the University of East Anglia for the degree of Doctor of Philosophy and has not been previously submitted at this or any other University for assessment or for any other degree. Except where stated and referenced or acknowledgment is given, this work is original and has been carried out by the author alone.

Marco Maurizio Daniele Cominetti

Part of this thesis has already been presented at the XXIII International Symposium on Medicinal Chemistry (EFMC-ISMC) and EFMC Young Medicinal Chemist Symposium, EFMC-YMCS, September 2014, Lisbon. Poster title: “Novel Multivalent Resorcinol Based Halophenols as Inhibitors of Reactive Oxygen Species.”

Abstract

The rationale behind this work is the discovery that a number of natural bromophenols from algae have antibiotic and antioxidant activities. Most natural compounds are based on phenol and catechol. Previous studies by the group investigated a novel class of halogenated compounds based on resorcinol dimers which showed a relatively high antimicrobial activity. In this work, the structures were modified further in order to develop a structure-activity relationship for these systems.

A novel synthetic approach to brominated resorcinol dimers was developed to allow efficient synthesis of the products without chromatographic purification. The method was additionally applied to the synthesis of a novel class of tetrameric and hexameric derivatives. Halogenation and dehalogenation methods were put in place to provide additional variety to the derivatives accessible. A set of simplified structures, including benzophenones and xanthenes, was also prepared for comparison.

The polyvalent structure of the tetramers and hexamers was investigated and exploited for the synthesis of dendrimeric multicalix[4]arene structures, including an octacalix[4]arene presenting thirty two amines, as proof of concept for the development of novel dendrimers, and among these new potential transfection agents and DNA binding structures.

The library of compounds thus obtained was screened for its effects on the viability of two cancer cell lines, MCF-7 and HL60. The results showed a varied profile, ranging from potent antiproliferative activity to compounds with very moderate effects. Additionally the potential antioxidant activity of the compounds was investigated with two *in vitro* assays and for their cytoprotective activity on MCF-7 cells.

Table of Contents

List of Figures	viii
List of Schemes	xiv
List of Tables.....	xvii
List of Abbreviations.....	xviii
Acknowledgments	1
1. Introduction	2
1.1 Antimicrobials and resistance	2
1.1.1 Drug Targets.....	3
1.1.2 Modes of Resistance and Transmission	4
1.1.3 Human Involvement.....	7
1.2 Bromophenols	7
1.2.1 Brominated bis-phenols as antimicrobials	9
1.3 Radicals, ROS and oxidative damage	15
1.3.1 ROS: a brief description	16
1.3.2 Cell defence against oxidative stress.....	18
1.3.3 Oxidative damage and pathologies.....	19
1.3.4 Antioxidants as therapeutic agents	22
1.4 Brominated bis-phenols as antioxidants.....	26
1.5 Previous Work.....	29
1.6 Aim of the Project	30
2. Dimers and Tetramers	31
2.1 Introduction to Resorcinol and Phloroglucinol Dimers	31
2.2 Introduction to Resorcinol Tetramers.....	32
2.3 Introduction to Resorcinol Hexamers.....	33
2.4 Synthesis of dimers	34

2.4.1 Synthesis of 4-bromoresorcinol	35
2.4.2 Synthesis of 2,4-dibromoresorcinol	35
2.4.3 Synthesis of 2,4-dibromophloroglucinol	35
2.4.4 Synthesis of phloroglucinol and resorcinol dimers	36
2.4.5 Synthesis of Dimers with Method 2	39
2.5 Synthesis of tetramers	42
2.5.1 4-Bromoresorcinol based tetramers	42
2.5.2 4-Chlororesorcinol based tetramers	44
2.5.3 By-products of 165 and their equilibrium	45
2.5.4 Method 1 for the synthesis of tetramers	52
2.5.5 Side reactions and scrambling	53
2.5.6 Aldehydes and mixed platforms	56
2.5.7 Crystallography	57
2.5.8 Dehalogenation of tetramers	60
2.5.9 Halogenation of tetramers	61
2.5.10 Biaryldicarboxaldehyde-based tetramers	62
2.5.11 Flexible tetramers	65
2.6 Synthesis of hexamers	65
2.7 Conclusions	67
2.8 Experimental	68
2.8.1 General	68
2.8.2 Crystal structure analyses	68
2.8.3 Synthesis	71
3. Bis-phenols, Benzophenones, Xanthenes and Xanthenes	145
3.1 Introduction to the structures	145
3.1.1 Synthetic approach	146
3.2 Synthesis	149
3.2.1 Synthesis of hydroxy benzophenones	149
3.2.7 Bromination of benzophenones	161

3.2.8 Cyclisation of benzophenones	163
3.2.9 Bromination of xanthenes	165
3.2.10 Reduction of benzophenones	166
3.2.11 Bromination of bis-resorcinols	168
3.2.12 Reduction of xanthenes	168
3.3 Conclusions	171
3.4 Experimental	173
3.4.1 General	173
3.4.2 Synthesis.....	173
4. Synthesis of dendrimers	188
4.1 Dendrimers	188
4.2 Calixarenes	189
4.3 Previous work.....	190
4.4 CuAAC, a quick overview	193
4.5 Functionalization of the Cores	195
4.5.2 Test of click reaction	199
4.5.3 Synthesis of a hindered model compound.....	202
4.5.4 Synthesis of a clickable tetra-amino calixarene	204
4.5.5 Synthesis of a functionalised dendrimer	206
4.6 Conclusions	208
4.7 Experimental	209
4.7.1 General	209
4.7.2 Synthesis.....	210
5. Biological evaluation.....	221
5.1 MTS assay	221
5.1.1 Cell Lines	222
5.2 Screening	222
5.2.1 Comparison of MCF-7 and HL60	223
5.2.2 Structures with low toxicity	225

5.2.3 Evaluation of tetramers	226
5.2.4 Antiproliferative compounds as potential anticancer agents?	228
5.3 Imaging	229
5.4 Conclusions	231
5.5 Experimental	233
5.5.1 Cell culture	233
5.5.2 Proliferation assay	233
5.5.3 Fluorescence Imaging	234
6. Antioxidant activity	235
6.1 Choice of the assay	235
6.1.1 Inhibition of induced lipid auto-oxidation	236
6.1.2 ORAC, TRAP and PABA assays	236
6.1.3 Ferric Reducing Ability of Plasma (FRAP) assay	237
6.1.4 Cupric reducing Antioxidant Capacity (CUPRAC) assay	238
6.1.5 Total Phenols Assay	238
6.1.6 2,2-Diphenyl-1-picrylhydrazyl (DPPH) radical Scavenging Capacity assay	239
6.1.7 Trolox Equivalent Antioxidant Capacity (TEAC) assay	240
6.1.8 <i>In Vivo</i> Cell Protection Assay	241
6.2 Results and Discussion	241
6.2.1 DPPH assay	241
6.2.2 TEAC assay	253
6.3 Biological evaluation of protective activity	270
6.4 Conclusions	273
6.5 Experimental	275
6.5.1 DPPH assay	275
6.5.2 TEAC assay	275
6.5.3 Cell culture	275
6.5.4 MTS with <i>tert</i> -butyl hydroperoxide	276

7. Conclusions and future work.....	277
8. References	279

List of Figures

Figure 1. Major classes of antibiotics with a representative example.....	2
Figure 2. Antibiotic targets ¹	3
Figure 3. Resistance mechanisms.....	5
Figure 4. Natural bromophenols (1-59) ¹⁶⁻²⁹	9
Figure 5. Isocitrate lyase (ICL) and tricarboxylic acid cycle (TCA) cycles	10
Figure 6. Classic ICL inhibitors	11
Figure 7. Natural brominated bis-phenols tested by Xu et al. ¹⁸	11
Figure 8. Natural and synthetic brominated bis-phenols tested by Oh <i>et al.</i> ²³	12
Figure 9. Potent chlorinated bis-phenol	13
Figure 10. Bromophenols as isocitrate lyase inhibitors. ³⁸ For each column, ICL inhibition increases going downwards.	13
Figure 11. Oxidative stress and its involvement in neurodegeneration and carcinogenesis. ⁴⁹	20
Figure 12. Example of DNA modification. ^{42,53}	21
Figure 13. Vitamin E and Trolox.	22
Figure 14. Examples of different polyphenols.	23
Figure 15. Examples of catalytic antioxidants.	23
Figure 16. <i>beta</i> -Carotene.....	24
Figure 17. Ubiquinone.....	25
Figure 18. Natural compounds involved in Nrf2 regulation.	25
Figure 19. Bromophenols with antioxidant activity and their reaction with DPPH radical	26
Figure 20 Brominated mono and bis-phenols with radical scavenging activity	26
Figure 21. Brominated mono- and bis-phenols with radical scavenging activity ^{27,28} ..	27
Figure 22. Halophenols as antioxidants and cytoprotective agents ⁷¹	28
Figure 23. Brominated bis-phenols with a side chain ⁷²	29
Figure 24. Previous and current work examples.	31
Figure 25. Tetramer with a central phenyl ring.....	32
Figure 26. Biaryl and flexible tetramers.....	33
Figure 27. Hexamers.	33
Figure 28. Long range coupling of the bridge in 131.....	38

Figure 29. Set of dimers. Black structures: obtained as pure compounds. Red structures: reaction leads to mixtures of products. Blue structures: a solvent or reagent could not be removed completely.	40
Figure 30. NMR of 153, with the signals of toluene highlighted. Recorded in DMSO-d ₆ at 400 MHz.	41
Figure 31. NMR of 156 and presence of aldehyde. Recorded in DMSO-d ₆ at 400 MHz.	42
Figure 32. NMR of 158. Recorded in DMSO-d ₆ at 400 MHz.	43
Figure 33. ¹ H NMRs of 165 (a), 164 (b) and 163 (c). All spectra were recorded in DMSO-d ₆ at 400 MHz.	45
Figure 34. Structures of 165, 166 and 167.	46
Figure 35. ¹ H-NMR of 167 (DMSO-d ₆ at 400 MHz).	46
Figure 36. ¹³ C-NMR of 167. Recorded in DMSO-d ₆ at 400 MHz.	47
Figure 37. Structure of 166, minimised with GAFF force field and rendered in UCSF Chimera.	47
Figure 38. ¹ H-NMR of 166. Recorded in DMSO-d ₆ at 400 MHz.	48
Figure 39. ¹³ C-NMR of 166. Recorded in DMSO-d ₆ at 400 MHz.	48
Figure 40. Crystal structure of 166. Top, a single molecule of 166 hydrogen bonded with a diethyl ether molecule and chain-like arrangement of 166 within the crystal, bottom.	49
Figure 41. ¹ H-NMR of the reaction mixture after 6 and 24 hours and spectra of 166 and 167 as reference compounds. All spectra were recorded in DMSO-d ₆ at 400 MHz.	50
Figure 42. Reaction of the closed acetal 166 (a) with 4-chlororesorcinol to give 165 (b) at 7 and 24 hours showing presence of 167 (c) during the reaction. All spectra were recorded in DMSO-d ₆ at 400 MHz.	51
Figure 43. Yield of some compounds with some favourable fragmentation points highlighted.	54
Figure 44. Scrambling of 163 (a) under Method 1 conditions with reference 4-bromo- and 4-chlororesorcinol. All spectra were recorded in DMSO-d ₆ at 400 MHz.	55
Figure 45. Scrambling of 163 (a) under Method 2 conditions with reference 4-bromo- and 4-chlororesorcinol. All spectra were recorded in DMSO-d ₆ at 400 MHz.	56
Figure 46. Crystal structures of 163, 164 and 165 and their arrangement within the crystal.	59
Figure 47. ¹ H-NMRs of 163 (a) and 183 (b).	61
Figure 48. ¹ H-NMR of 217 (a), 218 (b) and 219 (c).	67

Figure 49. View of a molecule of 163, indicating the atom numbering scheme and hydrogen-bonded atoms of neighbouring molecules. Thermal ellipsoids are drawn at the 50% probability level.	99
Figure 50. 163 molecules linked through hydrogen bonds in chains. The oxygen atoms of the hydrogen-bonded ether molecules are also included.	100
Figure 51. View of a molecule of 164. Thermal ellipsoids are drawn at the 50% probability level.....	103
Figure 52. Linking, through hydrogen bonds, of the 164 molecules, showing the ladder formation and the linking of pairs of ladders about centres of symmetry.....	104
Figure 53. View of a molecule of 165. Thermal ellipsoids are drawn at the 50% probability level.....	107
Figure 54. The molecules are linked through hydrogen bonds in chains (horizontally) about centres of symmetry, and in sheets and through methanol bridges.....	108
Figure 55. View of a molecule of 166 and hydrogen-bonded solvent (Et ₂ O) molecule, indicating the atom numbering scheme. Thermal ellipsoids are drawn at the 50% probability level.....	111
Figure 56. A chain of hydrogen-bond linked 166 and ether molecules.	111
Figure 57. Structures described in Chapter 2.	145
Figure 58. General structures of the compounds presented in Chapter 3.	146
Figure 59. ¹ H-NMR and ¹³ C-NMR of 222.	150
Figure 60. Comparison of the ¹³ C-NMR spectra of 224 (top) and 225 (bottom).....	151
Figure 61. ¹ H-NMR of 233.	156
Figure 62. ¹ H-NMR of the fragmentation of 225 (red) and spiking with 2,4-dimethoxybenzoic acid (blue).	158
Figure 63. ¹ H-NMRs of 220 (top), 241 (middle) and 242 (bottom).....	163
Figure 64. ¹ H-NMRs of 220 (top), 243 (bottom).	164
Figure 65. ¹ H-NMRs of 245 (A), reaction mixture for 245 before completion (B), 246 (C) and 244 (D).	165
Figure 66. ¹ H-NMR of 248.	167
Figure 67. ¹ H-NMR of 247 (a), 243 (b), 244 (c), 249 (d), 245 (e) and 250 (f).	170
Figure 68. ¹³ C-NMR of 247 (bottom) and 243 (top).....	170
Figure 69. Structures presented in the previous chapters and considered for the <i>in vitro/in vivo</i> testing in the following chapters.	172
Figure 70. Convergent and divergent synthesis of dendrimers.	188
Figure 71. Basic structure of calix[4]arenes and calix[4]resorcinarenes.	189

Figure 72. Conformations of calix[4]arenes.	190
Figure 73. 21 units multicalixarene built using click chemistry. ¹³⁵	192
Figure 74. Previously investigated resorcinarene-calixarene based multicalixarenes (A) ¹³⁶ and current work (B).	193
Figure 75. ¹ H-NMR of 183 (top), and 255 (bottom).	197
Figure 76. ¹ H-NMR of 256.	198
Figure 77. ¹ H-NMR of 257.	200
Figure 78. HSQC of of 257.	201
Figure 79. HMBC of of 257.	201
Figure 80. IR spectra of 259.	202
Figure 81. ¹ H-NMR of 260.	204
Figure 82. ¹ H-NMR of 255 (top), 265 (centre) and 264 (bottom).	207
Figure 83. ¹ H-NMR of 266.	208
Figure 84. Proliferation screening against MCF-7 and HL60, at 10 and 100 μ M concentrations for a three day treatment. Result expressed as percentage against control.	224
Figure 85. Compounds showing selectivity over the two cell lines.	225
Figure 86. Structures displaying low proliferation inhibition.	226
Figure 87. Effect of the central core of tetramers on cell viability.	226
Figure 88. Effect of the halogen substitution on cell viability.	227
Figure 89. Effect of geometry on cell viability.	227
Figure 90. Effect of the number of monomers on cell viability.	228
Figure 91. Tetramers with high anti proliferative activity.	228
Figure 92. Fluorescent compounds for imaging.	229
Figure 93. Fluorescence microscopy of MCF-7 cell treated with 187 and Hoescht 33342.	230
Figure 94. Fluorescence microscopy of MCF-7 cell treated with either 165, 187 or 143 and Hoescht 33342.	231
Figure 95. Autoxidation of linoleic acid monitored by UV absorbance. Initiator addition at point B, antioxidant addition at point C.	236
Figure 96. Structure of Trolox.	237
Figure 97. UV profile of the progressive conversion of DPPH into DPPHH.	240
Figure 98. Sample compounds for the initial evaluation of DPPH radical scavenging assay.	242

Figure 99. Time course profiles of the reaction between DPPH (150 μ M) and sample compounds monitored at 512 nm.	242
Figure 100. Comparison between the scavenging effect of two sample compounds and the decomposition of DPPH.	243
Figure 101. Compounds for the evaluation of halogen and geometry effects on DPPH scavenging activity.	245
Figure 102. Progress of the reaction between DPPH (150 μ M) and sample compounds (20 μ M) monitored at 512 nm.	246
Figure 103. DPPH consumed (initial concentration 150 μ M) by sample compounds (10 μ M) after 500 minutes. Measures in triplicate and error expressed as standard deviation.	246
Figure 104. Compound 183.	252
Figure 105. Decomposition of ABTS, starting from two different concentrations.	253
Figure 106. Different families of compounds, each with a representative structure.	255
Figure 107. ABTS scavenging activity of compound families' representative structures.	256
Figure 108. Xanthones.	256
Figure 109. ABTS scavenging activity of xanthones.	257
Figure 110. Benzophenones.	257
Figure 111. ABTS scavenging activity of benzophenones.	258
Figure 112. Bis-phenols.	258
Figure 113. ABTS scavenging activity of bis-phenols.	259
Figure 114. Dimers with different sidechains.	259
Figure 115. ABTS scavenging activity of dimers with different sidechains.	260
Figure 116. Dimers with different halogens.	261
Figure 117. ABTS scavenging activity of dimers with different halogens at 10 minutes and 600 minutes.	261
Figure 118. Tetramers with different halogens.	262
Figure 119. ABTS scavenging activity of tetramers with different halogens.	262
Figure 120. Tetramers with different geometries.	263
Figure 121. Activity of tetramers with different geometries.	264
Figure 122. Biaryl tetramers and shorter analogues.	264
Figure 123. ABTS scavenging activity of biaryl tetramers and shorter analogues.	265
Figure 124. Biaryl tetramers with different halogens.	265
Figure 125. ABTS scavenging activity of biaryl tetramers with different halogens.	266

Figure 126. Alkyl linked tetramers.	266
Figure 127. ABTS scavenging activity of alkyl linked tetramers.	267
Figure 128. Hexamers.	267
Figure 129. ABTS scavenging activity of hexamers.....	268
Figure 130. Effect of the bridge substituent in resorcinol dimers.	268
Figure 131. Effect of the number of resorcinol units on the activity.	269
Figure 132. Effect of the halogen on the activity.	269
Figure 133. Effect of the geometry of tetramers on the activity.	269
Figure 134. Effect of the central linker on the activity of tetramers.	270
Figure 135. Assay model.....	271
Figure 136. Effect of different <i>t</i> BuOOH concentrations on proliferation.....	271
Figure 137. Structures tested for protective effects.....	272
Figure 138. Effect of different compounds (at three different concentrations, each one in triplicate), on MCF-7 cells treated with <i>t</i> BuOOH. Error expressed as standard deviation.	273
Figure 139. Lead compounds by Zhao. ⁷¹	274

List of Schemes

Scheme 1. a) Fenton reaction. b) reduction of iron (III) to iron (II).	17
Scheme 2. Lipid peroxidation, adapted from Thanan. ⁴⁹	17
Scheme 3. Detoxification of superoxide and hydrogen peroxide. SOD (superoxide dismutase), CAT (catalase), GPX (glutathione peroxidase), GR (glutathione reductase), GST (glutathione <i>S</i> -transferase).	18
Scheme 4. Catalytic cycle of Ebselen.	24
Scheme 5. Retrosynthesis of dimers.	34
Scheme 6. Synthesis of 4-bromoresorcinol.	35
Scheme 7. Synthesis of 2,4-dibromoresorcinol.	35
Scheme 8. Synthesis of 2,4-dibromophloroglucinol (123). a) Possible routes to 2,4-dibromophloroglucinol. b) Approach used to synthesise 2,4-dibromophloroglucinol.	36
Scheme 9. Method 1.	37
Scheme 10. Synthesis of 131.	37
Scheme 11. Synthesis of 132.	38
Scheme 12. Synthesis of 134, 135 and 136.	38
Scheme 13. Bacci's synthesis of bis-phenols.	39
Scheme 14. Synthesis of 140.	39
Scheme 15. Synthesis of 158.	43
Scheme 16. Synthesis of 160 and attempted synthesis of X.	44
Scheme 17. Synthesis of 163, 164 and 165.	44
Scheme 18. Synthesis of 165 and 166.	50
Scheme 19. Equilibrium between 166 and 167.	51
Scheme 20. Retro-Friedel-Crafts fragmentation. General mechanism (a) and fragmentations observed by Bacci ⁷⁶ (b, c).	53
Scheme 21. Synthesis of 180, 181 and 182.	57
Scheme 22. Dehalogenation reactions.	60
Scheme 23. Halogenation of tetramers.	62
Scheme 24. Suzuki cross –coupling mechanism (a) and formation of an oxo-palladium complex (b). Adapted from Lennox. ⁸⁴	63
Scheme 25. Synthesis of 191, 192, 193 and 194.	64
Scheme 26. Synthesis of 197, 198 and 199.	64
Scheme 27. Synthesis of flexible tetramers.	65

Scheme 28. Synthesis of hexamers.	66
Scheme 29. Synthesis of benzophenones according to Hu. ⁹⁸	146
Scheme 30. Synthetic approach towards benzophenones, bis-phenols, xanthenes, xanthenes and their brominated analogues.....	147
Scheme 31. Bromination of 2,4-dihydroxybenzoic acid and similarity with benzophenones.	147
Scheme 32. Synthesis of 220.....	149
Scheme 33. Synthesis of 222.....	149
Scheme 34. Synthesis of 225 and 227.....	150
Scheme 35. Synthesis of 229 and attempted synthesis of 230.	151
Scheme 36. Retrosynthesis of 224.	152
Scheme 37. Acylation of aromatic compounds with P ₂ O ₅ /SiO ₂ , examples from Zarei. ¹⁰⁹	153
Scheme 38. Synthesis of 225.....	153
Scheme 39. Attempted synthesis of 231.	154
Scheme 40. Acylation of anisole with acetic acid in the presence of methanesulfonic acid and graphite reported by Sarvari. ¹¹⁴	154
Scheme 41. Acylation of 1,3-dimethoxybenzene with 2,6-dimethoxybenzoic acid. .	155
Scheme 42. Methylation of 220.	155
Scheme 43. Synthesis of 233 from 2,6-dimethoxybenzoic acid.	156
Scheme 44. Decarboxylation of 2,6-dimethoxybenzoic acid.....	156
Scheme 45. Acylation of 1,3-dimethoxybenzene with 2,6-dimethoxybenzoic acid, halted before rearrangement.....	157
Scheme 46. Synthesis of 233 from 1,3-dimethoxybenzene and 2,6-dimethoxybenzoic acid and subsequent rearrangement (a). Rearrangement of 225 to give 233 (b).....	157
Scheme 47. Fragmentation of 225.....	157
Scheme 48. Breakdown of 233 (a) and decarboxylation of 2,4-dimethoxybenzoic acid (b).	158
Scheme 49. Summary of the reactions involved in the synthesis of 225 and 233.	159
Scheme 50. Attempted synthesis of 231 with methane sulfonic acid and graphite. ..	159
Scheme 51. Attempted approaches for the synthesis of 231.....	160
Scheme 52. Potential alternative approach to the synthesis of 231.....	160
Scheme 53. Pettit's benzophenones synthesis. ¹¹⁸	161
Scheme 54. Synthesis of 224.....	161
Scheme 55. Synthesis of 240 and 241.....	161

Scheme 56. Synthesis of 241 and 242.....	162
Scheme 57. Synthesis of 243.....	163
Scheme 58. Synthesis of 244 and 245.....	164
Scheme 59. Synthesis of 245.....	165
Scheme 60. Synthesis of 246 (a) and 244 (b).....	166
Scheme 61. Synthesis of 247 described by Shi. ¹⁰⁰	166
Scheme 62. Synthesis of 248.....	166
Scheme 63. Different synthetic approaches to 135.	167
Scheme 64. Different synthetic approaches to 136.	168
Scheme 65. Synthesis of 136 by bromination.	168
Scheme 66. Synthesis of 247.....	169
Scheme 67. Synthesis of 249.....	169
Scheme 68. Synthesis of 250.....	169
Scheme 69. Dendrimers obtained by reaction of activated carboxylic acids and amines.	191
Scheme 70. Azide-alkyne cycloaddition.	194
Scheme 71. Mechanism of CuAAC. ¹⁴⁴	195
Scheme 72. Functionalization of the cores.....	196
Scheme 73. Synthesis of 255.....	196
Scheme 74. Synthesis of 256 and its 3D representation (the image is only meant to provide a better visualization of the structure, it is not a representative conformation. MarvinSketch and UCSF Chimera)	198
Scheme 75. Synthesis of test dendrimer 257.....	199
Scheme 76. Synthesis of 259.....	202
Scheme 78. Synthesis of 260.....	203
Scheme 79. Synthesis of 264.....	205
Scheme 80. Synthesis of 266.....	207
Scheme 81. Reduction of MTS to its chromogenic formazan derivative.	221
Scheme 82. Ferric-tripyridyltriazine complex, oxidised and reduced form.....	238
Scheme 83. Synthesis of ABTS ⁺	241
Scheme 84. HAT and ET reactions shown on eugenol.....	247
Scheme 85. Termination reactions for DPPH.	248
Scheme 86. Reactions of BHT with DPPH.....	249
Scheme 87. Reactions of eugenol with DPPH.	250

Scheme 88. DPPH mediated cyclization of garcinol. Only the relevant fragment is reported. ¹⁷⁵	250
Scheme 89. Proposed reactions for tetramer 163.	251
Scheme 90. Cyclization to fluorone.	252

List of Tables

Table 1. Reactive oxygen species ⁴²	15
Table 2. Comparison of yields of Method 1 and 2 for 107, 111 and 109.	41
Table 3. Yields of the reaction between 4-haloresorcinols and isomeric benzene dicarboxaldehydes under reaction conditions of Method 1 and 2.....	52
Table 4. Crystal data and structure refinement details for the four compounds 163 , 164 , 165 and 166	70
Table 5. Reaction conditions for the synthesis of 225.	154
Table 6. Results of the proliferation screening against MCF-7 and HL60, at 10 and 100 μ M concentrations for a three day treatment. Data expressed as percentage of proliferation compared to the control. Colour gradient from 0% proliferation (red) to white (50%) and blue (100%).	223
Table 7. Summary of the scavenging activity of the tested compounds (1 μ M), expressed as % of ABTS consumed, after 10 minutes and after 10 hours. Colour scale ranges from low activity (red) to high activity (blue). NaAsc = Sodium Ascorbate.	254

List of Abbreviations

AAPH:	2,2'-azobis(2-amidinopropane) dihydrochloride
ABTS:	2,2'-azino-bis(3-ethylbenzothiazoline-6-sulphonic acid)
AD:	Alzheimer's disease
ALS:	amyotrophic lateral sclerosis
AMD:	age-related macular degeneration
ARE:	antioxidant response element
BHT:	butylated hydroxytoluene
CAT:	catalase
DCE:	dichloroethane
DCM:	dichloromethane
CUPRAC:	cupric reducing antioxidant capacity
DIPEA:	diisopropylethylamine
DPPH:	1,1-diphenyl-2-picrylhydrazyl
EPR:	electron paramagnetic resonance
ET:	electron transfer
FRAP:	ferric reducing ability of plasma
GPX:	glutathione peroxidase
GSH:	glutathione
GSSG:	glutathione disulphide
HAT:	hydrogen atom transfer
HD:	Huntington's disease
HUVEC:	human umbilical vein endothelial cells
ICL:	isocitrate lyase
Keap1:	Kelch-like ECH-associated protein 1
LDL:	low-density lipoprotein
MDR:	multi drug resistant
MIC:	minimum inhibitory concentration
Mtb:	Mycobacterium tuberculosis
MTS:	([3-(carboxymethoxy)phenyl]-3-(4,5-dimethyl-2-thiazolyl)-2-(4-sulfo-phenyl)-2H-tetrazolium inner salt)
MTT:	(4,5-dimethyl-2-thiazolyl)-3,5-diphenyl-2H-tetrazolium bromide)
NaAsc:	sodium ascorbate

NAD: nicotinamide adenine dinucleotide
NBS: N-bromosuccinimide
NOS: nitric oxide synthase
Nrf2: nuclear factor erythroid 2–related factor 2
ORAC: oxygen radical absorbance capacity
PABA: 4-aminobenzoic acid
PD: Parkinson’s disease
PDC: pyridinium dichromate
ROS: reactive oxygen species
R-PE: R-phycoerythrin
RT: room temperature
SAR: structure-activity relationships
SOD: superoxide dismutase
TCA: tricarboxylic acid cycle
TDR: totally drug resistant
TEA: trimethylamine
TEAC: Trolox equivalent antioxidant capacity
TRAP: total peroxyl radical-trapping antioxidant parameter
UCSF: University of California, San Francisco

Acknowledgments

First of all, I would like to thank Susan Matthews for giving me the opportunity of working with her on this project and for her support during the course of my PhD. I would also like to thank Maria O'Connell for her supervision and teaching in the biology side of the project. I would also like to thank David Hughes for the crystallographic analysis of the compounds presented.

I would like to thank Zoe Waller for her support through the PhD, for believing in my skills. Thanks for pushing me forward and improving my teaching skills.

Colin Macdonald for the help with the NMR, both on the theoretical and the practical side of things.

Stephen Ashworth for the help with kinetics.

A big thank goes to all my family, who supported me through the (very long) course of my studies and had to put up with the distance.

My partner, Giulia, who has been with me and supported me during happy times and also when I was stressed or depressed.

Simone, Zoe and Qiran, for their friendship and help during the PhD. Anja, Noelia, Ivy, Shirley and Patricia for their help in the biology lab and their kind teaching. Jack, Antony, Alicia, Magda, Robert, Donald, Anissa, Janet and Jane the students who worked with me and bore with my improving and very harsh way of teaching.

Doroty, Desi, Hanae, Veronica, Melania, Henry, Ana, Luca, Sonia, Dani, Victor, Davide, Teresa, Yohan, Laura, Luigi, Paul, Carl and all the people I am sure I forgot to add. Thanks for the friendship, shopping, drinks, table football, barbecues and whatnot!

Mark Searcey, Lesley Howell, and my current lab mates. Thank you for believing in me.

Daniela Barlocco, Stefania Villa, Arianna Gelain, Daniela Masciocchi, Elena Cocchi and all the people in Milano, without your help I would have not been able to find a PhD in the first place.

1. Introduction

1.1 Antimicrobials and resistance

Antibiotics are undoubtedly one of the most important scientific achievements of the 20th century. Their introduction, beginning in the 30s with sulfonamides and β -lactams, revolutionised the treatment and prophylaxis of bacterial infections and paved the way for considerable medical progress (*e.g.* surgery and transplants). Following the first discoveries, a “golden age” of development led to the main antibiotic families still in use today, with the introduction of chloramphenicol, macrolides, tetracyclines, quinolones, aminoglycosides and aminocoumarins (**Figure 1**).¹⁻⁴

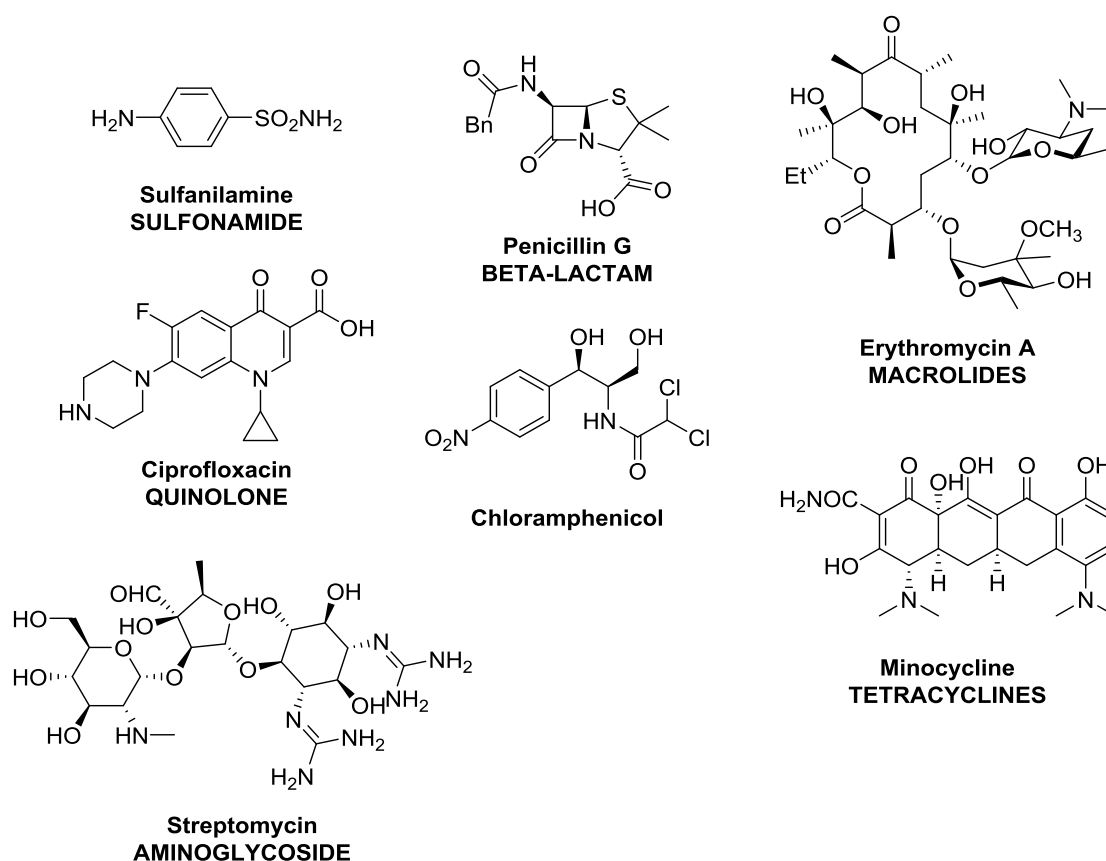


Figure 1. Major classes of antibiotics with a representative example

From the 70s, new classes of broad spectrum antibiotics have not been commercialised and only a few new compounds have been approved, often developed from older discoveries.

On the other hand, in 1942, immediately after the first discoveries, the problem of resistance emerged. Initially, it appeared a minor concern compared to the fast-paced development of new treatments. However, at present, it has become an area of major concern. Resistance has been identified for all available classes of compounds and multidrug-resistant (MDR) strains have been identified, with extreme cases of totally drug resistant (TDR) bacteria also now present.^{1,3}

1.1.1 Drug Targets

A range of different type of targets have been successfully exploited by antibiotics developed to date (**Figure 2**). β -Lactams produce their bactericidal effects by alteration of the homeostasis of the cell wall, a structure mainly sustained by a peptidoglycan composed of alternating *N*-acetylmuramic acid and *N*-acetylglucosamine. These structures are crosslinked through D-alanine pentapeptides protruding from the *N*-acetylmuramic units. The crosslinking reaction is catalysed by transpeptidases, which are the target of β -lactams. These are similar to the enzyme's substrate and irreversibly acylate it, leading to impaired wall synthesis. Without the wall, the cell is exposed to an hyperosmotic environment with subsequent cell death.⁵ A minor class of antibiotics, glycopeptides (*e.g.* Vancomycin), produce their activity by inhibition of both transglycopeptidases and transpeptidases by mimicking their structure.⁶ The absence of the cell wall in mammals drives the selectivity and the interest towards these approaches, and novel molecules, such as cationic peptides, are being developed to target this key structure.^{7,8}

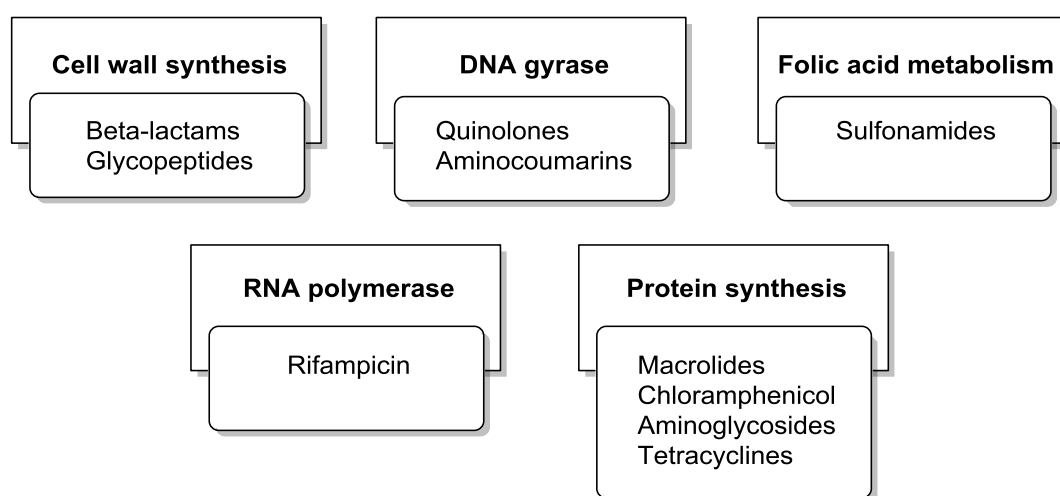


Figure 2. Antibiotic targets¹

Another important family of targets are DNA gyrase and topoisomerase IV. Bacterial DNA is normally a circular, single molecule, which is tightly packed into a supercoiled conformation. Access to DNA for replication, transcription and other processes, requires intervention of either gyrases or topoisomerases. These enzymes can introduce temporary breaks which allow unwinding and thus processing of DNA. By inhibiting these enzymes, there is impaired access to the genetic information, which leads to rapid death of the cell. These targets are also selective, as humans do not express the same types of topoisomerases.⁶

DNA-dependent RNA synthesis can also be targeted. Rifampicin, an antibiotic derived from structural modifications of natural metabolites of *Nocardia mediterranei*, is able to inhibit RNA synthesis. Its activity is due to binding within the main channel of bacterial DNA-dependent RNA polymerase and subsequent blocking of the elongation process of the forming RNA.⁹

Downstream of RNA synthesis, translation can additionally be targeted. Different families of antimicrobials can inhibit protein synthesis by interfering with different cellular structures. Bacterial ribosomes are different in humans and bacteria, and thus a rational target for antibiotics. Aminoglycosides, for example, bind to the 30S ribosomal unit and cause mistranslations, leading to the synthesis of nonsense proteins. Similarly to aminoglycosides, tetracyclines also bind to the 30S subunit (although other binding sites have been suggested to be involved in their action) but produce termination of the peptide growth. Macrolides and chloramphenicol, on the other hand, bind to the 50S subunit and prevent elongation, thus producing their bacteriostatic effect.⁶

Sulfonamides were among the first classes of antimicrobials discovered. They have a completely different mode of action, as 4-aminobenzoic acid (PABA) analogues they compete for dihydropteroate synthetase, an enzyme involved in folic acid synthesis. Differently from humans, who acquire folate through the diet, bacteria need to produce it. Folate is necessary for a variety of functions, and is essential for the synthesis of thymidine, without which the bacteria cannot multiply. Trimethoprim is another antimicrobial agent involved in folic acid metabolism; it acts downstream of the sulfonamides, and inhibits the reduction of dihydrofolic acid to tetrahydrofolic acid.⁶

1.1.2 Modes of Resistance and Transmission

Despite all these different mechanisms of action, bacteria have been able to develop a multifaceted array of survival adaptations and mechanisms of resistance for

every available antibiotic. Often, a single microorganism displays multiple forms of resistance against the same type of antibiotic.

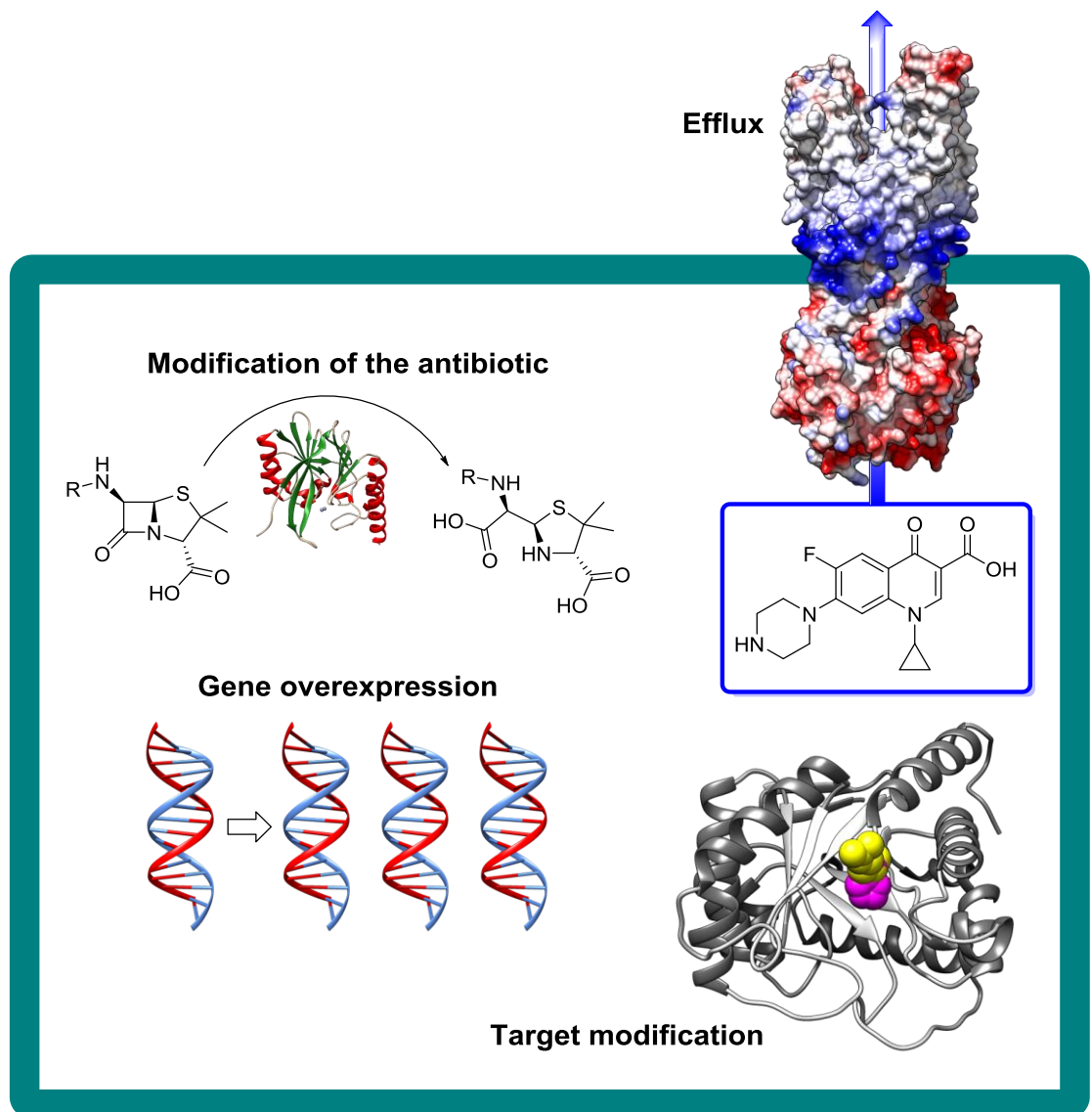


Figure 3. Resistance mechanisms

As illustrated in **Figure 3**, the ways in which bacteria exert resistance can be classified into four main modes of action:

- modification of the antibiotic
- modification of the target
- gene amplification
- efflux from the cell^{3,4}

A notable example of modification of antibiotics is through hydrolysis. Penicillins are substrates of β -lactamase, enzymes produced by the bacteria which inactivate the antibiotic by hydrolysis of the β -lactam ring. Macrolides are another example of family subject to hydrolytic enzymes. Alternatively, chloramphenicol is acetylated by a CoA-dependent chloramphenicol acetyltransferase. Another CoA-dependent acetyltransferase is responsible for the same transformation of aminoglycosides. These are also subject to *O*-phosphorylation and *O*-adenylation by ATP-dependant phosphotransferases and nucleotidyltransferases respectively.^{5,10,11}

Resistance by alteration of the target has spread to most classes of antimicrobials. It involves a change in the target of the antibiotic, for example a residue mutation in the sequence of an enzyme, which retains its activity while reducing the affinity for the antimicrobial. A single amino acid mutation in dihydropteroate synthase can lead to resistance, as in the case of specific *Escherichia coli* strains. In other species, *e.g. Staphylococcus haemolyticus* and *aureus*, multiple mutations cause resistance to the sulfonamides. Base repeats leading to modified tertiary structures have also been linked to altered response in *Streptococcus pneumoniae*. Quinolones, macrolides, aminoglycosides and β -lactams are other major examples of antimicrobials which can incur a resistance by alteration of the target.^{1,12}

Gene amplification produces overexpression of either the target protein or other systems involved in resistance (*e.g.* efflux pumps), thus reducing the effect of the antimicrobial. Sulfonamides and trimethoprim, for example, are susceptible to this type of resistance.^{3,13} Efflux pumps externalise solutes from the cytosol of the bacteria, effectively decreasing their intracellular concentration, with obvious consequences in the case of antibiotics. These systems become relevant when they are overexpressed (which can be substrate-induced) and/or mutated, thus increasing their effectiveness. The pumps can be specific for a substrate or be associated with multi drug resistance.¹³ Increased efflux and its consequent reduction of intracellular xenobiotic can facilitate the development of resistance either directly, by a combined effect with other resistance mechanisms, or indirectly by enhancement of gene transfer and recombination, partly by activation of the SOS response, radical mediated damage and subsequent repair mechanisms.^{3,14}

The genes responsible for resistance can be transmitted both vertically, by multiplication of the microorganism, and horizontally, by exchange of genetic information from one cell to another, thus maximising the potential of diffusion.

Horizontal gene transfer comprises a complex set of regulated functions, involving mobile genetic elements. Plasmids are probably the most relevant vectors, but viruses, transposons, integrons and naked DNA have been involved with resistance.^{3,15}

1.1.3 Human Involvement

Human activities have a great impact on development and maintenance of antibiotic resistance. Although misuse or abuse of antimicrobials for treatment or prophylaxis in humans is often perceived as a main factor in promoting and maintaining selection of resistant strains, there are many other factors to be accounted for. Treatment of household pets has to be considered as well, especially with the animal being in close contact with humans. Antibiotics are used in animal prophylaxis and treatment, and have also been used for growth production. Aquaculture and agriculture also take advantage of antibacterial products. Finally, cleaning products and research also contribute to resistance development.³

1.2 Bromophenols

Nature provides an incredibly varied range of substances, often with complex structures and different biological activities. Therefore, medicinal chemists frequently take inspiration from natural compounds. The idea behind this project comes from a group of brominated phenols isolated from red algae, which were harvested in the seas of China, Korea and Japan.

Figure 4 shows a set of representative bromophenols (**1-59**). These compounds were isolated from four families of red algae:

- *Rhodomela (confervoides*,¹⁶⁻²⁰ *larix*²¹)
- *Odonthalia (corymbifera*^{22,23})
- *Symphyocladia (latiscula*²⁴⁻²⁶)
- *Polysiphonia (urceolata*,²⁷⁻²⁹ *lanosa*³⁰)

These organisms all have a vanadium bromoperoxidase, a vanadate dependant enzyme, which is responsible for the synthesis of a profuse number of brominated substances.³¹ These products are involved in defence (antimicrobial and feeding-deterrent activities),^{22,31,32} signaling³¹ and scavenging H₂O₂ during oxidative stress.³³ The colour of the algae itself is due to a cuticle composed of polymerised bromophenols.³³

The structures presented in **Figure 4** are, for the most part, based on brominated catechols and present redundant side chains, especially alcohols, ethers, aldehydes, acids and esters. A small number of derivatives coupled with amino acids (**22**, **23**, **33**, **48**, **56**)^{17,19,26} or nucleosides (**24**)¹⁹ have also been discovered. Most of the isolated compounds are based on mono- and diaryl-bromophenols, only a few examples of tri- and tetra-aryl structures are currently known.³⁴

Of particular interest in this project are brominated bis-phenols such as **27-34**, produced by dimerisation of brominated catechols and extensively studied for their activities as antioxidants and antimicrobials (isocitrate lyase inhibitors). These compounds also present an interesting inhibitory activity against aldose reductase,²⁵ α -glucosidase³⁴ and tyrosine phosphatase 1B,³⁵ hence they possess a potential antidiabetic activity. Natural bis-phenols with these properties and their respective synthetic derivatives, already reported, will be individually discussed in the following sections.

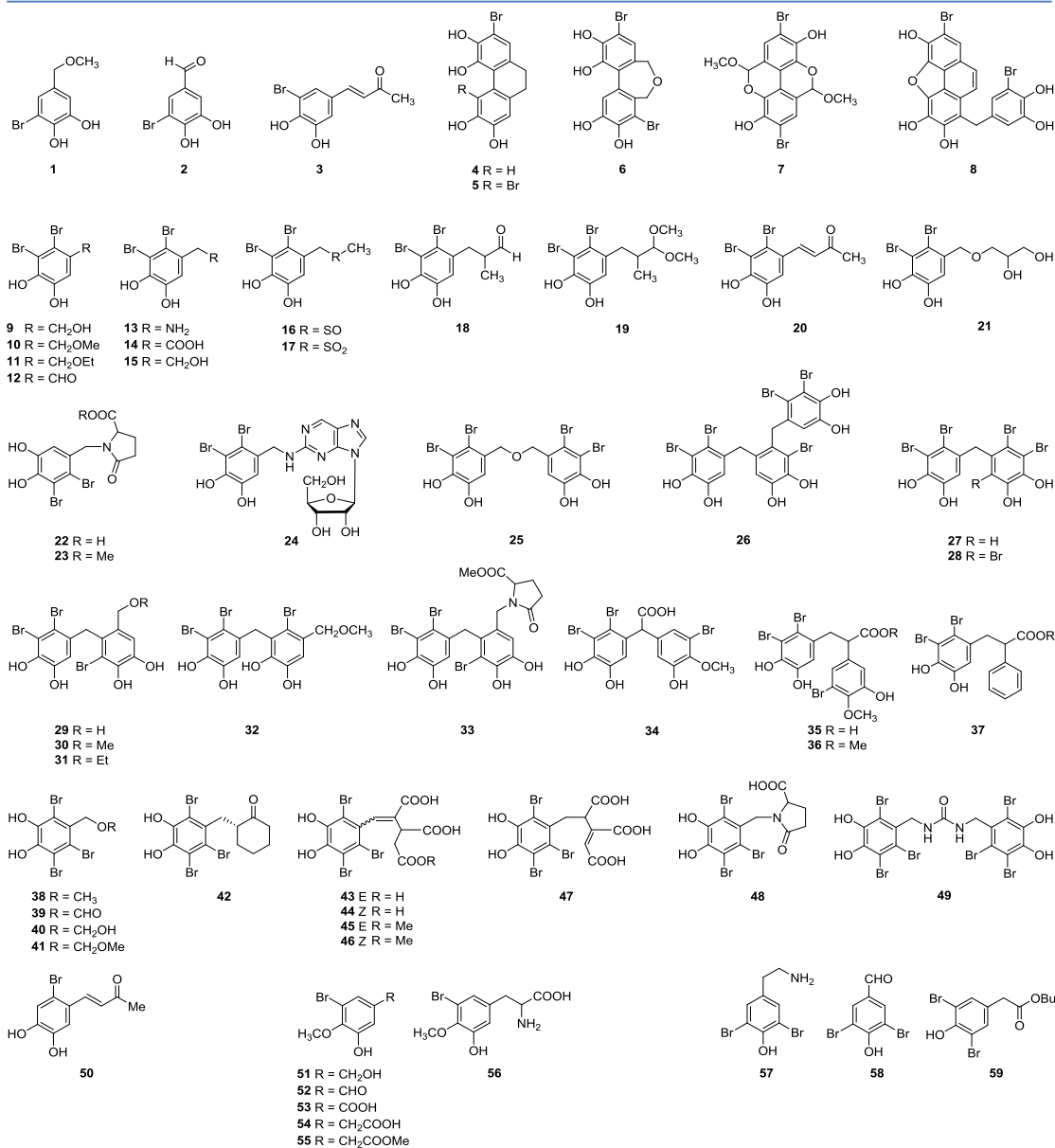


Figure 4. Natural bromophenols (1-59)¹⁶⁻²⁹

1.2.1 Brominated bis-phenols as antimicrobials

Some of the isolated and synthesised brominated phenols and their dimerised derivatives have displayed activity against a range of bacteria and fungi. Whilst the mechanism of action is not fully clear, isocitrate lyase (ICL) has been identified as a potential target.³⁶

1.2.1.1 Isocitrate Lyase

Isocitrate lyase is present in bacteria, fungi, some protists and plants. It is part of the glyoxylate cycle and mediates the conversion of isocitrate to succinate and glyoxylate (**Figure 5**). It is an anaplerotic path in the tricarboxylic acid cycle (TCA)

and allows the microorganism to assimilate 2-carbon compounds for catabolic reactions such as carbohydrate synthesis, bypassing the following limiting steps (mediated by isocitrate dehydrogenase and α -ketoglutarate dehydrogenase). Mammals do not have ICL, thus it represents an interesting, selective, target for the development of new antibiotics and biological tools.^{18,37-39}

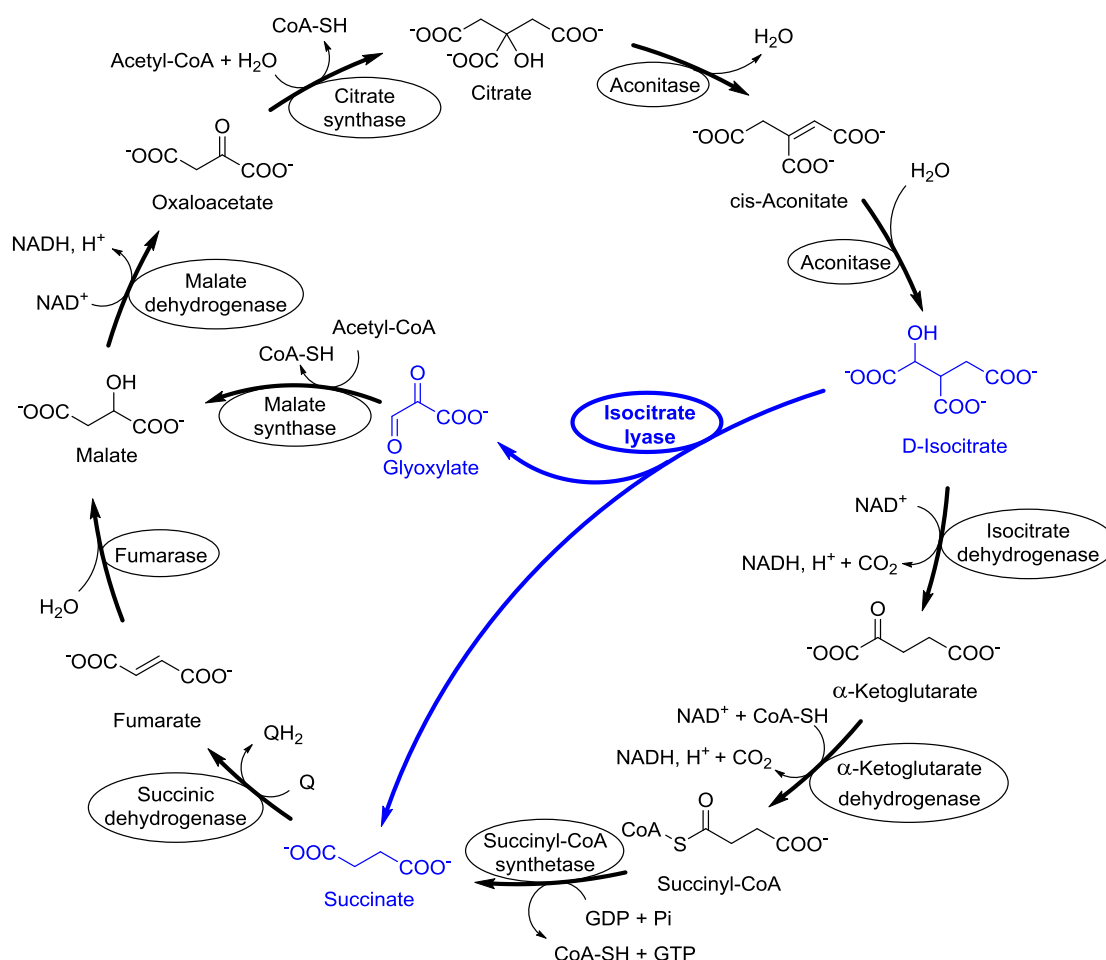


Figure 5. Isocitrate lyase (ICL) and tricarboxylic acid cycle (TCA) cycles

The role of ICL is critical in *Mycobacterium tuberculosis* (Mtb). The pathogen, which expresses two isoforms, ICL1 and ICL2, is dependent on their activity, notably during lung infection and within macrophages. Previous studies proved that deletion of both enzymes impairs intracellular replication of the pathogen and leads to its elimination from the lungs of mice.⁴⁰

Since the identification of ICL as target, a number of inhibitors have been reported. Recently, inhibition has been evaluated mostly on Mtb or *Candida albicans* ICL.³⁹

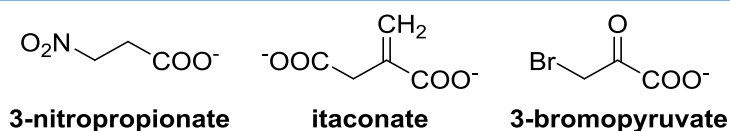


Figure 6. Classic ICL inhibitors

Classic inhibitors are substrate analogues, 3-nitropropionate, itaconate and 3-bromopyruvate (**Figure 6**). These are toxic compounds, they are aspecific and interact with other enzymes of the previously described cycles. 3-Bromopyruvate is also an alkylating agent. Their use is limited to that of tools to investigate the activity of the enzyme and 3-nitropropionate is usually exploited as a positive control for ICL inhibition. The large number of inhibitors discovered up to now have very different structures, and they are of both natural and synthetic origin. However, none of these compounds have been brought forward to clinical trials. Reviewing ICL inhibitors is beyond the scope of this thesis and, for a comprehensive review of these, we recommend the recent “Potential Inhibitors for Isocitrate Lyase of *Mycobacterium tuberculosis* and Non-M. tuberculosis: A Summary”, BioMed Research International (2015), by Lee.³⁹

1.2.1.2 Natural and synthetic bromophenols as antimicrobials

In 2003 Xu *et al.*¹⁸ reported the antimicrobial activity of a small set of natural brominated bis-phenols, shown in **Figure 7**. These were tested against different strains of Gram positive and Gram negative bacteria: *Pseudomonas aeruginosa*, *Escherichia coli*, *Staphylococcus aureus* and *Staphylococcus epidermidis*.

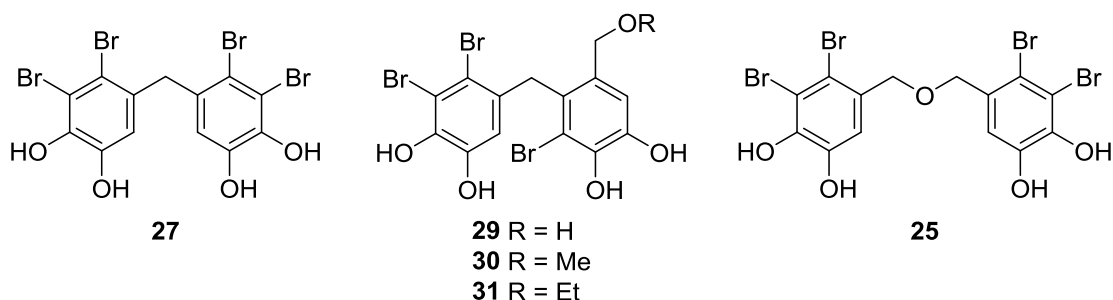


Figure 7. Natural brominated bis-phenols tested by Xu et al.¹⁸

The compounds display highest activity in the *Staphylococcus* family, with **30** and **25** showing the strongest inhibition, and are almost inactive against *Escherichia coli*. The only conclusion about the structure activity relationship is limited to compounds **29-31**: the optimal length of -R, for the activity against *Staphylococcus*, is one carbon.

In 2008 Oh *et al.*²³ described the antibacterial and antifungal activities of some natural bromophenols and synthetic derivatives (**Figure 8** – note: some compounds were previously discussed but the data cannot be related to that of Xu *et al.* because the strains and methods used are different). Concerning the antifungal activity, the natural compound **27** exhibited potent inhibition in all the four strains tested (*Candida albicans*, *Aspegillus fumigatus*, *Trichophyton rubrum*, *Trichophyton mentagrophytes*) with a minimum inhibitory concentration (MIC) two- to fourfold lower than the reference, Amphotericin B. Any change to the structure caused marked loss of activity, for example its regioisomer **68** and the derivatives with different numbers of hydroxyl groups are inactive.

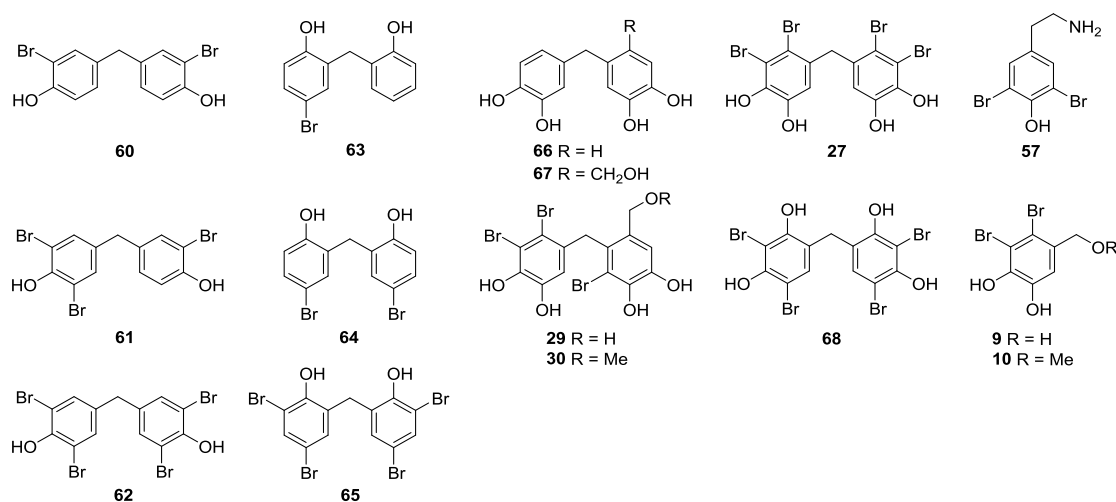


Figure 8. Natural and synthetic brominated bis-phenols tested by Oh *et al.*²³

The antimicrobial activity was tested against six strains of bacteria: *Staphylococcus aureus*, *Bacillus subtilis*, *Micrococcus luteus*, *Proteus vulgaris*, *Salmonella typhimurium* and *Escherichia coli*. *E. coli* showed resistance to all tested compounds. Molecules **64** and **65** can inhibit the growth of all the other strains and show a potent activity, especially the latter, whose MIC is comparable to that of Ampicillin. Analysing compounds **63-65**, it is interesting to note that the activity increases when the number of bromine atoms increases; the same trend can be observed for compounds **60** and **71** (which is a strong inhibitor). Surprisingly, and for unknown reasons, compound **62** is completely inactive.

In 2009 and 2010 the same research group published two more papers on the subject. The first one considers, for the most part, chlorinated compounds.⁴¹ A notable structure presented in this work is **69** (**Figure 9**): it is roughly two times more potent

than ampicillin (although, as seen with most molecules with this backbone, it is inactive against *E. coli*). This result suggests that the halogen is playing an important role in

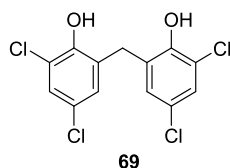


Figure 9. Potent chlorinated bis-phenol

activity and merits further investigation.

The second report³⁸ focused on brominated derivatives and, in addition to the previous antibacterial and antifungal activities, presents specific information about ICL inhibition. The tested compounds are shown in **Figure 10**.

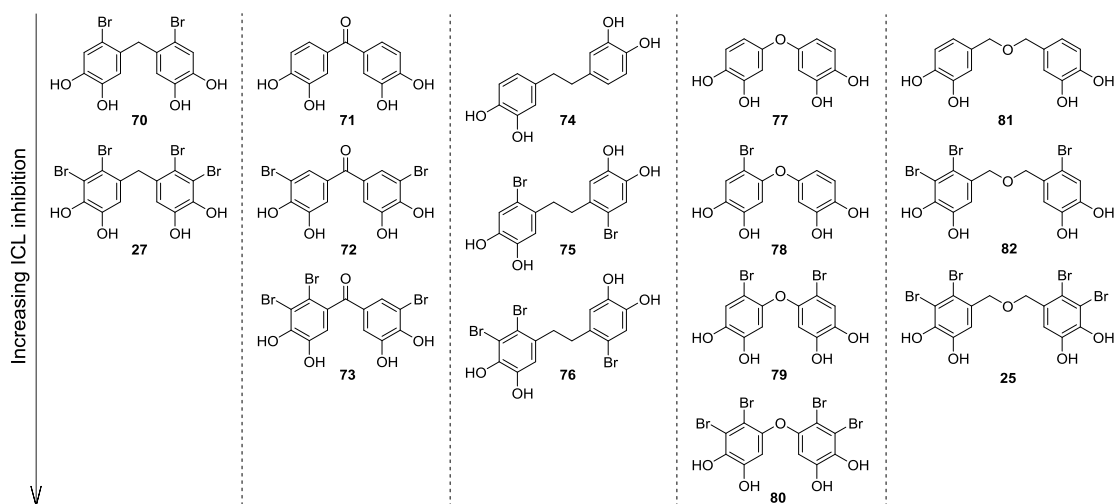


Figure 10. Bromophenols as isocitrate lyase inhibitors.³⁸ For each column, ICL inhibition increases going downwards.

All tested compounds, with the exception of the non-brominated **77** and **81**, show strong inhibition of ICL, with potency similar or higher than the reference, 3-nitropropionate. Compound **73** is the most active compound with an IC_{50} 20 times lower than the reference. The structure-activity relationships (SAR) for ICL inhibition that can be obtained from this work can be summarised as follows:

- the activity increases when the number of halogens increases (**Figure 10**), similarly to that seen for the antibacterial activity of compounds **63-65** (**Figure 8**).
- the benzophenone derivatives are more effective than their reduced counterparts (**71-73** vs. **70, 27**).

-
- on the contrary, replacement of the methylene bridge with an ether causes a small reduction of activity.
 - in the case of the ethers, changing the length of the bridge has little effect on the activity.

Despite the positive results for the inhibition of ICL, none of the new compounds show interesting activity when tested *in vitro*. Compound **27** is still the most potent: this result shows the importance of balancing enzyme-based and whole-organism studies to enable evaluation of the cell penetrating effects of new compounds.³⁸

1.3 Radicals, ROS and oxidative damage

“A free radical is defined as any atom or molecule that contains unpaired electrons and has independent existence (hence, the term free).”⁴² Bearing unpaired electrons translates into high reactivity. For this reason, radicals are usually short lived and tend to react, in a biological context, with different structures, ranging from membranes to DNA.

Oxygen- and nitrogen-centred radicals are often associated with closely related and highly reactive non-radical species and are often collectively termed Reactive Oxygen Species (ROS). The most important species are illustrated in **Table 1**.⁴²

Radicals	Non-radicals
Superoxide ($O_2^{\cdot-}$)	Hydrogen peroxide (H_2O_2)
Hydroperoxyl (HOO^{\cdot})	Alkyl hydroperoxides ($LOOH$)
Peroxyl (LOO^{\cdot})	Singlet oxygen (1O_2)
Alkoxyl (LO^{\cdot})	Ozone (O_3)
Hydroxyl (HO^{\cdot})	Hypochlorous acid ($HOCl$)
Nitric oxide (NO^{\cdot})	Peroxynitrite ($ONOO^{\cdot}$)
Nitrogen dioxide (NO_2^{\cdot})	

Table 1. Reactive oxygen species⁴²

The concept of oxidative stress was originally defined by Helmut Sies as “an imbalance between oxidants and antioxidants in favour of the oxidants, potentially leading to damage”.⁴² Cells are normally able to maintain an equilibrium between the production and the removal of radicals, and partially repair the damage caused by their activity. Alterations of these homeostasis processes have been identified in a number of pathological conditions.^{42,43}

Although radicals and the concept of oxidative stress are normally associated with cellular damage and pathological processes, it is important to remember that radicals are also involved in physiological processes. This consideration highlights the delicate equilibrium and the controversy that may arise in the evaluation of the activity of antioxidants, normally considered as protective agents but whose activity may reverse under different conditions.^{42,44-46}

1.3.1 ROS: a brief description

ROS generation is an intertwined, non-linear process. These species are produced through a number of different processes and their reactions can lead to other ROS.

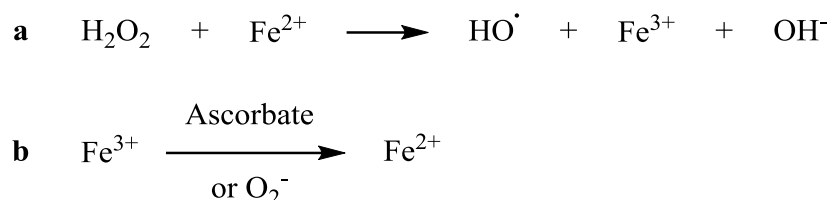
Superoxide radicals are mainly, but not exclusively, produced in the mitochondria through their electron transport system. They are also generated by autooxidation of small molecules (*e.g.* cysteine) and Fe^{2+} and its complexes. Cytochrome P450, cyclooxygenases and lipoxygenases are also among the enzymes able to produce this species. Superoxide is an interesting type of radical as it can either act as oxidising (*e.g.* NADH to NAD^+) or reducing (*e.g.* Fe^{3+} to Fe^{2+}) agent. Although its reaction with DNA, lipids and proteins is not biologically significant, its protonated form (hydroperoxyl radical, HOO^{\bullet}) and the intermediates of its reaction with Fe^{3+} can directly induce lipid peroxidation.^{42,47}

Superoxide is also a source of singlet oxygen and H_2O_2 by spontaneous dismutation. In the case of hydrogen peroxide, the conversion can also be catalysed by the enzymatic activity of superoxide dismutase (SOD), one of the enzymes involved in maintaining the cellular balance of oxidative species. Superoxide is also a source of peroxynitrite, which is produced by its reaction with nitric oxide.^{42,47,48}

Singlet oxygen is another important oxidant as it can directly oxidise guanine residues of nucleic acids, polyunsaturated fatty acids, and amino acids.^{42,48}

Hydrogen peroxide, also generated for the major part from superoxide radicals, is a poor oxidant, compared to its precursor, and is targeted by detoxification mechanisms, such as catalases, completing the activity of superoxide dismutase. Nonetheless, its activity must not be underestimated, its stability and permeability allows diffusion and subsequent action at other sites than its origin.^{42,47}

The effect of hydrogen peroxide is mediated by hydroxyl radicals (HO^{\bullet}) which are produced by interaction with transition metals (predominantly Cu^+ and Fe^{2+}). The reaction between these two species has become widely known as the Fenton reaction (**Scheme 1, a**).^{42,47}

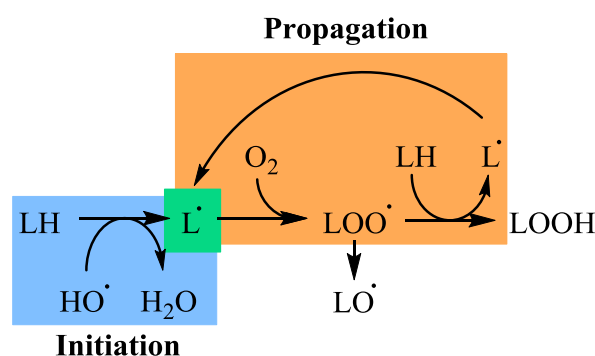


Scheme 1. a) Fenton reaction. b) reduction of iron (III) to iron (II).

It has to be noted that reconversion of Fe^{3+} to Fe^{2+} can be mediated by either superoxide radical or by other reducing agents, such as ascorbate. It is now evident how a reducing agent, widely considered as protective, can exert a pro-oxidant activity, allowing the cycle to continue. The reaction also provides a means to produce hydroxyl radicals *in situ* for model studies.^{42,48}

Hydroxyl radicals are extremely reactive, do not exclude almost any substrate, and often display rates of reaction above $2 \times 10^9 \text{ M}^{-1}\text{s}^{-1}$, which means the availability of a substrate and diffusion rate of the radical are the limiting steps of the reaction. They are therefore involved in lipid peroxidation, protein, DNA, RNA and carbohydrate damage.⁴²

Alkyl hydroperoxides (LOOH), alkyl peroxy (LOO $^\bullet$) radicals and alkoxy radicals (LO $^\bullet$) are generated prevalently during lipid peroxidation processes. It is a chain reaction which is initiated by interaction of a polyunsaturated fatty acid with a reactive radical, for example a hydroxyl radical (**Scheme 2, Initiation**).



Scheme 2. Lipid peroxidation, adapted from Thanan.⁴⁹

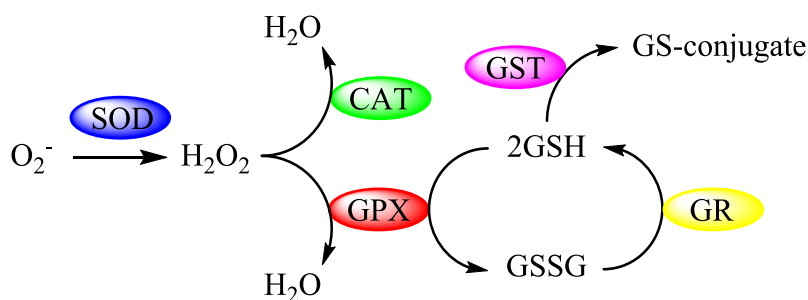
The reaction of the alkyl radical (L^\bullet) with oxygen to give a peroxy radical (LOO^\bullet , which can also convert to alkoxy, LO^\bullet) and subsequent regeneration of an alkyl radical sustain the reaction chain in a propagation step (**Scheme 2, Propagation**).^{42,49}

Nitrogen radicals are another relevant group of species. Of these, nitric oxide (NO^\bullet) is a particularly interesting molecule. It is produced by nitric oxide synthase under physiological condition and it is involved in regulation of vascular relaxation, but it is also related to inflammation processes. It can be converted to nitrogen dioxide (NO_2^\bullet) by reaction with oxygen. Rapid reaction with superoxide, on the other hand, generates peroxynitrite (ONOO^-) which is a highly toxic non-radical molecule, which can oxidise most biological structures.^{42,49}

1.3.2 Cell defence against oxidative stress

All organisms have developed a set of defence mechanisms to prevent, minimise and repair the damage caused by ROS. These mechanisms work at different levels and are of different nature.

Enzymes are a first line of defence. As previously described, superoxide dismutase converts superoxide into the less reactive hydrogen peroxide. This product is subsequently decomposed by catalase and glutathione peroxidase (GPX, **Scheme 3**). GPX and another enzyme, thioredoxin, can also decompose peroxynitrite. Glutathione peroxidase is part of a detoxifying system involving a number of auxiliary enzymes. GPX requires reduced glutathione (GSH) for its activity and converts it to the oxidised form (GSSG). Glutathione reductase, although not directly involved in ROS decomposition, is required to reconvert GSSG to GSH, allowing the cycle to continue. This suggests that the enzymes involved in the biosynthesis of GSH are part of the mechanism of protection. Glutathione *S*-transferase is also involved in protection from oxidative damage. It can conjugate products of lipid peroxidation, thus contributing to detoxification. Cells can overexpress this set of enzymes in response to increased oxidative activity as a means of protection.⁴²



Scheme 3. Detoxification of superoxide and hydrogen peroxide. SOD (superoxide dismutase), CAT (catalase), GPX (glutathione peroxidase), GR (glutathione reductase), GST (glutathione *S*-transferase).

An important consideration relevant to these enzymes is their dependence on metals. SODs are a diverse family, some are copper and zinc dependent, while others require manganese. Iron is required by catalase, while selenium is necessary for GPX. Iron and copper, in particular, can turn from pro-oxidants, by catalysing Fenton's reaction, to protective elements as part of detoxifying enzymes. To control the levels of metals further, many small molecules and proteins become involved in chelation of metals, thus contributing to regulate the oxidative stress related to their activities.⁴²

Together with glutathione, other small molecules have antioxidant activity. Some of these are produced by the organism as in the case of melanin, which protects the skin from ultraviolet radiation. Others are absorbed from the diet, this is the case of antioxidant vitamins such as ascorbate, vitamin E and carotenoids. Other substances, like plant derived polyphenols, also have antioxidant activity and will be discussed in **Chapter 1.3.4**.

A different system involved in controlling the oxidative stress of the cell is nuclear factor erythroid 2–related factor (Nrf2) / Kelch-like ECH-associated protein 1 (Keap1). Keap1 is responsible for controlling the activity of Nrf2, which is normally retained in the cytoplasm. As a consequence of increased oxidant stress, alteration of cysteine residues impairs the activity of Keap1, and Nrf2 is released. Subsequent translocation of Nrf2 into the nucleus and heterodimerization with other transcription factors allows binding to Antioxidant Response Element (ARE). Interaction with these promoters allows transcription of genes which are responsible for protection against antioxidants (SOD, among others) and xenobiotics.⁵⁰⁻⁵²

1.3.3 Oxidative damage and pathologies

Inflammation and oxidative stress are influenced by a number of environmental factors. As previously described, transition metals have pro-oxidant activities, and other chemical stimuli can lead to production of radical species. Infectious agents directly activate the immune response, a complex series of events which includes production of large quantities of radicals by activated phagocytes. Inflammation is a process involved in many different conditions, autoimmune pathologies, age related pathologies and cancers, for example (**Figure 11**).^{45,49}

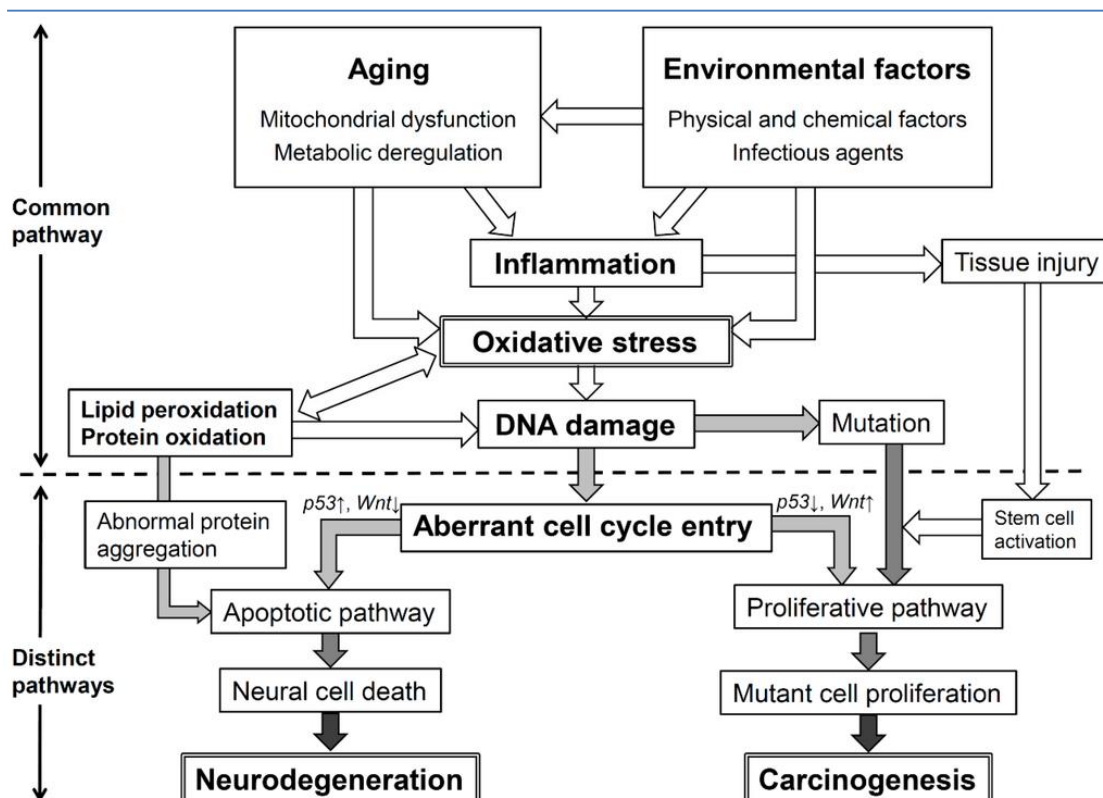


Figure 11. Oxidative stress and its involvement in neurodegeneration and carcinogenesis.⁴⁹

Aging and age-related pathologies are linked to environmental factors and genetic traits, and are interlinked with inflammation and oxidative stress. Alzheimer's, Parkinson's and other neurodegenerative diseases have been linked to increased protein oxidative damage. Carbonyl proteins derived from oxidative activity of ROS can contribute to the insurgence and progress of these pathologies. Their accumulation can impair critical cellular functions, such as lysosomal and proteasomal degradation, and increase ROS production by damaging mitochondria, for example, which may also induce apoptosis. Carbonyl proteins have also been found in protein aggregates typically found in synucleinopathies (*e.g.* Parkinson) and Alzheimer's disease. Increased oxidation of lipids, particularly abundant in neurons, has also been identified for most of these age related, neuronal pathologies. DNA damage is particularly relevant for the onset of these diseases. It is often strongly correlated with environmental factors, in particular exposition to high levels of transition metals. Damage to DNA, together with mitochondrial dysfunction, is a relevant step in induction of apoptosis.^{42,49}

Oxidative damage to lipids, proteins and, in particular, DNA, can drive mutagenesis and transformation of normal cells into cancer cells. The damage to DNA is particularly relevant in the case of nitrogen radicals, generated by inducible nitric

oxide synthases, whose expression is stimulated by infectious agents and other agents such as asbestos. Infectious agents related to cancer and DNA damage can be either bacterial (*e.g. Helicobacter pylori*), viral (*e.g. human papilloma virus* and *hepatitis virus*) and others (*e.g. Schistosoma haematobium*). Hydroxyl radicals are also involved in DNA damage (**Figure 12**). Fenton's reaction is the major source of this radical, iron bound to DNA produces the radical *in situ*, with consequent hydroxylation of DNA bases. Repair mechanisms can attempt to replace the modified bases, however it is an error-prone system, which may introduce a wrong base, thus generating a permanent mutation.^{42,49}

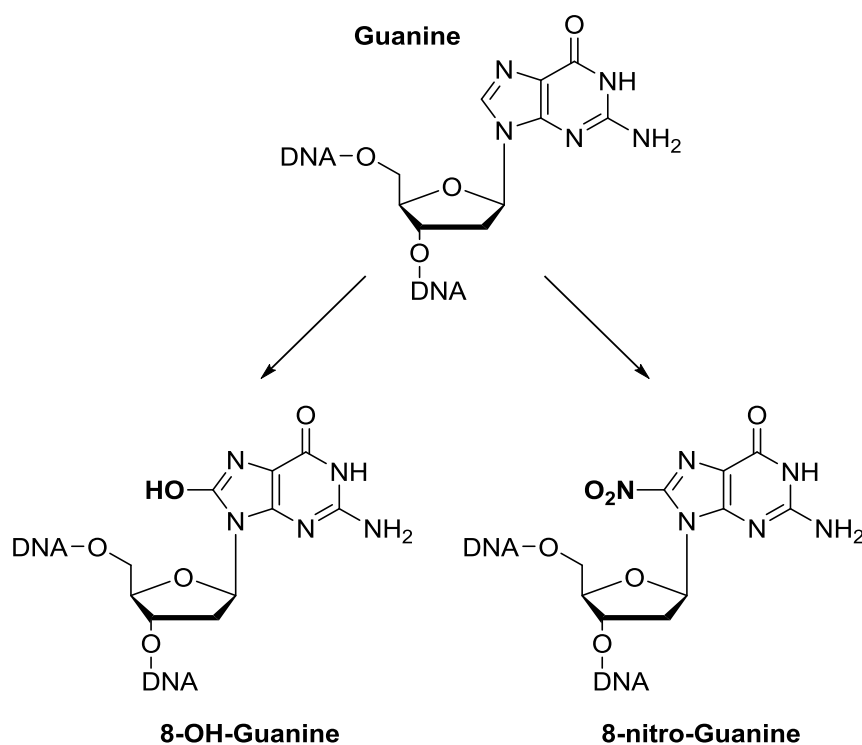


Figure 12. Example of DNA modification.^{42,53}

As previously discussed, oxidative stress can play multifaceted roles. Although nitritative DNA damage is undoubtedly related to mutagenesis, recent studies have highlighted that, in specific cases, progression of cancer can be favoured by antioxidants. As the cell, progressively deregulated, tries to cope with increased oxidative stress, ROS lose their role as promoters of transformation and become a threat, thus inverting the role of a supposedly protective agent.⁴⁶

1.3.4 Antioxidants as therapeutic agents

Due to the wide implications of radicals in aetiology and development of a number of pathologies, antioxidants have been the subject of extensive studies as preventative and therapeutic agents.

Antioxidants can be classified into two main categories, direct antioxidants which are able to react with radicals to break chain reactions, and indirect antioxidants, which do not react with radicals but help the cell to manage oxidative stress.⁵²

1.3.4.1 Direct antioxidants

Phenols, the main subject of this thesis, belong to the category of direct antioxidants, together with enzyme mimetics and polyenes. Phenols can also be subdivided into monophenols and polyphenols.⁵²

Among monophenols (**Figure 13**) key examples are vitamin E and its related tocopherols. Trolox, used as reference for some of the assays presented in this thesis, is an analogue of vitamin E.

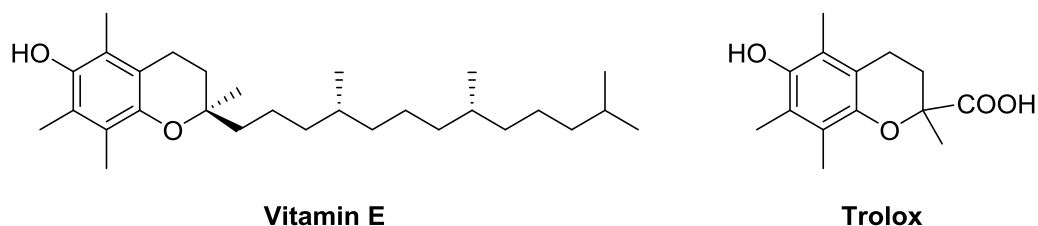


Figure 13. Vitamin E and Trolox.

Studies on the role of vitamin E in Alzheimer's disease (AD), Parkinson's disease (PD), Huntington's disease (HD) and amyotrophic lateral sclerosis (ALS) gave varying results. Whilst vitamin E proved effective in delaying ALS, in the case of AD, the results prove contradictory, and there is no clear indication for the use of vitamin E supplements. In the other diseases, it appears that it does not provide any beneficial effect but in combination with other antioxidants, slowed progression of age-related macular degeneration (AMD). On the other hand, potential negative effects of large doses of vitamin E, such as increased risk of prostate cancer, have also been identified.^{52,54-58}

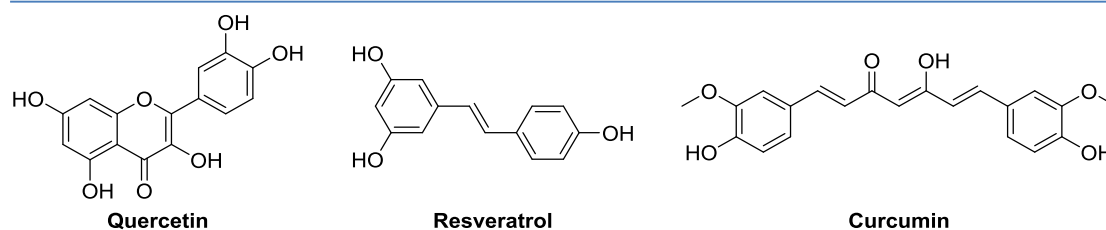


Figure 14. Examples of different polyphenols.

Stilbenoids like resveratrol, flavonoids like quercetin and other natural products like curcumin belong to the polyphenol group (**Figure 14**). The compounds synthesised during this work also belong to this family. This group of compounds is vast, if we consider that more than 8000 flavonoids are currently known. Many of these substances enter our diet daily, with flavonoids being probably the most relevant. These compounds, on top of their direct radical quenching ability, display metal chelating properties (thanks to the catechol and α -hydroxyketone), thus increasing their protective ability. Resveratrol and its analogues have been evaluated for their activity, in particular with AD, and proved to be an interesting starting point for development of novel therapeutic agents. Curcumin, a component of turmeric, has been widely evaluated for a number of pathologies. It showed ameliorating effects in cardiovascular diseases, where inflammation plays a major role. In atherosclerosis, where oxidation of lipids is a critical factor, ischaemia and reperfusion, and other cases, there are significant indications of positive effects from treatment with curcumin.⁵⁹⁻⁶²

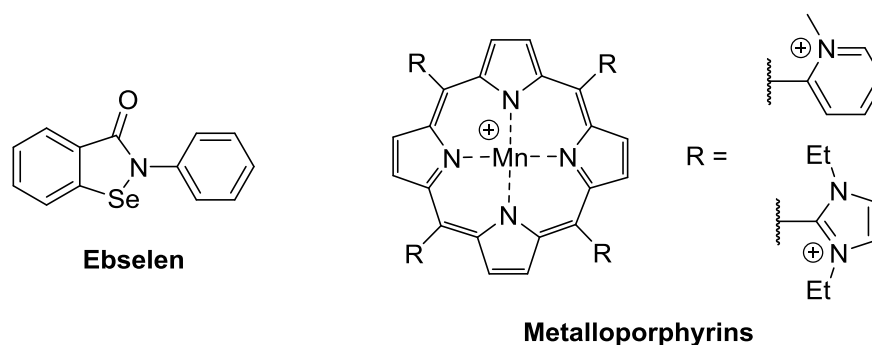
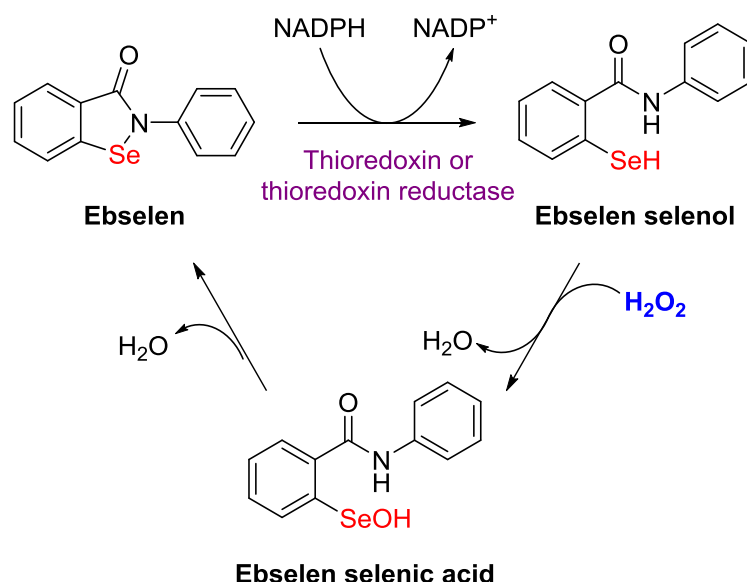


Figure 15. Examples of catalytic antioxidants.

Ebselen and its analogues belong to a different group of direct antioxidants, and display a catalytic activity (**Figure 15**). Ebselen is converted to its selenol by thioredoxin, thioredoxin reductase and GPX. In this form, it reacts quickly with hydrogen peroxide, which is decomposed to water, and it is converted to the corresponding selenic acid. Upon internal cyclisation and consequent loss of water

ebiselen is regenerated (**Scheme 4**). It can also inhibit nitric oxide synthase (NOS) and lipoxygenase among other enzymes, with additional antioxidant/anti-inflammatory effect. It is a promising agent, with potential activity in reducing oxidative damage associated with cardiovascular pathologies, diabetes, asthma and xenobiotic toxicity (cis-platin, cadmium, *etc*).^{52,63,64}



Scheme 4. Catalytic cycle of Ebiselen.

Ebiselen is not the only agent with catalytic activity, some manganese complexes also display antioxidant activity. Metalloporphyrins, such as the one reported in **Figure 15**, display SOD-like and catalase-like activities.^{52,64}

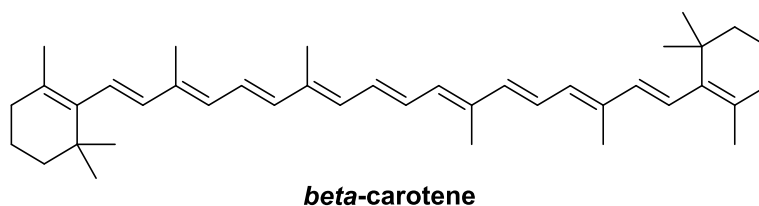
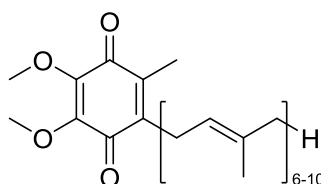


Figure 16. *beta*-Carotene.

The last group of direct antioxidants is constituted by the carotenoids (β -carotene, **Figure 16**) and similar polyene structures, commonly found in plants. They readily react with singlet oxygen and peroxy radicals forming stabilised radicals, thanks to their highly conjugated structures. Although these compounds display therapeutic effects in AD prevention, there is no evidence linking their mechanism of action with their antiradical properties.⁵²

1.3.4.2 Indirect antioxidants

In contrast to direct antioxidants, these compounds do not react with ROS, but support the mechanisms of protection of the cell.



Ubiquinone

Figure 17. Ubiquinone.

Quinones and their (poly)prenylated analogues (vitamin K group) are essential factors for varied physiological functions. Ubiquinone (**Figure 17**) is a notable member of this group and is involved in the mitochondrial electron transport chain. There are indications of potential beneficial effects in treatment of PD, HD and AD.^{52,65}

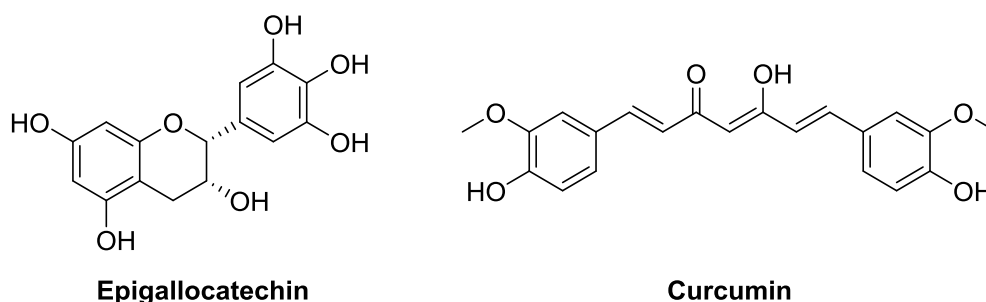


Figure 18. Natural compounds involved in Nrf2 regulation.

A different type of mechanism is the induction or repression of systems involved in oxidative stress protection. This is the case for some nitron spin labels. Although these molecules can indeed react with radicals and form adducts, the initial reason for interest in these molecules, they can also induce protective pathways. Interaction with the previously described Keap1/Nrf2 path, may produce a similar effect. Any substance able to induce Nrf2 activity would lead to translation of antioxidant enzymes, thus decreasing oxidative stress. Epigallocatechin and curcumin, which are also a direct antioxidants, are examples of natural products able to activate this regulatory pathway (**Figure 18**). In these two cases, Nrf2 activity is induced indirectly through phosphorylation by an upstream kinase (protein kinase C delta).^{52,66,67}

1.4 Brominated bis-phenols as antioxidants

As previously described, mono- and poly-phenols display direct antioxidant properties. Halogenated bromophenols belong to this family of compounds. Extracts from algae, isolated compounds and synthetic derivatives have been tested both *in vitro* and *in vivo* to evaluate their potential antioxidant potential. A brief summary of the most relevant results is herein presented.

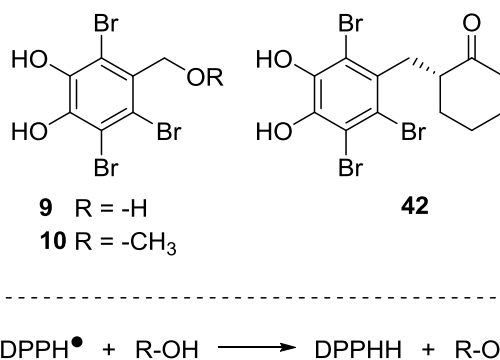


Figure 19. Bromophenols with antioxidant activity and their reaction with DPPH radical

In 1998, Park reported the antioxidant activity of a methanolic extract of *Symphyclocladia latiuscula*.⁶⁸ Subsequently, the same research group isolated, from the same alga, three bromophenols with 1,1-diphenyl-2-picrylhydrazyl (DPPH) radical scavenging activity (**Figure 19**).²⁴

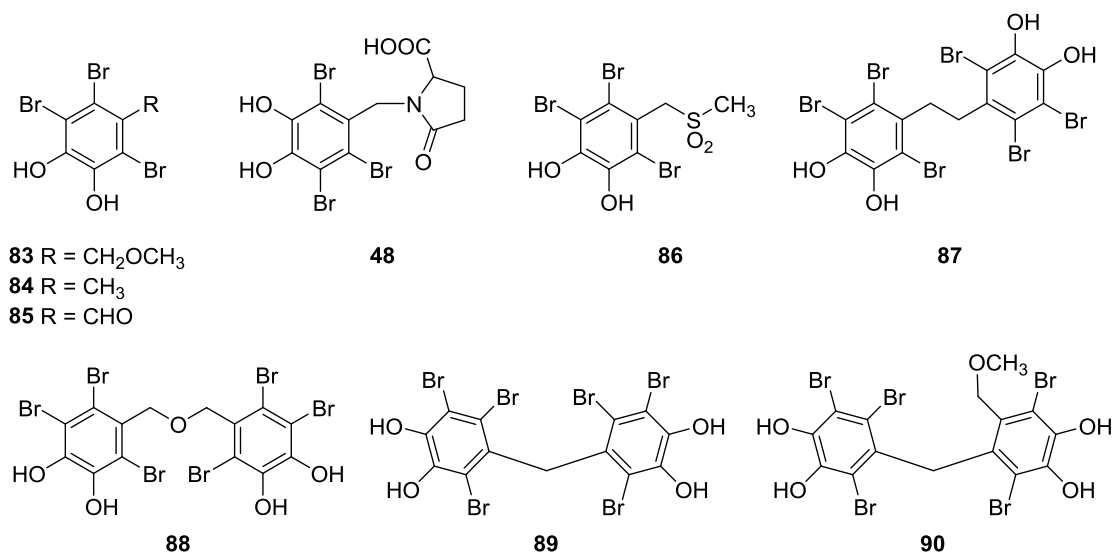


Figure 20 Brominated mono and bis-phenols with radical scavenging activity

In 2007, Duan tested a set of natural bromophenols isolated from *Symphycycladia latiuscula* (**Figure 20**) for their DPPH radical scavenging activity. The compounds were tested against the known antioxidant butylated hydroxytoluene (BHT), showing a potency 3.3- to 10-fold higher. From a SAR point of view, in agreement with previous observations by Son,⁶⁹ the activity increases with the number of hydroxyl groups: **87-90** are more potent than the monophenols **83-86** and **48**.⁷⁰

The same research group reported the antioxidant activity of other brominated phenols isolated from *Polysiphonia urceolata* (**Figure 21**) and confirmed the previous observation about the relationship between potency and number of hydroxyl groups (**Figure 21**).^{27,28}

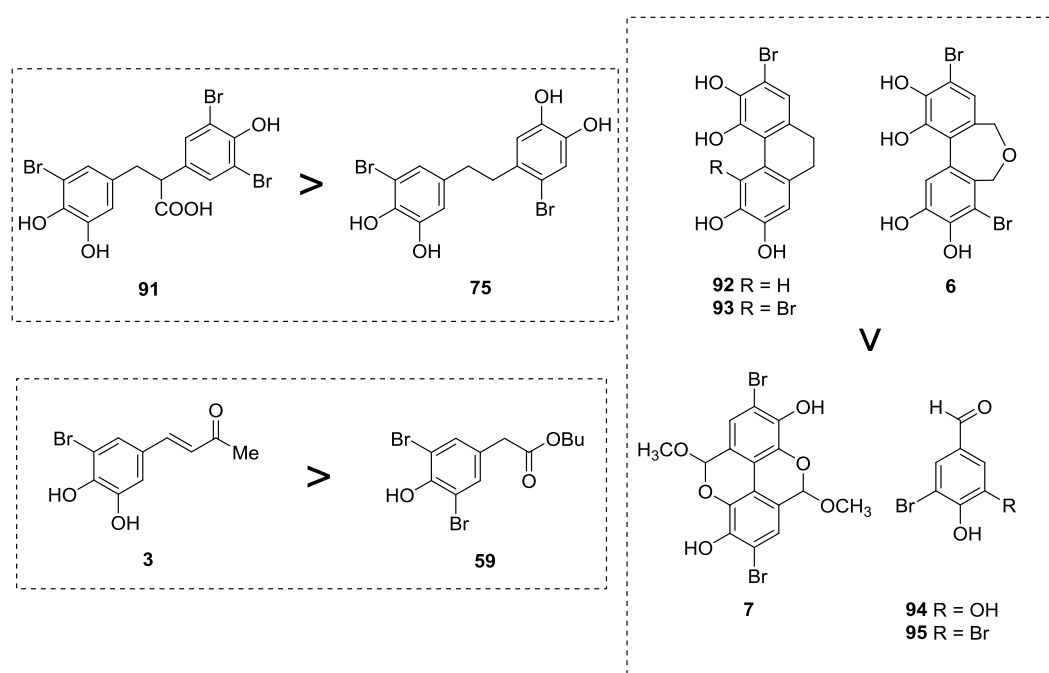


Figure 21. Brominated mono- and bis-phenols with radical scavenging activity^{27,28}

Following on from this, Zhao tested a large library of synthetic halophenols as antioxidants and cytoprotective agents (**Figure 22**).⁷¹ The compounds were tested for their DPPH radical scavenging activity. The chosen set demonstrated the importance of the hydroxyl groups for the activity: compounds **96-104b** and **96-104d** were active and most of them showed a potency higher than BHT (up to almost 3-fold for **98b**); on the contrary, their methoxy analogues (**96-104a** and **96-104c**) did not show any antioxidant activity.

The compounds were also evaluated *in vivo* for their cytoprotective activity against H₂O₂-induced injury in human umbilical vein endothelial cells (HUVEC). Some SAR considerations were drawn from the results:

- the methoxy compounds were not active, the presence of hydroxyl groups is necessary
- the presence of a bromine or chlorine is necessary
- unlike the radical scavenging activity, the potency *in vivo* does not increase with the number of hydroxyl groups (**100b,d**, **101b,d** are inactive)
- the position of the halogen can influence the activity (**104c**, with a chlorine in the *para* position is active, but its regioisomers do not provide protective activity)⁷¹

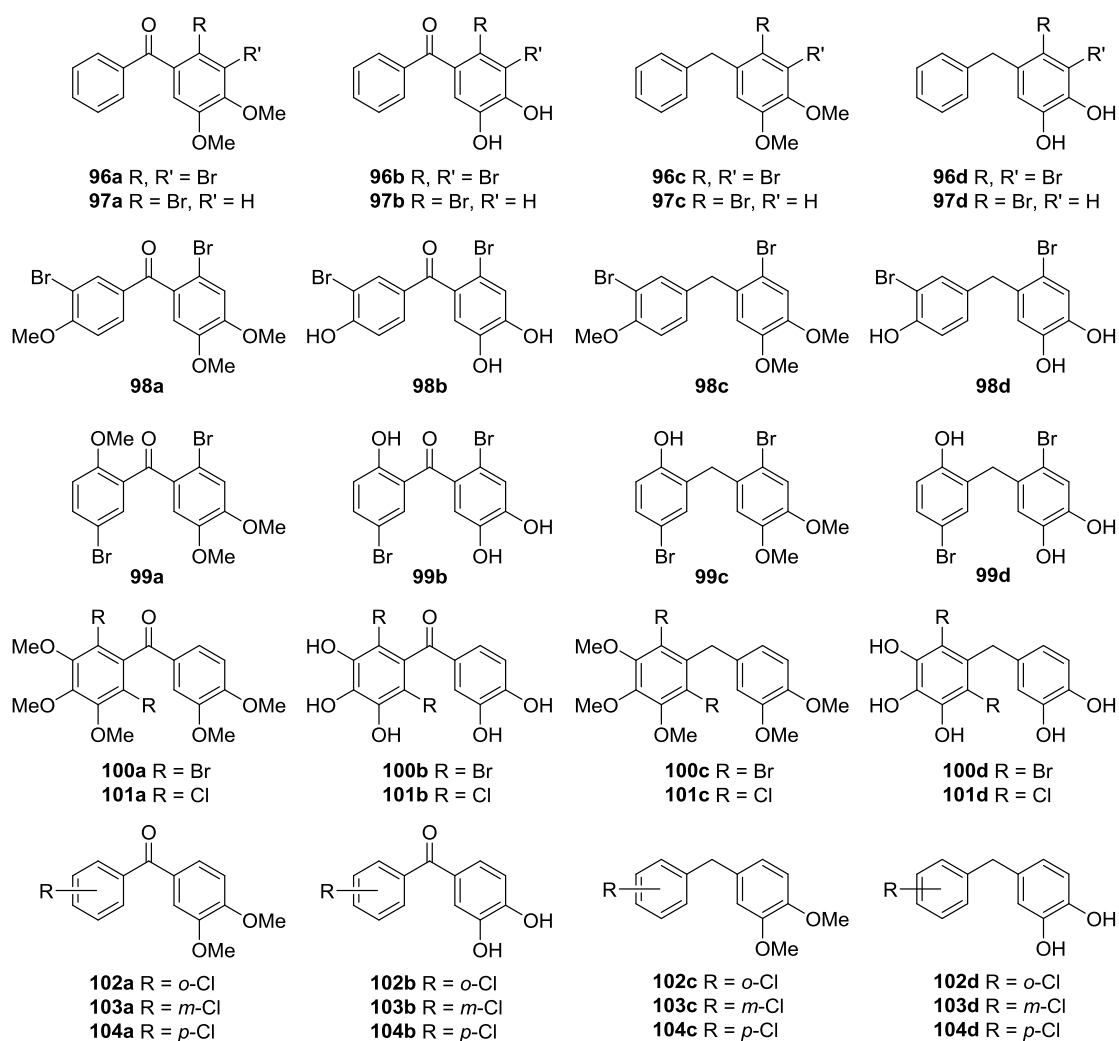


Figure 22. Halophenols as antioxidants and cytoprotective agents⁷¹

1.5 Previous Work

The work described in this thesis is a continuation of previous work of our research group, published in 2011.⁷² This study led to a set of interesting compounds, which are presented in **Figure 23**.

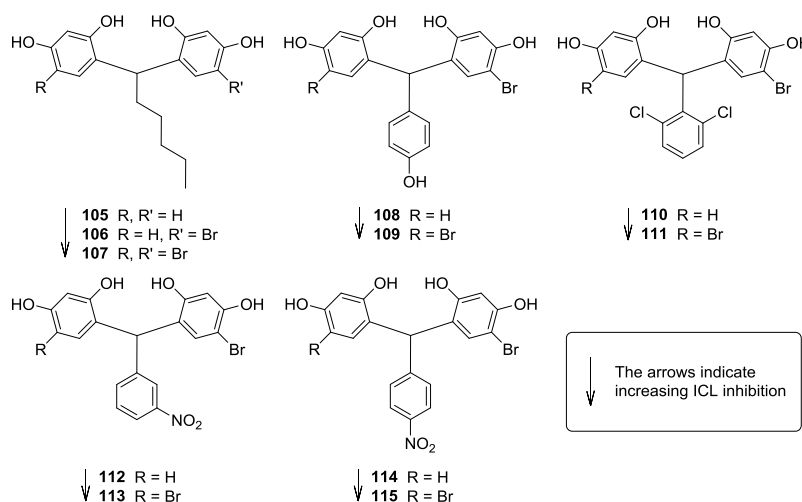


Figure 23. Brominated bis-phenols with a side chain⁷²

These new compounds present two main differences with the previous reports: they are based on resorcinol instead of catechol and phenol, the main building blocks of the natural compounds, and bear a side chain on the methylene bridge. For these compounds, the ICL inhibition follows the same trend described by Oh for the catechols:³⁸ higher number of halogens, higher potency. This is valid also for the side chain and different halogens: the most potent compound of the group is **111** and its activity is comparable with that of the natural compound **27**. The good activity of these compounds shows that resorcinol derivatives can also inhibit ICL and a catechol-based structure is not mandatory.

Compounds **107** and **109** possess high antibacterial activity, especially the latter, with an activity comparable to ampicillin. It is relevant to note that, exactly as described for ICL inhibition, the potency increases with the number of halogens.

Regarding the side chain on the bridging carbon, different substitutions lead to small variations in activity, indicating the possibility of further development of the bridging substituent to improve the receptor binding.

Also, it is immediately evident that they present four hydroxyl groups each. As previously described, these are directly related to the radical scavenging properties of

bromophenols and thus these molecules may also present antioxidant behaviour, although this has not yet been investigated.

These compounds are also interesting as they constitute rational building blocks toward the synthesis of substituted resorcarenes, an active area of research in the group. Cyclisation of two dimers with a differently substituted aldehyde has previously been described to obtain resorcarenes with alternating substituents on the bridge,⁷³ providing additional interest into these compounds.

1.6 Aim of the Project

Following our previous results, the aim of the present work is to prepare new families of resorcinol derivatives and investigate their activity as antimicrobials and antioxidants. The scope of the SAR of the previously synthesised resorcinol dimers will be expanded by variation of the number and type of halogens, the number of monomers will be increased to four and six, and simpler structures will also be included for comparison (**Chapters 2 and 3**). In addition, these novel, multivalent structures will be exploited as dendrimer cores, to prepare a new class of multicalixarenes (**Chapter 4**).

Since most of the compounds have never been prepared before, their antiproliferative activity will also be assessed (**Chapter 5**). Finally, simple antioxidant tests will be presented to evaluate potential radical scavenging properties (**Chapter 6**).

For simplicity, every chapter will introduce the rationale behind the synthesis or assays for the compounds under consideration.

2. Dimers and Tetramers

In this chapter, the synthesis of the first two main families of compounds will be presented. The first one, the dimers, is closely related to the compounds previously synthesised by our group, while the second is an extension to more complex, tetrameric structures.

2.1 Introduction to Resorcinol and Phloroglucinol

Dimers

Similarly to the compounds in our group's previous report, the dimers family consist of a set of bis-phenols with a bridging substituent (**Figure 24**). However, in this case, the compounds prepared bear up to four halogens, in various combinations, and these are not limited to bromine. The interest in chlorine lies in its similarity with bromine (electronegativity, lipophilicity, sigma-hole), although with a lower molecular mass. Chlororesorcinol is also readily available and offer some advantages over bromine, relative to its reactivity, as discussed in further chapters. 4-Fluororesorcinol based analogues have also been considered due to the low molecular weight and strong inductive effect of fluorine. Also, differently from bromine and chlorine, it does not present a sigma-hole.

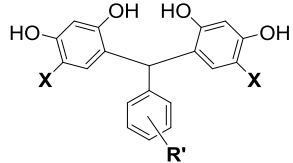
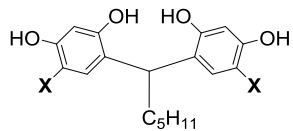
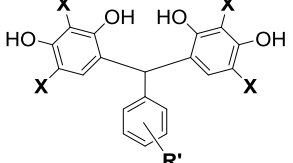
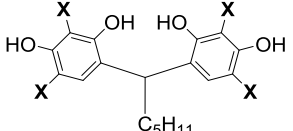
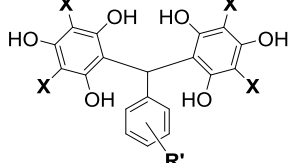
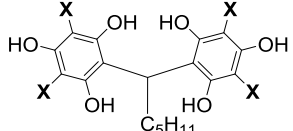
Previous work	Current work	
 <p>$R' = OH, Cl, NO_2$ $X = H, Br$</p> 	 <p>$R' = COOH, CHO, OH, Cl, Br$</p> 	 <p>$R' = COOH, CHO, OH, Cl, Br$</p>  <p>$X = H, Cl, Br$</p>

Figure 24. Previous and current work examples.

Initially, only the products with 4-hydroxybenzyl and pentyl substituents on the bridge were chosen. However, once the synthetic method was refined, allowing easy access to more products, other functional groups have been considered.

In addition, the synthesis of a phloroglucinol-based set was added, allowing evaluation of the effect of additional hydroxyl groups.

2.2 Introduction to Resorcinol Tetramers

The basic tetramers synthesised in this work are effectively presenting the same bis-resorcinol component twice, arranged around a central phenyl ring (**Figure 25**). Since the sidechain of dimers did not produce great variation in the activity, at least in the case of ICL binding,⁷² it is worth investigating whether a “doubled” structure can produce a better result. In the case of the antioxidant activity, since it is correlated with the number of available hydroxyl groups, tetrameric structures are expected to offer a significant advantage compared to their dimeric analogues.

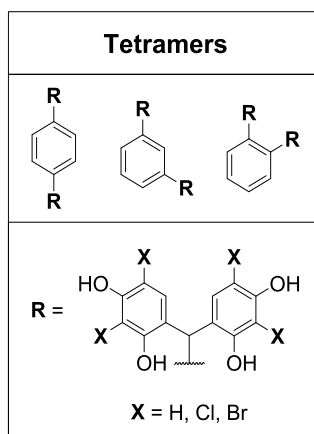


Figure 25. Tetramer with a central phenyl ring.

Additionally, since these structures present eight functionalizable hydroxyl groups, with a well organised topology, they could also be very interesting as potential dendrimer cores, allowing access to differently organised structures.

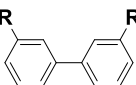
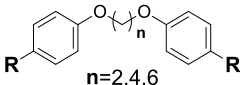
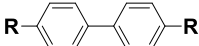
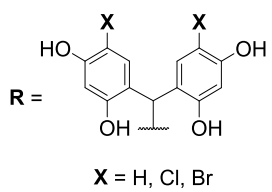
Biaryl-tetramers	Flexible tetramers
	
	

Figure 26. Biaryl and flexible tetramers.

In addition to the basic tetramers, built around a benzyl group, two additional sets of tetramers were planned (**Figure 26**). Biaryl-tetramers have a similar but longer, biaryl central structure, which maintain a certain degree or rigidity. Alternatively, flexible tetramers can be prepared by building around an alkyl chain, which allows control of the distance between the units and introduces considerable flexibility around its centre.

2.3 Introduction to Resorcinol Hexamers

Hexamers are the largest resorcinol-based structures considered (**Figure 27**). They are also the most interesting from the point of view of the raw number of functionalizable hydroxyl groups. With twelve anchoring points, uniformly distributed around a central phenyl ring, they constitute a very attractive, novel dendrimer core in addition to their medicinal chemistry applications.

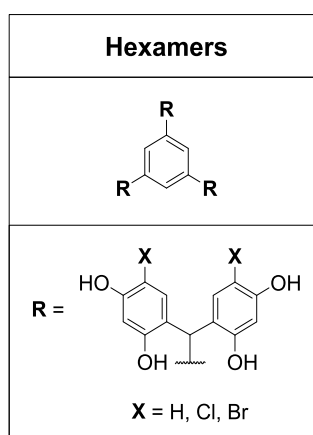
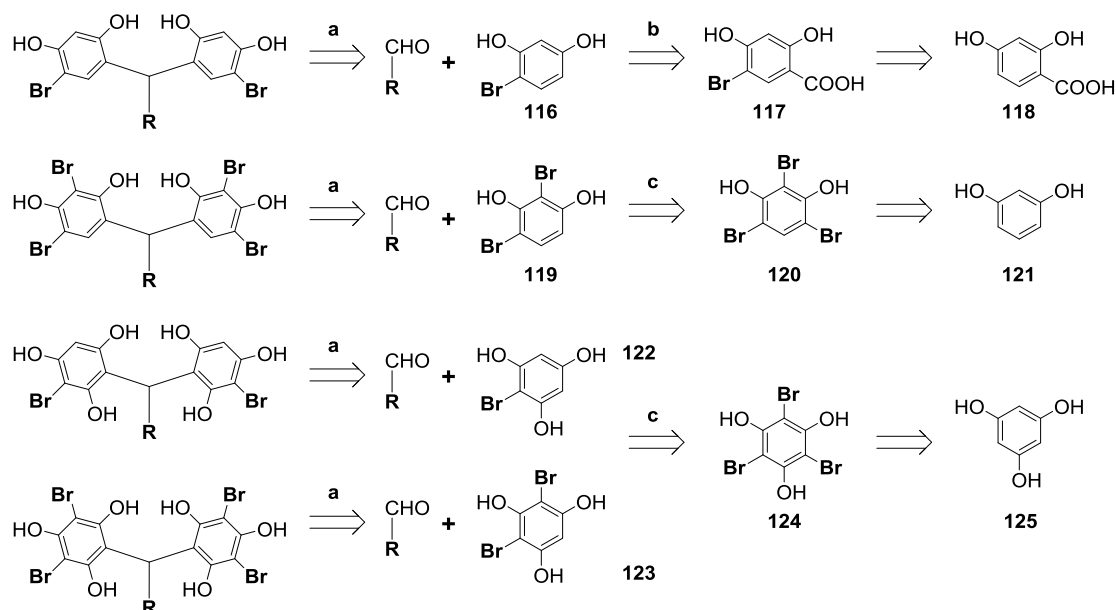


Figure 27. Hexamers.

2.4 Synthesis of dimers

The synthetic approach for this class was planned based on previous work by the group.⁷² Proceeding by retrosynthesis: for all compounds, the final and crucial step of the procedure is the condensation of an aldehyde (which bears the bridging sidechain) and the halogenated monomer (resorcinol/phloroglucinol-based) – **Scheme 5, a**. This key step is an acid-catalysed condensation. As subsequently described, it is strongly influenced by both the aldehyde and the reactivity of the resorcinol and a number of different conditions were investigated.



Scheme 5. Retrosynthesis of dimers.

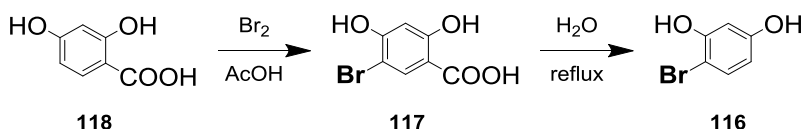
Whilst 4-fluoro/chloro/bromo resorcinols are commercially available, synthesis of 4-bromoresorcinol (**116**) is rapid and more cost-effective and was therefore employed. However, selective introduction of one bromine atom on activated aromatics such as resorcinol and phloroglucinol cannot be achieved directly, while polyhalogenation is rapid and leads to complex mixtures. For this reason, in the case of 4-bromoresorcinol, a carboxylic group is exploited as protecting group (**Scheme 5, b**), and it also reduces the reactivity of the resorcinol, thus allowing access to a monosubstituted product which can be conveniently decarboxylated.

For dibromoresorcinol (**119**) and mono- (**122**) and dibromophloroglucinol (**123**), dehalogenation of a fully brominated substrate (**124**) is more convenient

(**Scheme 5, c**). Synthesis of tribromo-resorcinol/phloroglucinol is rapid and convenient thanks to their high reactivity towards bromination.

2.4.1 Synthesis of 4-bromoresorcinol

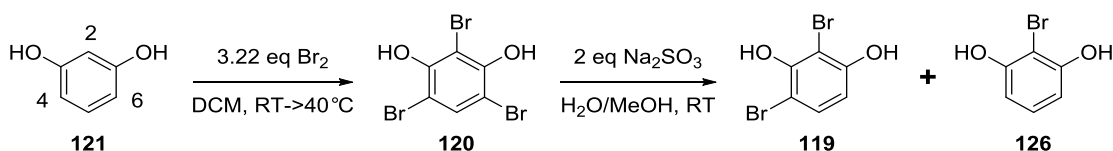
Synthesis of 4-bromoresorcinol was achieved with a method previously employed within the group and based on a work by Sandin (**Scheme 6**).⁷⁴ 2,4-Hydroxybenzoic acid is initially brominated to give **117**. The product is isolated by precipitation and subsequent thermal decarboxylation on the crude material produces **116** after flash chromatography, with an overall yield of 43%.



Scheme 6. Synthesis of 4-bromoresorcinol.

2.4.2 Synthesis of 2,4-dibromoresorcinol

Synthesis of compound **119** from resorcinol also requires two steps. Positions 4 and 6 are more reactive than position 2; therefore, to synthesise compounds which bear a bromine in position 2 such as **119** and **126**, complete substitution of all activated positions was initially pursued. Subsequently, a debromination approach similar to that reported by Kiehlmann⁷⁵ was used (**Scheme 7**) to yield the di-substituted compound.



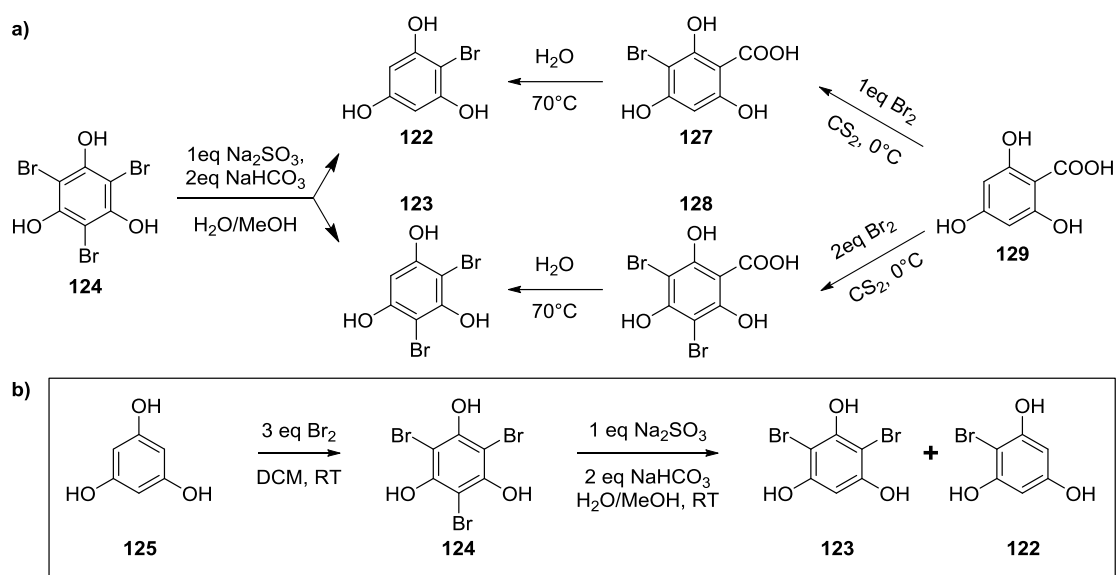
Scheme 7. Synthesis of 2,4-dibromoresorcinol.

The reaction conditions were not optimised but the chosen strategy offered a simple route to the desired products with a yield over two steps of 54% and 10%, for **119** and **126**, respectively.

2.4.3 Synthesis of 2,4-dibromophloroglucinol

Due to the strong activating effect of hydroxyl groups, bromination of phloroglucinol is fast and proceeds rapidly to the tribrominated product. Therefore, monobromo- and dibromo-phloroglucinol can be prepared either by debromination of

tribromophloroglucinol or bromination and deprotection of a phloroglucinol derivative (**Scheme 8, a**).⁷⁵



Scheme 8. Synthesis of 2,4-dibromophloroglucinol (**123**). a) Possible routes to 2,4-dibromophloroglucinol. b) Approach used to synthesise 2,4-dibromophloroglucinol.

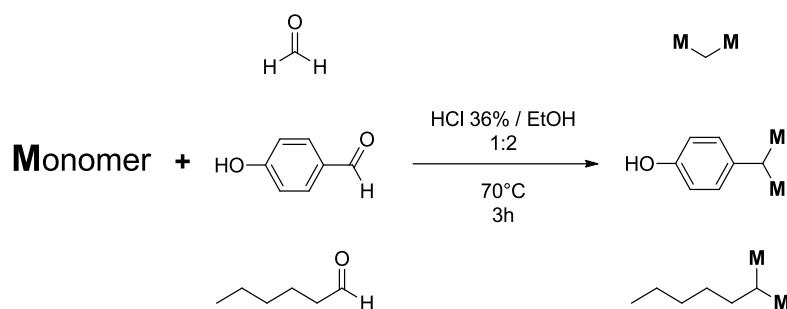
The debromination approach (**Scheme 8, b**) was chosen for a number of reasons. Firstly, mono- and dibromophloroglucinol can be easily separated by flash chromatography. Secondly, debromination can be performed on the crude tribromophloroglucinol and thus the procedure allows a simple, quick, two step procedure with only a final purification. Thirdly, monobromination of trihydroxybenzoic acid (which is also more expensive than phloroglucinol) is not truly selective, and the intermediate requires purification, increasing the number of steps required. Finally, CS₂ is not a convenient solvent, due to its toxicity.

The chosen procedure allows, in a few hours, the preparation of **123** and **122** with a yield over two steps of 14% and 12% respectively. Unreacted **124** is easily separated by filtration and can be recycled.

2.4.4 Synthesis of phloroglucinol and resorcinol dimers

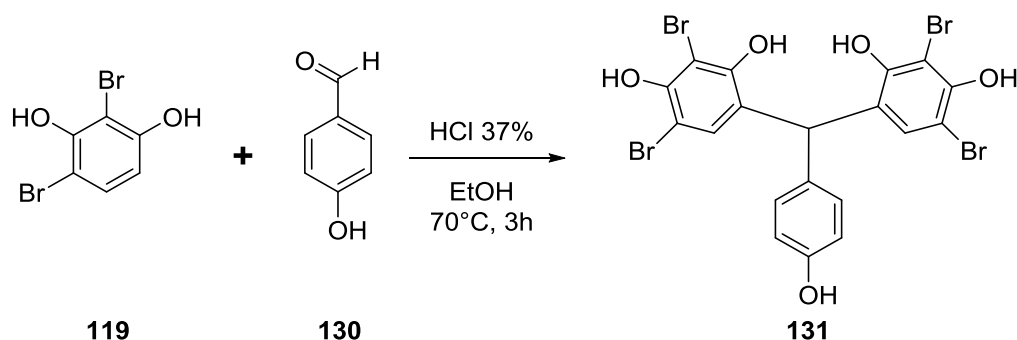
The synthesis of phloroglucinol and resorcinol dimers was investigated according to the procedure used by Bouthenet.⁷² Condensation of halogenated resorcinol or phloroglucinol (**Scheme 9, Monomer**) with an aldehyde was performed

in a 1:1 solution of ethanol and 37% hydrochloric acid at 70 °C over three hours (**Scheme 9**). For convenience, this method will be henceforth referred to as **Method 1**.



Scheme 9. Method 1.

Compound **131**, which is one of the novel dibromoresorcinol-based structures required, was chosen to test the reaction (**Scheme 10**). 4-Hydroxybenzaldehyde (**130**) was selected as condensation partner because the product would give two well defined doublets in the ^1H -NMR.



Scheme 10. Synthesis of **131**.

The expected compound was obtained, although only traces of product were isolated. The NMR data are consistent with the proposed structure. The molecule shows a potential plane of symmetry (**Figure 28**): hydrogens 1, 9 and 10 show three different peaks, each one integrating for two hydrogens. As expected, in the ^{13}C -NMR, eleven different peaks can be identified. The connectivity to the bridge was confirmed by HMBC: 3J couplings were observed between carbon 7 and hydrogens in positions 9 and 1.

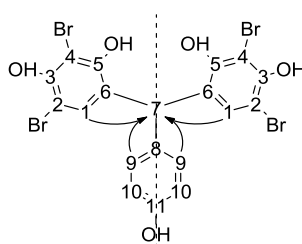
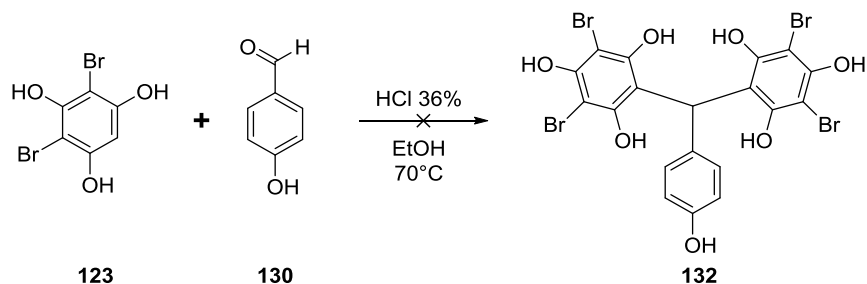


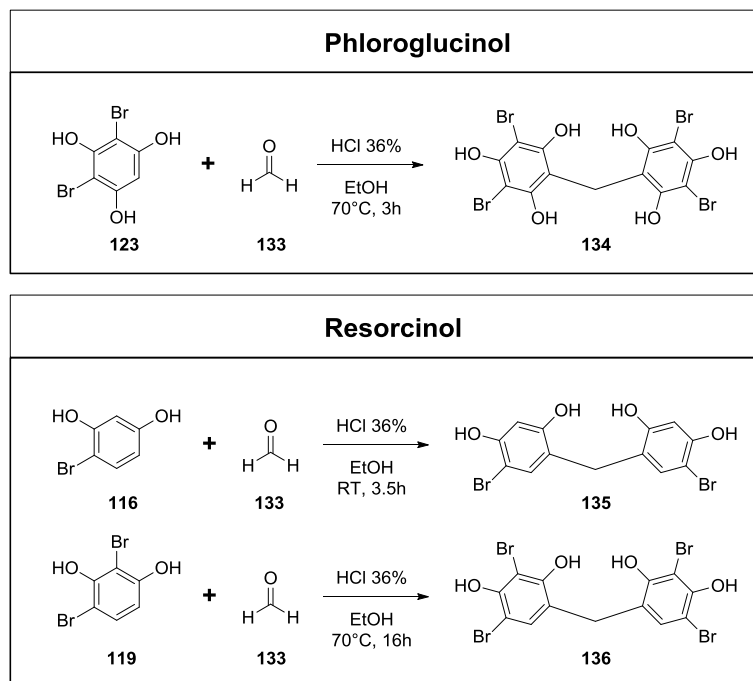
Figure 28. Long range coupling of the bridge in **131**.

The same conditions were then tested with **123**, however, the reaction did not give the expected compound, instead a complex mixture of undefined products was obtained (**Scheme 11**). Given that 4-hydroxybenzaldehyde might not be reactive enough and the product may be susceptible to retro Friedel-Crafts reaction, (**Chapter 2.5.5**.) dimerization with formaldehyde was considered. It is more reactive than its higher analogue, less hindered and not susceptible to electrophilic attack.



Scheme 11. Synthesis of **132**.

In this case, dimerisation of compound **123** with formaldehyde (**Scheme 12**), led to the expected compound, **134**, even though the yield is very low (4%). Dimerisation with formaldehyde worked with brominated resorcinols as well, allowing the preparation of **135** (3%) and **136** (20%).

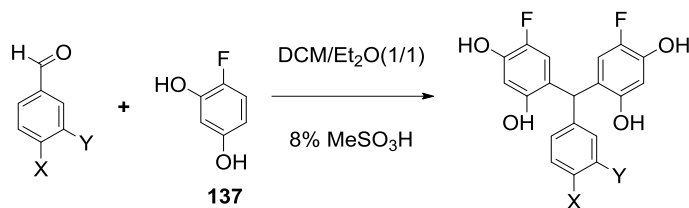


Scheme 12. Synthesis of **134**, **135** and **136**.

All these reactions provided complex mixtures, with consequently difficult and inefficient purification. It has to be noted that TLC/column chromatography on silica gel is not particularly suitable for these compounds; firstly, the compounds have a significant tendency to tailing, which is slightly controllable by addition of acid. Secondly, many products have high absorbance/fluorescence due to their aromatic nature, causing difficulties in discriminating relevant products/impurities. Considering the fact that reproducibility is also low, finding a new method with larger scope, better yields and easier purification was necessary.

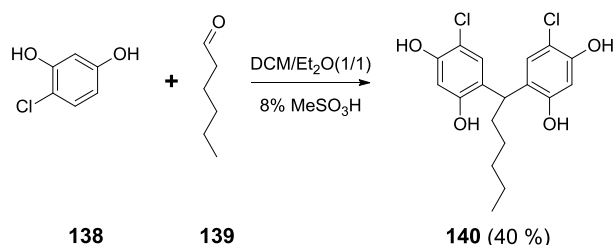
2.4.5 Synthesis of Dimers with Method 2

Bacci and co-workers reported a method for a two-step synthesis of fluorones through bis-phenols. The first condensation (**Scheme 13**), leading to a bis-resorcinol, involves a methanesulfonic acid-catalysed condensation in DCM/diethyl ether, which is a less polar system compared to the previously used water/ethanol media.⁷⁶



Scheme 13. Bacci's synthesis of bis-phenols.

This alternative reaction was tested with the synthesis of **140** (**Scheme 14**). One equivalent of aldehyde was condensed with an excess of 4-chlororesorcinol (2.5 equivalents), using a 1:1 solution of DCM:Et₂O with 8% of methanesulfonic acid as catalyst. Under these conditions the product was obtained in five hours: NMR of the reaction mixture shows only the product and the remaining excess of resorcinol.



Scheme 14. Synthesis of **140**.

The real improvement required for this reaction is the purification. Bacci used chromatographic methods, however a more convenient approach was sought. In most

cases these products do not precipitate from the reaction mixture and the excess of haloresorcinol cannot be removed by extraction.

In an attempt to avoid flash chromatography, an initial extraction to remove the acid and a subsequent crystallisation were attempted. Crystallisation from diethyl ether, DCM, methanol, hexane and their combinations could not be achieved, and it was clear would require optimisation for every compound.

Considering that monohalogenated resorcinols are soluble in water, a different and less conventional approach was used. The reaction mixture was diluted with diethyl ether to reduce its density below that of water and poured on distilled water. The multiphasic system was vigorously allowed to stir until the organic solvent evaporated completely, producing a solid suspension. The solid was collected on a Büchner filter and washed with further water to give the product. This method allows quick purification and removal of residual acid, which is essential to avoid degradation of the stored compound.

Using this method, a first set of dimers was produced (**Figure 29, black structures**). The products were obtained in yields ranging from 18 to 91%, with most reaction producing good, higher than 50%, yields. Compound **144** is a special case, it requires an additional crystallisation step, as the reaction is not as clean as the others, thus lowering the yield considerably.

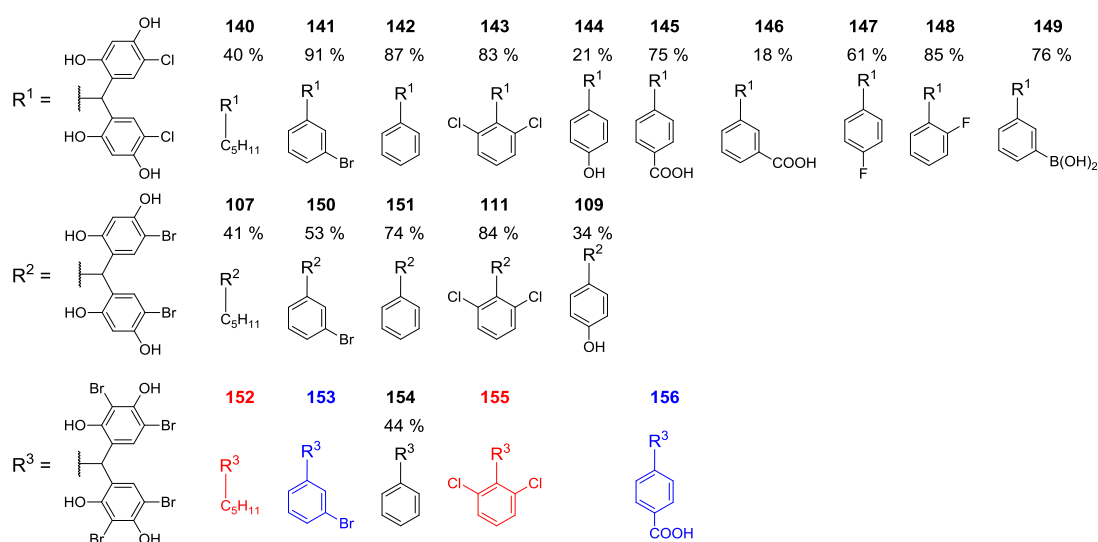


Figure 29. Set of dimers. Black structures: obtained as pure compounds. Red structures: reaction leads to mixtures of products. Blue structures: a solvent or reagent could not be removed completely.

The purification method employed, although very convenient and rapid, has a simple disadvantage: compounds with relatively good solubility in water provide lower

yields. All compounds show a marked tendency to retain water, which cannot be completely removed. Quantification of the water was attempted by thermogravimetric analysis however the compounds quickly decompose, preventing quantification. Calculation of water content was therefore performed indirectly: the product content in weighed samples was measured by quantitative NMR and the amount of water was obtained by difference.

Compared to **Method 1**, previously used in the group to synthesise **107**, **111** and **109**,⁷² the present approach is more convenient as it avoids purification by flash chromatography, allowing immediate access to the products. The yields (**Table 2**) are also superior, except in the case of **109**, probably as a consequence of the higher solubility provided by the additional phenol.

<i>Yield</i>	<i>Method 1 (%)</i>	<i>Method 2 (%)</i>
107	22	41
111	36	84
109	63	34

Table 2. Comparison of yields of **Method 1** and **2** for **107**, **111** and **109**.

As discussed in detail (**Chapter 2.5.5**), dibromoresorcinol requires longer reaction times. After ten days it was possible to isolate **154** and **153**. However, the reaction does not reach completion and removal of the aldehyde is necessary. To do so, following precipitation in water, toluene was used to wash the solid product. Unexpectedly, compound **153** displayed very high affinity with toluene (**Figure 30**). Repeated washes and co-evaporations with different solvents were not helpful, thus its purification was not possible. Chromatographic purification could lead to the pure product, however it was not pursued as a number of analogues were already available.

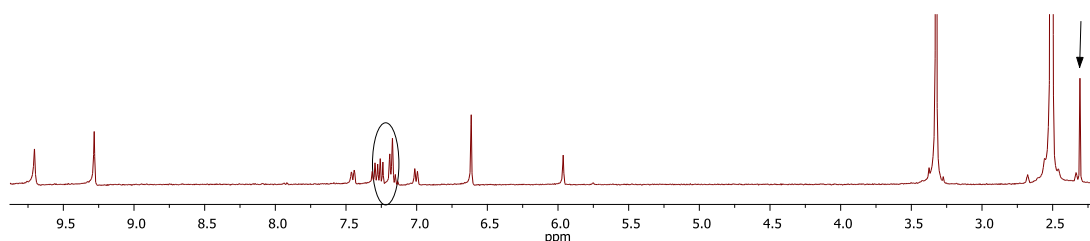


Figure 30. NMR of **153**, with the signals of toluene highlighted. Recorded in DMSO- d_6 at 400 MHz.

Compound **156** was also successfully synthesised, however the aldehyde cannot be removed from the mixture with toluene. The NMR (**Figure 31**) respects the canons dictated by all the other isolated compounds but the product could not be isolated in

pure form with the method in use. Preparative HPLC will have to be considered for its isolation, were it necessary.

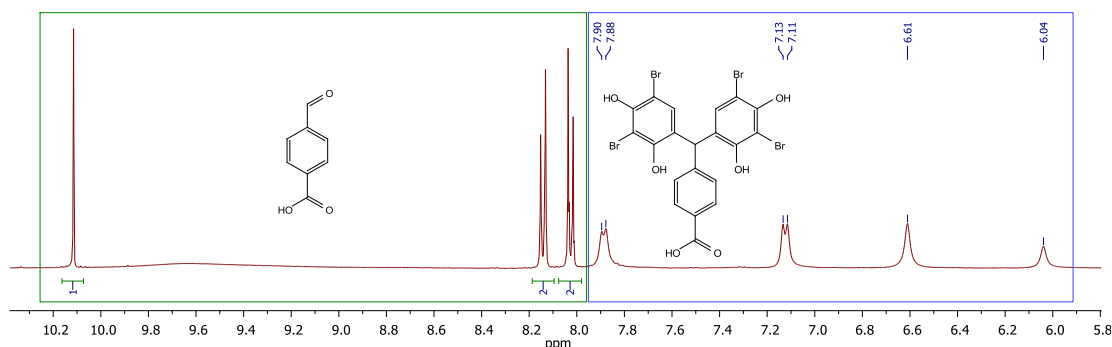


Figure 31. NMR of **156** and presence of aldehyde. Recorded in DMSO- d_6 at 400 MHz.

In contrast to those previously described, compounds **152** and **155** led to complex mixtures, in which the expected compound could not be clearly identified by NMR and purification was not pursued.

An alternative approach to the synthesis of tetrabrominated dimers would be the bromination of their dibrominated precursors by NBS (as in **Chapter 2.5.9** for tetramers), although this has not been attempted.

This synthetic approach using methanesulfonic acid as catalyst was extensively used throughout the project and, for convenience, will be henceforth referred to as **Method 2**. The effect of the solvent and side reactions leading to complex mixtures, together with a comparison between **Method 1** and **Method 2** will be discussed in (**Chapter 2.5.5**).

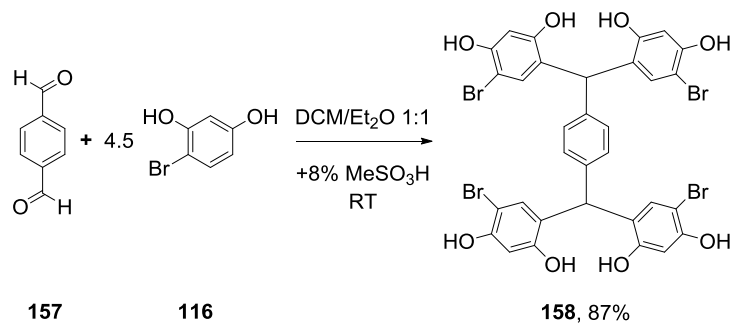
2.5 Synthesis of tetramers

As discussed in the introduction to this chapter, to evaluate whether increasing the number of halogenated resorcinol units produces better activity, synthesis of tetramers was also undertaken.

2.5.1 4-Bromoresorcinol based tetramers

Application of **Method 2** to the synthesis of tetramers was straightforward. Reaction of 1 equivalent of benzene-1,4-dicarboxaldehyde with 4.5 equivalents of 4-bromoresorcinol led to the expected product, **158**, in 87% yield (**Scheme 15**). The purification of this compound was different from that used for the dimers. The reaction mixture was diluted with diethyl ether and left overnight at 4 °C to give large crystals.

Identity of the compound was confirmed by NMR and high resolution mass spectrometry.



Scheme 15. Synthesis of **158**.

The molecule displays two planes of symmetry and thus the resulting ^1H -NMR spectrum is simple. Three singlets, at 6.8, 6.5 and 6.5, each assigned an integral of four, identify the aromatic hydrogens (**Figure 32. b, c, d**) and a singlet at 5.7, with an integral of two, represents the bridge's proton (**Figure 32. a**). Assignments were confirmed by HSQC and HMBC.

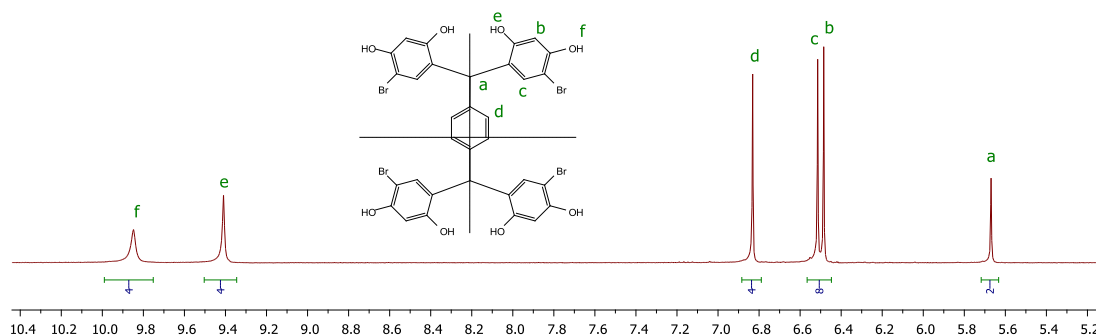
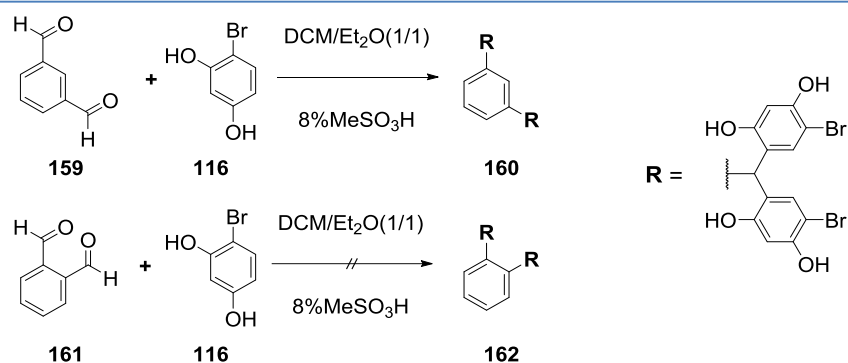


Figure 32. NMR of **158**. Recorded in DMSO- d_6 at 400 MHz.

To obtain the geometrical isomers, required for activity comparison and different presentation of hydroxyl groups for dendrimer development, the reaction was also performed with benzene-1,3- and benzene-1,2-dicarboxaldehyde (**Scheme 16**). The reaction with benzene-1,3-dicarboxaldehyde (**159**) readily proceeded to the expected product (**160**) in 61% yield.

However, under these conditions, the *ortho* isomer (**161**) did not lead to the expected product and the formation of a complex mixture was observed (**Scheme 16**).

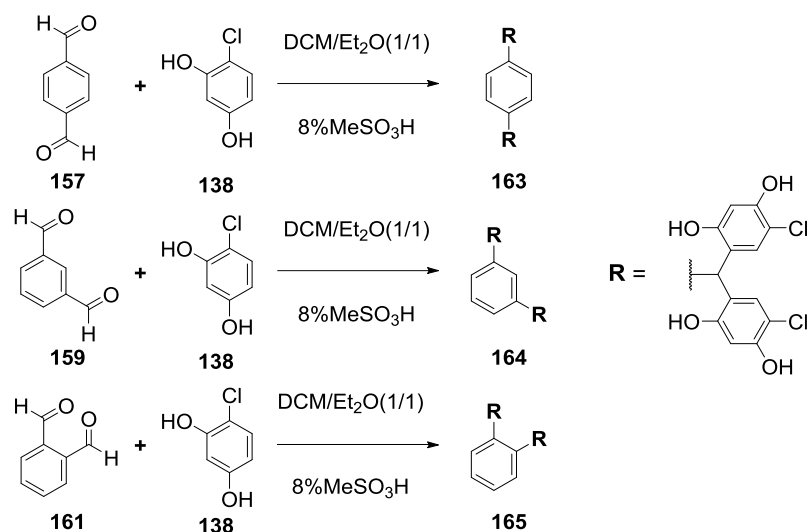


Scheme 16. Synthesis of **160** and attempted synthesis of **X**.

For these compounds, crystallisation from organic solvents is not ideal as a final purification step. The crystals include the solvent and a small amount of acid which shortens the shelf life of the product and has to be removed before testing in biological systems or *in vitro* assays. To obtain an acid-free product without solvents of crystallisation, trituration of the product in water is the ideal procedure and was used to prepare all samples required for testing.

2.5.2 4-Chlororesorcinol based tetramers

To prepare the chloro- substituted analogues, the same reactions were conducted using 4-chlororesorcinol. 4-Chlororesorcinol is commercially available and inexpensive, allowing scale-up and testing without the need of synthesising intermediates (**Scheme 17**).



Scheme 17. Synthesis of **163**, **164** and **165**.

Synthesis of **163** proceeded as expected and provided the product in 87% yield. Unexpectedly, **164** did not crystallise in a reproducible way, but the product could be

isolated by evaporation on water, as with the dimers. The product can be alternatively prepared as described in **Chapter 2.5.4**.

Compound **165** behaved rather differently from its analogues. Precipitation of the product in large quantities impaired the stirring and progress of the reaction, with subsequent formation of a relevant by-product (**Chapter 2.5.3**). The reaction was changed to provide better stirring and the volume of the solvent was also increased. Compound **165** was then obtained as a green solid in 94% yield.

After changing geometry, symmetry is maintained. In all cases, each resorcinol monomer is equivalent to the others in the molecule, thus giving two singlets for the aromatic hydrogens (**Figure 33**, 6.6 to 6.2 ppm) and two singlets for the hydroxyl groups (above 8.8 ppm). Between 7.2 and 6.6 ppm the peaks of the central ring are observed (**Figure 33**). Between 5.7 and 5.6 ppm the bridge singlet can be identified.

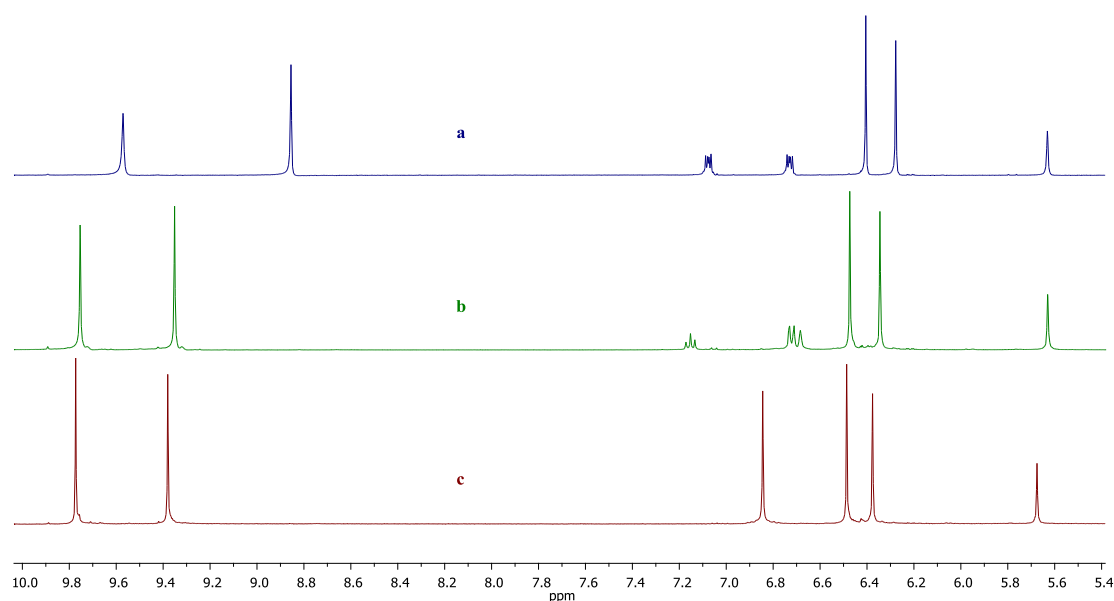


Figure 33. ^1H NMRs of **165** (a), **164** (b) and **163** (c). All spectra were recorded in DMSO- d_6 at 400 MHz.

2.5.3 By-products of **165** and their equilibrium

As previously stated, the initial conditions and set-up used for the synthesis of **165** led to a non-homogeneous mixture. Despite this, isolation of the product by filtration led to pure **165**, although in poor yields. The reaction was followed by ^1H -NMR to investigate whether it was slower than the previous reactions, potentially as a consequence of steric hindrance, and thus to optimise the reaction conditions. The aldehyde was quickly and completely consumed, but the presence of an unidentified

product was revealed. Since the product of the reaction is solid and insoluble, complete isolation of it by filtration was possible. The remaining liquor was slowly evaporated, producing crystallisation of the by-product – **166** (**Figure 34**).

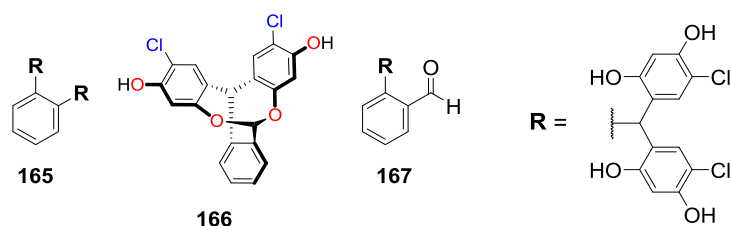


Figure 34. Structures of **165**, **166** and **167**.

In order to understand the reaction fully, **167** was synthesised. Phthalaldehyde reacted with two equivalents of 4-chlororesorcinol under **Method 2** conditions. The expected product was isolated by filtration. Interestingly, intermediate **166**, also visible in the ^1H -NMR, was collected by crystallisation of the remaining liquor.

For aldehyde **167** (**Figure 34**), three peaks are expected in the low field range of the ^1H NMR, two for the hydroxyl groups (**Figure 35**, **b**, **a**) and one, at highest ppm, for the aldehyde (**Figure 35**, **g**). Two singlets identify the hydrogens of the resorcinol (**Figure 35**, **e**, **f**). The open aldehyde exerts a strong deshielding effect on the bridge (**Figure 35**, **d**), causing an upfield shift of about 1.5 ppm, compared to its closed analogue. The presence of an aldehyde can also be clearly identified by ^{13}C -NMR: in **Figure 36**, the presence of a peak at 191.7 ppm is a distinctive trait of **167**.

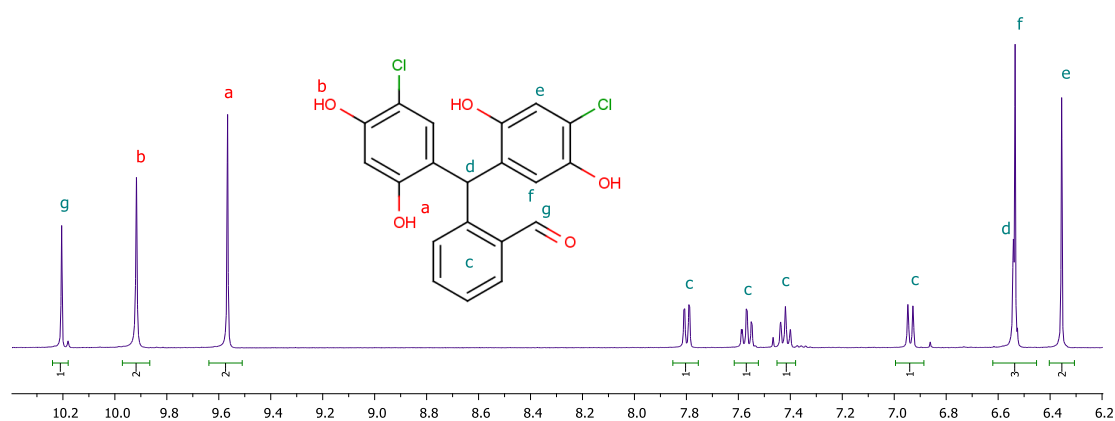


Figure 35. ^1H -NMR of **167** (DMSO- d_6 at 400 MHz).

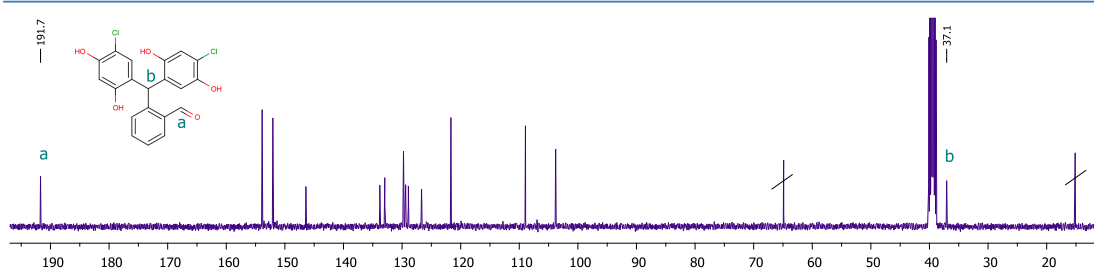


Figure 36. ^{13}C -NMR of **167**. Recorded in DMSO-d_6 at 400 MHz.

Considering the distances between the aldehyde and the hydroxyl groups, formation of an acetal was a reasonable hypothesis. The structure was drawn and minimised with GAFF force field in UCSF Chimera (**Figure 37**) and displayed reasonable angles and bond distances, suggesting that the acetal could be formed.

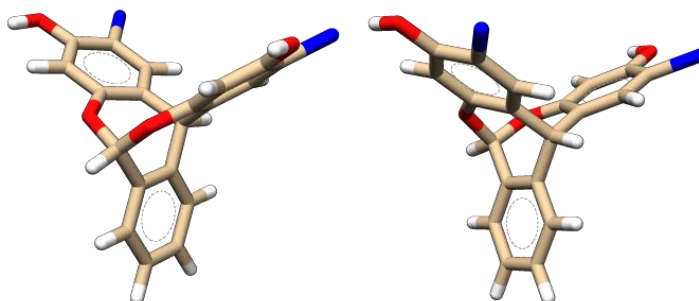


Figure 37. Structure of **166**, minimised with GAFF force field and rendered in UCSF Chimera.

Results from ^1H -NMR proved consistent with the proposed structure. In DMSO-d_6 (**Figure 38**), compound **166** displays a single peak above 9 ppm, corresponding to the hydroxyl groups. Two singlets identify the isolated hydrogens of the resorcinol groups (**Figure 38, c, e**). The position of the bridge is consistent with the other structures previously described (**Figure 38, f**). As expected, the hydrogen of the acetal lies in the region of the aromatics, downfield of the bridge (**Figure 38, d**). The connectivity of **166** was also confirmed by HMBC. NOESY interactions are also consistent.

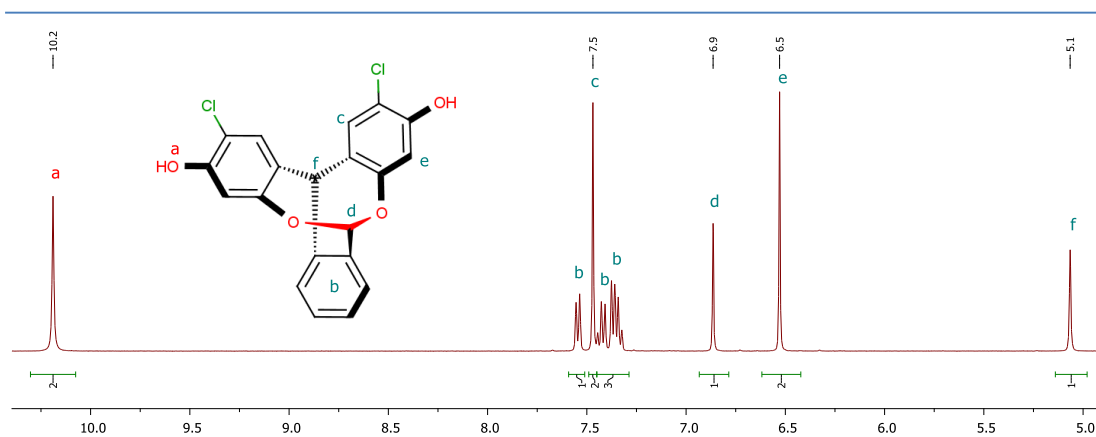


Figure 38. ^1H -NMR of **166**. Recorded in DMSO-d_6 at 400 MHz.

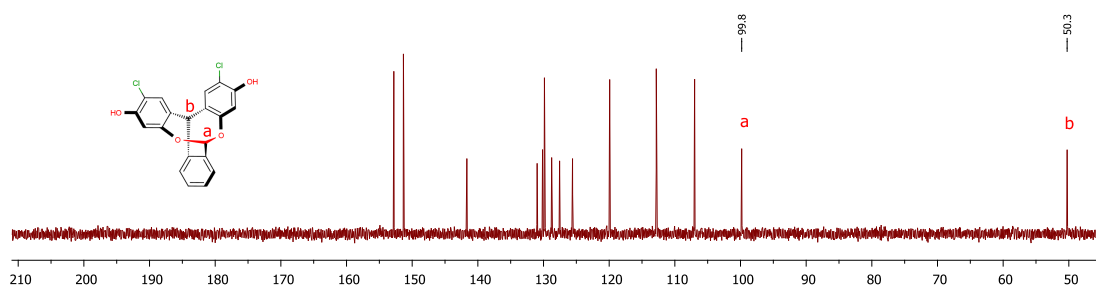


Figure 39. ^{13}C -NMR of **166**. Recorded in DMSO-d_6 at 400 MHz.

Since **166** has a unique bicyclic structure, crystallisation and X-ray diffraction was also used to confirm the structure and verify its topology. As expected from the initial modelling, the molecule displays a triplanar structure (**Figure 40, top**). The hydrogens of the hydroxyl groups are the only atoms out of any plane. They act as hydrogen bond donors towards a molecule of ether on one side, and towards another molecule of **166** on the other side, thus forming chains (**Figure 40, bottom**).

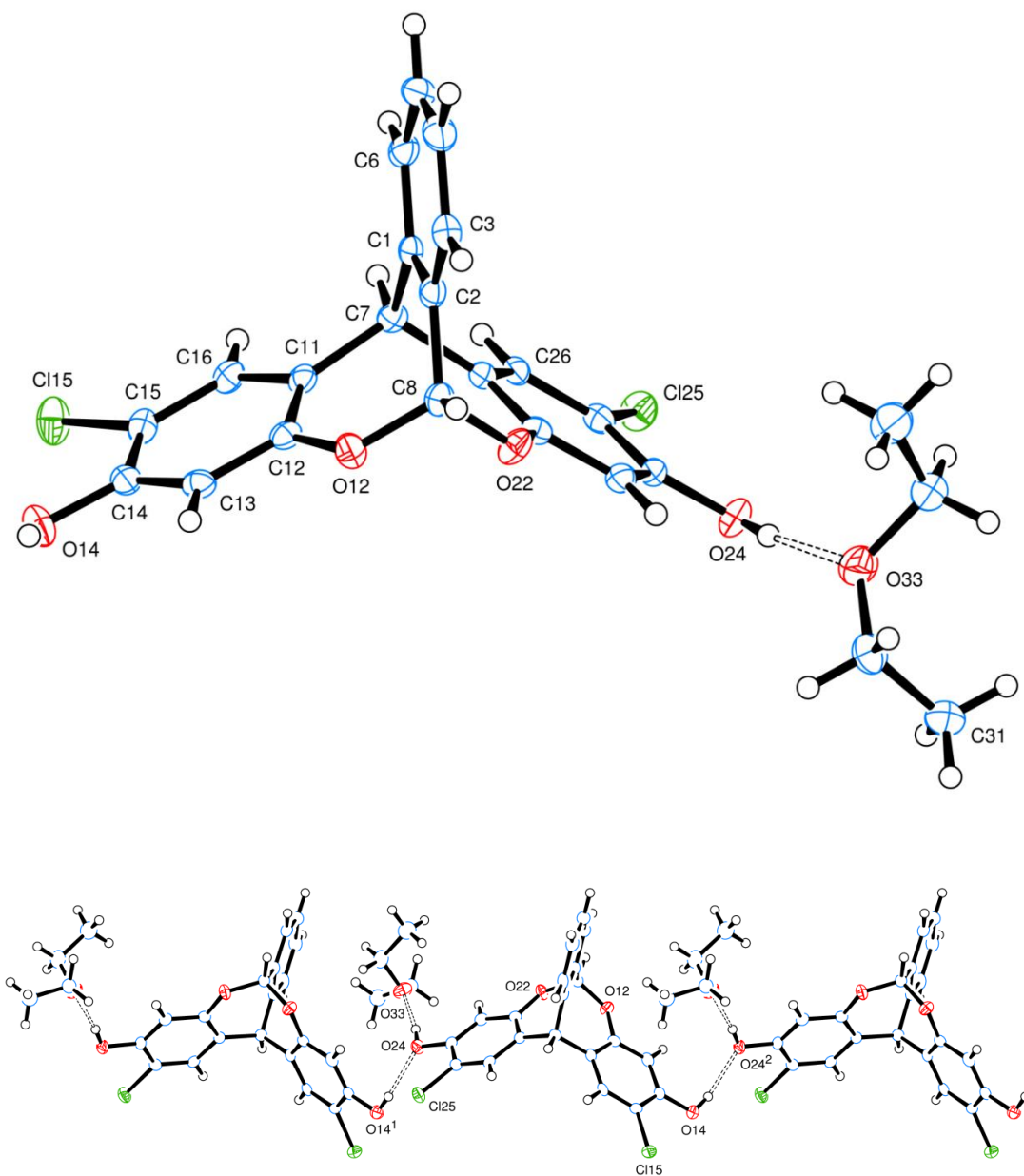
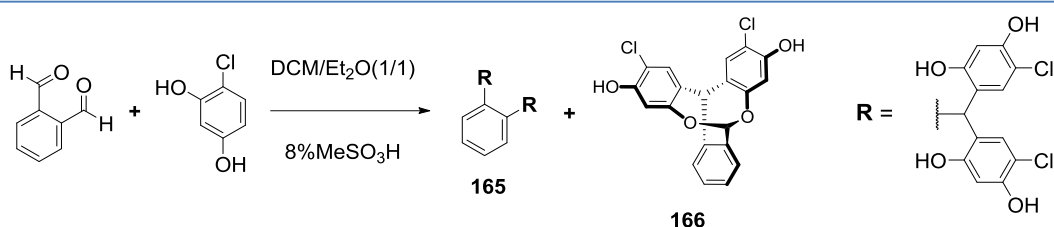


Figure 40. Crystal structure of **166**. Top, a single molecule of **166** hydrogen bonded with a diethyl ether molecule and chain-like arrangement of **166** within the crystal, bottom.

As previously said, using the first method employed to obtain **165**, a mixture of **166** and product was obtained (**Scheme 18**). Curiously, aldehyde **167** was not isolated from the reaction; it is an unexpected result because it is the obvious intermediate in the formation of **166**.



Scheme 18. Synthesis of **165** and **166**.

To investigate this anomaly, phthalaldehyde was treated with two equivalents of 4-chlororesorcinol and the reaction was followed by ^1H -NMR (**Figure 41**). Both **167** and **166** are present in the reaction mixture after 6 and 24 hours; the ratio between the two is stable and is 1.6 to 1, respectively (**Figure 41**).

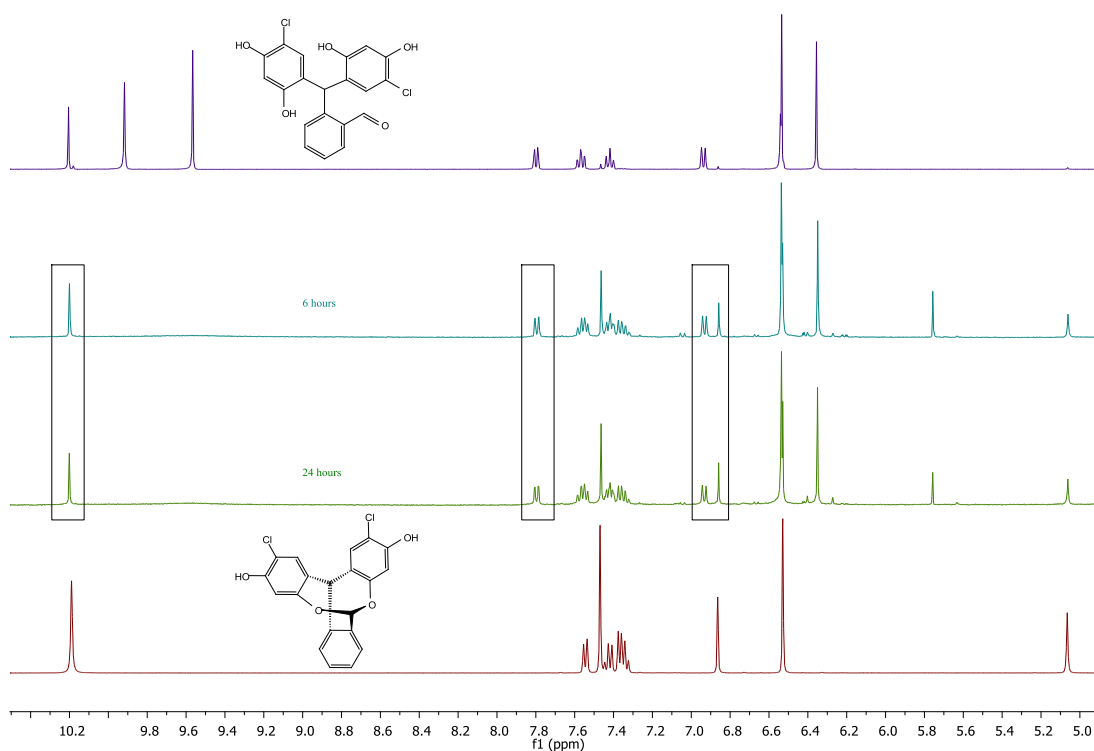


Figure 41. ^1H -NMR of the reaction mixture after 6 and 24 hours and spectra of **166** and **167** as reference compounds. All spectra were recorded in DMSO-d_6 at 400 MHz.

Additionally, reaction of the closed acetal **166** (**Figure 42, a**) with an excess of 4-chlororesorcinol led to the expected tetramer, **165** (**Figure 42, b**). Over the course of the reaction, the open aldehyde was also identified by ^1H -NMR (**Figure 42, c**).

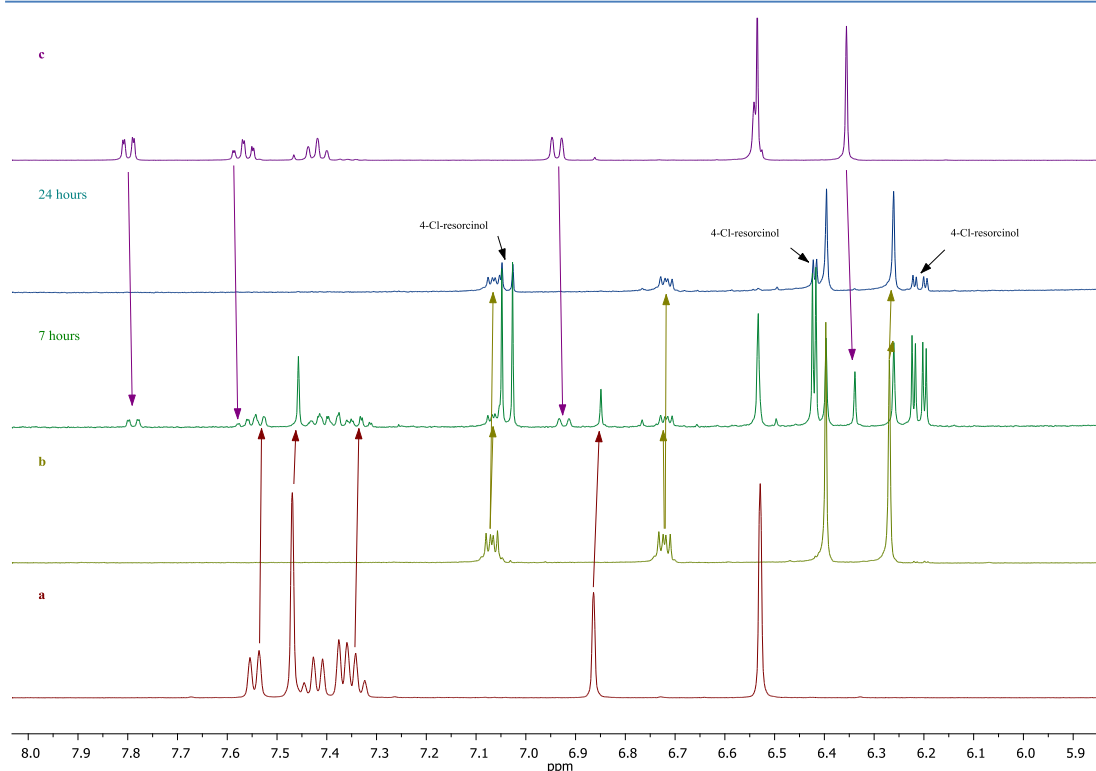
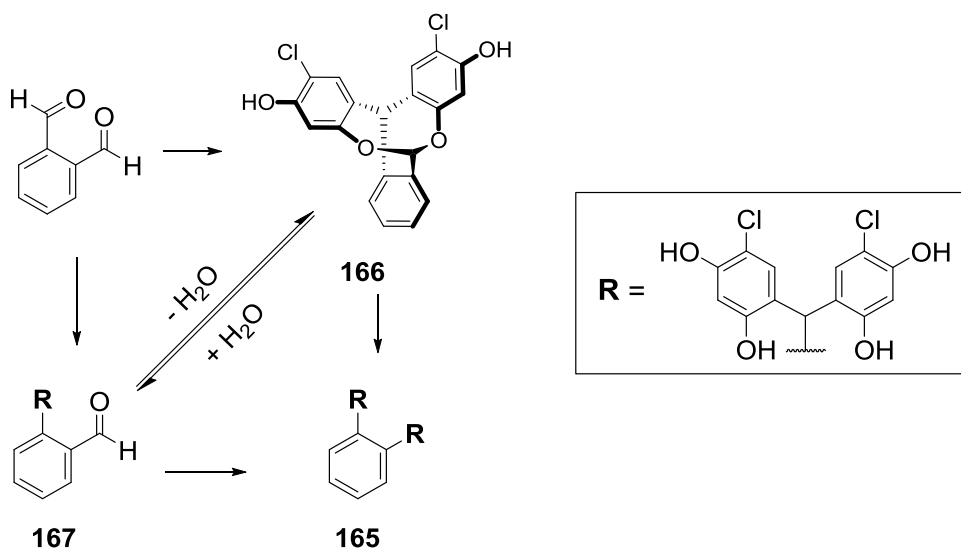


Figure 42. Reaction of the closed acetal **166** (a) with 4-chlororesorcinol to give **165** (b) at 7 and 24 hours showing presence of **167** (c) during the reaction. All spectra were recorded in DMSO- d_6 at 400 MHz.

These results suggest that the acetal is involved in an equilibrium with its aldehyde form. During the initial reaction for **165**, probably due to the large amount of product formed, which tends to bind water effectively, the equilibrium was likely to have been pushed towards acetal **166**, explaining why aldehyde **167** was not isolated (Scheme 19).



Scheme 19. Equilibrium between **166** and **167**.

2.5.4 Method 1 for the synthesis of tetramers

Despite the earlier failures with the use of **Method 1** for the synthesis of dimers, it was additionally investigated for the synthesis of tetramers. The results are listed in **Table 3**. With 4-bromoresorcinol, only **Method 2** provided results. Surprisingly, **Method 1** produced the expected compounds with good yields in the case of 4-chloro/fluororesorcinol based tetramers. This was particularly useful in the synthesis of **164**, which did not crystallise as easily as its regioisomers. Isolation of **164** using **Method 2** required evaporation of ether from a water mixture as seen for the dimers. This is not convenient for large scale reactions. With **Method 1**, evaporation of the solvent, resuspension of the solid in water and filtration provides the pure product in excellent yields (91%). However, except for the specific case of **164**, **Method 2** provides better yields and its scope additionally covers the bromoresorcinol derivatives.

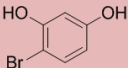
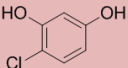
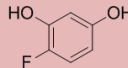
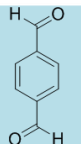
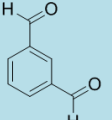
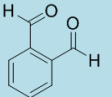
						
	8% MeSO ₃ H in Et ₂ O/DCM 1:1, RT	HCl 37%/EtOH 1:1, 70°C	8% MeSO ₃ H in Et ₂ O/DCM 1:1, RT	HCl 37%/EtOH 1:1, 70°C	8% MeSO ₃ H in Et ₂ O/DCM 1:1, RT	HCl 37%/EtOH 1:1, 70°C
	87%	mix	87%	66%	65%	35%
	61%	mix	NA	91%	NA	NA
	mix	mix	94%	80%	NA	NA

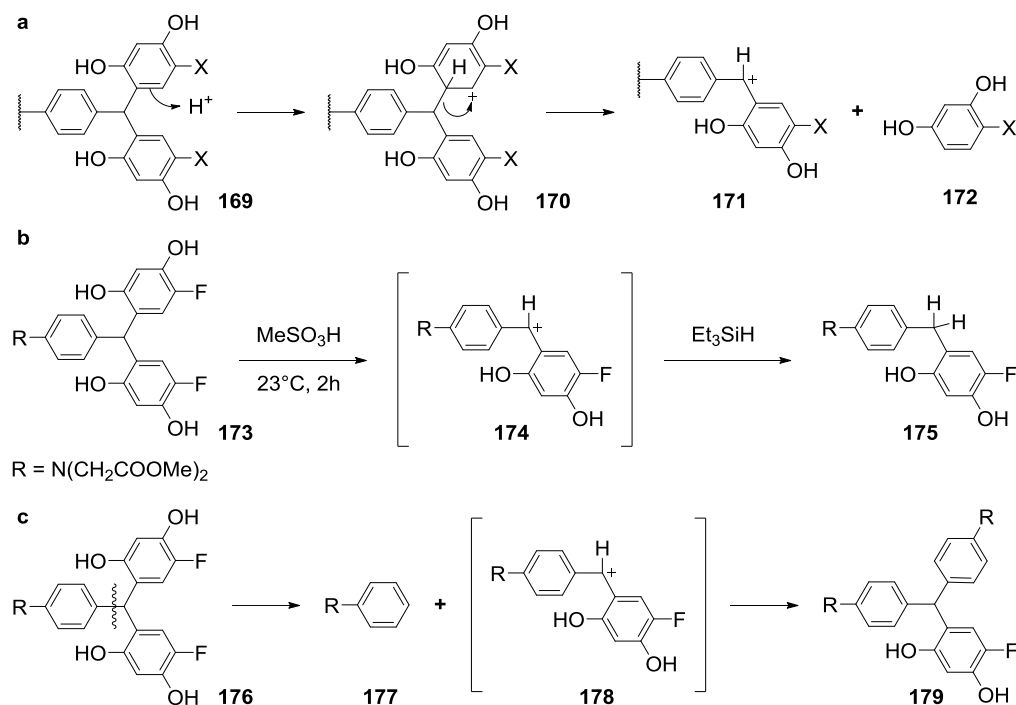
Table 3. Yields of the reaction between 4-haloresorcinols and isomeric benzene dicarboxaldehydes under reaction conditions of **Method 1** and **2**.

Fluoro-derivative **168** was prepared to evaluate the effects of fluorine as a substituent in the following biological and *in vitro* studies. Due to the cost of the starting material, only one example was prepared and further analogues will be synthesised if the substitution proves valuable. As opposed to its chloro- and bromo-analogues, its solubility in water is significantly higher and is probably the cause of the poor yield of the reaction, especially in the case of **Method 1**.

2.5.5 Side reactions and scrambling

The different behaviour of tetramers and dimers towards **Method 1** and **2** was further investigated. In the presence of strong acids, activated aromatic compounds are expected to undergo retro-Friedel-Crafts fragmentation (**Scheme 20, a**).

This behaviour was confirmed by Bacci with similar structures (**Scheme 20, b**).⁷⁶ Formation of highly reactive benzhydryl cations leads to unexpected products and polymerisation. In their experiments fluorinated bis-phenols were fragmented in neat methanesulfonic acid and the cation trapped using triethylsilane to obtain **175** in 81% yield. They also observed fragmentation on the aniline ring under **Method 2** conditions (**Scheme 20, c**).



Scheme 20. Retro-Friedel-Crafts fragmentation. General mechanism (a) and fragmentations observed by Bacci⁷⁶ (b, c).

Their results suggest that fragmentation is the main cause of poor yields and by-products formation. In light of this, it was interesting to review our previous results. The harsh conditions of **Method 1** favours formation of by-products: high polarity of the solvent stabilises the ionic intermediates, and high temperatures increase the rate of fragmentation. **Method 2** uses low polarity solvents and lower temperatures. This is particularly reflected in the synthesis of dimers, such as **131** (see page 37). 4-Hydroxybenzaldehyde is activated and prone to retro-Friedel-Crafts (**Figure 43**). If we also consider the fact that dibromoresorcinol is a relatively poor nucleophile, it is easy

to expect very low yields (traces in this case). However, with formaldehyde, which is more reactive and does not have a side chain susceptible to retro-Friedel-Crafts, dibromoresorcinol produces considerably better yields (**136**, 19.5%). Interestingly, when 4-bromoresorcinol reacts with formaldehyde to give **135** (see page 38), the yield is again very poor (2.6%), probably as a consequence of the susceptibility to protonation.

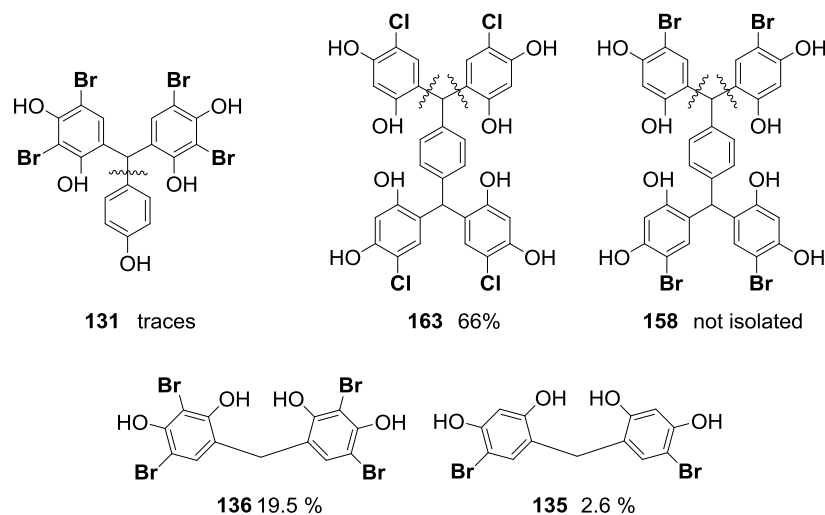


Figure 43. Yield of some compounds with some favourable fragmentation points highlighted.

Regarding tetramers, fragmentation by electrophilic addition to the central benzene is unlikely, as it is not activated. Therefore, fragmentation can be considered as directly dependent on resorcinol substitution. Chlorine is more electronegative than bromine, and the subsequently less electron-rich resorcinol displays slower fragmentation rates. This explains the difference between **158** and **163**. In fact, only the former has been isolated under **Method 1** conditions. One would expect even better results for fluororesorcinol, however, this cannot be verified by isolated yields as it is fairly soluble in water, with consequent product loss during purification.

Since Bacci isolated the sideproduct derived from fragmentation of his aniline sidechain in the conditions of **Method 2**, it was relevant to verify whether and to what extent chloro and bromoresorcinol were giving fragmentation in the case of our tetramers (especially considering that we obtained the pure products without the necessity of any chromatographic purification step).

Compound **163** was reacted with an excess of bromoresorcinol (5 eq) under both **Method 1** and **2** conditions, for five hours in both cases. The results are presented in **Figure 44** and **Figure 45**. It is immediately evident that **Method 1** leads to

fragmentation (presence of chlororesorcinol in the reaction mixture) and significant polymerisation (broad, undefined mounds). **Method 2** produces scrambling as well, although to an evidently lesser extent. This shows that aldehyde-dimers, like **167**, are unlikely to be useful for the synthesis of mixed tetramers as scrambling would occur, producing complex mixtures of different tetramers. To prepare mixed tetramers, a different approach will need to be used and will be discussed in the following paragraph.

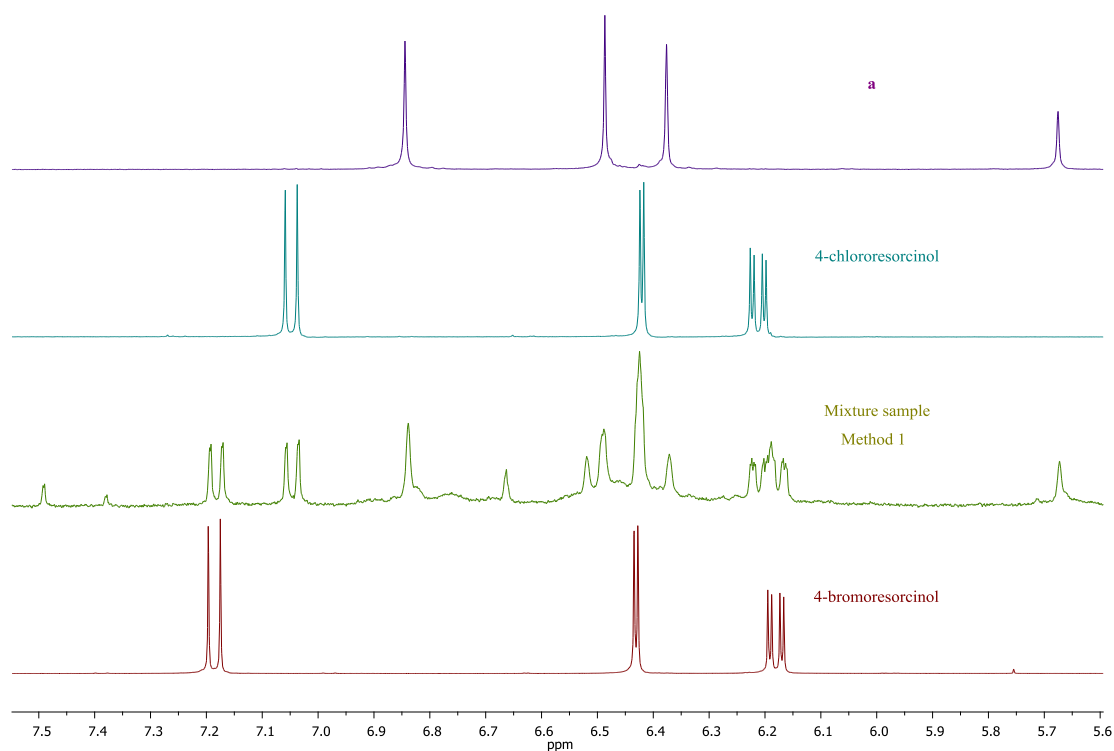


Figure 44. Scrambling of **163** (a) under **Method 1** conditions with reference 4-bromo- and 4-chlororesorcinol. All spectra were recorded in DMSO- d_6 at 400 MHz.

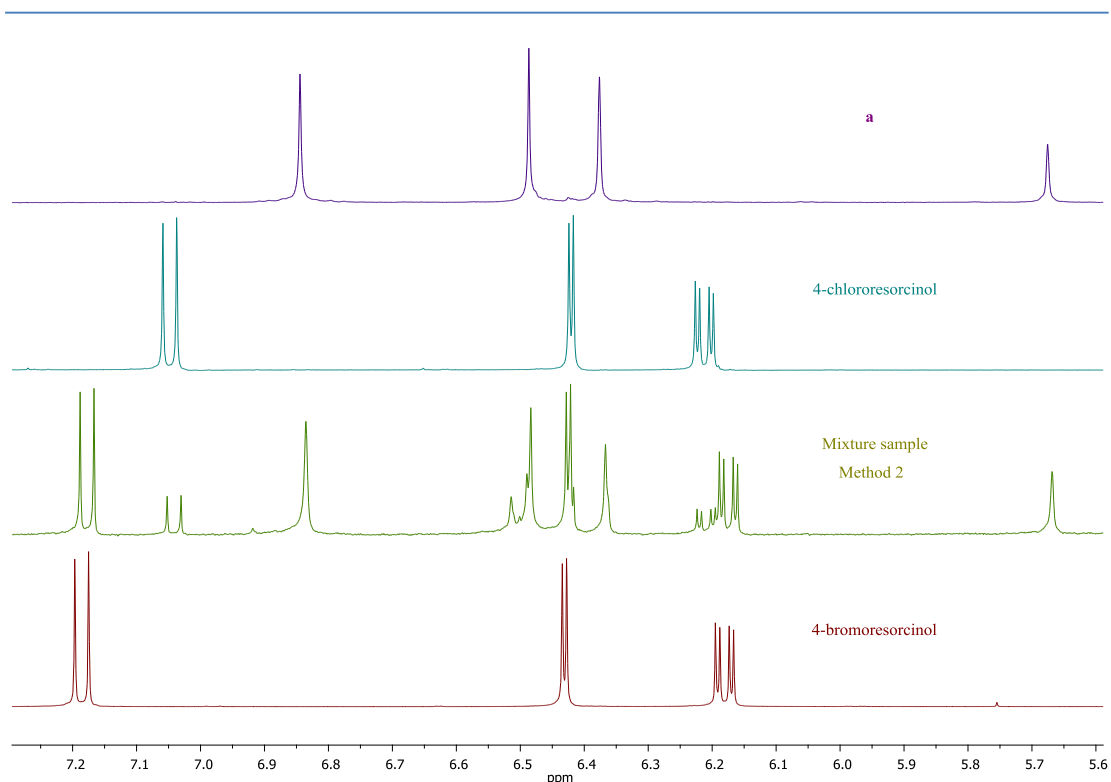
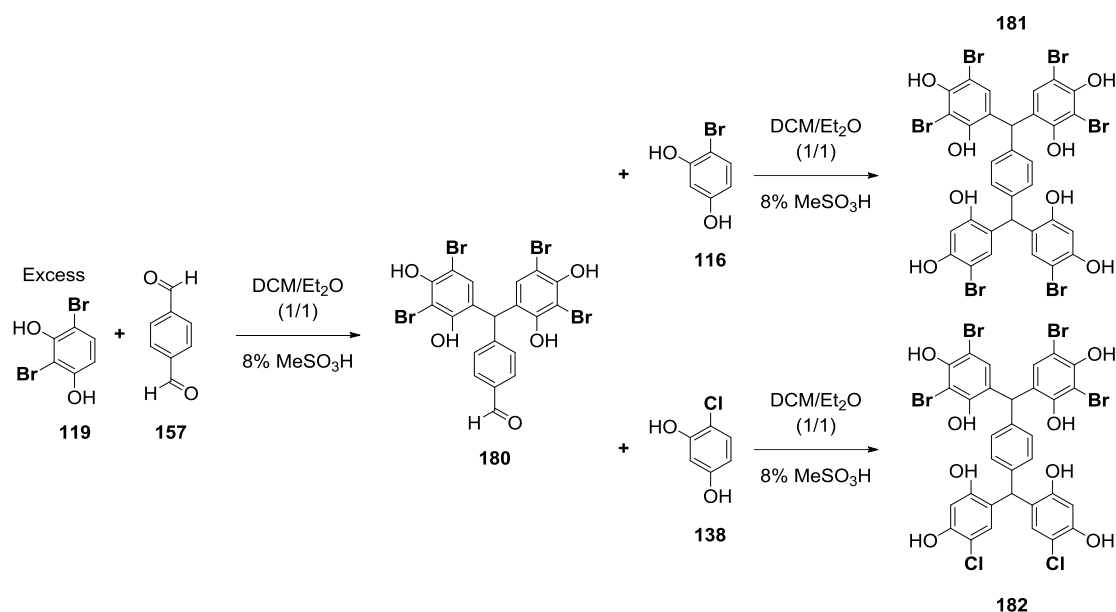


Figure 45. Scrambling of **163** (a) under **Method 2** conditions with reference 4-bromo- and 4-chlororesorcinol. All spectra were recorded in DMSO- d_6 at 400 MHz.

2.5.6 Aldehydes and mixed platforms

Isolation of a dimer presenting an aldehyde (**167**) was relevant for the preparation of mixed tetramers. Due to the reversibility of the reaction with monosubstituted resorcinols, obtaining aldehyde-dimer products was not normally possible. To ensure the reaction of only one aldehyde, the less reactive 2,4-dibromoresorcinol was employed. As expected, its reaction with benzene-1,4-dicarboxaldehyde produced **180** (**Scheme 21**). An excess (6 equivalents) of dibromoresorcinol was necessary, on top of eight days reaction time. Dibromoresorcinol is a very poor nucleophile and it does not appear to be significantly affected by retro Friedel-Crafts reactions. On top of this, its product **180** is poorly soluble in the reaction mixture, reducing the chances of a potential condensation of the second aldehyde and fragmentations. These effects might also be supported by a reduced reactivity of the second aldehyde, as a consequence of the electron-withdrawing effect of carbonyls, condensation of one aldehyde could slightly reduce the electrophilicity of the second.

Despite the poor solubility of **180**, it was possible for this to react with monohalogenated resorcinols and prepare the mixed platforms **181** and **182** (Scheme 21).



Scheme 21. Synthesis of **180**, **181** and **182**.

2.5.7 Crystallography

As the resorcinol tetramers were novel structures, we envisioned the possibility of using them as dendrimer cores and in supramolecular organic-inorganic frameworks, in addition to the Medicinal Chemistry applications. Single crystal X-ray diffraction was conducted to have absolute confirmation of the identity and further insight into the crystal arrangement and geometry/conformation. Structures of **163**, **164** and **165** were confirmed. All of them present the resorcinol rings on staggered planes. In every case, an extensively interconnected hydrogen-bond network leads to column or ladder-like structures, with solvent molecules (diethyl ether or methanol) bridging the chains of compounds and filling the spaces.

163 (Figure 46, a) forms columns, with each molecule stacked above the previous and hydrogen bonded to it through two hydroxyl groups, O14, O14¹. The other six hydroxyl groups form hydrogen bonds with diethyl ether, which intercalates the parallel running chains.

164 (Figure 46, b) is organised in a ladder-like structures, with two hydroxyl groups donating hydrogen bonds to the following molecule. The ladders organise in

pairs running alongside, with each tetramer lying about a point of symmetry in respect to the one in the adjacent ladder. These double chains are bridged with one another through methanol molecules.

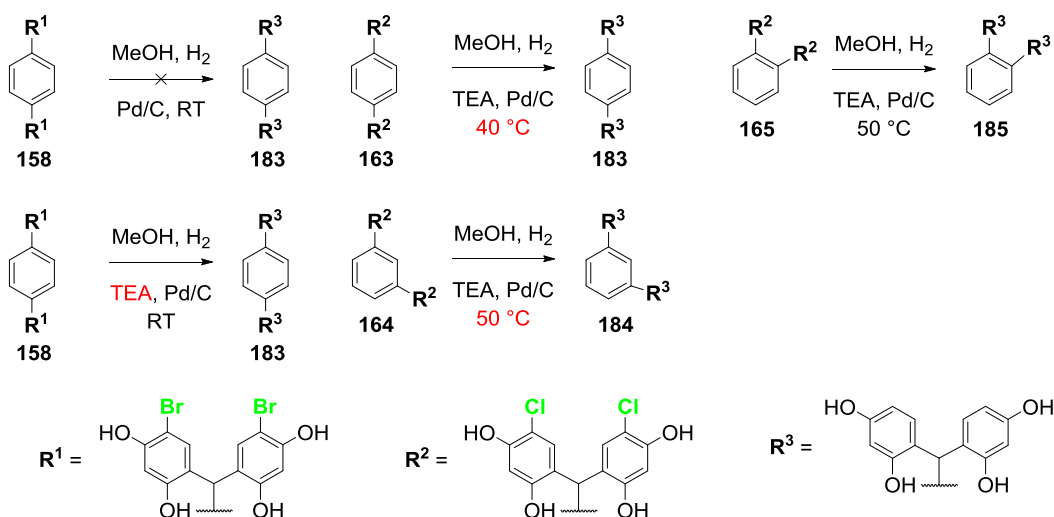
165 (Figure 46, c) displays a similar ladder system, with each molecule stacked on the preceding one. In this case, the ladders lie on the same plane and are bound to each other by double-bridging methanol molecules. It is interesting to note that the hydrogens of the bridge, unlike the other tetramers, are forced to point towards each other as a consequence of the steric hindrance.

The extensive binding of solvent by the compounds explains the difficulties found in removing solvents from the products. Even diethyl ether, *per se* extremely volatile, cannot be removed under high vacuum at 40 °C, which is impressive considering that its boiling point is 34.6 °C. Co-evaporation with water, which provides stronger hydrogen bonds, allows removal of organic solvents which would not leave otherwise. This is a necessary step for those compounds meant for biological testing. After a week of drying in the presence of silica gel and high vacuum, the products were analysed by quantitative ¹H-NMR to obtain exact sample purity, quantification is in any case necessary for yield calculation.

2.5.8 Dehalogenation of tetramers

Dehalogenation of tetramers is essential to obtain reference compounds for SAR studies. Moreover, these structures are suitable candidates for dendrimer cores. To be useful as such, a simple and scalable synthesis would be ideal to obtain the products in reasonable amounts for further studies. In previous work by our collaborators in South Korea, dehalogenation of bromoresorcinol dimers was obtained through hydrogenation in the presence of catalytic amounts of palladium over alumina, in methanol, at room temperature.⁷² The reaction yield is low (21-56%) and purification by RP-HPLC was employed.

The first dehalogenation attempted was the reduction of **158**. Palladium over carbon was used as catalyst due to its availability and the reaction was conducted in methanol at room temperature, however extensive polymerisation was observed. Since the reaction leads to hydrobromic acid as side-product, and the product would be expected to be very sensitive to acids (**Chapter 2.5.5**), it was therefore reasonable to see whether a base could scavenge the acid, thus preventing fragmentation. Triethylamine was chosen because it is soluble in the reaction conditions and acidic water (for purification purposes), and it is not reactive towards the product. As expected, with this modification, the reaction led to the pure product, in almost quantitative yields, after a simple extraction (**Scheme 22**).



Scheme 22. Dehalogenation reactions.

We then investigated the chloro-substituted analogues instead of bromoresorcinol-based tetramers, as chlororesorcinol is readily available and cheap, allowing the desired scale up. Additionally, **185** is only accessible through its

chlororesorcinol-based precursor **165**. As expected, chlorine is less reactive and the temperature had to be increased slightly to obtain complete dehalogenation. **183** was obtained at 40 °C in 96% yield. Probably, as a consequence of steric hindrance, reduction of **164** and **165** required a further increase in temperature, the products, **184** and **185**, were obtained at 50 °C in 62% and 69% yield, respectively.

Identification of the dehalogenated product, and completion of the reaction, can be easily verified by ^1H -NMR (**Figure 47**). The first thing to be noted is that, as one would expect, the symmetry observed before is maintained. The singlets belonging to the resorcinol are split in doublets (3J and 4J) and a new double doublet (3J , 4J) appears, indicating the hydrogen replacing the halogen. This pattern is typical for all non-halogenated tetramers.

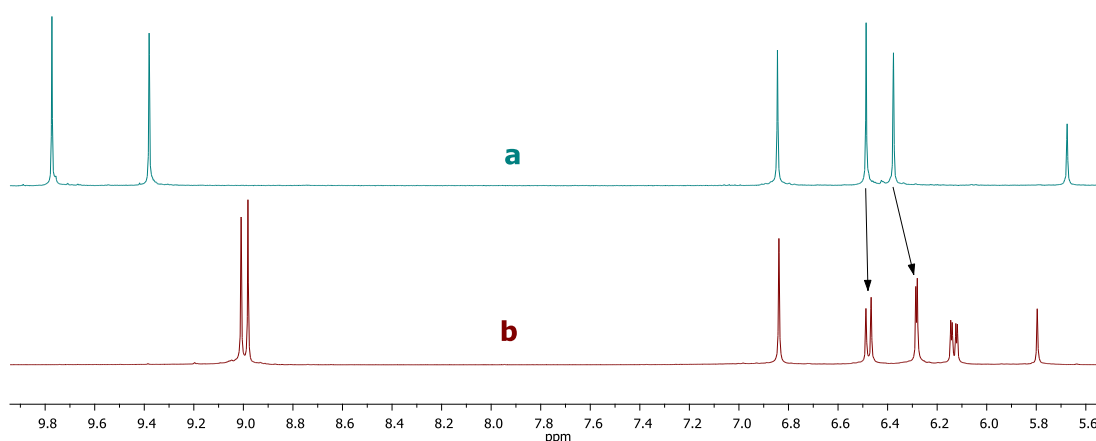


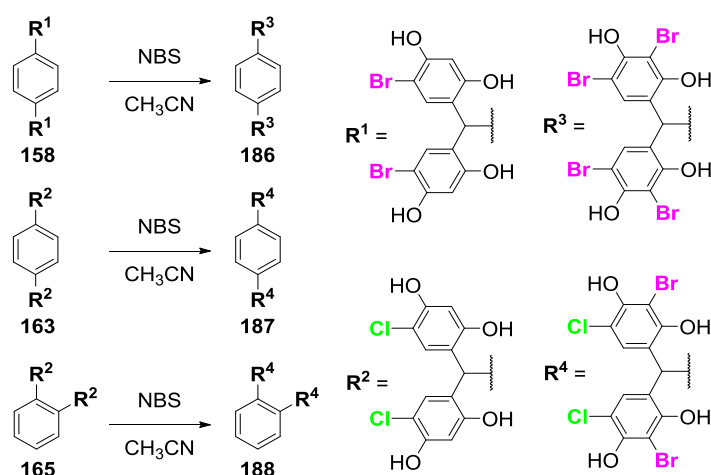
Figure 47. ^1H -NMRs of **163** (a) and **183** (b).

2.5.9 Halogenation of tetramers

Since formation of tetramers based on dibromoresorcinol is not possible using our first method, due to the fact that the reaction stops at the dimer as in the case of **180**, an alternative approach was necessary. The work by Das⁷⁷ was initially considered. The author used ammonium acetate to catalyse the selective bromination of phenolic compounds by *N*-bromosuccinimide (NBS). Decomposition of NBS by ammonia leads initially to Br_2 , which is then further reduced by ammonia to HBr .⁷⁸ Hydrobromic acid polarises the N-Br bond of NBS, facilitating electrophilic substitution of the aromatic compound but, unfortunately, presence of acid would likely lead to fragmentation.

Since the resorcinols are more reactive than the model compounds used by Dal, the reaction was attempted without the catalyst. Compound **158** was dissolved in acetonitrile and freshly crystallised NBS was added. Unexpectedly, the reaction

produced an immediate precipitation and reached completion in 25 minutes, giving **186** in 63% yield (**Scheme 23**). Similarly, **163** and **165** reacted with NBS to obtain **187** and **188**, respectively. Compounds with resorcinol units bearing mixed halogens were thus obtained. It has to be noted that these reactions can easily (and very rapidly) produce by-products and polymerisation, either as a consequence of acid formation or oxidation. For this reason, and with the additional issue of the reduced solubility of the products, development of other derivatives was postponed until after results from the biological tests on the already available compounds.



Scheme 23. Halogenation of tetramers.

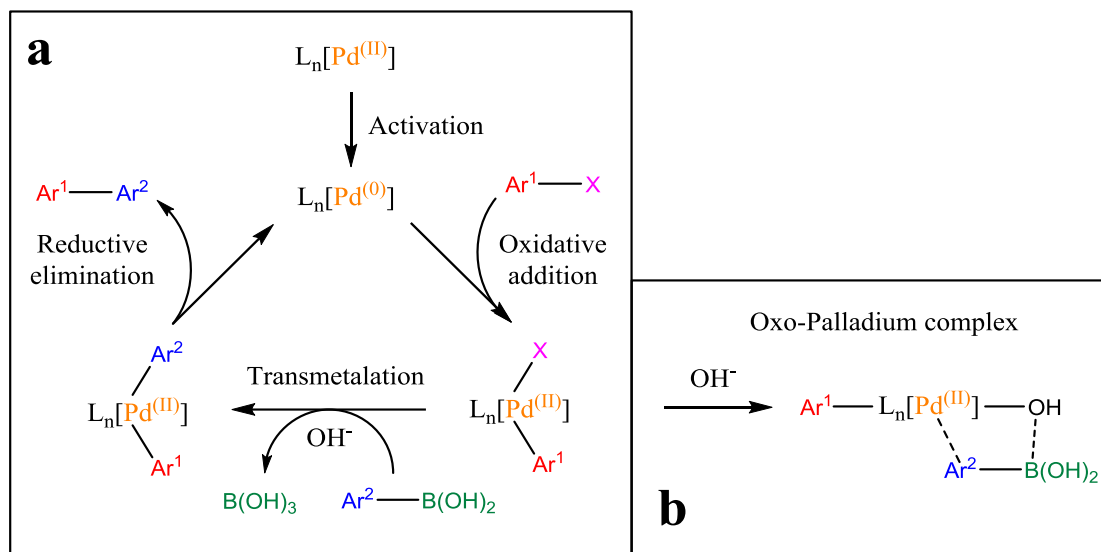
2.5.10 Biaryldicarboxaldehyde-based tetramers

To develop a further set of tetramers with a longer spacer while maintaining a (relatively) rigid and defined geometry, biaryldicarboxaldehydes were also considered as a bridging unit. To obtain the necessary aldehyde in one step from commercially available materials, a classical Suzuki coupling appeared to be the most convenient approach and some desired products were already described in the literature.^{79,80} Homocoupling reactions are also available,^{81,82} however they present the significant drawback of not allowing access to mixed products in case of further development (on top of the increased cost of the boron-based starting material).

2.5.10.1 Suzuki cross-coupling

In 1979, Suzuki and Miyaura reported the palladium-catalysed cross coupling of alkenyl/alkynyl halides with alkenylboranes. The reaction has since been developed and acquired a major role among the chemical tools available, leading to the award of a Nobel Prize to the author (joint with other major contributors to palladium-catalysed

cross coupling, R. E. Heck and E. Negishi).⁸³ To date, there are many variations on the original theme, the conditions have been improved and the scope of the reaction has been considerably extended.



Scheme 24. Suzuki cross –coupling mechanism (a) and formation of an oxo-palladium complex (b).

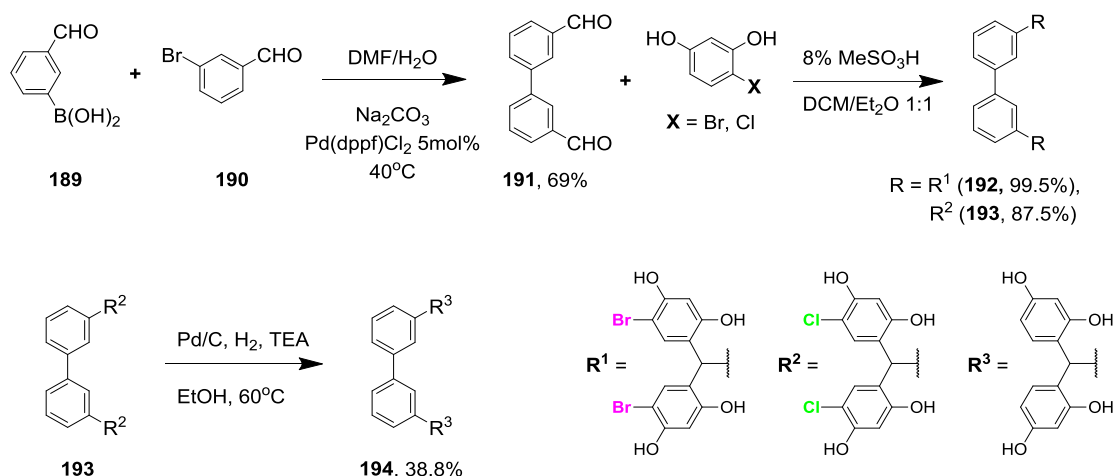
Adapted from Lennox.⁸⁴

A general mechanism for the reaction is reported in **Scheme 24, a**. The Palladium(0) catalyst reacts with a formally nucleophilic aryl substrate in the Oxidative Addition step, leading to a first Palladium(II) complex. Subsequent Transmetalation with a formally nucleophilic aryl boron, leads to a second Palladium complex. A last step, involving reduction of Pd(II) to Pd(0) and elimination of the cross-coupled product regenerated the catalyst bringing the cycle to its beginning. Different organoboron reagents have different pathways to undergo the transmetalation step. In the case of boronic acids, a base produces an Oxo-Palladium complex which is then able to transmetalate, as reported in **Scheme 24, b**.⁸³⁻⁸⁶

2.5.10.2 Synthesis of biaryl-tetramers

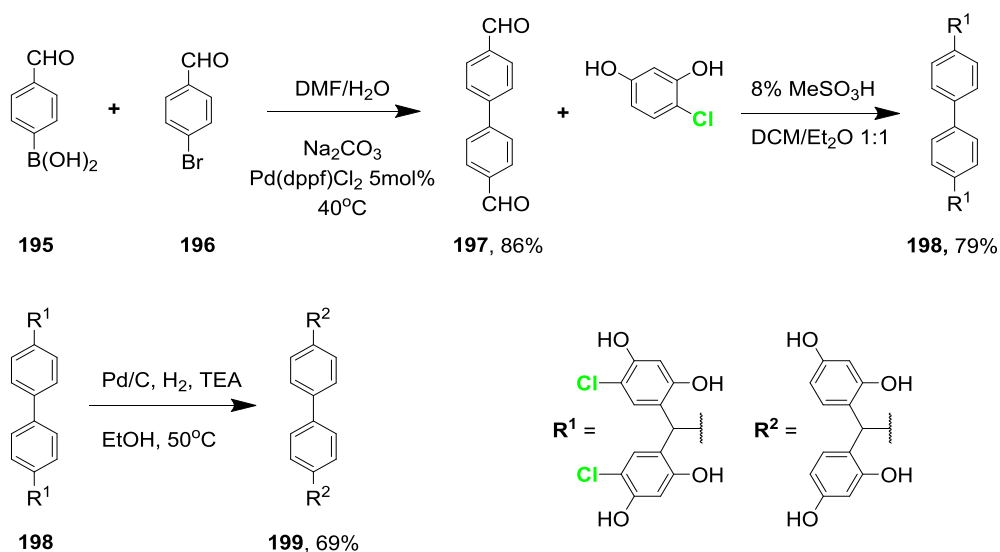
Aldehyde **191** was prepared in good yields (69%) from palladium-catalysed cross coupling of 3-formylphenylboronic acid with 3-bromobenzaldehyde. Despite the fact that Kuhnert⁷⁹ did not specify the procedure used, a tentative method led to the product in 69% yield, a result consistent with his 71%. The reaction was conducted in DMF-water medium, in the presence of sodium carbonate and [1,1'-bis(diphenylphosphino)ferrocene] dichloropalladium as catalyst, at 40 °C. The product was then purified by column chromatography. Subsequently, **Method 2** allowed access

to both chloro and bromo-resorcinol based tetramers in excellent yields, 87.5 and 99.5% respectively (**Scheme 25**). Dehalogenation of the product was obtained with the method previously described, however the conditions were not yet refined. The reaction was carried out at 60 °C instead of 50 °C, probably causing a loss of product and reducing the yield (38.8%).



Scheme 25. Synthesis of **191**, **192**, **193** and **194**.

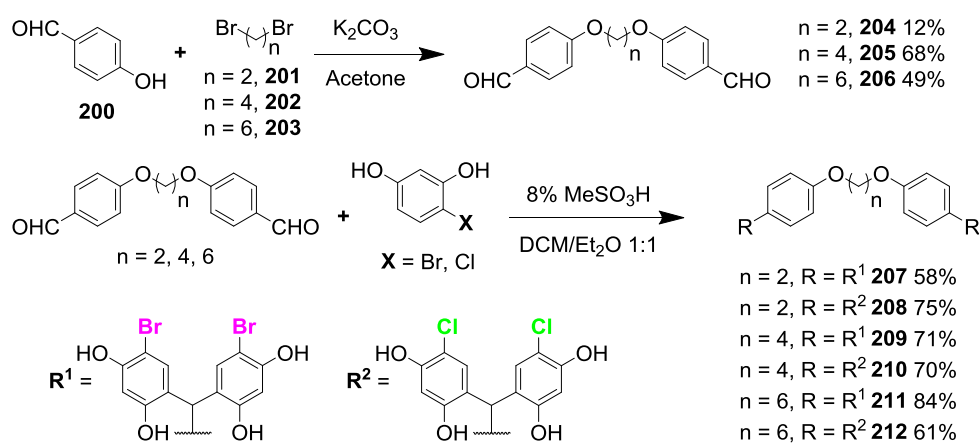
Similarly to that described above, aldehyde **197** was obtained by the Suzuki reaction in high yield (86%). Tetramer **198** was then prepared according to **Method 2** in excellent yield (79%). Subsequent dehalogenation led to the expected molecule (**199**) in 69% yield.



Scheme 26. Synthesis of **197**, **198** and **199**.

2.5.11 Flexible tetramers

An additional set of tetramers, presenting two dimers linked by a flexible chain of different lengths was also prepared. The linker consists of two 4-hydroxybenzaldehydes with an alkyl chain bridging the hydroxyl groups. To prepare the linker, similarly to the method reported by Narasimha,⁸⁷ 4-hydroxybenzaldehyde was reacted with dibromoalkanes of different lengths (two, four and six carbons) in the presence of a base and the expected products were obtained in poor to good yields (**Scheme 27**). Subsequent condensation of the aldehyde with 4-chloro/bromoresorcinol according to **Method 2** led to the expected products in good yields (58-84%).

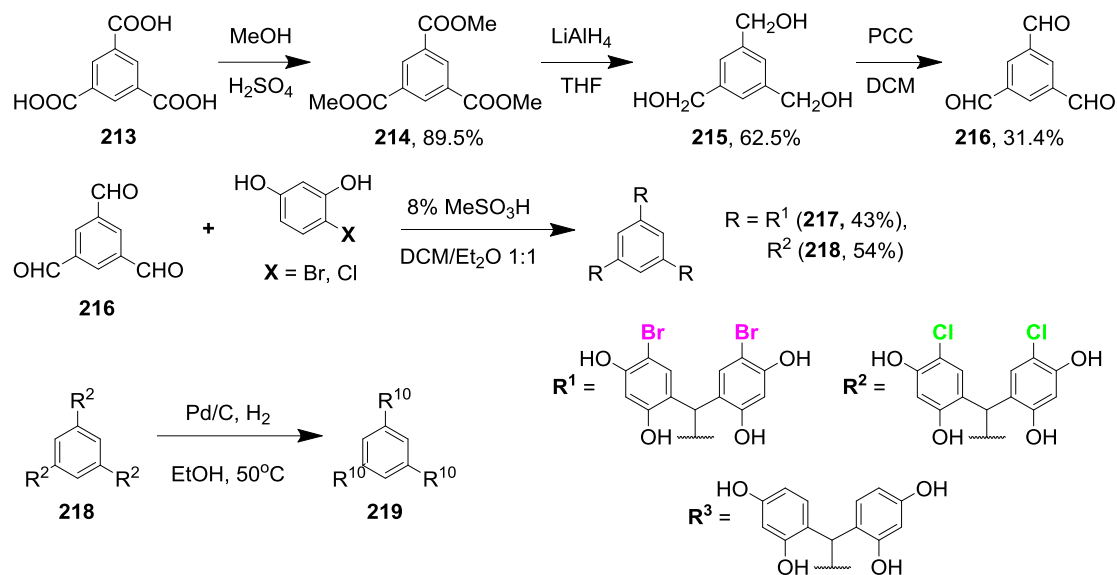


Scheme 27. Synthesis of flexible tetramers.

2.6 Synthesis of hexamers

We also saw the intriguing opportunity of preparing a hexamer, which would display twelve available hydroxyl groups. For this, synthesis of 1,3,5-triformylbenzene was undertaken. The synthesis was carried out according to the procedure by Kaur (**Scheme 28**).⁸⁸ Trimesic acid (benzene-1,3,5-tricarboxylic acid) is a cheap and readily available starting material. It was converted to its corresponding methyl ester (**214**) by heating at reflux in a solution of sulphuric acid in methanol. The clean product was obtained in very good yield (89.5%) after an extraction workup. The following reaction, which involves the reduction of the ester to alcohol (**215**), is the bottleneck of the procedure. Despite its acceptable yield (62.5%) it requires a very long reaction time, and totally unexpected, an even longer quenching time, far higher than the reported procedure. The reduction required three days (instead of four hours) and six equivalents of lithium aluminium hydride (instead of three). The author used a 1:1 mixture of celite and potassium hydrogensulfate to quench the reaction. Due to unavailability, sodium

hydrogensulfate was used instead. To quench the reaction properly, the ratio of NaHSO₄:celite was increased to 4:1 and the mixture was allowed to stir for 112 hours. Using diluted HCl was not a viable option, as it led to a viscous oil and no identifiable product. The oxidation of alcohol to aldehyde (**216**) with PCC proceeded as expected, although the yield obtained was lower than the reported one (31% versus 51%).



Scheme 28. Synthesis of hexamers.

Synthesis of the hexamers with **Method 2** proceeded as expected but the reaction time was increased to twenty-four hours to allow completion. The yields, however, were lower than for the tetramers, with only 43% and 54% for bromo and chloro-resorcinol based hexamers, respectively.

Unfortunately, dehalogenation of **218** to **219** did not yield a pure product. The expected compound could be clearly identified by ¹H-NMR but it was not possible to isolate it in a sufficiently pure form (**Figure 48, c**). Nonetheless, upon propargylation of the hydroxyl groups and subsequent purification, the crude can be used for the synthesis of a dodecavalent dendrimer core, as described in **Chapter 4.5.1**.

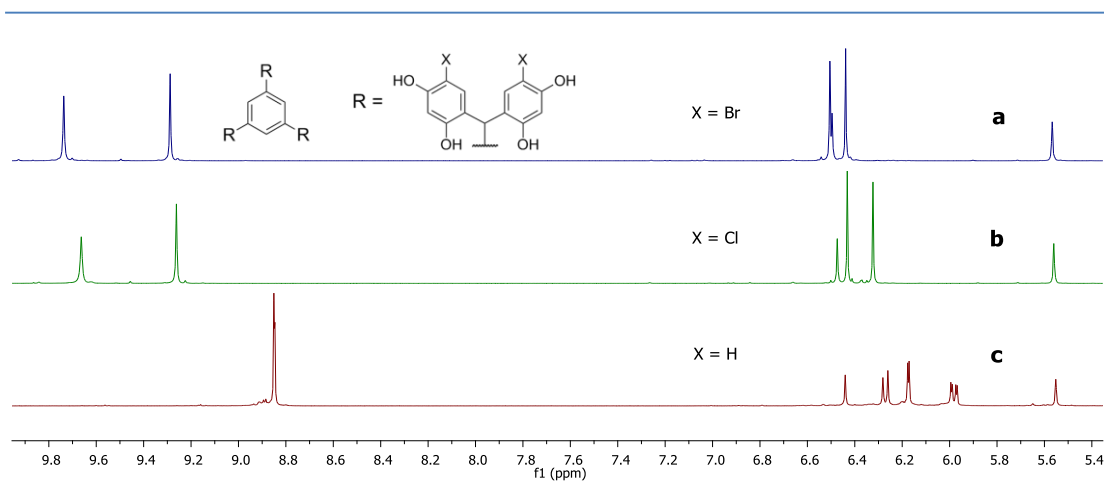


Figure 48. ^1H -NMR of **217** (a), **218** (b) and **219** (c).

From the ^1H NMR (**Figure 48, a, b**), both products present the same features as the tetramers, with equivalent hydrogens for all resorcinol units, producing two singlets, a singlet for the hydrogens of the core and a final one for the bridge. Two singlets represent the two hydroxyl groups. Similarly, as described before, dehalogenation produces new peaks and splitting of the pre-existing signals (**Figure 48, c**).

2.7 Conclusions

Two rapid and convenient methods for the synthesis of dimers and tetramers have been discussed. **Method 2**, in particular, allowed access to a large number of resorcinol derivatives, with significant improvements over the previously employed approach. The scope of the reaction has been extended and the new purification method developed, allowed access to the products without requiring chromatography, thus permitting large scale reactions. Application and study of **Method 2** provided better understanding of the limitation of the reaction as a consequence of the fragmentations described.

Study of **Method 2** also led to a novel polycyclic structure, **166**, previously unreported. It is an interesting spinner like structure, which can be interconverted between the open and closed conformation. However, similar structures could not be identified in the literature and potential biological activities cannot be suggested.

Three families of novel tetramers have been synthesised and characterised. These flexible structures are open to further modifications and, thanks to their well organised geometries, are also interesting as dendrimer cores, as discussed in **Chapter 4**.

Methods for further halogenation and dehalogenation of tetramers have been described, to provide access to additional analogues for SAR. In total, 40 structures have been added to those previously available, thus extending considerably the complexity of the accessible SAR. The library will be evaluated for antimicrobial and antioxidant activities with the compounds presented in **Chapter 3**.

2.8 Experimental

2.8.1 General

All reagents and solvents for synthesis were commercial and used without further purification. NMR spectra were recorded at 293 K, unless otherwise stated, using a 400 MHz Spectrometer. Shifts are calibrated relative to deuterated solvent residual peaks. Infrared spectra were recorded using an FT-IR spectrometer with ATR attachment. MS were run on an LTQ orbitrap XL and were recorded by the EPSRC Mass Spectrometry National facility. Thin-layer chromatography (TLC) was carried out on aluminium sheets coated with silica gel 60 F254 (Merck). TLC plates were inspected by UV light ($\lambda = 254$ nm). Silica gel column chromatography was performed with silica gel Si 60 (40–63 μm).

2.8.2 Crystal structure analyses

Crystal data and results from structure refinement for the four compounds are collated in **Table 4**. Analyses were performed by Dr David Hughes.

A crystal of each compound was mounted in oil on a glass fibre and fixed in the cold nitrogen stream on an Oxford Diffraction Xcalibur-3/Sapphire3-CCD diffractometer, equipped with Mo-K α radiation and graphite monochromator. Intensity data were measured by thin-slice ω - and ϕ -scans.

Data were processed using the CrysAlisPro-CCD and –RED⁸⁹ programs. The structures were determined by the direct methods routines in the SHELXS program⁹⁰ and refined by full-matrix least-squares methods, on F²'s, in SHELXL.⁹⁰

The non-hydrogen atoms of the principal molecule in each structure were refined with anisotropic thermal parameters. There are solvent molecules (ether and/or methanol) in all the crystals; in some cases, **163** and **166**, these are fully ordered but, in **164** and **165**, there are disordered with varying degrees of resolution; except for those of low site

occupancy (which were refined isotropically), the non-hydrogen atoms were refined anisotropically. Generally, the phenolic and hydroxyl hydrogen atoms were identified in difference maps and were refined freely; all other hydrogen atoms were added in idealised positions and set to ride on the parent carbon atoms. In compound **163**, however, all the hydrogen atoms were located in difference maps and refined freely.

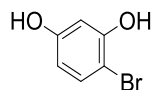
Scattering factors for neutral atoms were taken from reference⁹¹. Computer programs used in this analysis have been noted above, and were run through WinGX⁹² on a Dell Optiplex GX620 PC at the University of East Anglia.

Compound	163	164	165	166
Elemental formula	C ₃₂ H ₂₂ Cl ₄ O ₈ , 6(C ₄ H ₁₀ O)	C ₃₂ H ₂₂ Cl ₄ O ₈ , <i>ca</i> 7.5(C ₄ H ₄ O)	C ₃₂ H ₂₂ Cl ₄ O ₈ , <i>ca</i> 2(C ₄ H ₄ O), <i>ca</i> 5(C ₄ H ₁₀ O)	C ₂₀ H ₁₂ Cl ₂ O ₄ , C ₄ H ₁₀ O
Formula weight	1121.02	916.61	1111.0	461.32
Crystal system, space group	Monoclinic, I2/a	Triclinic, P-1	Triclinic, P-1	Monoclinic, P2 ₁ /n
Unit cell dimensions				
a (Å)	19.5798(5) Å	11.5190(3)	13.6713(5)	12.3214(6)
b (Å)	10.5855(2) Å	12.8094(5)	13.6859(4)	11.6802(5)
c (Å)	30.2255(8) Å	15.5844(4)	15.8507(5)	15.2837(6)
α (°)	90	79.044(3)	87.748(3)	90
β (°)	100.449(2)	77.462(2)	71.565(3)	107.433(4)
γ (°)	90 °	71.732(3)	84.007(3)	90
Volume (Å ³)	6160.7(3)	2112.99(11)	2798.10(16)	2098.54(16)
Z, Calculated density (Mg/m ³)	4, 1.209	2, 1.441	2, 1.319	4, 1.460
F(000)	2392	962	1184	960
Absorption coefficient (mm ⁻¹)	0.251	0.350	0.277	0.345 mm
Crystal colour, shape	pale brown block	colourless prism	pale yellow prism	colourless plate
Crystal size (mm)	0.36 x 0.24 x 0.18	0.40 x 0.12 x 0.10	0.32 x 0.13 x 0.12	0.12 x 0.10 x 0.05
Theta range for data collection (°)	3.03 to 27.50	2.99 to 22.49	3.09 to 22.50	3.07 to 25.00
Completeness to theta-max (%)	99.8	99.2	99.7	99.8
Max. and min. transmission	1.0 and 0.918	1.0 and 0.935	1.0 and 0.883	1.0 and 0.914
Reflections collected	50395	20695	30403	29087
No. of unique reflections, R(int)	7083, 0.040	5493, 0.054	7299, 0.060	3688, 0.071
No. of 'observed' reflections (I > 2σ _I)	5801	3401	5321	2842
Data / restraints / parameters	7083 / 0 / 498	5493 / 0 / 603	7299 / 0 / 768	3688 / 0 / 288
Goodness-of-fit on F ² , S	1.027	1.041	1.046	1.028
Final R indices ('observed' data)	R ₁ = 0.038, wR ₂ = 0.093	R ₁ = 0.074, wR ₂ = 0.191	R ₁ = 0.067, wR ₂ = 0.156	R ₁ = 0.038, wR ₂ = 0.078
Final R indices (all data)	R ₁ = 0.051, wR ₂ = 0.099	R ₁ = 0.138, wR ₂ = 0.240	R ₁ = 0.095, wR ₂ = 0.172	R ₁ = 0.058, wR ₂ = 0.083
Largest diff. peak and hole (e.Å ⁻³)	0.32 and -0.24	1.11 and -0.37	0.40 and -0.39	0.24 and -0.23

Table 4. Crystal data and structure refinement details for the four compounds **163**, **164**, **165** and **166**.

2.8.3 Synthesis

Compound 116^{74,75}



Prepared according the procedure by Sandin,⁷⁴ with minor modifications.

A stirring mixture of 2,4-dihydroxybenzoic acid (20 g, 85.83 mmol) in 160 mL of acetic acid was heated at 40 °C until complete dissolution of the solid. The solution was cooled to 30 °C and a solution of bromine (6.4 mL, 124.9 mmol) in 60 mL of acetic acid was added dropwise. The reaction was allowed to stir for one hour and then poured in 1.5 L of distilled water. After one night at 4 °C, the crystalline product (**117**) was collected by Büchner filtration. The crude **117** was suspended in distilled water and refluxed for 36 hours. The solution was cooled at room temperature and extracted with diethyl ether (3 x 300 mL). The organic layers were collected, dried over magnesium sulfate and evaporated under reduced pressure. The crude material was then purified by flash chromatography (30:1, DCM:MeOH) to give **116** as a white solid.

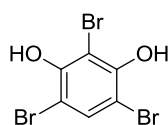
43% yield.

MP: 103-104 °C

¹H NMR (400 MHz, DMSO) δ 9.97 (s, 1H), 9.45 (s, 1H), 7.19 (d, J = 8.6 Hz, 1H), 6.43 (d, J = 2.7 Hz, 1H), 6.18 (dd, J = 8.6, 2.7 Hz, 1H).

¹³C NMR (101 MHz, DMSO) δ 157.78, 154.56, 132.67, 108.10, 103.57, 98.09.

Compound 120⁷⁵

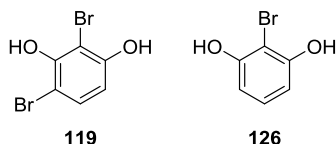


A solution of bromine (30 mL, 0.58 mol) in 200 mL of DCM was added dropwise to a solution of resorcinol (20 g, 0.18 mol) in DCM (200 mL) over 4 hours. The red solution was allowed to stir at 40 °C for 64 hours. Excess bromine was removed by bubbling air

through the mixture. The solvent was evaporated and the crude material was used without any further purification for the synthesis of **119** and **126**.

^1H NMR (400 MHz, DMSO) δ 9.98 (s, 2H, ArOH), 7.69 (s, 1H, ArH).

Compounds **119**⁷⁵ and **126**⁷⁵



A solution of sodium sulfite (45.79 g, 0.36 mol) in 210 mL of water/MeOH (2:1) was added to a allowed to stir mixture of **120** in 240 mL of the same solvent. The reaction was allowed to stir until **120** was completely consumed (TLC with DCM, I₂ staining). The yellow solution was extracted with diethyl ether; the organic layers were collected, dried over anhydrous magnesium sulfate and evaporated. Upon flash chromatography with DCM, **119** and **126** were isolated as white crystalline solids.

Compound **119**:

54% yield over two steps.

MP: 99-100 °C (lit. 92.8-93.7 °C)⁹³

^1H -NMR (400 MHz, DMSO) δ 10.34 (s, 1H, ArOH), 9.55 (s, 1H, ArOH), 7.29 (d, J=8.6, 1H, ArH), 6.46 (d, J=8.6, 1H, ArH).

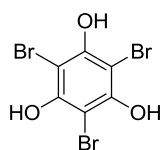
^{13}C -NMR (101 MHz, DMSO) δ 154.92, 151.45, 130.97, 108.73, 100.58, 100.04.

Compound **126**:

10% yield over two steps.

^1H -NMR (400 MHz, DMSO) δ 9.92 (s, 2H, ArOH), 6.92 (t, J=7.9, 1H, ArH), 6.40 (d, J=7.9, 2H, ArH).

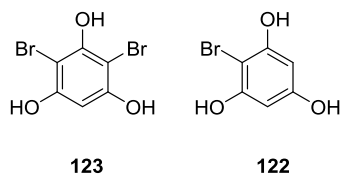
Compound **124**⁷⁵



Over one hour, a solution of bromine (6.1 mL, 0.12 mol) in DCM (20 mL) was added dropwise to a suspension of phloroglucinol (5 g, 0.04 mol) in 130 mL. Then the mixture

was allowed to stir at room temperature for one hour. Upon evaporation under reduced pressure of the solvent a solid product was obtained. The crude was used without further purification for the synthesis of **123** and **122**.

Compounds **123** and **122**⁷⁵



Crude **124** was suspended in a water/methanol solution (38 ml: 76 mL) and allowed to stir for 15 minutes. A solution of sodium sulphite (5 g, 0.04 mol) and sodium hydrogencarbonate (6.66 g, 0.08 mol) in water (112 mL) was added. The mixture was allowed to stir for 3 hours and then quenched with 60 mL of HCl 1.2 M. The solid was collected and washed with water to give clean **124**, which could be recycled. The water was extracted with diethyl ether, and then with ethyl acetate. The organic layers were combined, dried over anhydrous magnesium sulfate and evaporated. The crude product was purified by flash chromatography using 60:1 DCM/MeOH to elute **123** and then 55:1 DCM/MeOH for **122**.

Compound 123: 11.8% yield over two steps.

MP: 165-167 °C

¹H-NMR (400 MHz, DMSO) δ 10.08 (s, 2H, ArOH), 9.21 (s, 1H, ArOH), 6.27 (s, 1H, ArH).

¹³C NMR (101 MHz, DMSO) δ 154.10, 151.87, 95.44, 89.59.

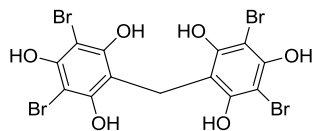
IR (ν_{max} , cm⁻¹): 3445, 3387, 1591, 1481, 1435, 1250, 1210, 1158, 1037, 806.

Compound 122: 14.2% yield over two steps.

¹H-NMR (400 MHz, DMSO) δ 9.69 (s, 2H, ArOH), 9.20 (s, 1H, ArOH), 5.92 (s, 2H, ArH).

¹³C NMR (101 MHz, DMSO) δ 157.32, 155.41, 94.74, 87.46.

Compound 134



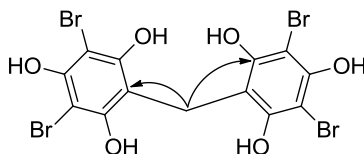
1.5 mL of HCl 37% (aq) were added to a suspension of **123** (0.5 g, 1.44 mmol) and formaldehyde (37% in water, 0.68 mmol) in 2 mL of ethanol. The mixture was allowed to stir for three hours at 70 °C. Subsequently, the reaction was neutralised with NaHCO₃ and extracted with ethyl acetate. The organic layers were collected, dried over sodium sulphate anhydrous and evaporated. The crude material was purified *via* flash chromatography (DCM/MeOH 8:2) to give **134**.

3.7% yield.

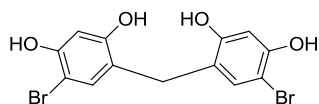
¹H-NMR (400 MHz, DMSO) δ 9.85 (b, 4H, ArOH), 9.46 (b, 2H, ArOH), 3.87 (s, 2H, Ar₂CH₂).

¹³C-NMR (101 MHz, DMSO) δ 151.08, 150.14, 108.90, 93.08, 20.8 (Ar₂CH₂).

HMBC correlations:



Compound 135



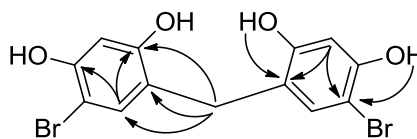
4 mL of HCl 37% (aq) were added to a solution of **116** (1 g, 5.29 mmol) and formaldehyde (37% in water, 2.51 mmol) in 8 mL of ethanol. The reaction was allowed to stir for 3.5 hours at room temperature. Subsequently, the yellow solution was neutralised with NaHCO₃ and extracted with ethyl acetate. The organic layers were collected, dried over sodium sulphate anhydrous and evaporated. The crude was purified *via* flash chromatography (DCM/MeOH 20:1) to give **135** as an off white solid.

2.6% yield.

¹H-NMR (400 MHz, DMSO) δ 9.78 (s, 2H, ArOH), 9.47 (s, 2H, ArOH), 6.93 (s, 2H, ArH), 6.50 (s, 2H, ArH), 3.52 (s, 2H, Ar₂CH₂).

^{13}C -NMR (101 MHz, DMSO) δ 155.01, 152.46, 132.80, 119.92, 103.32, 97.65, 27.54 (Ar_2CH_2).

HMBC correlations:

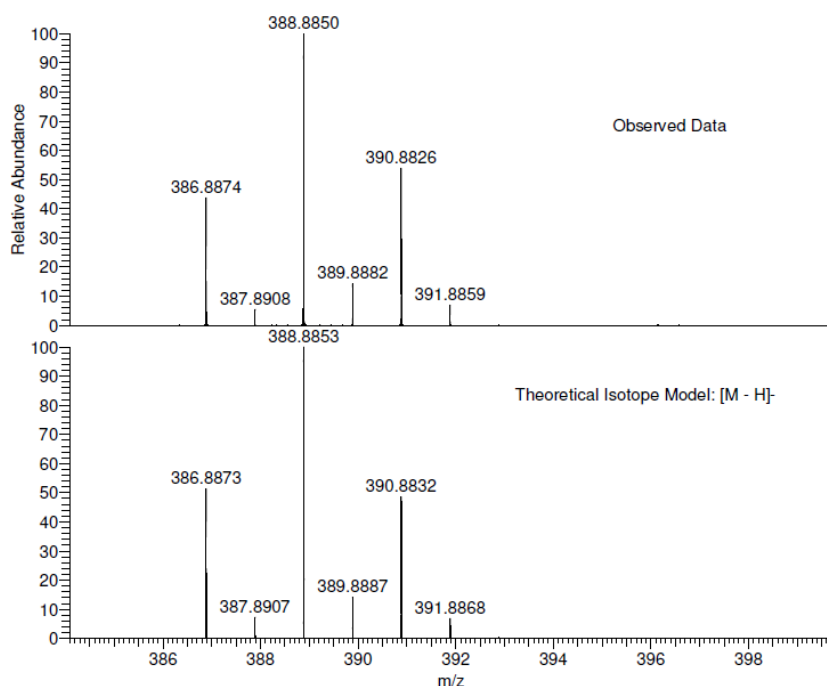


IR (ν_{max} , cm^{-1}): 3491, 3364, 1614, 1597, 1585, 1504, 1484, 1422, 1357, 1317, 1296, 1266, 1199, 1169, 1136, 1115, 1007, 922, 894, 878, 827, 804.

MC-22 MW=390?
C₁₃H₁₀Br₂O₄
(MeOH)/MeOH

EPSRC National Facility Swansea
LTQ Orbitrap XL

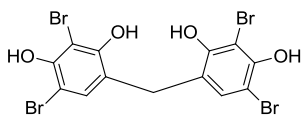
Marco Cominetti
04/09/2013 10:19:43



NL:
3.05E7
UEAMAT202-OJ-HNESN#61-
65 RT: 1.51-1.73 AV: 4 T:
FTMS - p NSI Full ms
[200.00-4000.00]

NL:
1.01E4
C₁₃H₉Br₂O₄:
C₁₃H₉Br₂O₄
p (gss, s/p:40) Chrg -1
R: 100000 Res .Pwr . @FWHM

Compound 136²³



3 mL of HCl 37% (aq) were added to a solution of **119** (1 g, 3.73 mmol) and formaldehyde (37% in water, 1.77 mmol) in 4 mL of ethanol. The reaction was allowed to stir for 16 hours at 70 °C. Subsequently, the solution was neutralised with NaHCO_3 and extracted with ethyl acetate. The organic layers were collected, dried over anhydrous magnesium sulfate and evaporated. The crude was purified *via* flash chromatography (DCM/ethanol 100:1) to **136** as a light pink solid.

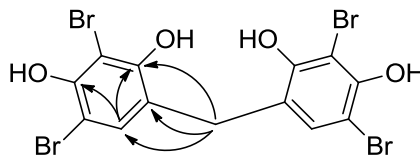
19.5% yield.

MP: 215 °C decomposition

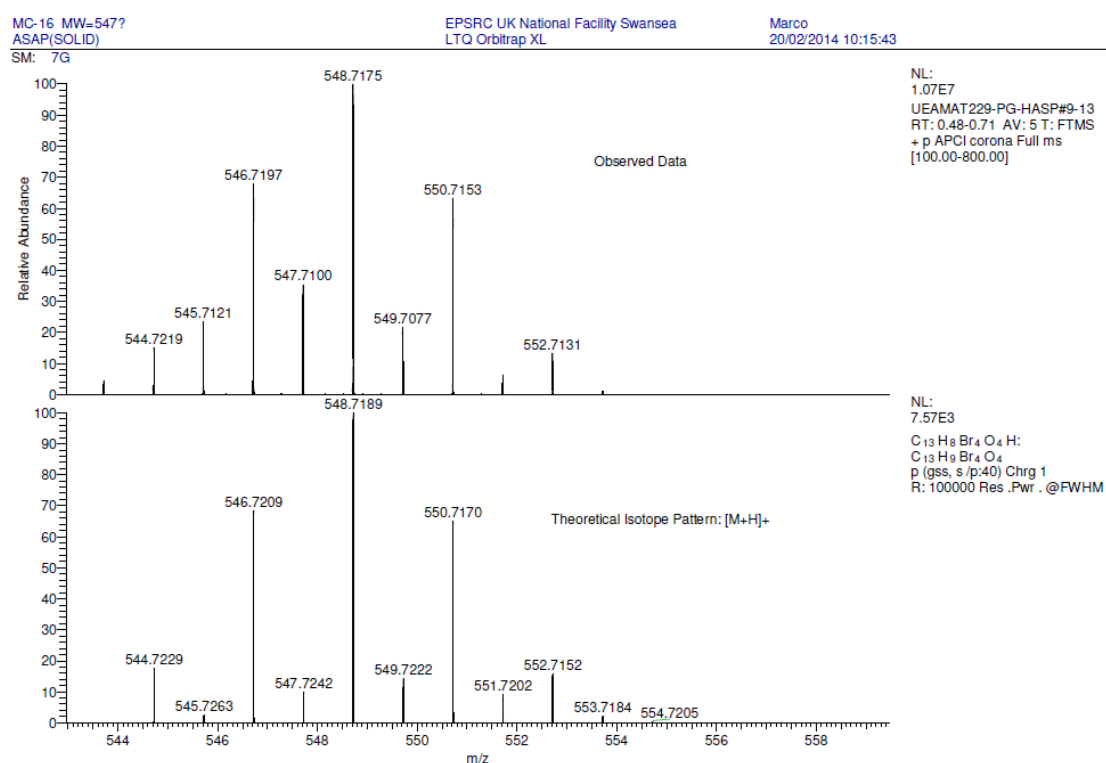
^1H -NMR (400 MHz, DMSO) δ 9.52 (s, 2H, ArOH), 9.27 (s, 2H, ArOH), 7.06 (s, 2H, ArH), 3.80 (s, 2H, Ar₂CH₂).

^{13}C -NMR (101 MHz, DMSO) δ 151.96, 149.60, 131.29, 121.74, 102.89, 100.89, 29.59 (Ar₂CH₂).

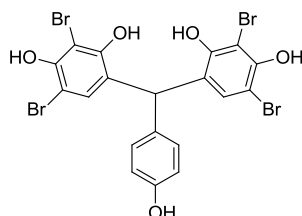
HMBC correlations:



IR (ν_{max} , cm^{-1}): 3474, 3353, 1594, 1569, 1467, 1455, 1428, 1349, 1310, 1250, 1231, 1204, 1169, 1141, 1033, 922, 894, 871, 834.



Compound 131



10 mL of HCl 37% (aq) was added to a solution of **119** (1.48 g, 5.52 mmol) and 4-hydroxybenzaldehyde (0.22 g, 1.8 mmol) in 20 mL of ethanol. The reaction was allowed to stir for 3 hours at 70 °C. Subsequently, the solution was neutralised with NaHCO₃ and extracted with ethyl acetate. The organic layers were collected, dried over

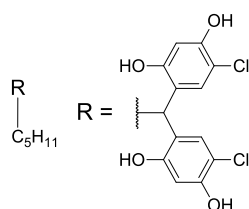
anhydrous magnesium sulfate and evaporated. The crude was purified *via* flash chromatography (DCM/MeOH gradient: 50:1→20:1) to give a red solid of **131**.

Yield < 1%.

^1H -NMR (400 MHz, DMSO) δ 9.59 (s, 2H, ArOH), 9.30 (s, 1H, ArOH), 9.13 (s, 2H, ArOH), 6.78 (d, $J=8.6$, 2H, ArH), 6.70 (d, $J=8.6$, 2H, ArH), 6.59 (s, 2H, ArH), 5.87 (s, 1H, Ar₃CH).

^{13}C -NMR (101 MHz, DMSO) δ 155.78, 151.72, 149.59, 131.95, 130.58, 129.80, 126.04, 115.17, 103.18, 100.44, 48.57 (Ar₃CH).

Compound 140



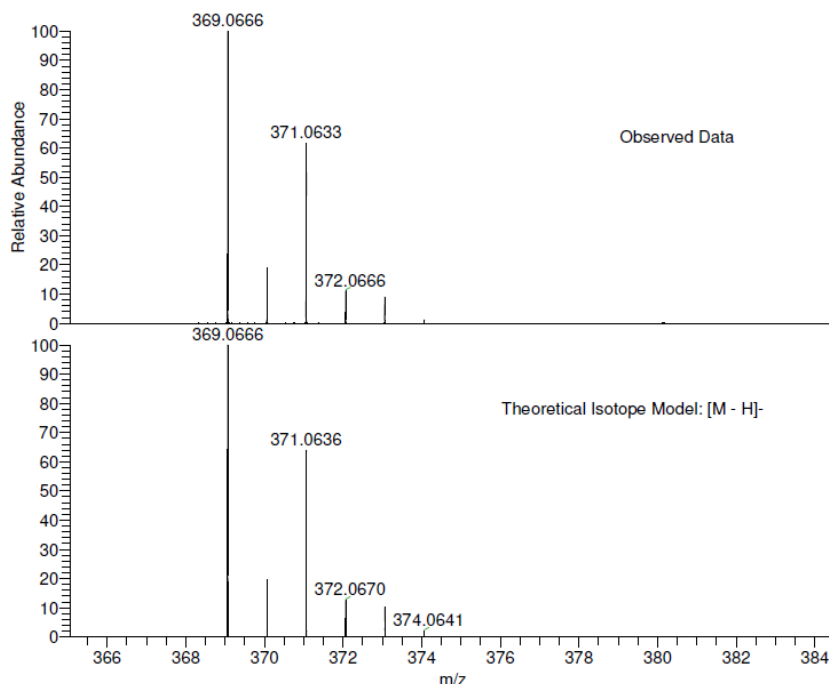
0.24 mL of methanesulfonic acid was added to a pre-cooled (0 °C) mixture of hexanal (250 mg, 2.5 mmol) and 4-chlororesorcinol (902.1 mg, 6.24 mmol) in 3 mL of Et₂O/DCM (1/1, v/v). The reaction vessel was sealed and the reaction allowed to stir for 5 h. The resulting mixture was diluted with diethyl ether, poured into distilled water and allowed to stir vigorously until a suspension was obtained. The product was collected by Büchner filtration, washed with abundant distilled water and dried in a desiccator to give a light orange powder.

Yield: 40% (calculated from NMR to account for solvent of crystallisation)

MP: 186-188 °C

^1H -NMR (400 MHz, DMSO) δ 9.66 (s, 2H), 9.27 (s, 2H), 6.86 (s, 2H), 6.44 (s, 2H), 4.26 (t, $J = 7.8$ Hz, 1H), 1.77 (q, $J = 7.8$ Hz, 2H), 1.28 – 1.12 (m, 6H), 0.82 (t, $J = 7.0$ Hz, 3H).

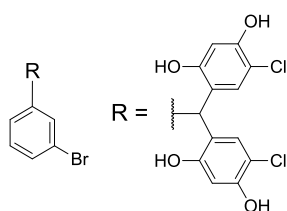
^{13}C -NMR (101 MHz, DMSO) δ 154.79, 151.52, 128.85, 123.86, 109.33, 104.10, 36.01, 33.82, 31.64, 27.71, 22.46, 14.40.



NL:
7.52E7
UEAMAT201-OJ-HNESN#1-5
RT: 0.20-0.43 AV: 4 T: FTMS -
p NSI Full ms [120.00-2000.00]

NL:
1.10E4
C₁₈ H₁₉ Cl₂ O₄:
C₁₈ H₁₉ Cl₂ O₄
p (gss, s/p:40) Chrg -1
R: 100000 Res .Pwr . @FWHM

Compound 141



0.64 mL of methanesulfonic acid was added to a pre-cooled (0 °C) mixture of 3-bromobenzaldehyde (0.315 mL, 2.7 mmol) and 4-chlororesorcinol (976.65 mg, 6.76 mmol) in 8 mL of Et₂O/DCM (1/1, v/v). The reaction vessel was sealed and the reaction allowed to stir for 5 h. The resulting mixture was diluted with diethyl ether, poured into distilled water and allowed to stir vigorously until a suspension was obtained. The product was collected by Büchner filtration, washed with abundant distilled water and dried in a desiccator to give an orange powder.

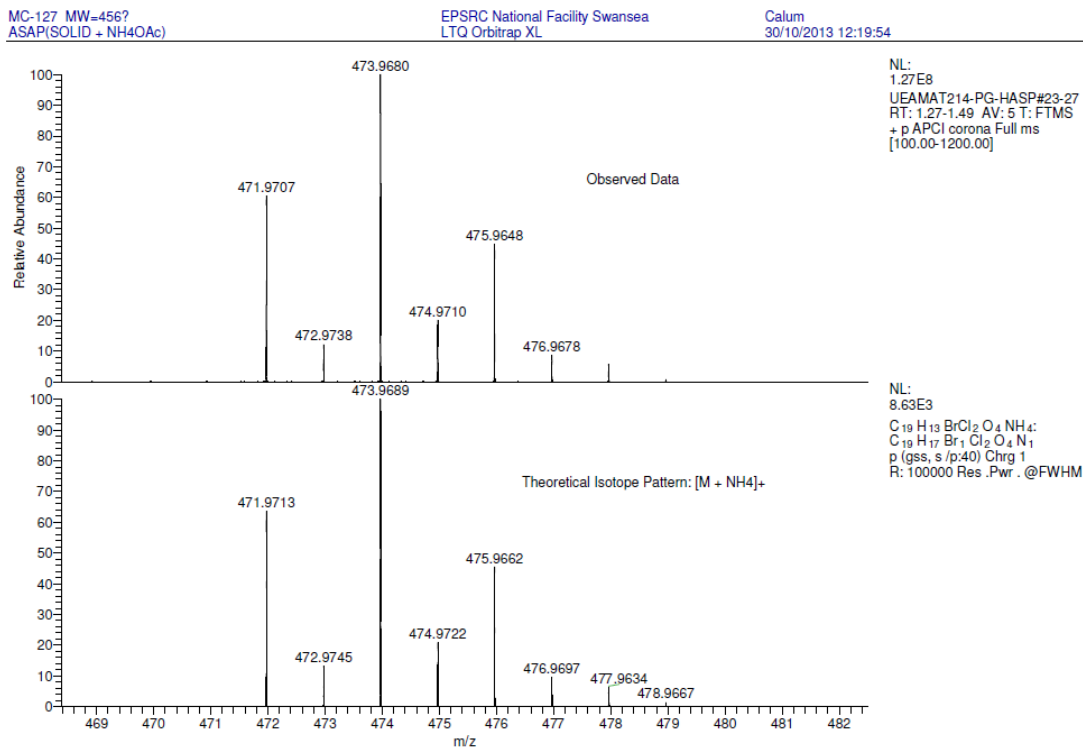
Yield: 90.6% (calculated from NMR to account for solvent of crystallisation)

MP: 230-232 °C

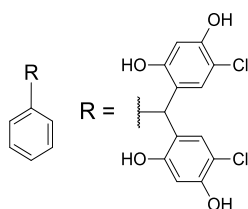
¹H-NMR (400 MHz, DMSO) δ 9.89 (s, 2H), 9.51 (s, 2H), 7.39 (d, *J* = 7.8 Hz, 1H), 7.24 (t, *J* = 7.8 Hz, 1H), 7.07 (s, 1H), 6.97 (d, *J* = 7.8 Hz, 1H), 6.52 (s, 2H), 6.41 (s, 2H), 5.69 (s, 1H).

^{13}C -NMR (101 MHz, DMSO) δ 154.68, 152.45, 147.26, 131.53, 130.79, 129.96, 129.25, 128.31, 122.06, 121.95, 109.32, 104.23, 42.20.

IR (ν_{max} , cm^{-1}): 3439, 1613, 1592, 1504, 1423, 1335, 1234, 1195, 1169, 1118, 1072, 1026, 1009, 899, 834.



Compound 142



0.24 mL of methanesulfonic acid was added to a pre-cooled (0 °C) mixture of benzaldehyde (250 mg, 2.36 mmol) and 4-chlororesorcinol (851.4 mg, 5.89 mmol) in 3 mL of Et₂O/DCM (1/1, v/v). The reaction vessel was sealed and the reaction allowed to stir for 5.5 h. The resulting mixture was diluted with diethyl ether, poured into distilled water and allowed to stir vigorously until a suspension was obtained. The product was collected by Büchner filtration, washed with abundant distilled water and dried in a desiccator to give an orange powder.

Yield: 87.2% (calculated from NMR to account for solvent of crystallisation)

MP: 105-108 °C

^1H -NMR (400 MHz, DMSO) δ 9.81 (s, 2H), 9.41 (s, 2H), 7.27 (t, $J = 7.3$ Hz, 2H), 7.17 (t, $J = 7.3$ Hz, 1H), 6.96 (d, $J = 7.3$ Hz, 2H), 6.50 (s, 2H), 6.39 (s, 2H), 5.71 (s, 1H).

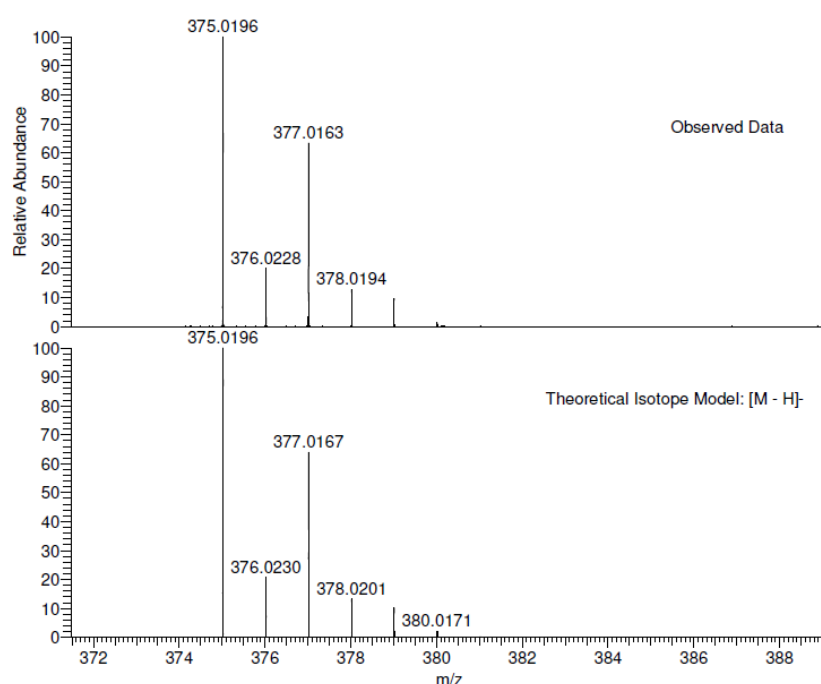
^{13}C -NMR (101 MHz, DMSO) δ 154.66, 152.15, 144.18, 129.98, 129.19, 128.56, 126.26, 123.01, 109.14, 104.16, 42.25.

IR (ν_{max} , cm^{-1}): 3584, 3416, 3267, 1617, 1601, 1523, 1493, 1425, 1377, 1338, 1303, 1271, 1248, 1192, 1134, 1073, 1028, 917, 903, 869, 839, 825.

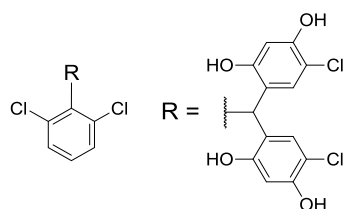
MC-120 MW=377?
C₁₉H₁₄Cl₂O₄
(MeOH)/MeOH

EPSRC National Facility Swansea
LTQ Orbitrap XL

Marco Cominetti
04/09/2013 10:22:35



Compound 143



1.2 mL of methanesulfonic acid was added to a pre-cooled (0 °C) mixture of 2,6-dichlorobenzaldehyde (500 mg, 2.86 mmol) and 4-chlororesorcinol (1.0325 g, 7.14 mmol) in 15 ml of Et₂O/DCM (1/1, v/v). The reaction vessel was sealed and the reaction allowed to stir for 6 h. The resulting mixture was diluted with diethyl ether, poured into distilled water and allowed to stir vigorously until a suspension was obtained. The

product was collected by Büchner filtration, washed with abundant distilled water and dried in a desiccator to give a pale orange powder.

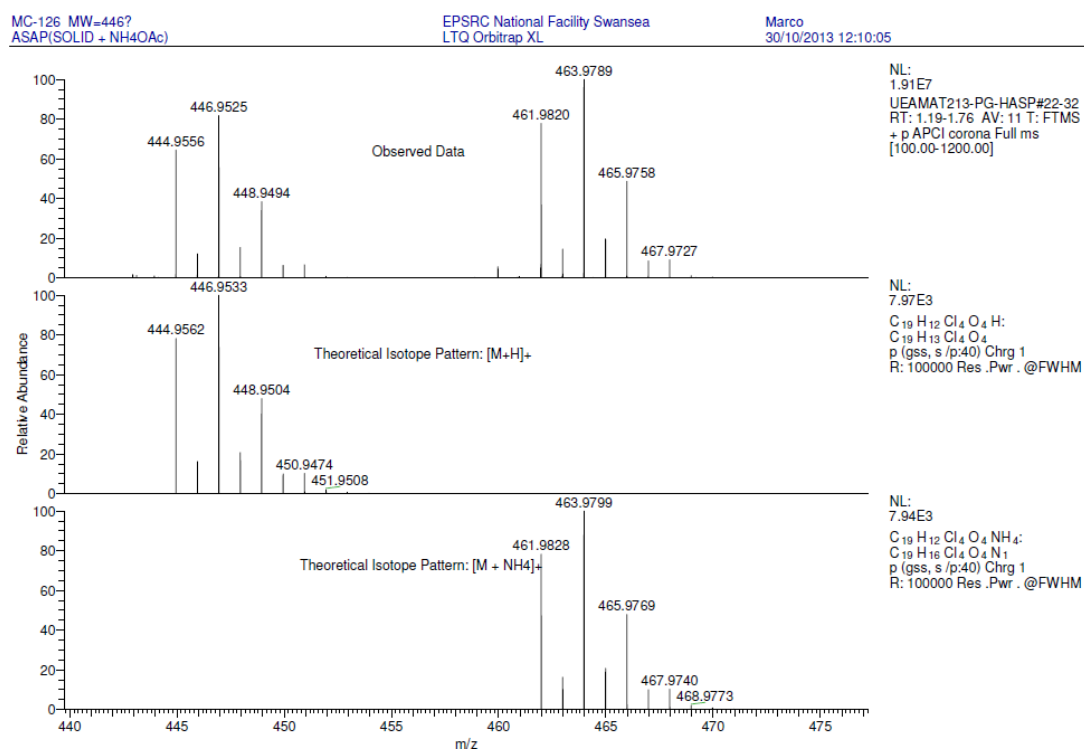
Yield: 83% (calculated from NMR to account for solvent of crystallisation)

MP: 238-240 °C

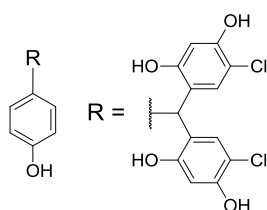
^1H -NMR (400 MHz, DMSO) δ 9.85 (s, 2H), 9.44 (s, 2H), 7.39 (d, J = 8.0 Hz, 2H), 7.25 (t, J = 8.0 Hz, 1H), 6.51 (s, 2H), 6.48 (s, 2H), 6.18 (s, 1H).

^{13}C -NMR (101 MHz, DMSO) δ 154.88, 152.48, 138.93, 135.73, 130.34, 129.89, 128.93, 119.25, 109.27, 103.82, 41.48.

IR (ν_{max} , cm^{-1}): 3642, 3520, 3498, 3428, 1612, 1599, 1555, 1502, 1428, 1329, 1261, 1229, 1206, 1169, 1123, 1083, 1026, 906, 871, 846, 827.



Compound 144



0.24 mL of methanesulfonic acid was added to a pre-cooled (0 °C) mixture of 4-hydroxybenzaldehyde (250 mg, 2.05 mmol) and 4-chlororesorcinol (739.8 g, 5.12 mmol) in 3 mL of Et₂O/DCM (1/1, v/v). The reaction vessel was sealed and the reaction allowed to stir for 5 h. The resulting mixture was diluted with diethyl ether, poured into distilled water and allowed to stir vigorously until a suspension was obtained. The product was collected by Büchner filtration, washed with abundant distilled water and DCM. The product was recrystallised from DCM/MeOH to give a light orange solid.

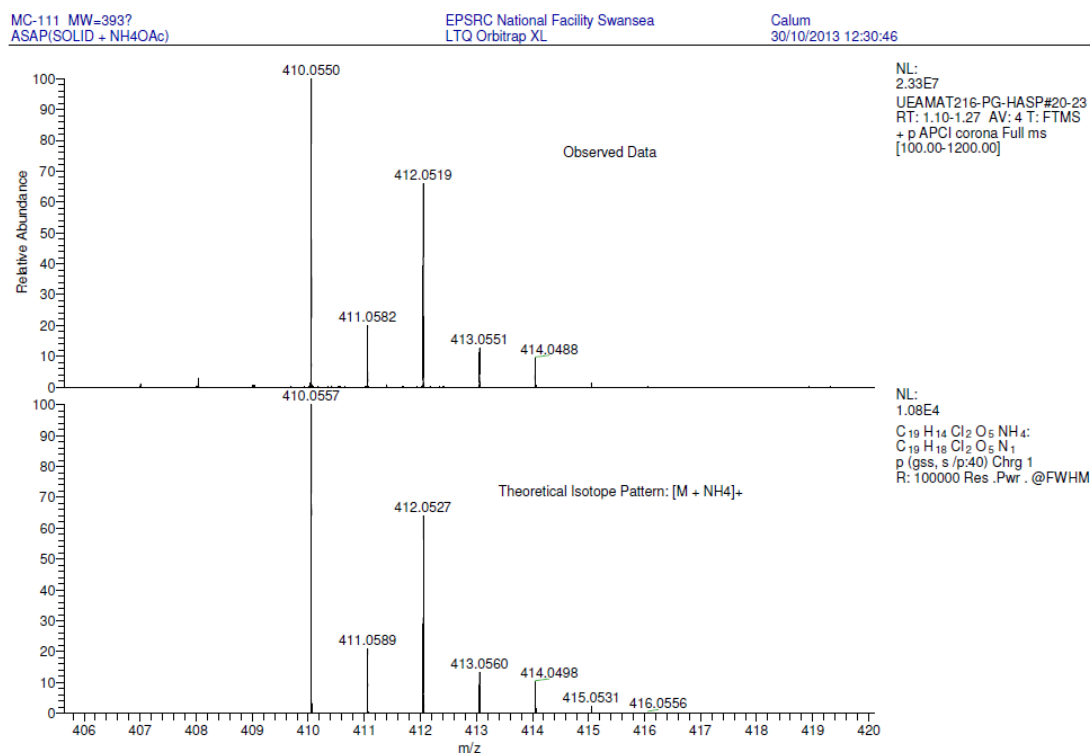
Yield: 20.5% (calculated from NMR to account for solvent of crystallisation)

MP: 226-228 °C

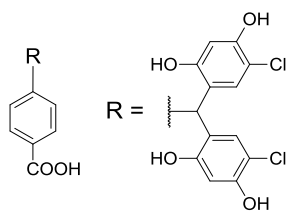
¹H-NMR (400 MHz, DMSO) δ 9.76 (s, 2H), 9.34 (s, 2H), 9.17 (s, 1H), 6.74 (d, *J* = 8.5 Hz, 2H), 6.66 (d, *J* = 8.5 Hz, 2H), 6.48 (s, 2H), 6.39 (s, 2H), 5.60 (s, 1H).

¹³C-NMR (101 MHz, DMSO) δ 155.76, 154.58, 151.96, 134.13, 130.07, 129.89, 123.72, 115.34, 109.04, 104.13, 41.36.

IR (ν_{max}, cm⁻¹): 3307, 1613, 1600, 1511, 1487, 1422, 1335, 1239, 1209, 1189, 1170, 1122, 1026, 902, 882, 870, 848, 830, 801.



Compound 145



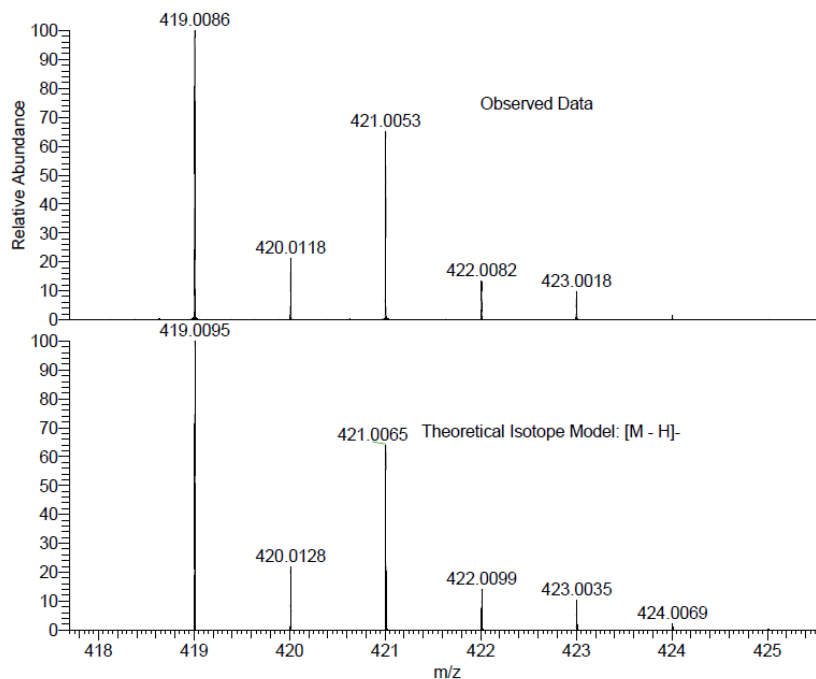
1.2 mL of methanesulfonic acid was added to a pre-cooled (0 °C) mixture of 4-formylbenzoic acid (500 mg, 3.33 mmol) and 4-chlororesorcinol (1.2036 g, 8.33 mmol) in 15 ml of Et₂O/DCM (1/1, v/v). The reaction vessel was sealed and the reaction allowed to stir for 6 h. The resulting mixture was diluted with diethyl ether, poured into distilled water and allowed to stir vigorously until a suspension was obtained. The product was collected by Büchner filtration, washed with abundant distilled water and dried in a desiccator.

Yield: 75% (calculated from NMR to account for solvent of crystallisation)

¹H-NMR (400 MHz, DMSO) δ 12.79 (s, 1H), 9.87 (s, 2H), 9.49 (s, 2H), 7.85 (d, *J* = 8.3 Hz, 2H), 7.08 (d, *J* = 8.3 Hz, 2H), 6.52 (s, 2H), 6.41 (s, 2H), 5.76 (s, 1H).

¹³C-NMR (101 MHz, DMSO) δ 167.73, 154.72, 152.40, 149.67, 130.00, 129.72, 129.29, 128.88, 122.19, 109.31, 104.21, 42.45.

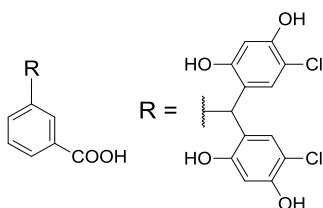
IR (ν_{max}, cm⁻¹): 3497, 3249, 1691, 1606, 1503, 1427, 1384, 1316, 1268, 1234, 1218, 1189, 1168, 1118, 1018, 899, 840.



NL:
2.78E7
UEAMAT215-OS-HNESN#15-
48 RT: 1.06-1.29 AV: 4 T:
FTMS - p NSI Full ms
[133.00-798.00]

NL:
1.07E4
C₂₀H₁₃Cl₂O₆:
C₂₀H₁₃Cl₂O₆:
p (gss, s /p:40) Chrg -1
R: 100000 Res .Pwr . @FWHM

Compound 146



0.24 mL of methanesulfonic acid was added to a pre-cooled (0 °C) mixture of 3-formylbenzoic acid (200 mg, 1.33 mmol) and 4-chlororesorcinol (481.4 mg, 3.33 mmol) in 3 ml of Et₂O/DCM (1/1, v/v). The reaction vessel was sealed and the reaction allowed to stir for 7 h. The resulting mixture was diluted with diethyl ether, poured into distilled water and allowed to stir vigorously until a suspension was obtained. The product was collected by Büchner filtration, washed with abundant distilled water and dried in a desiccator to give a light pink powder.

Yield: 18% (calculated from NMR to account for solvent of crystallisation)

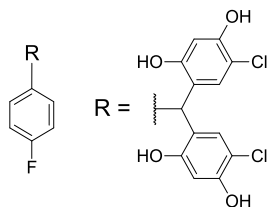
MP: 253-255 °C

¹H-NMR (400 MHz, DMSO) δ 12.91 (s, 1H), 9.88 (s, 2H), 9.49 (s, 2H), 7.77 (d, *J* = 7.7 Hz, 1H), 7.51 (s, 1H), 7.40 (t, *J* = 7.7 Hz, 1H), 7.23 (d, *J* = 7.7 Hz, 1H), 6.52 (s, 2H), 6.40 (s, 2H), 5.76 (s, 1H).

^{13}C -NMR (101 MHz, DMSO) δ 167.86, 154.71, 152.38, 144.82, 133.71, 130.96, 130.00, 129.67, 128.91, 127.41, 122.34, 109.29, 104.24, 42.25.

IR (ν_{max} , cm^{-1}): 3503, 1695, 1683, 1614, 1588, 1505, 1421, 1326, 1311, 1288, 1252, 1196, 1163, 1127, 1029, 1017, 931, 896, 884.

Compound 147



0.24 mL of methanesulfonic acid was added to a pre-cooled (0 °C) mixture of 4-fluorobenzaldehyde (200 mg, 1.61 mmol) and 4-chlororesorcinol (582.3 mg, 4.03 mmol) in 3 mL of Et₂O/DCM (1/1, v/v). The reaction vessel was sealed and the reaction allowed to stir for 7 h. The resulting mixture was diluted with diethyl ether, poured into distilled water and allowed to stir vigorously until a suspension was obtained. The product was collected by Büchner filtration, washed with abundant distilled water and dried in a desiccator to give a light yellow powder.

Yield: 61% (calculated from NMR to account for solvent of crystallisation)

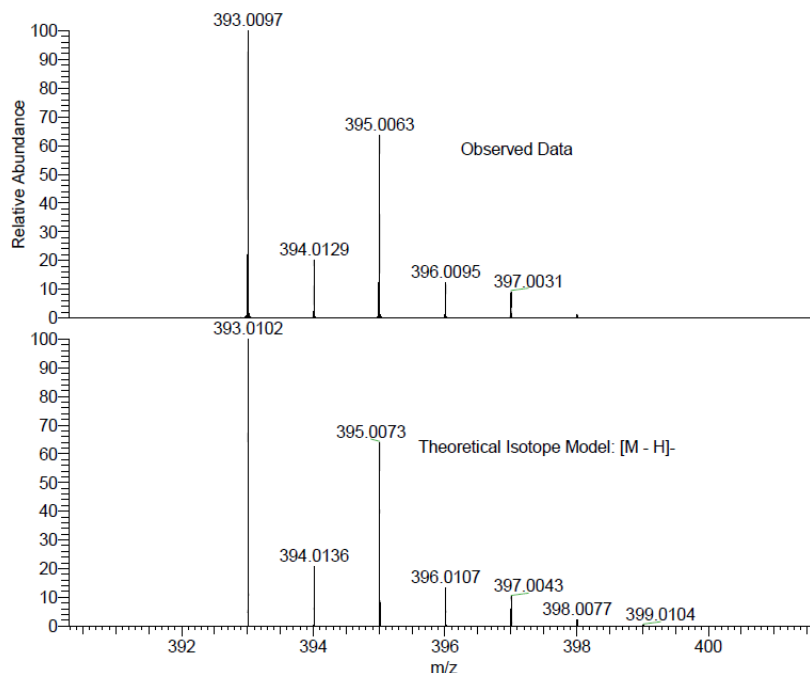
MP: 138-141 °C

^1H -NMR - F decoupled (400 MHz, DMSO) δ 9.83 (s, 2H), 9.43 (s, 2H), 7.08 (d, J = 8.8 Hz, 2H), 6.98 (d, J = 8.8 Hz, 2H), 6.51 (s, 2H), 6.40 (s, 2H), 5.70 (s, 1H).

^{13}C -NMR (101 MHz, DMSO) δ 160.92 (d, J = 241.6 Hz), 154.64, 152.27, 140.23, 130.83 (d, J = 8.0 Hz), 129.88, 122.83, 115.24 (d, J = 21.1 Hz), 109.23, 104.19, 41.62.

^{19}F -NMR (376 MHz, DMSO) δ -117.49 (tt, J = 8.9, 5.6 Hz).

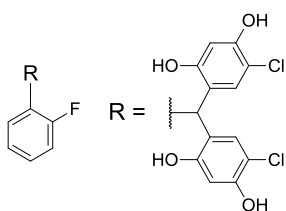
IR (ν_{max} , cm^{-1}): 3422, 3295, 1600, 1506, 1431, 1338, 1285, 1263, 1232, 1199, 1171, 1156, 1122, 1027, 894, 881.



NL:
5.14E7
UEAMAT242-OA-HNESN#2-18
RT: 0.01-0.45 AV: 16 T:
FTMS - p NSI Full ms
[140.00-1935.00]

NL:
1.09E4
C₁₉ H₁₂ Cl₂ FO₄:
C₁₉ H₁₂ Cl₂ F₁ O₄
p (gss, s/p:40) Chrg -1
R: 100000 Res .Pwr . @FWHM

Compound 148



0.24 mL of methanesulfonic acid was added to a pre-cooled (0 °C) mixture of 2-fluorobenzaldehyde (200 mg, 1.61 mmol) and 4-chlororesorcinol (582.3 mg, 4.03 mmol) in 3 ml of Et₂O/DCM (1/1, v/v). The reaction vessel was sealed and the reaction allowed to stir for 7 h. The resulting mixture was diluted with diethyl ether, poured into distilled water and allowed to stir vigorously until a suspension was obtained. The product was collected by Büchner filtration, washed with abundant distilled water and dried in a desiccator to give a white solid.

Yield: 85% (calculated from NMR to account for solvent of crystallisation)

MP: 200-203 °C

¹H-NMR - F decoupled (400 MHz, DMSO) δ 9.85 (s, 2H), 9.47 (s, 2H), 7.33 – 7.21 (m, 1H), 7.16 – 7.05 (m, 2H), 6.81 (dd, *J* = 7.6, 1.5 Hz, 1H), 6.52 (s, 2H), 6.38 (s, 2H), 5.93 (s, 1H).

^{13}C -NMR (101 MHz, DMSO) δ 160.48 (d, J = 244.7 Hz), 154.62, 152.4, 131.19 (d, J = 14.8 Hz), 130.37 (d, J = 4.2 Hz), 129.59, 128.45 (d, J = 8.2 Hz), 124.45 (d, J = 3.2 Hz), 121.50, 115.56 (d, J = 21.9 Hz), 109.22, 104.23, 35.38.

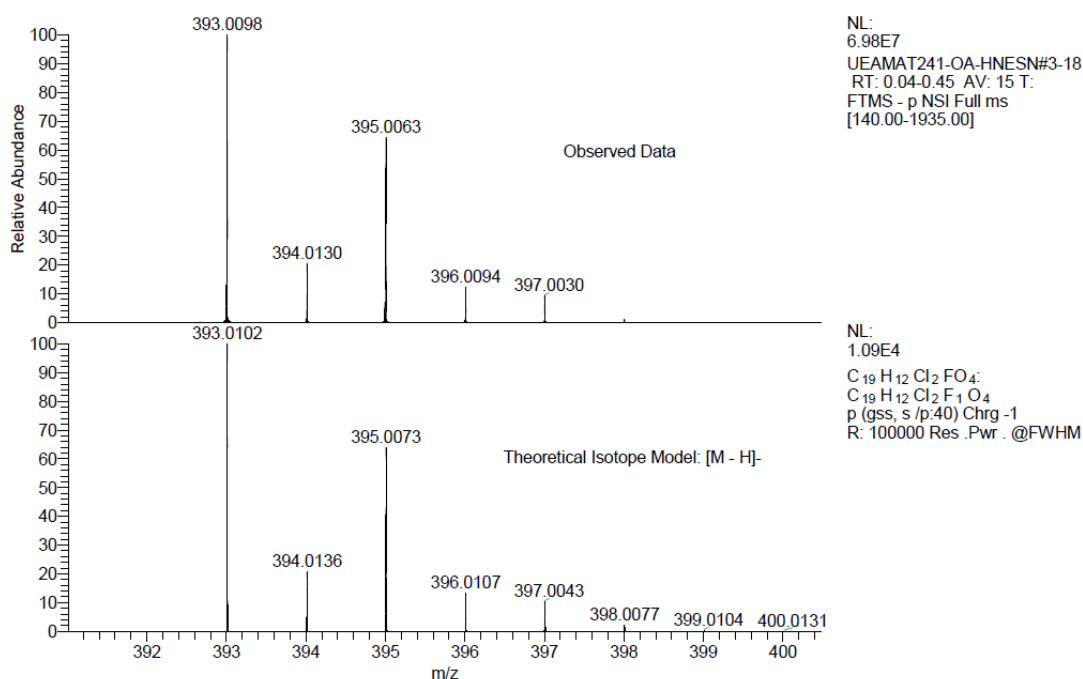
^{19}F NMR (376 MHz, DMSO) δ -117.06 (ddd, J = 10.4, 7.9, 5.5 Hz).

IR (ν_{max} , cm^{-1}): 3613, 3393, 3278, 1619, 1600, 1524, 1489, 1425, 1374, 1338, 1305, 1275, 1251, 1231, 1219, 1194, 1168, 1134, 1095, 1028, 904, 897.

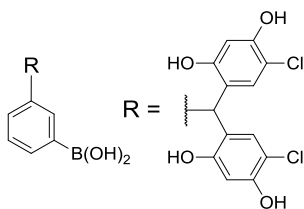
MC-175 MW=395?
C₁₉H₁₃Cl₂FO₄
(MeOH)/MeOH+DEA

EPSRC National Facility Swansea
LTQ Orbitrap XL

Marco Cominetti
19/12/2014 09:34:24 AM



Compound 149



0.24 mL of methanesulfonic acid was added to a pre-cooled (0 °C) mixture of 3-formylboronic acid (200 mg, 1.33 mmol) and 4-chlororesorcinol (482 mg, 3.33 mmol) in 3 mL of Et₂O/DCM (1/1, v/v). The reaction vessel was sealed and the reaction allowed to stir for 7 h. The resulting mixture was diluted with diethyl ether, poured into distilled water and allowed to stir vigorously until a suspension was obtained. The product was collected by Büchner filtration, washed with abundant distilled water and dried in a desiccator to give a white powder.

Yield: 76% (calculated from NMR to account for solvent of crystallisation)

MP: 400-405 °C

^1H -NMR (400 MHz, DMSO) δ 9.79 (s, 2H), 9.39 (s, 2H), 7.96 (s, 2H), 7.60 (d, J = 7.3 Hz, 1H), 7.47 (s, 1H), 7.23 (t, J = 7.5 Hz, 1H), 6.96 (d, J = 7.7 Hz, 1H), 6.50 (s, 2H), 6.41 (s, 2H), 5.72 (s, 1H).

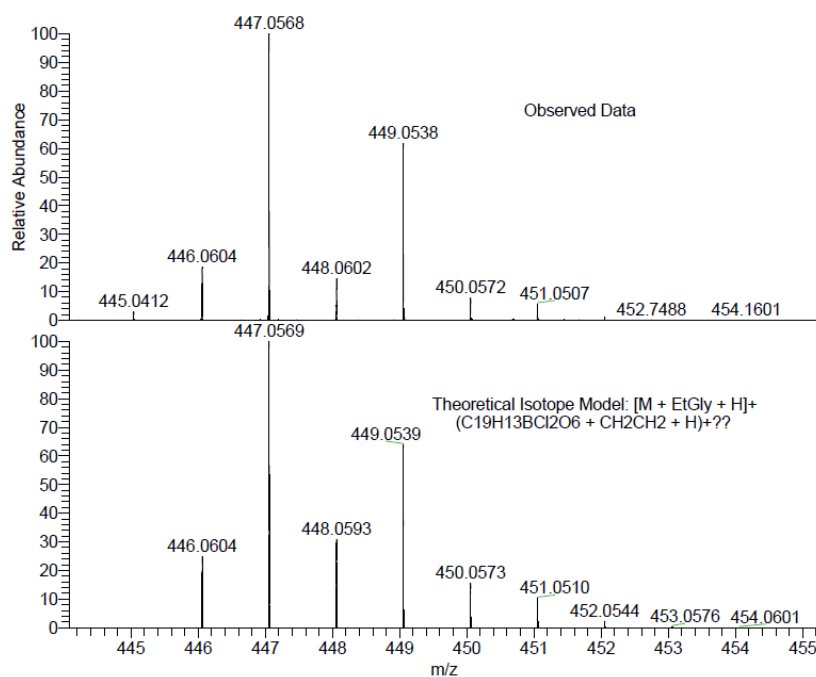
^{13}C -NMR (101 MHz, DMSO) δ 154.62, 152.06, 143.04, 135.26, 134.16, 132.12, 130.80, 130.10, 127.56, 123.20, 109.11, 104.14, 42.29.

IR (ν_{max} , cm^{-1}): 3561, 3509, 3440, 3301, 1614, 1510, 1424, 1355, 1331, 1245, 1199, 1118, 1048, 1025, 962, 904, 829.

MC-179 MW=421?
ASAP (MeOH _ EthGly + NH4OAc))

EPSRC National Facility Swansea
LTQ Orbitrap XL

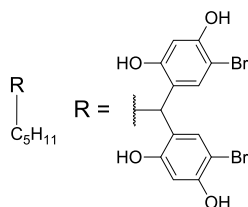
Marco
23/12/2014 12:34:28 PM



NL:
2.72E6
UEAMAT239-PG-HASP-2#115-
121 RT: 3.19-3.36 AV: 7 T:
FTMS + p APCI corona Full ms
[100.00-800.00]

NL:
8.47E3
C₁₉ H₁₃ BCl₂ O₆ C₂ H₄ H:
C₂₁ H₁₈ B₁ Cl₂ O₆
p (gss, s /p:40) Chrg 1
R: 100000 Res .Pwr . @FWHM

Compound 107⁷²



0.32 mL of methanesulfonic acid was added to a pre-cooled (0 °C) mixture of hexanal (250 mg, 2.5 mmol) and 4-bromoresorcinol (1.1793 g, 6.24 mmol) in 4 ml of Et₂O/DCM (1/1, v/v). The reaction vessel was sealed and the reaction allowed to stir

for 7 h. The resulting mixture was diluted with diethyl ether, poured into distilled water and allowed to stir vigorously until a suspension was obtained. The product was collected by Büchner filtration, washed with abundant distilled water and dried in a desiccator to give a light yellow powder.

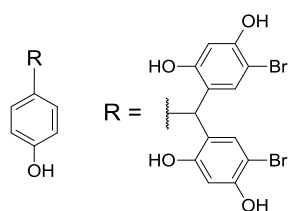
Yield: 41% (calculated from NMR to account for solvent of crystallisation)

MP: 125-126 °C (lit. 107-109 °C)⁷²

¹H-NMR (400 MHz, DMSO) δ 9.74 (s, 2H), 9.31 (s, 2H), 7.00 (s, 2H), 6.45 (s, 2H), 4.24 (t, J = 7.8 Hz, 1H), 1.77 (q, J = 7.8 Hz, 2H), 1.29 – 1.11 (m, 6H), 0.82 (t, J = 7.0 Hz, 3H).

¹³C-NMR (101 MHz, DMSO) δ 154.79, 151.52, 128.85, 123.86, 109.33, 104.10, 36.01, 33.82, 31.64, 27.71, 22.46, 14.40.

Compound 109⁷²



0.32 mL of methanesulfonic acid was added to a pre-cooled (0 °C) mixture of 4-hydroxybenzaldehyde (250 mg, 2.05 mmol) and 4-bromoresorcinol (1.7412 g, 9.21 mmol) in 4 ml of Et₂O/DCM (1/1, v/v). The reaction vessel was sealed and the reaction allowed to stir for 7 h. The resulting mixture was diluted with diethyl ether, poured into distilled water and allowed to stir vigorously until a suspension was obtained. The product was collected by Büchner filtration, washed with abundant distilled water and dried in a desiccator.

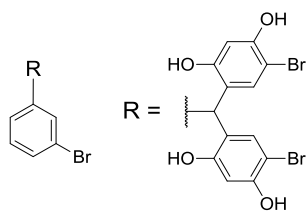
Yield: 34% (calculated from NMR to account for solvent of crystallisation)

MP: 200-202 °C (lit. 201-202 °C)⁷²

¹H-NMR (400 MHz, DMSO) δ 9.84 (s, J = 5.2 Hz, 2H), 9.37 (s, 2H), 9.17 (s, J = 5.7 Hz, 1H), 6.74 (d, J = 8.5 Hz, 2H), 6.66 (d, J = 8.5 Hz, 2H), 6.53 (s, 2H), 6.49 (s, 2H), 5.60 (s, 1H).

¹³C-NMR (101 MHz, DMSO) δ 155.76, 155.26, 153.03, 134.12, 132.67, 130.06, 124.38, 115.35, 104.00, 97.82, 41.36.

Compound 150



0.32 mL of methanesulfonic acid was added to a pre-cooled (0 °C) mixture of 3-bromobenzaldehyde (250 mg, 1.35 mmol) and 4-bromoresorcinol (683.5 mg, 3.62 mmol) in 4 ml of Et₂O/DCM (1/1, v/v). The reaction vessel was sealed and the reaction allowed to stir for 7 h. The resulting mixture was diluted with diethyl ether, poured into distilled water and allowed to stir vigorously until a suspension was obtained. The product was collected by Büchner filtration, washed with abundant distilled water and dried in a desiccator to give an orange powder.

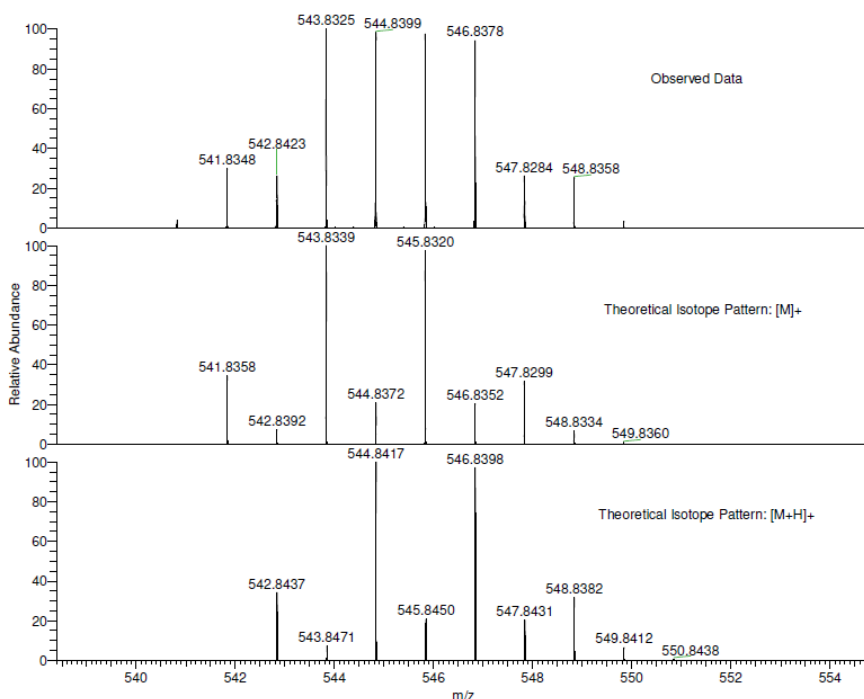
Yield: 53% (calculated from NMR to account for solvent of crystallisation)

MP: 101-104 °C

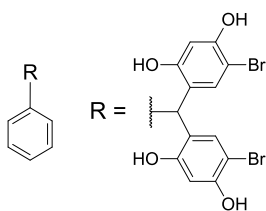
¹H-NMR (400 MHz, DMSO) δ 9.97 (s, 2H), 9.54 (s, 2H), 7.39 (dd, *J* = 8.0, 1.0 Hz, 1H), 7.25 (t, *J* = 7.8 Hz, 1H), 7.07 (t, *J* = 1.5 Hz, 1H), 6.97 (d, *J* = 7.8 Hz, 1H), 6.55 (s, 2H), 6.53 (s, 2H), 5.68 (s, 1H).

¹³C-NMR (101 MHz, DMSO) δ 155.36, 153.52, 147.26, 132.75, 131.52, 130.80, 129.27, 128.29, 122.73, 121.94, 104.10, 98.05, 42.21.

IR (ν_{max}, cm⁻¹): 3386, 1610, 1498, 1425, 1333, 1240, 1201, 1168, 1115, 1009, 900, 834.



Compound 151⁹⁴



0.32 mL of methanesulfonic acid was added to a pre-cooled (0 °C) mixture of benzaldehyde (250 mg, 2.36 mmol) and 4-bromoresorcinol (1.1132 g, 5.89 mmol) in 4 ml of Et₂O/DCM (1/1, v/v). The reaction vessel was sealed and the reaction allowed to stir for 7 h. The resulting mixture was diluted with diethyl ether, poured into distilled water and allowed to stir vigorously until a suspension was obtained. The product was collected by Büchner filtration, washed with abundant distilled water and dried in a desiccator to give a pale yellow powder.

Yield: 74% (calculated from NMR to account for solvent of crystallisation)

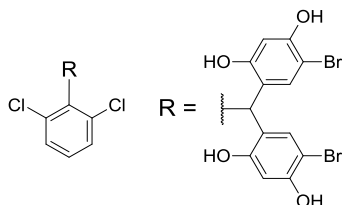
MP: 125-129 °C

¹H-NMR (400 MHz, DMSO) δ 9.90 (s, 2H), 9.46 (s, 2H), 7.27 (t, *J* = 7.4 Hz, 2H), 7.17 (t, *J* = 7.3 Hz, 1H), 6.95 (d, *J* = 7.3 Hz, 2H), 6.53 (s, *J* = 6.5 Hz, 2H), 6.51 (s, 2H), 5.71 (s, 1H).

^{13}C -NMR (101 MHz, DMSO) δ 155.33, 153.22, 144.16, 132.78, 129.18, 128.57, 126.29, 123.68, 104.04, 97.91, 42.25.

IR (ν_{max} , cm^{-1}): 3589, 3422, 3286, 1617, 1594, 1522, 1492, 1423, 1377, 1338, 1303, 1250, 1201, 1130, 1074, 1035, 1012, 917, 903, 866, 838, 832, 820.

Compound 111⁷²



0.32 mL of methanesulfonic acid was added to a pre-cooled (0 °C) mixture of 2,6-dichlorobenzaldehyde (250 mg, 1.43 mmol) and 4-bromoresorcinol (675 mg, 3.57 mmol) in 4 mL of Et₂O/DCM (1/1, v/v). The reaction vessel was sealed and the reaction allowed to stir for 7 h. The resulting mixture was diluted with diethyl ether, poured into distilled water and allowed to stir vigorously until a suspension was obtained. The product was collected by Büchner filtration, washed with abundant distilled water and dried in a desiccator to give a light orange powder.

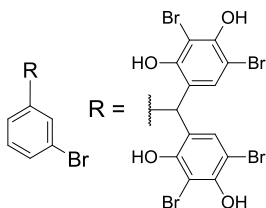
Yield: 84% (calculated from NMR to account for solvent of crystallisation)

MP: 238-240 °C (lit. 162-164 °C) The compound goes through different states, definition of a melting point by direct observation is misleading.

^1H -NMR (400 MHz, DMSO) δ 9.94 (s, 2H), 9.48 (s, 2H), 7.39 (d, J = 8.0 Hz, 2H), 7.25 (t, J = 8.0 Hz, 1H), 6.65 (s, 2H), 6.49 (s, 2H), 6.18 (s, 1H).

^{13}C NMR (101 MHz, DMSO) δ 155.54, 153.54, 138.93, 135.76, 133.16, 129.86, 128.94, 119.85, 103.68, 97.99, 41.43.

Compound 153

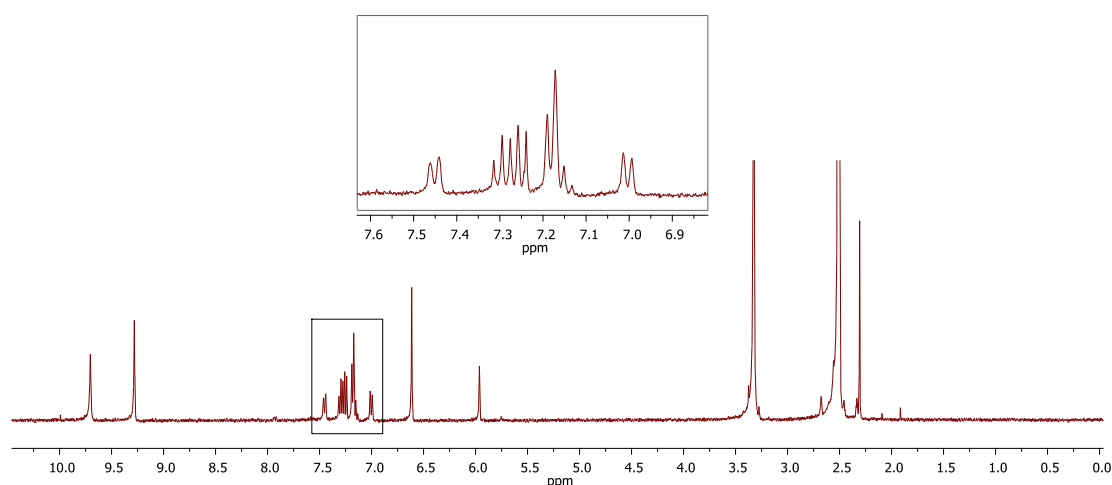


0.32 mL of methanesulfonic acid was added to a pre-cooled (0 °C) mixture of 3-bromobenzaldehyde (200 mg, 1.08 mmol) and 2,4-dibromoresorcinol (724 mg, 2.70

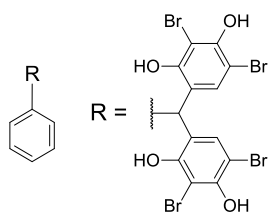
mmol) in 4 ml of Et₂O/DCM (1/1, v/v). The reaction vessel was sealed and the reaction allowed to stir for 10 days. The resulting mixture was diluted with diethyl ether, poured into distilled water and allowed to stir vigorously until a suspension was obtained. The product was collected by Büchner filtration, washed with abundant toluene, distilled water and dried in a desiccator.

Toluene cannot be removed by repeatedly washing with water or hexane, re-suspension in water and filtration is useful either. Co-evaporation with water or methanol does not remove the impurity.

A ¹H-NMR is reported for reference.



Compound 154



0.32 mL of methanesulfonic acid was added to a pre-cooled (0 °C) mixture of benzaldehyde (200 mg, 1.88 mmol) and 2,4-dibromoresorcinol (1.26 g, 4.71 mmol) in 4 ml of Et₂O/DCM (1/1, v/v). The reaction vessel was sealed and the reaction allowed to stir for 10 days. The resulting mixture was diluted with diethyl ether, poured into distilled water and allowed to stir vigorously until a suspension was obtained. The product was collected by Büchner filtration washed with abundant toluene, distilled water and dried in a desiccator to give a pink powder.

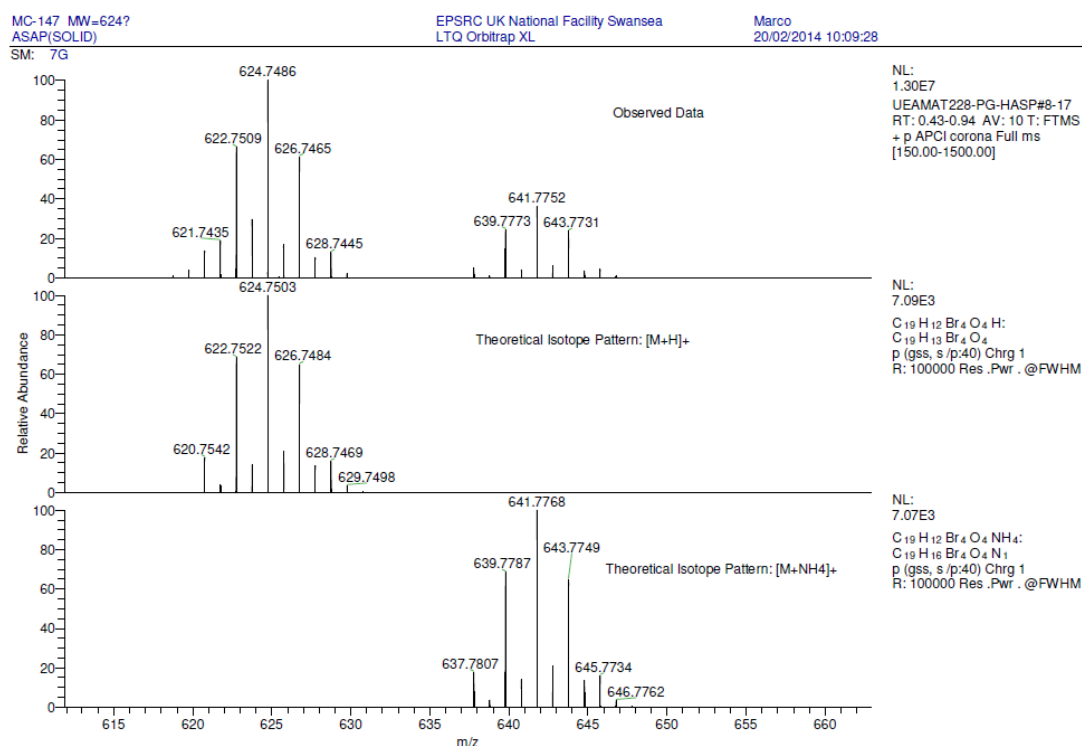
Yield: 44% (calculated from NMR to account for solvent of crystallisation)

MP: 390 °C dec.

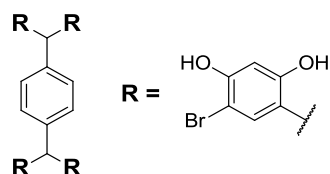
^1H -NMR (400 MHz, DMSO) δ 9.65 (s, 2H), 9.21 (s, 2H), 7.32 (t, J = 7.4 Hz, 2H), 7.24 (t, J = 7.3 Hz, 1H), 7.01 (d, J = 7.3 Hz, 2H), 6.60 (s, 2H), 5.99 (s, 1H).

^{13}C -NMR (101 MHz, DMSO) δ 152.32, 150.28, 142.58, 131.20, 129.35, 128.91, 126.91, 125.89, 103.74, 101.01, 44.15.

IR (ν_{max} , cm^{-1}): 3505, 3465, 1594, 1575, 1492, 1471, 1425, 1333, 1275, 1217, 1173, 1143, 1132, 1037, 929, 903, 882, 825.



Compound 158



Method 1

Product not isolated

Method 2

1.2 mL of methanesulfonic acid was added to a pre-cooled (0 °C) mixture of terephthalaldehyde (300 mg, 2.24 mmol) and 4-bromoresorcinol (1.90 g, 10.07 mmol)

in 15ml of Et₂O/DCM (1/1, v/v). The reaction vessel was sealed and the reaction allowed to stir for 7 h. The mixture was poured into 75 mL of Et₂O and cooled for 18 h at 4°C. The resulting solid was collected and washed with diethyl ether to give the white crystalline product (2.5583 g).

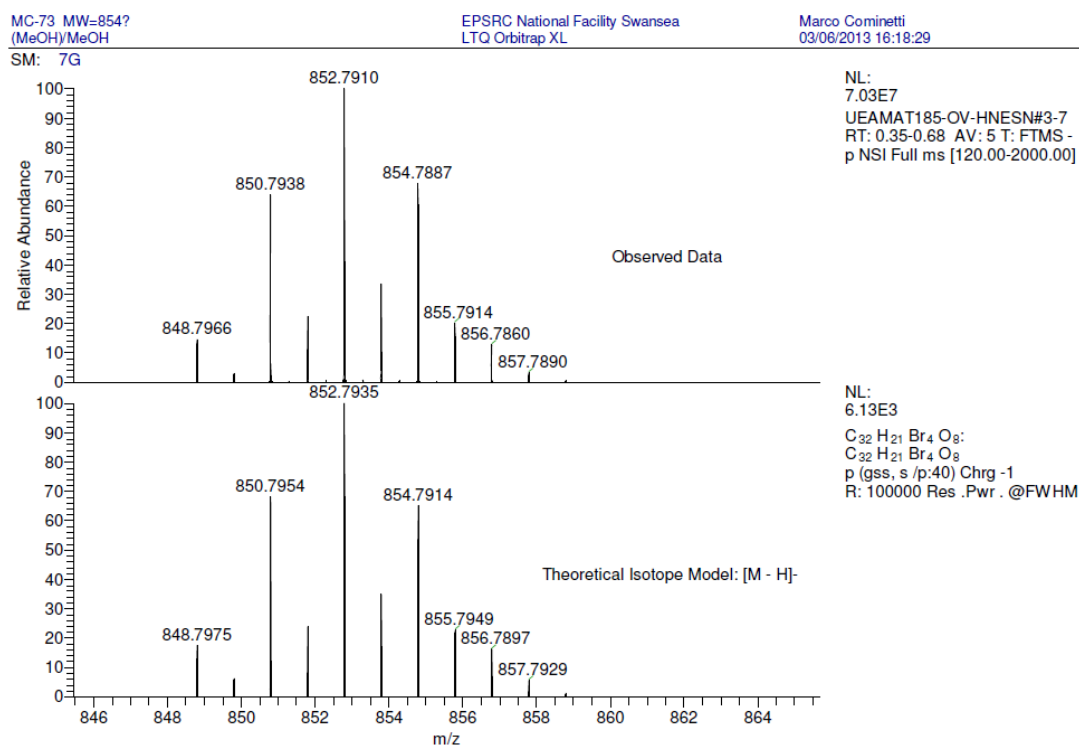
Yield: 87% (calculated from NMR to account for solvent of crystallisation)

MP: 149-151°C

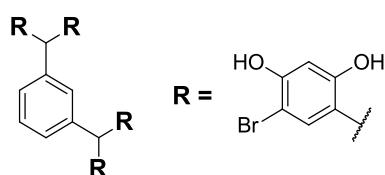
¹H-NMR (400 MHz, DMSO) δ 9.86 (s, 1H), 9.42 (s, 1H), 6.84 (s, 1H), 6.52 (s, 1H), 6.49 (s, 1H), 5.68 (s, 1H).

¹³C-NMR (101 MHz, DMSO) δ 154.77, 152.64, 141.02, 132.33, 128.39, 123.40, 103.52, 97.46, 41.27.

IR (ν_{max}, cm⁻¹): 3476.5, 3416.5, 1608, 1592, 1502, 1485.5, 1424, 1332.5, 1276.5, 1236, 1195, 1166.5, 1112.5, 1009, 888.5, 835.5.



Compound 160



Method 2

1.2 mL of methanesulfonic acid was added to a pre-cooled (0 °C) mixture of isophthalaldehyde (200 mg, 1.491 mmol) and 4-bromoresorcinol (1.26 g, 6.710 mmol) in 15 mL of Et₂O/DCM (1/1, v/v). The reaction vessel was sealed and the reaction allowed to stir for 6.5 h. The mixture was poured into 75 mL of Et₂O and cooled for 18h at 4°C. The resulting solid was collected and washed with diethyl ether to give a pale green powder (1.1071 g).

Yield: 61% (calculated from NMR to account for solvent of crystallisation)

MP:151-153°C

¹H-NMR (400 MHz, DMSO) δ 9.83 (s, 4H), 9.38 (s, 4H), 7.15 (t, *J* = 7.6 Hz, 1H), 6.77 – 6.65 (m, 3H), 6.50 (s, 4H), 6.48 (s, 4H), 5.63 (s, 2H).

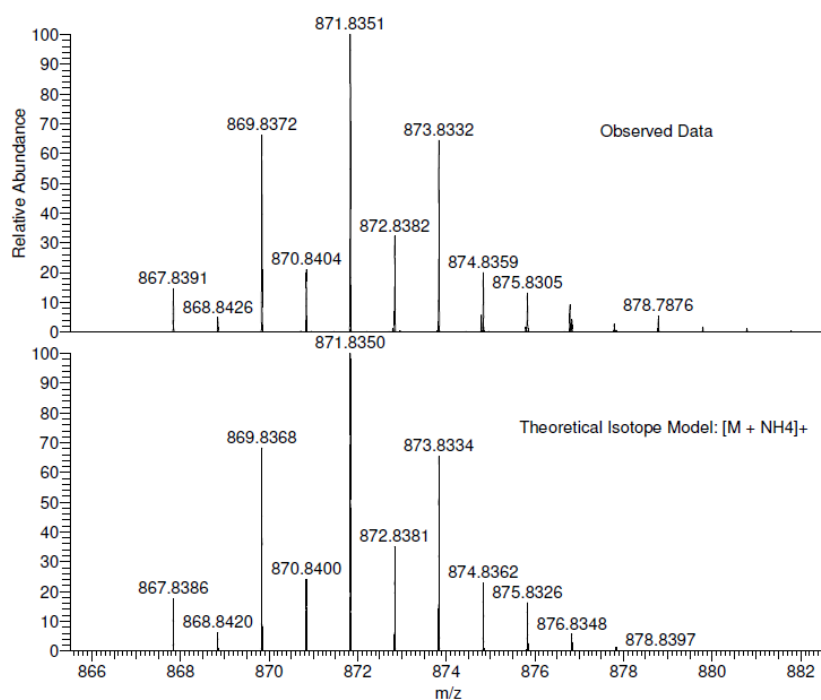
¹³C-NMR (101 MHz, DMSO) δ 154.71, 152.61, 143.25, 132.22, 129.69, 127.64, 126.09, 123.30, 103.54, 97.49, 41.58.

IR (ν_{max}, cm⁻¹): 3464.5, 3390.5, 1607, 1500.5, 1485, 1423.5, 1370, 1332, 1276.5, 1238.5, 1195.5, 1167.5, 1115.5, 1010, 896.5, 887.5, 834.

MC-84 MW=854?
(MeOH)/MeOH + NH₄OAc

EPSRC National Facility Swansea
LTQ Orbitrap XL

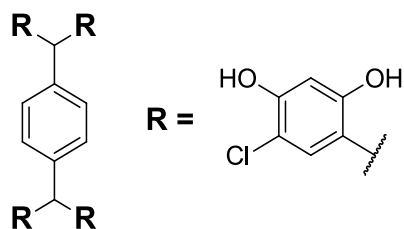
Marco Cominetti
19/07/2013 16:29:18



NL:
2.18E6
UEAMAT197-OJ-HNESP#32-
50 RT: 0.74-1.26 AV: 19 T:
FTMS + p NSI Full ms
[120.00-2000.00]

NL:
6.11E3
C₃₂H₂₂Br₄O₈NH₄:
C₃₂H₂₆Br₄O₈N₁
p (gss, s /p:40) Chrg 1
R: 100000 Res .Pwr . @FWHM

Compound 163



Method 1

A mixture of terephthalaldehyde (500 mg, 3.73 mmol) and 4-chlororesorcinol (2.42 g, 16.78 mmol) was dissolved in 15 ml of ethanol/HCl 37% (1/1, v/v) and allowed to stir at 70 °C for 5 h. The solvent was evaporated and the resulting orange solid obtained was suspended in water, collected by filtration and washed with water. To remove trace 3-chlororesorcinol, the solid was suspended in dichloromethane, allowed to stir for 15 minutes, collected by filtration and washed with dichloromethane. The orange powder was dried in the desiccator for one week to give 1.6505 g of product.

Yield: 66% (calculated from NMR to account for solvent of crystallisation)

Method 2

1.2 mL of methanesulfonic acid was added to a pre-cooled (0 °C) mixture of terephthalaldehyde (500 mg, 3.73 mmol) and 4-chlororesorcinol (2.42 g, 16.78 mmol) in 15 ml of Et₂O/DCM (1/1, v/v). The reaction vessel was sealed and the reaction allowed to stir for 5 h. The mixture was poured into 75 mL of Et₂O and cooled for 18 h at 4°C. The resulting solid was collected and washed with diethyl ether to give the orange crystalline product (2.8132 g).

Yield: 86% (calculated from NMR to account for solvent of crystallisation)

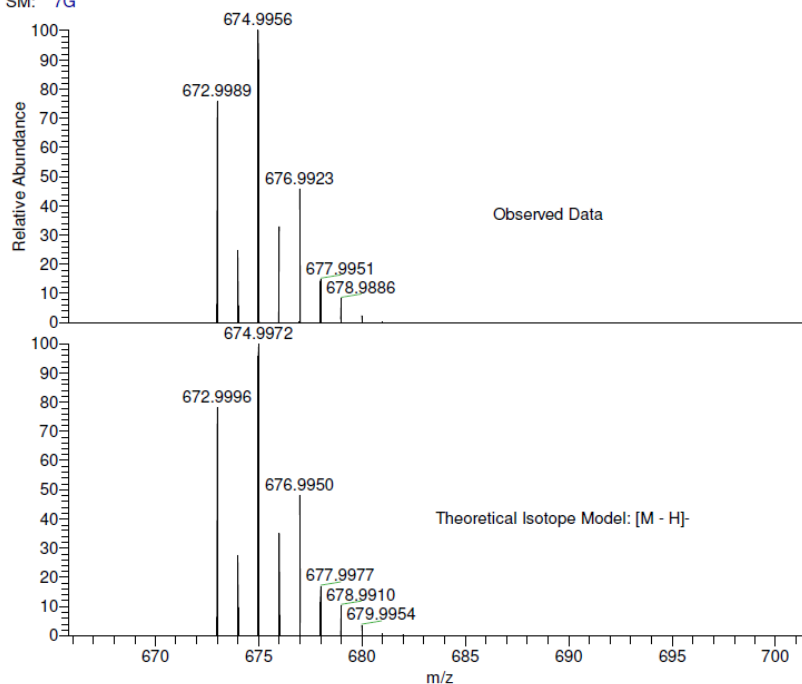
MP: 225-256°C

¹H-NMR (400 MHz, DMSO) δ 9.77 (s, 4H), 9.38 (s, 4H), 6.84 (s, 4H), 6.49 (s, 4H), 6.38 (s, 4H), 5.68 (s, 2H).

¹³C-NMR (101 MHz, DMSO) δ 154.10, 151.57, 141.03, 129.52, 128.39, 122.73, 108.67, 103.65, 41.31.

IR (ν_{max}, cm⁻¹): 3498.5, 3424.5, 3209.5, 1613, 1505, 1428.5, 1355.5, 1322, 1283.5, 1266.5, 1245, 1224, 1209, 1194.5, 1169.5, 1121.5, 1029, 905, 889.5, 840.5.

SM: 7G



NL:
4.33E7
UEAMAT190-OV-HNESN#2-7
RT: 0.26-0.68 AV: 6 T: FTMS -
p NSI Full ms [120.00-2000.00]

NL:
6.86E3
C₃₂H₂₁Cl₄O₈:
C₃₂H₂₁Cl₄O₈:
p (gss, s /p:40) Chrg -1
R: 100000 Res .Pwr . @FWHM

Crystallisation procedure

During preparation according to **Method 2**: the mixture obtained after 5 hours was poured in 75 mL of diethyl ether: the solid initially dissolved and then recrystallised after one night in the fridge at 4 °C. Crystals were taken directly from the solution.

Platform **163** (**Figure 49**) lies about a twofold symmetry axis, normal to the central C₆ ring and through the centre of that ring.

Each of the hydroxyl groups in this molecule is a hydrogen-bond donor, three (and the symmetry-related three) linked to ether (solvent) molecules, and the fourth (and its equivalent) forming a bond with an adjacent **163** molecule. These molecules thus form chains which run parallel to the crystallographic *b*-axis (**Figure 49**) in the form of columns of **163** molecules padded out by ether molecules.

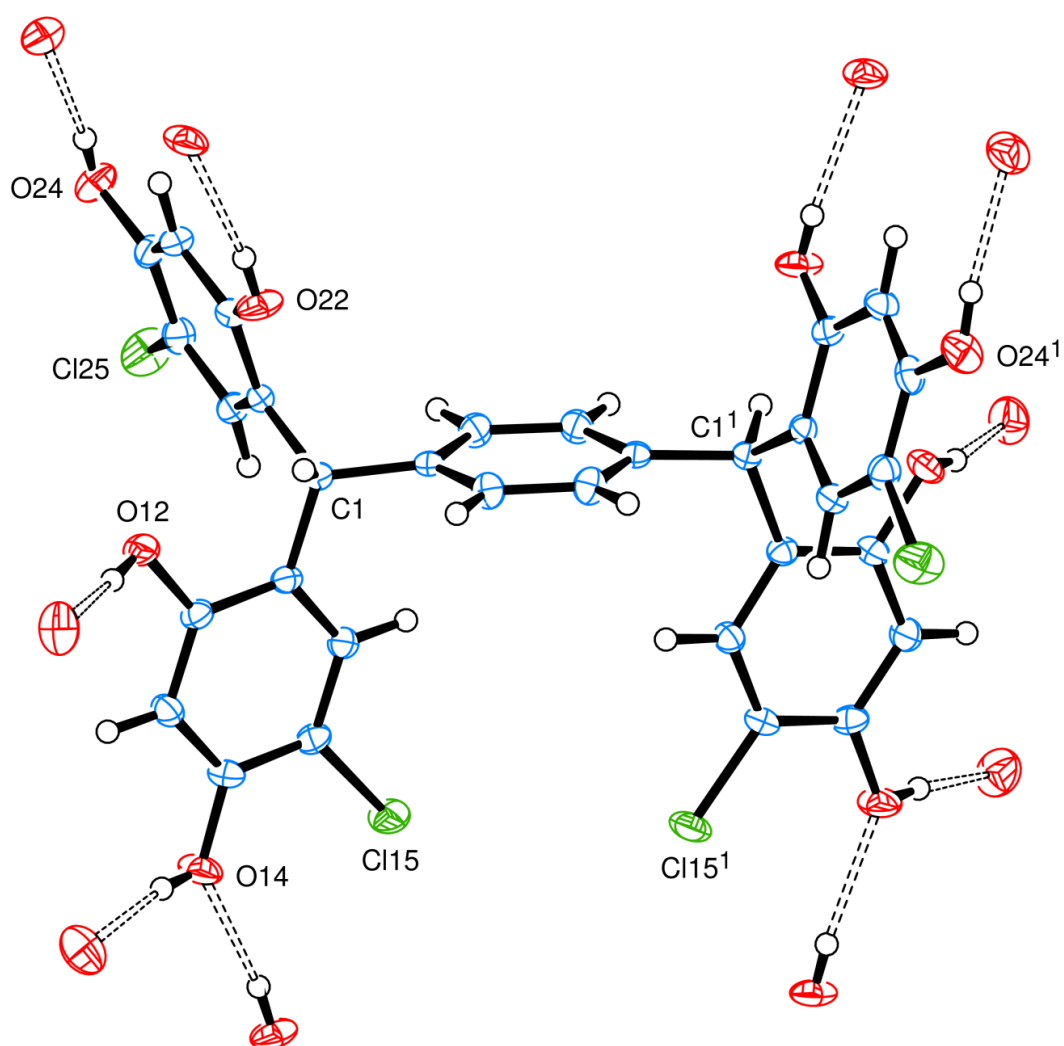


Figure 49. View of a molecule of **163**, indicating the atom numbering scheme and hydrogen-bonded atoms of neighbouring molecules. Thermal ellipsoids are drawn at the 50% probability level.

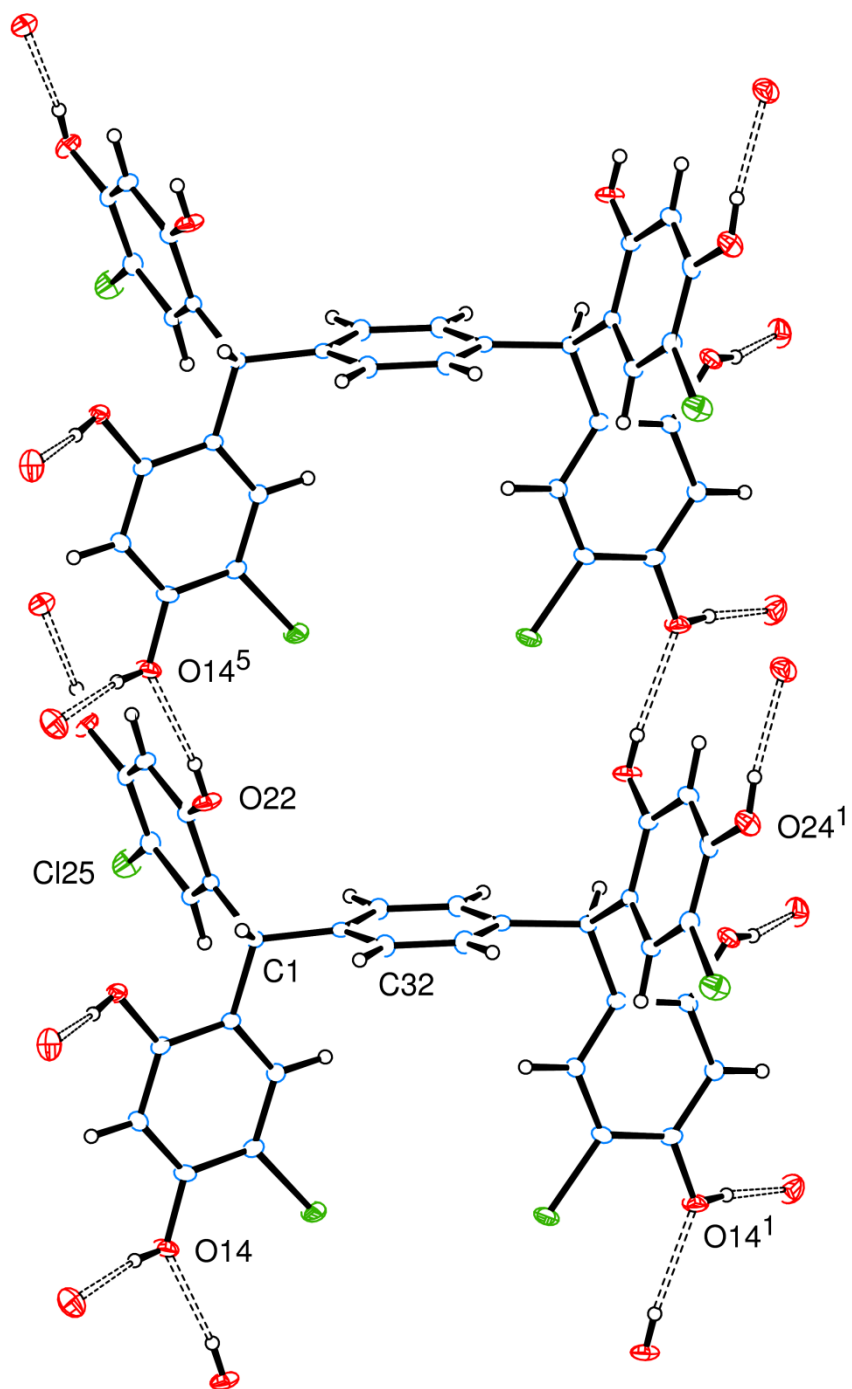
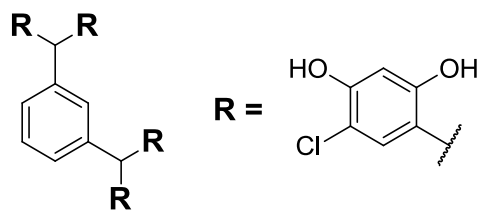


Figure 50. 163 molecules linked through hydrogen bonds in chains. The oxygen atoms of the hydrogen-bonded ether molecules are also included.

Compound 164



Method 1

A mixture of isophthalaldehyde (500 mg, 3.73 mmol) and 4-chlororesorcinol (2.42 g, 16.78 mmol) was dissolved in 15 ml of ethanol/HCl 37% (1/1, v/v) and allowed to stir at 70 °C for 5 h. The solvent was evaporated and the resulting orange solid obtained was suspended in water, collected by filtration and washed with water. To remove trace 3-chlororesorcinol, the solid was suspended in dichloromethane, allowed to stir for 15 minutes, collected by filtration and washed with dichloromethane. The orange powder was dried in the desiccator for one week to give 2.4721 g of product.

Yield: 91% (calculated from NMR to account for solvent of crystallisation)

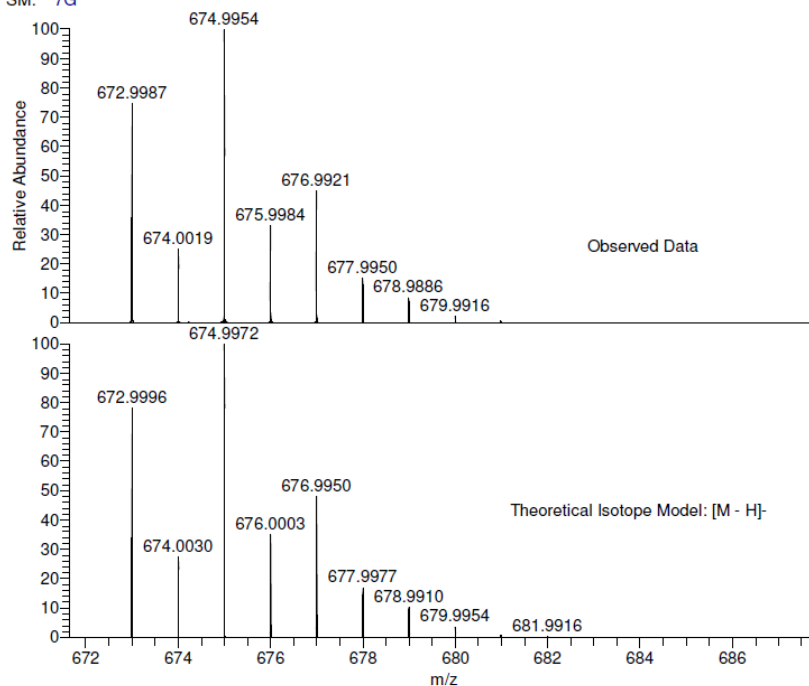
MP: 172-174 °C

$^1\text{H-NMR}$ (400 MHz, DMSO) δ 9.75 (s, 4H), 9.35 (s, 4H), 7.15 (t, $J = 7.6$ Hz, 1H), 6.72 (d, $J = 7.6$ Hz, 2H), 6.47 (s, 4H), 6.34 (s, 4H), 5.63 (s, 2H).

$^{13}\text{C-NMR}$ (101 MHz, DMSO) δ 154.03, 151.55, 143.26, 129.65, 129.42, 127.69, 126.12, 122.64, 108.73, 103.67, 41.61.

IR (ν_{max} , cm^{-1}): 3477.5, 3420.5, 3061, 1617, 1602, 1500, 1430, 1381, 1360.5, 1319.5, 1295.5, 1281.5, 1263, 1232, 1208.5, 1194.5, 1179, 1159.5, 1128, 1119, 1089, 1029.5, 900, 889.5, 839.5.

SM: 7G



NL:
3.66E7
UEAMAT189-OV-HNESN#4-7
RT: 0.43-0.68 AV: 4 T: FTMS -
p NSI Full ms [120.00-2000.00]

NL:
6.86E3
C₃₂H₂₁Cl₄O₈
C₃₂H₂₁Cl₄O₈
p (gss, s /p:40) Chrg -1
R: 100000 Res .Pwr .@FWHM

Crystallisation procedure

A sample of compound was suspended in a solution 1:1 of DCM:Et₂O and heated to reflux. The minimum amount of methanol necessary to obtain complete dissolution was added; the clear solution obtained was sealed in the tube and left at room temperature to obtain transparent needles.

Platform 164 molecules are linked, directly and through bridging methanol molecules, in an extensive hydrogen-bonded network. Principally, the octa-phenols are linked in ladder-like chains through O(24³)-H...O(14) and O(34)-H...O(44³) hydrogen bonds; there are also O(32)-H...O(42¹) hydrogen bonds, about centres of symmetry, that link these chains into double-ladder chains. These chains are linked through one or more bridging methanol molecules.

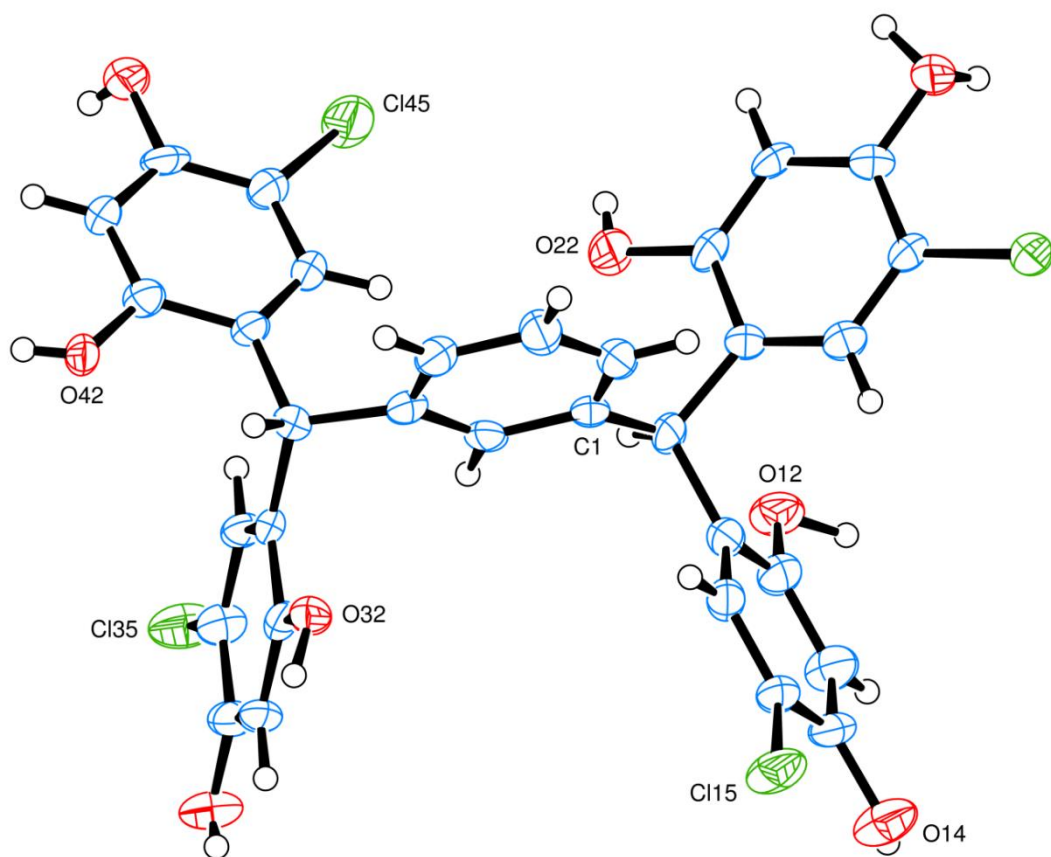


Figure S1. View of a molecule of **164**. Thermal ellipsoids are drawn at the 50% probability level.

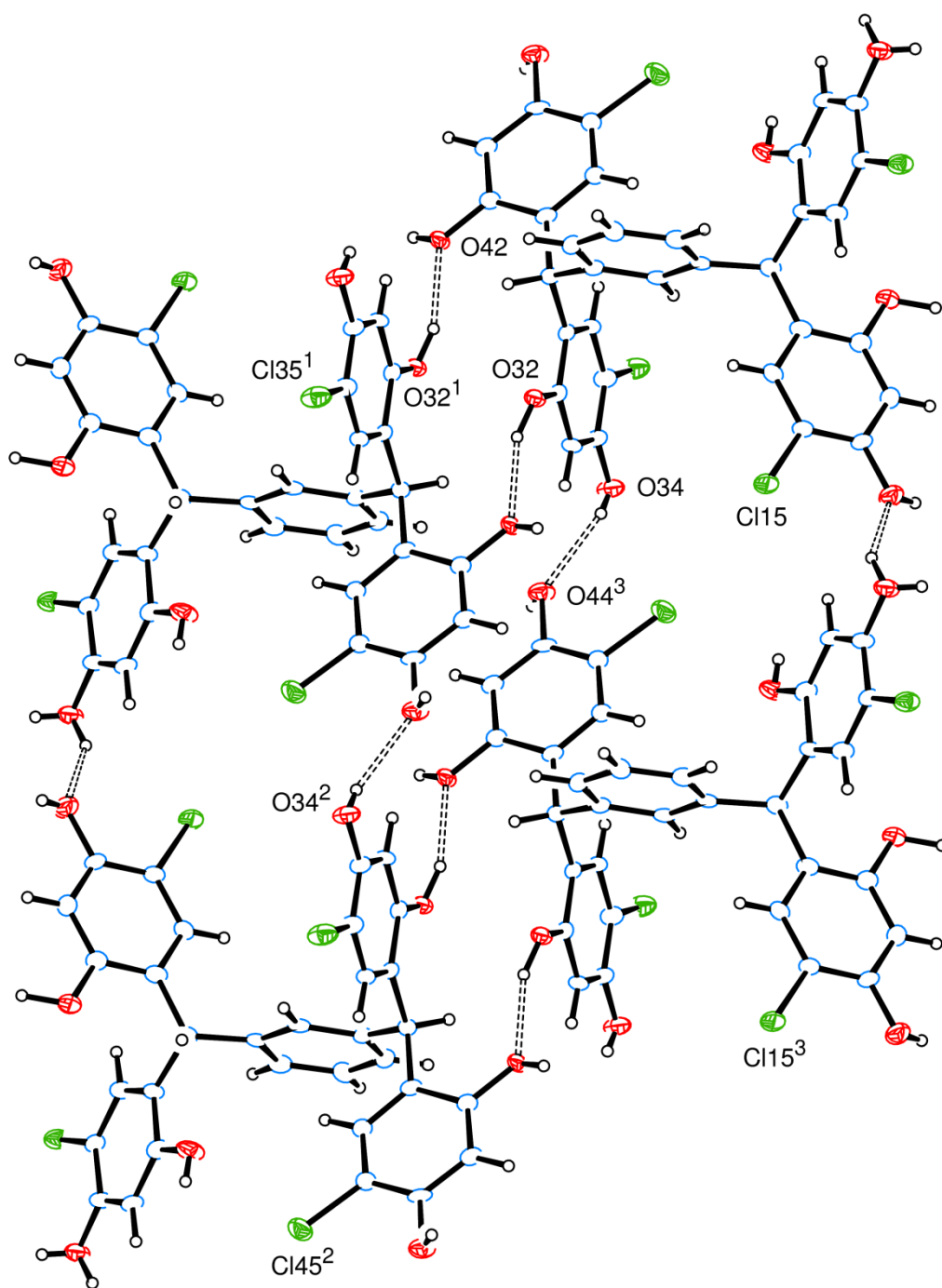
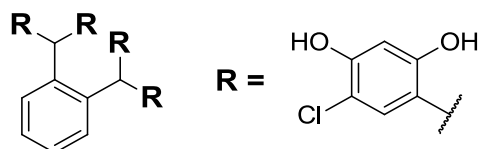


Figure 52. Linking, through hydrogen bonds, of the **164** molecules, showing the ladder formation and the linking of pairs of ladders about centres of symmetry.

Compound 165



Method 1

A mixture of phthaldialdehyde (500 mg, 3.73 mmol) and 4-chlororesorcinol (2.425 g, 16.78 mmol) was dissolved in 15 ml of ethanol/HCl 37% (1/1, v/v) and allowed to stir at 70 °C for 6.5 h. The solvent was evaporated and the resulting orange solid obtained was suspended in water, collected by filtration and washed with water. To remove trace 3-chlororesorcinol, the solid was suspended in dichloromethane, allowed to stir for 15 minutes, collected by filtration and washed with dichloromethane. The orange powder was dried in the desiccator for one week to give 2.4915 g of product.

Yield: 80% (calculated from NMR to account for solvent of crystallisation)

Method 2

1.2 mL of methanesulfonic acid was added to a pre-cooled (0 °C) mixture of phthaldialdehyde (500 mg, 3.73 mmol) and 4-chlororesorcinol (2.425 g, 16.78 mmol) in 15 ml of Et₂O/DCM (1/1, v/v). The reaction vessel was sealed and the reaction allowed to stir vigorously for 6 h. The mixture was poured into 75 mL of Et₂O and cooled for 18 h at 4 °C. The resulting solid was collected and washed with diethyl ether to give a pale yellow powder (398.1 mg).

Note stirring must be vigorous, the amount of precipitate formed can give uneven stirring and isolation of **11**; use of reaction tubes is discouraged.

Yield: 94% (calculated from NMR to account for solvent of crystallisation)

MP: 282-283 °C

¹H-NMR (400 MHz, DMSO) δ 9.57 (s, 4H), 8.86 (s, 4H), 7.08 (dd, *J* = 5.7, 3.5 Hz, 2H), 6.73 (dd, *J* = 5.7, 3.5 Hz, 2H), 6.41 (s, 4H), 6.28 (s, 4H), 5.63 (s, 2H).

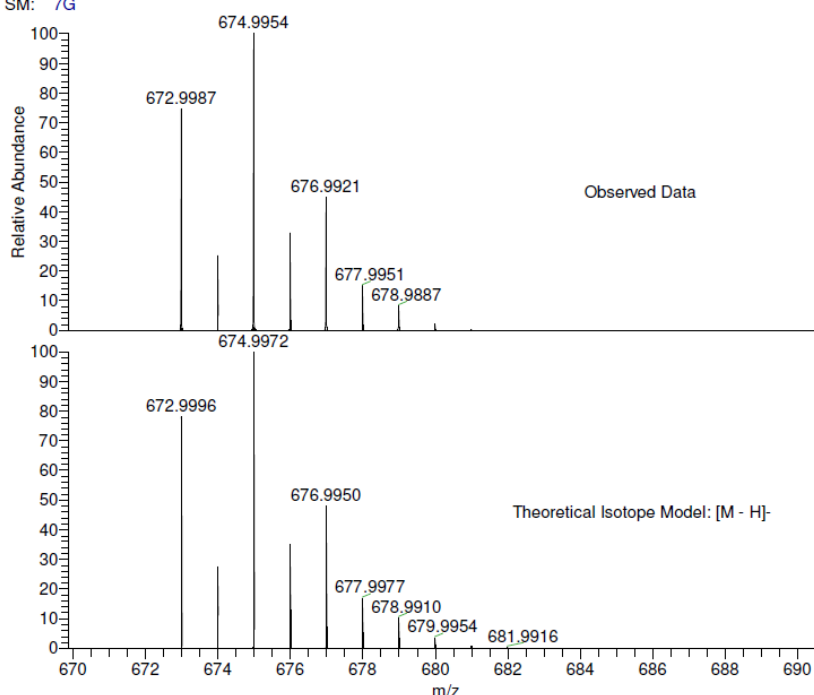
¹³C-NMR (101 MHz, DMSO) δ 154.32, 151.18, 141.82, 129.76, 128.72, 125.39, 122.41, 108.34, 103.50, 39.1. (The peak at 39.6 is overlaid with DMSO and was assigned by HSQC)

IR (ν_{max} , cm^{-1}): 3492, 3397, 1614, 1598.5, 1502.5, 1424, 1367.5, 1334, 1248, 1191.5, 1126.5, 1029, 905, 895, 876.5, 864, 836.5, 822.

MC-93 MW=676?
(MeOH)/MeOH
SM: 7G

EPSRC National Facility Swansea
LTQ Orbitrap XL

Marco Cominetti
03/06/2013 16:30:55



NL:
8.53E7
UEAMAT188-OV-HNESN#3-7
RT: 0.35-0.68 AV: 5 T: FTMS -
p NSI Full ms [120.00-2000.00]

NL:
6.86E3
C₃₂H₂₁Cl₄O₈:
C₃₂H₂₁Cl₄O₈:
p (gss, s /p:40) Chrg -1
R: 100000 Res .Pwr . @FWHM

Crystallisation procedure

A sample of compound was suspended in diethyl ether and heated to reflux. The minimum amount of methanol necessary to obtain complete dissolution was added; the clear solution obtained was sealed in the tube and left at room temperature to obtain transparent needles.

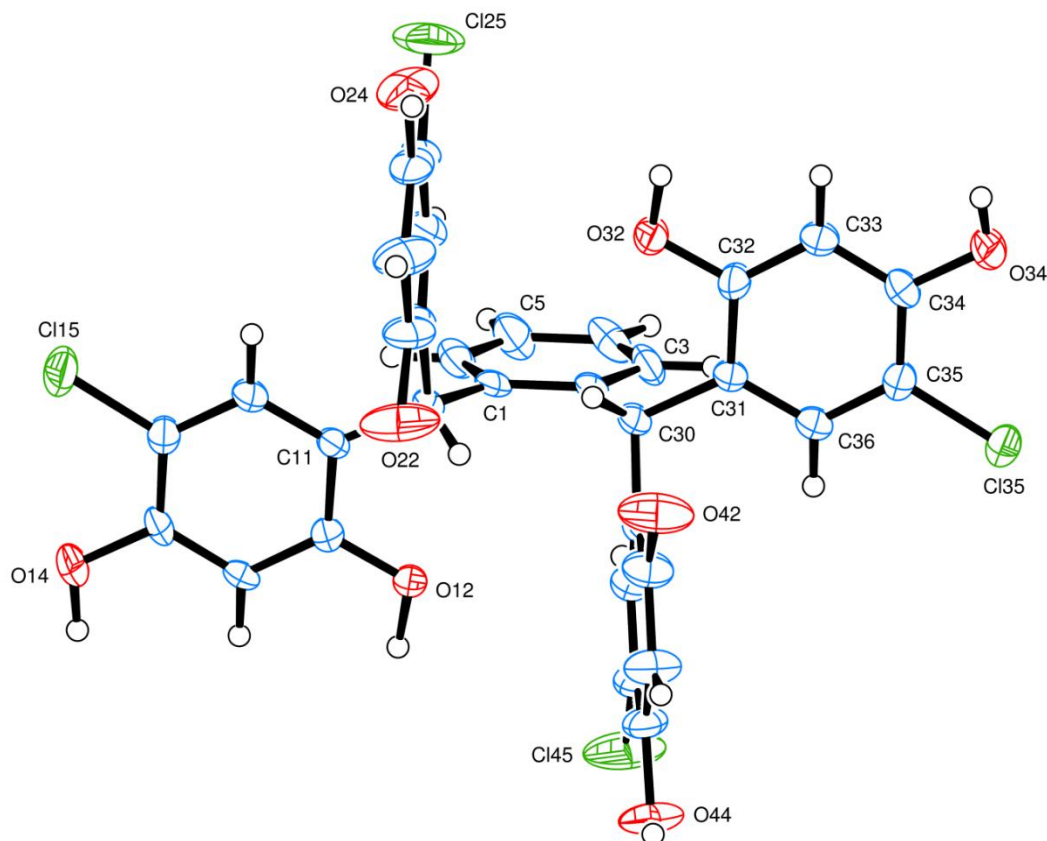


Figure 53.

All eight phenolic groups are donors in hydrogen bonds, and several are also acceptor atoms. The O(12) and O(32) each form pairs of links about centres of symmetry with neighbouring **165** molecules and thus form ladder-like chains through the crystal, (horizontally in **Figure 54**).

The two principal methanol molecules combine in a double bridging link between chains, forming a “square” hydrogen bonding cycle, **Figure 54**, thus forming sheets of linked molecules.

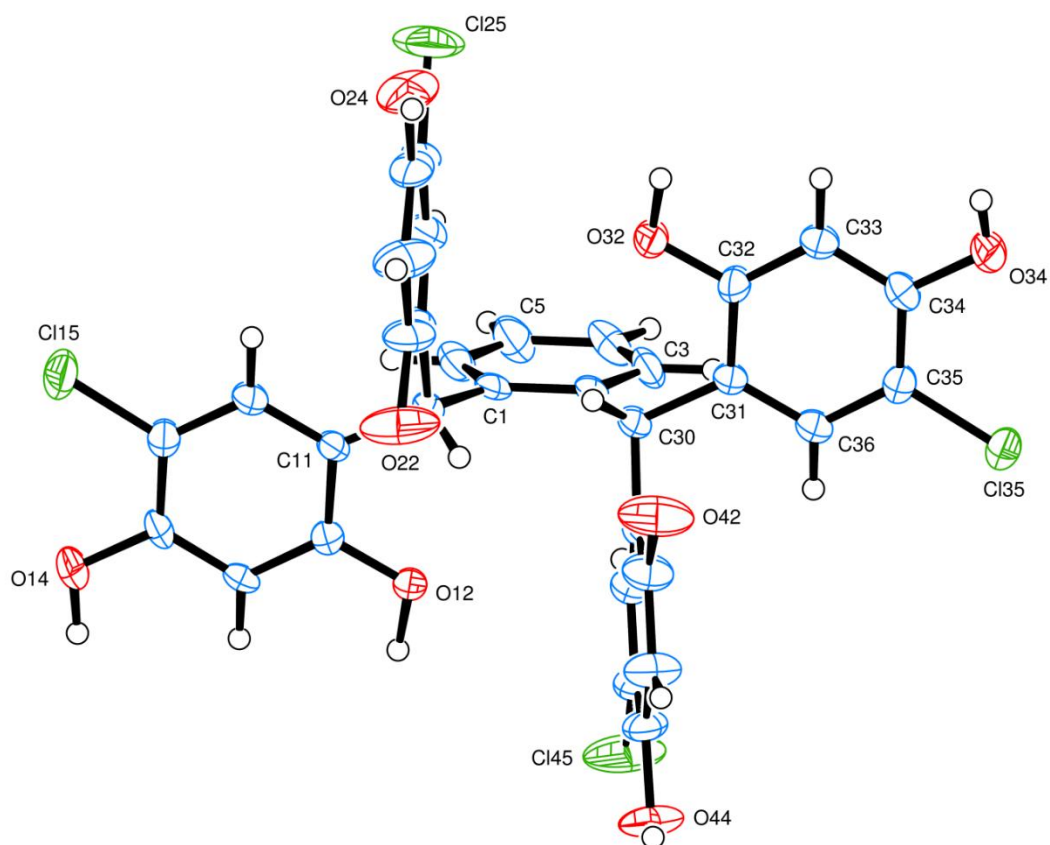


Figure 53. View of a molecule of **165**. Thermal ellipsoids are drawn at the 50% probability level.

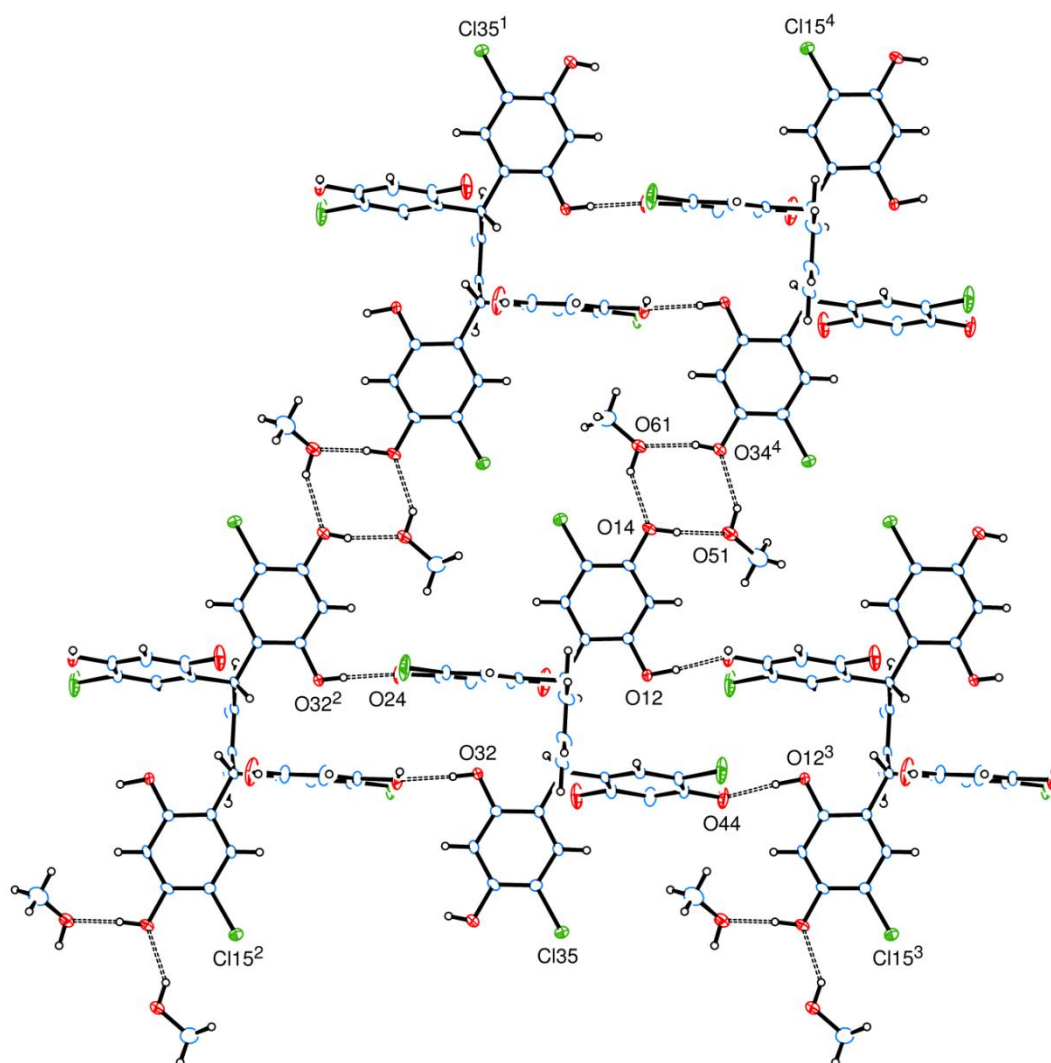
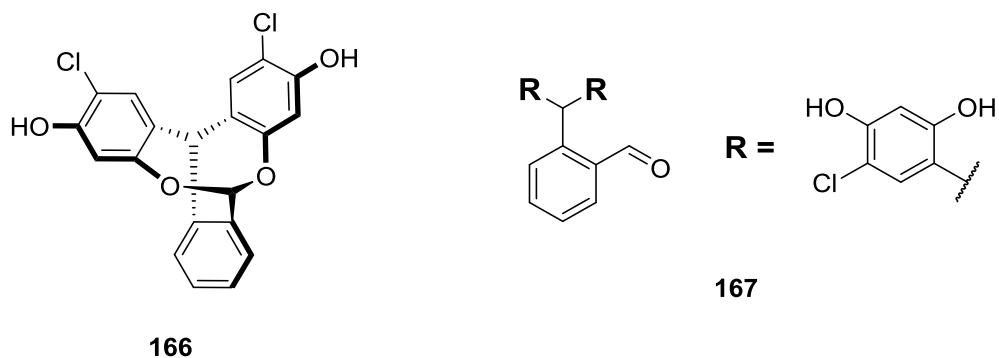


Figure 54. The molecules are linked through hydrogen bonds in chains (horizontally) about centres of symmetry, and in sheets and through methanol bridges.

Compound 166 and 167



1.2 mL of methanesulfonic acid was added to a pre-cooled (0 °C) mixture of phthalaldialdehyde (500 mg, 3.73 mmol) and 4-chlororesorcinol (1.07 g, 7.46 mmol) in

15 ml of Et₂O/DCM (1/1, v/v). The reaction vessel was sealed and the reaction allowed to stir vigorously for 6 h. The mixture was poured into 75 mL of Et₂O and cooled for 18 h at 4 °C. The resulting solid was collected and washed with diethyl ether. The product was dried in the oven at 60 °C for 18 h to give 773.2 mg of **167** as a white powder

Yield: 44% (calculated from NMR to account for solvent of crystallisation)

To isolate **166**: after collecting the solid **167**, the remaining liquor was washed with a solution of 1.55 g of NaHCO₃ in 20 mL of water and then with brine. The organic layer was dried over MgSO₄ and the product was crystallised by solvent evaporation.

Compound 166

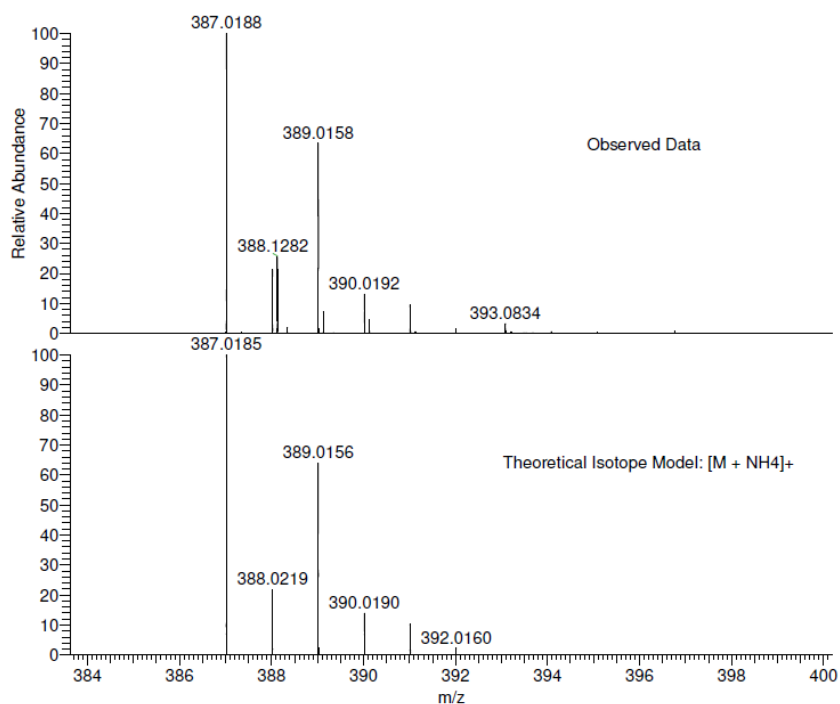
Yield: 11%

MP: 259-260 °C

¹H-NMR (400 MHz, DMSO) δ 10.19 (s, 2H), 7.55 (d, *J* = 7.3 Hz, 1H), 7.47 (s, 2H), 7.45 – 7.31 (m, 3H), 6.86 (s, 1H), 6.53 (s, 2H), 5.07 (s, 1H).

¹³C-NMR (101 MHz, DMSO) δ 152.80, 151.33, 141.67, 130.97, 130.15, 129.86, 128.76, 127.55, 125.58, 119.92, 112.82, 106.99, 99.82, 50.26.

IR (ν_{max}, cm⁻¹): 3476.5, 3427.5, 1612, 1486.5, 1431, 1319, 1278, 1240, 1218.5, 1210, 1145, 1122.5, 1067.5, 1042, 978.5, 953.5, 940.5, 923, 901, 870.5, 858.5, 840.5, 822.5.



NL:
8.04E5
UEAMAT194-OJ-HNESP#32-
50 RT: 0.75-1.26 AV: 19 T:
FTMS + p NSI Full ms
[120.00-2000.00]

NL:
1.07E4
C₂₀ H₁₂ Cl₂ O₄ H:
C₂₀ H₁₃ Cl₂ O₄
p (gss, s/p:40) Chrg 1
R: 100000 Res .Pwr .@FWHM

The compound forms a rigid triplanar molecule which crystallises with an ether (solvent) molecule.

The only atoms that do not lie on one of the three planes are the phenolate hydrogen atoms which are directed in forming hydrogen bonds which link the diphenolate molecules in chains and to the ether molecules.

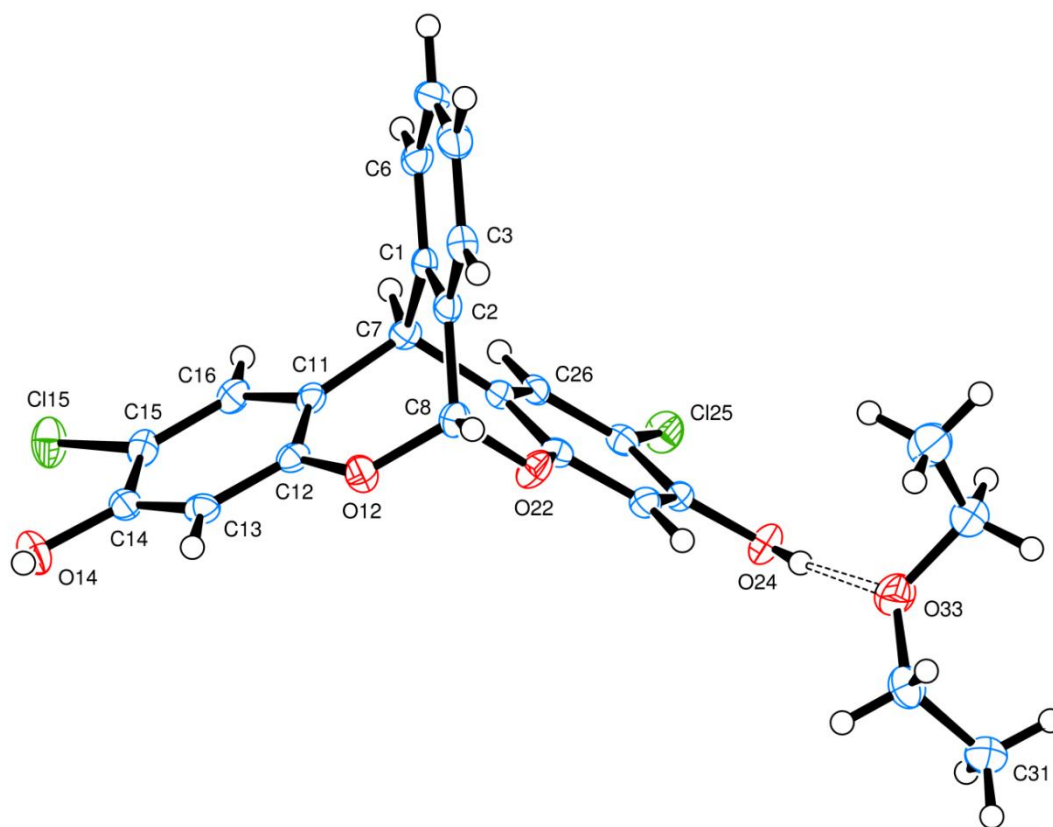


Figure 55. View of a molecule of **166** and hydrogen-bonded solvent (Et₂O) molecule, indicating the atom numbering scheme. Thermal ellipsoids are drawn at the 50% probability level.

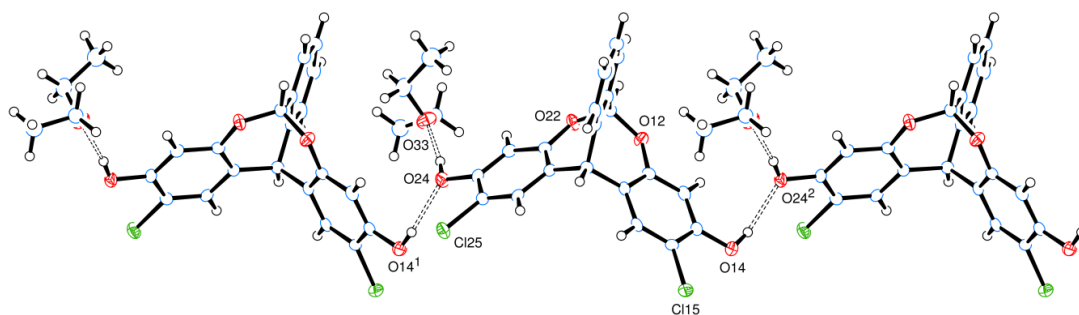


Figure 56. A chain of hydrogen-bond linked **166** and ether molecules.

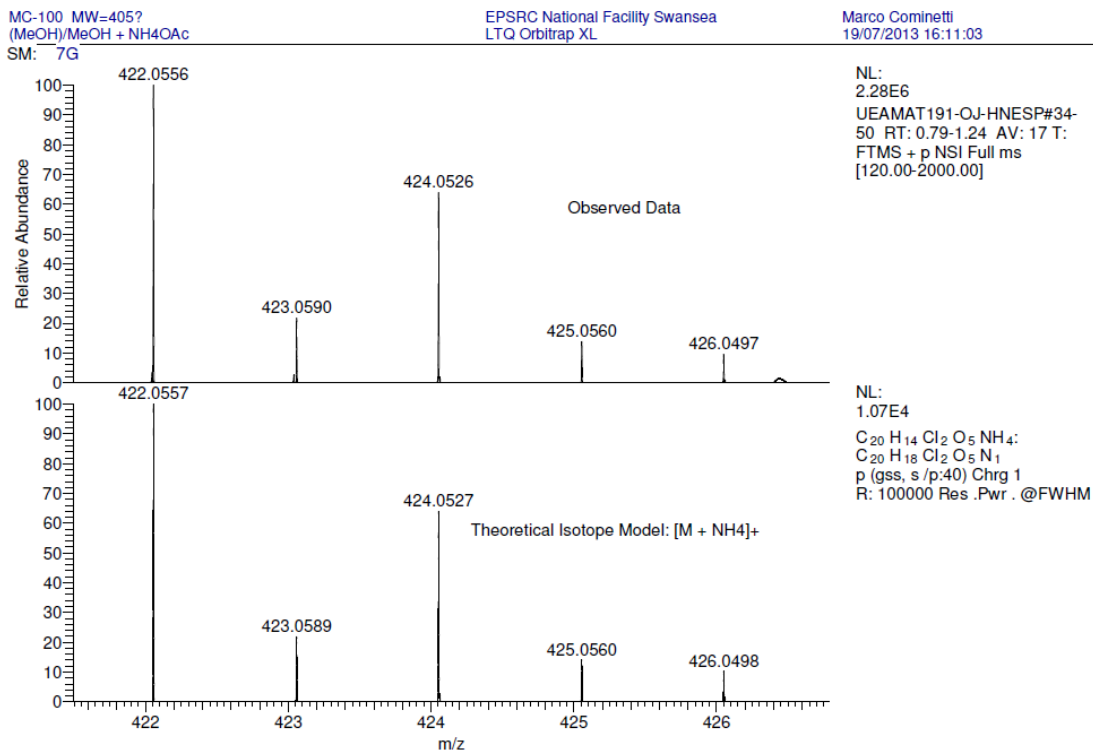
Compound 167

MP: 214-216 °C

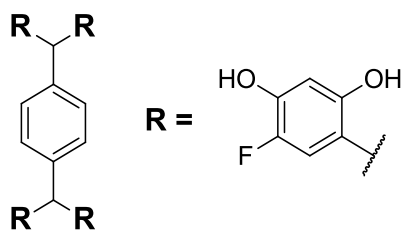
¹H-NMR (400 MHz, DMSO) δ 10.20 (s, 1H), 9.92 (s, 2H), 9.57 (s, 2H), 7.80 (dd, *J* = 7.6, 1.4 Hz, 1H), 7.56 (dt, *J* = 7.7, 1.4 Hz, 1H), 7.42 (adt, *J* = 7.6 Hz, 1H), 6.94 (add, *J* = 7.7 Hz, 1H), 6.55 – 6.53 (m, 3H), 6.36 (s, 2H).

^{13}C -NMR (101 MHz, DMSO) δ 191.70, 153.88, 152.05, 146.41, 133.80, 132.95, 129.76, 129.39, 128.92, 126.67, 121.67, 108.95, 103.79, 37.06.

IR (ν_{max} , cm^{-1}): 3420.5, 3366, 3168, 1649, 1613.5, 1594.5, 1521, 1420.5, 1366, 1274, 1251.5, 1217.5, 1194.5, 1174, 1132.5, 1090, 1030.5, 903.5, 895, 866.5, 832.5.



Compound 168



Method 1

A mixture of terephthalaldehyde (116.3 mg, 0.87 mmol) and 4-fluororesorcinol (500 mg, 3.90 mmol) was dissolved in 3 ml of ethanol/HCl 37% (1/1, v/v) and allowed to stir at 70 °C for 5 h. The solvent was evaporated and the resulting orange solid obtained was suspended in water, collected by filtration and washed with water. The light orange powder was dried in the desiccator for one week to give 238.9 mg of product.

Yield: 35% (calculated from NMR to account for solvent of crystallisation)

Method 2

0.56 mL of methanesulfonic acid was added to a pre-cooled (0 °C) mixture of terephthalaldehyde (104.7 mg, 0.78 mmol) and 4-fluororesorcinol (500 mg, 3.90 mmol) in 7 mL of Et₂O/DCM (1/1, v/v). The reaction vessel was sealed and the reaction allowed to stir for 7 h. The mixture was poured into 75 mL of Et₂O and cooled for 18 h at 4 °C. The resulting solid was collected and washed with diethyl ether to give a pale yellow powder (398.1 mg).

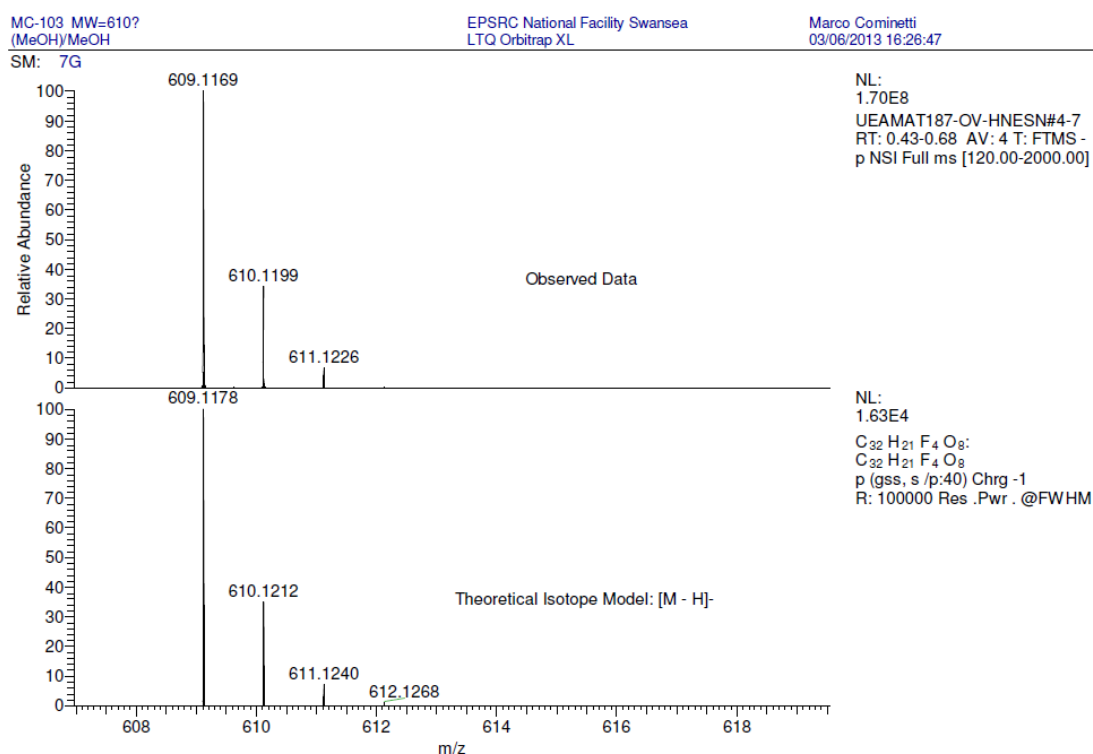
Yield: 65% (calculated from NMR to account for solvent of crystallisation)

MP: 194-195 °C

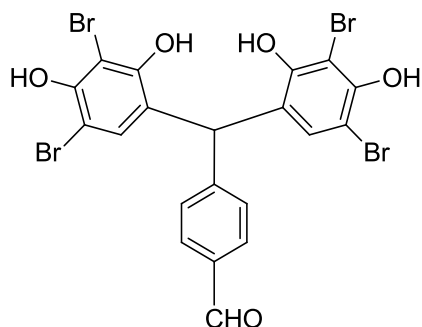
¹H-NMR - F decoupled (400 MHz, DMSO) δ 9.45 (s, 4H), 9.04 (s, 4H), 6.84 (s, 4H), 6.42 (s, 4H), 6.25 (s, 4H), 5.70 (s, 2H).

¹³C-NMR (101 MHz, DMSO) δ 144.07 (d, *J* = 230.0 Hz), 142.82 (d, *J* = 13.4 Hz), 120.88 (d, *J* = 4.6 Hz), 116.03 (d, *J* = 20.1 Hz), 104.41 (d, *J* = 1.5 Hz).

IR (ν_{max}, cm⁻¹): 3360, 1631, 1526, 1510.5, 1441, 1326, 1265.5, 1240, 1227, 1209.5, 1158.5, 1090.5, 901, 878.5, 844, 820.5.



Compound 180



1.28 mL of methanesulfonic acid was added to a pre-cooled (0 °C) mixture of terephthalaldehyde (500 mg, 3.73 mmol) and 2,4-dibromoresorcinol (6 g, 22.40 mmol) in 16 ml of Et₂O/DCM (1/1, v/v). The reaction vessel was sealed and the reaction allowed to stir vigorously for 8 d. The resulting solid was collected and washed with dichloromethane. The product was dried in the oven at 60 °C for 3 d to give 2.2748 g of **180** as a white powder

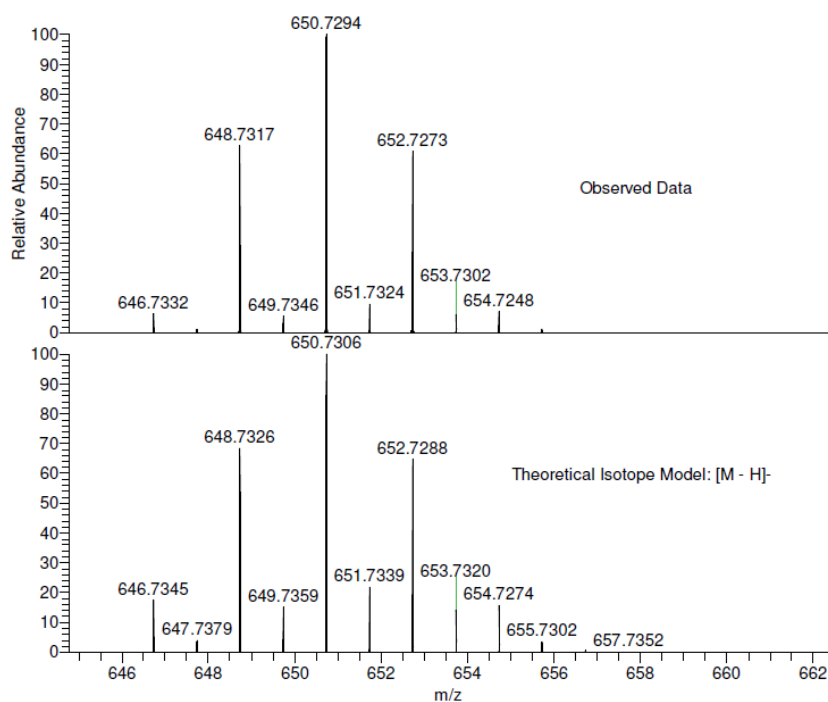
Yield: 85% (calculated from NMR to account for solvent of crystallisation)

MP: 244-245 °C

¹H-NMR (400 MHz, DMSO) δ 9.98 (s, 1H), 9.71 (s, 2H), 9.30 (s, 2H), 7.86 (d, *J* = 8.3 Hz, 2H), 7.24 (d, *J* = 8.3 Hz, 2H), 6.62 (s, 2H), 6.06 (s, 1H).

¹³C-NMR (101 MHz, DMSO) δ 192.61, 151.92, 150.09, 149.44, 134.63, 130.74, 129.70, 129.57, 124.44, 103.34, 100.69, 43.99.

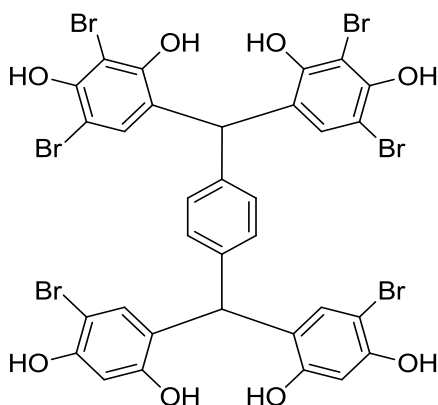
IR (ν_{max}, cm⁻¹): 3492.5, 3469.5, 2759, 1575, 1311, 1276.5, 1253, 1237.5, 1112, 1033.5, 1014.5, 982, 912.5, 871, 850.5.



NL:
6.63E6
UEAMAT183-OV-HNESN#2-7
RT: 0.26-0.68 AV: 6 T: FTMS -
p NSI Full ms [120.00-2000.00]

NL:
7.00E3
C₂₀H₁₁Br₄O₅:
C₂₀H₁₁Br₄O₅
p (gss, s /p:40) Chrg -1
R: 100000 Res .Pwr . @FWHM

Compound 181



0.72 ml of methanesulfonic acid was added to a pre-cooled (0 °C) mixture of **180** (400 mg, 0.61 mmol) and 4-bromoresorcinol (289.9 g, 1.534 mmol) in 9 ml of Et₂O/DCM (1/1, v/v). The reaction vessel was sealed and the reaction allowed to stir for 3 d. The mixture was poured into distilled water and extracted with ethyl acetate three times. The organic layers were combined, washed with brine and dried over anhydrous Na₂SO₄. The solvent was evaporated and the resulting solid was suspended in 50 mL of water. The mixture was allowed to stir vigorously for 15 minutes before being centrifuged (8500 rpm for 10 min). The supernatant solution was removed and the solid was washed two more times with a total of 100 mL of distilled water. The pink solid was dried in the desiccator for one week (485.6 mg).

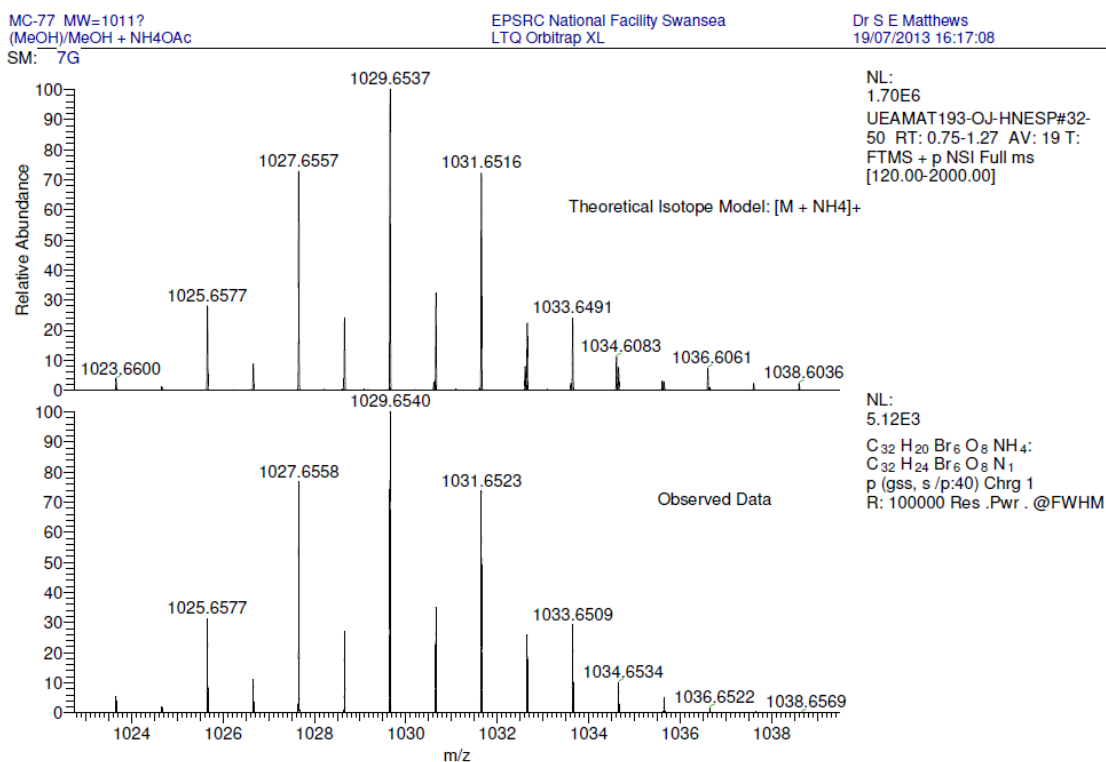
Yield: 75.64% (calculated from NMR to account for solvent of crystallisation)

MP: 189-191 °C

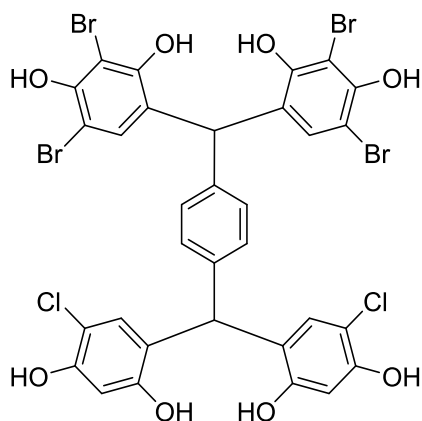
^1H -NMR (400 MHz, DMSO) δ 9.87 (s, 2H), 9.61 (s, 2H), 9.43 (s, 2H), 9.19 (s, 2H), 6.89 (s, 4H), 6.58 (s, 2H), 6.53 (s, 2H), 6.50 (s, 2H), 5.95 (s, 1H), 5.69 (s, 1H).

^{13}C -NMR (101 MHz, DMSO) δ 154.78, 152.70, 151.76, 149.71, 141.80, 139.48, 132.34, 130.78, 128.72, 128.57, 125.57, 123.26, 103.52, 103.18, 100.55, 97.50, 43.21, 41.32.

IR (ν_{max} , cm^{-1}): 3477.5, 1606, 1595.5, 1503.5, 1471, 1427, 1329, 1274.5, 1189.5, 1170, 1133, 1115.5, 1038, 1010.5, 892.5, 837.5.



Compound 182



0.96 mL of methanesulfonic acid was added to a pre-cooled (0 °C) mixture of **180** (500 mg, 0.77 mmol) and 2-chlororesorcinol (277.2 mg, 1.91 mmol) in 12 mL of Et₂O/DCM (1/1, v/v). The reaction vessel was sealed and the reaction allowed to stir for 2 d. The mixture was poured into distilled water and extracted with ethyl acetate three times. The organic layers were combined, washed with brine and dried over anhydrous Na₂SO₄. The solvent was evaporated and the resulting solid was suspended in 50 mL of water. The mixture was allowed to stir vigorously for 15 minutes before being centrifuged (8500 rpm for 10 min). The supernatant solution was removed and the solid was washed two more times with a total of 100 mL of distilled water. The solid was dried in the desiccator for one week.

MP: 184-186 °C

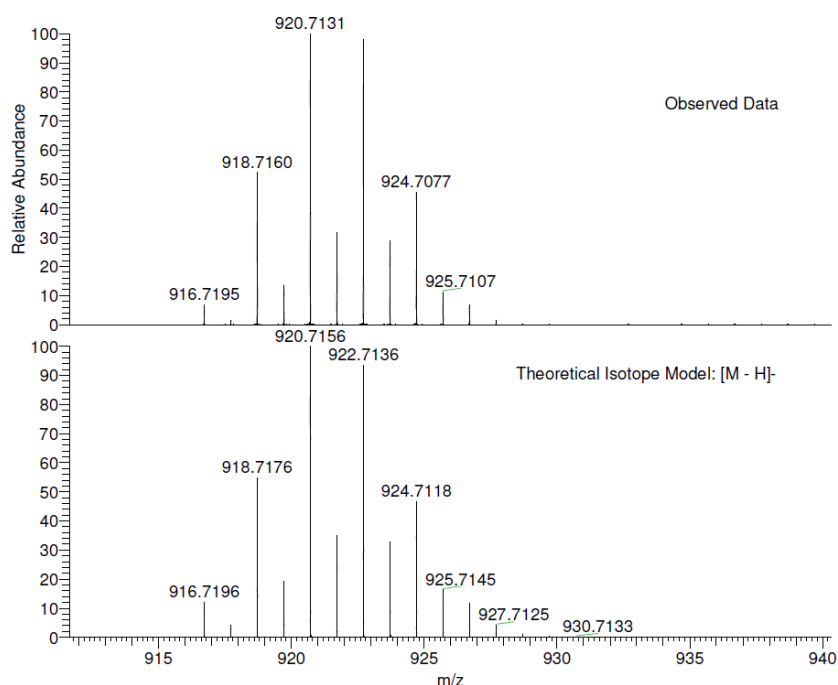
¹H-NMR (400 MHz, DMSO) δ 9.79 (s, 2H), 9.61 (s, 2H), 9.40 (s, 2H), 9.20 (s, 2H), 6.89 (s, 4H), 6.58 (s, 2H), 6.49 (s, 2H), 6.38 (s, 2H), 5.95 (s, 1H), 5.69 (s, 1H).

¹³C-NMR (101 MHz, DMSO) δ 154.61, 152.27, 152.12, 150.21, 142.29, 139.97, 131.27, 130.02, 129.22, 129.04, 126.06, 123.08, 109.22, 104.14, 103.68, 101.02, 43.72, 41.83.

MC-116 MW=923?
C₃₂H₂₀Br₄Cl₂O₈
(MeOH)/MeOH

EPSRC National Facility Swansea
LTQ Orbitrap XL

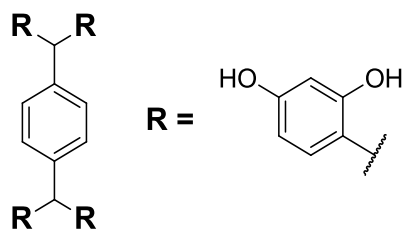
Marco Cominetti
04/09/2013 10:13:52



NL:
1.62E8
UEAMAT200-OJ-HNESN#1-5
RT: 0.20-0.43 AV: 4 T: FTMS -
p NSI Full ms [120.00-2000.00]

NL:
5.09E3
C₃₂H₁₉Br₄Cl₂O₈:
C₃₂H₁₉Br₄Cl₂O₈
p (gss, s/p:40) Chrg -1
R: 100000 Res .Pwr . @FWHM

Compound 183



Palladium over carbon (catalytic) was added to a solution of **163** (3.18 mmol) and triethylamine (12.37 mL, 88.72 mmol) in 150 mL of methanol. A hydrogen atmosphere was applied and the mixture was allowed to stir at 40 °C for 18 h. The catalyst was removed by filtration and the solution was dried under reduced pressure. The product was suspended in HCl 1.2 M and extracted with ethyl acetate three times. The organic layers were combined, washed with HCl 1.2 M, brine and dried over Na₂SO₄. Upon evaporation of the solvent the product was obtained as an orange powder (1.9341 g).

Note: the reaction can be carried out using **158** as substrate and comparable yields can be obtained at room temperature in the same timescale.

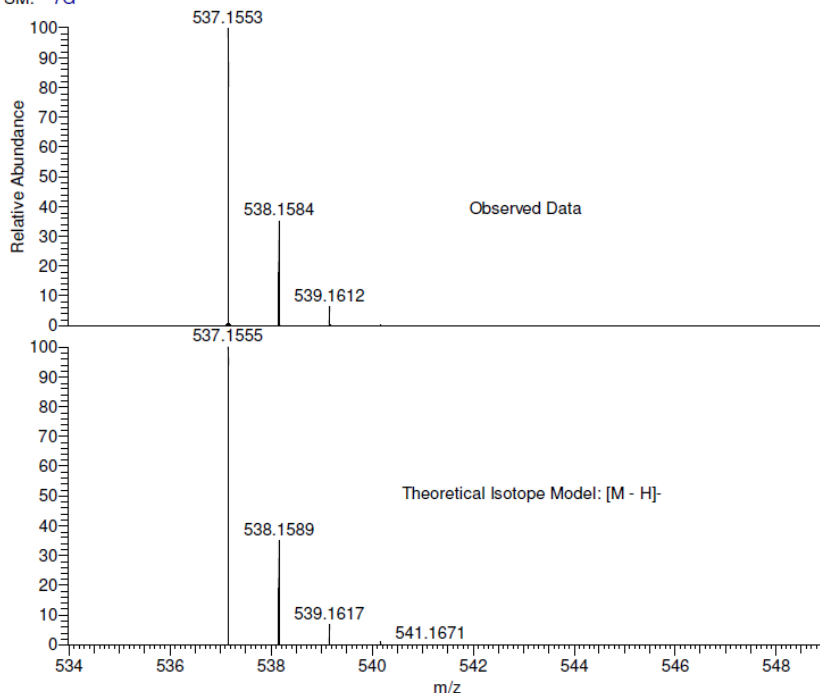
Yield: 96% (calculated from NMR to account for solvent of crystallisation)

MP: 178-180 °C

¹H NMR (400 MHz, DMSO) δ 8.94 (s, 4H), 8.92 (s, 4H), 6.78 (s, 4H), 6.41 (d, *J* = 8.3 Hz, 4H), 6.22 (d, *J* = 2.3 Hz, 4H), 6.07 (dd, *J* = 8.3, 2.3 Hz, 4H), 5.73 (s, 2H).

¹³C NMR (101 MHz, DMSO) δ 156.52, 155.74, 142.49, 130.49, 128.62, 122.10, 105.80, 102.79, 41.21.

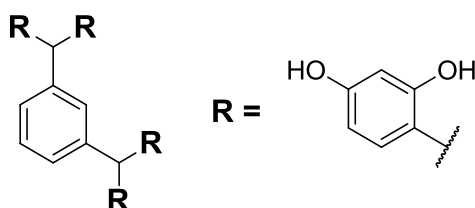
IR (ν_{max}, cm⁻¹): 3291, 1601, 1512.5, 1504.5, 1452, 1374.5, 1298.5, 1248, 1197, 1158.5, 1091, 972, 834.5.



NL:
6.08E7
UEAMAT186-OV-HNESN#2-6
RT: 0.26-0.60 AV: 5 T: FTMS -
p NSI Full ms [120.00-2000.00]

NL:
1.63E4
C₃₂ H₂₅ O₈:
C₃₂ H₂₅ O₈:
p (gss, s /p:40) Chrg -1
R: 100000 Res .Pwr . @FWHM

Compound 184



Palladium over carbon (catalytic) was added to a solution of **164** (0.34 mmol) and triethylamine (1.24 mL, 8.87 mmol) in 20 mL of ethanol. A hydrogen atmosphere was applied and the mixture was allowed to stir at 60 °C for 18 h. The catalyst was removed by filtration and the solution was dried under reduced pressure. The product was suspended in HCl 1.2 M and extracted with ethyl acetate three times. The organic layers were combined, washed with HCl 1.2 M, brine and dried over Na₂SO₄. Upon evaporation of the solvent the product was obtained as an orange powder (160.9 mg).

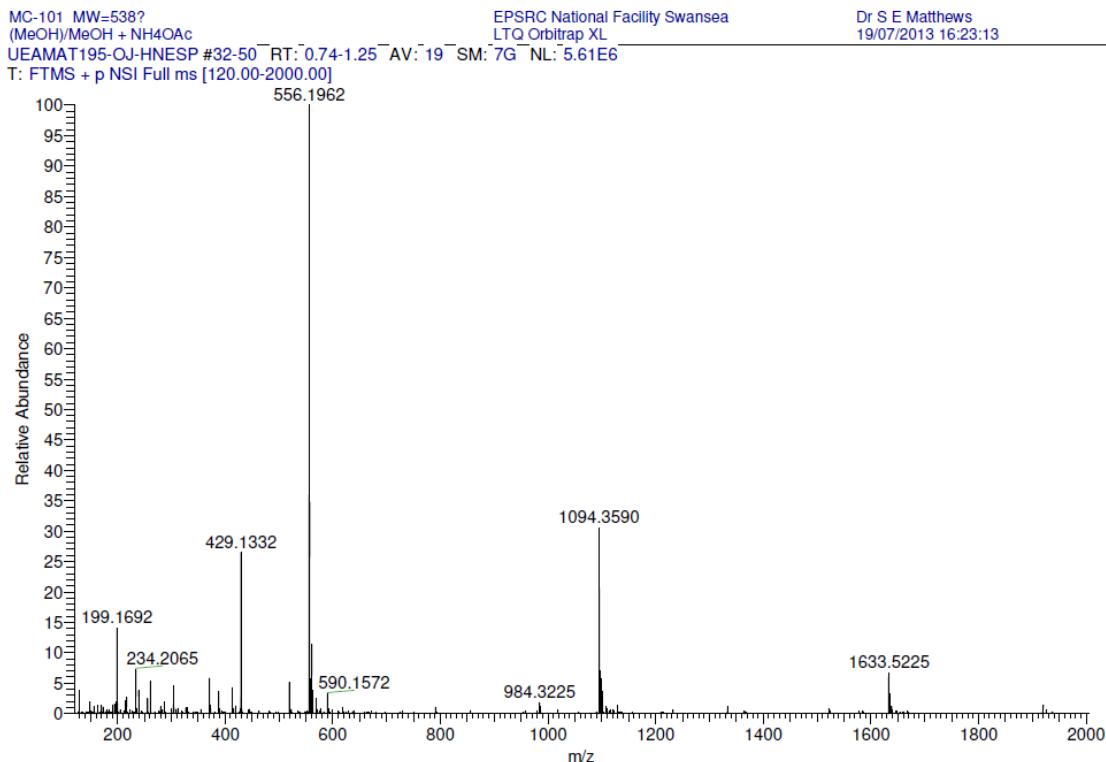
Yield: 62% (calculated from NMR to account for solvent of crystallisation)

MP: 165-167 °C

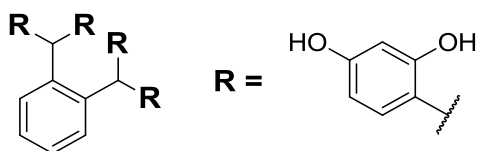
¹H NMR (400 MHz, DMSO) δ 8.98 (d, 4H), 8.91 (s, 4H), 7.01 (t, *J* = 7.8 Hz, 1H), 6.71 (s, 1H), 6.64 (d, *J* = 7.8 Hz, 2H), 6.34 (d, *J* = 8.3 Hz, 4H), 6.21 (d, *J* = 2.2 Hz, 4H), 6.04 (dd, *J* = 8.3, 2.2 Hz, 4H), 5.67 (s, 2H).

^{13}C NMR (101 MHz, DMSO) δ 156.49, 155.72, 145.03, 130.66, 130.49, 127.24, 126.15, 122.08, 105.70, 102.80, 41.77.

IR (ν_{max} , cm^{-1}): 3302.5, 1600.5, 1515.5, 1506, 1451.5, 1297.5, 1246.5, 1155.5, 1090.5, 972, 833.5.



Compound 185



Palladium over carbon (catalytic) was added to a solution of **165** (0.23 mmol) and triethylamine (0.99 mL, 7.10 mmol) were dissolved in 12 mL of ethanol. A hydrogen atmosphere was applied and the mixture was allowed to stir at 60 °C for 18 h. The catalyst was removed by filtration and the solution was dried under reduced pressure. The product was suspended in HCl 1.2 M and extracted with ethyl acetate three times. The organic layers were combined, washed with HCl 1.2 M, brine and dried over Na₂SO₄. Upon evaporation of the solvent the product was obtained as an orange powder (101.6 mg).

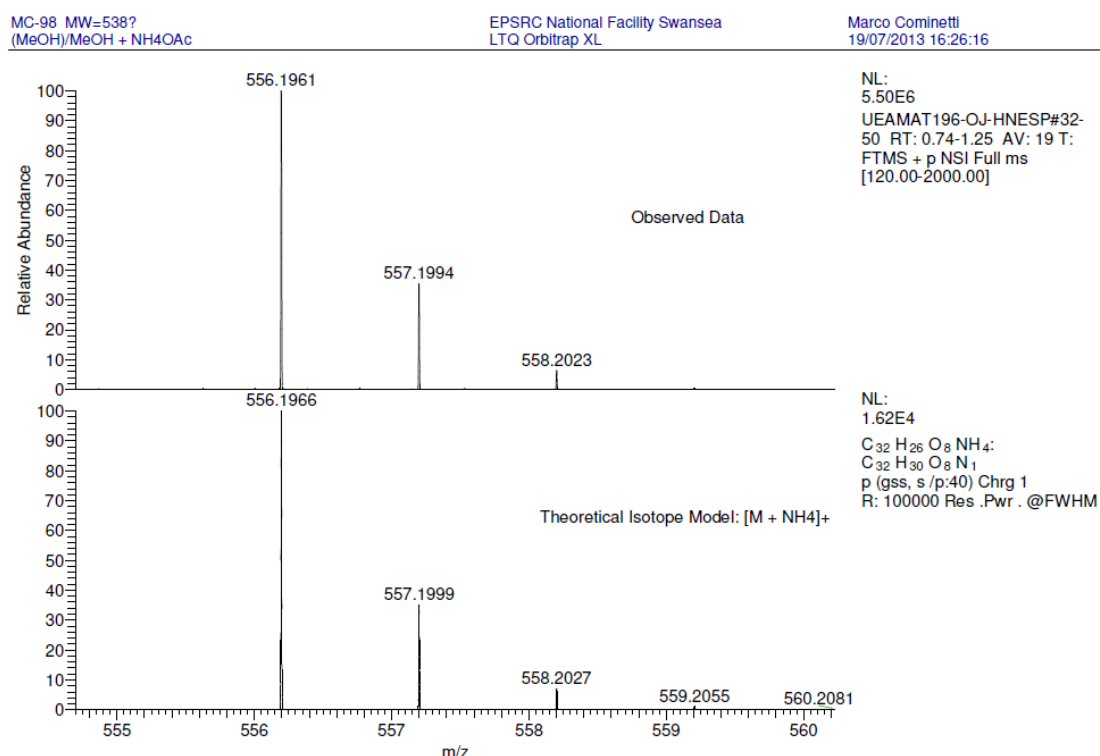
Yield: 69% (calculated from NMR to account for solvent of crystallisation)

MP: 216-218 °C

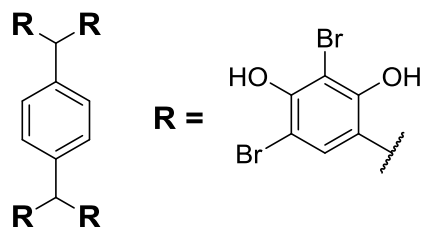
^1H NMR (400 MHz, DMSO) δ 8.79 (s, 4H), 8.20 (s, 4H), 6.98 (dd, $J = 5.7, 3.5$ Hz, 2H), 6.74 (dd, $J = 5.7, 3.5$ Hz, 2H), 6.26 (d, $J = 8.3$ Hz, 4H), 6.14 (d, $J = 2.4$ Hz, 4H), 5.99 (dd, $J = 8.3, 2.4$ Hz, 4H), 5.73 (s, 2H).

^{13}C NMR (101 MHz, DMSO) δ 155.89, 155.33, 142.77, 130.07, 129.01, 124.67, 121.08, 104.95, 102.20, 38.8. (The peak at 38.8 is overlaid with DMSO and was assigned by HSQC)

IR (ν_{max} , cm^{-1}): 3501.5, 3306.5, 1599, 1516.5, 1505.5, 1454, 1373.5, 1336.5, 1291.5, 1249.5, 1214.5, 1182, 1168, 1150.5, 1092.5, 970.5, 834.



Compound 186



A solution of freshly recrystallised NBS (0.5 g, 0.585 mmol) in 10 mL of acetonitrile was added to a stirring solution of **163** (0.5 g, 2.81 mmol) in 10 mL of acetonitrile. After 25 minutes the solid product was collected by Büchner filtration and thoroughly washed with water. The solid was dried under vacuum to give the product as a red-orange powder.

Yield: 63% (calculated from NMR to account for solvent of crystallisation)

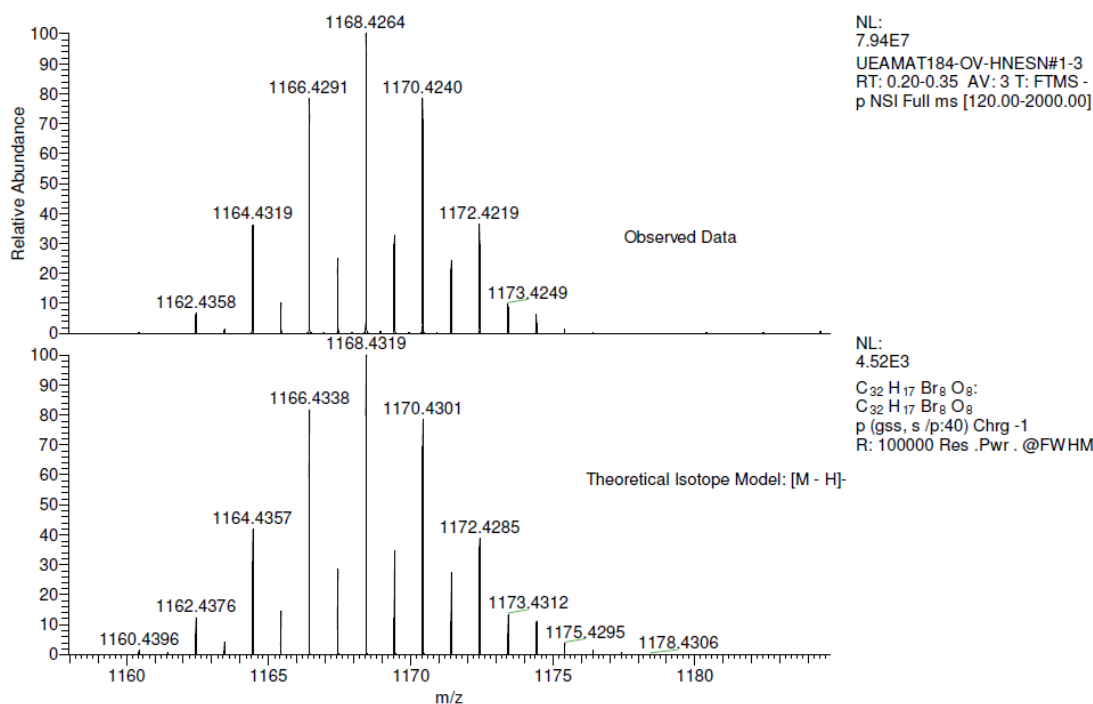
^1H -NMR (400 MHz, DMSO) δ 9.63 (s, 4H), 9.21 (s, 4H), 6.96 (s, 2H), 6.60 (s, 2H), 5.97 (s, 1H).

^{13}C -NMR (101 MHz, DMSO) δ 152.26, 150.26, 140.72, 131.26, 129.38, 125.93, 103.68, 101.07, 43.73.

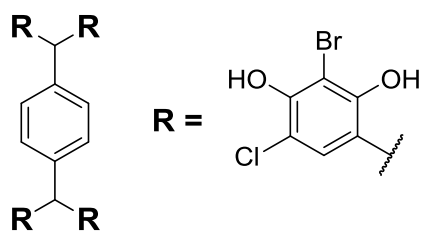
MC-75 MW=1169?
(MeOH)/MeOH

EPSRC National Facility Swansea
LTQ Orbitrap XL

Marco Gominetti
03/06/2013 16:14:21



Compound 187



NBS (505.3 mg, 2.84 mmol) was added to a stirring solution of **163** (400 mg, 0.59 mmol) in 16 mL of acetonitrile. After 30 minutes the reaction was diluted with water. The solid product was collected by Büchner filtration and thoroughly washed with water. The solid was dried under vacuum to give the product as a light orange powder.

Yield: 39.3% (calculated from NMR to account for solvent of crystallisation)

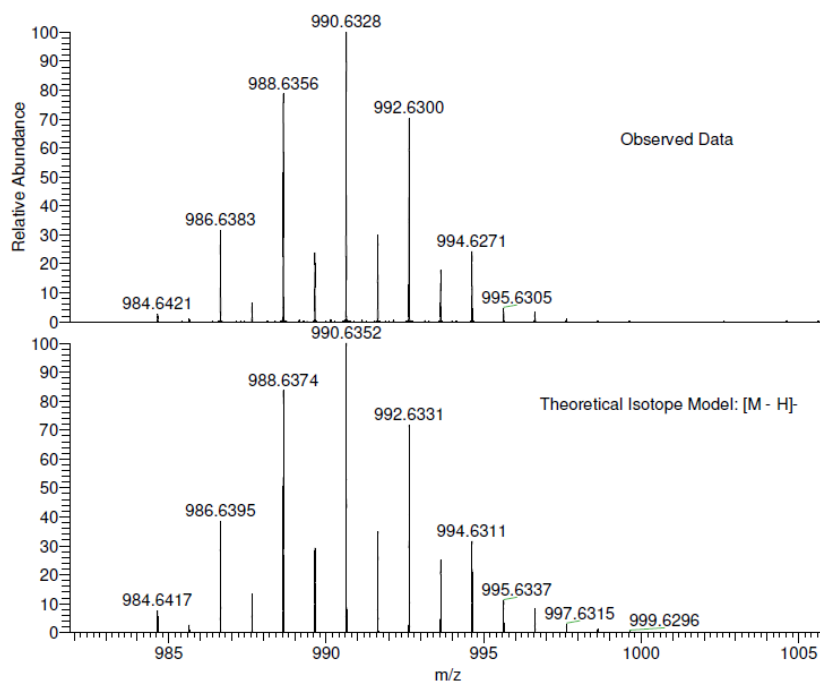
^1H -NMR (400 MHz, DMSO) δ 9.78 (s, 2H), 9.17 (s, 2H), 6.94 (s, 2H), 6.44 (s, 2H), 5.97 (s, 1H).

^{13}C -NMR (101 MHz, DMSO) δ 151.75, 149.38, 140.72, 129.37, 128.37, 125.09, 111.89, 103.53, 43.74.

MC-114 MW=991?
C₃₂H₁₈Br₄Cl₄O₈
(MeOH)/MeOH

EPSRC National Facility Swansea
LTQ Orbitrap XL

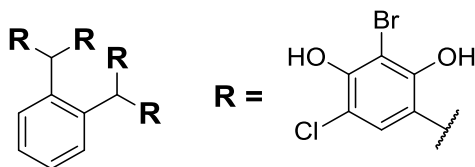
Marco Cominetti
04/09/2013 10:34:11



NL:
1.22E8
UEAMAT207-OJ-HNESN#1-4
RT: 0.20-0.43 AV: 4 T: FTMS -
p NSI Full ms [120.00-2000.00]

NL:
4.76E3
C₃₂ H₁₇ Br₄ Cl₄ O₈:
C₃₂ H₁₇ Br₄ Cl₄ O₈:
p (gss, s /p:40) Chrg -1
R: 100000 Res .Pwr . @FWHM

Compound 188

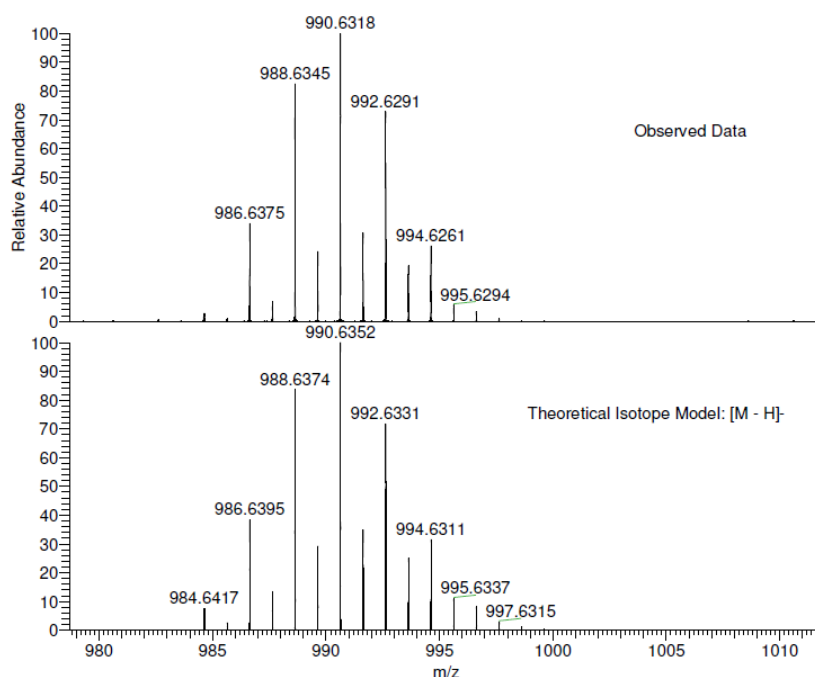


A solution of freshly recrystallised NBS (107.9 mg, 0.601 mmol) in 2 mL of acetonitrile was added to a stirring solution of **165** (100 mg, 0.148 mmol) in 2 mL of acetonitrile. After 20 minutes the reaction was quenched with 70 mg (0.555 mmol) of phloroglucinol, and diluted with water. The solid product was collected by Büchner filtration and thoroughly washed with water. The solid was dried under vacuum to give the product as a brown powder.

Yield: 84.3% (calculated from NMR to account for solvent of crystallisation)

^1H -NMR (400 MHz, DMSO) δ 9.53 (s, 2H), 8.46 (s, 2H), 7.25 – 7.13 (m, 2H), 6.89 – 6.79 (m, 2H), 6.28 (s, 2H), 6.23 (s, 1H).

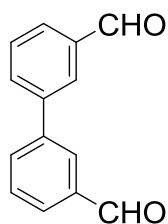
^{13}C -NMR (101 MHz, DMSO) δ 151.49, 149.05, 140.92, 129.57, 128.46, 126.82, 124.06, 111.52, 103.08, 40.81.



NL:
1.20E8
UEAMAT204-OJ-HNESN#1-5
RT: 0.20-0.43 AV: 4 T: FTMS -
p NSI Full ms [120.00-2000.00]

NL:
4.76E3
C₃₂ H₁₇ Br₄ Cl₄ O₈:
C₃₂ H₁₇ Br₄ Cl₄ O₈:
p (gss, s/p:40) Chrg -1
R: 100000 Res .Pwr . @FWHM

Compound 191⁹⁵



To a allowed to stir solution of 3-formylphenylboronic acid (1.0 g, 6.669 mmol), 3-bromobenzaldehyde (0.778 mL, 6.669 mmol), DMF (160 mL) and Na₂CO₃ (4.241 g, 40.014 mmol) in water (16 mL), a catalytic amount of 5% Pd(dppf)Cl₂ (0.033 mmol) was added. The flask was flushed with argon and the reaction mixture was allowed to stir for 18 hours at 40 °C. The solvent was removed under reduced pressure and the product was purified by column chromatography (DCM/Hexane 1:1) to give **191** as a white solid.

Yield: 69%

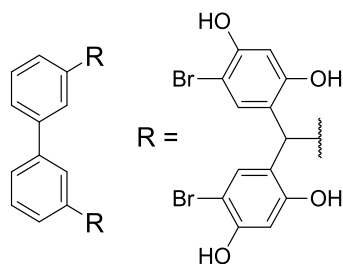
[M+NH₄]⁺ = 228.1016 (Calculated: 228.1019)

MP: 93-95 °C (lit. 92-94 °C)⁹⁵

¹H-NMR (400 MHz, CDCl₃) δ 10.14 (s, 1H), 8.18 (s, 1H), 8.04 – 7.86 (m, 2H), 7.69 (t, *J* = 7.7 Hz, 1H).

^{13}C -NMR (101 MHz, CDCl_3) δ 192.03, 140.71, 137.10, 132.99, 129.80, 129.47, 128.01.

Compound 192



0.16 mL of methanesulfonic acid was added to a pre-cooled (0 °C) mixture of **191** (100.6 mg, 0.48 mmol) and 4-bromoresorcinol (406.4 mg, 2.15 mmol) in 2 mL of $\text{Et}_2\text{O}/\text{DCM}$ (1/1, v/v). The reaction vessel was sealed and the reaction allowed to stir for 6 h. The resulting mixture was diluted with diethyl ether, poured into distilled water and allowed to stir vigorously until a suspension was obtained. The product was collected by Büchner filtration, washed with abundant distilled water and dried in a desiccator to give an orange powder.

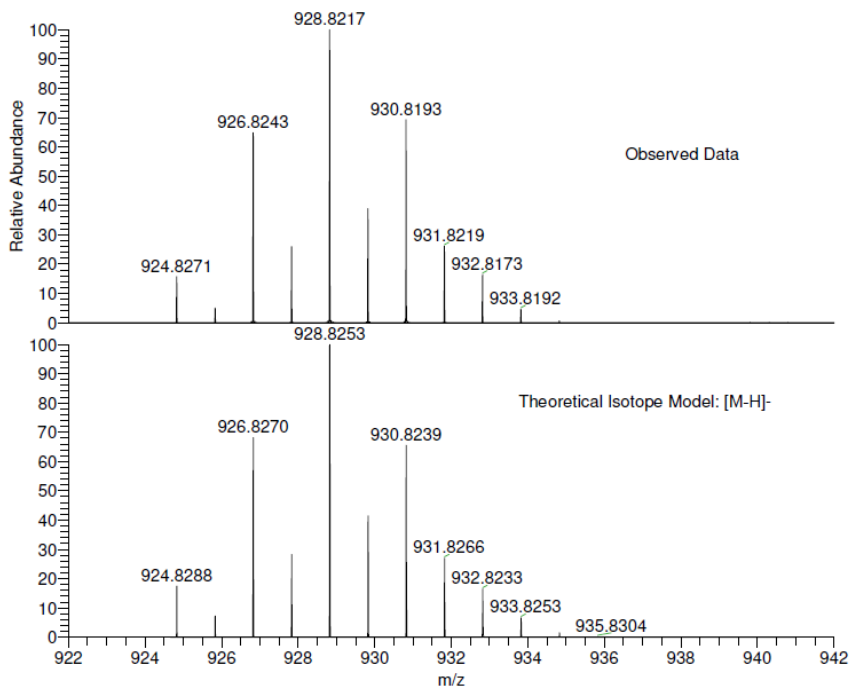
Yield: 87.5% (calculated from NMR to account for solvent of crystallisation)

MP: 257-258 °C

^1H -NMR (400 MHz, DMSO) δ 9.90 (s, 4H), 9.46 (s, 4H), 7.39 – 7.31 (m, 4H), 7.22 (s, 2H), 6.94 – 6.87 (m, 2H), 6.61 (s, 4H), 6.51 (s, 4H), 5.76 (s, 2H).

^{13}C -NMR (101 MHz, DMSO) δ 155.35, 153.28, 144.93, 140.46, 132.75, 129.22, 128.24, 127.61, 124.72, 123.48, 104.12, 97.99, 42.55.

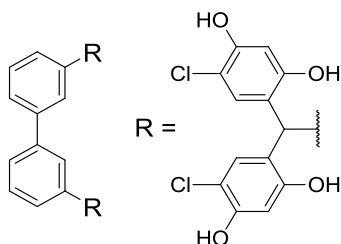
IR (ν_{max} , cm^{-1}): 3624, 3526, 3480, 3278, 1606, 1591, 1501, 1488, 1430, 1393, 1335, 1277, 1211, 1190, 1161, 1116, 1010, 904, 836, 823.



NL:
7.26E7
UEAMAT221-OJ-HNESN#59-
62 RT: 1.51-1.73 AV: 4 T:
FTMS - p NSI Full ms
[200.00-4000.00]

NL:
5.76E3
C₃₈ H₂₅ Br₄ O₈:
C₃₈ H₂₅ Br₄ O₈
p (gss, s/p:40) Chrg -1
R: 100000 Res .Pwr .@FWHM

Compound 193



0.16 mL of methanesulfonic acid was added to a pre-cooled (0 °C) mixture of **191** (101.2 mg, 0.48 mmol) and 4-chlororesorcinol (310.5 mg, 2.15 mmol) in 2 mL of Et₂O/DCM (1/1, v/v). The reaction vessel was sealed and the reaction allowed to stir for 6 h. The resulting mixture was diluted with diethyl ether, poured into distilled water and allowed to stir vigorously until a suspension was obtained. The product was collected by Büchner filtration, washed with abundant distilled water and dried in a desiccator to give an off yellow powder.

Yield: 99.5% (calculated from NMR to account for solvent of crystallisation)

MP: 261-270 °C

¹H-NMR (400 MHz, DMSO) δ 9.82 (s, 4H), 9.43 (s, 4H), 7.33 (m, 4H), 7.21 (s, 2H), 7.00 – 6.84 (m, 2H), 6.50 (s, 4H), 6.47 (s, 4H), 5.76 (s, 2H).

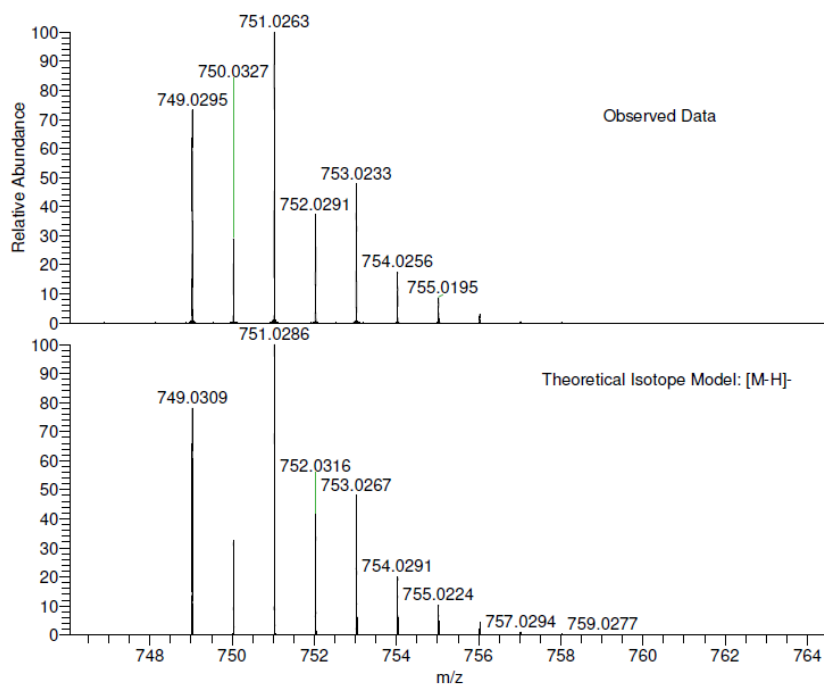
^{13}C -NMR (101 MHz, DMSO) δ 154.67, 152.21, 144.93, 140.47, 129.96, 129.22, 128.26, 127.59, 124.71, 122.82, 109.24, 104.24, 42.53.

IR (ν_{max} , cm^{-1}): 3526, 3491, 1612, 1595, 1491, 1434, 1335, 1278, 1244, 1226, 1214, 1189, 1160, 1148, 1117, 1023, 905, 859, 836.

MC-136 MW=752?
C₃₈H₂₆Cl₄O₈
(MeOH)/MeOH

EPSRC National Facility Swansea
LTQ Orbitrap XL

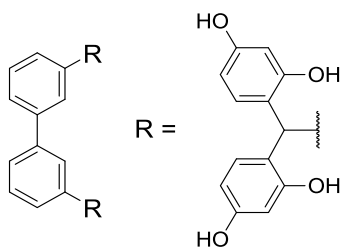
Marco Cominetti
05/12/2013 13:19:54



NL:
9.27E7
UEAMAT222-OJ-HNESN#44-
49 RT: 1.51-1.73 AV: 4 T:
FTMS - p NSI Full ms
[200.00-4000.00]

NL:
6.44E3
C₃₈H₂₅Cl₄O₈:
C₃₈H₂₅Cl₄O₈
p (gss, s/p:40) Chrg -1
R: 100000 Res .Pwr . @FWHM

Compound 194



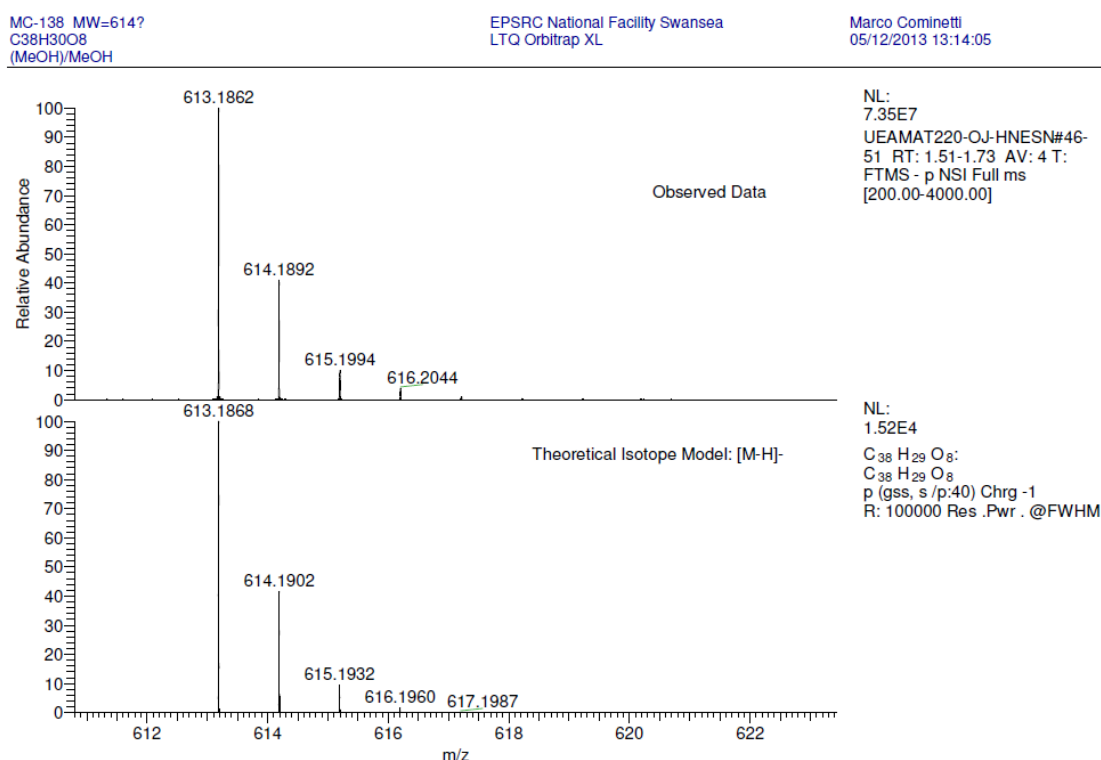
Palladium over carbon (catalytic) was added to a solution of **193** (0.97 mmol) and triethylamine (3.55 mL, 25.5 mmol) in 48 mL of ethanol. A hydrogen atmosphere was applied and the mixture was allowed to stir at 50 °C for 18 h. The catalyst was removed by filtration and the solution was dried under reduced pressure. The product was suspended in HCl 1.2 M and extracted with ethyl acetate three times. The organic layers were combined, washed with HCl 1.2 M, brine and dried over Na₂SO₄. The solvent was removed under reduced pressure and the solid obtained was suspended in water, collected by Büchner filtration and washed thoroughly with water. The product was then dried in a desiccator to give an orange powder.

Yield: 38.8% (calculated from NMR to account for solvent of crystallisation)

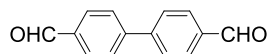
^1H -NMR (400 MHz, DMSO) δ 9.01 (s, 4H), 8.97 (s, 4H), 7.31 – 7.19 (m, 4H), 7.11 (s, 2H), 6.91 (d, J = 7.3 Hz, 2H), 6.45 (d, J = 8.3 Hz, 4H), 6.25 (d, J = 2.3 Hz, 4H), 6.11 (dd, J = 8.3, 2.3 Hz, 4H), 5.83 (s, 1H).

^{13}C -NMR (101 MHz, DMSO) δ 156.70, 155.79, 146.66, 140.46, 130.54, 128.72, 128.35, 127.63, 124.03, 121.59, 105.95, 102.89, 41.97.

IR (ν_{max} , cm^{-1}): 3307, 1601, 1518, 1506, 1453, 1298, 1157, 1090, 973, 834.



Compound 197



To a allowed to stir solution of 4-formylphenylboronic acid (1.0 g, 6.669 mmol), 4-bromobenzaldehyde (1.3 g, 6.8 mmol), DMF (160 mL) and Na₂CO₃ (4.3 g, 0.04 mol) in water (16 mL), a catalytic amount of 5% Pd(dppf)Cl₂ (0.033 mmol) was added. The flask was flushed with argon and the reaction mixture was allowed to stir for 18 hours at 40 °C. The solvent was removed under reduced pressure and the product was purified by column chromatography (DCM/Hexane 1:1) to give **197** as white solid.

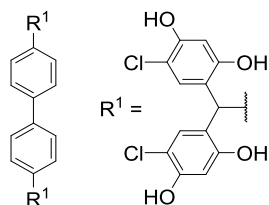
Yield: 86% (calculated from NMR to account for solvent of crystallisation)

MP: 155-158 °C

^1H NMR (400 MHz, DMSO) δ 10.10 (s, 2H), 8.10 – 7.98 (m, 8H).

^{13}C NMR (101 MHz, DMSO) δ 193.29, 144.86, 136.28, 130.67, 128.40.

Compound 198



0.56 mL of methanesulfonic acid was added to a pre-cooled (0 °C) mixture of **197** (0.3 g, 1.2 mmol) and 4-chlororesorcinol (0.8 mg, 5.4 mmol) in 7 ml of Et₂O/DCM (1/1, v/v). The reaction vessel was sealed and the reaction allowed to stir for 18 h. The resulting mixture was diluted with diethyl ether, poured into distilled water and allowed to stir vigorously until a suspension was obtained. The product was collected by Büchner filtration, washed with abundant distilled water and dried in a desiccator to give an orange powder.

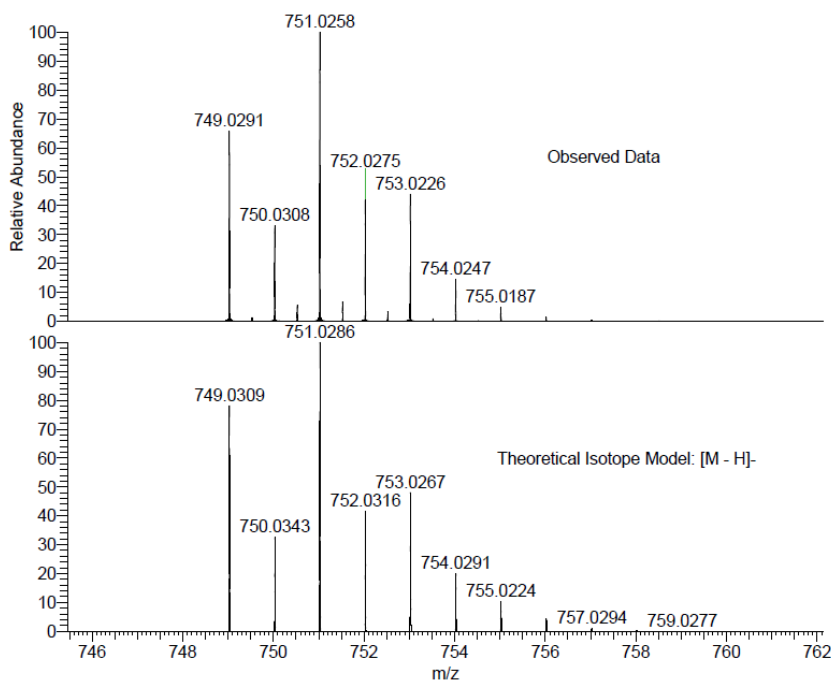
Yield: 79% (calculated from NMR to account for solvent of crystallisation)

MP: 195-200 °C

^1H -NMR (400 MHz, DMSO) δ 9.83 (s, 4H), 9.45 (s, 4H), 7.56 (d, J = 8.3 Hz, 4H), 7.03 (d, J = 8.3 Hz, 4H), 6.52 (s, 4H), 6.45 (s, 4H), 5.74 (s, 2H).

^{13}C -NMR (101 MHz, DMSO) δ 154.69, 152.21, 143.28, 137.93, 129.97, 129.73, 126.73, 122.91, 109.21, 104.22, 41.99.

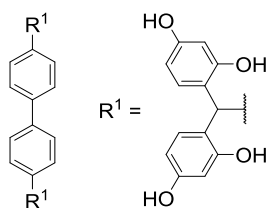
IR (ν_{max} , cm^{-1}): 3335, 2359, 2361, 2338, 1612, 1492, 1432, 1330, 1275, 1233, 1169, 1122, 1025, 1007, 896, 882, 867.



NL:
3.74E7
UEAMAT243-OA-HNESN#3-18
RT: 0.04-0.44 AV: 15 T:
FTMS - p NSI Full ms
[140.00-1935.00]

NL:
6.44E3
C₃₈H₂₅Cl₄O₈:
C₃₈H₂₅Cl₄O₈
p (gss, s /p:40) Chrg -1
R: 100000 Res .Pwr . @FWHM

Compound 199



Palladium over carbon (catalytic) was added to a solution of **198** (300 mg, 0.348 mmol) and triethylamine (1.33 mL, 9.57 mmol) in 20 mL of ethanol. A hydrogen atmosphere was applied and the mixture was allowed to stir at 50 °C for 5 h. The catalyst was removed by filtration and the solution was dried under reduced pressure. The product was suspended in HCl 1.2 M and extracted with ethyl acetate three times. The organic layers were combined, washed with HCl 1.2 M, brine and dried over Na₂SO₄. The solvent was removed under reduced pressure and the solid obtained was suspended in water, collected by Büchner filtration and washed thoroughly with water. The product was then dried in a desiccator to give an orange powder.

Yield: 68.7% (calculated from NMR to account for solvent of crystallisation)

MP: 180-185 °C

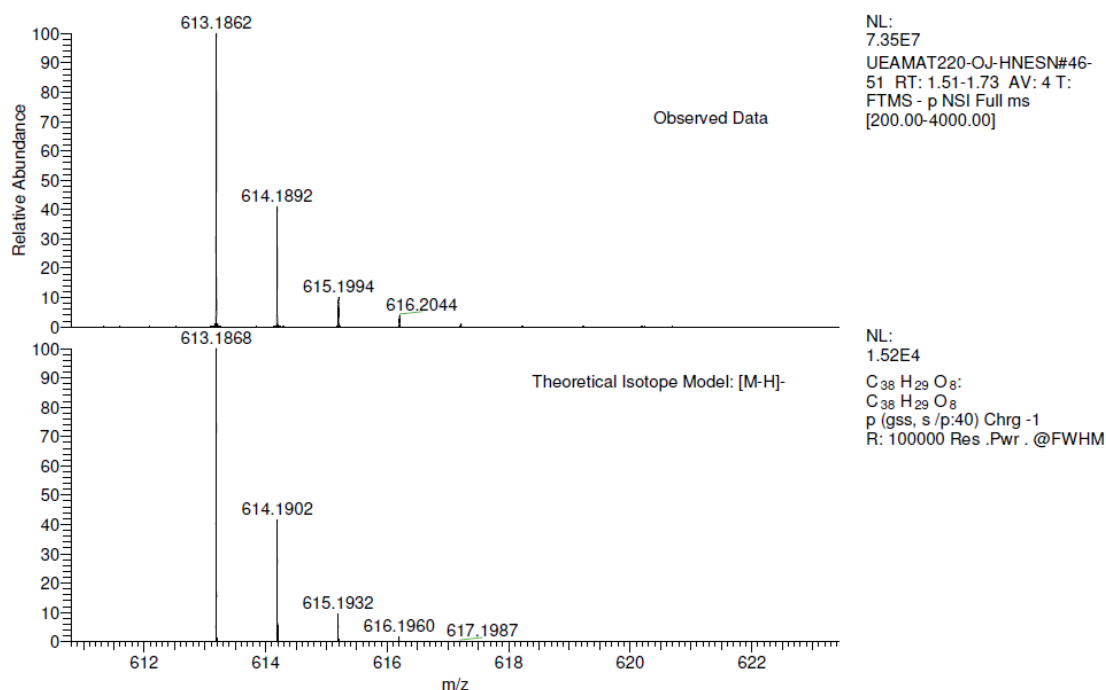
^1H NMR (400 MHz, DMSO) δ 9.02 (s, 4H), 8.97 (s, 4H), 7.46 (d, J = 8.3 Hz, 4H), 7.00 (d, J = 8.3 Hz, 4H), 6.45 (d, J = 8.3 Hz, 4H), 6.26 (d, J = 2.4 Hz, 4H), 6.10 (dd, J = 8.3, 2.4 Hz, 4H), 5.81 (s, 2H).

^{13}C NMR (101 MHz, DMSO) δ 156.71, 155.83, 144.95, 137.67, 130.54, 129.75, 126.31, 121.69, 105.88, 102.85, 41.55.

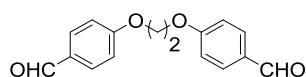
MC-138 MW=614?
C₃₈H₃₀O₈
(MeOH)/MeOH

EPSRC National Facility Swansea
LTQ Orbitrap XL

Marco Cominetti
05/12/2013 13:14:05



Compound 204⁸⁷



A stirring mixture of 4-hydroxybenzaldehyde (5 g, 40.94 mmol) and potassium carbonate (14.1 g, 102 mmol) in acetone (250 mL) was boiled under reflux for 1 hour. 1,2-Dibromoethane (1.41 mL, 16.376 mmol) was added and the mixture was allowed to stir overnight. The solid residue was removed by filtration and washed with DCM. The filtrates were combined and evaporated under reduced pressure. The product was purified by column chromatography (DCM).

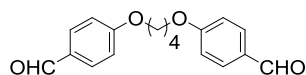
Yield: 12%

MP: 120-122 °C (lit. 127-129 °C)⁸⁷

$^1\text{H-NMR}$ (400 MHz, CDCl_3) δ 9.84 (s, 1H), 7.89 – 7.74 (m, 2H), 7.09 – 6.94 (m, 2H), 4.38 (s, 2H).

$^{13}\text{C-NMR}$ (101 MHz, CDCl_3) δ 190.76, 163.40, 132.04, 130.43, 114.89, 66.51.

Compound 205⁹⁶



A stirring mixture of 4-hydroxybenzaldehyde (5 g, 40.94 mmol) and potassium carbonate (14.1 g, 102 mmol) in acetone (250 mL) was boiled under reflux for 1 hour. 1,4-Dibromobutane (1.96 mL, 16.376 mmol) was added and the mixture was allowed to stir overnight. The solid residue was removed by filtration and washed with DCM. The filtrates were combined and evaporated under reduced pressure. The product was purified by column chromatography (DCM).

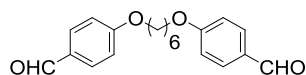
Yield: 68.2%

MP: 275-277 °C

$^1\text{H-NMR}$ (400 MHz, CDCl_3) δ 9.92 (s, 1H), 7.94 – 7.80 (m, 2H), 7.08 – 6.96 (m, 2H), 4.26 – 4.08 (m, 2H), 2.14 – 1.94 (m, 2H).

$^{13}\text{C-NMR}$ (101 MHz, DMSO) δ 190.78, 163.96, 132.02, 129.98, 114.73, 67.76, 25.81.

Compound 206⁸⁷



A stirring mixture of 4-hydroxybenzaldehyde (5 g, 40.94 mmol) and potassium carbonate (14.1 g, 102 mmol) in acetone (250 mL) was refluxed for 1 hour. 1,6-Dibromohexane (2.52 mL, 16.376 mmol) was added and the mixture was allowed to stir overnight. The solid residue was removed by filtration and washed with DCM. The filtrates were combined and evaporated under reduced pressure. The product was purified by column chromatography (DCM).

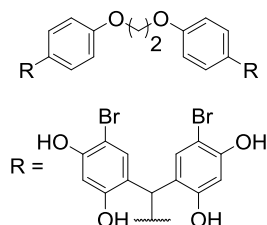
Yield: 48.5%

MP: 109-111 °C (lit. 113-115 °C)⁸⁷

^1H -NMR (400 MHz, CDCl_3) δ 9.91 (s, 1H), 7.93 – 7.78 (m, 2H), 7.08 – 6.95 (m, 2H), 4.09 (t, J = 6.4 Hz, 2H), 1.96 – 1.80 (m, 2H), 1.63 – 1.57 (m, 2H).

^{13}C -NMR (101 MHz, CDCl_3) δ 190.81, 164.16, 132.01, 129.85, 114.74, 68.18, 29.00, 25.78.

Compound 207



0.16 mL of methanesulfonic acid was added to a pre-cooled (0 °C) mixture of **204** (136.1 mg, 0.50 mmol) and 4-bromoresorcinol (443.6 mg, 2.35 mmol) in 2 ml of $\text{Et}_2\text{O}/\text{DCM}$ (1/1, v/v). The reaction vessel was sealed and the reaction allowed to stir for 24 h. The resulting mixture was diluted with diethyl ether, poured into distilled water and allowed to stir vigorously until a suspension was obtained. The product was collected by Büchner filtration, washed with abundant distilled water and dried in a desiccator to give an orange powder.

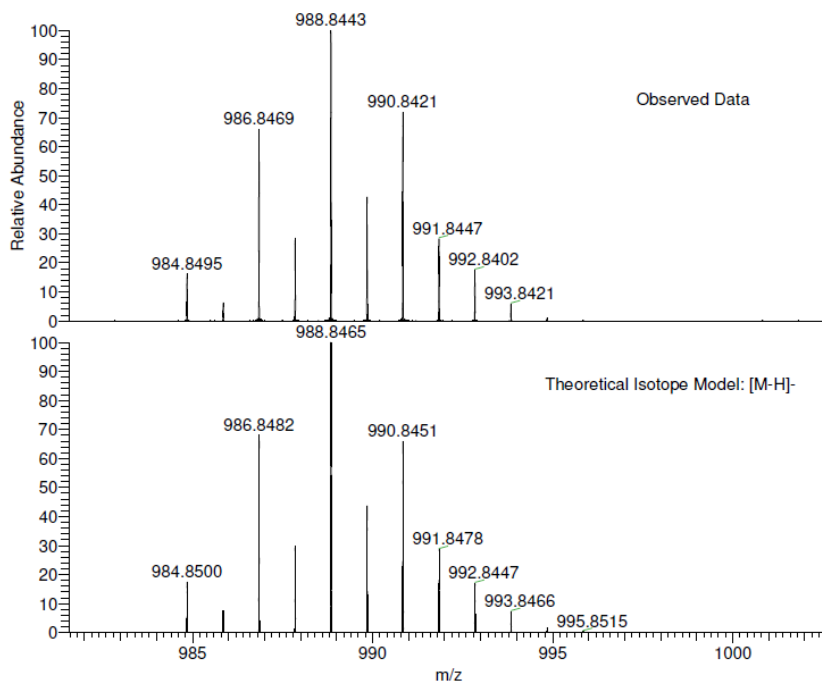
Yield: 57.9% (calculated from NMR to account for solvent of crystallisation)

MP: 180-182 °C

^1H -NMR (400 MHz, DMSO) δ 9.87 (s, 4H), 9.41 (s, 4H), 6.88 (m, 8H), 6.54 (s, 4H), 6.50 (s, 4H), 5.65 (s, 2H), 4.26 (s, 4H).

^{13}C -NMR (101 MHz, DMSO) δ 156.90, 155.30, 153.14, 136.20, 132.67, 130.16, 124.07, 114.53, 104.04, 97.88, 66.70, 41.44.

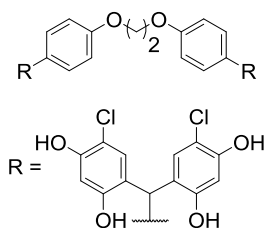
IR (ν_{max} , cm^{-1}): 3543, 3434, 1607, 1507, 1418, 1331, 1242, 1224, 1209, 1189, 1174, 1114, 1073, 1058, 1010, 930, 898, 871, 830.



NL:
1.88E7
UEAMAT219-OJ-HNESN#44-
47 RT: 1.51-1.73 AV: 4 T:
FTMS - p NSI Full ms
[200.00-4000.00]

NL:
5.63E3
C₄₀ H₂₉ Br₄ O₁₀:
C₄₀ H₂₉ Br₄ O₁₀
p (gss, s/p:40) Chrg -1
R: 100000 Res.Pwr. @FWHM

Compound 208



0.32 mL of methanesulfonic acid was added to a pre-cooled (0 °C) mixture of **204** (199.7 mg, 0.74 mmol) and 4-chlororesorcinol (492 mg, 3.4 mmol) in 4 ml of Et₂O/DCM (1/1, v/v). The reaction vessel was sealed and the reaction allowed to stir for 24 h. The resulting mixture was diluted with diethyl ether, poured into distilled water and allowed to stir vigorously until a suspension was obtained. The product was collected by Büchner filtration, washed with abundant distilled water and dried in a desiccator to give an orange powder.

Yield: 75.1% (calculated from NMR to account for solvent of crystallisation)

MP: 162-163 °C

¹H-NMR (400 MHz, DMSO) δ 9.79 (s, 4H), 9.37 (s, 4H), 6.88 (s, 8H), 6.49 (s, 4H), 6.40 (s, 4H), 5.65 (s, 2H), 4.26 (s, 4H).

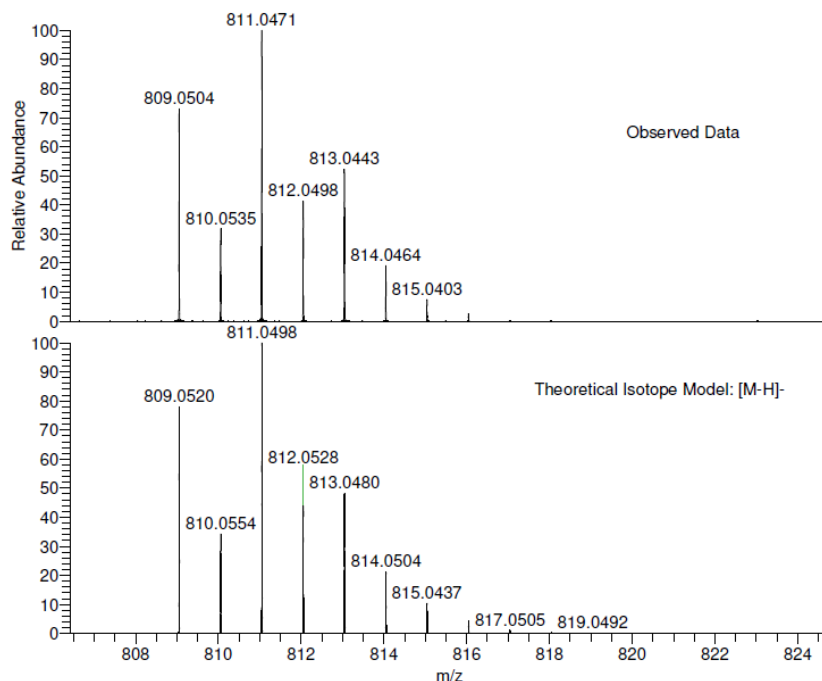
^{13}C -NMR (101 MHz, DMSO) δ 156.90, 154.62, 152.07, 136.22, 130.17, 129.89, 123.40, 114.52, 109.12, 104.16, 66.71, 41.45.

IR (ν_{max} , cm^{-1}): 3538, 3503, 3422, 1606, 1509, 1423, 1333, 1241, 1225, 1209, 1181, 1118, 1072, 1060, 1028, 931, 897, 878, 866, 836.

MC-135 MW-812?
C₄₀H₃₀Cl₄O₁₀
(MeOH)/MeOH

EPSRC National Facility Swansea
LTQ Orbitrap XL

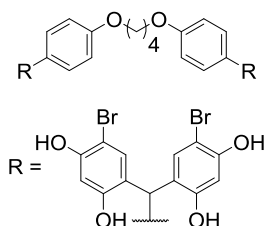
Marco Gominetti
05/12/2013 13:22:46



NL:
7.33E7
UEAMAT223-OJ-HNESN#49-
50 RT: 1.65-1.73 AV: 2 T:
FTMS - p NSI Full ms
[200.00-4000.00]

NL:
6.28E3
C₄₀ H₂₉ Cl₄ O₁₀:
C₄₀ H₂₉ Cl₄ O₁₀
p (gss, s/p:40) Chrg -1
R: 100000 Res. Pwr. @FWHM

Compound 209



0.16 mL of methanesulfonic acid was added to a pre-cooled (0 °C) mixture of **205** (130.6 mg, 0.44 mmol) and 4-bromoresorcinol (285.2 mg, 1.97 mmol) in 2 mL of Et₂O/DCM (1/1, v/v). The reaction vessel was sealed and the reaction allowed to stir for 24 h. The resulting mixture was diluted with diethyl ether, poured into distilled water and allowed to stir vigorously until a suspension was obtained. The product was collected by Büchner filtration, washed with abundant distilled water and dried in a desiccator to give an orange powder.

Yield: 70.7% (calculated from NMR to account for solvent of crystallisation)

MP: 219-220 °C

^1H -NMR (400 MHz, DMSO) δ 9.86 (s, 4H), 9.40 (s, 4H), 6.84 (s, 8H), 6.54 (s, 4H), 6.49 (s, 4H), 5.64 (s, 2H), 3.99 (s, 4H), 1.86 (s, 4H).

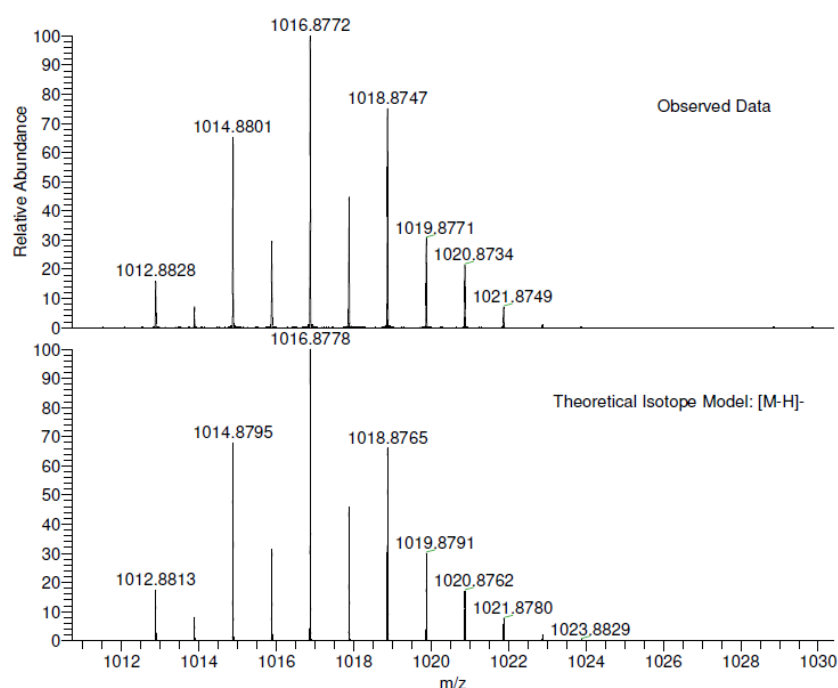
^{13}C -NMR (101 MHz, DMSO) δ 157.19, 155.29, 153.12, 135.86, 132.66, 130.10, 124.12, 114.48, 104.04, 97.87, 67.49, 41.43, 26.05.

IR (ν_{max} , cm^{-1}): 3480, 3382, 1610, 1585, 1511, 1492, 1425, 1414, 1386, 1328, 1271, 1245, 1192, 1167, 1148, 1113, 1051, 1009, 975, 906, 869, 836, 809.

MC-140 MW=1018?
C₄₂H₃₄Br₄O₁₀
(MeOH)/MeOH

EPSRC National Facility Swansea
LTQ Orbitrap XL

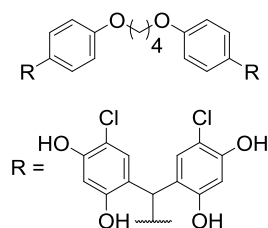
Marco Cominetti
05/12/2013 13:08:18



NL:
3.06E6
UEAMAT218-OJ-HNESN#61-
64 RT: 1.51-1.75 AV: 4 T:
FTMS - p NSI Full ms
[200.00-4000.00]

NL:
5.52E3
C₄₂ H₃₃ Br₄ O₁₀:
C₄₂ H₃₃ Br₄ O₁₀
p (gss, s/p:40) Chrg -1
R: 100000 Res.Pwr. @FWHM

Compound 210



0.16 mL of methanesulfonic acid was added to a pre-cooled (0 °C) mixture of **205** (100.1 mg, 0.34 mmol) and 4-chlororesorcinol (218.3 mg, 1.51 mmol) in 2 mL of Et₂O/DCM (1/1, v/v). The reaction vessel was sealed and the reaction allowed to stir for 24 h. The resulting mixture was diluted with diethyl ether, poured into distilled water and allowed to stir vigorously until a suspension was obtained. The product was

collected by Büchner filtration, washed with abundant distilled water and dried in a desiccator to give an orange powder.

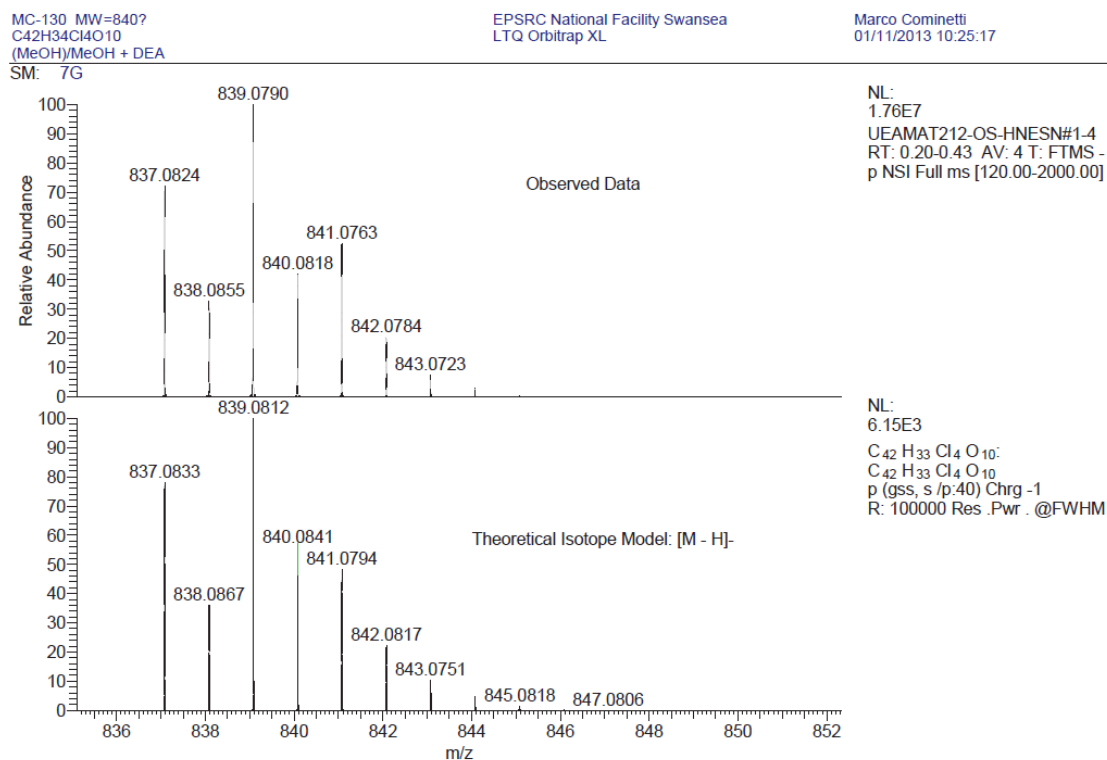
Yield: 69.7% (calculated from NMR to account for solvent of crystallisation)

MP: 294-295 °C

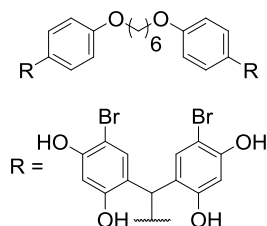
^1H -NMR (400 MHz, DMSO) δ 9.78 (s, 4H), 9.36 (s, 4H), 6.84 (s, 8H), 6.49 (s, 4H), 6.40 (s, 4H), 5.64 (s, 2H), 3.99 (s, 4H), 1.85 (s, 4H).

^{13}C -NMR (101 MHz, DMSO) δ 157.19, 154.61, 152.05, 135.87, 130.11, 129.88, 123.45, 114.48, 109.10, 104.16, 67.48, 41.43, 26.05.

IR (ν_{max} , cm^{-1}): 3584, 3491, 3382, 1610, 1588, 1504, 1424, 1387, 1330, 1244, 1234, 1194, 1174, 1117, 1051, 1028, 974, 905, 873, 838, 828.



Compound 211



0.24 mL of methanesulfonic acid was added to a pre-cooled (0 °C) mixture of **206** (151.5 mg, 0.46 mmol) and 4-bromoresorcinol (391 mg, 2.1 mmol) in 3 mL of Et₂O/DCM (1/1, v/v). The reaction vessel was sealed and the reaction allowed to stir for 24 h. The resulting mixture was diluted with diethyl ether, poured into distilled water and allowed to stir vigorously until a suspension was obtained. The product was collected by Büchner filtration, washed with abundant distilled water and dried in a desiccator to give an orange powder.

Yield: 83.8% (calculated from NMR to account for solvent of crystallisation)

MP: 184-185 °C

¹H-NMR (400 MHz, DMSO) δ 9.86 (s, 4H), 9.40 (s, 4H), 6.93 – 6.74 (m, 8H), 6.53 (s, 4H), 6.49 (s, 4H), 5.64 (s, 2H), 3.92 (t, *J* = 6.3 Hz, 4H), 1.72 (bs, 4H), 1.47 (bs, 4H).

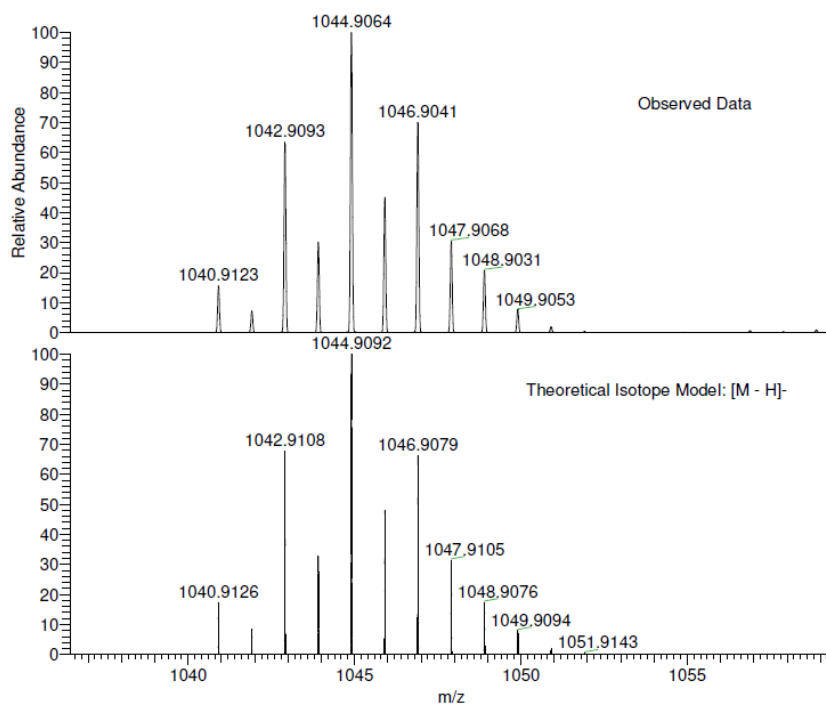
¹³C-NMR (101 MHz, DMSO) δ 157.23, 155.28, 153.11, 135.78, 132.66, 130.09, 124.12, 114.45, 104.03, 97.86, 67.70, 41.41, 29.25, 25.89.

IR (ν_{max}, cm⁻¹): 3474, 2937, 2862, 1608, 1592, 1506, 1425, 1333, 1234, 1194, 1171, 1116, 1007, 901, 876, 834.

MC-141 MW=1046?
(MeOH)/MeOH

EPSRC National Facility Swansea
LTQ Orbitrap XL

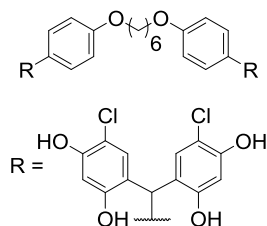
Marco cominetti
05/12/2013 16:11:12



NL:
3.95E7
UEAMAT217-OJ-HNESN-2#40-
83 RT: 0.96-2.02 AV: 44 T:
FTMS - p NSI Full ms
[150.00-2000.00]

NL:
5.41E3
C₄₄H₃₇Br₄O₁₀:
C₄₄H₃₇Br₄O₁₀
p (gss, s/p:40) Chrg -1
R: 100000 Res .Pwr .@FWHM

Compound 212



0.32 mL of methanesulfonic acid was added to a pre-cooled (0 °C) mixture of **206** (199.7 mg, 0.61 mmol) and 4-chlororesorcinol (398.9 mg, 2.76 mmol) in 4 ml of Et₂O/DCM (1/1, v/v). The reaction vessel was sealed and the reaction allowed to stir for 24 h. The resulting mixture was diluted with diethyl ether, poured into distilled water and allowed to stir vigorously until a suspension was obtained. The product was collected by Büchner filtration, washed with abundant distilled water and dried in a desiccator to give a red powder.

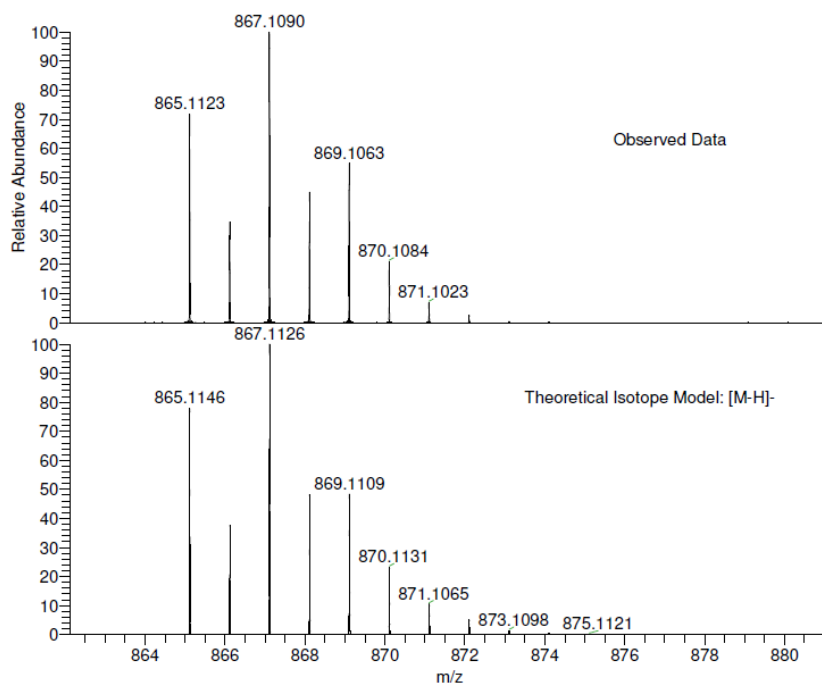
Yield: 60.7% (calculated from NMR to account for solvent of crystallisation)

MP: 132-133 °C

¹H-NMR (400 MHz, DMSO) δ 9.78 (s, 4H), 9.37 (s, 4H), 6.92 – 6.76 (m, 8H), 6.49 (s, 4H), 6.40 (s, 4H), 5.64 (s, 2H), 3.92 (t, *J* = 6.3 Hz, 4H), 1.72 (bs, 4H), 1.47 (bs, 4H).

¹³C-NMR (101 MHz, DMSO) δ 157.23, 154.61, 152.05, 135.79, 130.10, 129.88, 123.46, 114.45, 109.10, 104.16, 67.70, 41.42, 29.26, 25.89.

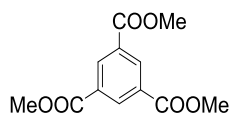
IR (ν_{max}, cm⁻¹): 3399, 1607, 1504, 1427, 1335, 1235, 1198, 1171, 1118, 1024, 1010, 899, 881, 870, 836.



NL:
5.96E7
UEAMAT224-OJ-HNESN#48-
49 RT: 1.65-1.73 AV: 2 T:
FTMS - p NSI Full ms
[200.00-4000.00]

NL:
6.02E3
C₄₄ H₃₇ Cl₄ O₁₀:
C₄₄ H₃₇ Cl₄ O₁₀
p (gss, s /p:40) Chrg -1
R: 100000 Res .Pwr . @FWHM

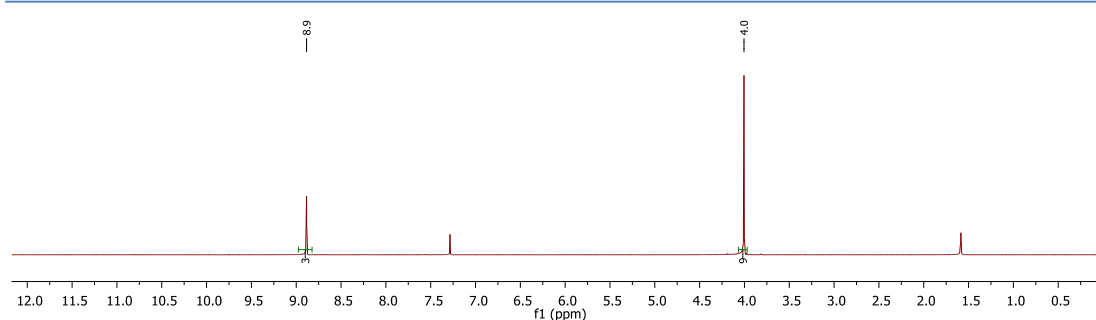
Compound 214⁹⁷



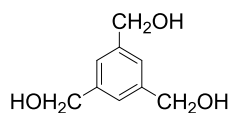
Prepared according to Dimick.⁹⁷

Concentrated sulphuric acid (2.5 mL) was added to a stirring solution of benzene-1,3,5-tricarboxylic acid (10 g, 47.62 mmol) in methanol (175 mL) and the solution was heated at reflux for 24 hours. The solvent was removed under reduced pressure and the residue was dissolved in chloroform. The organic phase was washed twice with a saturated solution of sodium bicarbonate, dried over magnesium sulfate and then evaporated under reduced pressure to give the product.

Product was used as crude for the synthesis of **215**, ¹H-NMR (CDCl₃) is reported for reference.



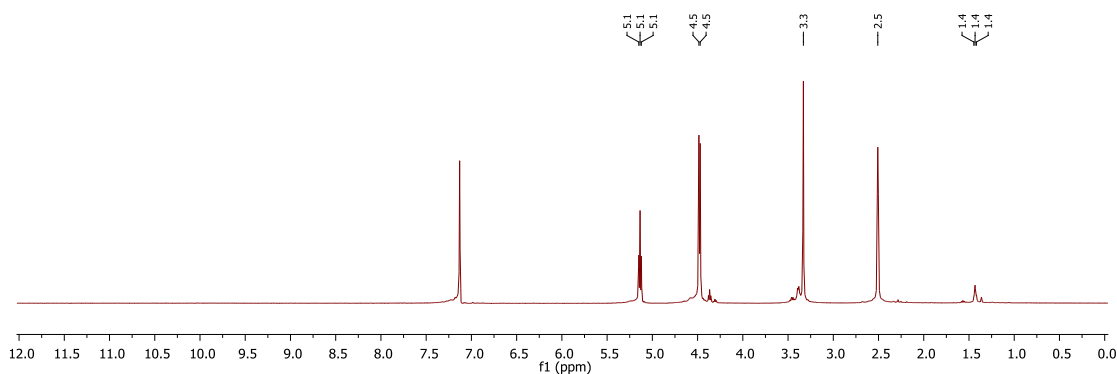
Compound 215⁸⁸



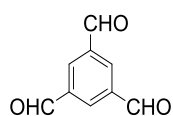
Prepared according to Kaur,⁸⁸ with minor modifications.

154R (5 g, 19.84 mmol) in dry THF (75 mL) and added drop-wise to a mixture of LiAlH_4 (4.6 g, 121.2 mmol) in anhydrous THF (165 mL) and allowed to stir for 36 hours. The reaction was quenched by addition of a mixture of NaHSO_4 and Celite (4:1). After 112 hours of stirring at room temperature, the mixture was filtered and washed with ethanol. The filtrate was evaporated under reduced pressure to give **215**.

The product was used as crude for the synthesis of **216**, a ^1H -NMR (CDCl_3) is reported for reference.



Compound 216⁸⁸



Prepared according to Kaur.⁸⁸

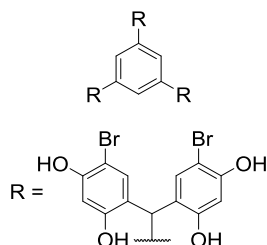
Pyridinium chlorochromate (11.661 g, 54.1 mmol) was slowly added to a stirring mixture of **215** (2.0487 g, 12.18 mmol) in dichloromethane (50 mL). After 30 minutes the mixture was diluted with acetone (20 mL) and allowed to stir for 3 hours. The solid residue was removed by filtration and washed with DCM. The organic layers were collected, washed with three times with a saturated solution of sodium carbonate, dried over sodium sulfate and evaporated under reduced pressure. The residue was purified by flash chromatography (DCM).

Yield: 31.4%

$^1\text{H-NMR}$ (400 MHz, DMSO) δ 10.23 (s, 1H), 8.67 (s, 1H).

$^{13}\text{C-NMR}$ (101 MHz, DMSO) δ 189.82, 137.82, 134.79.

Compound 217



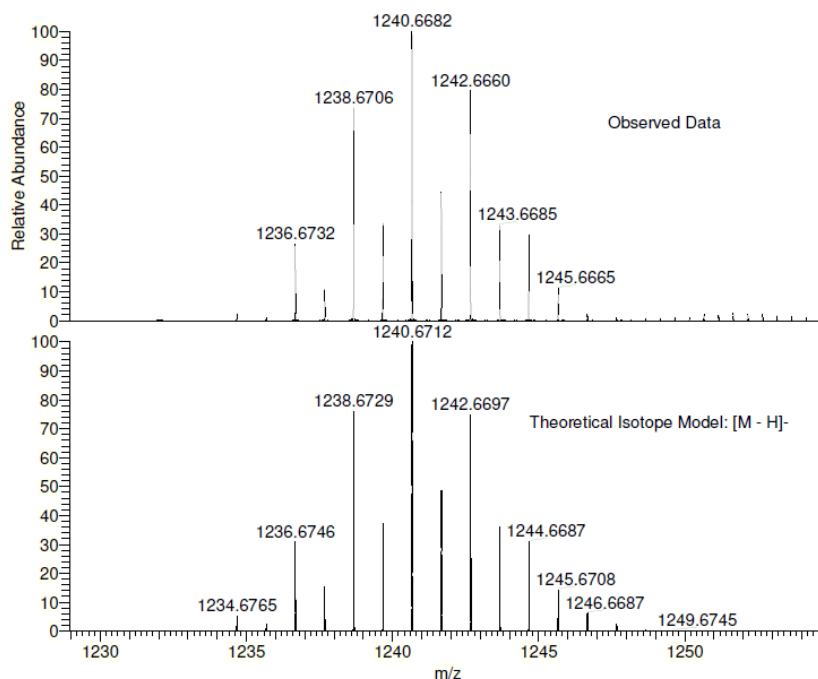
0.48 mL of methanesulfonic acid was added to a pre-cooled (0 °C) mixture of **216** (100 mg, 0.6 mmol) and 4-bromoresorcinol (816.5 mg, 4.32 mmol) in 6 ml of Et₂O/DCM (1/1, v/v). The reaction vessel was sealed and the reaction allowed to stir for 24 h. The resulting mixture was diluted with diethyl ether, poured into distilled water and allowed to stir vigorously until a suspension was obtained. The product was collected by Büchner filtration, washed with abundant distilled water and dried in a desiccator to give a yellow powder.

Yield: 57.6% (calculated from NMR to account for solvent of crystallisation)

$^1\text{H-NMR}$ (400 MHz, DMSO) δ 9.74 (s, 6H), 9.29 (s, 6H), 6.51 (s, 6H), 6.50 (s, 3H), 6.44 (s, 6H), 5.57 (s, 3H).

$^{13}\text{C-NMR}$ (101 MHz, DMSO) δ 155.01, 152.93, 142.85, 132.65, 127.73, 123.98, 104.03, 98.13, 41.83.

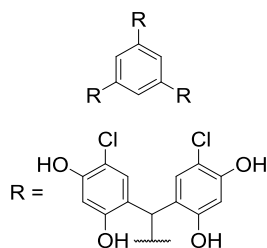
IR (ν_{max} , cm⁻¹): 3526, 3462, 3376, 3179, 1632, 1505, 1427, 1411, 1245, 1195, 1176, 1118, 1012, 915, 894, 880, 838, 822.



NL:
1.15E7
UEAMAT226-OC-HNESN-2#2-
6 RT: 0.26-0.52 AV: 4 T:
FTMS - p NSI Full ms
[120.00-2000.00]

NL:
4.52E3
C₄₅ H₂₉ Br₆ O₁₂
C₄₅ H₂₉ Br₆ O₁₂
p (gss, s /p:40) Chrg -1
R: 100000 Res .Pwr . @FWHM

Compound 218



0.48 mL of methanesulfonic acid was added to a pre-cooled (0 °C) mixture of **216** (100 mg, 0.6 mmol) and 4-chlororesorcinol (624 mg, 4.32 mmol) in 6 ml of Et₂O/DCM (1/1, v/v). The reaction vessel was sealed and the reaction allowed to stir for 24 h. The resulting mixture was diluted with diethyl ether, poured into distilled water and allowed to stir vigorously until a suspension was obtained. The product was collected by Büchner filtration, washed with abundant distilled water and dried in a desiccator to give a yellow powder.

Yield: 68.5% (calculated from NMR to account for solvent of crystallisation)

¹H-NMR (400 MHz, DMSO) δ 9.66 (s, 6H), 9.26 (s, 6H), 6.47 (s, 3H), 6.43 (s, 6H), 6.32 (s, 6H), 5.56 (s, 3H).

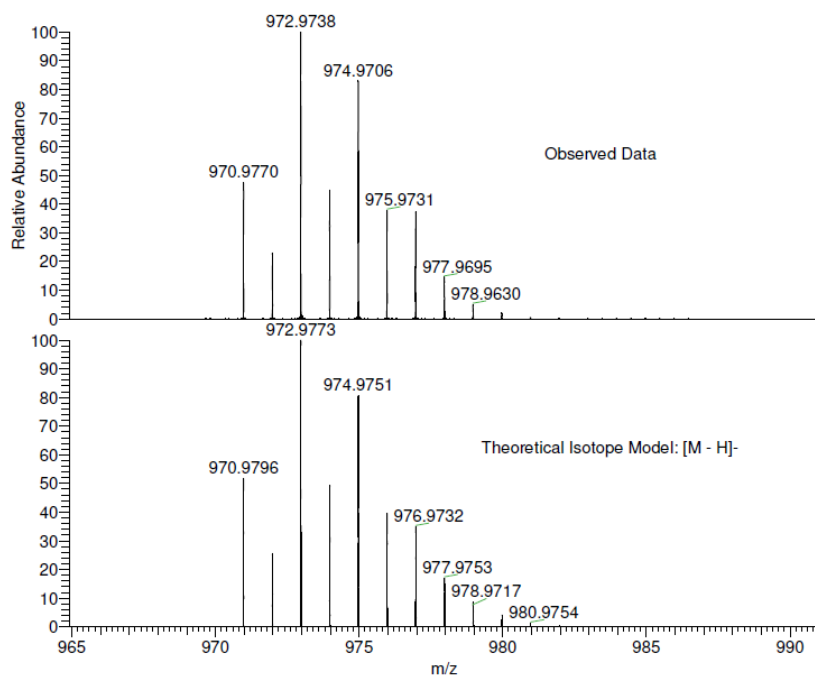
¹³C-NMR (101 MHz, DMSO) δ 154.34, 151.88, 142.96, 129.83, 127.66, 123.31, 109.34, 104.14, 41.88.

IR (ν_{max} , cm^{-1}): 3549, 3439, 3347, 3203, 1614, 1506, 1430, 1417, 1338, 1242, 1195, 1176, 1126, 1031, 973, 912, 894, 883, 838, 823.

MC-144 MW=975?
C₄₅H₃₀Cl₆O₁₂
(MeOH)/MeOH+DEA

EPSRC National Facility Swansea
LTQ Orbitrap XL

Marco Cominetti
23/02/2014 12:32:56



NL:
9.04E7
UEAMAT227-OC-HNESN#50
RT: 1.72 AV: 1 T: FTMS - p
NSI Full ms [200.00-4000.00]

NL:
5.12E3
C₄₅ H₂₉ Cl₆ O₁₂
C₄₅ H₂₉ Cl₆ O₁₂
p (gss, s /p:40) Chrg -1
R: 100000 Res .Pwr . @FWHM

Scrambling experiments

Method 1: A mixture of **163** (50 mg, 0.07 mmol) and *4-bromoresorcinol* (55.9 mg, 0.30 mmol) was dissolved in 3ml of ethanol/HCl 37% (1/1, v/v). The solution obtained was allowed to stir at 70 °C for 5 hours; a sample was dried with compressed air and analysed with ¹H-NMR.

Method 2: A mixture of **163** (50 mg, 0.07 mmol) and *4-bromoresorcinol* (55.9 mg, 0.30 mmol) was dissolved in 3ml of Et₂O/DCM (1/1, v/v); 0.24 mL of *methanesulfonic acid* were added, and the reaction vessel was sealed. The mixture was allowed to stir for five hours; a sample was dried with compressed air and analysed with ¹H-NMR.

3. Bis-phenols, Benzophenones, Xanthenes and Xanthenes

3.1 Introduction to the structures

Bis-phenols have simplified structure compared to the previously reported natural products and synthesised compounds. Both dimers and tetramers are substantially based on two resorcinol units bridged by a methylene group. This unit is adorned with a substituent on the bridge, either aliphatic or aromatic, possibly leading to a tetrameric structure.

The bis-phenol family is a simplified version, where the bis-phenol unit does not have a substituent on the bridge (**Figure 57**). Its purpose is to provide the basic model compound and assess whether a sidechain produces any improvement in activity.

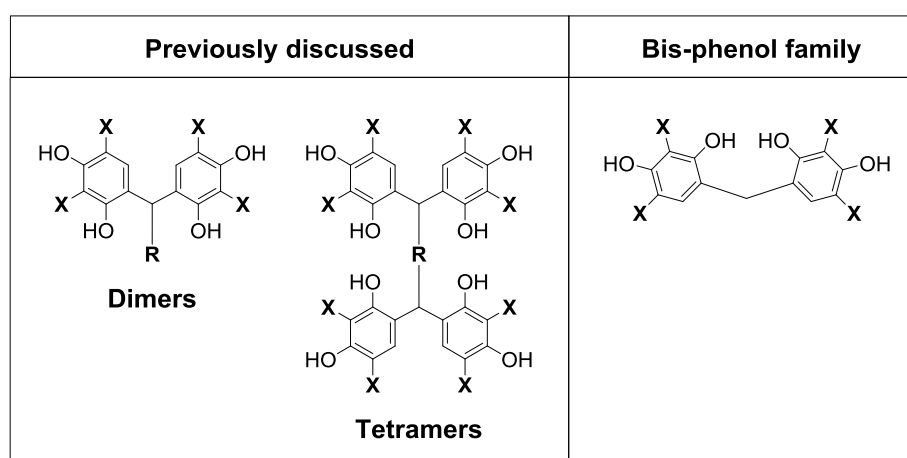


Figure 57. Structures described in **Chapter 2**.

A specific approach was chosen to access the bis-phenol family, such that intermediates would constitute interesting compounds to extend the investigable SAR. Benzophenones are the starting point for the synthesis and offer an additional oxygen on the bridge (**Figure 58**), which introduces extended conjugation and potential intramolecular hydrogen bonding, producing conformational effects and altering the pK_a of the hydroxyl groups.

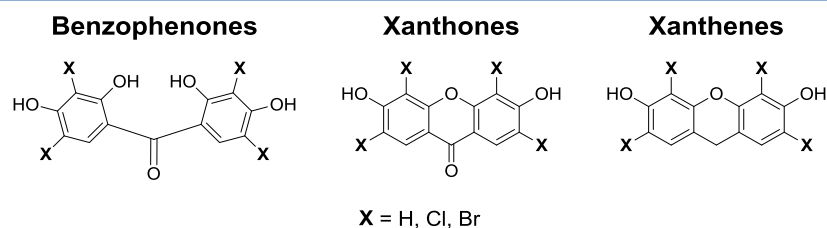
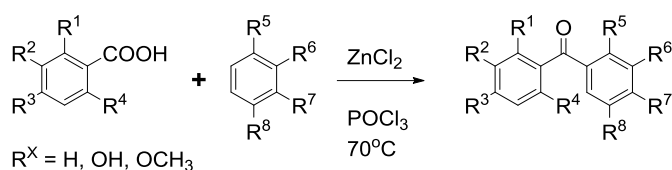


Figure 58. General structures of the compounds presented in **Chapter 3**.

With benzophenones at hand, cyclisation to xanthenes and subsequent reduction to xanthenes leads to fundamentally flat structures, with only two hydroxyl groups, and allows easy access to a different halogenated motif for our investigations.

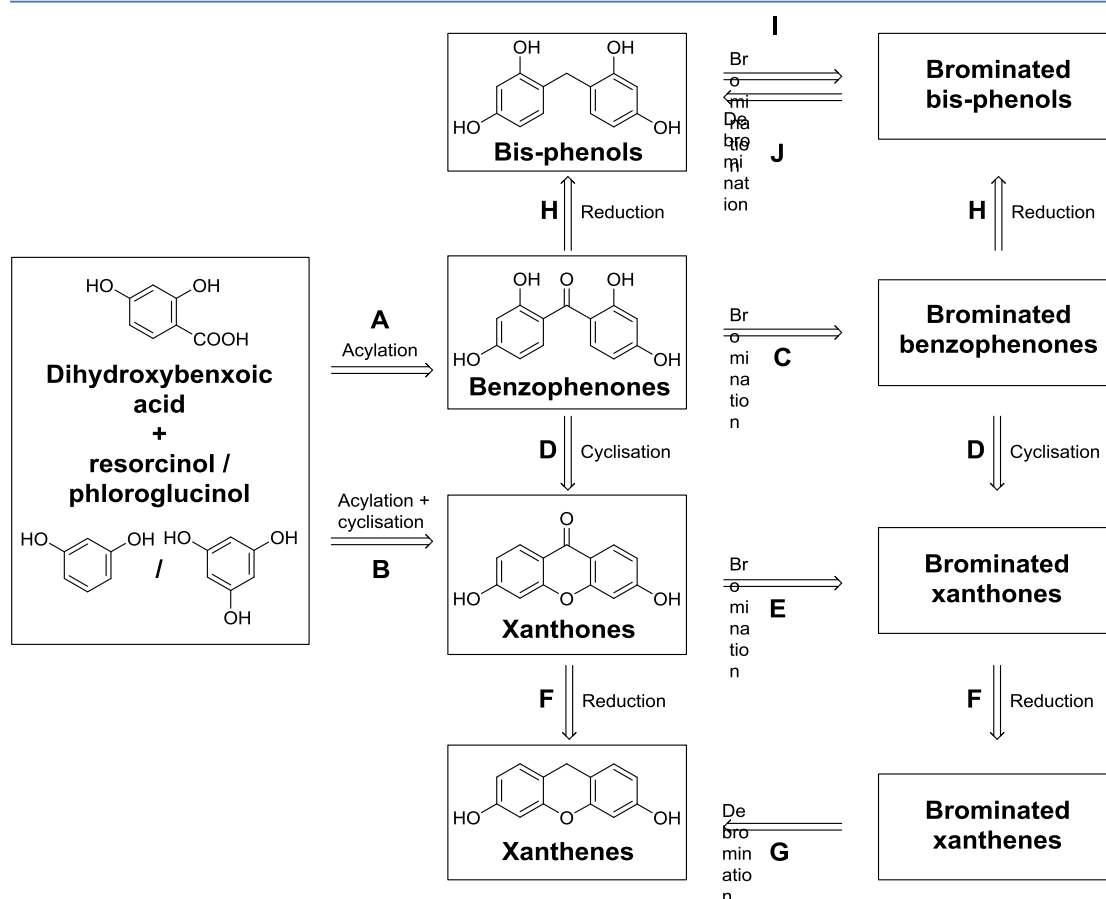
3.1.1 Synthetic approach

The idea which drove the design of the synthetic approach for this family of compounds came from a report by Hu. He described a facile synthesis of hydroxybenzophenones as α -Glucosidase Inhibitors. One step preparation of the product benzophenones was obtained by Friedel-Crafts acylation in $POCl_3$ with $ZnCl_2$ as catalyst (**Scheme 29**) and purification was carried out by simple crystallisation.⁹⁸



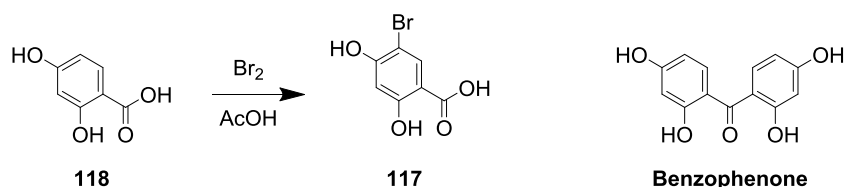
Scheme 29. Synthesis of benzophenones according to Hu.⁹⁸

A solid base to work with is fundamental and hydroxybenzophenones appeared to be a flexible starting point for a number of structural modifications. Moreover, Hu's method allows access to varied starting compounds, extending the scope of the method (**Scheme 30, A**).



Scheme 30. Synthetic approach towards benzophenones, bis-phenols, xanthenes, xanthenes and their brominated analogues.

The significant difference in reactivity due to the activating effect of hydroxyl groups, reported in the literature⁷⁵ and experienced directly for the synthesis of 4-bromoresorcinol, could be exploited to achieve selective bromination of benzophenones (**Scheme 30, C**). The carbonyl of the benzophenone is expected to act similarly to the carboxylic group in the previously described synthesis of 4-bromoresorcinol (**Chapter 2**), where it acts as “protecting group” and reduces the reactivity of the resorcinol, allowing convenient access to a monohalogenated derivative (**Scheme 31**).



Scheme 31. Bromination of 2,4-dihydroxybenzoic acid and similarity with benzophenones.

As previously reported, benzophenones and their brominated derivatives with matching hydroxyl groups (positions 2 and 2') can be cyclised (**Scheme 30, D**) in very high yields.^{99,100} The reaction is performed in a sealed tube with water at high temperatures (220 °C) and without any additional reactant. The reaction can also be catalysed by addition of a base, as reported by Azuma.¹⁰¹ Whilst alternative methods for cyclisation are available, high temperatures are always required and additional reactants are employed. The reaction can be catalysed with acids, such as Py·HCl,¹⁰⁰ Eaton's reagent^{102,103} and polyphosphoric acid.¹⁰⁴ Other methods, using bases such as tetramethylammonium hydroxide have also been reported.¹⁰⁵ Considering that polyphosphoric acid and Eaton's reagent can catalyse the cyclisation, it is reasonable to propose the possibility of acylating and cyclising in one step, shortening the path to xanthenes (**Scheme 30, B**).

Bromination of xanthenes (**Scheme 30, E**) offers an alternative route to the synthesis of their halogenated analogues.

Xanthenes and their halogenated derivatives can be reduced (**Scheme 30, F**) in high yields with borane, as previously reported by Shi.^{100,106} Borane is not a strong base and the reduction is favoured. In these examples, reductions are performed with a slight excess of reagent.^{100,106}

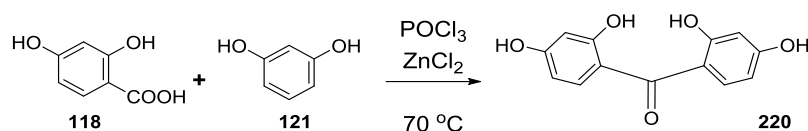
Direct reduction of benzophenones (**Scheme 30, H**) has not been described often, especially concerning highly hydroxylated or halogenated compounds. The challenge, in the case of halogenated derivatives, is complicated by potential debromination. Olah reported a series of ionic reductions using triethylsilane.^{107,108} However, all these reducing systems involve the use of acids (HF·Pyridine, trifluoroacetic acid or trifluoromethanesulfonic acid) and the model compounds used are much less activated than the poly-hydroxybenzophenones of interest. The resulting bis-phenols, similarly to the tetramers, would undergo acid-catalysed fragmentation. On the other hand, borane appears to be a feasible option; it is not reported in the literature for the reduction of benzophenones but, despite the different electronic density of the aromatic rings and their spatial arrangement compared to xanthenes, it remains a suitable route for exploration.

Bromination and debromination of bis-phenols (**Scheme 30, J**) could also be alternative strategies to allow access to particular products if more elegant synthetic routes were not successful.

3.2 Synthesis

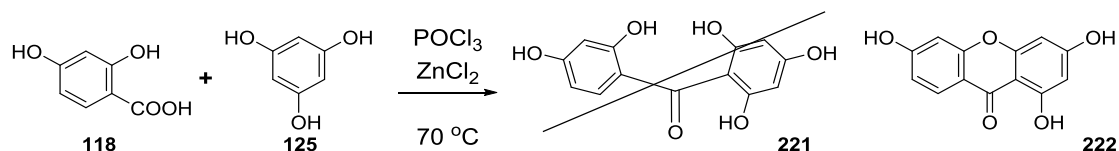
3.2.1 Synthesis of hydroxy benzophenones

Synthesis of a first family of benzophenones was attempted according to the procedure by Hu.⁹⁸ All three different structural isomers of 2,4-dihydroxybenzoic acid reacted with both resorcinol and phloroglucinol in the presence of anhydrous zinc chloride (II) and phosphorus oxychloride, at 70 °C.



Scheme 32. Synthesis of **220**.

Synthesis of compound **220**, which is known and also commercially available, was used as a test for the reaction (**Scheme 32**). Due to possible cyclisation of adjacent hydroxyl groups, it enabled verification of the selectivity of the reaction. Identification was also possible by comparing the product with an authentic sample. The acylation was achieved using phosphorus oxychloride as solvent and reactant, in the presence of excess zinc chloride at 70 °C over the course of 3 hours. Upon quenching of the POCl_3 , the product was isolated by filtration in 40% yield. Since the reaction successfully led to the expected product, it was tested with phloroglucinol and with different regioisomers of dihydroxybenzoic acid, to obtain a portfolio of starting products with a different hydroxyl group distribution.



Scheme 33. Synthesis of **222**.

To begin with, the same 2,4-dihydroxybenzoic acid was treated with phloroglucinol. However, in contradiction to the report by Hu,⁹⁸ the benzophenone product was not isolated as it is directly cyclised to the corresponding xanthone, **222**, in 91 % yield (**Scheme 33**).

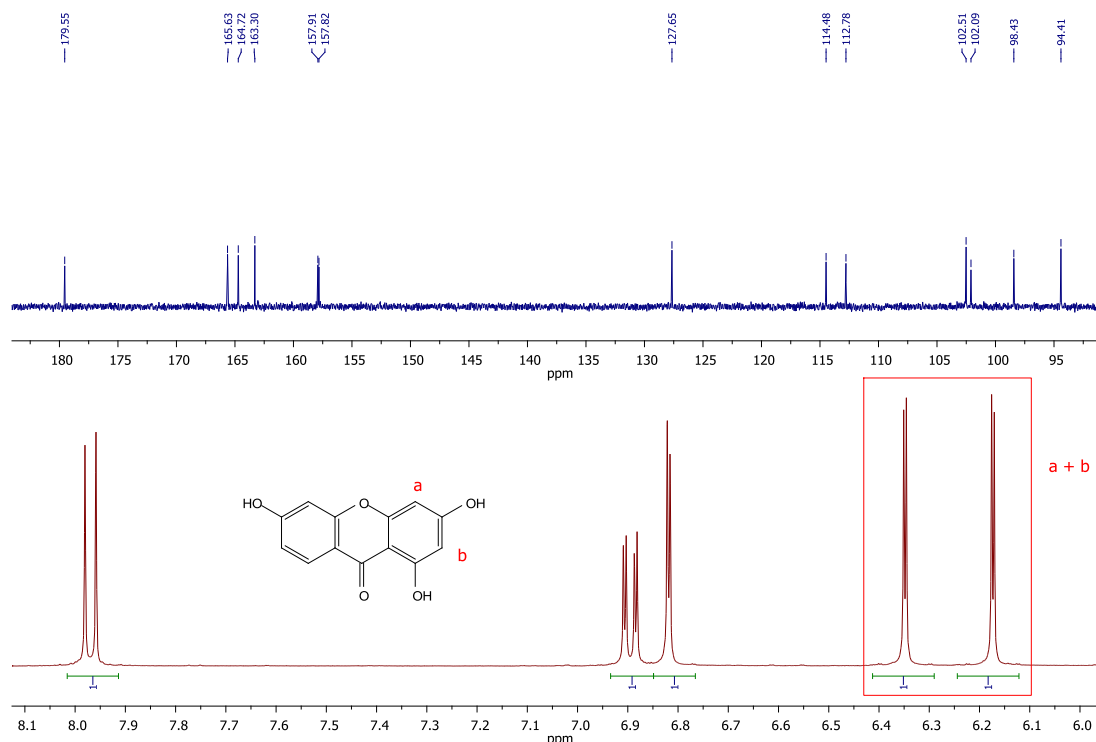
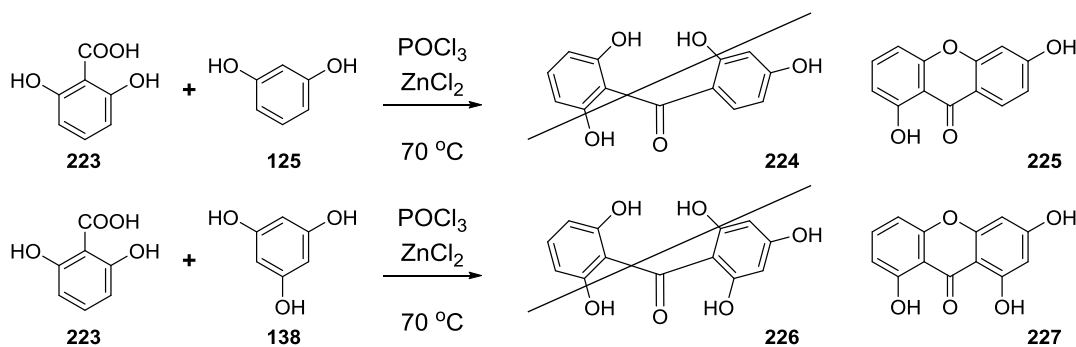


Figure 59. ^1H -NMR and ^{13}C -NMR of **222**.

Cyclization is evident in both ^1H -NMR and ^{13}C -NMR. The carbon NMR presents 13 signals, suggesting that there is no element of symmetry within the molecule and that carbons **a** and **b** are different (**Figure 59**). The hydrogens on the same positions are also different, displaying about 0.2 ppm difference in shift and a long range coupling between each other.



Scheme 34. Synthesis of **225** and **227**.

As expected from the cyclization of **222**, reaction of 2,6-dihydroxybenzoic acid with both resorcinol and phloroglucinol leads to the xanthenes **225** and **227**, in 27 % and 9.4 % yield respectively (**Scheme 34**). The presence of two hydroxyl groups facing the acylated partner is likely to facilitate the ring closure.

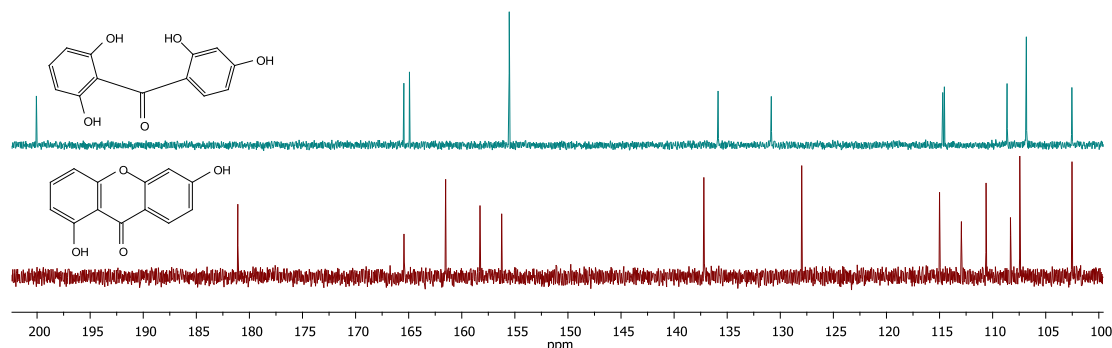
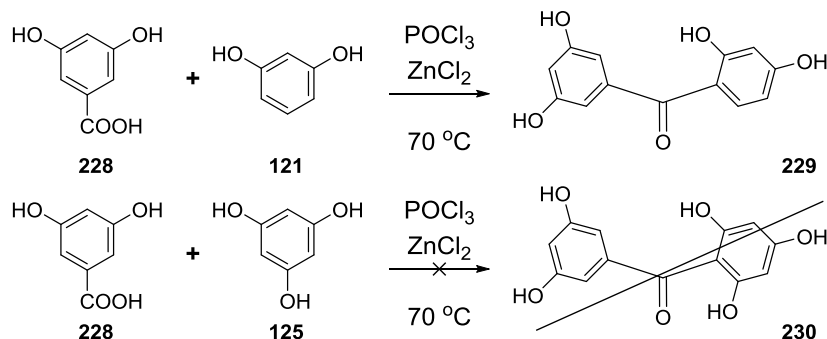


Figure 60. Comparison of the ^{13}C -NMR spectra of **224** (top) and **225** (bottom).

As discussed for **222**, cyclization of a potentially symmetric unit, increases the number of signals in the carbon NMR. In **Figure 60**, **224** and **225** (see **Chapter 3.2.6** for synthesis) are compared. Cyclization increases the number of signals from 11 to 13 due to the 2,6-dihydroxyphenyl unit losing its symmetry.



Scheme 35. Synthesis of **229** and attempted synthesis of **230**.

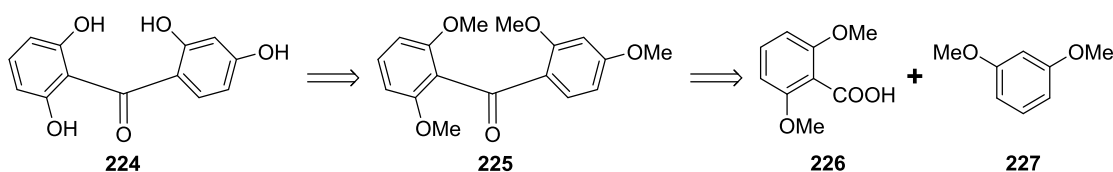
Interestingly, 3,5-dihydroxybenzoic acid did not appear to be particularly reactive under these conditions, and led to **229** in low yield (5%) by reaction with resorcinol. Intact starting material was also recovered from the reaction. Reaction of the same acid with phloroglucinol did not provide any product, thus isolation of **230** was not possible, and starting materials were recovered from the reaction mixture, even after 22 hours (compared to the usual 2-8 hours) (**Scheme 35**).

Although the results did not lead to all expected benzophenones, they are nonetheless interesting, and allowed direct access to two benzophenones and three xanthenes.

3.2.2 Synthesis of methoxy benzophenones

The previous approach did not lead, in some cases, to the expected benzophenones. Moreover, it has a number of drawbacks. Phosphorus oxychloride is a dangerous compound, being both corrosive and toxic, and the reaction is quenched with ice-water, with which it reacts violently, producing toxic gases. Also, the reaction mixture is very viscous, with consequent setup limitations.

Alternative approaches to the synthesis of benzophenones normally require protected hydroxyl groups, both to reduce potential side reactions and avoid interference/quenching of catalysts. Methoxy groups were chosen due to their resorcinol and phloroglucinol precursors being readily available and cheap (**Scheme 36**).



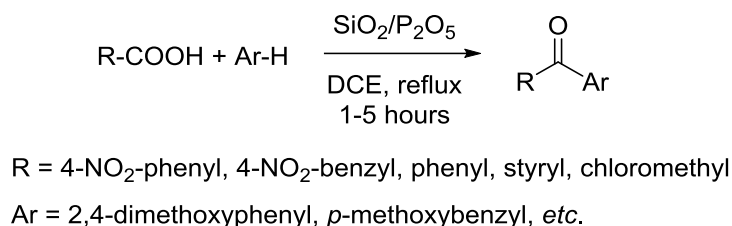
Scheme 36. Retrosynthesis of **224**.

A traditional approach could be a Friedel-Crafts acylation. The acid is firstly converted to acyl chloride and then, with the aid of a Lewis acid, undergo electrophilic substitution on the aromatic partner. This approach requires two steps and anhydrous conditions to prevent decomposition of the chloride. Eaton's reagent (7.7% phosphorus pentoxide in methanesulfonic acid) is a valid alternative, it is a relatively stable reagent and it is commercially available. Due to its better performance and handling ease, it replaced the previously used polyphosphoric acid. However, it requires anhydrous conditions.⁹⁹

Among various reports, two methods drew our attention. They both involve a heterogeneous catalyst and offer, at least on the presented model compounds, high yields and selectivity, simple handling and purification. Also, they do not require transition metals and employ compounds with low toxicity.

3.2.3 Synthesis of methoxy benzophenones with SiO₂-P₂O₅

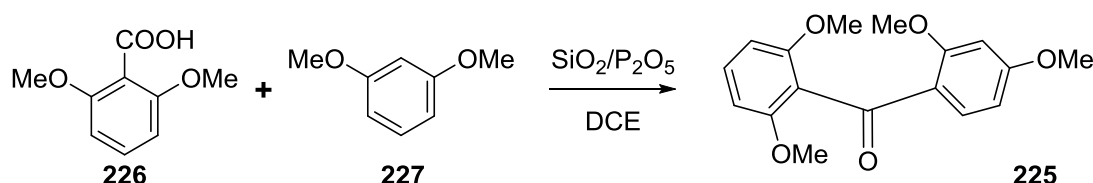
The acylation of aromatic compounds with carboxylic acids in the presence of P₂O₅/SiO₂ was reported by Zarei in 2008 (**Scheme 37**).¹⁰⁹ The same type of catalyst has other applications and was reported to catalyse the Ritter reaction,¹¹⁰ deprotection of diacetates,¹¹¹ condensation of indoles with carbonyl compounds¹¹² and to prepare benzimidazoles.¹¹³ The catalyst was used in solvent-free conditions for some of the mentioned applications.



Scheme 37. Acylation of aromatic compounds with P₂O₅/SiO₂, examples from Zarei.¹⁰⁹

The catalyst was readily prepared from silica (for column chromatography) and P₂O₅ and it is stable for long periods of time.¹⁰⁹

Since the model compounds reported by Zarei are very different from our methoxy derivatives, a model reaction to refine the conditions was necessary. Synthesis of **225**, whose unprotected analogue was not obtained with phosphorus oxychloride, was first investigated (**Scheme 38**).



Scheme 38. Synthesis of **225**.

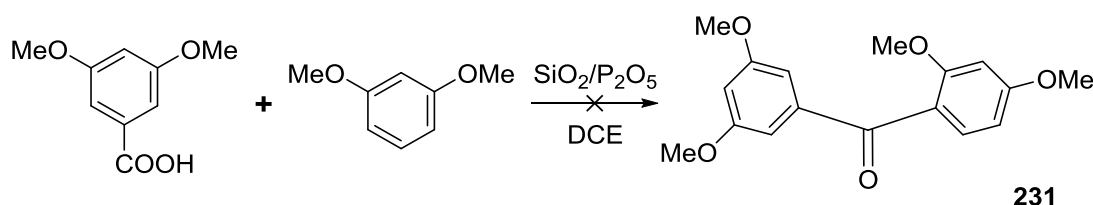
The reaction was tested with different combinations of temperature (RT, 40, 70 and 90 °C) with different amounts of catalyst (0.4 to 1.5 g of catalyst per mmol of acid) and different reaction times (**Table 5**).

Temperature (°C)	Catalyst (g/mmol of acid)	Time (hours)	Yield (%)
90	0.4	2	26
70	0.4	2	19
40	0.73	24	50

40	0.73	72	52
40	1.5	72	43
RT	0.4	24	0

Table 5. Reaction conditions for the synthesis of **225**.

The best result was obtained at 40 °C with 0.73 g_{catalyst}/mmol_{acid} and 72 hours reaction time, with a yield of 52%. However, with only one day of reaction, the yield is just 2% lower. The reaction time was preferred over the small increase in yield and the method was adjusted accordingly. On a larger scale, the reaction produces a total yield of 66%. Of this 66%, a part was immediately recovered by extraction and trituration (45%) and the remaining by decomposition of the catalyst, which traps a good amount of product, and column filtration of the crude with DCM (21%). The additional amount of product which can be recovered from the catalyst was not considered during the small scale tests under different conditions.

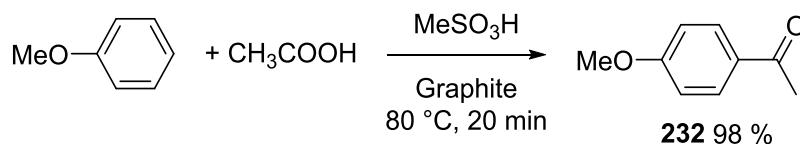


Scheme 39. Attempted synthesis of **231**.

Unfortunately, the method did not provide any product when 3,5-dimethoxybenzoic acid was used (**Scheme 39**). The reaction was attempted at higher temperature as well (70 °C) without any success.

3.2.4 Synthesis of methoxy benzophenones with graphite-MeSO₃H

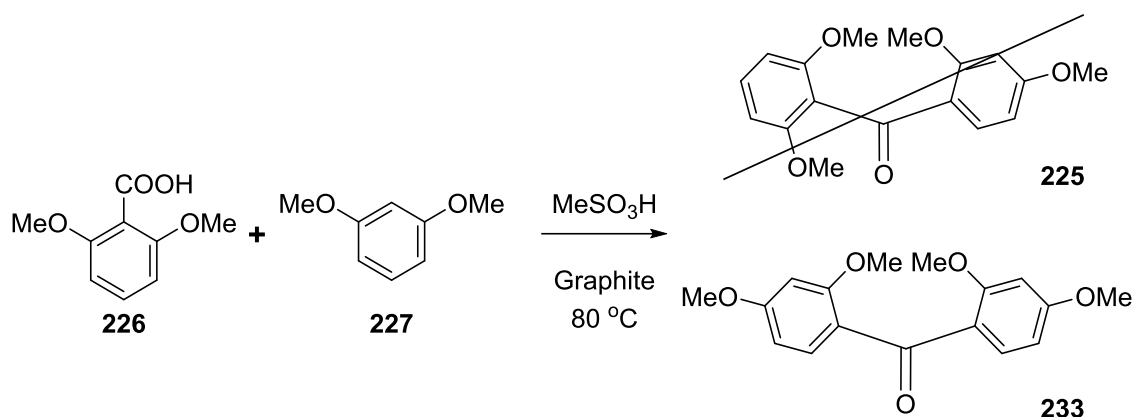
The acylation of aromatic ethers with methanesulfonic acid in presence of graphite, was initially reported by Sarvari¹¹⁴ in 2004. The author optimised the conditions of the reaction for anisole and acetic acid and then evaluated the scope of the reaction with a short series of different coupling partners.



Scheme 40. Acylation of anisole with acetic acid in the presence of methanesulfonic acid and graphite reported by Sarvari.¹¹⁴

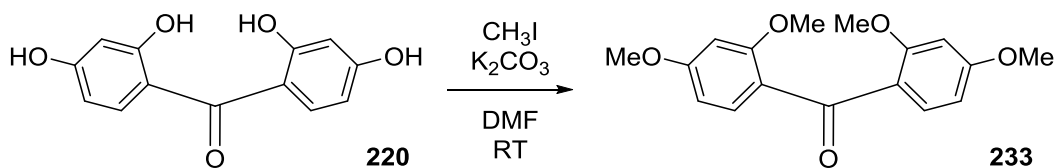
The reaction was performed in neat methanesulfonic acid at 80 °C in the presence of graphite (**Scheme 40**). The scope of the reaction covers differently substituted benzoic acids, including 2-hydroxybenzoic acid, suggesting compatibility with unprotected hydroxyl groups, and produces in all tested cases excellent (80-90%) yields.¹¹⁴

Since the reaction was optimised for relatively different compounds, the synthesis of **225** was used again to test the reaction conditions. Initially, the reaction was performed at 80 °C, as in the original procedure, and instead of the expected compounds we were surprised to find that a rearrangement had occurred (**Scheme 41**). The same result was also obtained at 40 °C. Isolation of the product is straightforward and quick, without any chromatographic process involved. Upon dilution with DCM, graphite can be removed from the reaction by filtration and any excess of acid can be neutralised with sodium hydrogen carbonate, which also neutralises the methanesulfonic acid. After evaporation of the organic solvent, a simple trituration with hexane, which can dissolve dimethylresorcinol but not the product, leads to the pure compound.



Scheme 41. Acylation of 1,3-dimethoxybenzene with 2,6-dimethoxybenzoic acid.

The compound isolated proved to be **233**. For reference, this compound was also synthesised by alkylation of **220** with methyl iodide (**Scheme 42**).



Scheme 42. Methylation of **220**.

Both ^1H -NMRs (**Figure 61**), which are superimposable, shows only two singlets for the methoxy groups, confirming that the structure is consistent with **233**.

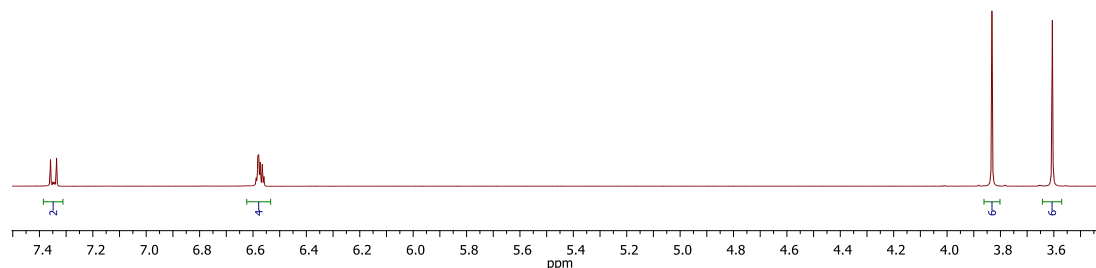
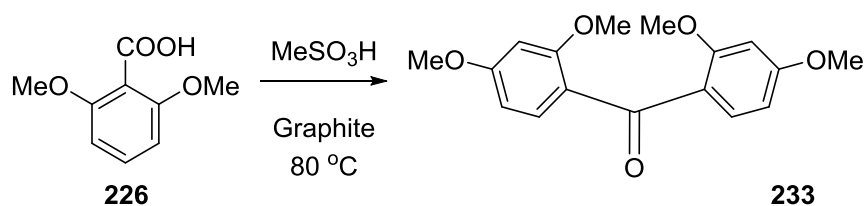


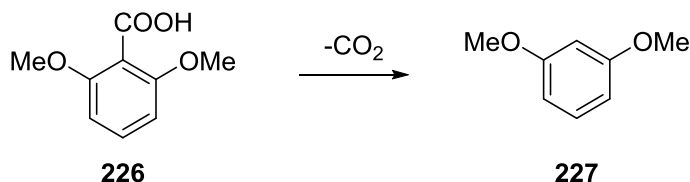
Figure 61. ^1H -NMR of **233**.

Since **233** was also obtained with the reaction at 40 °C, the behaviour of the reaction was studied at this temperature. In particular, the destiny of 2,6-dimethoxybenzoic acid in the presence of methanesulfonic acid and graphite was investigated (**Scheme 43**). Interestingly, after two days, the reaction led to the isolation of **233** despite the absence of the partner resorcinol.



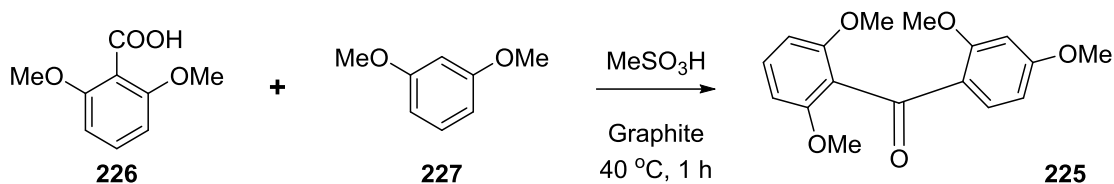
Scheme 43. Synthesis of **233** from 2,6-dimethoxybenzoic acid.

Decarboxylation of 2,6-dimethoxybenzoic acid leads to dimethyl resorcinol (**Scheme 44**). It has to be noted that the reaction is immediately evident due to effervescence of the mixture and the product has a characteristic sweet smell.



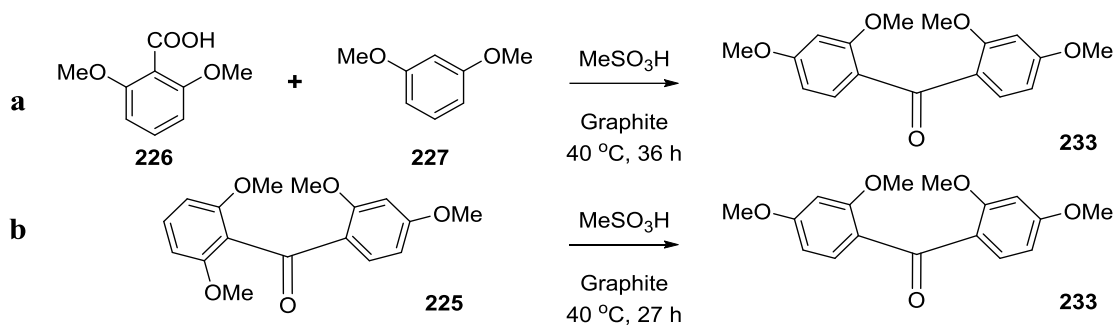
Scheme 44. Decarboxylation of 2,6-dimethoxybenzoic acid.

As previously seen, reaction of dimethyl resorcinol with the initial acid leads to **233** (**Scheme 42**). However, if the reaction is halted after 1 hour, **225** can be conveniently isolated (**Scheme 45**), suggesting that **225** is a kinetic product of the reaction.



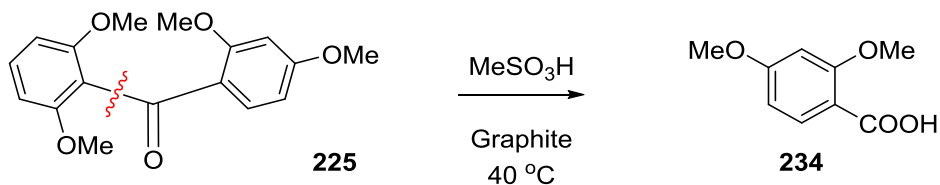
Scheme 45. Acylation of 1,3-dimethoxybenzene with 2,6-dimethoxybenzoic acid, halted before rearrangement.

If the reaction is allowed to proceed for longer, in order to lead to **233** (**Scheme 46, a**), as previously observed, formation of 2,4-dimethoxybenzoic acid is necessary. This leads to the supposition that **225**, upon breakage of the bond on the 2,6-dimethoxy side, releases 2,4-dimethoxybenzoic acid. This also implies that, as experimentally verified, decomposition of **225** alone leads to **233** (**Scheme 46, b**).



Scheme 46. Synthesis of **233** from 1,3-dimethoxybenzene and 2,6-dimethoxybenzoic acid and subsequent rearrangement (a). Rearrangement of **225** to give **233** (b).

The formation of 2,4-dimethoxybenzoic acid (**234**) from decomposition of **225** (**Scheme 47**) can be verified by NMR. A sample of the reaction can be directly diluted with DMSO- d_6 and tested. Due to the presence of methanesulfonic acid, the shift of the peaks can be variable. To confirm the presence of the acid, the NMR is recorded before and after the addition of a sample of the pure analyte (**Figure 62**).



Scheme 47. Fragmentation of **225**.

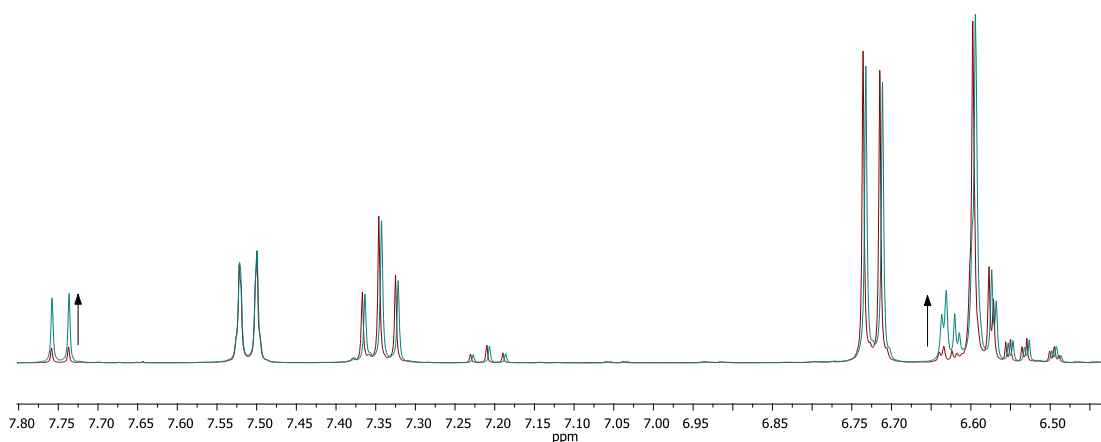
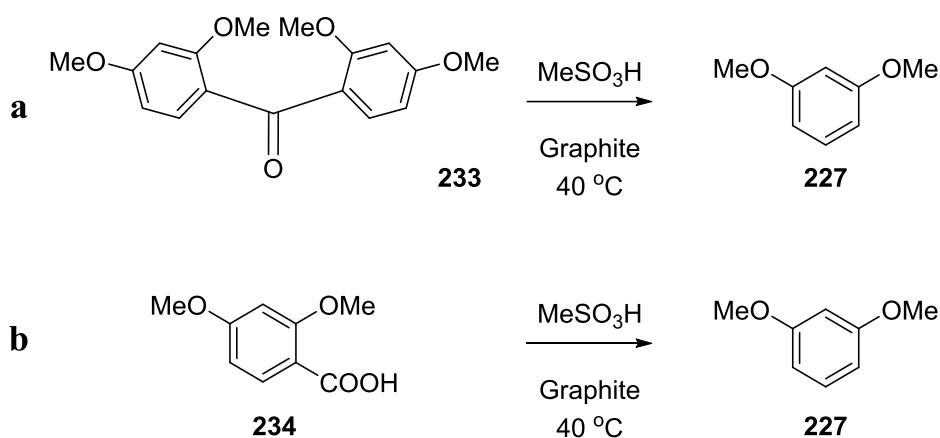


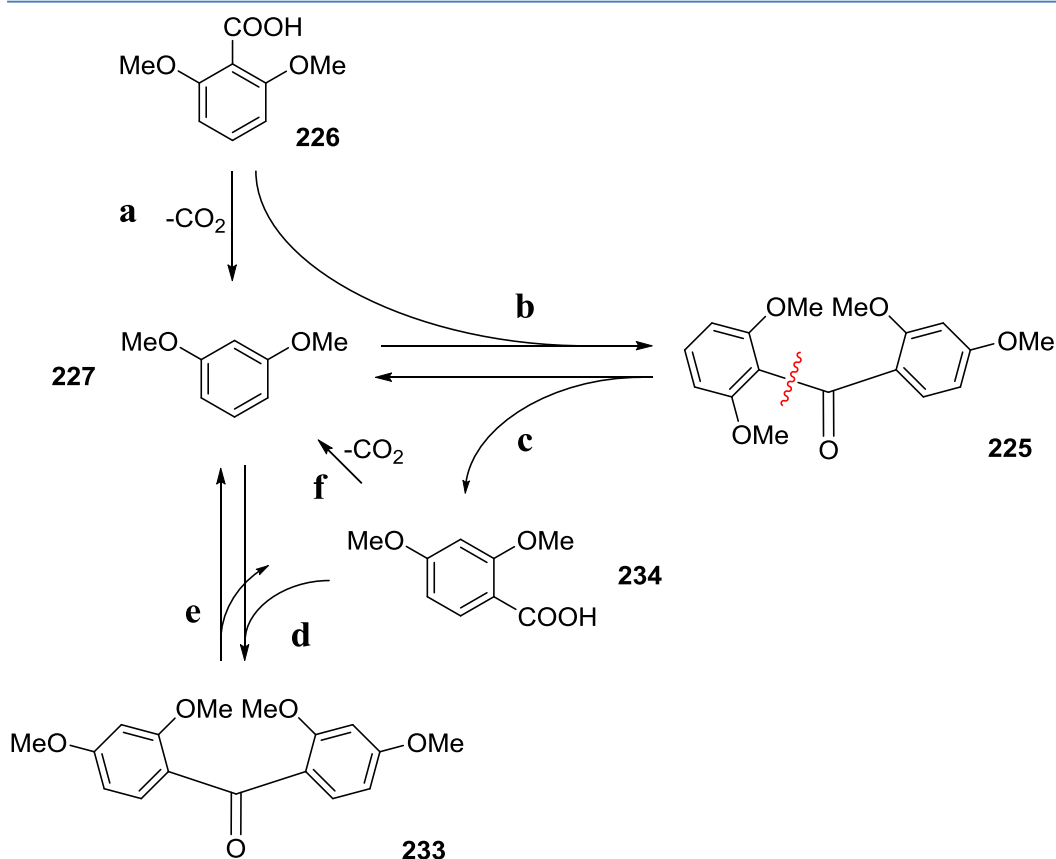
Figure 62. ^1H -NMR of the fragmentation of **225** (red) and spiking with 2,4-dimethoxybenzoic acid (blue).

Breakdown of **233** (Scheme 48, a) and decarboxylation of 2,4-dimethoxybenzoic acid (Scheme 48, b) have also been observed. Prolonged exposure of these to the reaction conditions lead to dimethylresorcinol.



Scheme 48. Breakdown of **233** (a) and decarboxylation of 2,4-dimethoxybenzoic acid (b).

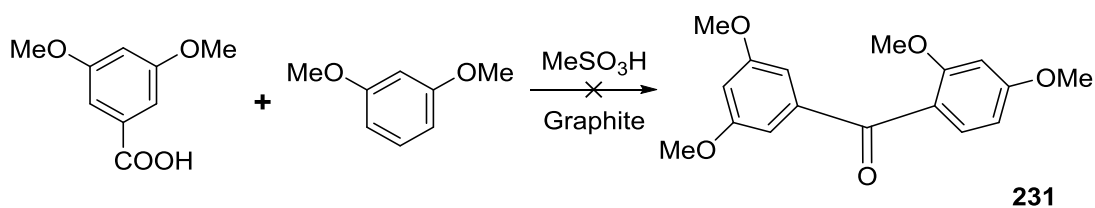
All these results can be summarised in a single scheme, highlighting the concurrent transformations observed. Decarboxylation of 2,6-dimethoxybenzoic acid leads to dimethylresorcinol (Scheme 49, a). Friedel-Crafts acylation leads to **225** (Scheme 49, b). Fragmentation of the newly formed benzophenone leads to 2,4-dimethoxybenzoic acid (Scheme 49, c), allowing access to **233** (Scheme 49, d).



Scheme 49. Summary of the reactions involved in the synthesis of **225** and **233**.

An extensive search of the literature, indicated that this rearrangement has previously been seen in the work of Kasbekar¹¹⁵ and Hosangadi¹¹⁶ when using polyphosphoric acid at 80 °C. However, here, using this catalyst, the temperature can be lowered to 40 °C and the method allows isolation of the kinetic and the thermodynamic product.

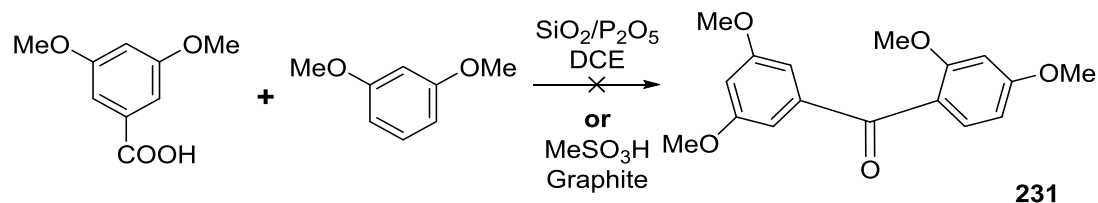
Reaction of dimethylresorcinol and 3,5-dimethoxybenzoic acid in presence of methanesulfonic acid and graphite did not lead to the expected compound, **231** (**Scheme 50**). The reaction was attempted both at 40 and 80 °C but the starting material proved to be unreactive and was recovered from the reaction mixture.



Scheme 50. Attempted synthesis of **231** with methane sulfonic acid and graphite.

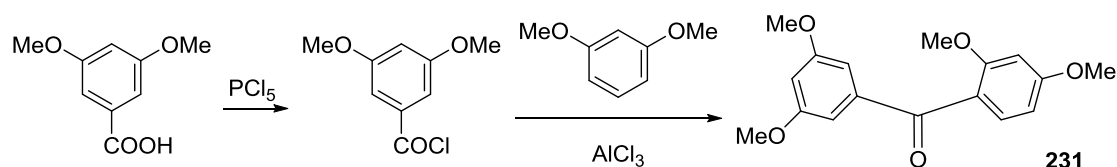
3.2.5 Compound 231

Since compound **231** was not obtained with either of the acylation procedures attempted (**Scheme 51**), it is relevant to note that its synthesis has only been reported once in 1913 by Mauthner.¹¹⁷



Scheme 51. Attempted approaches for the synthesis of **231**.

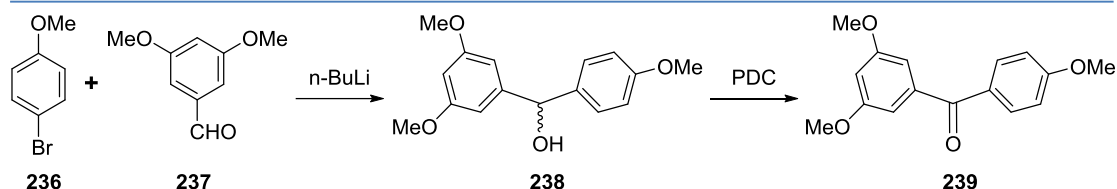
In this paper it was synthesised from the acid, which was firstly converted to acyl chloride and subsequently converted to the benzophenone by Friedel-Crafts acylation in the presence of AlCl_3 (**Scheme 52**).¹¹⁷



Scheme 52. Potential alternative approach to the synthesis of **231**.

Since the analytical data is limited to the procedures available at the time, it may be interesting to attempt the synthesis and prove whether the reaction actually leads to the expected compound.

Other strategies to prepare these compounds are available, such as the one employed by Pettit and co-workers.¹¹⁸ They prepared one of the compounds reported in Mauthner's work using a completely different synthetic approach. They used butyllithium to prepare 4-methoxyphenyllithium from its parent bromide and subsequently obtain a benzhydrol (**Scheme 53**, **238**) by nucleophilic attack to an aldehyde. The benzophenone (**Scheme 53**, **239**) was then obtained by oxidation of **238** with pyridinium dichromate (PDC).

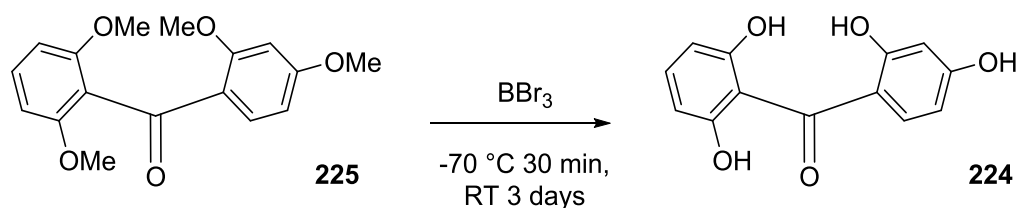


Scheme 53. Pettit's benzophenones synthesis.¹¹⁸

This strategy would be considered if any further development of these products is required.

3.2.6 Deprotection of methoxybenzophenones

Dealkylation of aryl methyl ethers with boron tribromide is a well known and established method.^{119,120} Compound **225** was used as a model to test the reaction. The deprotection required low temperatures (-70 °C) during the addition of BBr₃, thus preventing fragmentation. It also required long reaction times to remove all methyl groups. The product was isolated in 67% yield (**Scheme 54**).

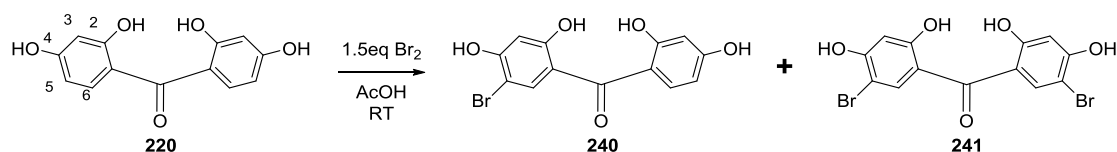


Scheme 54. Synthesis of **224**.

Since the reaction did not lead to significant scrambling or cyclisation, it is a reasonable way to complete the synthesis of the hydroxybenzophenones.

3.2.7 Bromination of benzophenones

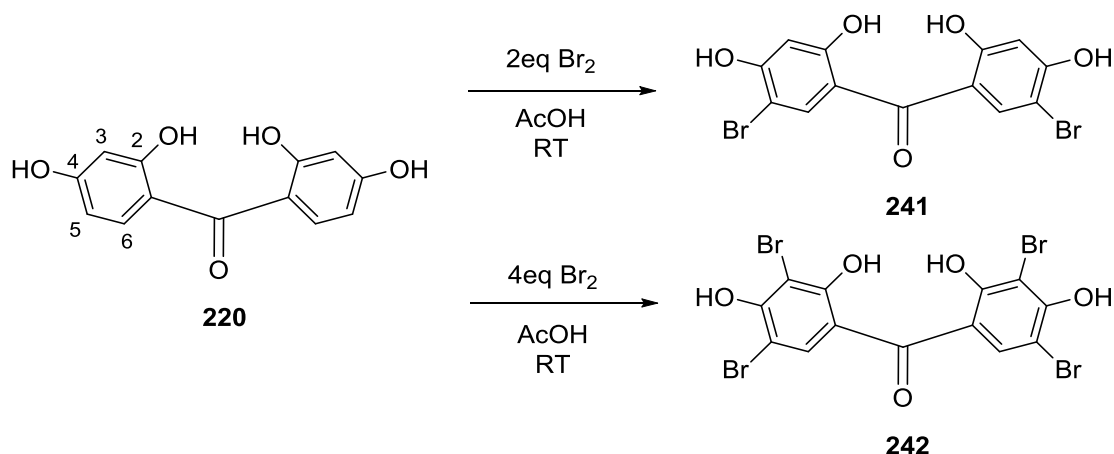
We initially focused on the bromination of **220**, the most simple of resorcinol based benzophenones. It is commercially available and allows access to the first family of derivatives.



Scheme 55. Synthesis of **240** and **241**.

Bromination was achieved by reaction with bromine at room temperature, using acetic acid as solvent (**Scheme 55**), as described for the synthesis of 5-bromo-2,4-dihydroxybenzoic acid (**117**, **Chapter 2**). Initially, partial bromination of **220** with 1.5 equivalents of bromine and subsequent isolation of both **240** and **241** with silica gel chromatography was attempted. However, it was evident that such an approach was not providing good results as the products tend to tail and co-elute upon chromatography.

Therefore, addition of stoichiometric amounts of bromine was investigated (**Scheme 56**). Using two or four equivalents of bromine led specifically to **241** and **242**, respectively. It has to be noted that control of the reaction leading to **241** is not trivial: NBS could be an interesting alternative, since it is easier to handle and less reactive than bromine. Nonetheless, the reactions produced the expected compounds in adequately pure form for further use; the result suggests that, as expected, the selectivity of bromination in position 5,5' of the benzophenone is significantly higher than in 3,3'.



Scheme 56. Synthesis of **241** and **242**.

By substitution of equivalent hydrogens on **220** (**Figure 63, top**), the ^1H -NMR of **241** loses a signal and the splitting of **a**, which is not coupled to **c** anymore (**Figure 63, middle**). In **242** only one aromatic signal is left (**Figure 63, bottom**). Progressive addition of bromine also produces a shift downfield of hydrogen **a**.

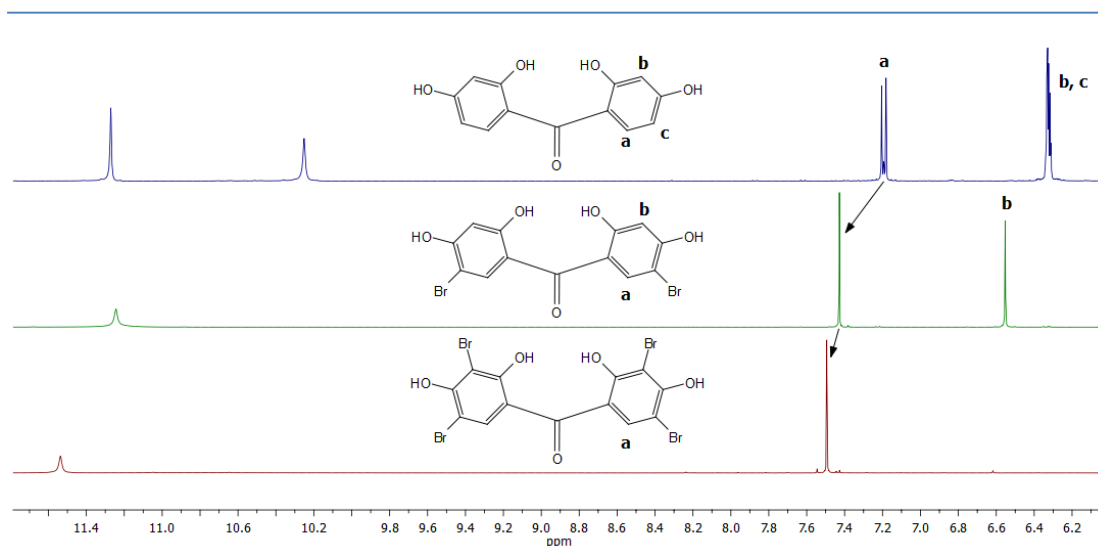
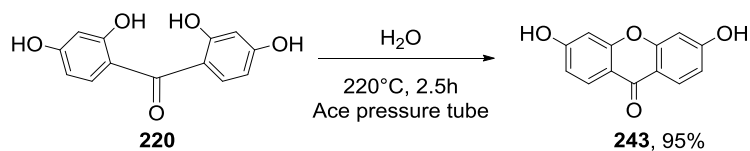


Figure 63. ^1H -NMRs of **220** (top), **241** (middle) and **242** (bottom).

3.2.8 Cyclisation of benzophenones

Cyclisation was conducted as previously reported by Kurduker⁹⁹ and Shi.¹⁰⁰ Parent benzophenones were suspended in water, sealed in a pressure tube and thermally induced cyclisation was achieved at 220 °C. Cyclisation of **220** proceeded as expected from literature, giving the pure product, **243**, in crystalline form and almost quantitative yield (**Scheme 57**).



Scheme 57. Synthesis of **243**.

Cyclisation induces a significant downfield shift of the aromatic protons, as a consequence of the bridging oxygen being conjugated to two rings instead of one (**Figure 64**).

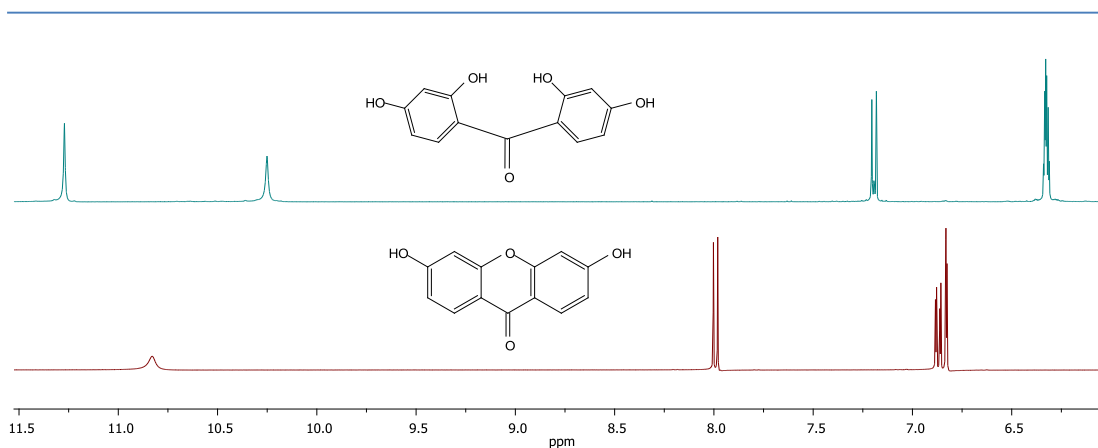
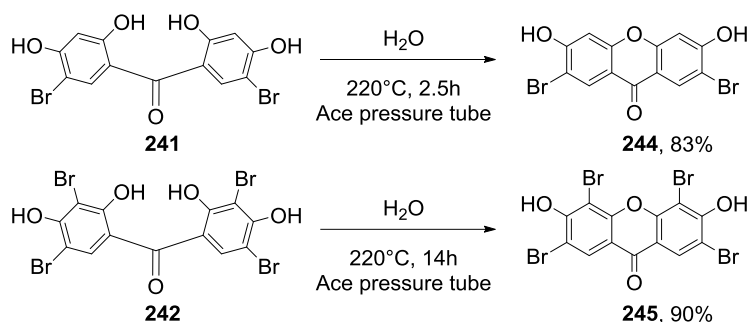


Figure 64. ^1H -NMRs of **220** (top), **243** (bottom).

Using the same approach, **244** and **245** were also obtained in high yields, 83 and 90%, respectively (**Scheme 58**). However, the method proved impractical, the sealed tube was heated in the oven and the rubber seal, due to the temperature, quickly broke down or deformed, leading to evaporation of the water and decomposition of the product.

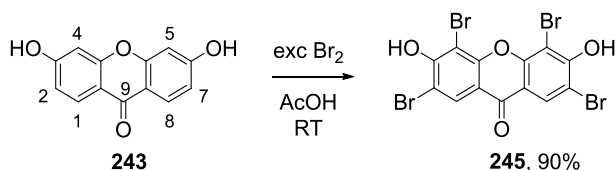


Scheme 58. Synthesis of **244** and **245**.

To avoid the problem, a sand bath was used to obtain the required temperatures, leaving the seal and stopper outside the heating block, thus preventing damage to the rubber. Unfortunately, uneven heating required the temperature to be raised to 230 °C, which is the highest limit attainable with water, and an increase in the reaction time (about 18 hours). Under these conditions, synthesis of **245** was not possible, as the reaction does not reach completion and some decomposition is observed. On the other hand, preparation of **243**, whose precursor is commercially available, became more convenient, as it could be easily monitored (the colour changes from yellow to colourless) and was not subject to technical failures.

3.2.9 Bromination of xanthenes

As **245** could not be readily prepared by this route, while **243** can be, we then considered obtaining **245** through the bromination of **243**. Full bromination to give **245** was easily achieved in 90% yield by reaction of **243** with a large excess of bromine in acetic acid over about one week (**Scheme 59**). Purification of any remaining, incomplete, product could be achieved by hot filtration of a boiling mixture of the product in water. The reaction's progress was monitored by NMR.



Scheme 59. Synthesis of **245**.

Interestingly, two sets of doublets were often identified before the reaction reached completion. The presence of doublets (**Figure 65, B**) suggests that either positions 1 and 2 or 7 and 8 are untouched. **244**, which is also a reasonable intermediate pre-**245**, displays only 2 singlets (**Figure 65, D**).

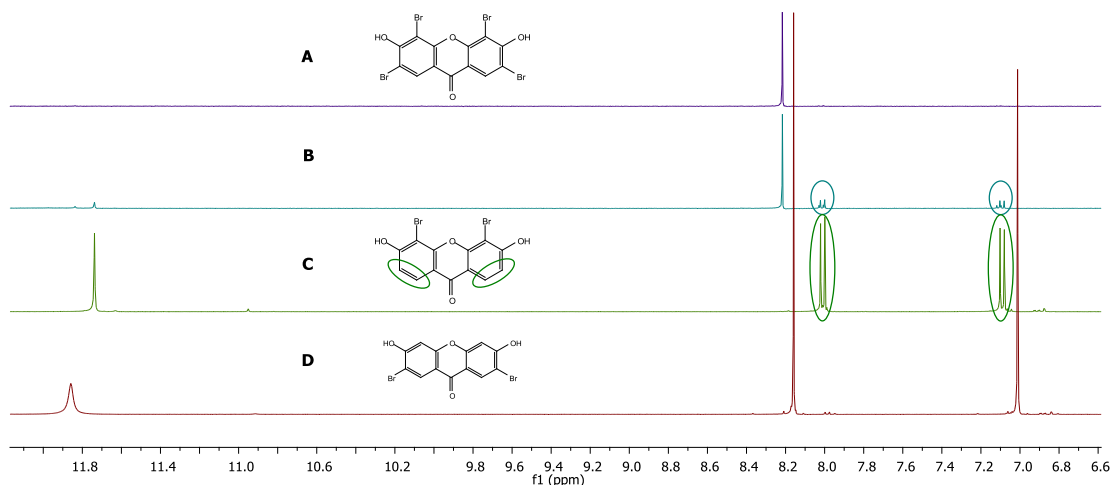
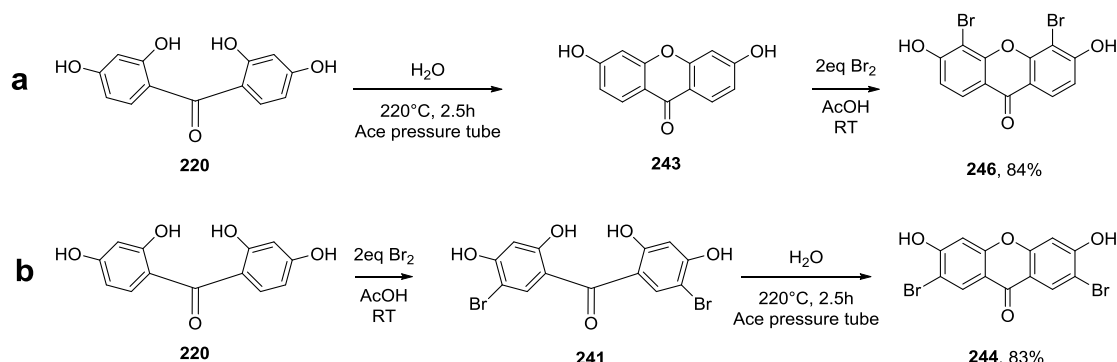


Figure 65. ^1H -NMRs of **245** (A), reaction mixture for **245** before completion (B), **246** (C) and **244** (D).

To investigate this potential selectivity, which would lead to an unreported product, partial bromination of **243** with 2 equivalents of bromine was attempted and led to **246**, in close-to-absolute selectivity. Out of curiosity, the reaction was repeated in DCM to verify whether an aprotic solvent led to a different result; however, it appears that selectivity is maintained. By swapping the order of the steps, cyclisation-

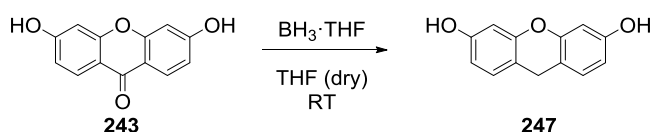
bromination (**Scheme 60, a**) and bromination-cyclisation (**Scheme 60, b**) of a benzophenone, we were able to isolate the two different, partially brominated, isomers.



Scheme 60. Synthesis of **246** (a) and **244** (b).

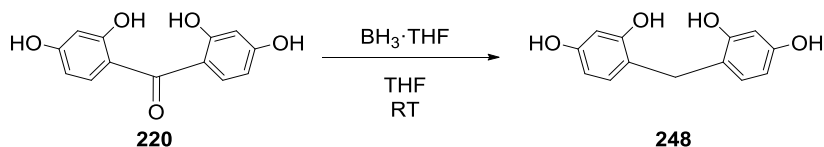
3.2.10 Reduction of benzophenones

Reductive deoxygenation of xanthenes using borane-THF complex was described by Shi (**Scheme 61**).¹⁰⁰



Scheme 61. Synthesis of **247** described by Shi.¹⁰⁰

The reduction was directly obtained on unprotected xanthenes, suggesting that it might be applicable to our benzophenones in the same way, although a larger excess of reducing agent might be necessary to compensate for the number of interfering hydroxyl groups.¹⁰⁰ Reduction of benzophenones with this method was employed for the synthesis of **248** and **135**.



Scheme 62. Synthesis of **248**.

Benzophenone **220** was reduced at room temperature with borane-THF complex in anhydrous THF, under inert atmosphere (**Scheme 62**). Compound **248** was obtained in poor yield (16%). As **Figure 66** shows, the crude of the product is reasonably pure;

however, a great part of the material is lost during column chromatography, which is a necessary step to obtain a product suitably pure for biological applications.

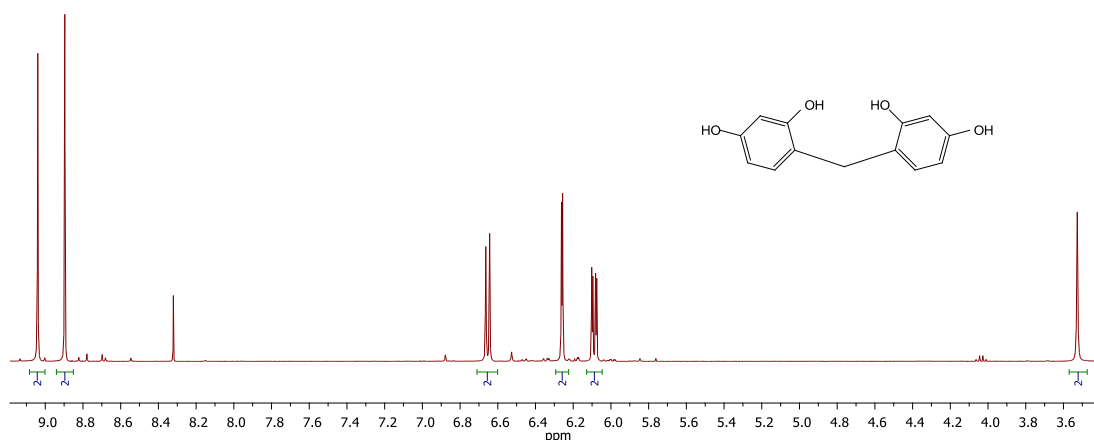
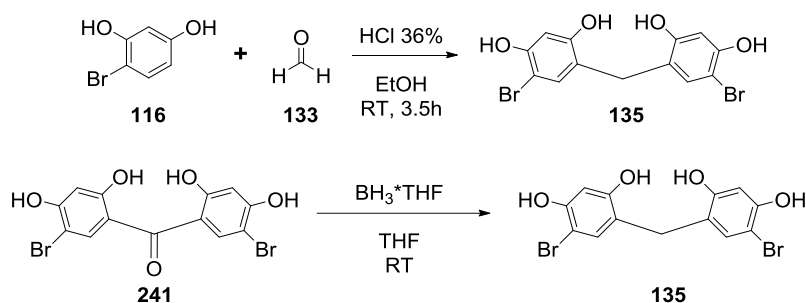


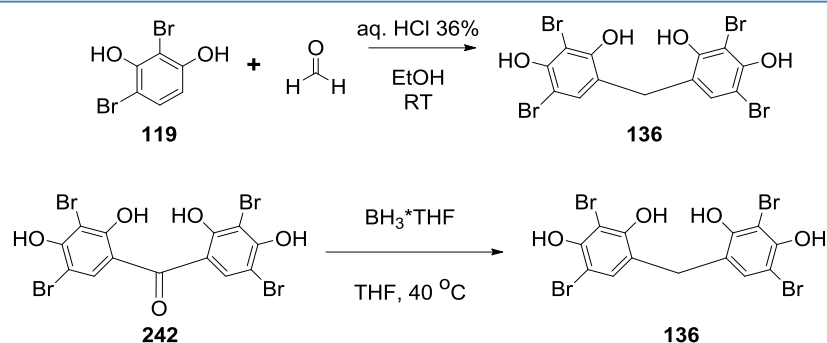
Figure 66. ¹H-NMR of **248**.

Compound **135** was previously synthesised by condensation of 4-bromoresorcinol with formaldehyde (**Scheme 63**), as described in **Chapter 2**. However, due to the low yield of the previous method, its synthesis by reduction was attempted. Following the procedure for the reduction of **220**, preparation of **135** provided a considerably better yield (39%) than the acid-catalysed dimerization (3%)



Scheme 63. Different synthetic approaches to **135**.

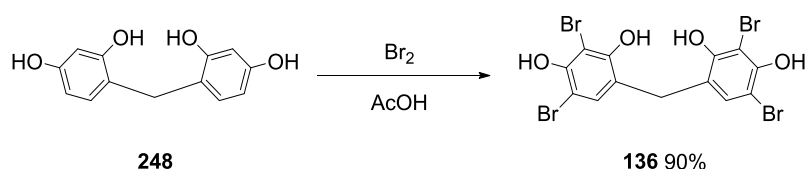
Synthesis of **136** was previously achieved by condensation in 20% yield, as described in **Chapter 2**. Its reduction by borane-THF complex was possible, although it required heating at 40 °C (**Scheme 64**). Purification proved more tedious than in the case of the condensation and the method was thus abandoned.



Scheme 64. Different synthetic approaches to **136**.

3.2.11 Bromination of bis-resorcinols

Since all brominated bis-phenols have previously been obtained by condensation or reduction, bromination of bis-resorcinols has not been attempted. However, this method has been employed by Oh for the synthesis of **136**. The method employed is the same as we used for the bromination of benzophenones and xanthenes, involving bromination with Br_2 in acetic acid. The published method claims a yield of 90% after reverse phase HPLC purification.²³ Thus, it appears that bromination of bis-resorcinol is indeed feasible and high yielding, offering an applicable alternative, were it necessary.

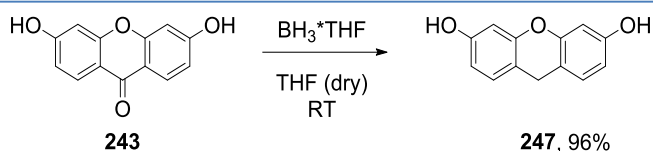


Scheme 65. Synthesis of **136** by bromination.

3.2.12 Reduction of xanthenes

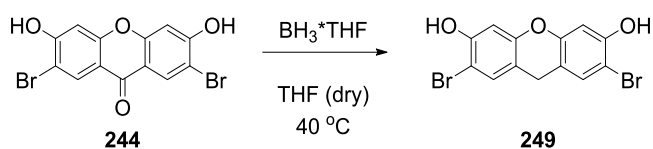
As previously illustrated in the introduction to this chapter, reduction of xanthenes has been achieved by reaction with borane in dry THF and described by Shi.¹⁰⁰

Reduction of **243** with borane-THF complex in dry THF proceeded at room temperature to yield **247**, as expected from literature (**Scheme 66**) in excellent yield (96%). After reaction the solvent was evaporated under reduced pressure and the solid residue was treated with diluted HCl, leading to a dark yellow product which can be conveniently isolated by filtration.



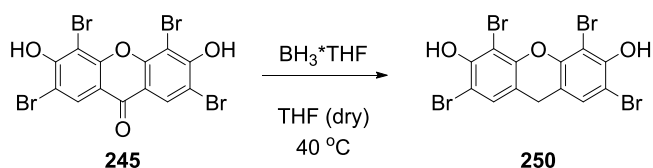
Scheme 66. Synthesis of **247**.

On the other hand, synthesis of **249** (**Scheme 67**) was not as smooth. It required heating at 45 °C and 7 equivalents of reducing agent. In contrast to **247**, the quality of the product after precipitation is not acceptable, and further purification is required. However, column chromatography led to isolation of traces of product. The product also appears to be decomposing during elution, leading to mixed fractions with lower purity than the starting material. Moreover, the product appeared to degrade pretty when exposed to natural light or as a consequence of heating.



Scheme 67. Synthesis of **249**.

As expected from the previous result, due to a poorly activated starting material, deoxygenation of **245** to **250** required a large excess of borane (9 eq) and 12 hours of reaction at 40 °C (**Scheme 68**). Once again, the compound is not very stable and its formation was identified by ¹H-NMR but its purification by flash chromatography led to a product with worse quality than the starting crude.



Scheme 68. Synthesis of **250**.

The ¹H-NMR profile is consistent in all cases: reduction of the xanthone leads to a high field shift in the position of all aromatic and hydroxyl protons. The appearance of a peak around 3.4-4 ppm is diagnostic of a successful deoxygenation (**Figure 67**).

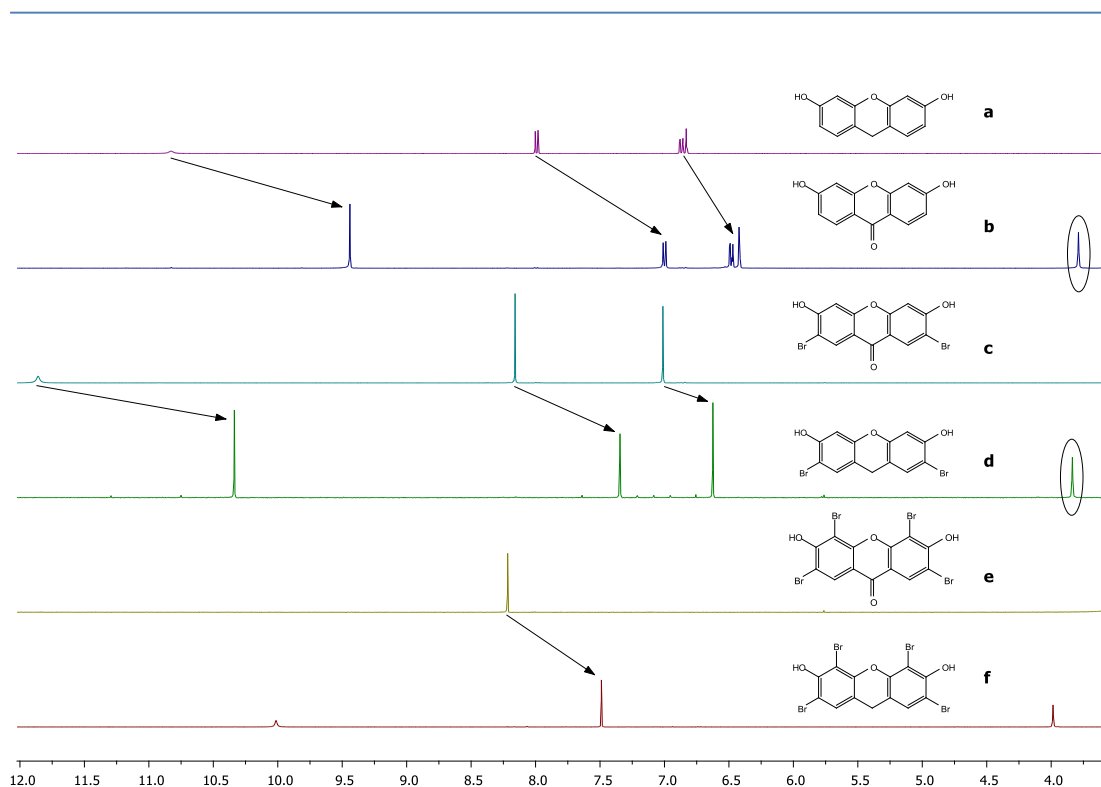


Figure 67. ^1H -NMR of **247** (a), **243** (b), **244** (c), **249** (d), **245** (e) and **250** (f).

The reduction of the carbonyl is blatant in the ^{13}C -NMR, with the reduced carbon shifting from 175 ppm to 25 ppm (**Figure 68**).

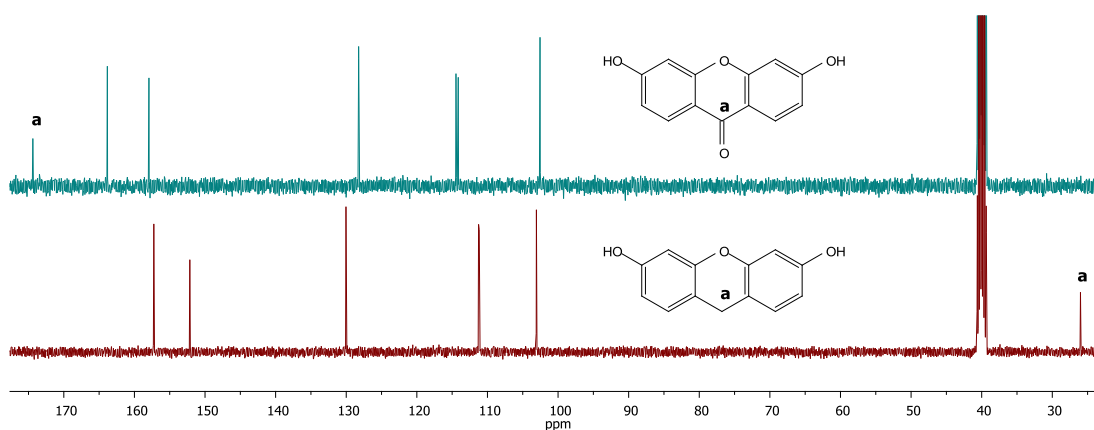


Figure 68. ^{13}C -NMR of **247** (bottom) and **243** (top).

Since the purification and the stability of **249** and **250** were not ideal, the xanthene group was not considered for further development and testing. The results presented come from explorative reactions, therefore, yields and full characterisation of **249** and **250** are not reported and further investigation and optimisation are necessary if the compounds were to become of interest.

3.3 Conclusions

In **Chapters 2** and **3**, the synthesis of a number of novel structures have been described. Most notable among these are the tetramers and hexamers, interesting both for their potential biological application and for the construction of dendrimers, as described in the following chapter. The simpler structures, bis-resorcinols, benzophenones and xanthenes presented in this chapter are interesting as comparison against the dimers and tetramers. A flexible approach for their synthesis has been presented and discussed. The presented compounds which will be investigated in **Chapters 5** and **6** are summarised in **Figure 69**.

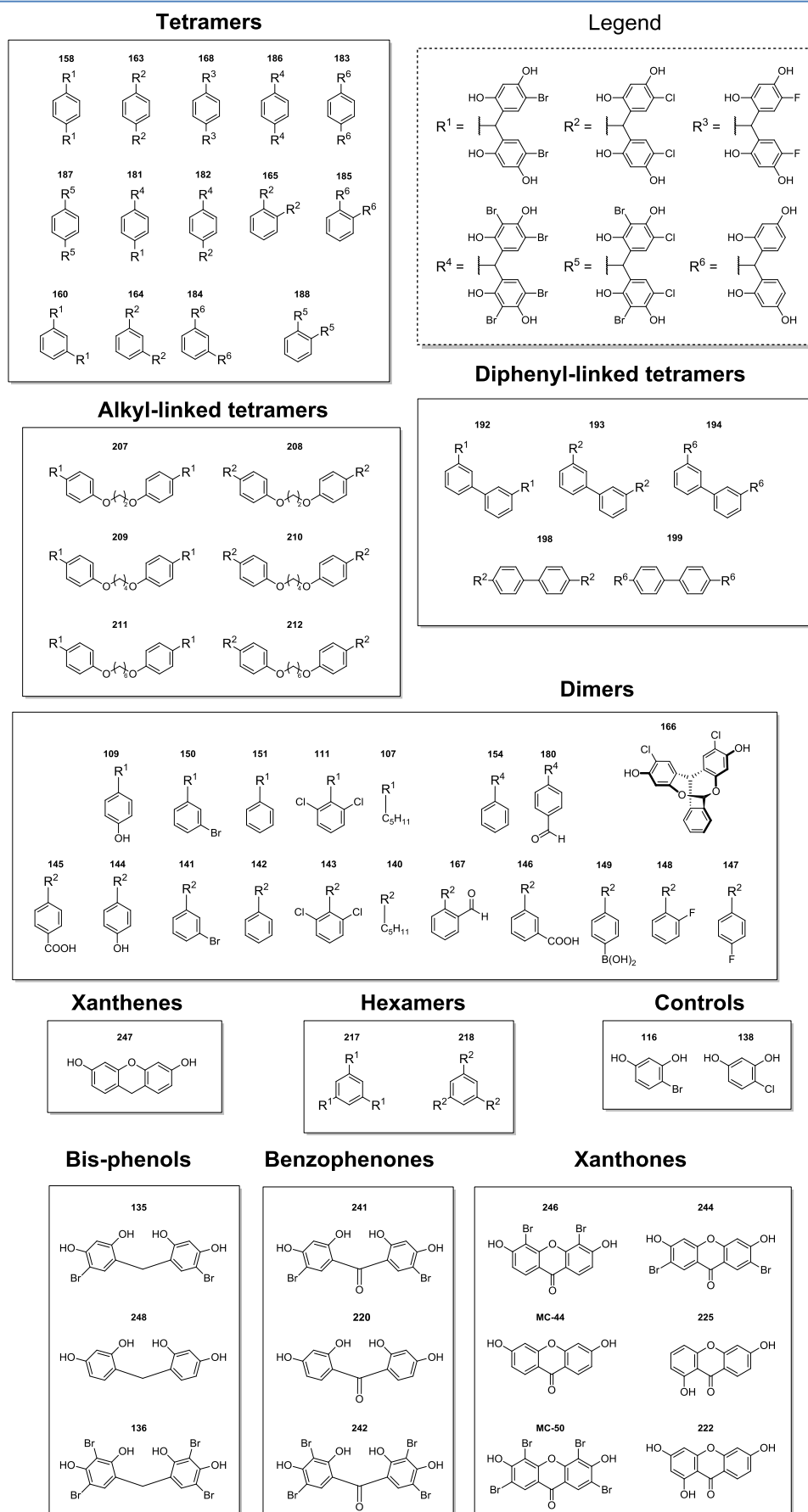


Figure 69. Structures presented in the previous chapters and considered for the *in vitro/in vivo* testing in the following chapters.

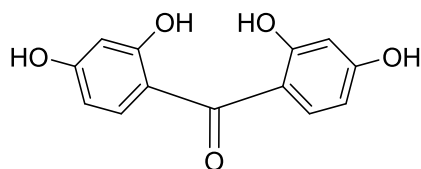
3.4 Experimental

3.4.1 General

All reagents and solvents for synthesis were commercial and used without further purification. NMR spectra were recorded at 293 K, unless otherwise stated, using a 400 MHz Spectrometer. Shifts are referenced relative to deuterated solvent residual peaks. Infrared spectra were recorded using an FT-IR spectrometer with ATR attachment. MS were run on an LTQ orbitrap XL and were recorded by the EPSRC Mass Spectrometry National facility. Thin-layer chromatography (TLC) was carried out on aluminium sheets coated with silica gel 60 F254 (Merck). TLC plates were inspected by UV light ($\lambda = 254$ nm). Silica gel column chromatography was performed with silica gel Si 60 (40–63 μm).

3.4.2 Synthesis

Compound 220¹²¹



A mixture of 2,4-dihydroxybenzoic acid (3.1 g, 20.11 mmol), resorcinol (2 g, 18.16 mmol) and zinc chloride (12 g, 88.05 mmol) in 15 mL of POCl_3 was allowed to stir at 70 °C for 3 hours. The reaction was poured on ice and allowed to stir for an hour. The solid was collected, washed with cold water and dried in the oven (60 °C) to give a yellow powder.

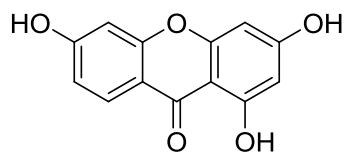
Yield: 40.1%

^1H -NMR (400 MHz, DMSO) δ 11.27 (s, 2H, ArOH), 10.25 (s, 2H, ArOH), 7.19 (d, $J=9.2$, 2H, ArH), 6.37 – 6.28 (m, 4H, ArH).

^{13}C -NMR (101 MHz, DMSO) δ 199.24, 162.77, 160.62, 133.48, 115.20, 107.29, 102.38.

MP = 199-202 °C (lit. 200-201 °C)¹²¹

Compound 222¹²²



A mixture of 2,4-dihydroxybenzoic acid (2 g, 20.11 eq), phloroglucinol (1.5 g, 11.89 mmol) and zinc chloride (6.5 g, 47.7 mol) in 7.5 mL of POCl₃ was allowed to stir at 70 °C for 3 hours. The reaction was poured on ice and allowed to stir for an hour. The solid was collected, washed with cold water and dried in the oven (60 °C) to give a yellow powder.

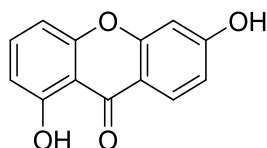
Yield: 90.5%

¹H-NMR (400 MHz, DMSO) δ 13.11 (s, 1H, ArOH), 11.04 (b, 2H, ArOH), 8.03 (d, J =8.7, 1H, ArH), 6.95 (dd, J =8.7, 2.2, 1H, ArH), 6.88 (d, J =2.2, 1H, ArH), 6.41 (d, J =2.1, 1H, ArH), 6.23 (d, J =2.1, 1H, ArH).

¹³C-NMR (101 MHz, DMSO) δ 179.55, 165.63, 164.72, 163.30, 157.91, 157.82, 127.65, 114.48, 112.78, 102.51, 102.09, 98.43, 94.41.

MP = 295 °C decomp. (lit. 323-324 °C)¹²²

Compound 225¹²³



A mixture of 2,6-dihydroxybenzoic acid (3.1 g, 20.11 mmol), resorcinol (2 g, 18.16 mmol) and zinc chloride (12 g, 88.05 mmol) in 15 mL of POCl₃ was allowed to stir at 70 °C for 3 hours. The reaction was poured on ice and allowed to stir for an hour. The solid was collected, washed with cold water and extracted with ethyl acetate. The organic layer was washed with brine, dried on magnesium sulfate and the solvent was removed under reduced pressure. The solid was purified by flash chromatography on silica gel using 40/1 DCM/MeOH as eluent to give a yellow powder.

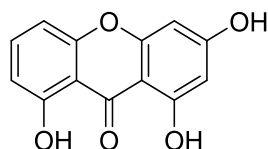
Yield: 26.5%

^1H -NMR (400 MHz, DMSO) δ 12.85 (s, 1H, ArOH), 11.20 (s, 1H, ArOH), 8.05 (d, $J=8.8$, 1H, ArH), 7.68 (t, $J=8.3$, 1H, ArH), 7.03 (d, $J=8.3$, 1H, ArH), 6.95 (dd, $J=8.8$, 2.1, 1H, ArH), 6.88 (d, $J=2.1$, 1H, ArH), 6.79 (d, $J=8.3$, 1H, ArH).

^{13}C -NMR (101 MHz, DMSO) δ 180.61, 164.95, 161.03, 157.80, 155.75, 136.71, 127.50, 114.51, 112.45, 110.13, 107.83, 106.96, 102.04.

MP: 258-261 °C (lit. 258-259 °C)¹²³

Compound 227



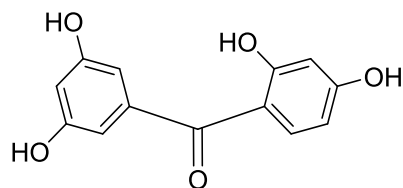
A mixture of 2,6-dihydroxybenzoic acid (4 g, 25.95 mmol), phloroglucinol (3 g, 23.79 mmol) and zinc chloride (13 g, 95.39 mmol) in 15 mL of POCl_3 was allowed to stir at 70 °C for 3 hours. The reaction was poured on ice and allowed to stir for an hour. The solid was collected, washed with cold water and extracted with ethyl acetate. The organic layer was washed with brine, dried on magnesium sulfate and the solvent was removed under reduced pressure. The solid was purified by flash chromatography on silica gel using 40/1 DCM/MeOH as eluent to give a yellow powder.

Yield: 9.4%

^1H -NMR (400 MHz, DMSO) δ 11.86 (s, 1H, ArOH), 11.82 (s, 1H, ArOH), 11.26 (s, 1H, ArOH), 7.70 (t, $J=8.3$, 1H, ArH), 7.01 (d, $J=8.3$, 1H, ArH), 6.81 (d, $J=8.3$, 1H, ArH), 6.41 (d, $J=2.1$, 1H, ArH), 6.24 (d, $J=2.1$, 1H, ArH).

^{13}C -NMR (101 MHz, DMSO) δ 183.43, 166.52, 162.16, 160.26, 157.46, 155.48, 137.21, 110.59, 107.08, 106.86, 101.16, 98.54, 94.33.

Compound 229



A mixture of 3,5-dihydroxybenzoic acid (3.1 g, 20.11 mmol), resorcinol (2 g, 18.16 mmol) and zinc chloride (12 g, 88.05 mmol) in 15 mL of POCl_3 was allowed to stir at

70 °C for 2 hours. The reaction was poured on ice and allowed to stir for 24 hours. The precipitate was collected by Büchner filtration, washed with a 3% solution of NaHCO₃ and dried in the oven (60 °C). The solid was dispersed in water, the solution was saturated with NaHCO₃ and the product was extracted with ethyl acetate. The organic layer was dried over sodium sulfate, and the solvent was removed to give **229**.

Yield: 4.9%

[M+H]⁺ = 247.0601 (Calculated: 247.0601)

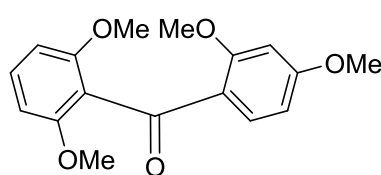
¹H-NMR (400 MHz, DMSO) δ 12.23 (s, 1H, ArOH), 10.70 (s, 1H, ArOH), 9.64 (s, 2H, ArOH), 7.43 (d, *J*=8.8, 1H, ArH), 6.42 (s, 3H, ArH), 6.38 (dd, *J*=8.8, 2.3, 1H, ArH), 6.34 (d, *J*=2.3, 1H, ArH).

¹³C-NMR (101 MHz, DMSO) δ 198.84, 164.79, 164.52, 158.24, 139.69, 135.24, 112.26, 107.98, 106.59, 105.42, 102.66.

SiO₂/P₂O₅ catalyst

Prepared according to the method by Zarei, with minor modifications.¹⁰⁹ Silica gel was washed with 10% HCl and dried in the oven at 120 °C over three days. Three grams of silica were then mixed with 3 grams of P₂O₅ using a glass rod for 10 minutes to give a very thin powder, which was then dried in the oven for 1 hour. The catalyst was stored in a sealed plastic box.

Compound 225



Method with SiO₂/P₂O₅

A mixture of 2,6-dimethoxybenzoic acid (2.5 g, 13.7 mmol), 1,3-dimethoxybenzene (3.792 g, 27.4 mmol) and SiO₂/P₂O₅ (10 g) in DCE (50 mL) was allowed to stir for 24 hours at 40 °C. The resulting mixture was shaken vigorously with DCM (50 mL) and the liquid was decanted. The procedure was repeated three times. The solid was then suspended with 50 mL of DCM and removed by filtration. The solid was washed a last time with 50 mL of DCM and the organic layers were combined. The organic extract was washed with a saturated solution of NaHCO₃, brine and dried over sodium sulfate.

The solvent was removed under reduced pressure and the resulting oil was triturated with hexane to give the product (1.82 g) as white solid.

To recover a larger amount of product, the solid residue previously discarded was treated with a saturated solution of NaHCO_3 in water, and the resulting mixture was extracted with ethyl acetate. The organic layer was washed with brine, dried over sodium sulfate and the solvent was removed under reduced pressure. Upon purification by flash chromatography (DCM) an additional 0.86 g of product were collected.

Total yield: 65.7%

Method with MeSO_3H and graphite

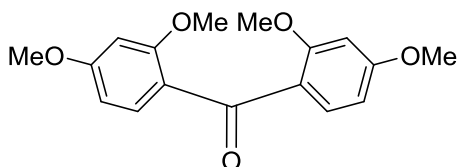
A mixture of 2,6-dimethoxybenzoic acid (364.3 mg, 2 mmol), 1,3-dimethoxybenzene (0.26 mL, 2 mmol), graphite (0.2 g) in MeSO_3H (0.6 mL, 8 mmol) was heated at 40 °C for 1 hour. The mixture was diluted with DCM and graphite was removed by filtration. The solution was treated with saturated NaHCO_3 and the organic layer was separated, washed with saturated NaHCO_3 twice, with brine and dried over sodium sulfate. The solvent was removed under reduced pressure and the residue was triturated with hexane to give **225**.

^1H NMR (400 MHz, DMSO) δ 7.50 (d, J = 8.5 Hz, 1H), 7.31 (t, J = 8.4 Hz, 1H), 6.70 (d, J = 8.4 Hz, 2H), 6.61 – 6.53 (m, 2H), 3.83 (s, 3H), 3.64 (s, 9H).

^{13}C NMR (101 MHz, DMSO) δ 190.95, 164.97, 162.00, 156.82, 134.36, 130.24, 121.51, 120.63, 106.07, 104.67, 99.32, 56.19, 56.14, 56.05.

MP: 130-132 °C

Compound **233**¹²⁴



Method with MeI

A mixture of 2,2',4,4'-tetrahydroxybenzophenone (4g, 16.2 mmol), K_2CO_3 (23.4g, 169.3 mmol), and MeI (6 mL, 96.4 mmol) in 200 mL of DMF was allowed to stir at room temperature for 41 hours. 600 mL of distilled water were added and allowed to

stir for 15 minutes. The white precipitate was collected by Büchner filtration and washed with 800 mL of distilled water. The solid was dissolved in 400 mL of ethyl acetate and washed with 400 mL of water, 400 mL of brine and dried over sodium sulfate. The solvent was evaporated under reduced pressure to give 4.3 g of white product.

Yield: 87.5%

Method with 2,4-dimethoxybenzoic acid and 1,3-dimethoxybenzene

A mixture of 2,4-dimethoxybenzoic acid (364.3 mg, 2 mmol), 1,3-dimethoxybenzene (0.26 mL, 2 mmol), graphite (0.2 g) in MeSO₃H (0.6 mL, 8 mmol) was heated at 40 °C for 62 hours. The mixture was diluted with DCM and graphite was removed by filtration. The solution was treated with saturated NaHCO₃ and the organic layer was separated, washed with saturated NaHCO₃ twice, with brine and dried over sodium sulfate. The solvent was removed under reduced pressure and the residue was triturated with hexane to give **233**.

Method with 2,6-dimethoxybenzoic acid and 1,3-dimethoxybenzene

A mixture of 2,6-dimethoxybenzoic acid (364.3 mg, 2 mmol), 1,3-dimethoxybenzene (0.26 mL, 2 mmol), graphite (0.2 g) in MeSO₃H (0.6 mL, 8 mmol) was heated at 40 °C for 36 hours. The mixture was diluted with DCM and graphite was removed by filtration. The solution was treated with saturated NaHCO₃ and the organic layer was separated, washed with saturated NaHCO₃ twice, with brine and dried over sodium sulfate. The solvent was removed under reduced pressure and the residue was triturated with hexane to give **233**.

Method with 2,6-dimethoxybenzoic acid alone

Same as previous method, without 1,3-dimethoxybenzene.

Method from 225

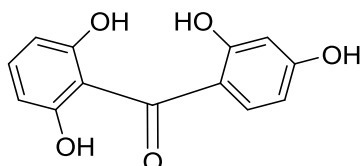
A mixture of **225** (180 mg, 0.6 mmol), graphite (0.1 g) in MeSO₃H (0.3 mL, 4 mmol) was heated at 40 °C for 27 hours. The mixture was diluted with DCM and graphite was removed by filtration. The solution was treated with saturated NaHCO₃ and the organic layer was separated, washed with saturated NaHCO₃ twice, with brine and dried over sodium sulfate. The solvent was removed under reduced pressure and the residue was triturated with hexane to give **233**.

^1H NMR (400 MHz, DMSO) δ 7.35 (m, 2H), 6.62 – 6.53 (m, 4H), 3.83 (s, 6H), 3.61 (s, 6H).

^{13}C NMR (101 MHz, DMSO) δ 192.05, 163.58, 160.19, 132.09, 123.66, 105.50, 98.76, 56.05, 55.91.

MP: 124-125 °C (lit. 138-140 °C)¹²⁴

Compound 224



Within a sealed system, saturated with Argon, a solution of BBr_3 (2.55 mL, mmol) in 17 mL of DCM was added (over 30 minutes) to a stirring solution of **225** (850 mg, mmol) in 17 mL DCM, and the temperature was maintained at -78 °C. After 30 minutes the cold bath was removed and the reaction was allowed to reach room temperature. The reaction was allowed to stir for three days and then cooled to 0 °C. Ice-cold water (40 mL) was slowly added to the mixture and DCM was subsequently evaporated under reduced pressure. The solid product was collected by Büchner filtration.

Yield: 66.9%

Note: the product decomposed after being exposed for prolonged times to air and light, and was purified by flash chromatography with DCM/MeOH 12/1.

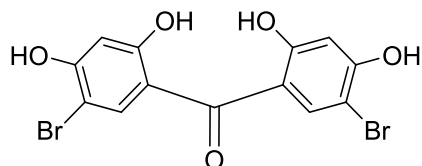
^1H -NMR (400 MHz, DMSO) δ 12.63 (s, 1H), 10.65 (s, 1H), 9.57 (s, 2H), 7.13 (d, J = 8.5 Hz, 1H), 7.05 (t, J = 8.2 Hz, 1H), 6.38 (d, J = 8.2 Hz, 2H), 6.34 – 6.27 (m, 2H).

^{13}C -NMR (101 MHz, DMSO) δ 200.06, 165.46, 164.93, 155.53, 135.86, 130.85, 114.70, 114.55, 108.64, 106.82, 102.54.

MP = 254 -260 °C

$[\text{M}+\text{H}]^+ = 247.0602$ (Calculated: 247.0601)

Compound 241⁹⁹



A solution of bromine (0.83 mL, 16.24 mmol) in acetic acid (12 mL) was added drop wise to a allowed to stir solution of **220** (2 g, 8.12 mmol) in acetic acid (20 mL). Two hours after completing the addition of bromine, the reaction was poured in ice water. The solid was collected by Büchner filtration and washed with distilled water. The product was purified by filtration from boiling water and then, if necessary, by column chromatography (30/1 DCM/MeOH) to give a yellow powder.

Note: dissolution of **220** in acetic acid requires heating to 40-50 °C. After complete dissolution, the mixture is allowed to cool down below 30 °C.

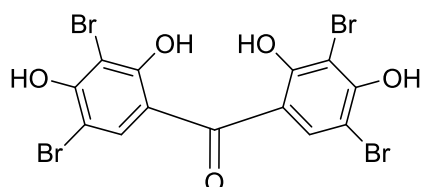
Yield: 94%

¹H NMR (400 MHz, DMSO) δ 11.24 (s, 4H), 7.43 (s, 2H), 6.55 (s, 2H).

¹³C NMR (101 MHz, DMSO) δ 196.93, 159.73, 159.66, 135.85, 117.12, 103.82, 99.96.

MP: 224-228 °C (lit. 211 °C)⁹⁹

Compound 242⁹⁹



A solution of bromine (0.83 mL, 16.24 mmol) in acetic acid (4 mL) was added drop wise to a stirring solution of **220** (1 g, 4.6 mmol) in acetic acid (8 mL) at 50 °C. The mixture was allowed to stir for 4 hours and then it was poured in ice water. The solid was collected by Büchner filtration and washed with distilled water. The product was purified by filtration from boiling water to give a yellow solid.

Yield: 61.6%

¹H NMR (400 MHz, DMSO) δ 11.54 (s, 2H), 7.49 (s, 2H).

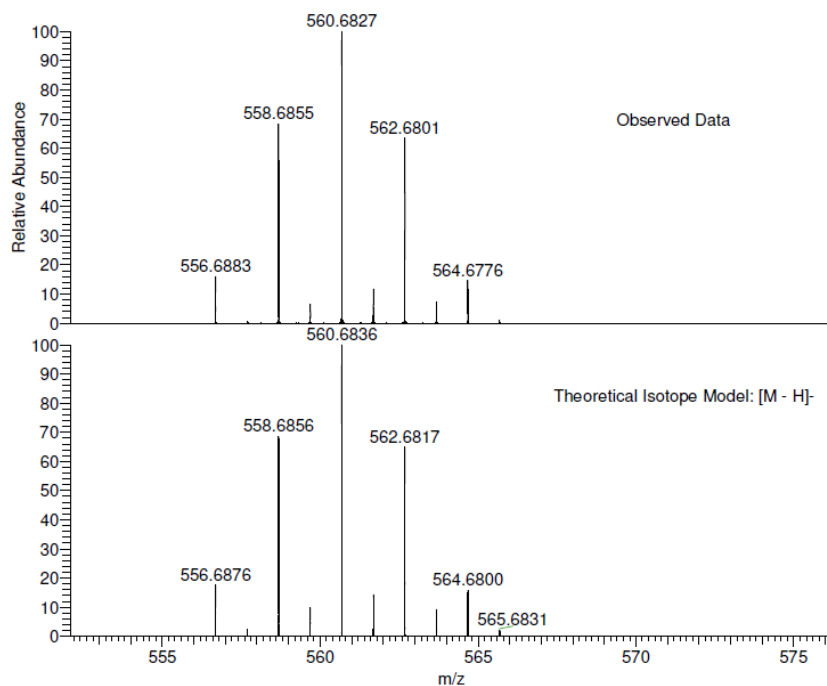
¹³C NMR (101 MHz, DMSO) δ 195.93, 156.06, 155.95, 133.48, 117.26, 101.30, 101.00.

MP: 275-277 °C (254 °C)⁹⁹

MC-27 MW-561?
C₁₃H₅Br₄O₅
(MeOH)/MeOH

EPSRC National Facility Swansea
LTQ Orbitrap XL

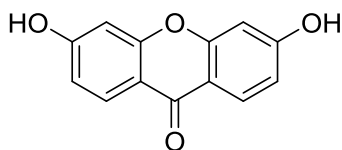
Marco Cominetti
04/09/2013 10:31:17



NL:
2.52E8
UEAMAT206-OJ-HNESN#59-
62 RT: 1.51-1.73 AV: 4 T:
FTMS - p NSI Full ms
[200.00-4000.00]

NL:
7.55E3
C₁₃ H₅ Br₄ O₅:
C₁₃ H₅ Br₄ O₅
p (gss, s /p:40) Chrg -1
R: 100000 Res .Pwr . @FWHM

Compound 243



A mixture of **220** (200 mg, 0.876 mmol) in distilled water (6 mL) was heated to 220-230 °C in an Ace pressure tube fitted with a silicone back seal using a preheated sand bath at 230 °C. When a completely colourless solution was obtained, the tube was removed and allowed to cool down slowly to room temperature. The tube was then cooled down to 4 °C in the fridge to complete the crystallization of the product. The solid was then collected by Büchner filtration and washed with cold water to give white needles.

Note 1: silicone is the material of choice as it provides the highest working temperatures. However, the reaction temperature is close to its limits. Worn out seals and higher temperatures have to be avoided. If the seal fails, a jet of steam is produced: adequate shielding and attention is required.

Note 2: reaction duration is not provided as very different times were experienced, colour proved to be an effective way to check the reaction progress.

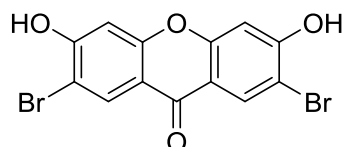
Yield: 94.8%

MP: > 350 °C

^1H NMR (400 MHz, DMSO) δ 10.83 (s, 2H), 7.99 (d, J = 8.7 Hz, 2H), 6.87 (dd, J = 8.7, 2.2 Hz, 2H), 6.83 (d, J = 2.2 Hz, 2H).

^{13}C NMR (101 MHz, DMSO) δ 173.88, 163.33, 157.44, 127.74, 113.95, 113.63, 102.05.

Compound 244⁹⁹



A mixture of **241** (100 mg, 0.259 mmol) in distilled water (6 mL) was heated to 220-230 °C in an Ace pressure tube fitted with a silicone back seal using a preheated sand bath at 230 °C. The tube was removed after 18 hours and allowed to cool down slowly to room temperature. The solid was then collected by Büchner filtration and washed with cold water to give a white solid.

Note 1: silicone is the material of choice as it provides highest working temperatures. However, the reaction temperature is close to its limits. Worn out seals and higher temperatures have to be avoided. If the seal fails, a jet of steam is produced: adequate shielding and attention is required.

Note 2: 18 hours is indicative, very different times were experienced. The reaction progress can be easily checked by NMR and the reaction can be allowed longer times.

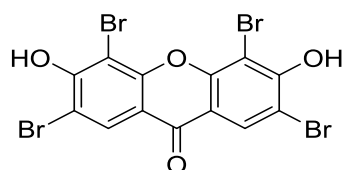
Yield: 83.3%

^1H NMR (400 MHz, DMSO) δ 11.86 (s, 2H), 8.16 (s, 2H), 7.01 (s, 2H).

^{13}C NMR (101 MHz, DMSO) δ 172.65, 160.23, 156.63, 130.33, 115.18, 107.80, 103.73.

MP: 377-380 °C (lit. 330 °C)⁹⁹

Compound 245⁹⁹



Method with sealed tube

A mixture of **242** (200 mg, 0.356 mmol) in distilled water (6 mL) was heated to 220 °C in an Ace pressure tube fitted with a silicone back seal using an oven. The tube was removed after 14 hours and allowed to cool down slowly to room temperature. The solid was then collected by Büchner filtration and washed with cold water.

Yield: 89.7%

Method by bromination

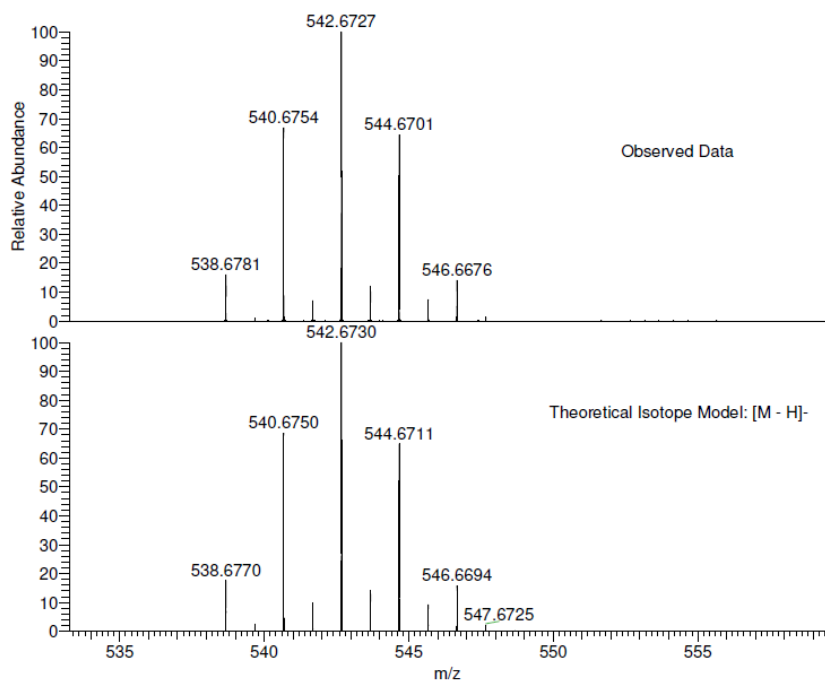
A solution of bromine (0.38 mL, 7.362 mmol) in acetic acid (2 mL) was slowly added to a mixture of **243** (400 mg, 1.753 mmol) in acetic acid (4 mL) and allowed to stir at room temperature. The reaction was checked daily by ¹H-NMR to verify its completion. An excess of bromine was always maintained in the reaction by addition of further 0.38 mL of bromine when the solution lost its light orange colour. Upon completion, air was bubbled through the mixture to remove any excess of bromine the solid was collected by Büchner filtration and washed with distilled water. The product was purified by filtration from boiling water to give a white solid.

Yield: 90.6%

¹H NMR (400 MHz, DMSO) δ 8.22 (s, 2H).

¹³C NMR (101 MHz, DMSO) δ 172.3, 157.7 (uncertain), 153.5, 109.2, 100.2.

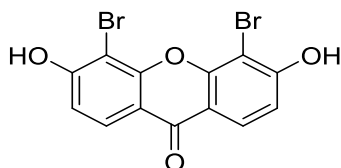
MP: 330-332 °C (lit. 281 °C)⁹⁹



NL:
1.06E8
UEAMAT205-OJ-HNESN#64-
65 RT: 1.57-1.65 AV: 2 T:
FTMS - p NSI Full ms
[200.00-4000.00]

NL:
7.57E3
C₁₃ H₃ Br₄ O₄:
C₁₃ H₃ Br₄ O₄
p (gss, s /p:40) Chrg -1
R: 100000 Res .Pwr . @FWHM

Compound 246



A solution of bromine (0.45 mL, 8.76 mmol) in acetic acid (100 mL) was added drop wise to a stirring solution of **243** (1 g, 4.38 mmol) in acetic acid (120 mL). The mixture was allowed to stir for 18 hours at room temperature and then it was poured in ice water. The solid was collected by Büchner filtration and washed with distilled water. The product was purified by filtration from boiling water to give a white solid.

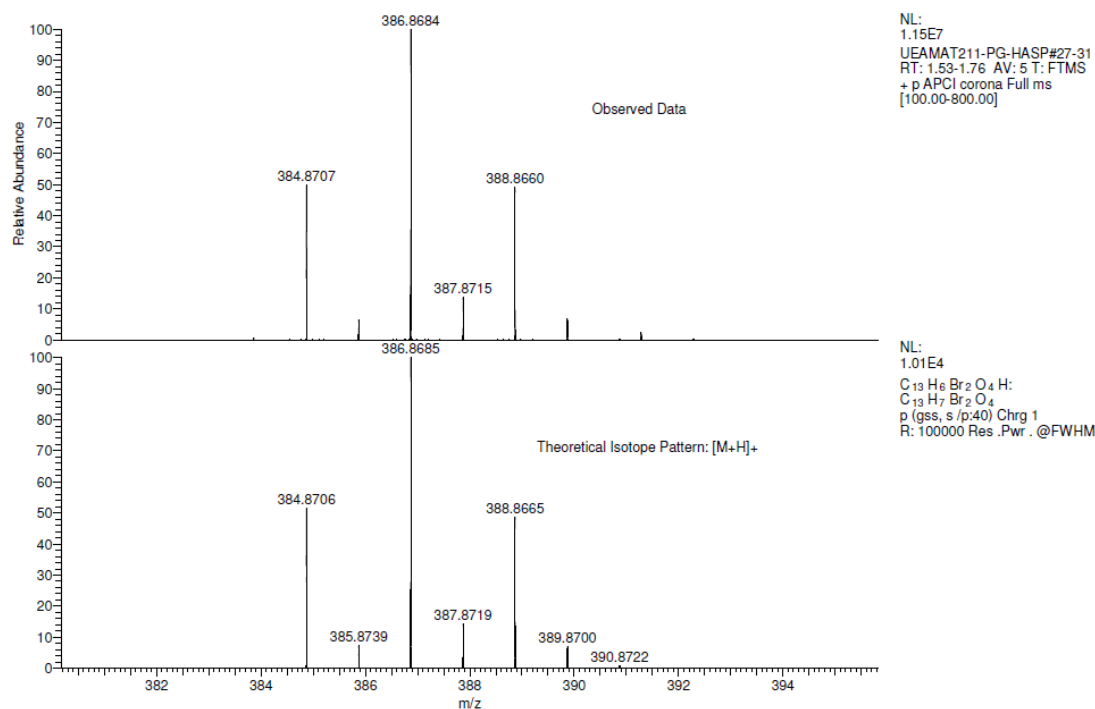
Yield: 83.7%

¹H NMR (400 MHz, DMSO) δ 11.74 (s, 2H), 8.01 (d, *J* = 8.8 Hz, 2H), 7.09 (d, *J* = 8.8 Hz, 2H).

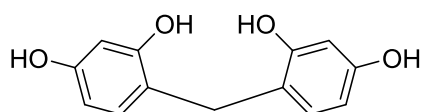
¹³C NMR (101 MHz, DMSO) δ 173.91, 161.06, 154.48, 126.73, 114.97, 113.95, 97.43.

IR (ν_{max}, cm⁻¹): 3463, 3081, 1599, 1570, 1425, 1353, 1335, 1305, 1206, 1176, 1124, 1047, 843, 775.

MP = 329-332 °C



Compound 248¹²⁵



A solution of $\text{BH}_3 \cdot \text{THF}$ 1M (14 mL, 14 mmol) was added to a allowed to stir solution of **220** (1.55 g, 6.3 mmol) in 100 mL of dry THF under argon. The mixture was allowed to stir overnight, then THF was removed under reduced pressure. The solid was dissolved in a solution of aq. NaOH and precipitated by acidification with HCl. The solid was collected by Büchner filtration and purified by flash chromatography using 15/1 DCM/MeOH as eluent to give an off white powder.

Yield: 16%

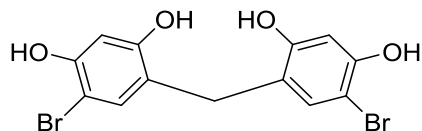
^1H -NMR (400 MHz, DMSO) δ 9.04 (s, 2H), 8.89 (s, 2H), 6.65 (d, $J=8.2$, 2H), 6.26 (d, $J=2.4$, 2H), 6.09 (dd, $J=8.2$, 2.4, 2H), 3.52 (s, 2H).

^{13}C -NMR (101 MHz, DMSO) δ 156.08, 155.47, 130.27, 118.03, 105.82, 102.18, 27.80 (Ar_2CH_2).

IR (ν_{max} , cm^{-1}): 3203, 1612, 1601, 1511, 1462, 1433, 1405, 1326, 1314, 1305, 1268, 1220, 1167, 1106, 970, 850, 839, 825.

MP: 207-210 °C (250 °C)¹²⁵

Compound 135

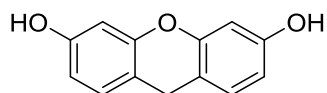


A solution of $\text{BH}_3 \cdot \text{THF}$ 1M (3.1 mL, 3.1 mmol) was added to a allowed to stir solution of **241** (500 mg, 1.24 mmol) in 30 mL of dry THF under argon. The mixture was allowed to stir overnight, then THF was removed under reduced pressure. The solid was dissolved in a solution of aq. NaOH and precipitated by acidification with HCl. The solid was collected by Büchner filtration and purified by flash chromatography using 20/1 DCM/MeOH as eluent to give an off white solid.

Yield: 39%

See **Chapter 2** for an alternative method and analytical data.

Compound 247¹⁰⁰



Prepared according to the procedure by Shi.¹⁰⁰

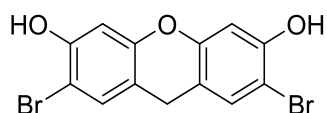
Yield: 96.3%

^1H NMR (400 MHz, DMSO) δ 9.44 (s, 2H), 7.00 (d, J = 8.2 Hz, 2H), 6.48 (dd, J = 8.2, 2.4 Hz, 2H), 6.42 (d, J = 2.4 Hz, 2H), 3.79 (s, 2H).

^{13}C NMR (101 MHz, DMSO) δ 157.25, 152.15, 130.04, 111.26, 111.16, 103.06, 26.01.

MP: 215-218 °C

Compound 249

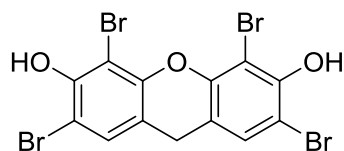


BH_3 -THF complex 1 M in THF (7 mL, 7 mmol) was slowly added to a allowed to stir solution of **244** (400 mg, 1.04 mmol) in 30 mL of dry THF. The reaction was performed under argon and after addition of the reducing agent was allowed to stir for 2.5 hours at 45 °C. The solvent was carefully removed by evaporation and the residue was treated

with 20 mL of HCl 1M. The mixture was allowed to stir for two hours and solid product was collected by Büchner filtration.

^1H NMR (400 MHz, DMSO) δ 10.34 (s, 2H), 7.35 (s, 2H), 6.62 (s, 2H), 3.84 (s, 2H).

Compound 250



BH_3 -THF complex 1 M in THF (1.65 mL, 1.65 mmol) was slowly added to a allowed to stir solution of **245** (100 mg, 0.184 mmol) in 10 mL of dry THF. The reaction was performed under argon and after addition of the reducing agent was allowed to stir for 12 hours at 40 °C. The solvent was carefully removed by evaporation and the residue was treated with 20 mL of HCl 1M. The mixture was allowed to stir for two hours and then extracted with ethyl acetate (3 x 20 mL). The organic layers were dried with magnesium sulfate and evaporated under reduced pressure. The solid obtained was resuspended in HCl 1M and collected by Büchner filtration.

^1H NMR (400 MHz, DMSO) δ 10.01 (s, 2H), 7.49 (s, 2H), 3.99 (s, 2H).

4. Synthesis of dendrimers

4.1 Dendrimers

As the etymology of the word suggests, dendrimers are branched structures, somewhat resembling a tree. They are characterised by a central core and present one or more layers (generations) of branches. Differently from polymers, they are well defined structures. They are often synthesised with repetitive reaction sequences (**Figure 70**), proceeding either from the core and adding fragments outwards (divergent synthesis) or, *viceversa*, external fragments can be built and eventually bound to the core (convergent synthesis).^{126,127}

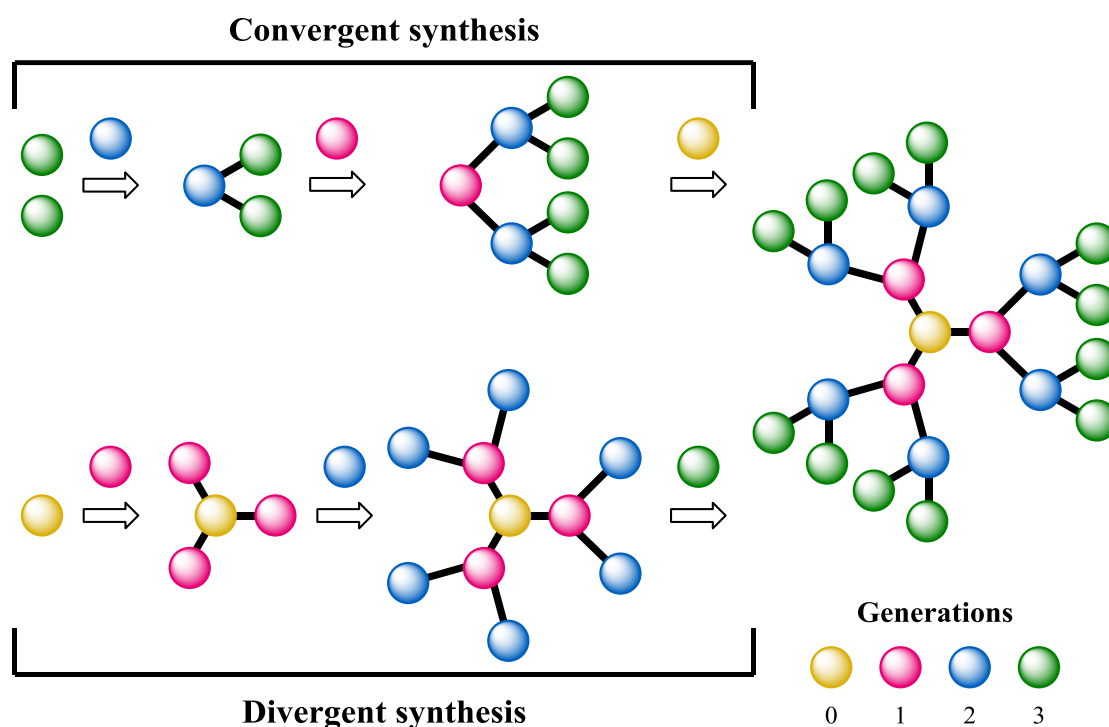


Figure 70. Convergent and divergent synthesis of dendrimers.

Dendrimers and multivalent structures have applications in a wide range of fields. Being able to carry different structures, they can be adapted to interact with a range of biological and non-biological targets and with well-defined structures they can also be used to build supramolecular structures and in crystal engineering.¹²⁸⁻¹³⁰

4.2 Calixarenes

Within our research group, dendrimers have been developed in a number of ways using calixarenes as key building blocks.^{131,132} Calixarenes are macrocyclic structures obtained by reaction of phenols with aldehydes.¹³³ As the name suggests, calix[*n*]arenes are constituted by *n* phenolic units to form a chalice-like structure. The two main types of structures employed within the group are calix[4]arenes based on phenol (and henceforth, simply addressed as calixarene) and calix[4]resorcinarenes (resorcinarene), based on resorcinol (**Figure 71**). The tetramers previously described can be considered as an “open” form of a calix[4]resorcinarene, and the hexamer an “open” calix[6]resorcinarene.

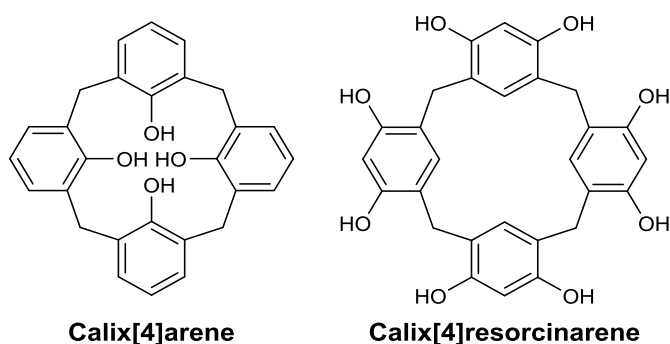


Figure 71. Basic structure of calix[4]arenes and calix[4]resorcinarenes.

Calixarenes are easily accessible on large scales and are extremely flexible building blocks. They can be conveniently and selectively functionalised at the upper rim, lower rim and methylene bridges. Also, upon introduction of sterically hindering groups, they can be locked into specific conformations, providing access to differently presented and well organised structures (**Figure 72**).

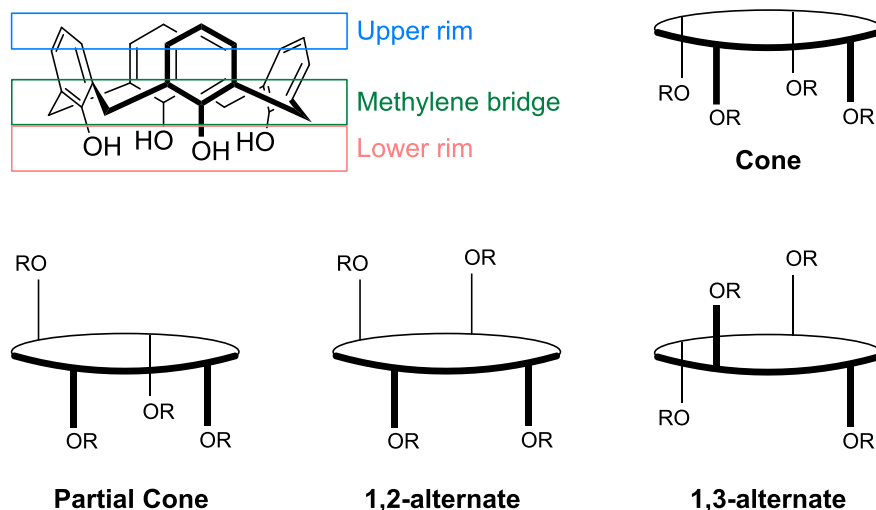
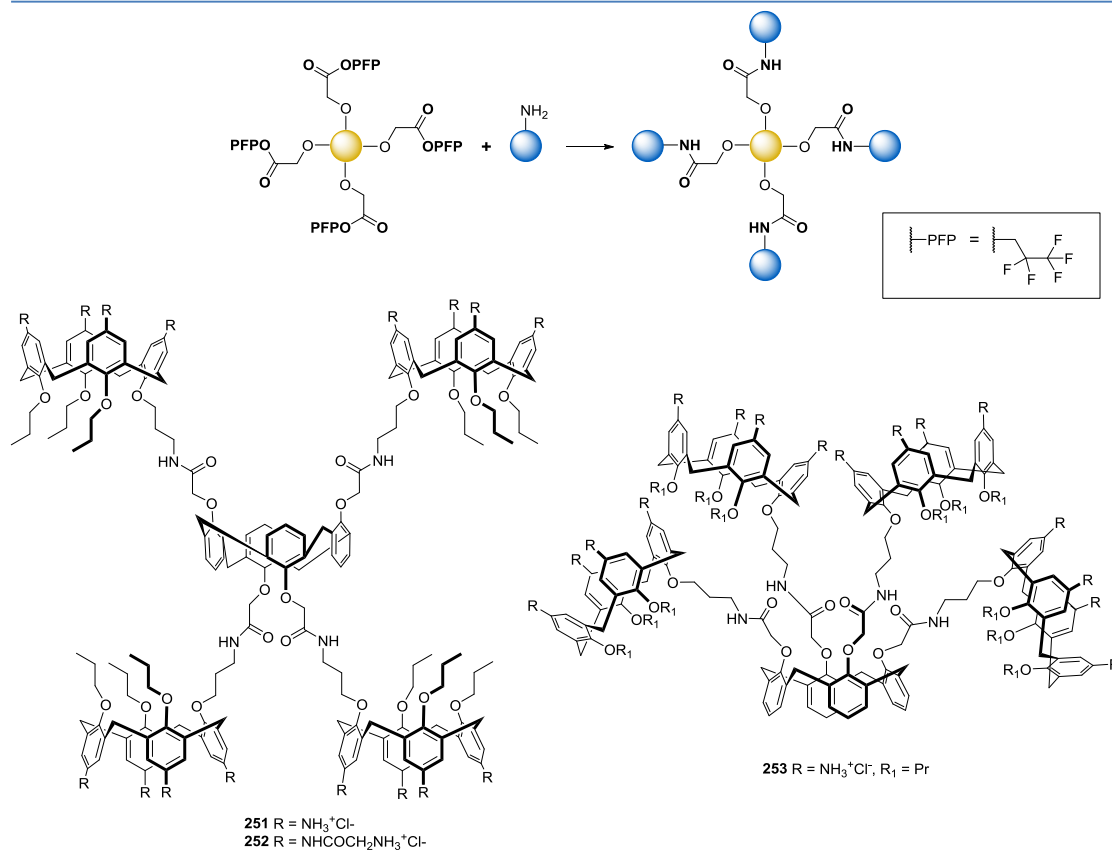


Figure 72. Conformations of calix[4]arenes.

4.3 Previous work

Previous work in our research group investigated the synthesis and potential biological applications of calixarene and resorcinarene dendrimers. The first type of dendrimers investigated were based on cone and 1,3-alternate calixarenes. In contrast to the work presented in this thesis, growth of the dendrimer was obtained by reaction of activated carboxylic acids and amines (Error! Reference source not found.). The approach also allowed access to the convergent synthesis of a large dendrimer, with 21 calixarenes on the third generation.^{131,132,134}



Scheme 69. Dendrimers obtained by reaction of activated carboxylic acids and amines.

More importantly, a set of dendrimers based on amino-functionalised calixarenes were also synthesised and were shown to bind effectively to DNA. These studies highlighted how the binding is related to both charge and structure.^{131,134} The ability to bind DNA was subsequently exploited to investigate the ability of cationic calix dendrimers to transfect cells. For this purpose, a library of calix dendrimers was synthesised using a click chemistry approach. The results showed that all the compounds are able to internalise a plasmid, and they are especially efficient when bearing aliphatic amines.¹³⁵

Subsequent investigations evaluated synthetic routes to multicalixarene glycoconjugates. The rationale behind the synthesis of these molecules lies in the potential ability of targeting specific cells through the glycosides (*e.g.* bacterial lectins) and thus, deliver a specific DNA sequence or drug with high selectivity.¹³⁵

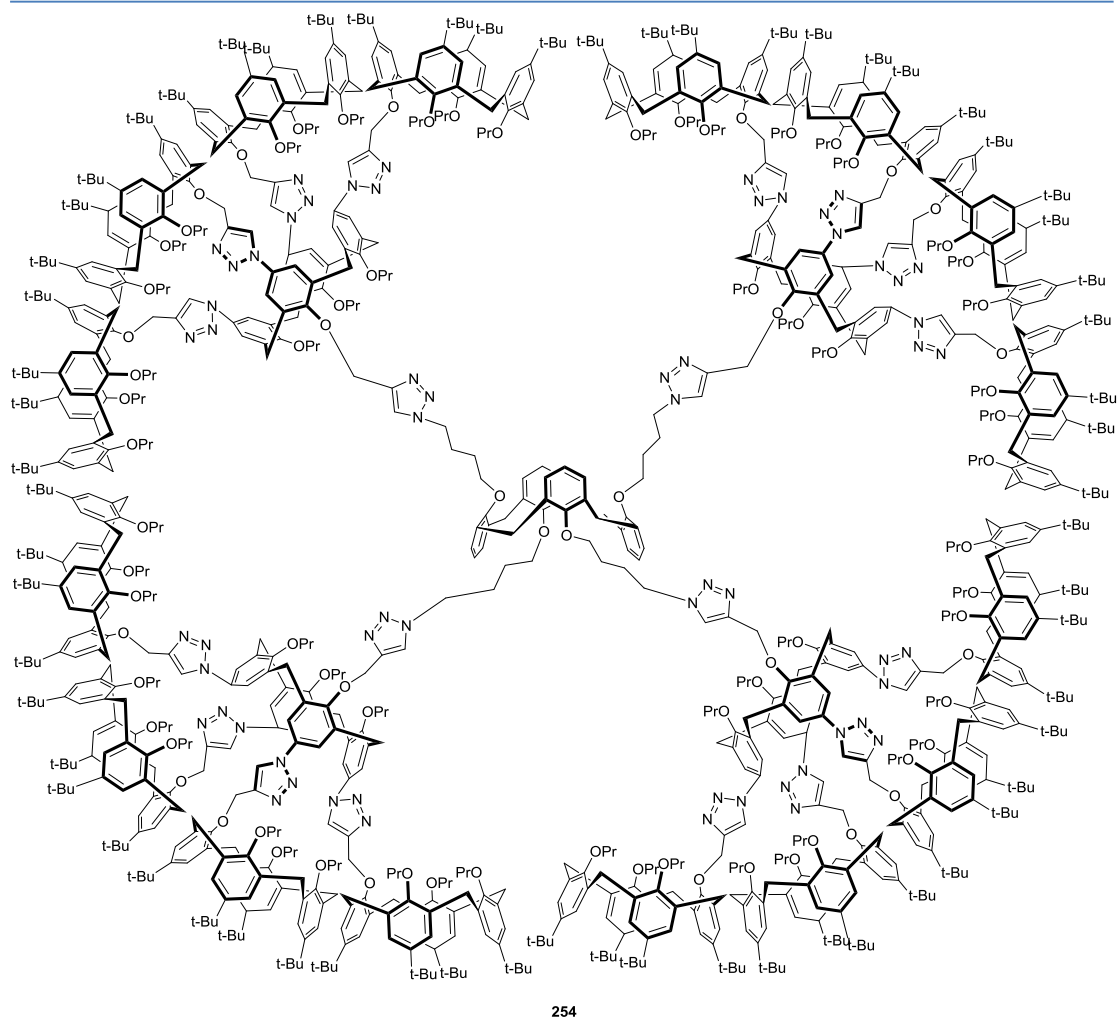


Figure 73. 21 units multicalixarene built using click chemistry.¹³⁵

With the intent of building larger and even more complex dendrimers, the potential of click chemistry was also exploited to build different 21 unit multicalixarenes such as **254**, represented in **Figure 73**, proving that construction of larger and more varied structures is possible by the click chemistry approach.¹³⁵

Mixed resorcinarene-calixarene based multicalixarenes such as those reported in **Figure 74 (A)** have also been investigated. They are based on click chemistry and bear a resorcinol-based core, with the dendrimer developing on the lower rim of the resorcinarene.¹³⁶

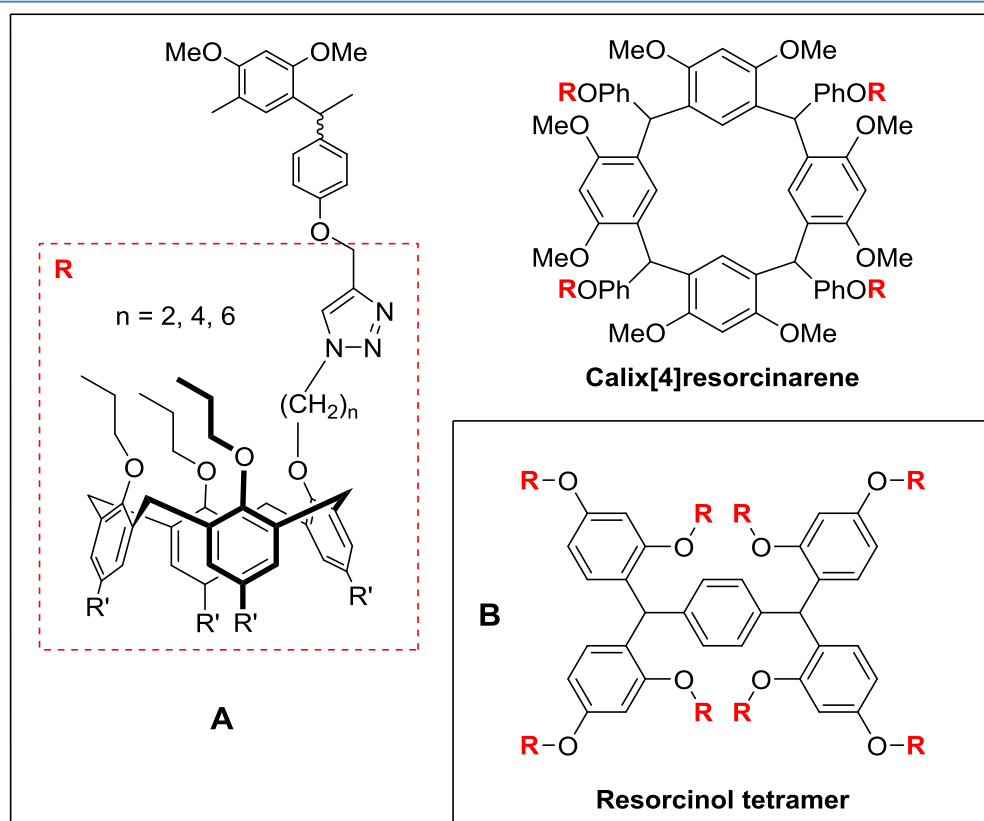


Figure 74. Previously investigated resorcinarene-calixarene based multicalixarenes (A)¹³⁶ and current work (B).

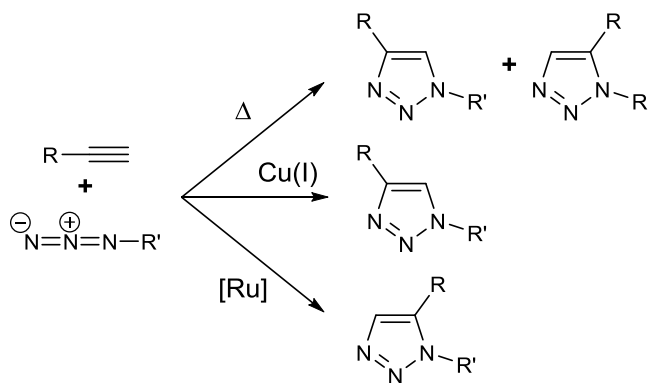
Our novel resorcinol-based platforms **Figure 74 (B)** present an alternative distribution of anchors for the growth of the dendrimers. The resorcinol units, instead of being cyclised, are arranged in couples around a phenyl core (which can also be substituted with variable length spacers, as described for compounds **208**, **210** and **212**, **Chapter 2**). The attachment to the central ring is variable, allowing three different regioisomers (*ortho*, *meta*, *para*) to present the dendrimer branches in different orientations. Despite lacking (at the moment) a viable option for convenient functionalization of the bridges, as in resorcinarenes, they are very simple to obtain and functionalise in high yields. The functionalization of the cores and synthesis of octa-calixarene dendrimers (**Figure 74 (B)**) will be discussed in this chapter.

4.4 CuAAC, a quick overview

Working with large structures provides a number of challenges, ranging from low yields to purification, characterization and solubility issues. To minimise yield and purification problems, robust reaction methodologies, with high yields and selectivity are required. Click chemistry encompasses a range of reactions endowed with these

features.¹³⁷⁻¹³⁹ The most representative of these reactions is probably the Copper-Catalysed Azide-Alkyne Cycloaddition (CuAAC). It is reliable, simple and high yielding, with varied applications, high tolerance to different solvents and accommodates both homogeneous and heterogeneous phases.^{137,139}

Cycloaddition of an azide with an alkyne to give 1,2,3-triazoles can be achieved by thermal activation: the reaction is known as the Huisgen 1,3-dipolar cycloaddition. The reaction did not initially attract much attention due to its poor regioselectivity, leading to mixtures of products. The reaction also required high temperatures, and long reaction times, all of these limiting the potential scope of the reaction. More interest was placed on the reaction when subsequent studies by Sharpless and Meldal^{140,141} revealed that copper (I) could catalyse the reaction, not only allowing a reduction of the operating temperature, but also leading to high regioselectivity (**Scheme 70**). The reaction can also be catalysed by silver¹⁴² and ruthenium. The latter, most importantly, selectively leads to the 1,5-regioisomer.¹⁴³

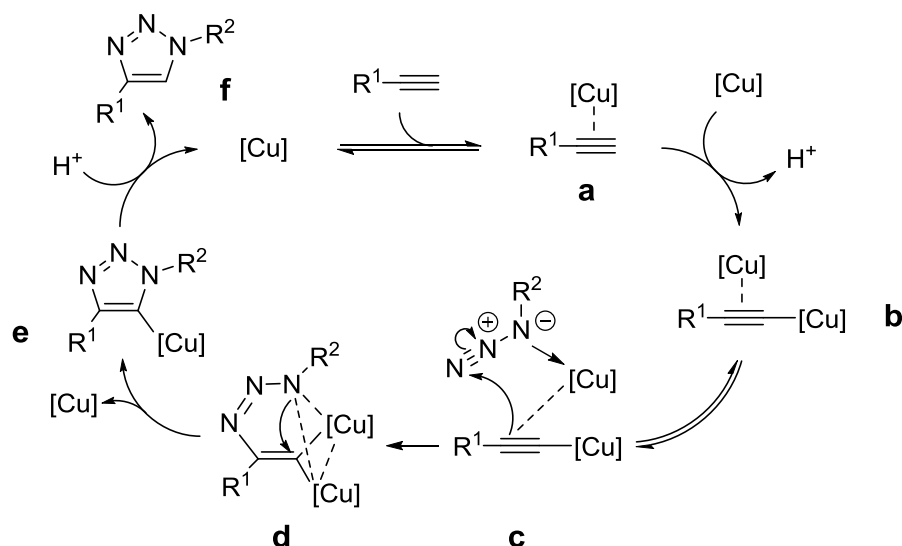


Scheme 70. Azide-alkyne cycloaddition.

A further improvement to the reaction, is the production *in situ* of the copper catalyst, often generated from copper (II) sulphate, which can be achieved by addition of sodium ascorbate. The presence of an excess of sodium ascorbate allows an easier setup, as the oxygen in the air can oxidise Cu(I) to Cu(II), quickly reducing the amount of catalyst. The presence of a reducing agent, which reconverts the catalyst, prevents the necessity of working under inert atmosphere.

The mechanism of the reaction (**Scheme 71**) had been elusive and was recently clarified by Worrell. Initially, formation of a π -bound Cu-alkyne complex occurs (**a**), which allows deprotonation and formation of a σ -bound complex (**b**). Recruitment of a second copper atom is required to form the catalytic complex (**c**). This step is critical, the

authors proved the necessity of the recruitment of a second copper atom using a stable alkyne-Cu σ -bound complex as reagent and noted that reaction does not proceed unless additional catalyst is added. In the following step, the copper atoms become equivalent (**d**) and upon elimination of a copper atom (**e**) and subsequent protonation of the triazole (**f**) the cycle is closed. The equivalence of the two copper in step d was demonstrated using an enriched copper catalyst with the stable alkyne-Cu σ -bound complex, which produces an enriched triazole-Cu σ -bound complex.¹⁴⁴



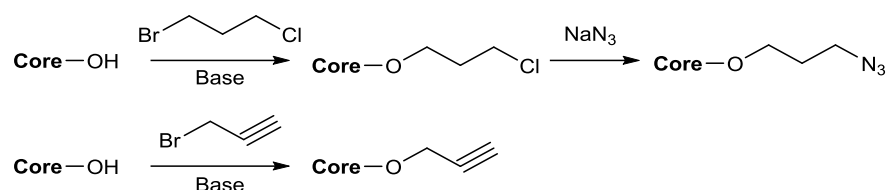
Scheme 71. Mechanism of CuAAC.¹⁴⁴

4.5 Functionalization of the Cores

Initially, to evaluate whether the scaffolds were suitable for dendrimer construction through click chemistry, we decided to functionalise a core and test the click reaction with a simple and readily available materials. Since functionalization of the calixarene units with either an azide or alkyne is simple, the choice for the core is open to both functional groups. Hence, the initial functionalization of the core must be chosen based on the ease of purification and scalability. Two options were thus considered (**Scheme 72**). A first option is the alkylation with a bifunctional alkane, such as 1-bromo-3-chlorobutane, and subsequent substitution of the terminal chlorine with azide. The second option requires propargyl bromide as an alkylating agent. Despite its toxicity, it allows direct access to the functionalised core in one step and the purification is simple.

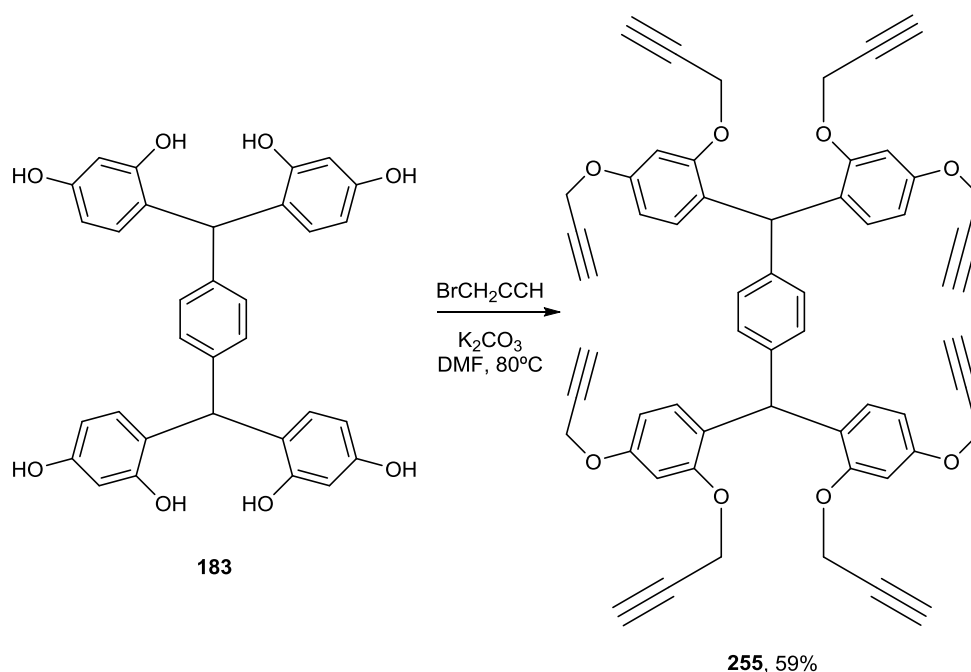
The first option provided a complicated mixture, probably as a consequence of crosslinking. Since the ¹H-NMR did not reveal any clear evidence of the product and

the TLC did not identify a specific product, the route was discounted in favour of the second option.



Scheme 72. Functionalization of the cores.

Alkylation of **183** with propargyl bromide was achieved in the presence of potassium carbonate, at 80 °C in DMF (**Scheme 73**). The purification of **255** by flash chromatography is very simple. However, for the sake of obtaining an optimal starting material for the subsequent reactions, which may increase the complexity and thus the difficulty of purification, only the main fractions were collected. The isolated yield (59%) is good but not excellent, and is probably lower than the true reaction yield.



Scheme 73. Synthesis of **255**.

Examining the $^1\text{H-NMR}$ (**Figure 75**) it is possible to highlight how the features of the core remain intact and its peaks are only slightly shifted as a consequence of the alkylation. As expected, the signals of the hydroxyl groups are lost in exchange for the newly introduced propargyl groups. Probably as a consequence of steric hindrance around the bridge, their signals are not equivalent, resulting in two sets of signals, one for the *ortho* and one for the *para* position chains.

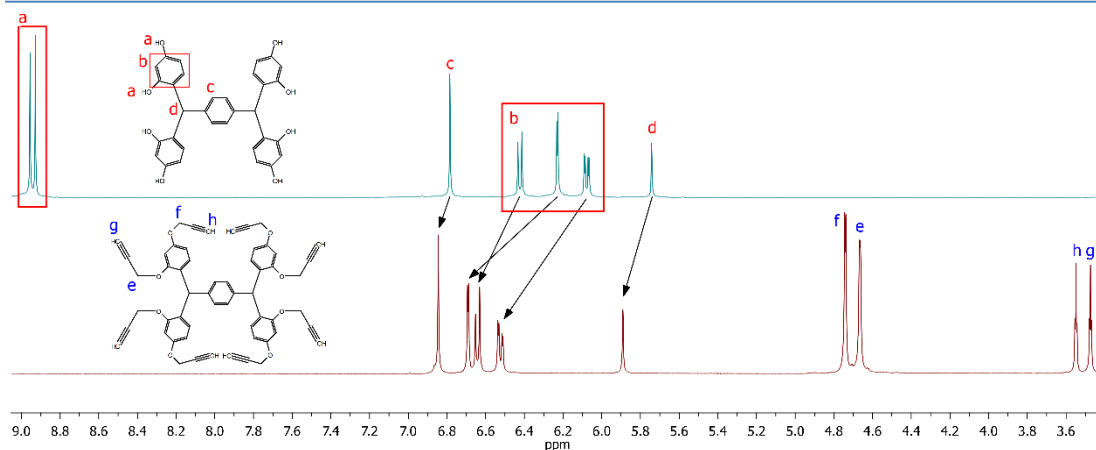
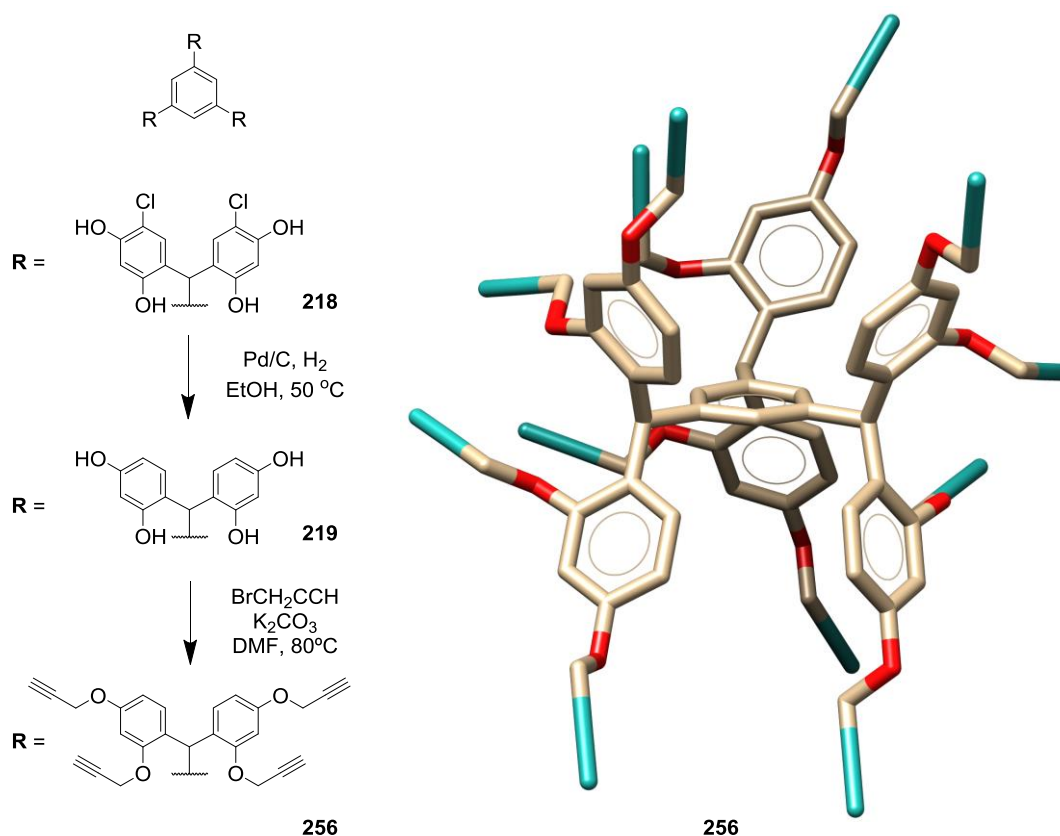


Figure 75. ¹H-NMR of **183** (top), and **255** (bottom).

4.5.1 Hexameric Core

Compound **219** is arguably the most interesting core structure available from this work, presenting twelve extremities to be functionalised. In the previous chapter, **219** was prepared by dehalogenation of its chloro-substituted analogue **218**, but the purity of the product was not acceptable, at least for biological evaluation. Purification of the hexamer is not practical, however, the reaction of the crude with propargyl bromide leads to an easy to purify product, allowing access to **256** in 32% yield over two steps (Scheme 74).



Scheme 74. Synthesis of **256** and its 3D representation (the image is only meant to provide a better visualization of the structure, it is not a representative conformation. MarvinSketch and UCSF Chimera)

The ^1H -NMR profile (**Figure 76**) is similar to that of **255**. Propargyl substituents present two sets of signals, each with a triplet for the terminal hydrogen (2.32 ppm, 2.46 ppm) and a doublet for the $-\text{CH}_2-$ (2.30 ppm, 2.57 ppm). The bridge hydrogens are all equivalent and show a singlet (5.72 ppm). Similarly, the central ring produces a singlet (6.44 ppm). The remaining signals, partly overlapped, represent the resorcinol aromatic hydrogens.

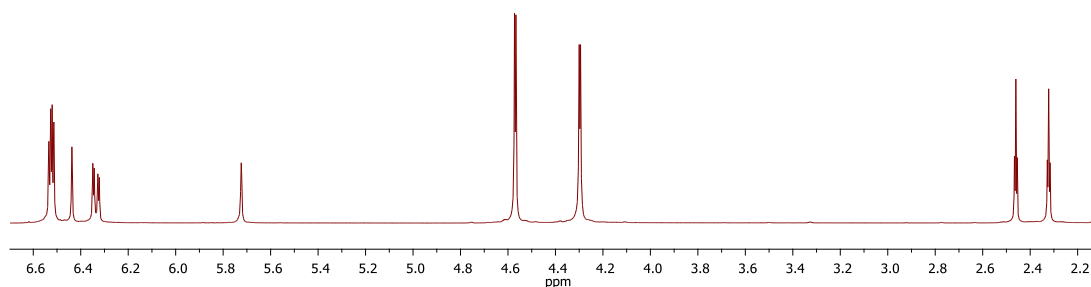
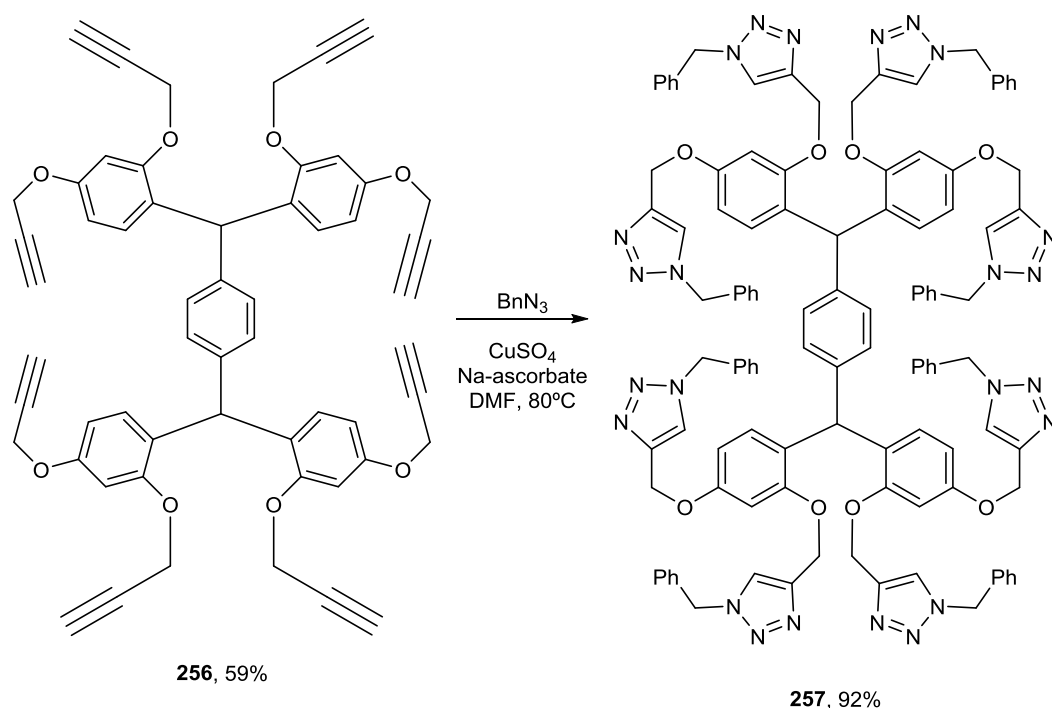


Figure 76. ^1H -NMR of **256**.

The approach thus provides access to a method to recover insufficiently clean phenolic precursors, paving the way to additional dendrimer cores.

4.5.2 Test of click reaction

The click reaction of a simple azide (benzyl azide) was used to test the optimal conditions for the reaction. In the presence of copper sulphate and sodium ascorbate in DMF at 80 °C, the reaction proceeded in a few hours, leading to the expected product in 92% (**Scheme 75**). The yield is surprising considering that eight individual cyclisation reactions are necessary for each product molecule.



Scheme 75. Synthesis of test dendrimer **257**.

The ^1H -NMR of **257** retains the characteristic features of the previously described **183**. Observing **Figure 77**, it is possible to see that the symmetry is not lost, the bridge (**a**), the three peaks of the resorcinol unit (**b**) and the core (**c**) are immediately identifiable. Correlation between the hydrogens of the resorcinol can also be confirmed by COSY. Integration according to these peaks reveals that the signal at 8.1 ppm (**i**), which can be assigned to a triazole due to its deshielded position, represents only four of the moieties. This is an expected result since chains **e-f-g** and **h-i-j** (**Figure 77**) reside in different environments, as previously observed with **255**.

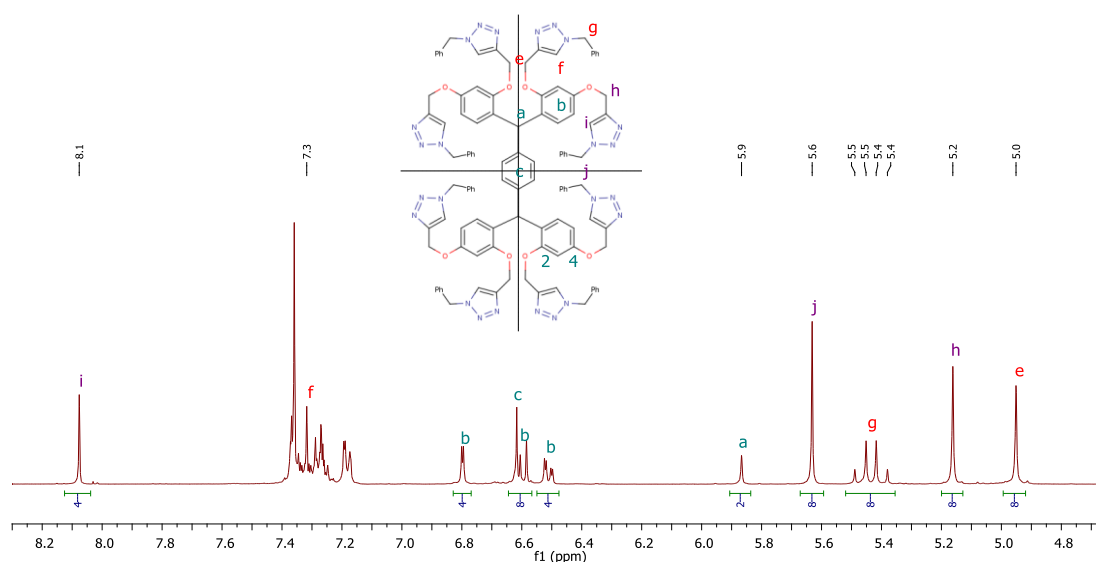


Figure 77. ^1H -NMR of **257**.

Using a combination of HSQC (**Figure 78**) and HMBC (**Figure 79**), all signals were assigned. Chain **e-f-g** was identified by HMBC correlation: the hydrogen of the bridge has a 3J relationship with only one carbon bearing an oxygen (these have typically shifts around 160 ppm in our resorcinol based platforms). The same carbon is three bonds away from hydrogens **e**. Moving along the chain, **f** and **g** were also identified. In a similar fashion, **h-i-j** were identified starting from the interaction of the second (and last) ^{13}C signal around 160 ppm and hydrogen **h**.

Chain **e-f-g** (**Figure 77**) is interesting, as the hydrogen of the triazole (**f**) is particularly shielded, 0.8 ppm more than **i**. Also, the benzylic hydrogens **g** are diastereotopic, which is surprising as **e**, supposedly more hindered, is not. This could be a consequence of π -stacking between two equivalent **e-f-g** chains.

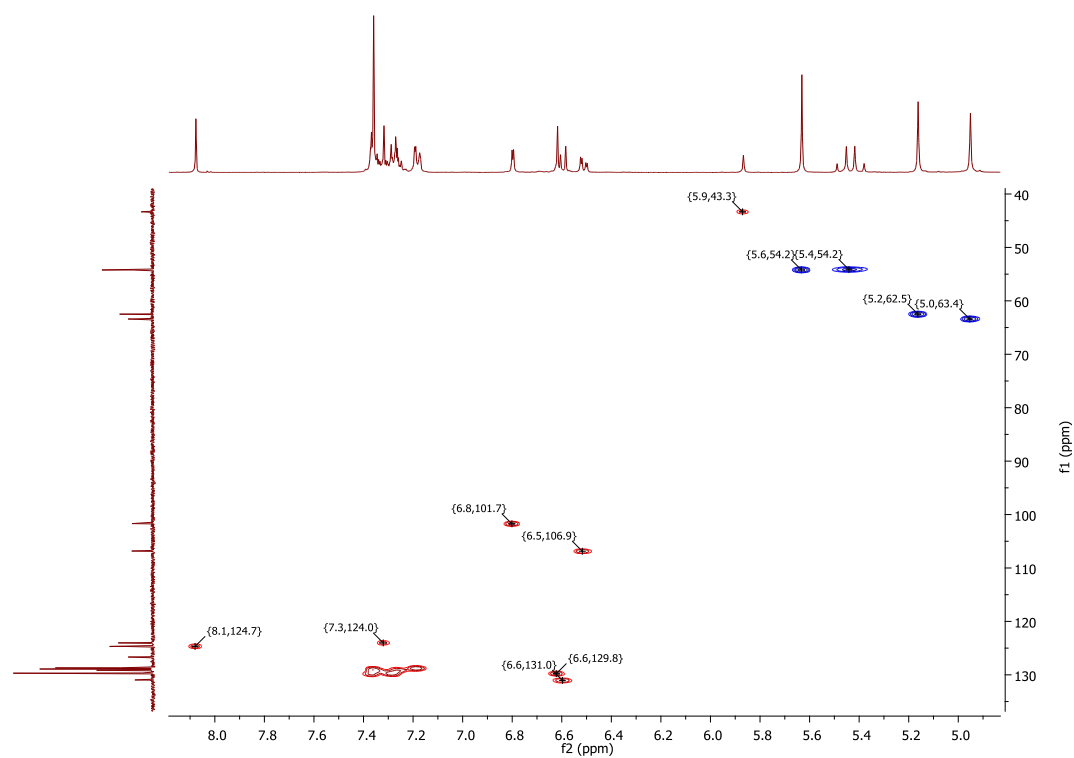


Figure 78. HSQC of of **257**.

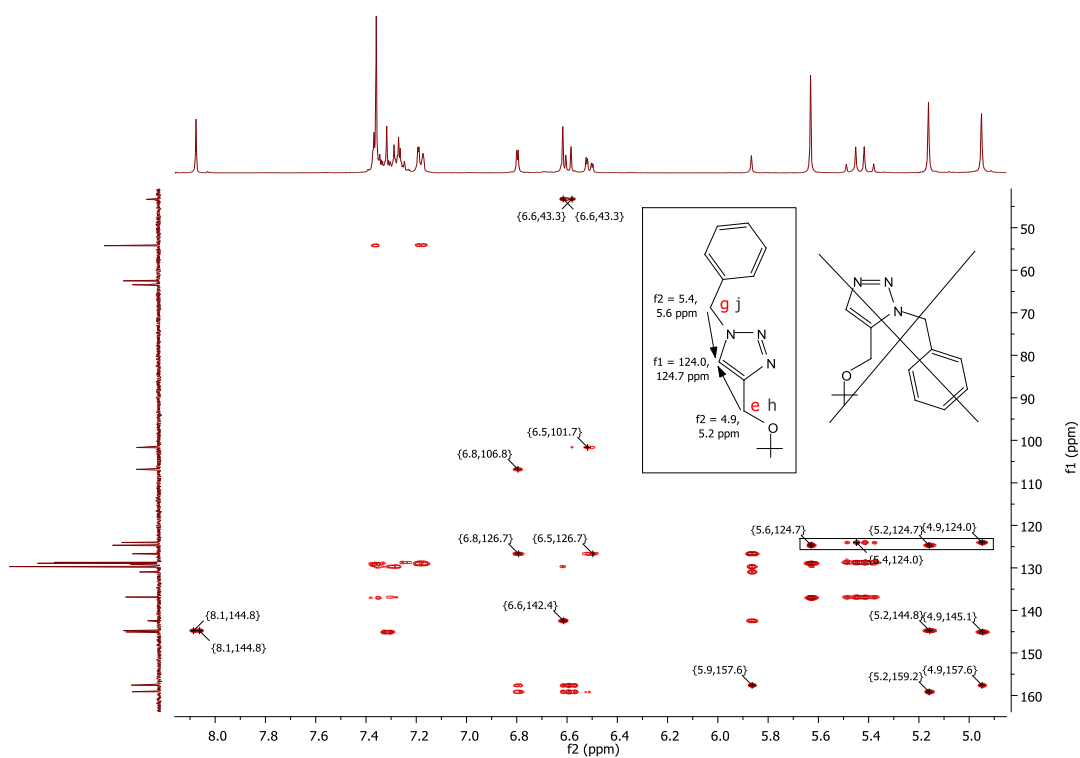
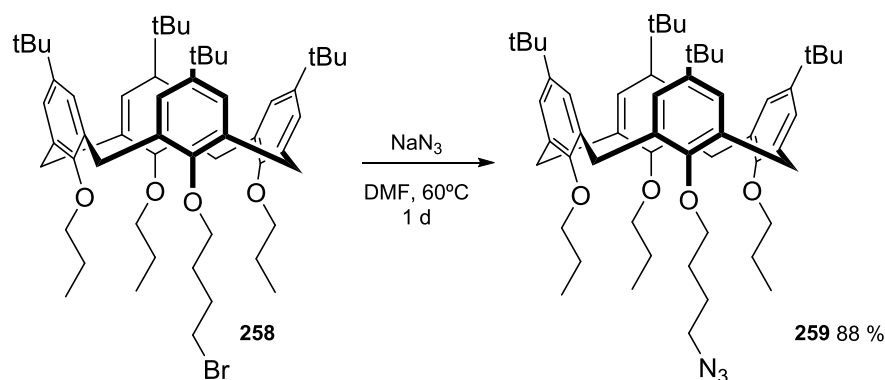


Figure 79. HMBC of of **257**.

4.5.3 Synthesis of a hindered model compound

To evaluate potential limitations due to the steric hindrance of the molecules clicked onto the core, a model calixarene was synthesised. Compound **258** was prepared according to the procedure reported by Regayeg¹⁴⁵ from material available within the group. Substitution of the bromine with an azide was achieved by stirring the precursor with sodium azide in DMF at 60 °C, thus obtaining the clickable product **259** (**Scheme 76**). The reaction was clean and produced a product of ideal quality by simple filtration. Since the substitution only produces a shift in the hydrogen signals, NMR analysis was supported by IR spectroscopy to confirm the introduction of the azide, which produces a clear signal around 2100 cm⁻¹ (**Figure 80**).



Scheme 76. Synthesis of **259**.

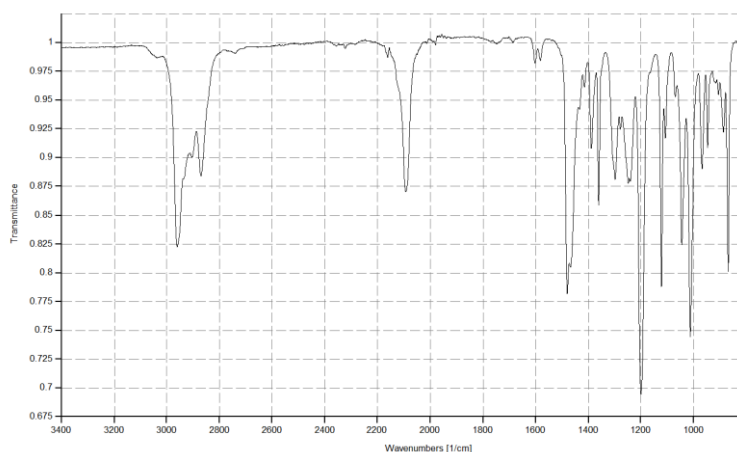
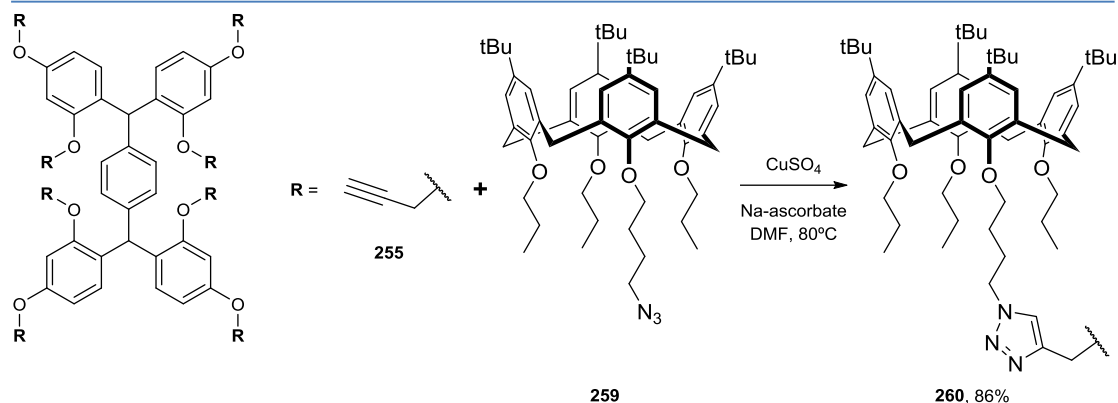


Figure 80. IR spectra of **259**.

Click reaction of the calixarene onto the core was undertaken with the same procedure described for the first model compound and produced the expected dendrimer in excellent yield: 86% (Error! Reference source not found.).



Scheme 77. Synthesis of **260**.

The ^1H -NMR of this dendrimer bears similarities with that of the previously described dendrimer **257**, with the additional complexity of the calixarenes (**Figure 81**). The triazoles have two distinct peaks (**a**), exactly as in the previous model dendrimer. The structure of the core is still identifiable, although the signal is poor. Central ring **b**, resorcinol units (**d**) and bridge **e** do not overlap with the hydrogens of the calixarene (**c**) and their relationship can be identified using COSY and HMBC. The bridging methylenes of the former propargyl group (**f**) stand out at around 5 ppm and can be confirmed by long range coupling with the carbons of the core. As it is usual for cone calixarene conformations, the hydrogens of the bridges are diastereotopic and split (**g**). Hydrogens **h**, **i** and **j** are the last signals around 4 ppm and were confirmed by HMBC. The remaining peaks were assigned to the alkyl chains.

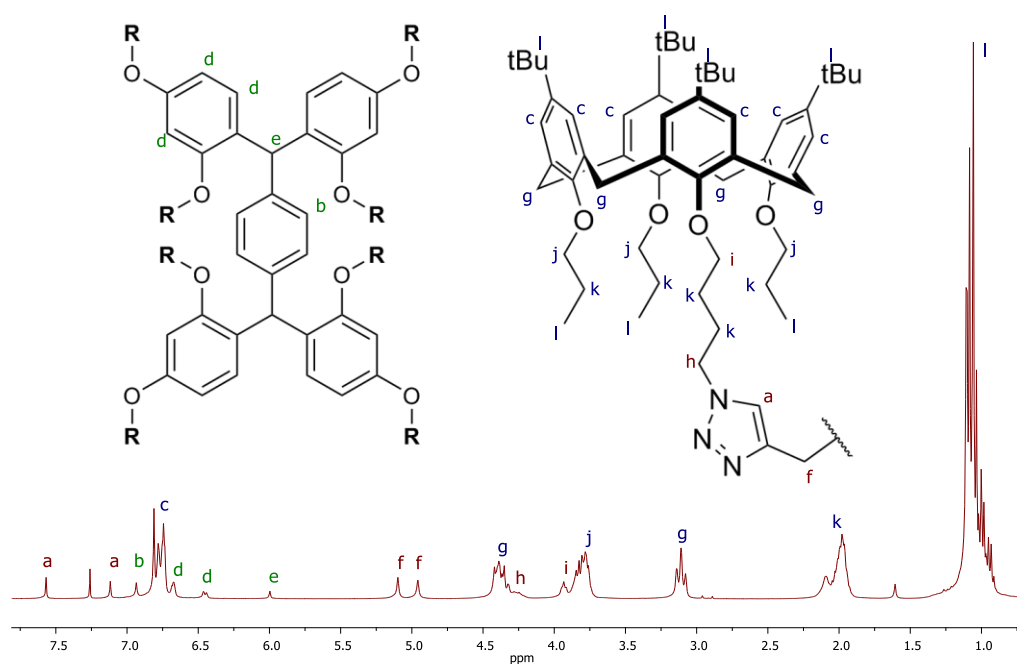


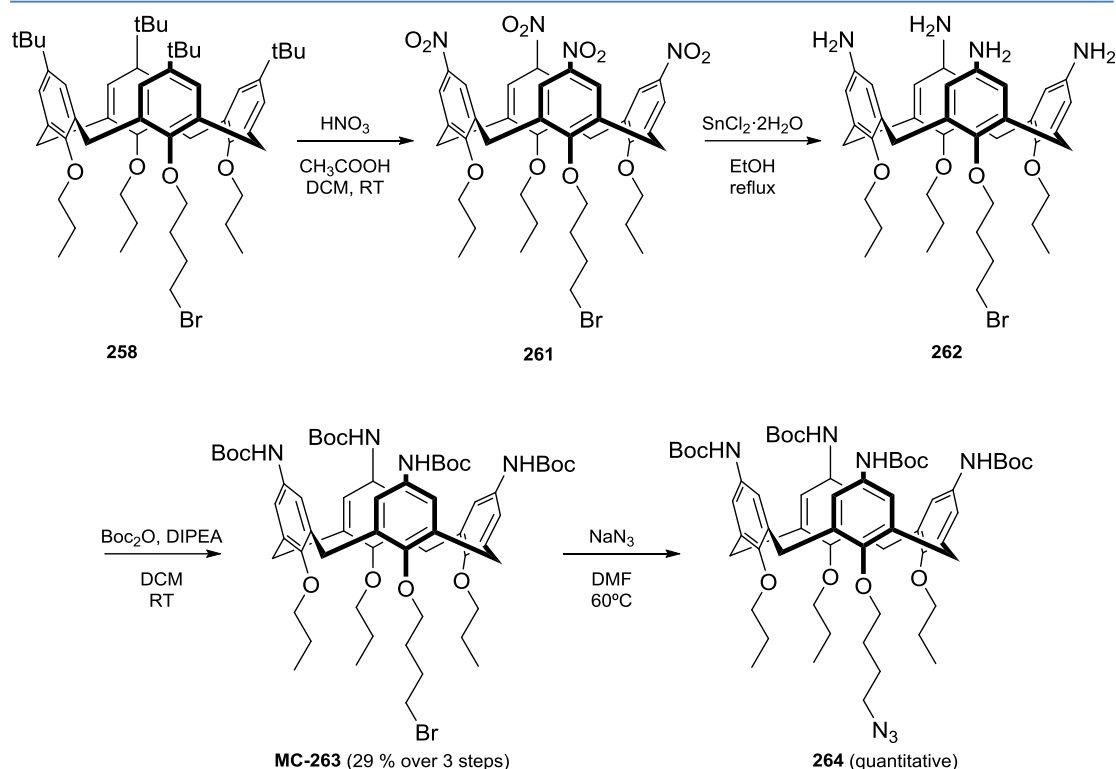
Figure 81. ^1H -NMR of **260**.

The result shows that clicking bulky extremities to the core is feasible and it was therefore possible to move to a practical application.

4.5.4 Synthesis of a clickable tetra-amino calixarene

As described in the introduction to this chapter, cationic multicalixarenes are interesting DNA-binding platforms.¹³¹ The approach used for the synthesis of **260** was thus employed to prepare a novel octa-tetraminocalixarene.

Compound **258** was also used as a starting material to prepare a calixarene which bears four protected amines on the upper rim and an azide on the lower rim (**Scheme 78**). The ipso nitration to substitute the *tert*-butyl group with a nitro group, originally described by Verboom,¹⁴⁶ was also employed by Regayeg.¹⁴⁵ The reaction with nitric acid and acetic acid in dichloromethane is rapid and leads to the product in 1-6 hours (the colour turns from black to light brown and is a good indication of the reaction progress). In contrast to Regayeg, the crude material was not crystallised but triturated in methanol producing a very clean product which was directly used for the following reaction.



Scheme 78. Synthesis of **264**.

For the reduction of the nitro group, a consolidated method widely used within the group, and previously reported by Budka,¹⁴⁷ was employed. A mixture of **261** and tin(II) chloride in ethanol was heated at reflux for 48 hours to yield the expected compound. The extraction of the product from the reaction mixture is tedious as a consequence of the presence of large amounts of salts and foaming.

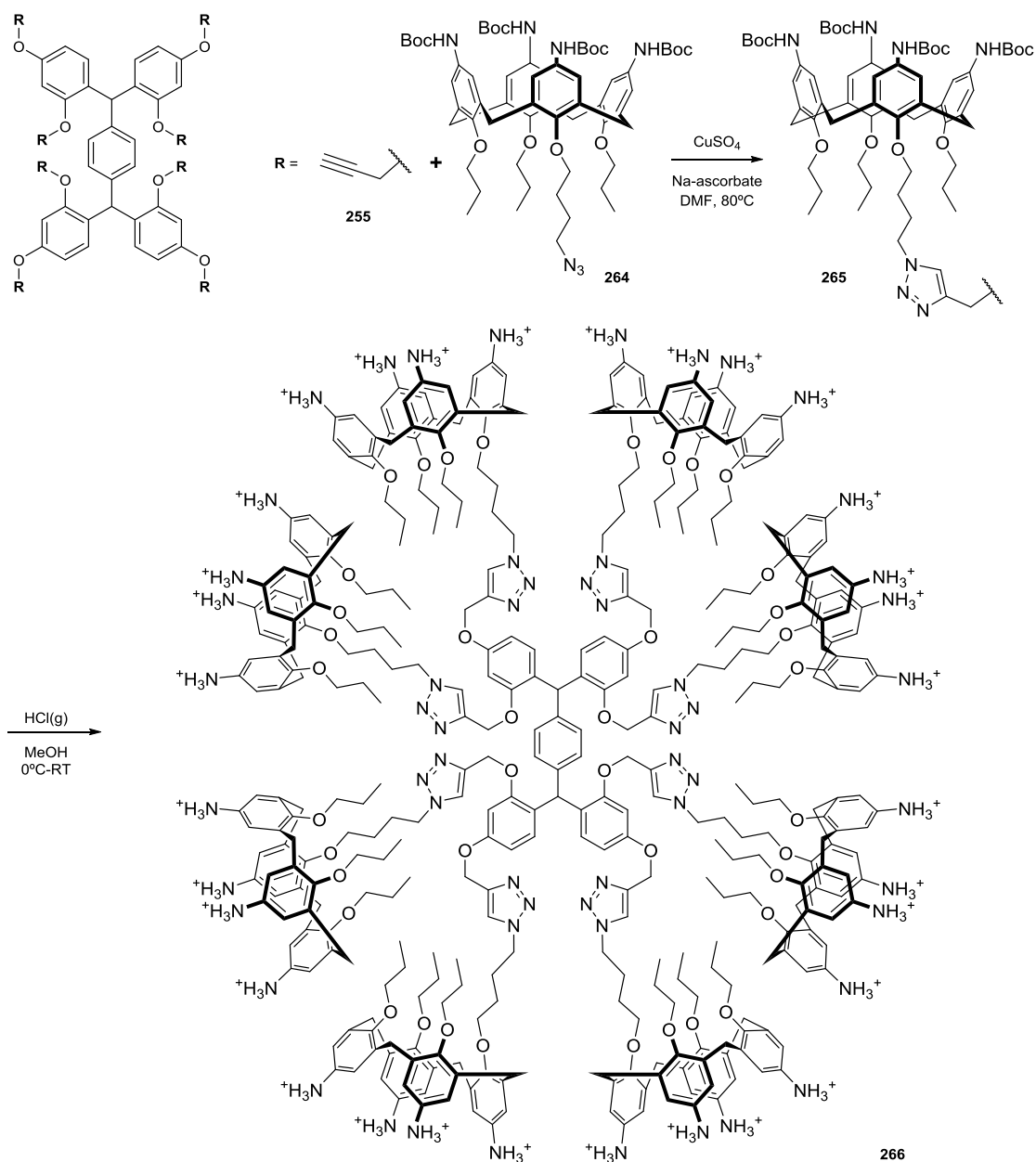
A subsequent protection of the amino groups is necessary for two reasons: firstly, if left unprotected they would interfere with the click reaction by coordinating the copper catalyst. Secondly, the product cannot be conveniently purified by flash chromatography on silica gel. For these reasons, the amines were protected with di-tert-butyl dicarbonate, according to a method reported by Saadioui,¹⁴⁸ and the product was then purified by chromatography to give **263** in 29% yield over three steps. The choice of the protecting group might appear odd, since Boc is removed with acids. However, it can be removed under mild conditions, and it provides an interesting evaluation of whether the deprotection of acid-labile groups is feasible despite the relative instability of the cores to acid-catalysed retro-Friedel-Crafts reaction. Boc protection is a well known method, it has been used within the group, and has the additional advantage of

allowing access to selective, partial protection of calixarenes,¹⁴⁸ thus increasing the potential scope of the attainable derivatives.

Finally, the bromine was substituted with sodium azide, as previously described for **259**, to give the clickable product **264** in quantitative yield.

4.5.5 Synthesis of a functionalised dendrimer

Azide **264** was clicked onto the core using the same method used for the previous tetramers to obtain **265** in 77% yield (**Scheme 79**). Because a two-fold excess of azide was used, it is relevant to note that such excess can be recovered in 93% yield during the purification of the product, thus minimising the loss of the building block.



Formation of the triazole is confirmed by appearance of typical deshielded peaks (**a**, **Figure 82**), and disappearance of the alkyne terminal hydrogens (**b**, **Figure 82**). Other characteristic peaks from the core, are slightly shifted in their positions (**c**, **d**, **Figure 82**), especially the linker to the triazole (**e**, **Figure 82**). The remaining peaks, although quite broad, originate from the newly attached calixarene.

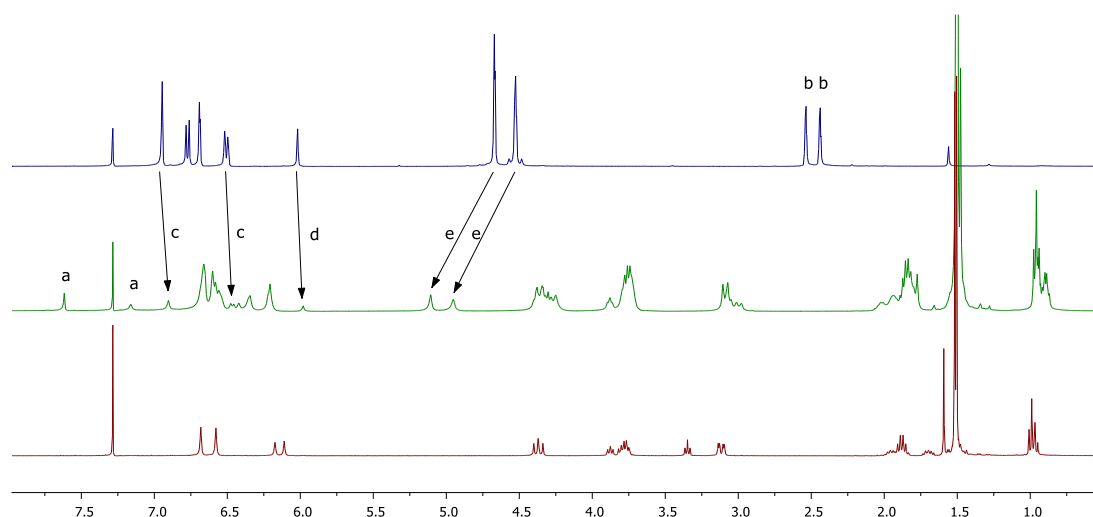


Figure 82. ^1H -NMR of **255** (top), **265** (centre) and **264** (bottom).

The product was then deprotected. HCl deprotection is a critical step (**Scheme 79**), as previously discussed, because of potential retro-Friedel-Crafts reactions. With the hydroxyl groups “protected” as ethers, the nucleophilicity of the resorcinol fragments is partially reduced. The starting material is dissolved in DCM and deprotected by HCl, which is bubbled into the solution. Salification of the newly formed amines, produces precipitation, blocking the reaction. To complete it, addition of methanol, which re-dissolves the partially reacted product, is required. This step is critical: dissolution of hydrochloric acid in methanol is an exothermic process. To minimise potential fragmentation, the temperature is controlled with an ice bath and the amount of methanol is maintained at the minimum necessary, which also helps maintain the polarity as low as possible, contributing to the reduction of the rate of retro-Friedel-Crafts. The product was purified by preparative RP-HPLC to give the product in 79% yield. The identity of the compound was confirmed by high resolution mass spectrometry and by NMR, which shows a similar profile to that of **265**, although some peaks are covered by the solvent (**Figure 83**). The result confirms the possibility of

using this approach to remove acid-labile protecting groups without significant loss of material.

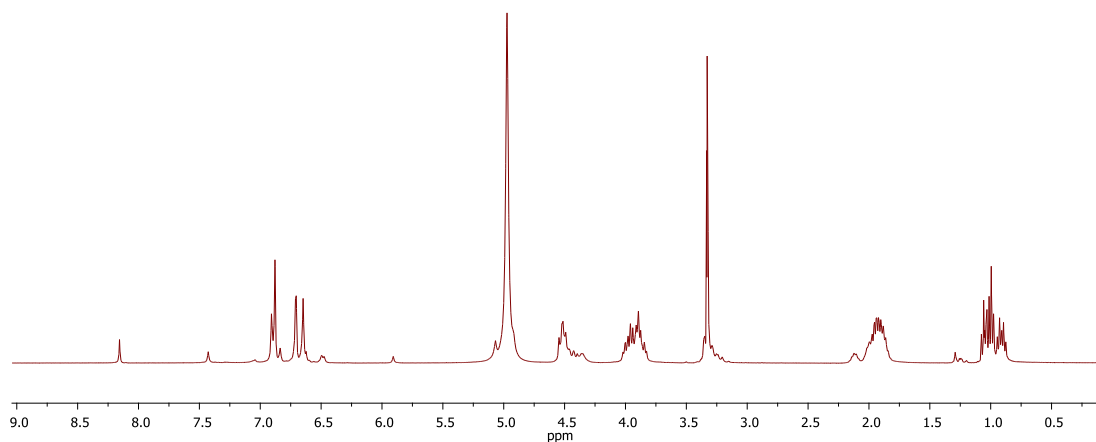


Figure 83. ^1H -NMR of **266**.

4.6 Conclusions

In this Chapter, a suitable method for the functionalization of our multivalent core structures with alkyne sidechains have been presented. The method also allowed derivatization and subsequent purification of the hexameric core (**219**), for further use in dendrimer synthesis.

A sample core have been functionalised with model compounds and subsequently with tetra-aminocalix[4]arenes, producing a first-generation octacalix with 32 exposed amines. This work is a proof of concept and first step toward new, potential DNA binding structures.

In conclusion, an efficient procedure for the functionalization of our novel octa- and dodeca-valent dendrimer cores has been developed, allowing easy access to a new range of resorcinol based dendrimers.

4.7 Experimental

4.7.1 General

All reagents and solvents for synthesis were commercial and used without further purification. NMR spectra were recorded at 293 K, unless otherwise stated, using a 400 MHz Spectrometer. Shifts are referenced relative to deuterated solvent residual peaks. Infrared spectra were recorded using an FT-IR spectrometer with ATR attachment. MS were run on an LTQ orbitrap XL and were recorded by the EPSRC Mass Spectrometry National facility. Thin-layer chromatography (TLC) was carried out on aluminum sheets coated with silica gel 60 F254 (Merck). TLC plates were inspected by UV light ($\lambda = 254$ nm). Silica gel column chromatography was performed with silica gel Si 60 (40–63 μm).

Purification by preparative RP-HPLC was performed on an Agilent 1260 Infinity using an Agilent Eclipse XDB-C18 column, 21.2 x 150mm, 5 μM .

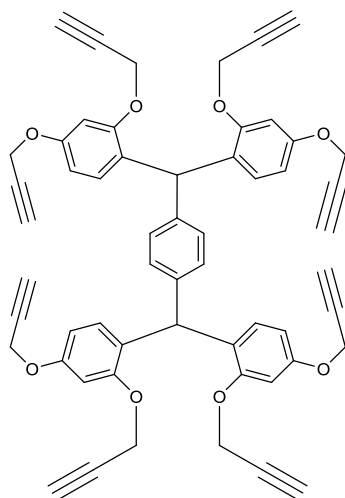
Solvent A: 5% methanol in water + 0.05% TFA.

Solvent B: 5% water in methanol + 0.05% TFA.

Gradient: Solvent A to Solvent B in 20 minutes. Flow rate = 20 mL/min. Detection wavelength = 254 nm.

4.7.2 Synthesis

Compound 255



A mixture of **183** (3.26 mmol), anhydrous potassium carbonate (10.4236 g, 75.42 mmol), and propargyl bromide (5.5446 g, 57.46 mmol) in 100 ml of DMF was allowed to stir at 70 °C for 5 h and then for 18 h at 80 °C. The solvent was evaporated under reduced pressure and the resulting solid suspended in water and extracted three times with diethyl ether. The organic layers were combined, washed with NaHCO₃, brine and then dried over MgSO₄. The crude product obtained upon evaporation of the solvent was purified via flash chromatography on silica gel (DCM as eluent) and dried in the oven at 120 °C. A pale yellow solid was obtained (1.6239 g).

Yield: 59%

[M+NH₄]⁺ = 860.3217 (Calculated: 860.3218)

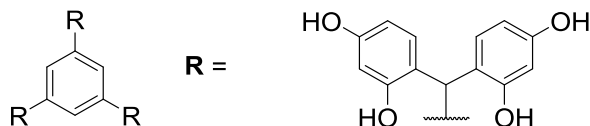
MP: 135-137 °C

¹H-NMR (400 MHz, DMSO) δ 6.84 (s, 4H), 6.69 (d, *J* = 2.3 Hz, 4H), 6.64 (d, *J* = 8.5 Hz, 4H), 6.52 (dd, *J* = 8.5, 2.3 Hz, 4H), 5.89 (s, 2H), 4.74 (d, *J* = 2.3 Hz, 8H), 4.67 (d, *J* = 2.3 Hz, 8H), 3.55 (t, *J* = 2.3 Hz, 4H), 3.47 (t, *J* = 2.3 Hz, 4H).

¹³C-NMR (101 MHz, DMSO) δ 156.61, 155.46, 140.93, 129.91, 128.42, 125.55, 105.94, 101.22, 79.24, 79.16, 78.18, 78.00, 56.07, 55.50, 41.01.

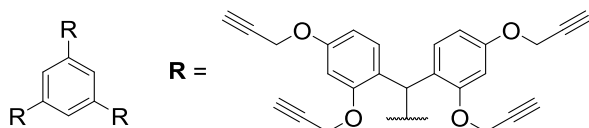
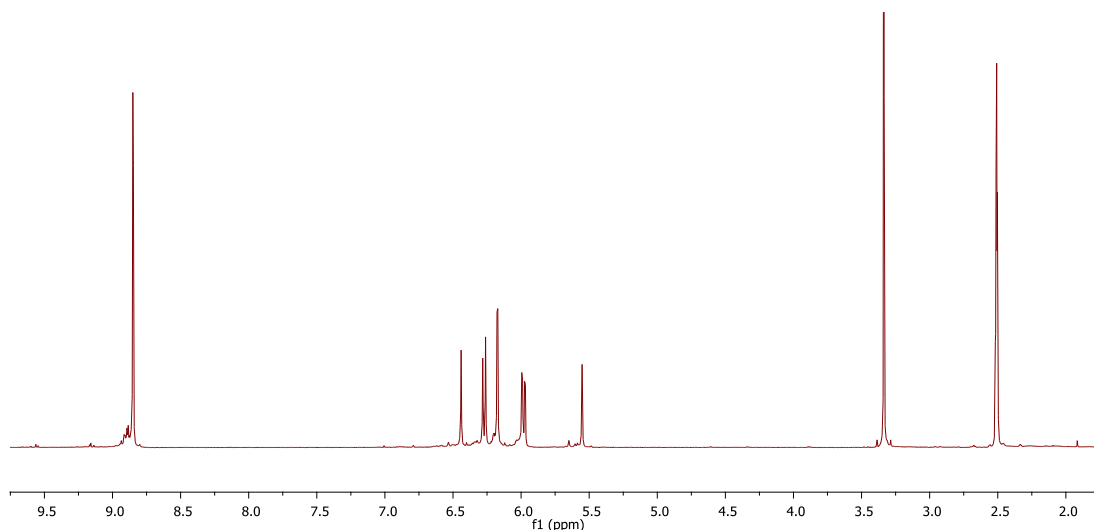
IR (ν_{max}, cm⁻¹): 3286, 1607.5, 1586, 1498, 1451, 1428, 1370.5, 1285, 1247, 1162.5, 1109, 1025, 941.5, 920.5, 832, 800.

Compound **219** and **256**



Palladium over carbon (catalytic) was added to a solution of **218** (0.33 mmol) and triethylamine (1 mL, 7.17 mmol) were dissolved in 24 mL of ethanol. A hydrogen atmosphere was applied and the mixture was allowed to stir at 50 °C for 5 h. The catalyst was removed by filtration and the solution was dried under reduced pressure. The product was suspended in HCl_{aq} 10% v/v and extracted with ethyl acetate three times. The organic layers were combined, washed with HCl_{aq} 10% v/v, brine and dried over Na₂SO₄. Upon evaporation, 260 mg of crude were obtained as an orange powder.

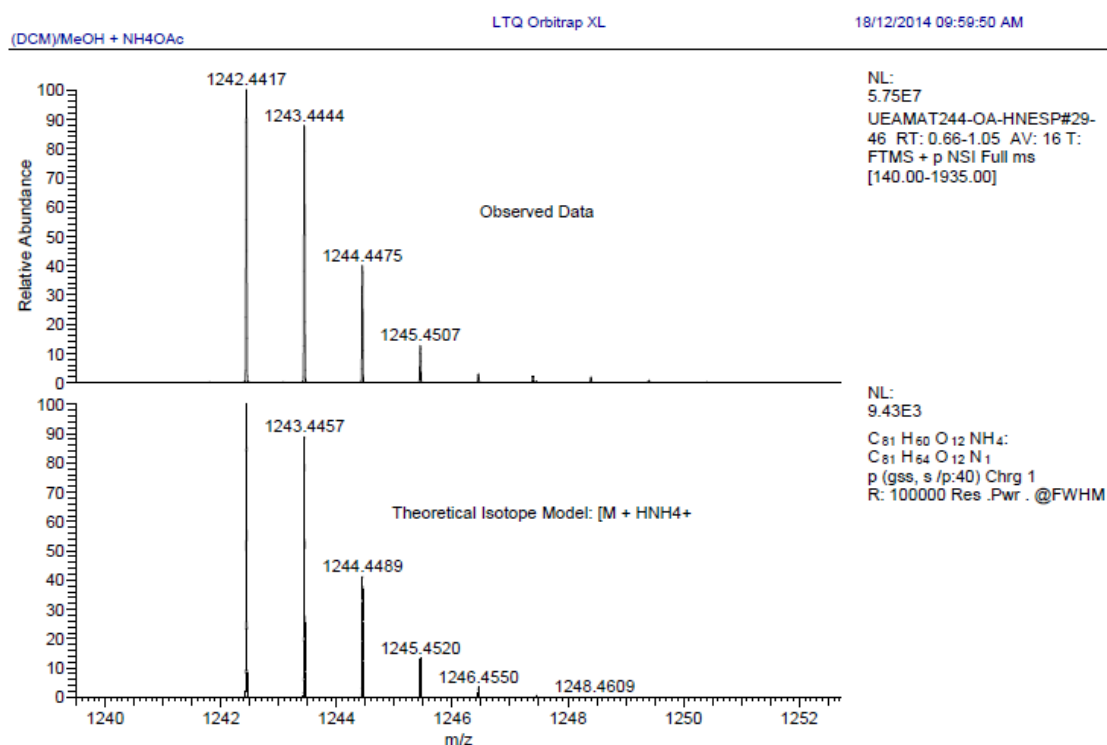
The crude was used without any further purification for the synthesis of **256**. A ¹H-NMR is reported for reference.



A mixture of crude **219** (160 mg), anhydrous potassium carbonate (948.7 mg, 6.86 mmol), and propargyl bromide 80 % in toluene (680.9 mg, 4.58 mmol) in 10 ml of DMF was allowed to stir at 70 °C for 5 h and then for 18 h at 80 °C. The solvent was evaporated under reduced pressure and the resulting solid suspended in water and extracted three times with diethyl ether. The organic layers were combined, washed with NaHCO₃, brine and then dried over MgSO₄. The crude product obtained upon

evaporation of the solvent was purified via flash chromatography on silica gel (DCM as eluent).

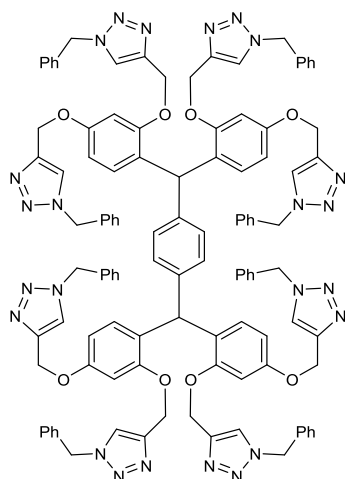
Yield: 31.8% over two steps



¹H-NMR (400 MHz, CDCl₃) δ 6.56 – 6.47 (m, 12H), 6.44 (s, 3H), 6.34 (dd, *J* = 8.5, 2.4 Hz, 6H), 5.72 (s, 3H), 4.57 (d, *J* = 2.4 Hz, 12H), 4.30 (d, *J* = 2.4 Hz, 12H), 2.46 (t, *J* = 2.4 Hz, 6H), 2.32 (t, *J* = 2.4 Hz, 6H).

¹³C-NMR (101 MHz, CDCl₃) δ 156.85, 156.20, 142.69, 130.52, 128.02, 127.11, 106.09, 101.55, 79.04, 78.82, 75.52, 75.33, 56.66, 55.99, 42.58.

Compound 257



Benzylazide (0.51 mL, 3.80 mmol) was added to a mixture of **255** (200 mg, 0.24 mmol), CuSO₄·5H₂O (5.9 mg, 0.02 mmol) and sodium ascorbate (18.8mg, 0.09 mmol) in 4 ml of DMF under argon. The mixture was slowly heated to 80 °C. After 3 h at 80 °C, the DMF was evaporated under reduced pressure. The dark yellow product was suspended in chloroform absorbed onto silica and purified by flash chromatography (ethyl acetate/acetone 9:1 and acetone) to give 0.4158 g of a pale yellow product

Yield: 92%

[M+2H]²⁺ = 954.9080 (Calculated: 954.9087)

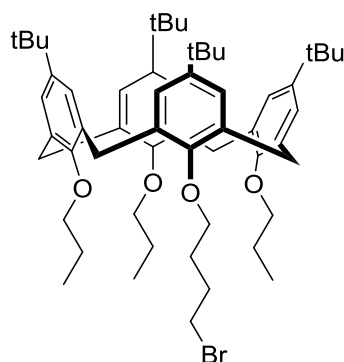
MP: 89-90 °C

¹H-NMR (400 MHz, Acetone) δ 8.08 (s, 4H), 7.44 – 7.11 (m, 44H), 6.80 (s, 4H), 6.79 (s, 4H), 6.62 (s, 4H), 6.59 (d, *J* = 8.5 Hz, 4H), 6.51 (dd, *J* = 8.5, 2.4 Hz, 4H), 5.87 (s, 2H), 5.63 (s, 8H), 5.47 (d, *J* = 15.0 Hz, 4H), 5.40 (d, *J* = 15.0 Hz, 4H), 5.16 (s, 8H), 4.95 (s, 8H).

¹³C-NMR (101 MHz, Acetone) δ 159.12, 157.59, 145.06, 144.75, 142.42, 137.00, 136.86, 130.96, 129.71, 129.69, 129.14, 129.07, 128.91, 128.71, 126.67, 124.68, 124.02, 106.83, 101.69, 63.40, 62.49, 54.22, 54.15, 43.34.

IR (ν_{max}, cm⁻¹): 1606, 1585, 1497, 1455, 1432, 1284, 1253.5, 1221.5, 1167.5, 1108.5, 1049, 1031.5, 1015.5, 823.5, 799.

Compound **258**¹⁴⁵



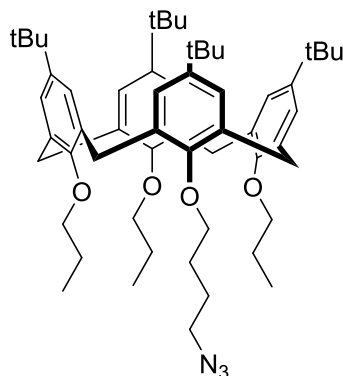
Prepared according to Regayeg.¹⁴⁵

MP: 184-186 °C (180 °C)¹⁴⁵

¹H-NMR (400 MHz CDCl₃, ppm): δ 6.80 (s, 4H), 6.74 (m, 4H), 4.39 (t, *J* = 12.4 Hz, 4H), 3.89 (t, *J* = 7.6 Hz, 2H), 3.81 (m, 6H), 3.50 (t, *J* = 6.8, 2H), 3.12 (m, 4H), 2.16 (m, 2H), 2.01 (m, 8H), 1.06 (m, 45H).

¹³C NMR (101 MHz, CDCl₃) δ 153.74, 153.60, 153.54, 144.49, 144.24, 144.19, 134.00, 133.93, 133.68, 133.50, 125.02, 124.93, 124.80, 76.90, 74.08, 33.85, 33.84, 33.79, 33.56, 31.50, 31.49, 31.44, 31.08, 31.07, 29.83, 29.06, 23.40, 23.28, 10.39, 10.33.

Compound 259

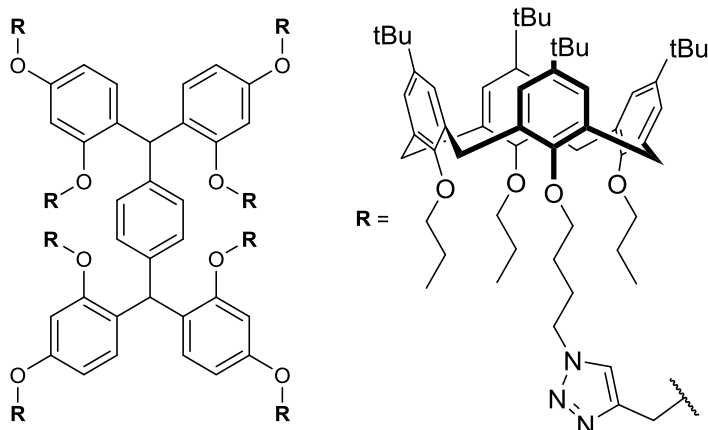


Sodium azide (0.43 g, 6.62 mmol) was added to a solution of **258** (4.00 g, 4.40 mmol) in DMF (80 mL) and allowed to stir at 60 °C for 18 hours. The mixture was then diluted with water and extracted with DCM. The organic layers were combined and washed three times with 3.6% HCL (100 mL), once with brine (100 mL) and then dried with MgSO₄. The solvent was removed under reduced pressure, to give the expected compound.

Yield: 88.4%

¹H-NMR (400 MHz, CDCl₃) δ 6.83 (s, 4H), 6.72 (m, 4H), 4.39 (t, *J* = 12.4 Hz, 4H), 3.90 (t, *J* = 7.6 Hz, 2H), 3.81 (m, 6H), 3.37 (t, *J* = 7.2, 2H), 3.12 (m, 4H), 2.13 (m, 2H), 2.00 (m, 8H), 1.74 (m, 2H), 1.07 (m, 45H).

Compound 260

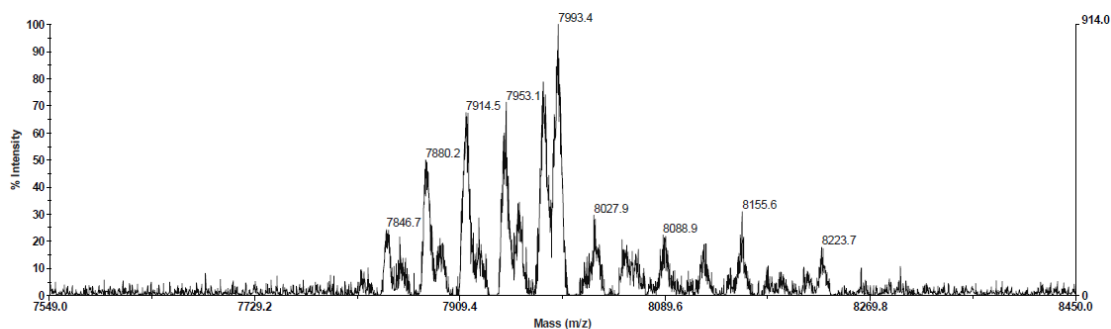


259 (741.8 mg, 0.850 mmol) was added to a mixture of **255** (44.8 mg, 53.1 μmol), $\text{CuSO}_4 \cdot 5\text{H}_2\text{O}$ (1.3 mg, 5.31 μmol) and sodium ascorbate (2.1 mg, 10.62 μmol) in 7 ml of DMF under argon. The mixture was slowly heated to 80 $^\circ\text{C}$. After 4 h at 80 $^\circ\text{C}$, the DMF was evaporated under reduced pressure. The dark yellow product was suspended in DCM, absorbed onto silica and purified by flash chromatography (DCM until the remaining **259** has been recovered, then DCM/MeOH 70/1).

Yield: 85.7%

^1H NMR (400 MHz, CDCl_3) δ 7.49 (s, 4H), 7.04 (s, 4H), 6.86 (s, 4H), 6.69 (m, 64H), 6.60 (m, 8H), 6.37 (m, 4H), 5.92 (s, 2H), 5.02 (s, 8H), 4.88 (s, 8H), 4.38 – 4.11 (m, 48H), 3.90-3.63 (m, 64H), 3.03 (t, $J = 12.8$ Hz, 32H), 2.07 – 1.78 (m, 80H), 1.16 – 0.78 (m, 360H).

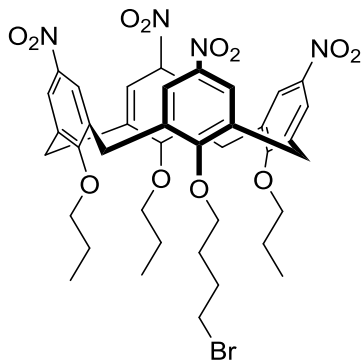
^{13}C NMR (101 MHz, CDCl_3) δ 158.07, 156.74, 153.68, 153.54, 153.48, 153.40, 153.30, 144.61, 144.42, 144.25, 143.95, 143.91, 133.96, 133.86, 133.74, 133.66, 133.42, 130.37, 129.12, 126.40, 125.09, 124.99, 124.81, 122.45, 105.40, 100.83, 77.23, 76.90, 74.11, 73.94, 62.80, 62.09, 50.44, 50.27, 33.86, 33.84, 33.82, 33.79, 31.49, 31.45, 31.09, 27.35, 27.28, 27.22, 23.42, 23.34, 23.32, 10.46, 10.41, 10.39, 10.37.



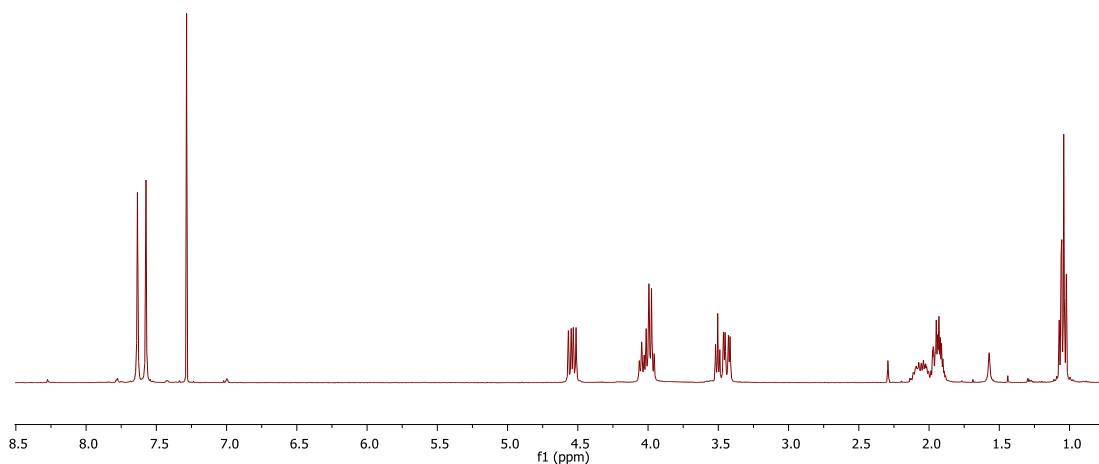
Acquired: 14:06:00, February 20, 2014
M Cominetti MC-159 MWt=7821? DCM Gold1 PosRef [1.29] (DCTB,DCM)
D:\2014\Feb14\UEAMAT225-VA-MAP-2_0001.dat

Printed: 07:07, February 21, 2014

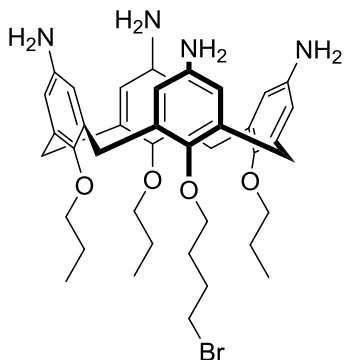
Compound 261¹⁴⁵



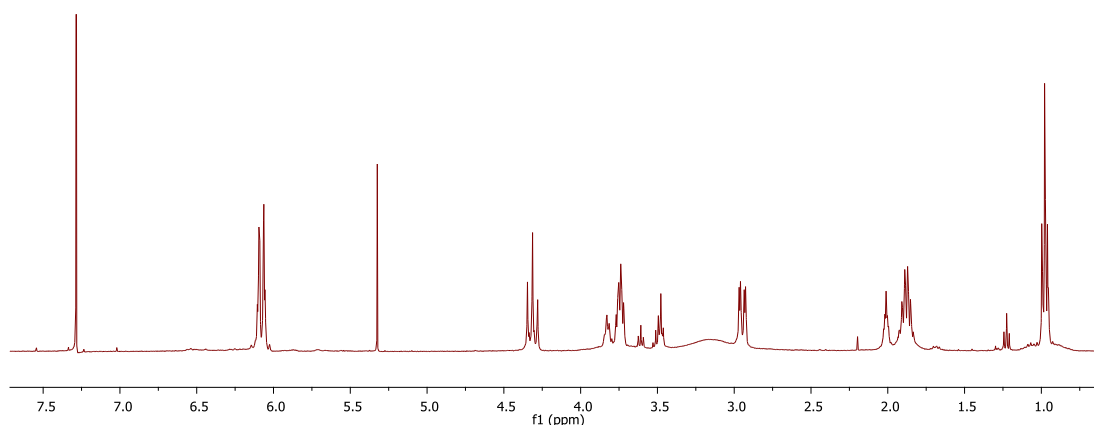
To a stirring solution of **258** (2 g, 2.2 mmol) in DCM (138 mL) were added, in sequence, glacial acetic acid (13.8 mL) and concentrated nitric acid (13.8 mL). After 6 hours, the reaction was diluted with 350 mL of distilled water, the organic layer was collected, washed with distilled water (twice), with brine (once) and dried with MgSO_4 . The solvent was removed under reduced pressure and the residue was triturated with methanol to give **261** (1.72 g). The white solid obtained was used for the synthesis of **262** without any further purification. A ^1H -NMR (400 MHz, CDCl_3) is reported for reference.



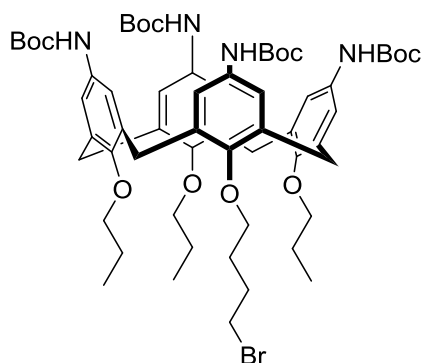
Compound 262



A mixture of crude **261** (1.70 g) and tin chloride dihydrate (11.31 g, 50.1 mmol) in ethanol (110 mL) was allowed to stir at reflux for 48 hours. The solvent was removed under reduced pressure and the result was treated with 350 mL of a solution of 10% NaOH in water. The mixture was then extracted with DCM three times. The organic layers were collected, washed with distilled water (twice), brine (once) and dried with MgSO₄. The solvent was removed under reduced pressure to give 1.18 g of brown solid. The crude was used directly for the synthesis of **263**. A ¹H-NMR (400 MHz, CDCl₃) is reported for reference.



Compound 263



Boc-anhydride (10.83 g, 49.6 mmol) was added to a stirring solution of crude **262** (1.17 g) and DIPEA (6.41 g, 49.6 mmol) in 40 mL of DCM and allowed to stir for 60 hours at room temperature. The resulting mixture was diluted with DCM and the organic layer was washed with water (twice), brine (once) and dried with MgSO₄. The solvent was removed under reduced pressure and the residue was purified by column chromatography (ethyl acetate/DCM 1/20) to give **263**.

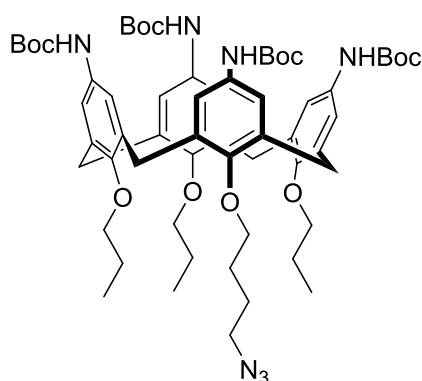
Yield: 29% over three steps, from **258**

[M+NH₄]⁺ = 1164.5651 (Calculated: 1164.5670)

^1H NMR (400 MHz, CDCl_3) δ 6.69 – 6.56 (m, 8H), 6.22 – 6.11 (m, 4H), 4.44 – 4.30 (m, 4H), 3.91 – 3.83 (m, 2H), 3.83 – 3.73 (m, 6H), 3.60 (t, J = 6.6 Hz, 1H), 3.47 (t, J = 6.3 Hz, 1H), 3.18 – 3.06 (m, 4H), 2.08 – 1.96 (m, 4H), 1.96 – 1.81 (m, 6H) 1.60 – 1.41 (m, 36H), 1.03 – 0.93 (m, 9H).

^{13}C NMR (101 MHz, CDCl_3) δ 153.38, 153.37, 153.35, 152.86, 152.84, 152.78, 152.65, 152.61, 135.30, 135.21, 135.03, 132.20, 132.00, 119.96, 119.91, 119.83, 80.06, 80.01, 77.23, 76.79, 73.90, 44.86, 33.36, 31.11, 29.69, 29.50, 28.84, 28.45, 27.57, 23.16, 23.09, 10.35.

Compound 264



Sodium azide (0.12 g, 1.85 mmol) was added to a solution of **263** (0.6 g, 0.52 mmol) in DMF (10 mL) and allowed to stir at 60 °C for 18 hours. The mixture was then diluted with water and the solid was collected by Büchner filtration. The product was washed with abundant distilled water and dried in air.

Yield: quantitative

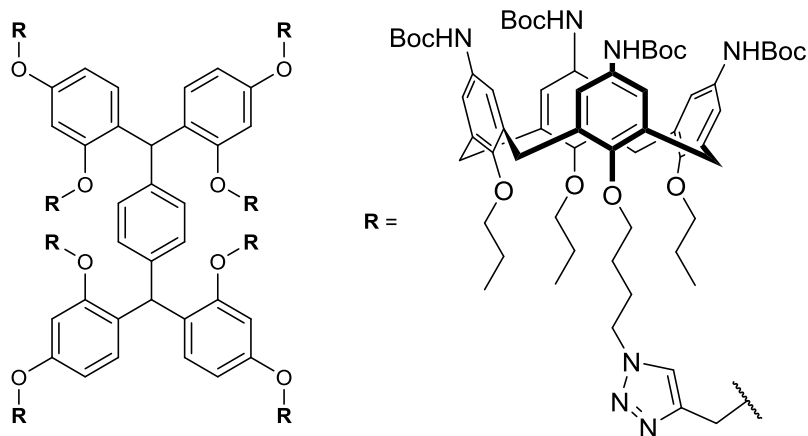
$[\text{M}+\text{NH}_4]^+ = 1125.6575$ (Calculated: 1125.6594)

^1H NMR (400 MHz, CDCl_3) δ 6.68 (s, 4H), 6.58 (s, 4H), 6.17 (s, 2H), 6.11 (s, 2H), 4.42 – 4.30 (m, 4H), 3.91 – 3.84 (m, 2H), 3.84 – 3.71 (m, 6H), 3.35 (t, J = 6.9 Hz, 2H), 3.17 – 3.05 (m, 4H), 2.03 – 1.79 (m, 8H), 1.77 – 1.63 (m, 2H), 1.50 (dd, J = 10.5, 5.0 Hz, 36H), 1.07 – 0.91 (m, 9H).

^{13}C NMR (101 MHz, CDCl_3) δ 153.41, 153.36, 153.35, 152.89, 152.71, 152.64, 135.41, 135.36, 135.08, 134.92, 132.22, 132.04, 132.00, 119.99, 119.89, 119.81, 80.07, 80.03, 80.00, 77.23, 76.80, 74.19, 51.51, 31.13, 31.10, 28.45, 27.26, 25.70, 23.17, 23.07, 10.36, 10.30.

IR (ν_{max} , cm^{-1}): 2977, 2931, 2873, 2096, 1700, 1601, 1522, 1472, 1416, 1367, 1291, 1241, 1215, 1149, 1066, 1037, 1004, 964, 872, 770.

Compound 265



Compound **264** (600 mg, 0.541 mmol) was added to a mixture of **255** (28.5 mg, 33.8 μmol), $\text{CuSO}_4 \cdot 5\text{H}_2\text{O}$ (25 mg, 0.1 mmol) and sodium ascorbate (250 mg, 1.26 mmol) in 7 ml of DMF under argon. The mixture was slowly heated to 80 $^\circ\text{C}$. After 4 h at 80 $^\circ\text{C}$, the DMF was evaporated under reduced pressure. The dark yellow product was suspended in DCM, absorbed onto silica and purified by flash chromatography (DCM/ethyl acetate 10/1 until the remaining **264** has been recovered, then DCM/MeOH 20/1 to elute the product).

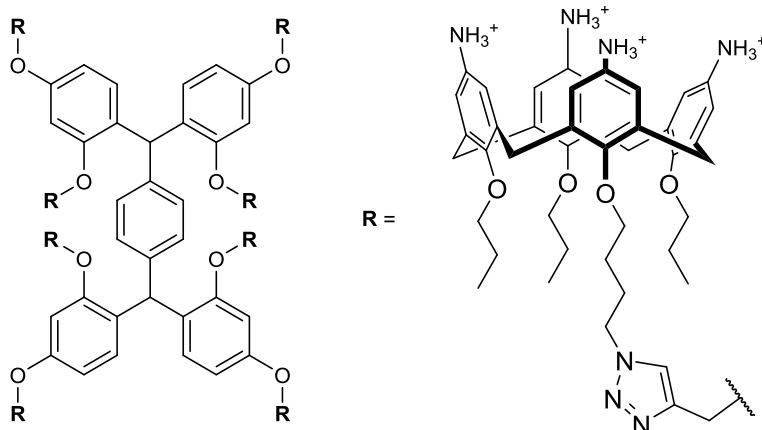
Yield: 76.8%. Excess of **264** was recovered in 92.5% yield.

$[\text{M}+(\text{NH}_4)_5]^{5+} = 1959.8908$ (Calculated: 1959.8962)

^1H NMR (400 MHz, CDCl_3) δ 7.59 (s, 4H), 7.14 (s, 4H), 6.88 (s, 4H), 6.71 – 6.48 (m, 68H), 6.44 (d, $J = 8.4$ Hz, 4H), 6.40 (s, 4H), 6.32 (s, 16H), 6.18 (s, 16H), 5.96 (s, 2H), 5.08 (s, 8H), 4.93 (s, 8H), 4.44 – 4.15 (m, 48H), 3.91 – 3.63 (m, 64H), 3.17 – 2.90 (m, 32H), 2.07 – 1.70 (m, 80H), 1.57 – 1.33 (m, 288H), 1.07 – 0.79 (m, 72H).

^{13}C NMR (101 MHz, CDCl_3) δ 158.04, 153.49, 153.44, 153.41, 153.39, 152.83, 152.79, 152.75, 152.68, 152.40, 152.30, 143.86, 135.34, 135.31, 135.28, 135.19, 135.11, 135.09, 135.00, 134.86, 132.41, 132.35, 132.08, 131.98, 122.61, 122.60, 120.12, 120.04, 120.02, 119.94, 119.88, 100.88, 80.00, 79.96, 79.89, 77.23, 73.93, 73.79, 62.03, 62.01, 50.30, 50.15, 31.10, 28.47, 28.46, 27.24, 27.16, 27.08, 23.16, 23.12, 23.09, 10.48, 10.42, 10.41, 10.32.

Compound 266



HCl_(g) was bubbled in a solution of **265** (82 mg, mmol) in DCM (2 mL) until a white precipitate formed. The mixture was cooled at 0 °C with an ice bath and MeOH was added dropwise to dissolve the precipitate. After one hour the source of HCl_(g) was removed and argon was bubbled in the mixture for sixty minutes. The solvent was then removed under reduced pressure. The residue was dissolved in 16 mL of HPLC Solvent A, filtered and purified by preparative RP-HPLC.

Yield: 78.8% (Calculated as TFA salt)

[M+(NH₄)₅]⁵⁺ = 1302.1327 (Calculated: 1302.1328)

¹H NMR (400 MHz, MeOD) δ 8.13 (d, *J* = 20.2 Hz, 4H), 7.43 (s, 4H), 7.04 (s, 4H), 6.96 – 6.80 (m, *J* = 14.2 Hz, 34H), 6.79 – 6.57 (m, 38H), 6.49 (d, *J* = 8.5 Hz, 4H), 5.91 (s, 2H), 4.62 – 4.28 (m, 48H), 4.10 – 3.74 (m, 64H), 2.20 – 2.07 (m, 8H), 2.07 – 1.79 (m, 72H), 1.14 – 0.81 (m, 72H).

¹³C NMR (101 MHz, MeOD) δ 161.24, 160.88, 160.52, 160.16, 156.65, 156.26, 156.10, 156.01, 136.70, 136.61, 136.53, 136.05, 135.99, 135.88, 135.80, 125.07, 125.04, 122.86, 122.84, 122.80, 122.51, 122.44, 122.35, 77.22, 77.13, 77.07, 74.66, 74.61, 74.59, 61.14, 49.85, 30.36, 30.31, 26.85, 23.00, 22.94, 9.58, 9.47, 9.26.

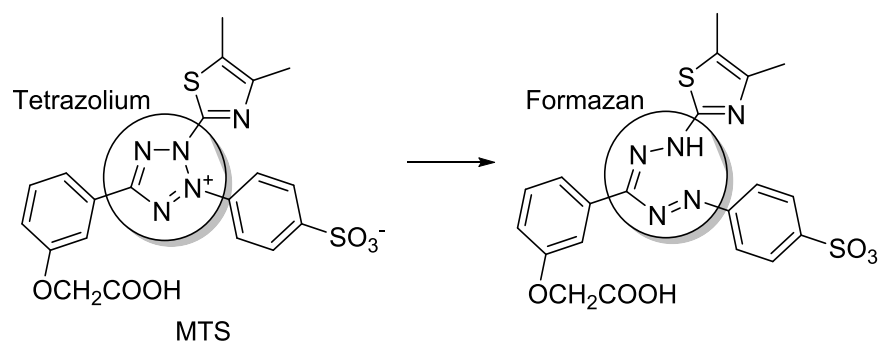
IR (ν_{max}, cm⁻¹): 2966, 2931, 2873, 2625, 1667, 1467, 1184, 1064, 1036, 999, 959, 839, 798, 721, 703.

5. Biological evaluation

The great majority of the compounds synthesised in the previous chapters are novel and thus there are no available data regarding their effect on cell viability. Evaluation of the effects on proliferation is a relevant step required to understand the potential of these new molecules. Potential antioxidant or antimicrobial compounds are expected to have low impact on the viability of human cells. On the other hand, potent inhibitors could be interesting leads toward the development of anticancer drugs. For this reason, the effect of these compounds on the proliferation of two human cancer cell lines was undertaken.

5.1 MTS assay

Formazan dyes are the basis of a number of biological assays. These dyes are characterised by a central tetrazole ring with a quaternary nitrogen, adorned with three aromatic substituents. Upon reduction, the colourless tetrazolium substrate is converted to a chromogenic formazan (Scheme 80), thus allowing spectrophotometric detection.^{149,150}



Scheme 80. Reduction of MTS to its chromogenic formazan derivative.

The nature of the substituents on the tetrazolium ring affects the biophysical properties of the dye. MTT (4,5-dimethyl-2-thiazolyl)-3,5-diphenyl-2H-tetrazolium bromide), one of the most widely used reagents, produces an insoluble formazan dye. On the other hand, MTS ([3-(carboxymethoxy)phenyl]-3-(4,5-dimethyl-2-thiazolyl)-2-(4-sulfo-phenyl)-2H-tetrazolium inner salt), gives a soluble dye. Ability to cross the membrane is also affected by the substituents and reagents that do not enter the

cytoplasm have additionally been developed. All these properties influence the methods and the applicability of the different reagents to different type of assays.

MTT and MTS are reduced intracellularly by NAD(P)H-dependent oxidoreductases and dehydrogenases (other enzymes are also involved to a minor extent) of viable cells. It has been demonstrated that, under controlled conditions, there is a correlation between the number of viable cells and the reduction of the tetrazolium reagent. The application of these dyes to microplate screening application made these methods rather popular, thanks to their simplicity and rapidity. MTT assay has been widely used to determine the effect of drugs and other substances on cell proliferation. Being a measure of the metabolic activity, the assay can be adjusted to probe the method of action of the drug itself by application of stimuli or modification of the assay conditions.

The principal difference between MTT and MTS assay is the solubility of the dye itself. In the case of MTT, a washing and solubilisation step is required, while MTS produces a soluble formazan, which can directly be measured (which also allows measurement at different time points rather than being a purely end-point assay). The disadvantage of MTS is the higher risk of interference caused by coloured compounds, which may interfere with the colorimetric detection. The MTS assay has been widely applied within the group and was chosen as an initial method for the screening of the effects on cell viability.

5.1.1 Cell Lines

For the screening two cancer cell lines were employed. MCF-7 cell are adherent cells of breast cancer origin, while HL60 grow in suspension and are human promyelocytic leukaemia cells. The choice of the two lines lies in the fact that MCF-7 express p53, a key tumour suppressor protein, whilst the gene for its expression in HL60 presents major deletion and it is thus non-functional. The difference allows potential discrimination of compounds interfering with the activity of p53.^{151,152}

5.2 Screening

Inhibition of cell proliferation was evaluated at two different concentrations for a three day treatment, in both MCF-7 and HL60 cell lines. Proliferation is reported

compared to the control, reported as percentage. A summary of the results is reported in **Table 6**.

	HL60		MCF-7			HL60		MCF-7	
	100 μ M	10 μ M	100 μ M	10 μ M		100 μ M	10 μ M	100 μ M	10 μ M
107	5	11	8	66	182	24	125	15	95
109	5	82	5	101	183	0	89	7	99
111	4	68	NA	NA	184	25	106	28	124
116	109	103	96	106	185	31	110	28	102
135	18	78	13	99	186	24	103	23	86
136	16	107	106	100	187	16	129	16	106
138	100	100	93	91	188	12	105	24	107
140	3	53	NA	NA	192	3	61	NA	NA
141	5	44	NA	NA	193	3	78	0	54
142	4	61	2	92	194	6	99	0	96
143	4	68	3	100	207	7	3	9	4
144	4	78	NA	NA	208	4	4	6	4
145	73	88	56	90	209	6	3	8	5
150	8	34	NA	NA	210	6	5	6	3
151	5	95	3	106	211	8	9	9	8
158	4	106	10	100	212	4	3	7	3
160	9	90	13	89	217	18	103	14	101
163	5	102	7	107	218	26	105	9	94
164	6	63	5	78	220	62	93	23	109
165	8	72	10	58	241	7	47	NA	NA
166	0	83	3	108	242	82	94	92	105
167	0	89	3	100	243	30	77	43	99
168	67	112	102	117	244	36	87	78	104
180	28	110	30	102	246	6	84	48	93
181	19	115	17	96	248	88	97	95	83

Table 6. Results of the proliferation screening against MCF-7 and HL60, at 10 and 100 μ M concentrations for a three day treatment. Data expressed as percentage of proliferation compared to the control. Colour gradient from 0% proliferation (red) to white (50%) and blue (100%).

5.2.1 Comparison of MCF-7 and HL60

The first discussion is related to the behaviour of the two different cell lines against the library of compounds. As visualised in **Figure 84**, both at 10 and 100 μ M concentrations, the compounds display a lack of selectivity, producing similar effects on both breast cancer and leukaemia type cells.

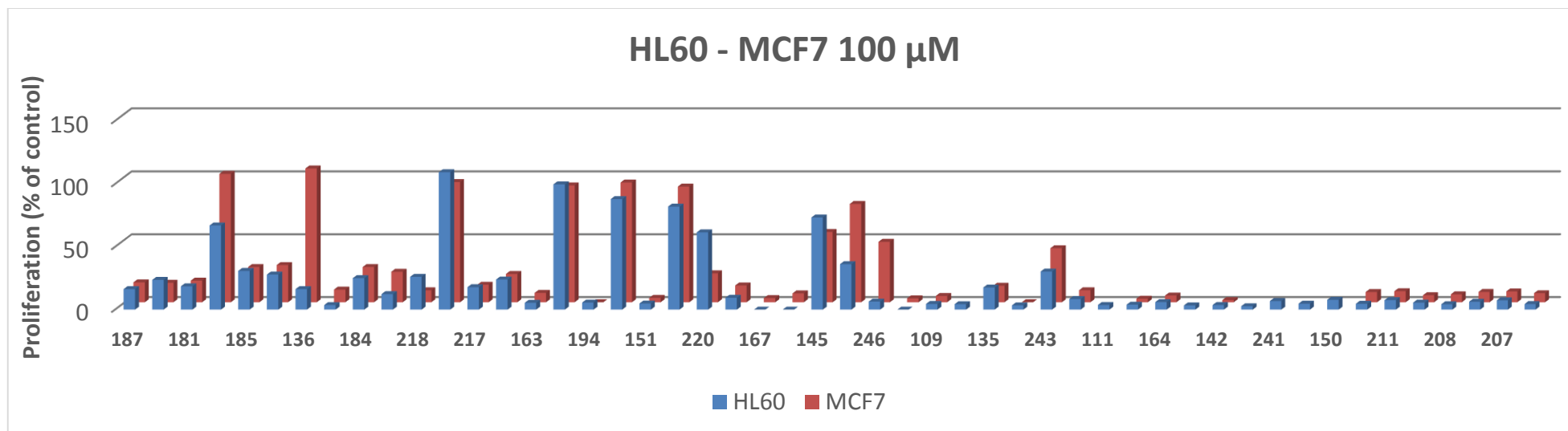
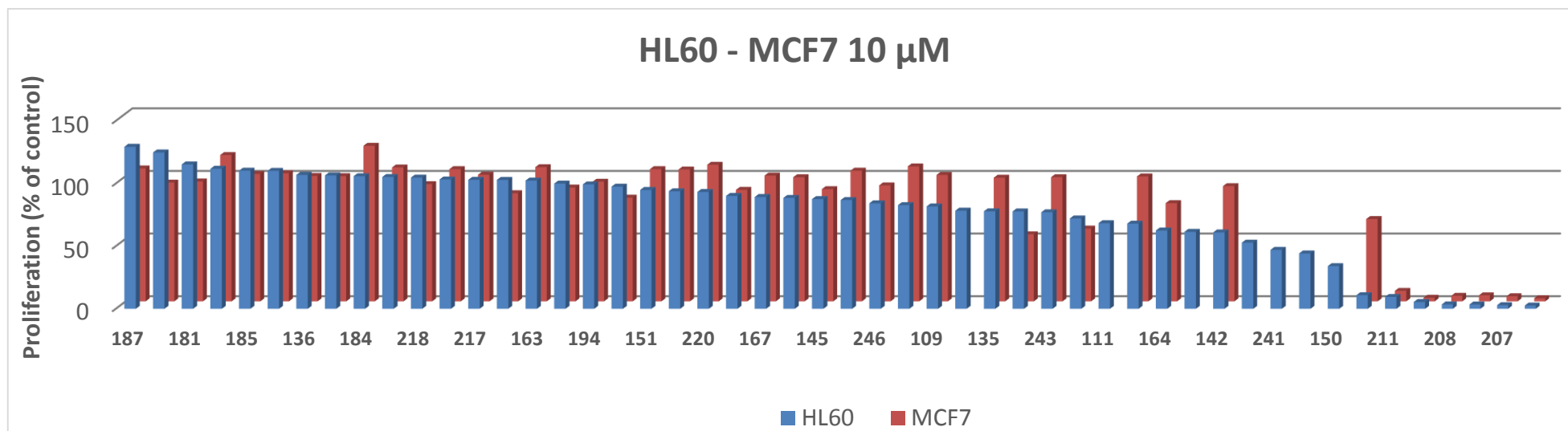


Figure 84. Proliferation screening against MCF-7 and HL60, at 10 and 100 μ M concentrations for a three day treatment. Result expressed as percentage against control.

Only **136**, **168**, **244** and **246** (**Figure 85**) produce a degree of selectivity across the two lines, at least at the concentrations considered. Of these, **136** is the most relevant, with HL60 almost completely inhibited (16% proliferation) and no effect on MCF-7 proliferation at 100 μ M concentration. In the case of xanthenes, **246** and **244**, the selectivity is limited to about 40% effect on the proliferation. This makes these compounds potentially interesting subject for further studies.

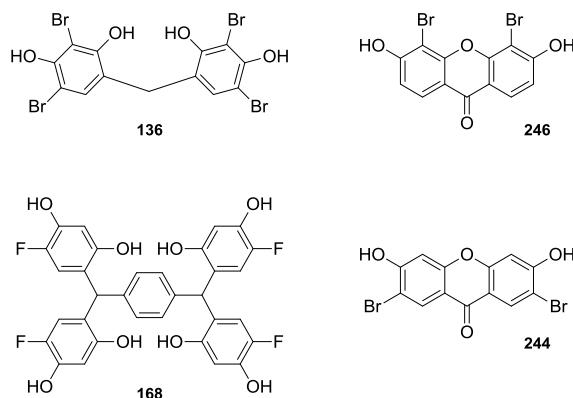


Figure 85. Compounds showing selectivity over the two cell lines.

5.2.2 Structures with low toxicity

In general, for both cell lines, as one can notice from **Figure 84**, a good number of the compounds display an IC_{50} between 10 and 100 μ M, which is relatively low compared to a typical anticancer drug like doxorubicin (125 nM, positive control). A few compounds, on the other hand, display an even lower inhibitory effect. The reference resorcinol monomers, 4-chlororesorcinol and 4-bromoresorcinol, both have substantially no effect on either cell lines at 100 μ M. Structures **168** and **136**, although only with MCF-7, display no inhibitory effect at the highest concentration used. Compounds **242**, **248**, **220**, **145** and **194** are also interesting for their low effect on cell viability.

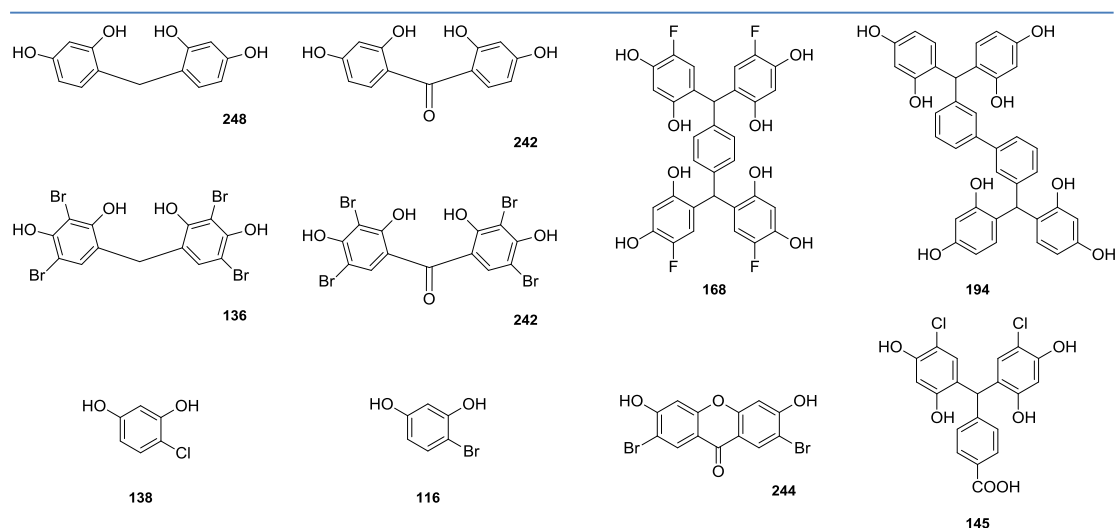


Figure 86. Structures displaying low proliferation inhibition.

Observing these structures (**Figure 86**), it is evident that lowest proliferation inhibition is mainly related to simple structures, monomers, benzophenones and bisphenols in particular, while tetramers and higher analogues lead to higher toxicity.

5.2.3 Evaluation of tetramers

The tetramers synthesised (**Figure 87**), can be classified into three groups: tetramers with a central phenyl ring (**a**), diphenol based tetramers (**b**) and with aryloxy-alkyl linked structures (**c**).

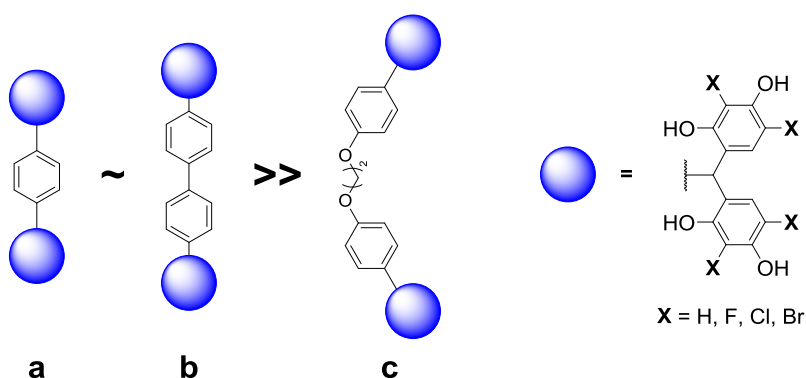


Figure 87. Effect of the central core of tetramers on cell viability.

The first group of tetramers (**a**), for the most part, do not display inhibitory effects at 10 μM concentrations, except for a few compounds. At 100 μM , on the other hand, they produce almost complete inhibition, suggesting an IC_{50} between 10 μM and 100 μM . For the second group (**b**), the trend is the same, implying that changing a

central phenyl ring to a diphenyl does not affect the activity. The situation changes dramatically with group **c**, which displays the highest toxicity in the library, with complete inhibition at 10 μ M. This group will be discussed further in the next chapter.

Effect of halogen substitution (**Figure 88**) on proliferation is less clear. Indeed, whilst it appears that fluoro-substitution (**a**) reduces the toxicity, it is however a single example in the library and a similar substitution on a geometric equivalent would be necessary to confirm the hypothesis.

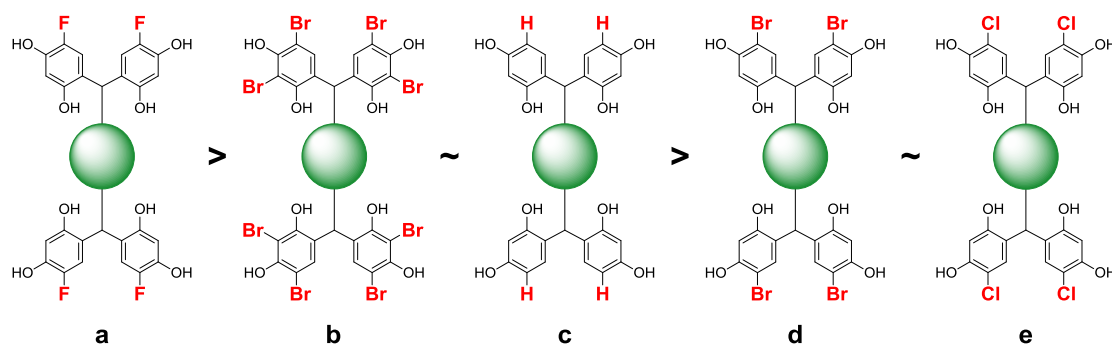


Figure 88. Effect of the halogen substitution on cell viability.

In general, compounds with more than four halogens (**b**), or without halogens (**c**), appear to be just slightly less toxic compared to their tetra-bromo (**d**) and tetra-chloro (**e**) analogues.

In the case of tetramers with a central phenyl ring, it appears that the geometry is not particularly relevant (**Figure 89**).

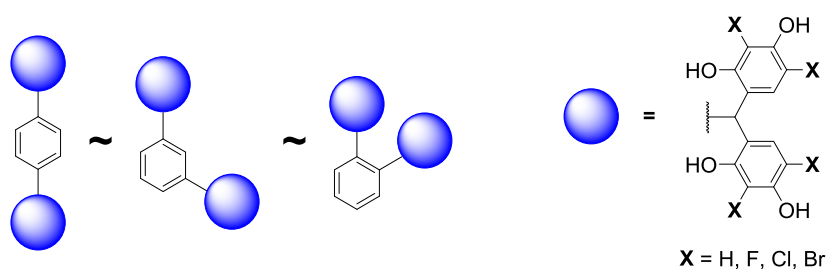


Figure 89. Effect of geometry on cell viability.

It is also interesting to note that increasing the number of monomers from four to six (**Figure 90**) results in less proliferation inhibition, while a reduction decreases cell viability.

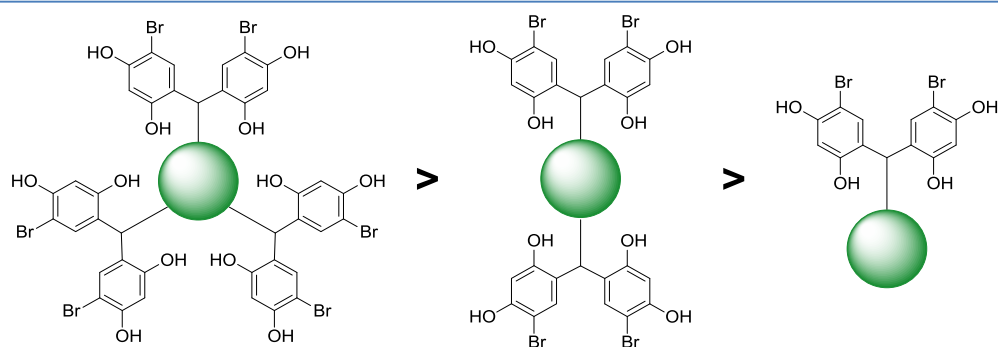


Figure 90. Effect of the number of monomers on cell viability.

5.2.4 Antiproliferative compounds as potential anticancer agents?

A small number of compounds caused complete inhibition of proliferation at 10 μM concentration (**Figure 91**). The structures are closely related and characterised by an alkyl linker between the dimeric units. To evaluate their potential as antiproliferative agents, the IC_{50} of **207**, **209**, **210** and **212**, was evaluated in HL60 cells.

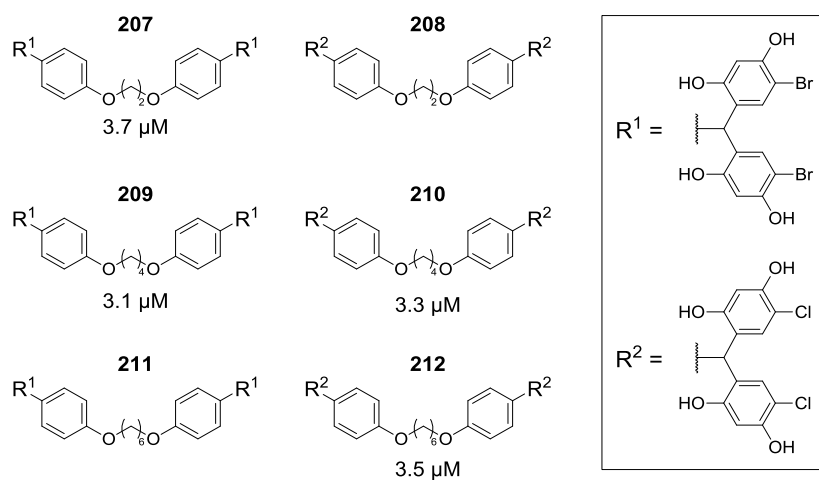


Figure 91. Tetramers with high anti proliferative activity.

The IC_{50} of the compounds tested, ranges between 3.1 and 3.7 μM , about one order of magnitude higher than doxorubicin (0.125 μM). More interesting is the fact that the structures present a substantially identical effect despite the length of the alkyl linker and the type of halogen.

5.3 Imaging

Since the great majority of the compounds studied are novel and display a certain degree of inhibition of proliferation, it was interesting to evaluate whether these can enter the cells effectively. A number of compounds are fluorescent, and are therefore easy to visualise by fluorescence microscopy. Their cell penetration was evaluated in MCF-7 cells, which are convenient for their size (compared to HL60) and the fact that they are adherent.

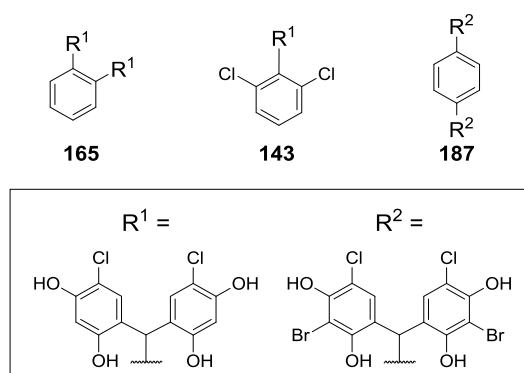


Figure 92. Fluorescent compounds for imaging.

The compounds shown are **165**, **187** and **143** (**Figure 92**). These are archetypal structures in the library, allowing us to assess penetration of basic tetramers (**165**), highly halogenated structures (**187**) and bis-phenols (**143**).

The cells were treated at 500 μ M concentration for 15 minutes, washed with media and then mounted on slides. Preliminary images appeared to show the compound concentrating in the nucleus, and thus a nuclear stain (Hoechst 33342) was employed to confirm the localisation. The counter-stain chosen is a DNA intercalator which emits blue fluorescence, which is different from the green or red fluorescence displayed by the test compounds.

Compound **187**, as every other highly halogenated compound in the library, exhibits strong fluorescence in DMSO and the colour changes by varying the pH. The effect is probably due to the acidic moieties and the effect is shared by other compounds in the library. It is also interesting to note that, differently from **165**, its fluorescence is not specific to a single channel, and displays fluorescence in both green and red channels.

The images in **Figure 93**, show penetration of compound **187** within MCF-7 cells and a control. All cells are effectively stained by the compound. In contrast to what was expected from the preliminary evaluation, the compound appears to be localising mainly in the cytosol, without particular penetration through the nuclear membrane. The inside of the nucleus is fainter compared to its immediate surroundings.

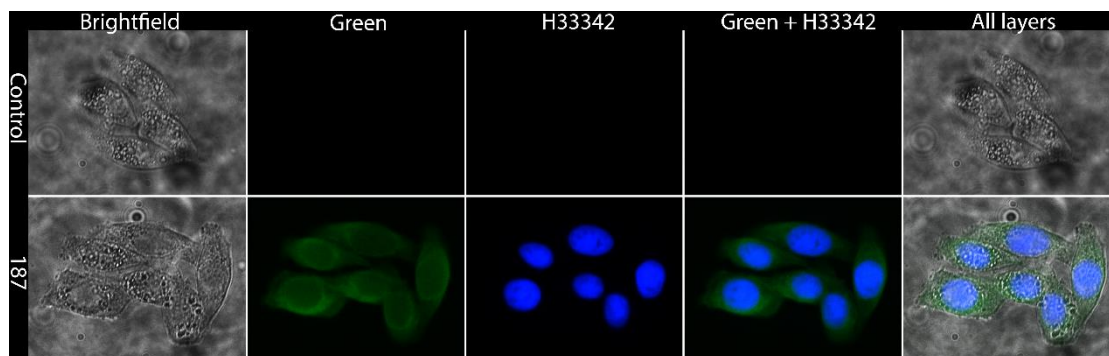


Figure 93. Fluorescence microscopy of MCF-7 cell treated with **187** and Hoescht 33342.

187 displays the same behaviour under the red filter (**Figure 94**). Similarly, **MC 126**, also in red, localises mainly in the cytosol. Exactly as described for **187**, the inside of the nucleus appears to be fainter. Compound **165**, which is particularly bright, appears to be localising in the cytosol but also on the surface of the nucleus. Its fluorescence is also more specific and does not appear in the red channel. It could be an interesting compound for further investigation, to evaluate whether the staining is specific to particular structures (*e.g.* endoplasmic reticulum) and useful as a fluorescent probe, since it is cheap and easy to produce.

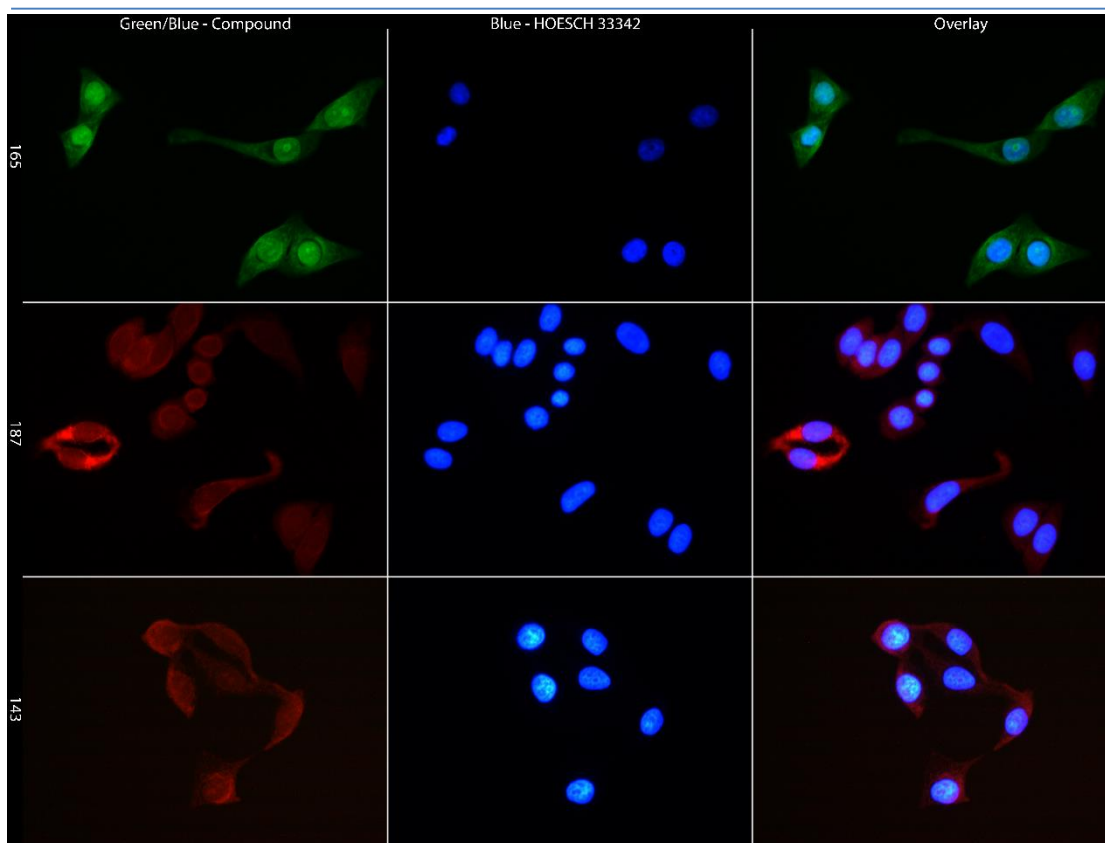


Figure 94. Fluorescence microscopy of MCF-7 cell treated with either **165**, **187** or **143** and Hoescht 33342.

Since it is confirmed that the compounds are able to penetrate the cells effectively and rapidly, both in the case of larger tetramers (more or less halogenated) and in the case of smaller dimers, it is reasonable to conclude that the antiproliferative effects observed may not be simply limited by their permeability and intracellular activity is very likely to be involved.

5.4 Conclusions

The library was screened to evaluate the antiproliferative effects of the compounds available. A varied profile has been identified, with compounds displaying high proliferation inhibition ($IC_{50} \sim 3 \mu M$) and compounds without effects on viability at the tested concentrations ($IC_{50} > 100 \mu M$).

Compounds with lower toxicity are relevant for the development of antibacterial and antioxidant drugs. The small set of compounds with high antiproliferative activity may be an interesting lead to investigate a new class of potent xenobiotics.

The ability of these compounds to permeate the cell has also been proven by fluorescence microscopy. Co-staining with a DNA targeting dye allowed verification that the compounds do not penetrate the nucleus. The prevalently perinuclear localisation of the compounds is worth further study to identify a potentially specific distribution to a defined cellular compartment.

5.5 Experimental

5.5.1 Cell culture

Both HL60 and MCF-7 cell lines were obtained from the European Collection of Cell Cultures.

HL60 cells were cultured in RPMI-1640 medium (HyClone Laboratories), supplemented with 10% Fetal Bovine Serum (PAA Laboratories), 2 mM L-glutamine (HyClone Laboratories), 100 U/mL Penicillin and 100 µg/mL Streptomycin (HyClone Laboratories).

MCF-7 cells were cultured in DMEM High Glucose medium (HyClone Laboratories) supplemented with 10% Fetal Bovine Serum (PAA Laboratories), 2 mM L-glutamine (HyClone Laboratories), 100 U/mL Penicillin and 100 µg/mL Streptomycin (HyClone Laboratories).

Cells were maintained at 37 °C in a humidified atmosphere with 5% CO₂ and passaged at 1/20 dilution (HL60) or 1/10 dilution (MCF-7) twice a week.¹⁵³

Cell counting was carried out using a 1/2 dilution of cells with 0.4% trypan blue solution (Sigma-Aldrich) and a Malassez haemocytometer.

5.5.2 Proliferation assay

MCF-7 (8000 per well, 100 µL) or HL60 (30000 per well, 100 µL) in 96 well plates (Thermo-Scientific) were treated with 1 µL of serial dilutions of sample compounds or vehicle control (DMSO). The plates were subsequently incubated for 72 hours in a humidified atmosphere at 37 °C and 5% CO₂. Cells treated with vehicle control were used as reference for 100% proliferation.

The cells were then treated with 10 µL of CellTiter 96[®] AQueous One Solution Cell Proliferation Assay (MTS) (Promega) and incubated for either 1.5 hours (MCF-7) or 4 hours (HL-60). Absorbance was measured using the POLARstar OPTIMA plate reader (BMG Labtech) at 492 nm. Data analysis was performed with Microsoft Excel (percentage proliferation) and GraphPad Prism V6.0 (IC₅₀ values).

5.5.3 Fluorescence Imaging

2 mL of MCF-7 cells (15000 cells/mL) were added to 6 well plates (Thermo-Scientific) with one coverslip in each well. After 24 hours of incubation, each well was treated with either, or a combination of, 10 μ L of sample (100 mM in DMSO), 4 μ L of Hoechst 33342 (2.5 mg/mL in water) or vehicle. After 15 minutes of incubation, the cells were washed with fresh media and the coverslips were mounted on slides using DPX Mounting Medium (Fisher Scientific). Images were immediately recorded using a Leica DMII HC microscope. Image processing and postproduction was performed with Leica's software and Adobe Photoshop CS6.

6. Antioxidant activity

Evaluation of the antioxidant effect of a substance is not a trivial problem, especially in a biological context. This is due to the complexity of the system under observation: the different origins of radicals, the varied type of radicals and pro/anti-oxidant enzymes influence the results. Even compounds without significant reactivity versus radicals can act as cofactors of antioxidant enzymes (*e.g.* selenium in glutathione peroxidase), induce the expression or inhibit anti- or pro-oxidant enzymes or chelate metals with a resulting *in-vivo* activity. Additionally, the toxicity of the compound itself has to be taken into consideration.

Due to the multifaceted nature of the problem, a range of different assays have been published over the years. Many *in vitro* assays aim at measuring the activity of samples against model radicals, however, correlation with their activity *in vivo* may not be possible.

In this chapter, the results of a preliminary evaluation of the products previously synthesised against model radicals will be presented. Subsequently, a selection of compounds was tested for their *in vivo* protection against oxidative stress and the results are reported.

6.1 Choice of the assay

As previously discussed (**Chapter 1**), for phenol-based structures reported in the literature, the activity *in vitro* is correlated with the number of hydroxyl groups. For this reason, the first assay was chosen to evaluate whether the trend is maintained with the compounds prepared and what influence the halogens have on these activities. For this reason, a simple and commonly used assay was required.

Different assays to evaluate the antioxidant capacity of compounds, natural extracts or food samples have been published. In the following paragraphs, the assays will be described very briefly and discussed for their suitability as a starting point to evaluate the behaviour of the compounds presented in this thesis.

6.1.1 Inhibition of induced lipid auto-oxidation

This assay evaluates the relative antioxidant efficiency of a sample, compared to that of α -tocopherol. Autooxidation of linoleic acid (or LDL) is induced by Cu(II) or 2,2'-azobis(2-amidinopropane) dihydrochloride (AAPH) and progress of the reaction is monitored by UV absorbance at 234 nm (peak of maximum absorbance of diene peroxides). Before addition of the initiator, the absorbance remains constant (**Figure 95, A-B**). After initiation, the autooxidation proceeds and the absorbance increases (**Figure 95, B-C**). The rate of the reaction is reduced by introduction of an antioxidant (**Figure 95, C-D**), and after its consumption the rate goes back to its original value (**Figure 95, D-E**). The authors defined the antioxidant efficiency as the slope of segment C-D (**Figure 95**) and can be reported as relative to a reference (α -tocopherol).¹⁵⁴

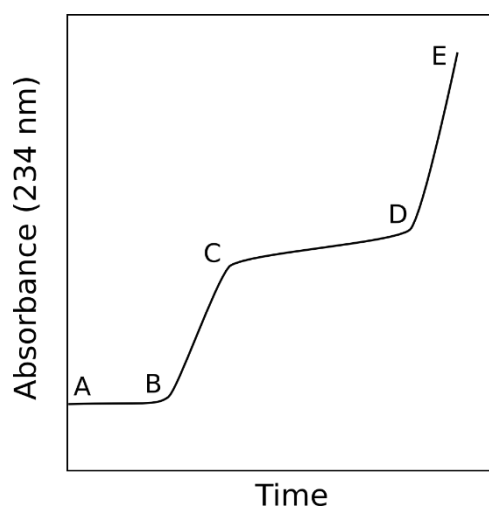


Figure 95. Autooxidation of linoleic acid monitored by UV absorbance. Initiator addition at point B, antioxidant addition at point C.

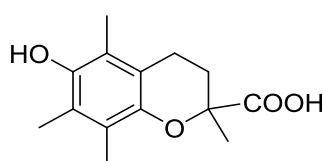
The assay, despite the (apparently) interesting direct protection of a lipid type of substrate, has a number of major drawbacks. The first and main one is the wavelength used for monitoring the reaction. It is a limiting condition as many organic compounds (or their products) can display absorption around 234 nm.¹⁵⁵ Secondly, measuring the change in rate might be difficult and require optimization.¹⁵⁵ Given the chromophore of our compounds, this assay was discounted.

6.1.2 ORAC, TRAP and PABA assays

This group of assays involves the use of fluorescent probes to monitor the progress of the different radical reactions of interest. The oxygen radical absorbance

capacity (ORAC) assay underwent varied modifications to improve its performance and applicability. Naguib¹⁵⁶ used a fluorescent reagent (6-carboxyfluorescein) which allows monitoring of reaction progress by spectrometry. AAPH initiates production of peroxy radicals that consume the fluorescent probe over time, progressively reducing the emission to zero. The area under the kinetic curve obtained is linearly correlated to the concentration of a standard sample (usually α -tocopherol) used for calibration.

The Total Peroxyl Radical-Trapping Antioxidant Parameter (TRAP) assay is a related assay which involves a fluorescent probe, R-phycoerythrin (R-PE, $\lambda_{em} = 575$), and AAPH. As with the lipid autoxidation assay, the reaction is slowed upon addition of a radical scavenger. In this case, the lag time is measured and reported as a function of the reference lag phase (Trolox, **Figure 96**).



Trolox

Figure 96. Structure of Trolox.

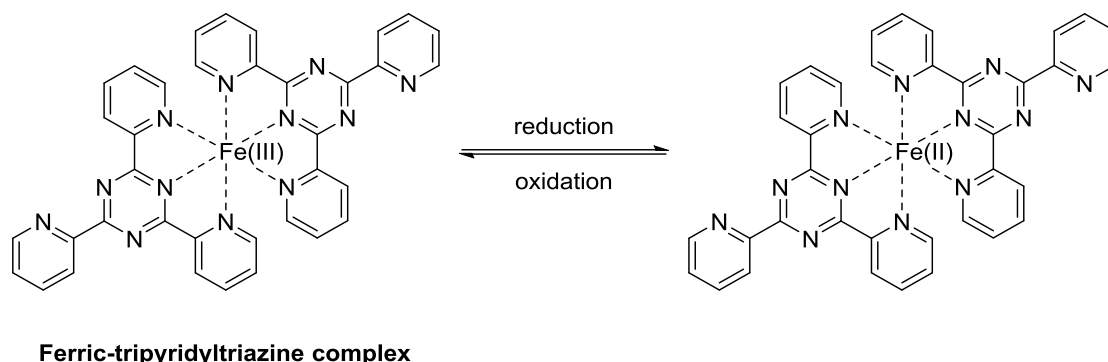
The use of fluorescent probes, quenched by a radical and protected by a scavenger, is still being developed. 4-Aminobenzoic acid (PABA) assay has been published in 2014 and uses the same concept, although fluorescence is measured at a fixed time point, with a resulting different type of analysis.¹⁵⁷

Compared to the inhibition assay (**Chapter 6.1.1**), these methods are more practical, as they allow preparation of the sample and measurement, without intermediate steps. On the other hand, despite the availability of different fluorescent probes, the methods may result in potential interference by different compounds in the library (and their oxidation products). It is important to note that many of the products prepared in our study display fluorescence, of different nature and indeed variable with pH. In addition, considering the potential fluorescence of the oxidation products (among which could be fluorone like substances), fluorescence monitoring is not ideal.

6.1.3 Ferric Reducing Ability of Plasma (FRAP) assay

In this assay, a ferric-tripyridyltriazine complex develops colour upon reduction and the reaction is monitored at 593 nm (**Scheme 81**). The assay is run under acidic

conditions, differently from other assays such as the Total Phenols Assay, which is conducted at basic pH.



Scheme 81. Ferric-tripyridyltriazine complex, oxidised and reduced form.

This assay was not suitable for our compounds for two reasons. Firstly, the presence of an excess of Fe(III) might interfere with the compounds in the library through co-ordination with the hydroxyl groups. Secondly, under acidic conditions the compounds display very poor solubility.¹⁵⁸

6.1.4 Cupric Reducing Antioxidant Capacity (CUPRAC) assay

In a similar fashion to the FRAP assay, the CUPRAC method is based on a chelated metal complex, in this case bis(neocuproine)copper(II) cation. The chromogenic probe turns orange yellow upon reduction of Cu(II) to Cu(I). Differently from FRAP, the working pH in this case is neutral.¹⁵⁹

The method has been developed extensively and presents varied modifications, including on-line HPLC applications.¹⁵⁹ However, the colour of the chromophore is similar to that of many compounds in the library and, similarly to FRAP, interference because of the excess of metal raises doubts about the use of this method.

6.1.5 Total Phenols Assay

Despite its name, the total phenols assay by Folin–Ciocalteu reagent effectively measures the reducing capacity of a sample. The reagent, commercially available, is composed of yellow mixed heteropolyphosphotungstates-molybdates and turns blue (760-765nm) by addition of a reducing agent.^{160,161}

The reaction is relatively slow, the colour develops slowly, reaches a maximum and then tends to fade. Nonetheless, with proper precautions readings between 1 and 6 hours give similar analytical results. Despite the time required by the reaction, the method is flexible and can be scaled to the plate reader, making it very convenient. The assay has also been widely used on a variety of samples and is widely accepted, making it an interesting candidate for an initial screening, especially considering that none of the compounds in the library has absorbance in the same range.^{160,161}

6.1.6 2,2-Diphenyl-1-picrylhydrazyl (DPPH) radical

Scavenging Capacity assay

2,2-Diphenyl-1-picrylhydrazyl radical (DPPH) is a relatively stable, nitrogen centred, radical and is commercially available as a solid crystalline material. DPPH solutions exhibit a strong purple colour with an absorption maximum at 512 nm. Reaction with a scavenger reduces the absorption at the maximum, with the solution turning progressively yellow. The progress of the reaction, activity of the sample and other parameters have been reported in different ways. A typically reported parameter is IC₅₀ (or EC₅₀), representing the concentration of sample required to decrease the initial absorbance of DPPH by 50% at a specific time.¹⁶² The time is usually chosen between 1 and 10 minutes, making the assay very quick and accessible.

Absorption vs Wavelength - multiple timesteps

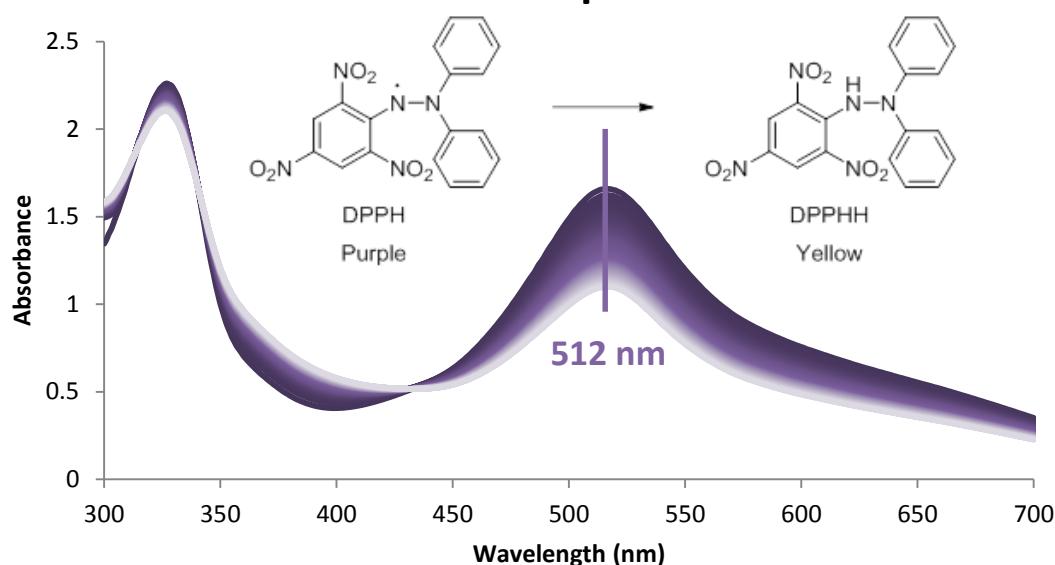


Figure 97. UV profile of the progressive conversion of DPPH into DPPHH.

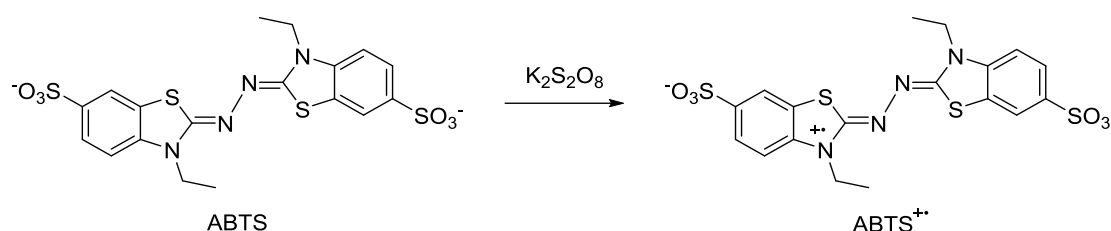
This assay has been widely used to test natural products, some of these have been discussed in the introduction (**Chapter 1**). An interesting feature of DPPH is that, due to its nature, it can be also identified and quantified by electron paramagnetic resonance (EPR), which offers an alternative and potentially discriminating quantitation approach against colourful samples or reaction products.¹⁶³ Alternatively, an amperometric determination method is available.^{164,165}

However, it is necessary to note that this approach is not useful for prediction of the *in vivo* protective effects of a sample, especially when emphasis is given to reaction stoichiometry rather than reaction kinetics and antioxidant chemistry.¹⁶⁶ Nonetheless, our initial attention was focused precisely on stoichiometry, to evaluate the ability of different, but closely related, structures to scavenge a model radical. As subsequently presented, *in vivo* protective studies evaluate the real protective effect in cells. The assay was chosen as a starting point and will be further discussed in context with the results.

6.1.7 Trolox Equivalent Antioxidant Capacity (TEAC) assay

The TEAC assay is based on another stable radical, prepared by oxidation of 2,2'-Azino-bis(3-ethylbenzothiazoline-6-sulfonic acid) (ABTS) diammonium salt with potassium persulfate in water (**Scheme 82**). The reaction produces a strong green-blue solution of ABTS^{•+}. A stock solution of radical is stable for a few weeks (dark, 4 °C)

and working solutions can be prepared when necessary. The absorption spectrum presents two main peaks, at 415 and 734 nm, with the latter being particularly relevant as most interference happens at shorter wavelengths.¹⁶⁷



Scheme 82. Synthesis of ABTS^{•+}.

The parameter usually reported for reference is the TEAC, which is the concentration of sample giving the same percentage inhibition of 1 mM Trolox. This is normally evaluated at fixed time points, usually less than 30 minutes.^{166,167}

Due to the nature of the radical, as in the case of DPPH, there are limitations to be considered and thus, this assay was used as alternative to DPPH. Further information about these issues will be provided with the results.

6.1.8 *In Vivo* Cell Protection Assay

Because of the difficulties in estimating potential protective effects from *in vitro* assays, some of the compounds were directly evaluated for their potential protective effects in cell lines using an adapted MTS assay.

6.2 Results and Discussion

6.2.1 DPPH assay

DPPH assays have been run in different protic solvents including methanol, methanol and water (also buffered or pH adjusted) and ethanol, although other studies have been conducted in aprotic solvents, *e.g.* acetone and benzene.^{162-166,168} In these studies, ethanol was chosen as it can dissolve all, but one, of the compounds in the library, thus maintaining constant conditions for all samples.

6.2.1.1 Initial evaluation

The first step was to compare the total scavenging capacity of all compounds. However, the reaction of DPPH with reducing agents is not always as fast as would be expected of strong reducing agents. For this reason, initial time course studies were run to evaluate whether the reaction reaches completion within a reasonable amount of time.

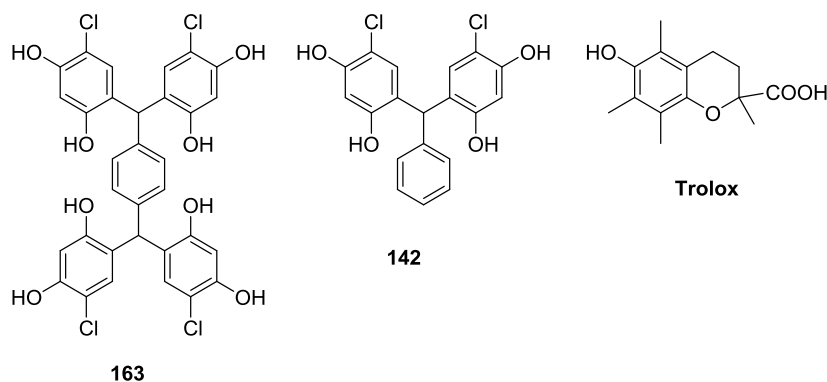


Figure 98. Sample compounds for the initial evaluation of DPPH radical scavenging assay.

The compounds chosen were **163** and **142**, being model structures of almost the entire library (**Figure 98**). The test compounds at 10 μM concentration were allowed to react with DPPH (150 μM) and the reaction was followed at 512 nm for 10 hours. In **Figure 99**, the percent of DPPH consumed (calculated as in **Equation 1**) is plotted against time.

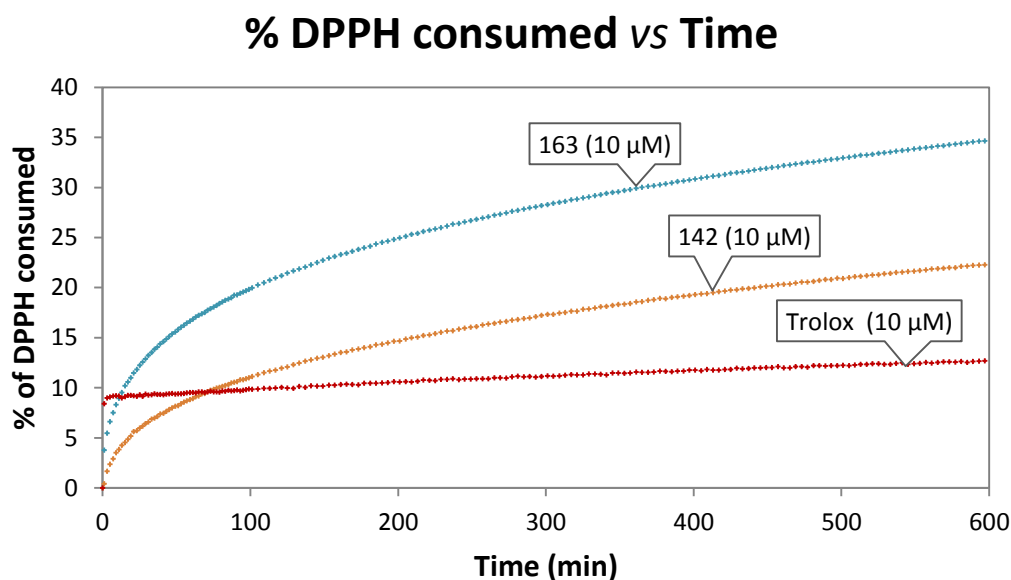


Figure 99. Time course profiles of the reaction between DPPH (150 μM) and sample compounds monitored at 512 nm.

$$\% \text{ of DPPH consumed} = 100 - (A_t \times 100 / A_{t=0}) \quad (1)$$

A_t = absorbance measured at time t

$A_{t=0}$ = initial absorbance

Equation 1. Calculation of the percent of DPPH consumed.

From **Figure 99**, it is clear that the reaction does not reach a plateau, which means it is not complete within the time frame of the analysis. The rate of the overall consumption of DPPH is not constant over time and progressively decreases. Since the radical is relatively stable, the decrease in absorbance might be due, in part or completely, to its decomposition. This is evident for Trolox, for which the reaction is complete almost immediately. **Figure 100** shows decomposition of DPPH over time, in the same conditions, **142** and Trolox are reported again for scale comparison.

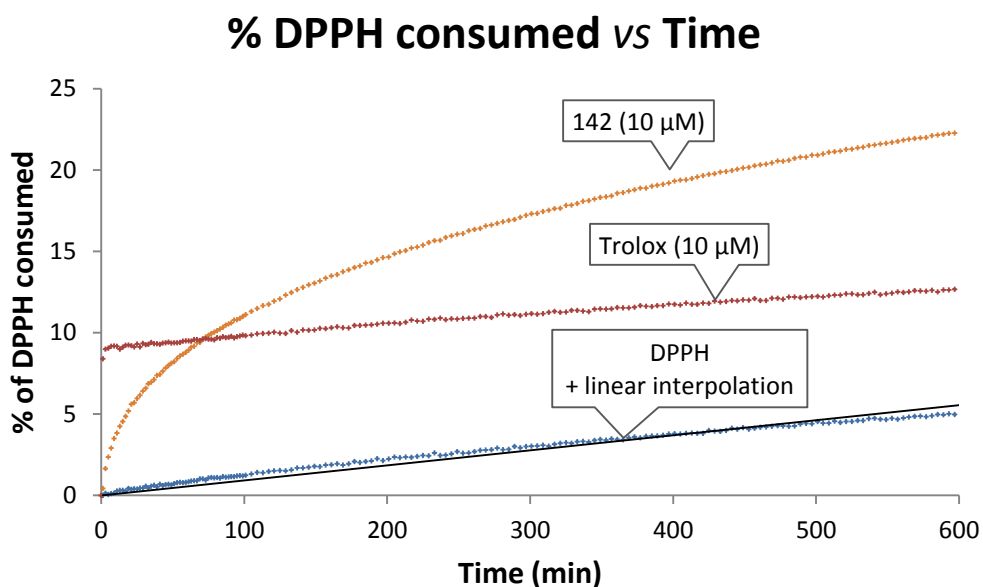


Figure 100. Comparison between the scavenging effect of two sample compounds and the decomposition of DPPH.

At 600 minutes, the decomposition of DPPH reached 5%, which is considerable compared to the 22% consumption seen with sample **142**. The rate of decomposition of DPPH slows down over time, as highlighted by a linear correlation in **Figure 100**. Consistently with what has been previously reported, the decomposition of DPPH in ethanol follows an overall pseudo-second order kinetic. The authors of the study

reported that the decomposition is slowed down by reaction products (undefined) between DPPH and solvent.¹⁶⁹ Decomposition of DPPH is faster in the presence of light and oxygen,¹⁷⁰ hence using degassed solvent, inert atmosphere and reduction of sampling might help to partially reduce the decomposition of DPPH, although a different solvent would probably be a better solution to the problem, especially considering that the use of ethanol has the result of reducing the effective amount of DPPH available for the reaction, as previously reported.¹⁶⁴

Since the decomposition of the probe is significant, subtraction of its contribution from the sample could be attempted to evaluate whether the steady state of the reaction is not reached as a consequence of DPPH behaviour. However, since the decomposition is concentration-dependent, the effect on the sample would be approximate and not consistent from sample to sample. The sample would react with DPPH consuming a part of it, thus altering the decomposition rate of DPPH itself.

6.2.1.2 Effect of Halogen and Geometry

Despite the considerable limits of the assay, a small set of compounds (**Figure 101**) was tested to evaluate the effect of different geometry and halogen substitution on the reactivity towards DPPH. Since a steady state cannot be reached, the compounds were all tested at the same concentration and the progress of the reaction was followed for a fixed three hours.

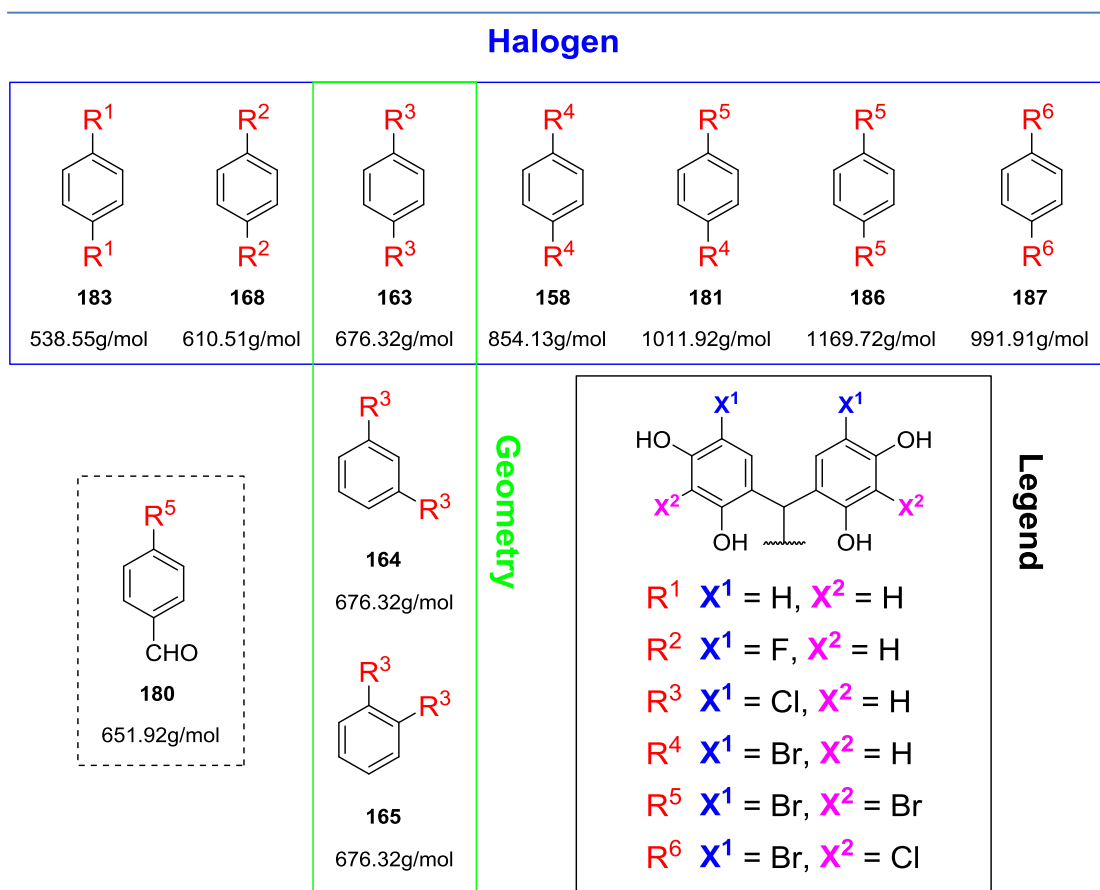


Figure 101. Compounds for the evaluation of halogen and geometry effects on DPPH scavenging activity.

From the results shown in **Figure 102**, the activity of the compounds is split into two clusters. Non-halogenated **183** and fluoro derivative **168** have about twice as much activity as the other compounds. Lack of substitution might increase the reactivity towards DPPH due to reduced steric hindrance, a limiting factor, as previously described. Additionally, an activated position is also available for further reaction, as described for eugenol and proposed for these compounds in **Chapter 6.2.1.3**. Fluorine-substituted compounds might display such high activity due to their higher acidity. Since dissociation influences the reaction, higher phenolate concentration produces higher rates. In fact, it appears that during the initial phase of the reaction the rate of DPPH depletion is higher in the case of **168**, whilst **183** reacts slower but eventually reaches a higher value.

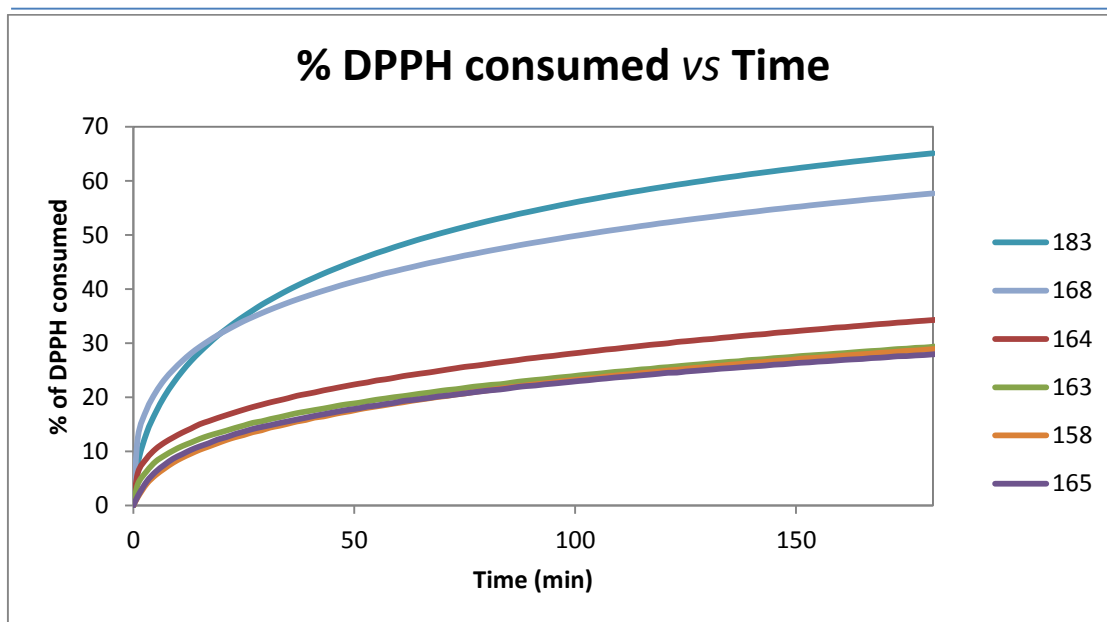


Figure 102. Progress of the reaction between DPPH (150 μ M) and sample compounds (20 μ M) monitored at 512 nm.

Geometrical isomerism does not appear to be significant, with **163**, **164** and **165** behaving almost identically, with only **164** displaying a slightly higher activity. This might be due to its inability to oxidise to a quinoid type structure. For these compounds, at 500 minutes (**Figure 103**), the activity profile is the same.

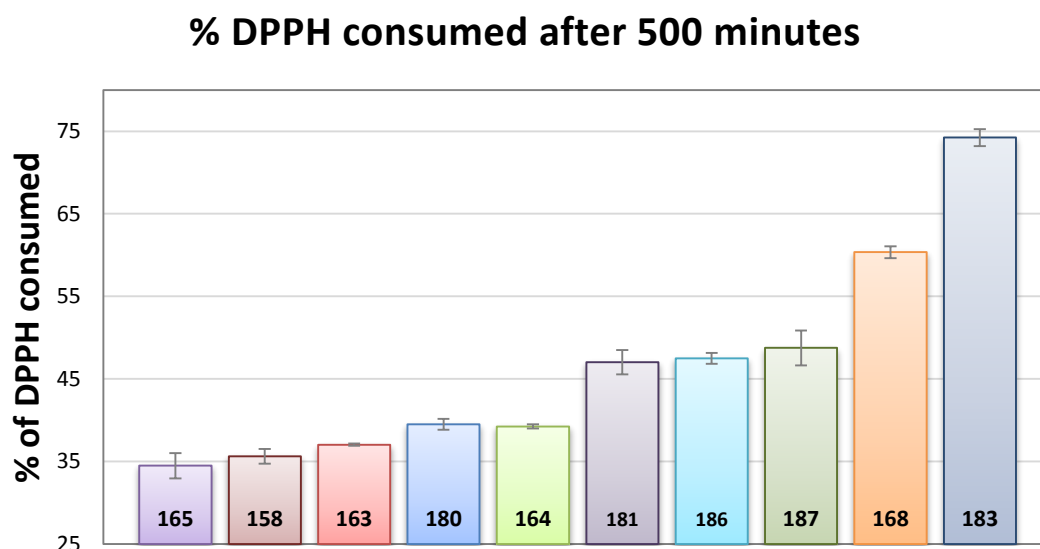


Figure 103. DPPH consumed (initial concentration 150 μ M) by sample compounds (10 μ M) after 500 minutes. Measures in triplicate and error expressed as standard deviation.

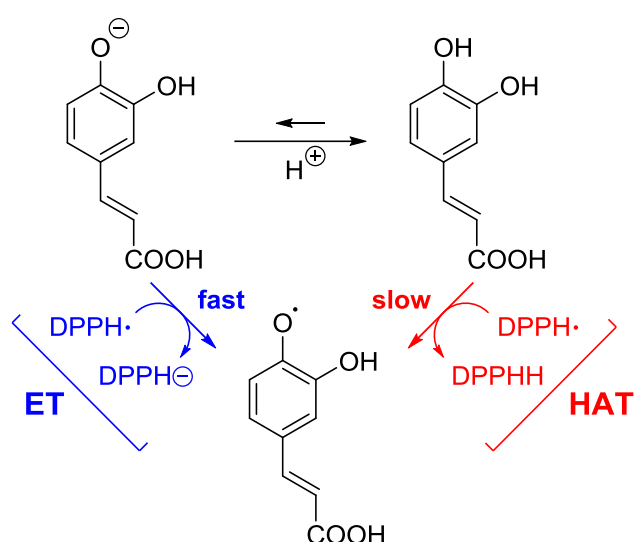
From these results, however, it is interesting to note how increased activity is linked to additional halogenation, as in the case of **181**, **186** and **187**. For these

compounds, all activated positions on the bis-resorcinols are substituted with halogens. A possible explanation of this might be, as in the case of **168**, linked to the acidity of the hydroxyl groups. Electron withdrawing groups increase the acidity of the hydroxyl groups, thus increasing their reactivity. The activity, however, may be limited by the increased steric hindrance of the halogens or the fact that additional reactive positions are occupied, explaining the relatively poorer performance of **181**, **186** and **187**. Additionally, the nature of the halogen is not relevant, substitution of chlorine atoms with bromine produced no effect (**181**, **186** and **187**).

Compound **180** is interesting as it suggests that, at least within the timeframe considered, a large bis-resorcinol unit may be replaced with a smaller, different substituent whilst retaining its total scavenging activity.

6.2.1.3 Solvent effects and Reactions with DPPH

To explain the slow reactivity of the sample compounds, the chemistry of the reaction of DPPH with phenols will be described. A first element to consider is the structure of DPPH. The access to the N-centred radical is limited by the considerable steric hindrance of the substituents it bears. This is also a contributing factor to the stability of the radical itself, together with delocalisation. The molecules in this study are complex and present hardly accessible sites, thus reducing the interaction possibilities.

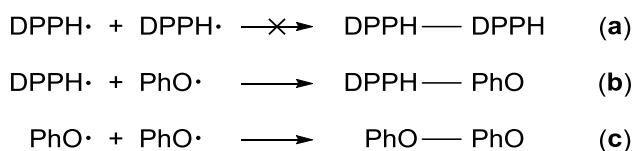


Scheme 83. HAT and ET reactions shown on eugenol.

Analysis of samples in different solvents revealed that reaction rates of phenolic compounds changed in different solvents, in particular it increases in hydrogen bonding

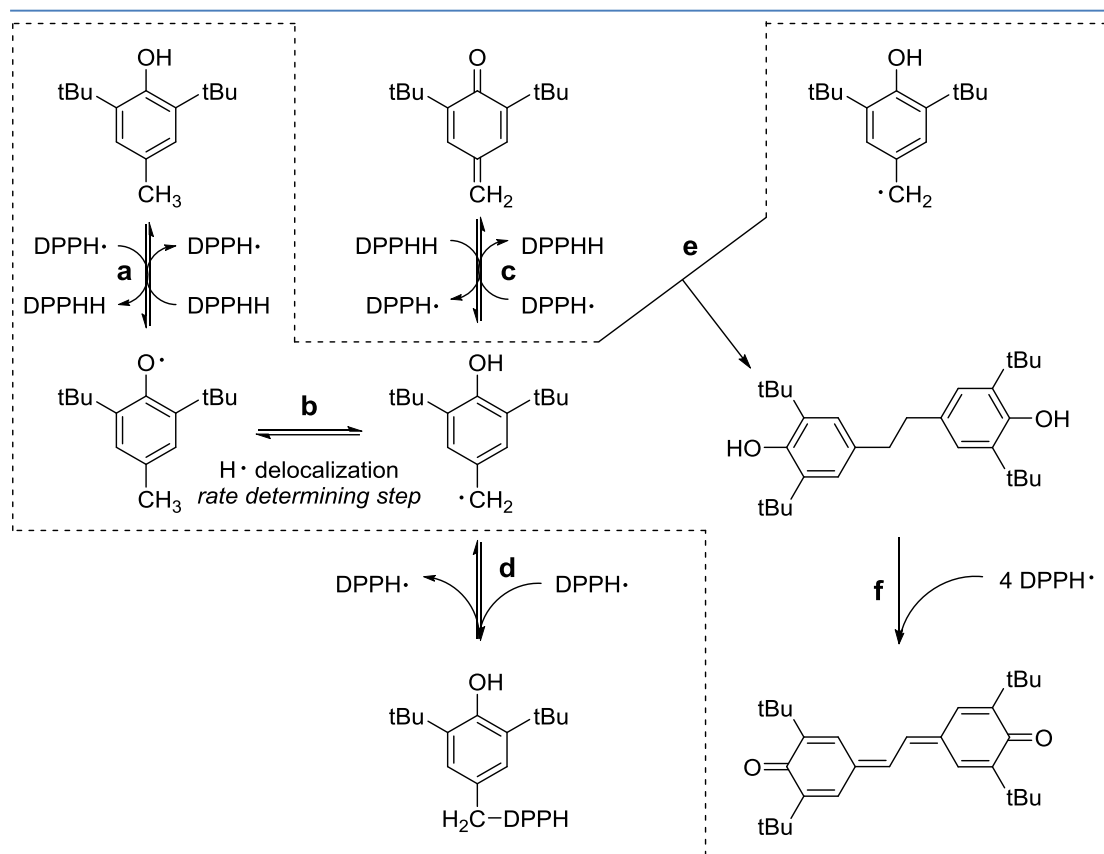
solvents.¹⁷¹ In methanol and ethanol, reaction of DPPH with phenols appears to be predominantly of electron transfer (ET) nature, with the rate-determining step being the transfer of an electron from the phenoxide anion to DPPH, rather than a hydrogen atom transfer (HAT) (**Scheme 83**). This is relevant as pH and its changes during the reaction might lead to different results and also highlights the potential effect of acidic or basic impurities.¹⁷¹⁻¹⁷³ On the other hand, if necessary, the reaction might be investigated at different pH (or in a non-hydrogen-bonding solvent) to evaluate the contribution of the different mechanisms, in particular of HAT, which is considered the terminating process for biologically relevant peroxy radicals.^{166,172}

Simple chain-terminating reactions, proposed by the original author of the assay, should end the reaction by dimerization. Since termination by dimerization of DPPH (**Scheme 84, a**) is forbidden by steric hindrance, the remaining options are reaction of aroxyl radical with itself (**Scheme 84, b**) or with DPPH (**Scheme 84, c**).¹⁶²



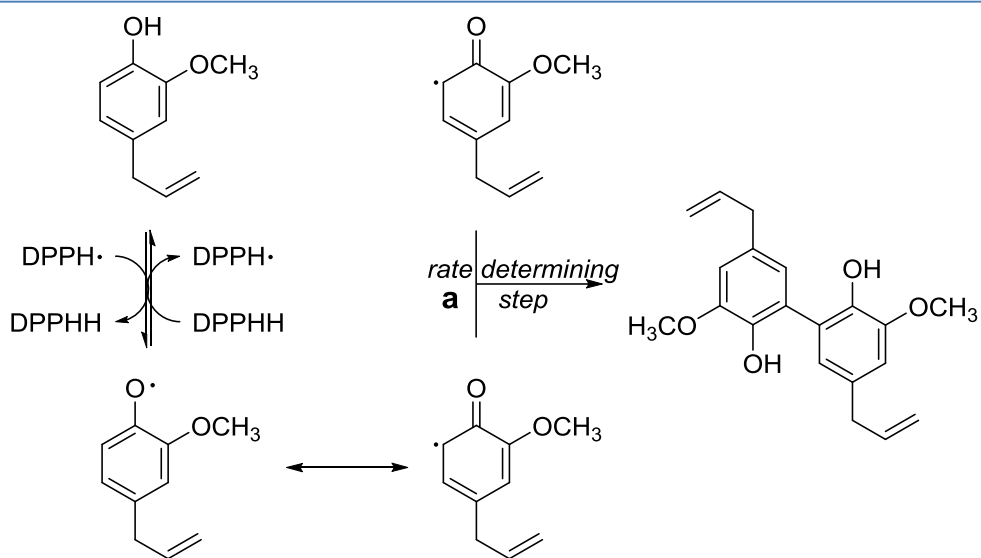
Scheme 84. Termination reactions for DPPH.

However, in the case of non-minimal structures or weak reducing agents, some of these transformations can be slow and/or reversible, becoming limiting in the kinetics of the process, and other reactions can be involved. An example is a relatively simple phenol, butylated-hydroxytoluene (BHT), its reaction being complete after 5 hours in methanol.¹⁷⁴



Scheme 85. Reactions of BHT with DPPH.

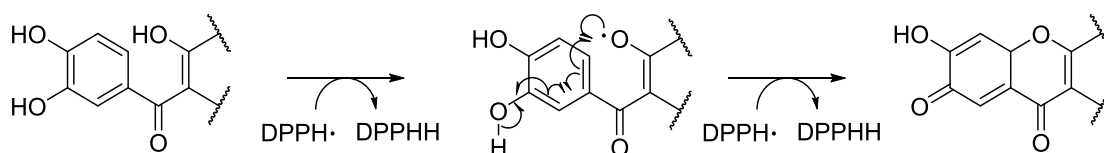
The reaction, represented in **Scheme 85**, involves a number of routes, mostly reversible. Initial and reversible reaction of BHT with DPPH leads to an aroxyl radical (**a**), which can delocalise a hydrogen atom in a slow reaction, which is rate-determining (**b**). Reaction with a second equivalent of DPPH leads to either a quinoid compound (**c**) or a DPPH bound structure (**d**). Alternatively, a dimerization step can occur (**e**), eventually leading to an oxidised bi-quinoid structure (**f**). The path is consistent with an experimental stoichiometric ratio DPPH/BHT of 2.8 (calculated is 3).¹⁷⁴



Scheme 86. Reactions of eugenol with DPPH.

A mechanism has also been proposed for eugenol (**Scheme 86**). In this case, excluding equilibrium reactions similar to those of BHT, in which DPPH binds the reagent, a radical aromatic coupling is proposed (**a**).¹⁷⁴ This is an additional interesting possibility to account for in regards to the compounds to be discussed.

An interesting cyclisation of garcinol by reaction with DPPH was reported by Sang (**Scheme 87**).¹⁷⁵ This is a further point of inspiration, as potential cyclisation steps may be involved. In particular, considering that DDQ mediated oxidative cyclisation is known to convert bis-resorcinols to their fluorone derivatives, as reported by Bacci.⁷⁶

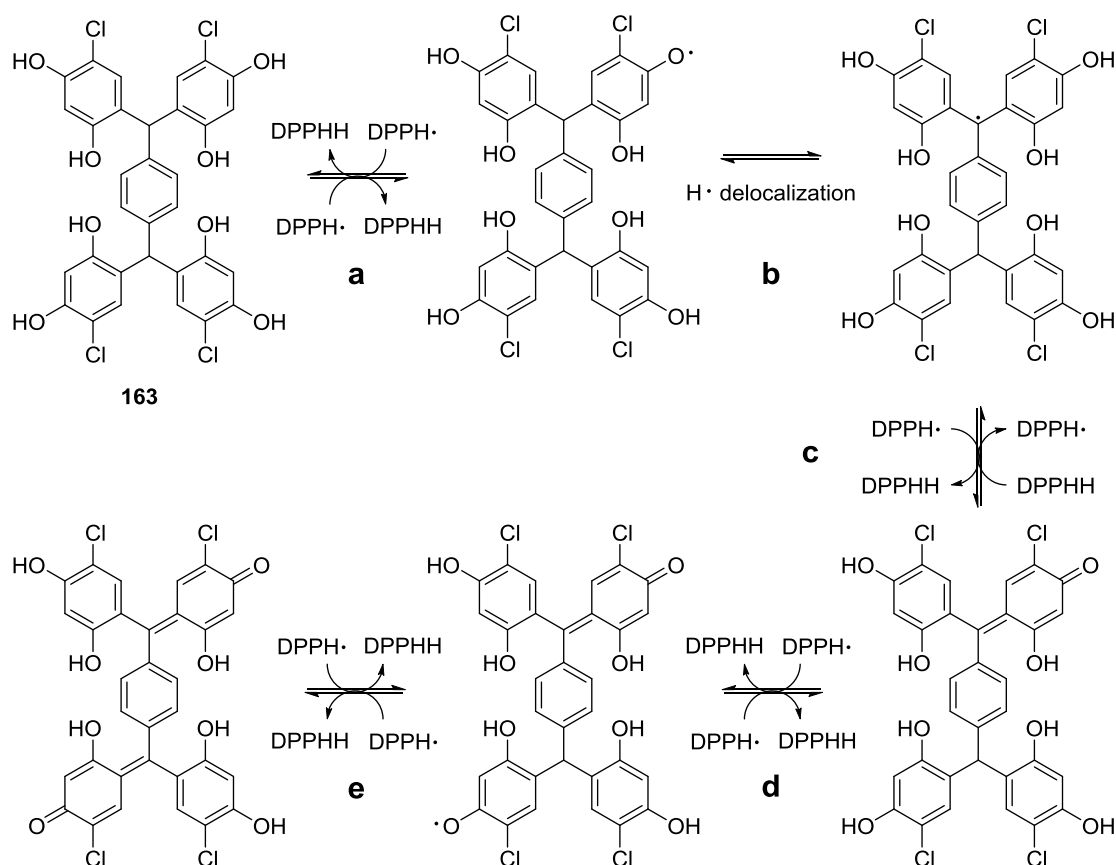


Scheme 87. DPPH mediated cyclization of garcinol. Only the relevant fragment is reported.¹⁷⁵

Other authors have proposed additional reactions, including oxidation of catechol and gallate derivatives to their quinones,¹⁷⁶ and substitution of nitro groups of DPPH by syringaldehyde/methyl syringate.¹⁷⁷

Based on the described studies, an oxidation mechanism for an example compound is proposed in **Scheme 88**. Similarly to BHT, abstraction of an electron from a hydroxyl group (**a**) and subsequent delocalization of a hydrogen (**b**) could lead to a triarylmethyl radical, the most classic type of organic radical (triphenylmethyl radical

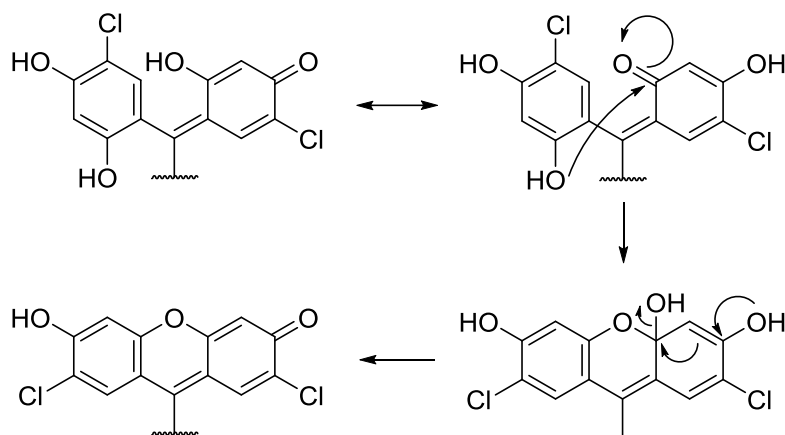
was the first organic radical discovered).¹⁷⁸ Upon abstraction of a second electron (**c**), a quinoid structure can be obtained. Repetition of the first two steps (**d,e**) could produce an equivalent quinoid structure on the other half of the tetramer. Up to this point, 4 equivalents of DPPH are theoretically consumed. After 500 minutes, from the data previously presented, it is possible to calculate that almost 3 equivalents of DPPH have been consumed by **163**. To push the reaction to completion and better evaluate the stoichiometry, it could be necessary to reduce the amount of sample in the reaction, prolong the reaction time and change the solvent to methanol. Use of basic conditions could also speed up the reaction, although different reactions might be observed. Identification or isolation of intermediates would also be ideal to prove the proposed mechanism.



Scheme 88. Proposed reactions for tetramer **163**.

However, the reaction probably produces an additional range of products. Undoubtedly, intermolecular cyclisation to xanthone by nucleophilic attack of a hydroxyl group (**Scheme 89**) to an adjacent carbonyl is possible, although the rate is probably limited by the absence of an acid catalyst, which would increase the rate of

proton delocalization and water elimination. Additional reactions may involve dimerizations and less favoured intermediates.



Scheme 89. Cyclization to fluorone.

Compound **168**, at 500 minutes, has consumed about 4 equivalents of DPPH, suggesting that this stoichiometry can indeed be matched. Due its higher reactivity, this compound may be a better model than **163**.

Differently from **163**, the amount of DPPH consumed by **183** after 500 minutes is about 5 equivalents. The higher reactivity is probably due to the lower steric hindrance in the absence of the chlorine substituent and the additional, highly activated positions available in its stead (**Figure 104**). This position suggests possible intermolecular reactions similar to those illustrated for eugenol, pushing the stoichiometry of the reaction beyond that accessible by its halogenated analogues.

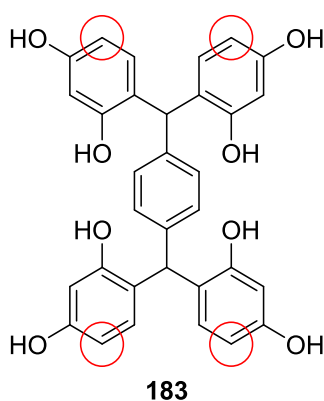


Figure 104. Compound **183**.

6.2.2 TEAC assay

TEAC assay, based on the reaction with ABTS^{•+}, was chosen as the second option for the screening of the library. It is a convenient assay but the mechanistic aspects of its reactivity are not as well-known as in the case of DPPH and different behaviours towards the same antioxidants have been identified. Thus, it makes an interesting element of comparison. However, as with DPPH, it must not be considered predictive of *in vivo* activities, and only as a method to compare reactivity.

In the case of ABTS^{•+}, instead of preparing a solution of known concentration as in the DPPH assay, the standard approach consists of preparing a stock solution, which is then diluted to obtain an absorbance of 0.7 ± 0.02 (734 nm) for the working solution (water as solvent).¹⁶⁷ The assay for the screening involves incubation of 1 mL of ABTS^{•+} with 10 μ L of sample/reference in ethanol (or ethanol only for the blank) at 30 °C and reading of absorbance (734 nm) after a predetermined amount of time.

6.2.2.1 Initial evaluation

Initially, since DPPH displayed a significant and non-linear decomposition within the considered timeframe, the behaviour of ABTS^{•+} was evaluated. ABTS^{•+} solutions were prepared at two different concentrations, one being half of the other and incubated with a blank of ethanol for 10 hours (**Figure 105**).

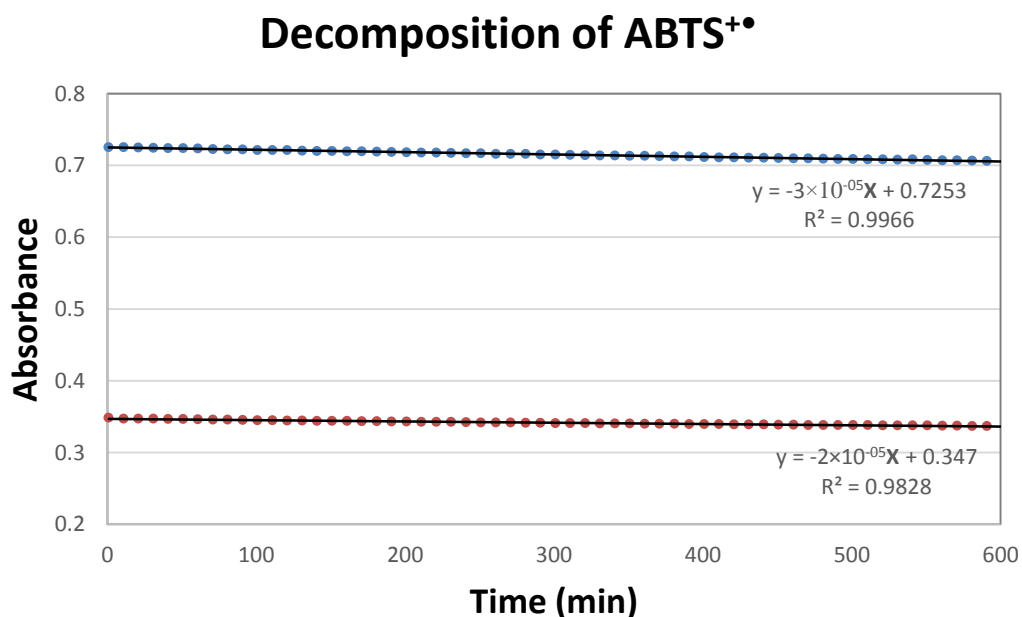


Figure 105. Decomposition of ABTS, starting from two different concentrations.

Decomposition of the probe is reasonably linear, with a total variation of 2.6-3.4% over 10 hours. The rate of decomposition is also very similar at different concentrations, suggesting that subtraction of ABTS^{•+} contribution to a sample's activity may be a reasonable approximation.

6.2.2.2 Screening

The course of the reaction for a set of compounds was followed over ten hours to verify whether the reaction reaches completion. As with DPPH, the progress of the reaction is slow and plateau is not reached. Since the process is time consuming and not in line with a simple screening, a different approach was considered. Each sample in the library was tested, using the same method, at the same concentration (1 μ M), at 10 minutes and 10 hours providing a general trend for comparison. Since the decomposition of ABTS^{•+} is substantially linear, its contribution to the sample activity is considered equal for all samples and thus ignored. The results of the screening is reported in **Table 7** and then discussed in detail.

Name	10 min	10 h	Name	10 min	10 h	Name	10 min	10 h
107	14	30	158	21	57	198	21	26
109	19	31	160	21	40	207	21	46
111	15	22	163	22	62	208	24	47
116	14	18	164	23	46	209	22	47
135	20	25	165	20	46	210	17	45
136	10	41	166	6	12	211	19	50
138	13	13	167	16	23	212	20	52
140	12	33	168	26	41	217	36	76
141	15	29	180	10	24	218	35	63
142	16	30	181	24	47	220	14	33
143	13	31	182	23	51	222	5	25
144	16	34	183	40	82	225	1	7
145	12	28	184	37	50	241	9	25
146	18	26	185	34	60	242	7	8
147	17	22	186	22	37	243	0	4
148	15	23	187	19	31	246	0	1
149	20	22	188	20	41	248	26	31
150	15	29	192	17	50	NaAsc	3	3
151	16	28	193	15	45	Trolox	5	4
154	10	22	194	35	57			

Table 7. Summary of the scavenging activity of the tested compounds (1 μ M), expressed as % of ABTS consumed, after 10 minutes and after 10 hours. Colour scale ranges from low activity (red) to high activity (blue). NaAsc = Sodium Ascorbate.

6.2.2.3 Family comparison

A first comparison can be made for the different families, to evaluate whether the increase in complexity leads to an increased scavenging activity. From every family a compound with the same halogenation pattern was chosen for the comparison (**Figure 106**).

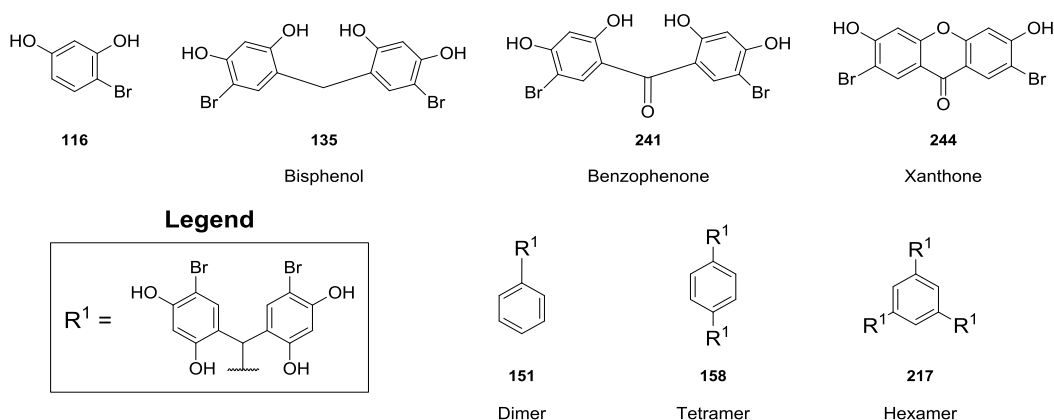


Figure 106. Different families of compounds, each with a representative structure.

Overall, as illustrated in **Figure 107**, activity increases progressively from the monomer (**116**), through the bis-phenol (**135**), tetramer (**158**), and hexamer (**217**). It is interesting to note, however, that at 10 minutes the difference between bis-phenol and tetramer is minimal, suggesting that although the tetramer can eventually consume a larger amount of radical, it does it at an apparently slower rate. A phenyl sidechain on the bis-phenol, as in dimer **151**, produces a lower initial rate, while increasing the total amount scavenged at 10 hours. The benzophenone **241** has a considerably slower rate at the beginning, losing about 10% activity against its parent bis-phenol. Compound **244** could not be compared as it is the only sample not soluble in ethanol. Arguably, as a consequence of the number of hydroxyl groups, the hexamer is the top-performing scaffold, with about 20% more activity over the tetramer. It appears that by increasing the number of bis-phenol units, the ABTS radical scavenging activity is indeed improved.

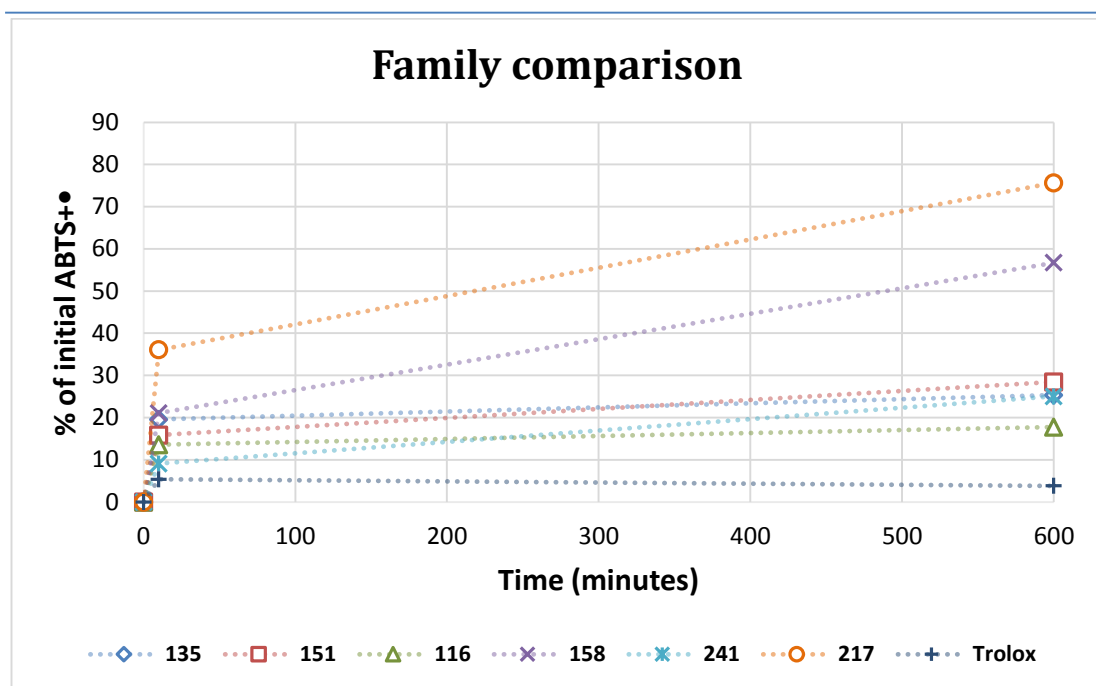


Figure 107. ABTS scavenging activity of compound families' representative structures.

6.2.2.4 Xanthenes comparison

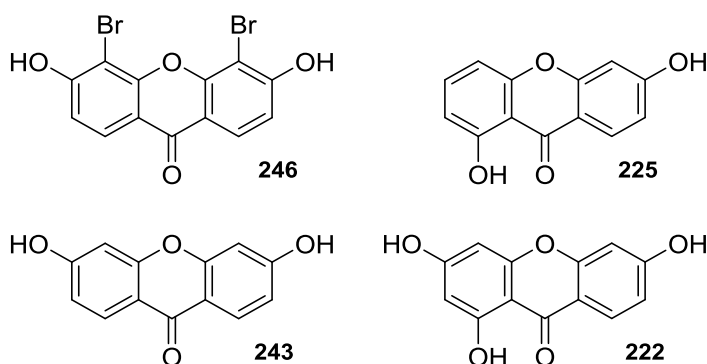


Figure 108. Xanthenes.

Xanthone **244**, due to its unexpectedly poor solubility, could not be tested with the previous compounds. On the other hand, its structural isomer **246** is soluble in ethanol. Compounds **246** and **243** have negligible activity, with only 1% and 4% inhibition, respectively, at ten hours. By inference, **244** is also probably inactive, making the xanthone group the least interesting for the activity against ABTS^{•+}. Only **222**, bearing three hydroxyl groups instead of two, has an average activity of 25% after 10 hours (**Figure 109**).

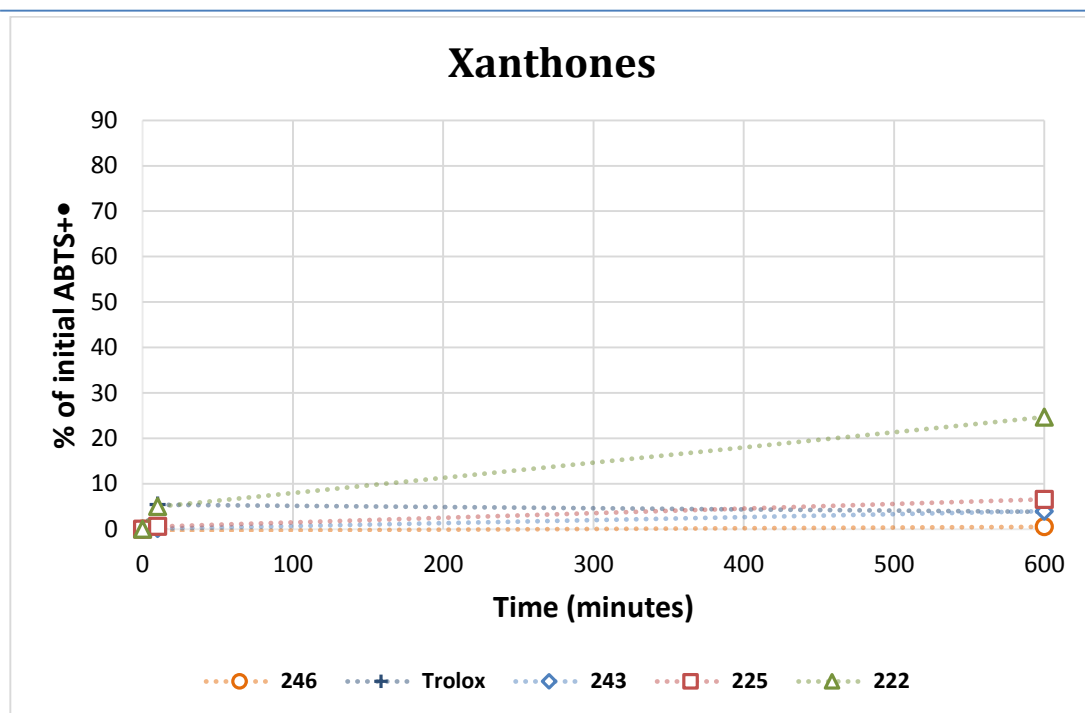


Figure 109. ABTS scavenging activity of xanthones.

6.2.2.5 Benzophenones comparison

The open analogues of xanthones, benzophenone (**Figure 110**), provide a slightly better profile. The best compound of the group, **220**, consumes 14 % DPPH and reaches 33 % inhibition after 10 hours (**Figure 111**).

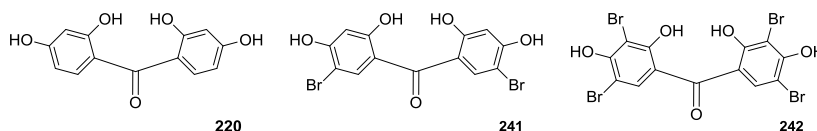


Figure 110. Benzophenones.

Interestingly, the activity decreases with an increasing number of halogens. The behaviour is diametrically opposed to that observed with DPPH, which is scavenged better by highly halogenated derivatives. In the present case, however, the increased steric hindrance caused by introduction of halogens might be hindering the progress of the reaction. An additional/alternative possibility is related to the acidity. Presence of more electron-withdrawing groups increases the acidity of the compound. If the reactions with ABTS were mainly driven by HAT processes, the reactivity would be lower due to the increased dissociation.

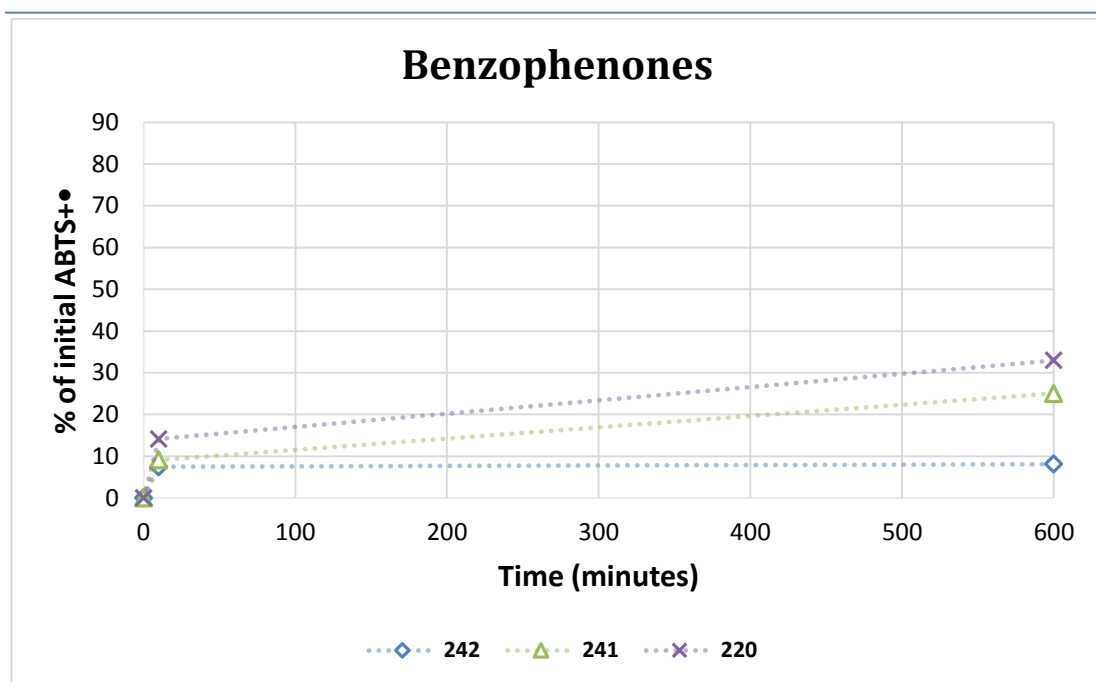


Figure 111. ABTS scavenging activity of benzophenones.

6.2.2.6 Bis-phenols comparison

Reduction of the benzophenones to bis-phenols in **Figure 112**, produces a better ABTS^{•+} scavenging activity with a minimum of 10% for **136** at ten minutes, which appears to be reacting slower than its analogues but reaches a higher total amount of scavenged radical after 10 hours. The compound without bromine substituents, **248**, appears to be the best performing at 10 minutes, with 26% inhibition (**Figure 113**).

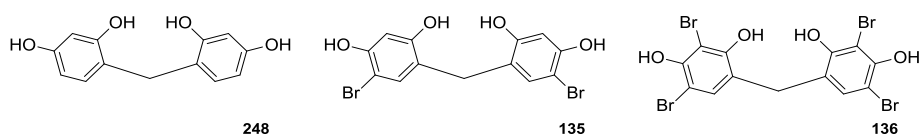


Figure 112. Bis-phenols.

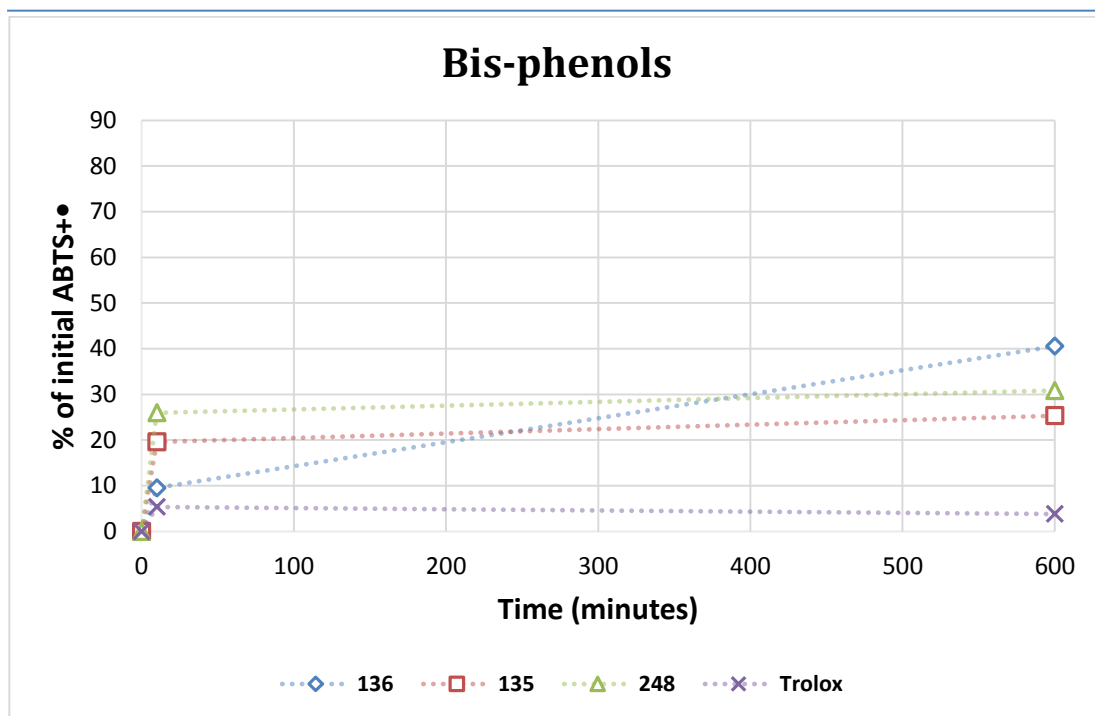


Figure 113. ABTS scavenging activity of bis-phenols.

6.2.2.7 Dimers comparison

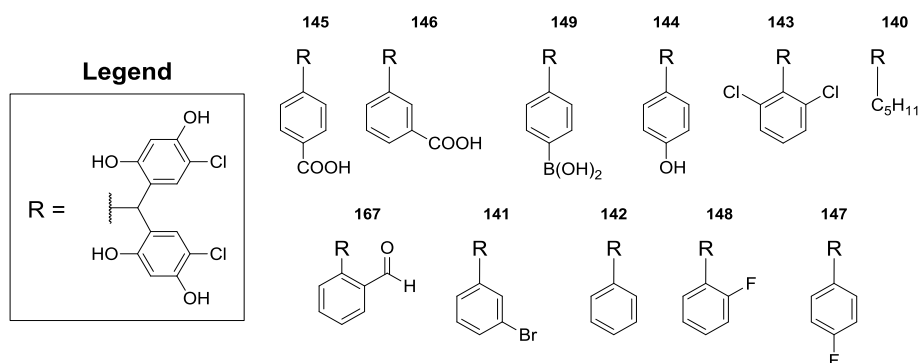


Figure 114. Dimers with different sidechains.

A substitution on the bridge of bis-phenols with a sidechain, as in the case of dimers (**Figure 114**), does not provide any real advantage over bis-phenols, at least for the activity at 10 minutes. However, they have a better profile at 10 hours, with inhibitions between 22% (**149**) and 34% (**144**), suggesting that the sidechain might increase the total amount of radical that can be scavenged. Compound **149** (highlighted in **Figure 115**) is interesting as it is the only example of a complete reaction at 10 minutes. It tops all other samples at 10 minutes but has a smaller total scavenging capacity, when its activity at ten hours is compared with that of its analogues. It might be an interesting compound to further evaluate the chemistry of the reaction, thanks to its complete, rapid reaction.

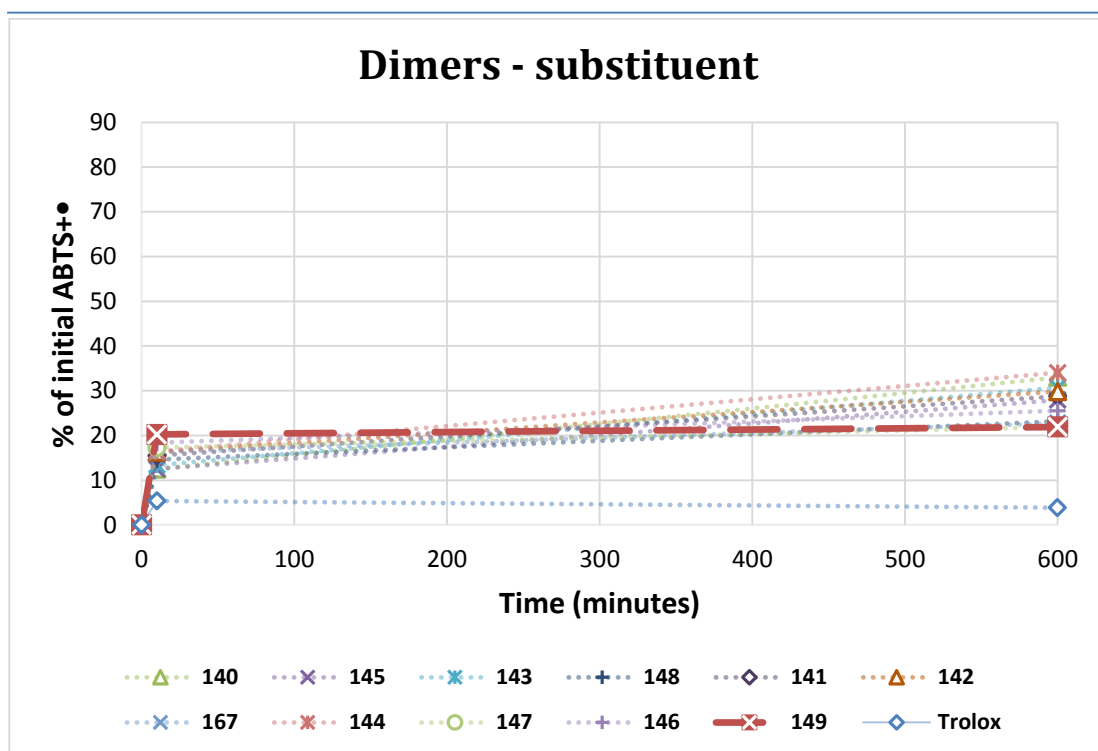


Figure 115. ABTS scavenging activity of dimers with different sidechains.

The position of the substituent on the aromatic ring, at least for the compounds evaluated, does not seem to play a relevant role on the activity, with **145** and **146** producing very similar results despite bearing the carboxylic acid in *para* and *meta*, respectively. The same can be said for **148** and **147**, with a fluorine substituent in *ortho* and *para*, respectively.

Compound **140** is interesting as it does not bear an aromatic sidechain. Although it provides the poorest activity within the group, along with **145**, at 10 minutes (12%), it is also the second best scavenger of the group, with 33% ABTS^{•+} consumption after ten hours. Thus, it appears that the type of aromatic groups used is not particularly important in increasing the total consumption of radical after 10 hours.

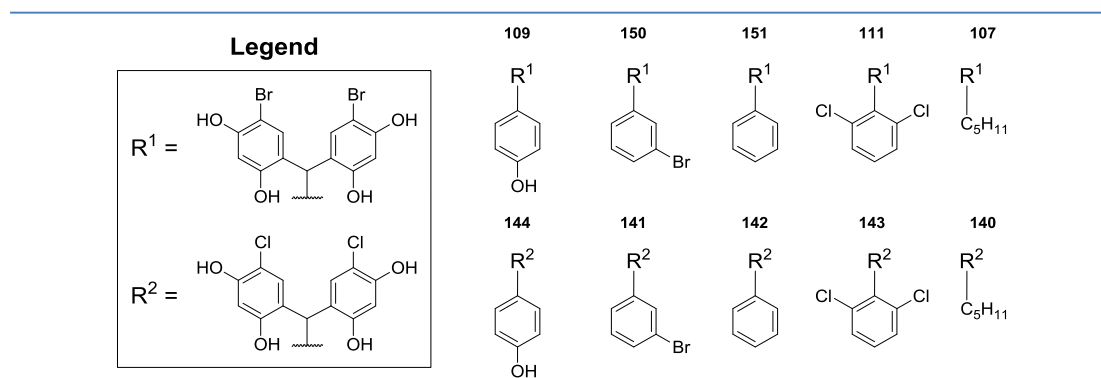


Figure 116. Dimers with different halogens.

Regarding the difference between bromine and chlorine substituents (**Figure 116**), it has to be noted that there is only a few percentage points difference between the compounds with either halogen (**Figure 117**). More relevant is the fact that bromine appears to produce in most cases an initially slightly higher rate (**109** > **144**, **107** > **140**, **111** > **143**) but smaller final activity. The suggestion would have to be confirmed with more data to verify if the difference is statistically significant.

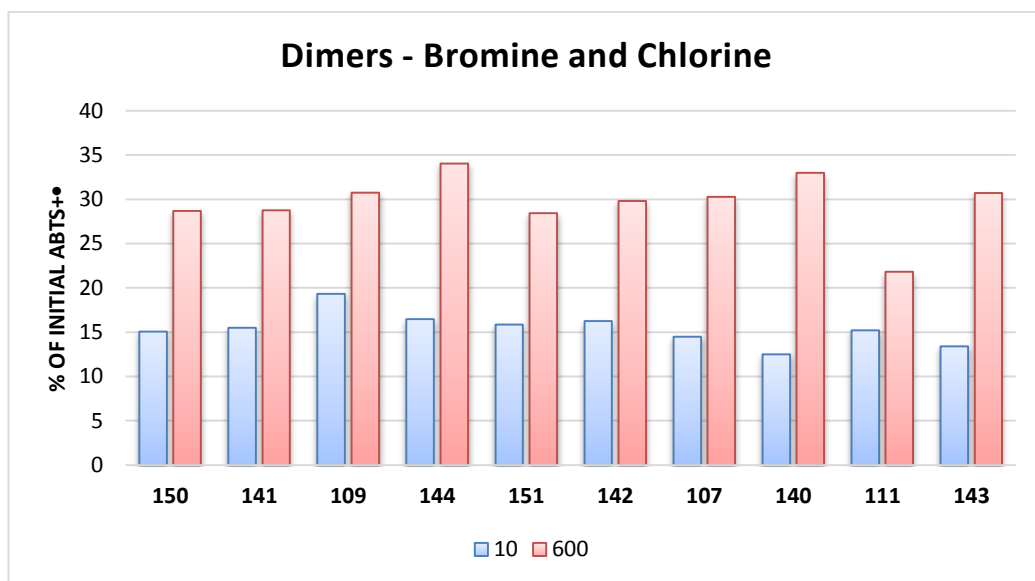


Figure 117. ABTS scavenging activity of dimers with different halogens at 10 minutes and 600 minutes.

6.2.2.8 Tetramers comparison

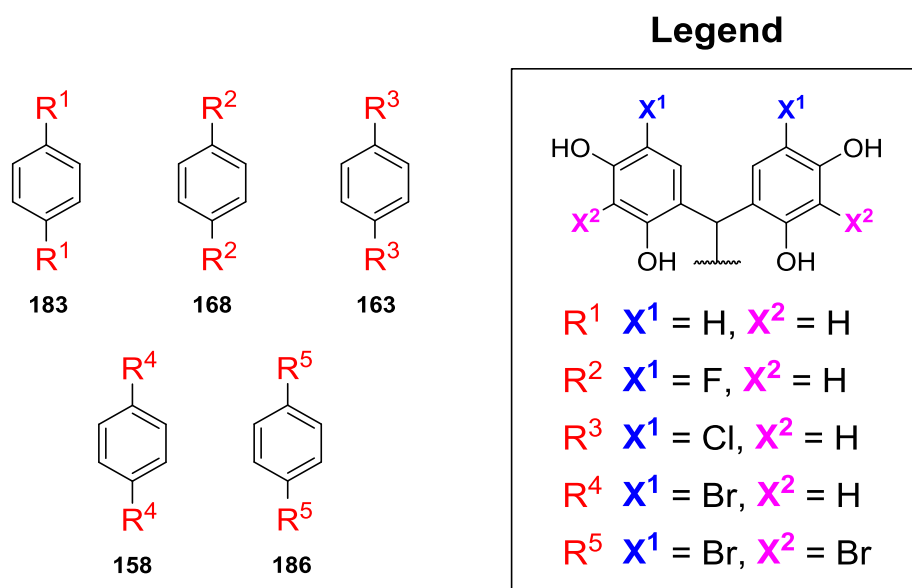


Figure 118. Tetramers with different halogens.

As previously said in the comparison between families, increasing the number of resorcinol units from two to four yields a good improvement in activity. In the case of tetramers (**Figure 118**), at 10 minutes the activity ranges between 20% and 40% of ABTS^{•+} inhibition and after 10 hours is between 30% and 80% (**Figure 119**).

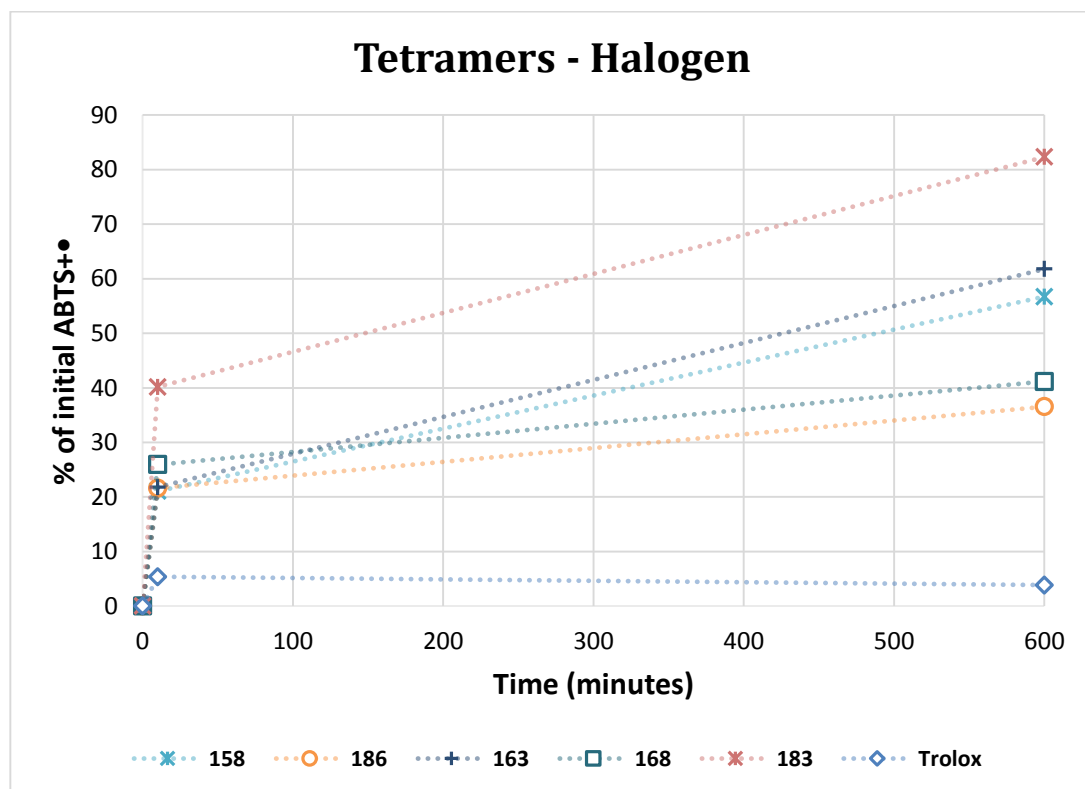


Figure 119. ABTS scavenging activity of tetramers with different halogens.

In this class we found the best performing compound, **183**, with 40% inhibition at 10 minutes and 82% at 10 hours. It is the compound with the highest apparent radical consumption rate at the beginning and presents the best sample-ABTS⁺⁺ stoichiometric ratio. This might not be simply related to the scarce steric hindrance compared to chloro and bromo derivatives. The fluoro substituted **168** does not perform anywhere near it, with 26% and 41% inhibition, respectively at 10 and 600 minutes. It is interesting to note that also **186**, very hindered and with two electron withdrawing groups, performs similarly to **168**.

In the DPPH assay, the fluorinated **168** and the octa-halogenated **186** perform better than their tetra-chloro and -bromo analogues, **163** and **158** respectively. As discussed for benzophenones, the increased acidity conferred by strong electron-withdrawing groups (fluorine, for **168**) or increased number of halogens (for **186**), could reduce the reactivity towards ABTS, suggesting that hydrogen atom transfers are more relevant to this reaction than electron transfer mechanisms.

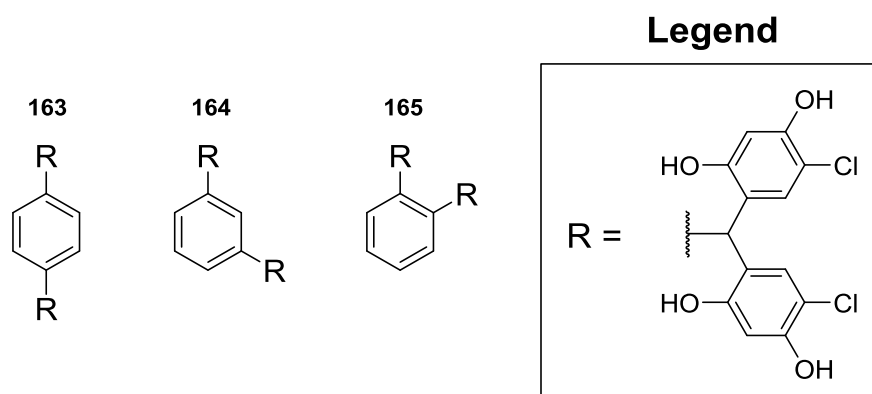


Figure 120. Tetramers with different geometries.

Geometry (**Figure 120**) does not affect the activity as much as halogen substitution. At 10 minutes, compounds **163**, **164** and **165** display a very similar behaviour, with about 22% inhibition. Only at 10 hours, **163**, the *para* isomer, displays a slightly higher activity (62%) than **164** and **165** (46%) (**Figure 121**).

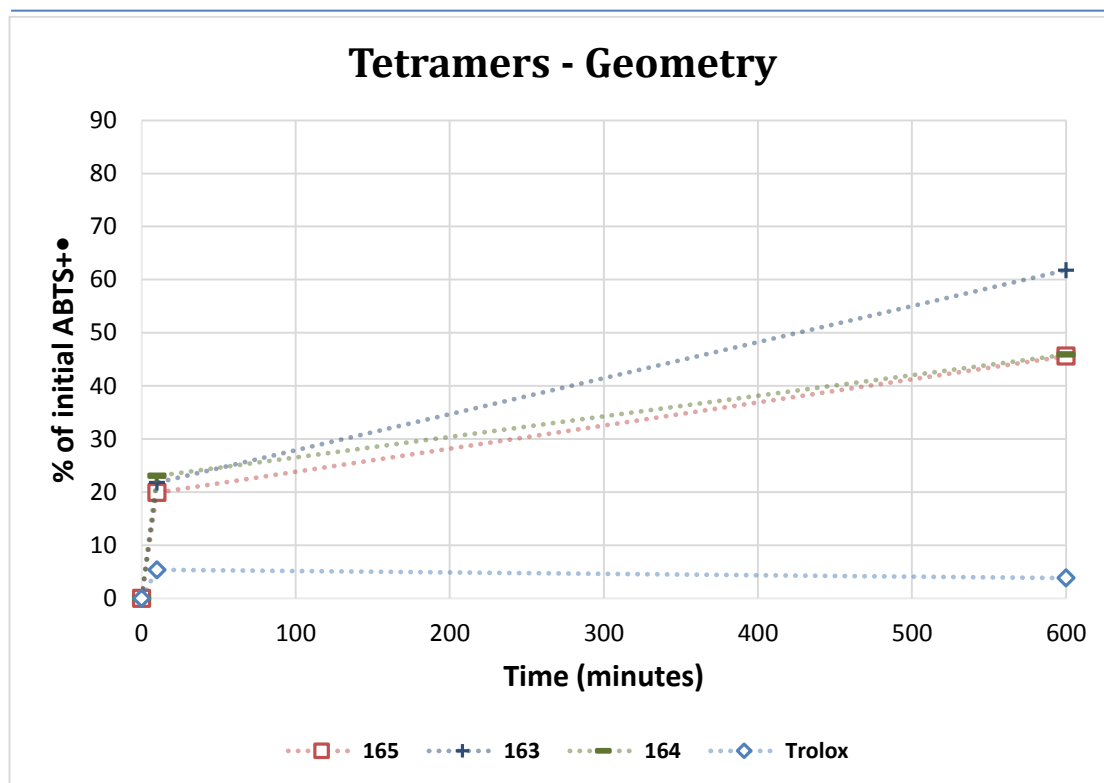


Figure 121. Activity of tetramers with different geometries.

6.2.2.9 Biaryls comparison

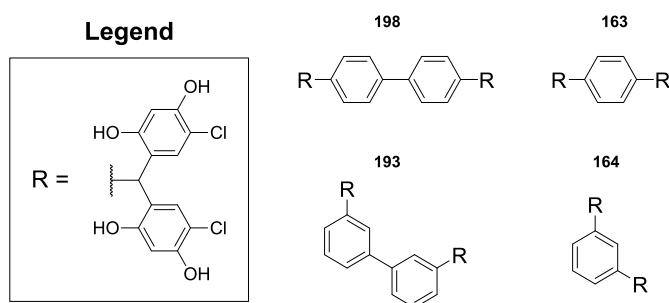


Figure 122. Biaryl tetramers and shorter analogues.

Replacement of the phenyl core of the previous tetramers with a biaryl (**Figure 122**) does not provide any beneficial effect (**Figure 123**). If we compare **163** with **198**, the activity after 10 minutes is similar, but the final consumption of ABTS⁺ for **163** is superior by 36%. In the case of **164** and **193**, the substitution of the phenyl ring with a biaryl produces a lower activity (-8%) at 10 minutes. Surprisingly, considering that a *meta* substituted core is unlikely to oxidise as a *para* substituted one, **193** provided a better activity at 10 hours than **198**.

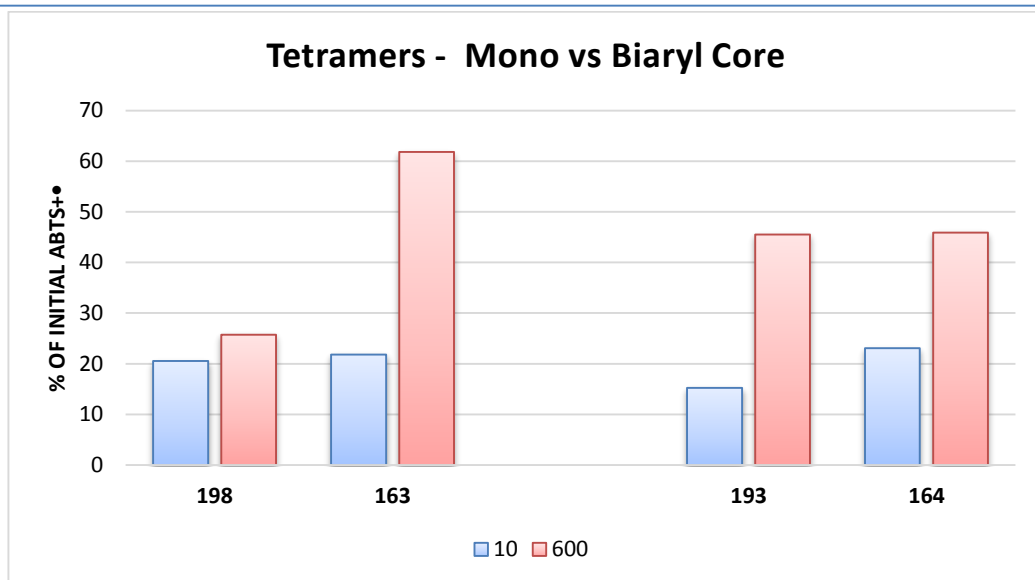


Figure 123. ABTS scavenging activity of biaryl tetramers and shorter analogues

As for the phenyl-core tetramers, 4-chloro- and 4-bromoresorcinol based biaryl tetramers (**193** and **192**, respectively) show similar profiles (**Figure 124**, **Figure 125**). Their dehalogenated analogue (**194**), on the other hand, produces a much better profile especially at 10 minutes. The result is in line with all the other non-halogenated tetramers.

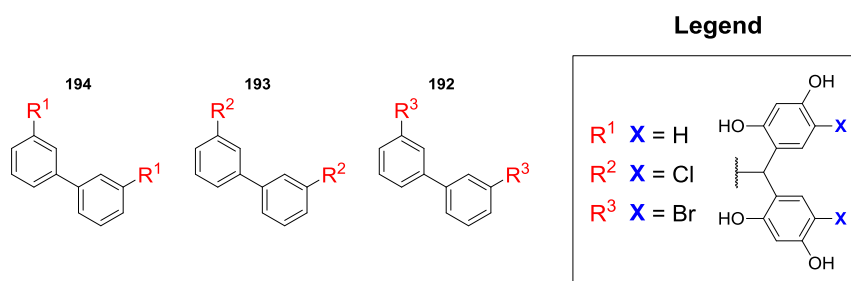


Figure 124. Biaryl tetramers with different halogens.

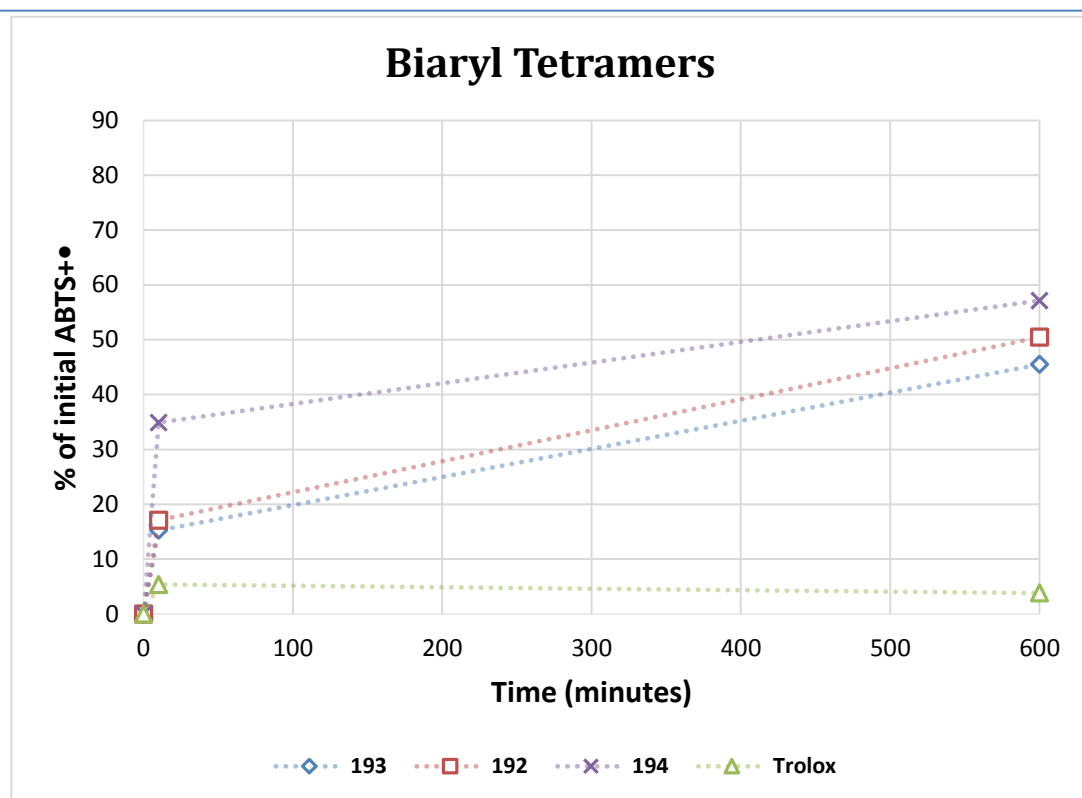


Figure 125. ABTS scavenging activity of biaryl tetramers with different halogens.

6.2.2.10 Alkyl-linked Tetramers Comparison

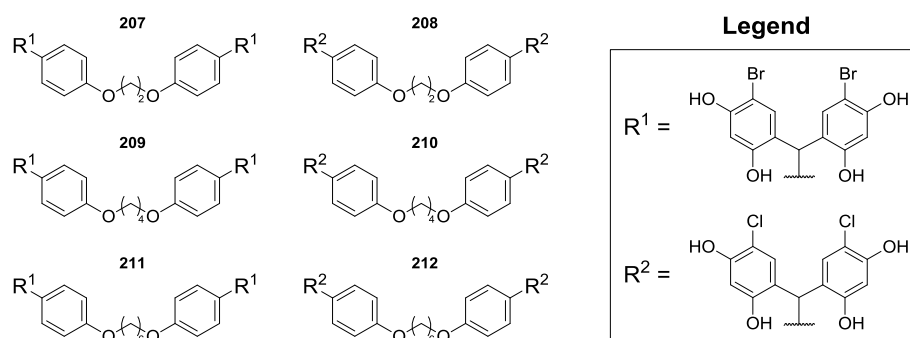


Figure 126. Alkyl linked tetramers.

The last group of tetramers is constructed around alkyl-linked aryls (**Figure 126**). All the compounds in the series produce a very similar profile, with about 20% activity at 10 minutes and 45% at 10 hours (**Figure 127**). As expected, the length of the alkyl linker does not affect significantly the reactivity, since it is unlikely to undergo oxidation. The result also underlines again that the difference produced by substituting bromine with chlorine is minimal.

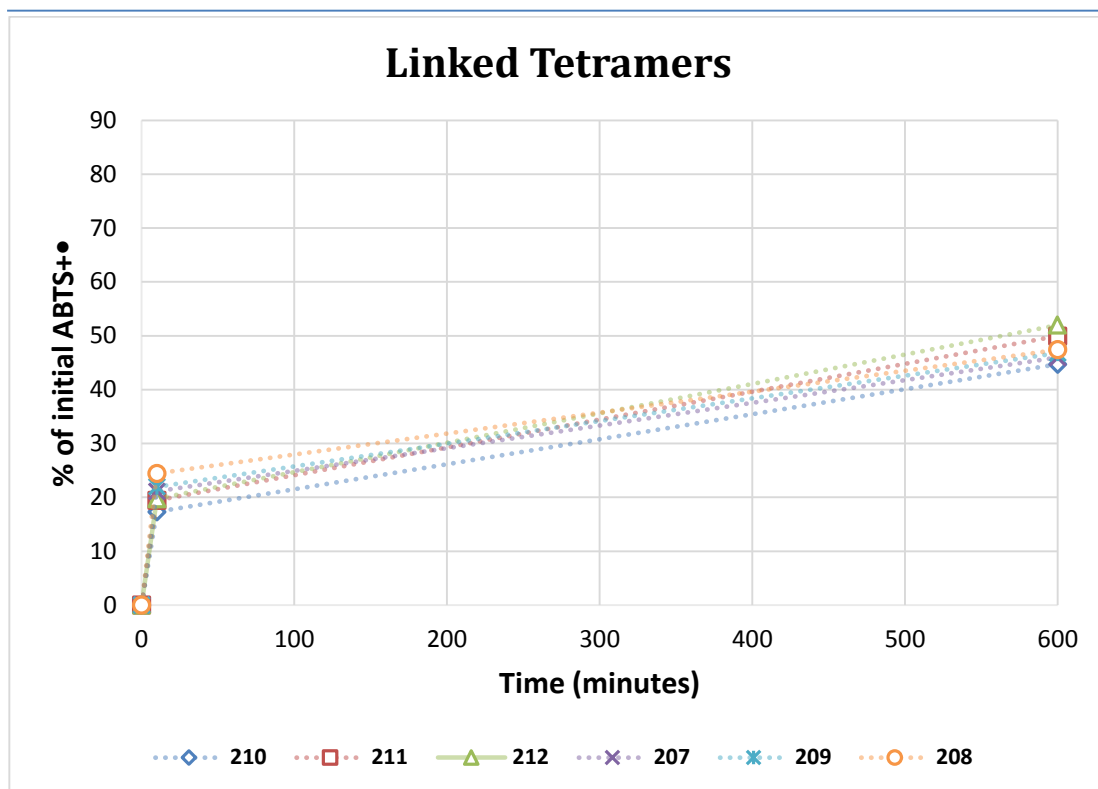


Figure 127. ABTS scavenging activity of alkyl linked tetramers.

6.2.2.11 Hexamers Comparison

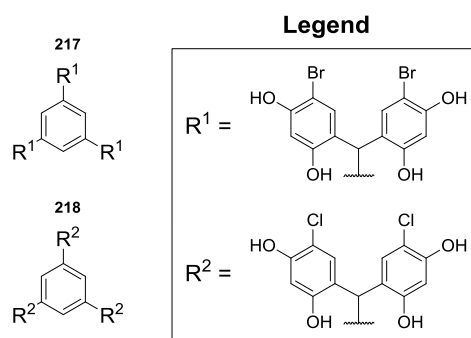


Figure 128. Hexamers.

The last group of compounds evaluated was the hexamers. These compounds bear six resorcinol units and, despite the halogen substituents, provide considerable ABTS^{•+} scavenging activity (**Figure 128**, **Figure 129**). The activity at 10 minutes of both structures ranks among the non-halogenated tetramers, providing some of the best results. At 10 hours, compounds **217** and **218** are the second and third most active compounds, arguably as a consequence of the raw number of resorcinol units.

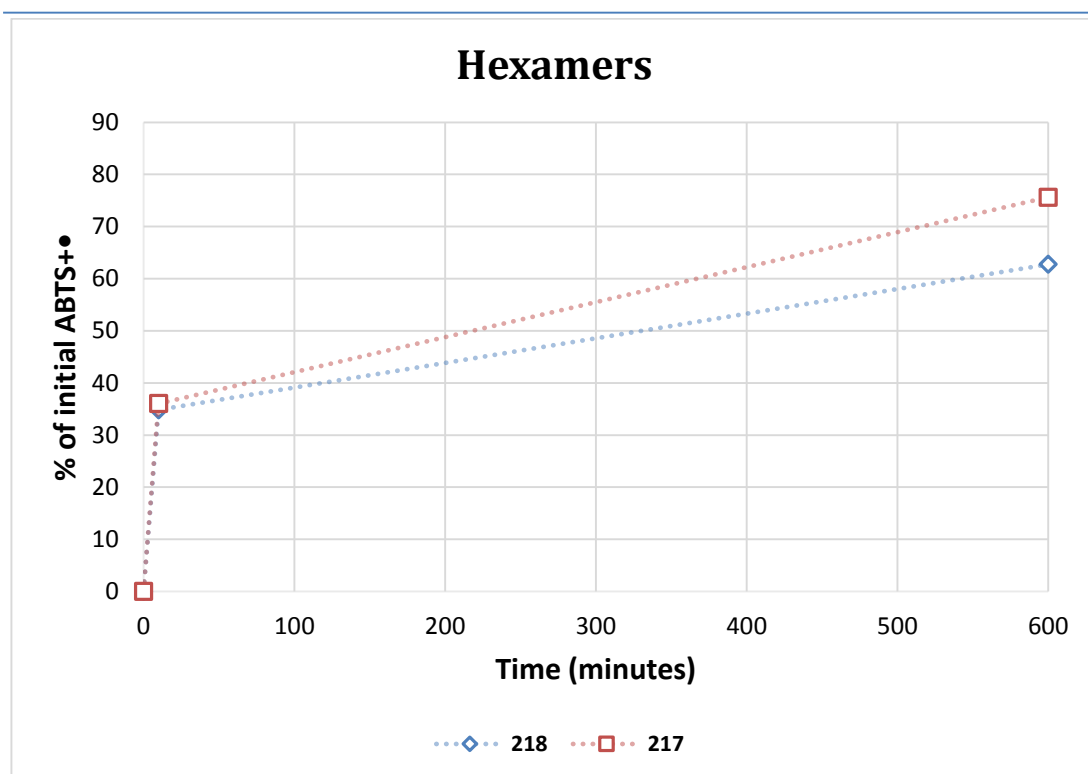


Figure 129. ABTS scavenging activity of hexamers.

6.2.2.12 SAR summary

The discussed reactivity with $\text{ABTS}^{+\bullet}$ can be generalised and summarised as follows. For resorcinol dimers (**Figure 130**), the activity increases from benzophenone to bis-phenol. The activity of the bis-phenol is comparable to that of its analogues with an aromatic sidechain.

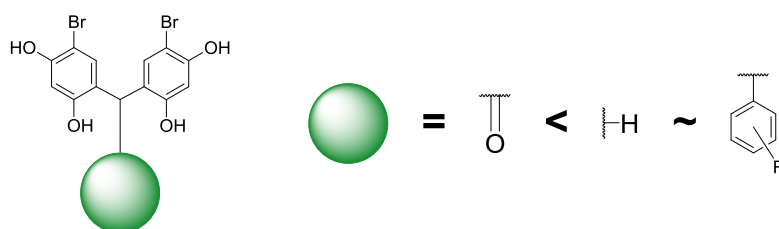


Figure 130. Effect of the bridge substituent in resorcinol dimers.

The number of resorcinol units (**Figure 131**) is critical for the activity, which increases with the number of units built into the structure.

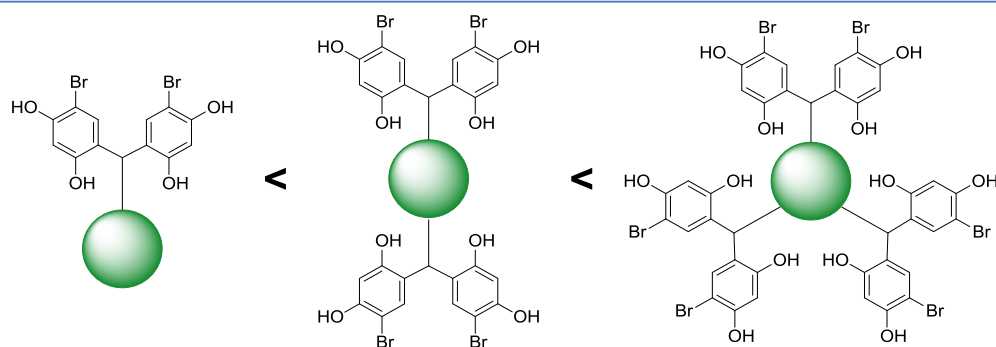


Figure 131. Effect of the number of resorcinol units on the activity.

The halogen substituent (**Figure 132**) is important to the activity, with dihalogenated and fluorinated structures providing the lowest activity. A better profile is provided by chloro and bromo derivatives, having similar activities. Non-halogenated compounds are clearly superior to the previous in their scavenging activity.

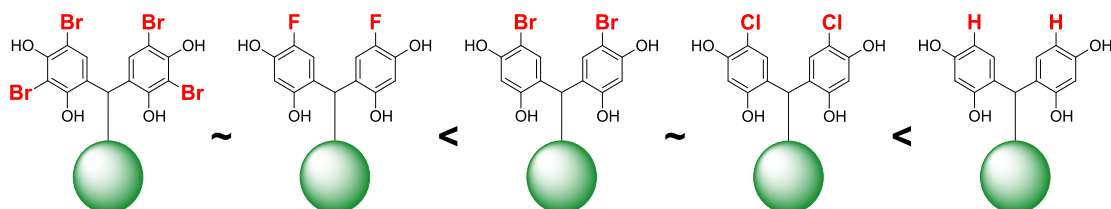


Figure 132. Effect of the halogen on the activity.

Geometry of the tetramers is relevant (although only at 10 hours), with the *para* substituted structures providing the best results, while *meta* and *ortho* have comparable activity (**Figure 133**).

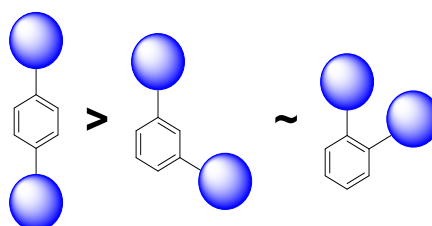


Figure 133. Effect of the geometry of tetramers on the activity.

Replacement of the phenyl ring of tetramers with biaryls or alkyl-linked aryls does not result in enhanced scavenging activity (**Figure 134**).

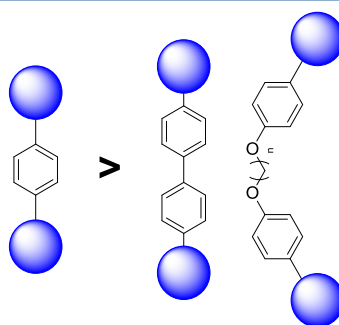


Figure 134. Effect of the central linker on the activity of tetramers.

6.3 Biological evaluation of protective activity

Although the previous assays provide a guideline about the ability of our compounds to scavenge specific radicals, the real protective effect *in vivo* cannot be simply correlated to the data available and requires evaluation in a biological system. For this purpose, the previously described MTS assay (**Chapter 5**) was adapted to measure the potential protective effect of a selected set of compounds. The method employed is based on approaches reported by Liu¹⁷⁹ and Zhao.⁷¹ In Liu's report, ARPE-19 cells were treated with serial dilutions of the test compound, incubated for 24 hours, and then stressed with *tert*-butylhydroperoxide (*t*BuOOH) for 4 hours. After washing the cells, and an additional 20 hours of incubation, the proliferation was measured by MTT assay and compared with the control (untreated cells, 100% proliferation) and the reference (stressed cells without test compound). A similar approach, with HUVEC cells and hydrogen peroxide, was used by Zhao to test the protective effects of natural brominated phenols, as described in the introduction.

In contrast to these methods, in our experiments the cancer cell line MCF7 was used as this had previously been used in proliferation experiments and allowed us to choose compounds with a proven, low antiproliferative effect. MCF7 are also adherent cells, which allows washing the cells after treatment. The second modification to the method is relative to the time of incubation with the sample compound before the stress event. In the published record by Liu,¹⁷⁹ the activity of the compounds is related to the expression of antioxidant enzymes. In our case, the compounds are expected to be, first of all, direct antioxidants, due to their similarities with natural phenol-based antioxidants. For this reason, the incubation with the sample compound was reduced to 4 hours, which appeared a reasonable amount of time to obtain through diffusion of the sample. The same incubation time was also used by Zhao⁷¹ for their assay with

brominated phenols. Finally, the reagent used was MTS, as previously employed with the initial proliferation assessment.

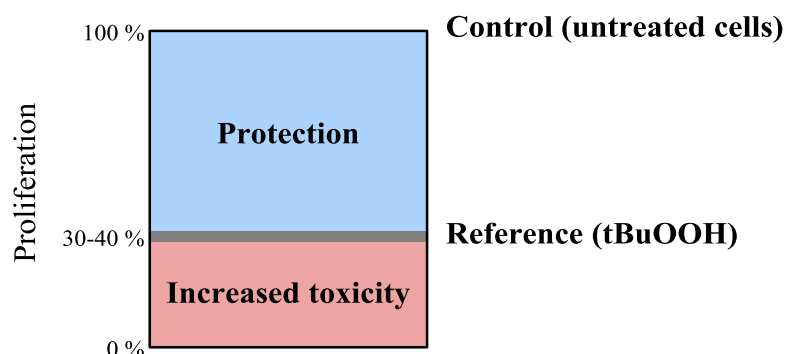


Figure 135. Assay model.

To be able to identify a protective effect or an increased cytotoxicity caused by the combined effects of the pro-oxidant *t*BuOOH and the sample compound, an idoneous concentration of hydroperoxide has to be identified. As illustrated in **Figure 135**, we aimed to identify a concentration which reduced the proliferation to about 40%. With this reference, it is possible to observe both a protective effect and a cytotoxic effect, with a slightly larger chromatic range for the first.

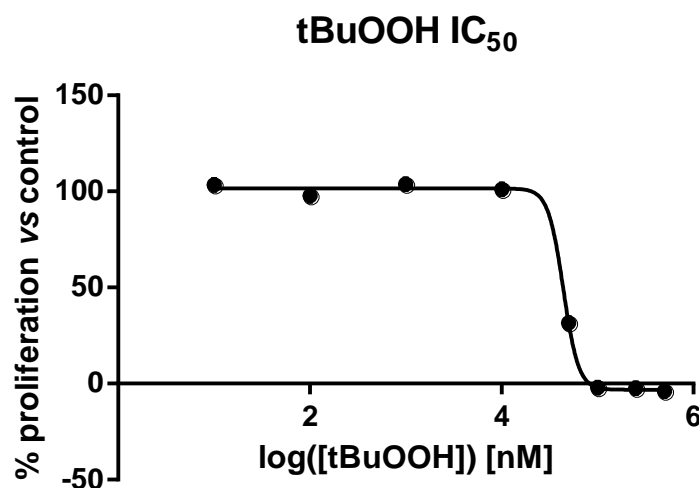


Figure 136. Effect of different *t*BuOOH concentrations on proliferation.

To identify such a concentration, the IC_{50} of *t*BuOOH was initially measured (**Figure 136**). With an IC_{50} of 44 μ M, initial assessment of protective effect was evaluated with a peroxide concentration of 50 μ M. Unexpectedly, the proliferation *versus* the control was higher than before and measured 88%. The result may be a consequence of the combined effect of the relative stability of peroxide solutions and

changes in the cell line over time. For this reason, the execution time was reduced to a minimum, with all compounds tested on a single day, from the same stock of peroxide. The required concentration of peroxide was found at 70 μ M, providing a proliferation of 48%, and a small set of compounds (**Figure 137**) was evaluated. These were chosen among those with poor antiproliferative effect against MCF7 and were tested at three different concentrations, to highlight potential concentration dependent trends. The basic 4-bromoresorcinol (**116**) was also tested as a reference. The results are summarised in **Figure 138** and reported separately for each individual plate, instead of normalised, for clarity of information.

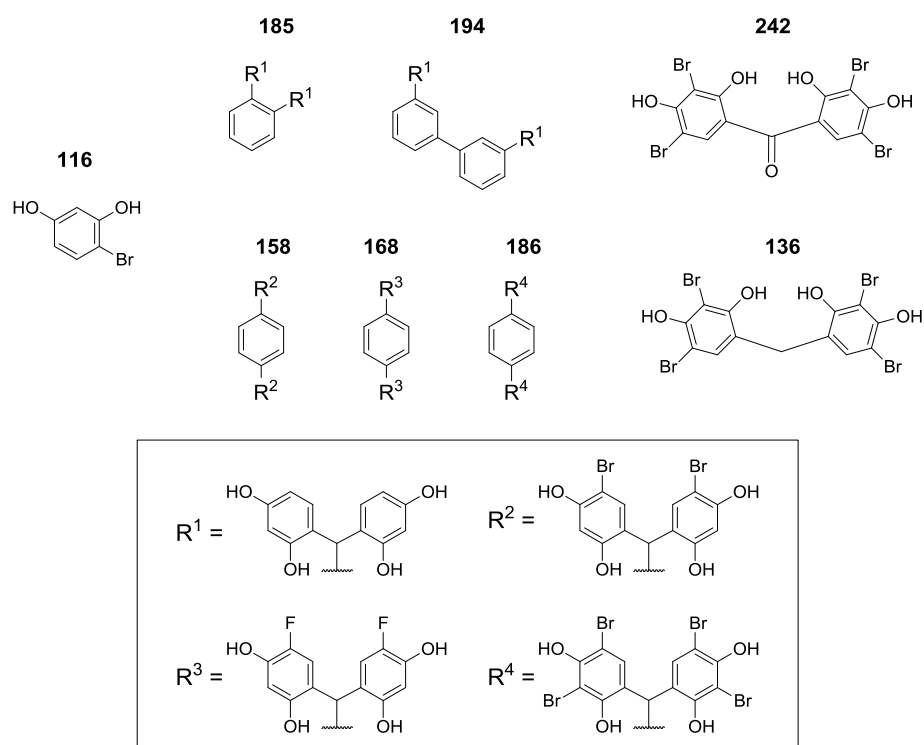


Figure 137. Structures tested for protective effects.

Compound **136**, a simple tetrabrominated bis-resorcinol, showed a protective effect at 10 μ M and 20 μ M, with an improvement in proliferation from 48% to 65% and 88%, respectively.

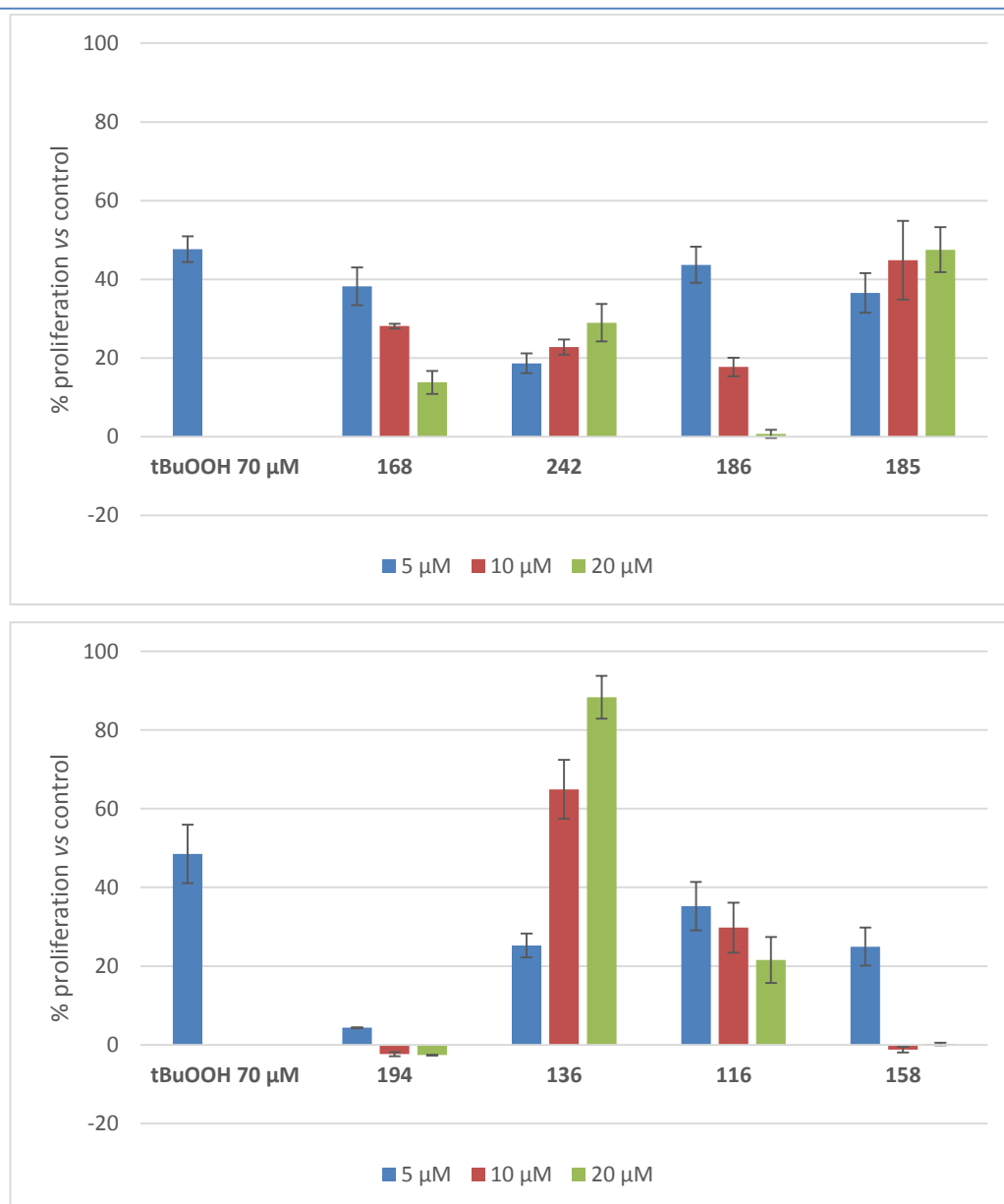


Figure 138. Effect of different compounds (at three different concentrations, each one in triplicate), on MCF-7 cells treated with *t*BuOOH. Error expressed as standard deviation.

Unfortunately, all other compounds presented a lower proliferation compared to the reference peroxide. It is interesting to note how **194** displayed a strong synergistic effect with *t*BuOOH. As reported in **Chapter 5**, the proliferation in MCF7 treated with **194** is 96% at 10 μM concentration. In the presence of *t*BuOOH, all tested concentrations including 5 μM, produced complete cell death.

6.4 Conclusions

The library of compounds available was tested for its radical scavenging activity *versus* two model compounds and for its potential *in vivo* protective effect.

In both DPPH and ABTS radical scavenging assays, the compounds demonstrated a relatively slow reaction rate but higher activity compared to the reference, thus demonstrating potentially interesting as antioxidants.

On the other hand, the small set of compounds tested *in vivo* did not provide the desired results, with only one compound, **136**, providing protection against oxidative stress. It would be interesting to evaluate additional analogues and more concentrations to identify more active compounds and potentially, a structure activity relationship to better understand the required functionalities. The compounds could also be tested after longer incubation times, to allow evaluation of potential changes in expression leading to different results.

Compound **194** may be an interesting compound to investigate further due to its interesting synergic effect with the oxidant, which is unexplained at present and might lead to a specific mechanism of action.

Considering the similarity of some of the compounds in the library with the compounds tested by Zhao,⁷¹ the results are disappointing. Among his compounds, **99b** and **96b** (**Figure 139**), display considerable protective effects, with an EC₅₀ of 0.4 μ M and 0.8 μ M, respectively.

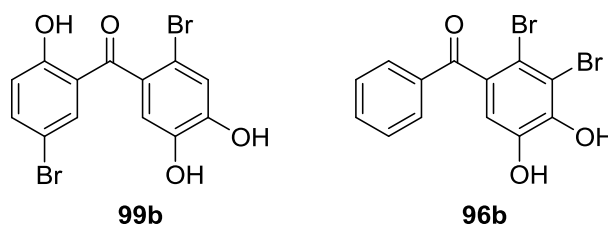


Figure 139. Lead compounds by Zhao.⁷¹

It is probably worth investigating a larger number of compounds and extend the trial to other types of cells, HUVEC (as in Zhao's work) or ARPE-19, which are possibly more suitable for this type of investigation, compared to MCF-7.

Despite the poor results *in vivo* obtained to date, these compound may be also interesting as radical scavengers/antioxidants or photo resistant additives in materials.¹⁸⁰

6.5 Experimental

Chemicals and reference compounds were purchased from Sigma-Aldrich, Fisher Scientific and Alfa Aesar. UV-Vis measures were recorded on a Agilent Technologies Cary 60 UV-Vis with Quantum North West TC1 temperature controller for the DPPH assays, and on a Hitachi U3010 Spectrophotometer for the TEAC assays. Water solutions were prepared with Milli-Q water.

6.5.1 DPPH assay

DPPH scavenging activity was determined as previously described by Balaydin,¹⁸¹ with minor modifications. Briefly, a 200 μ M solution of DPPH was freshly prepared on the day and kept in the dark. Samples were prepared as 10 mM stocks in ethanol and diluted to working solutions at 80 μ M concentration. For the measures, 250 μ L of sample, or ethanol for the reference, were added to 750 μ L of DPPH and vortexed for 20 seconds. In the case of time-courses, the sample was transferred to a cuvette, sealed, and readings were started at 60 seconds. In the case of single time-point measures, the sample was kept in the dark and read at the appropriate time. Absorbance was recorded at 512 nm.

6.5.2 TEAC assay

ABTS scavenging activity was recorded as previously described by Re,¹⁶⁷ with minor modifications. ABTS stock solution was prepared by reaction of an aqueous solution of ABTS diammonium salt (14 μ M) with an aqueous solution of potassium persulfate (4.90 μ M) in 1:1 ratio for 16 hours. The stock solution was diluted to an absorbance of 0.7 with water. Samples were prepared in ethanol. For the measures, 1 mL of ABTS working solution was equilibrated at 30 °C and then 10 μ L of sample, or ethanol for the reference, were added and vortexed for 10 seconds. Samples were then incubated in the dark at 30 °C for the required amount of time. Absorbance was then read at 734 nm.

6.5.3 Cell culture

MCF-7 cell line was obtained from the European Collection of Cell Cultures.

MCF-7 cells were cultured in DMEM High Glucose medium (HyClone Laboratories) supplemented with 10% Fetal Bovine Serum (PAA Laboratories), 2 mM

L-glutamine (HyClone Laboratories), 100 U/mL Penicillin and 100 µg/mL Streptomycin (HyClone Laboratories).

Cells were maintained at 37 °C in a humidified atmosphere with 5% CO₂ and passaged at 1/10 dilution twice a week.¹⁵³

Cell counting was carried out using a 1/2 dilution of cells with 0.4% trypan blue solution (Sigma-Aldrich) and a Malassez haemocytometer.

6.5.4 MTS with *tert*-butyl hydroperoxide

96 well plates (Thermo-Scientific) were prepared with MCF-7 cells (10000 per well, 100 µL) in serum free media. After 24 hours, the cells were treated with serial dilutions of sample compounds or vehicle control and incubated for 4 hours. After treatment with *tert*-butyl hydroperoxide or vehicle control the cells were incubated for an additional 4 hours. The cells were washed twice with serum free media and incubated for 18 hours. The cells were then treated with 10 µL of CellTiter 96[®] AQueous One Solution Cell Proliferation Assay (MTS) (Promega) and incubated for 4 hours. Absorbance was measured using a POLARstar OPTIMA plate reader (BMG Labtech) at 492 nm. Data analysis was performed with Microsoft Excel and GraphPad Prism V6.0 (IC₅₀ values).

7. Conclusions and future work

A simple, efficient method for the synthesis and purification of resorcinol dimers, tetramers and hexamers have been developed and applied to the synthesis of a library of compounds. Further halogenation and dehalogenation methods have been identified to allow access to a wider variety of derivatives. All methods employed have been developed to be scalable and avoid chromatographic purification, allowing easy access to the required derivatives. Novel derivatives, in the form of tetramers and hexamers with different halogens (not only bromine as before) and a more varied number and combination of halogens are now available and more are accessible with the methods presented.

A simplified set of structures, benzophenones, bis-phenols, xanthenes and xanthenes have been prepared, adding new approaches to the previously described literature methods and novel structures. These structures add additional variations on the previously evaluated dimers. The absence of a side chain and the cyclic structure of xanthenes contribute to the extent of the SAR evaluation.

Among these compounds, tetramers and hexamers, a previously unreported class of compounds, and in particular their dehalogenated derivatives, constitute interesting starting points for the development of dendrimers. These are a novel class of “open resorcinarenes”. The functionalization of these structures have been presented with model compounds and tested for the synthesis of an octacalixarene with thirty two amines, a proof of concept for future work on DNA binding compounds and transfection agents.

The compounds displayed interesting activities against DPPH and ABTS displaying notable activity, especially in scavenging the latter radical. Unfortunately, poor results have been obtained *in vivo*, with only one of the examples tested to date showing interesting, concentration dependent protection. On the other hand, a synergistic activity with tBuOOH have been identified for one of the derivatives, and may be worth further investigation. However, the model used may not be ideal and the cytoprotective activity will be further investigated in different cell lines.

The activity of these compounds against mycobacterial isocitrate lyase is currently being investigated through a collaboration with Dr Eva Novotná, from the

Faculty of Pharmacy in Hradec Králové (Charles University) and Prof. Ho Ki-Bong
from Seoul National University.

8. References

- (1) Lewis, K. *Nature Reviews Drug Discovery* **2013**, *12*, 371.
- (2) Cantas, L.; Shah, S. Q. A.; Cavaco, L. M.; Manaia, C. M.; Walsh, F.; Popowska, M.; Garelick, H.; Bürgmann, H.; Sørsum, H. *Frontiers in Microbiology* **2013**, *4*, 96.
- (3) Davies, J.; Davies, D. *Microbiology and Molecular Biology Reviews : MMBR* **2010**, *74*, 417.
- (4) Morar, M.; Wright, G. D. *Annual Review of Genetics* **2010**, *44*, 25.
- (5) Drawz, S. M.; Bonomo, R. A. *Clinical Microbiology Reviews* **2010**, *23*, 160.
- (6) Foye, W. O.; Lemke, T. L.; Williams, D. A. *Foye's Principles of Medicinal Chemistry*; Lippincott Williams & Wilkins, 2008.
- (7) Koh, J.-J.; Lin, S.; Aung, T. T.; Lim, F.; Zou, H.; Bai, Y.; Li, J.; Lin, H.; Pang, L. M.; Koh, W. L.; Salleh, S. M.; Lakshminarayanan, R.; Zhou, L.; Qiu, S.; Pervushin, K.; Verma, C.; Tan, D. T. H.; Cao, D.; Liu, S.; Beuerman, R. W. *Journal of Medicinal Chemistry* **2015**, *58*, 739.
- (8) Zou, H.; Koh, J.-J.; Li, J.; Qiu, S.; Aung, T. T.; Lin, H.; Lakshminarayanan, R.; Dai, X.; Tang, C.; Lim, F. H.; Zhou, L.; Tan, A. L.; Verma, C.; Tan, D. T. H.; Chan, H. S. O.; Saraswathi, P.; Cao, D.; Liu, S.; Beuerman, R. W. *Journal of Medicinal Chemistry* **2013**, *56*, 2359.
- (9) Campbell, E. A.; Korzheva, N.; Mustaev, A.; Murakami, K.; Nair, S.; Goldfarb, A.; Darst, S. A. *Cell* **2001**, *104*, 901.
- (10) Shaw, W. V.; Packman, L. C.; Burleigh, B. D.; Dell, A.; Morris, H. R.; Hartley, B. S. *Nature* **1979**, *282*, 870.
- (11) Davies, J.; Wright, G. D. *Trends in Microbiology* **1997**, *5*, 234.
- (12) Sköld, O. *Drug Resistance Updates* **2000**, *3*, 155.
- (13) Piddock, L. J. V. *Clinical Microbiology Reviews* **2006**, *19*, 382.
- (14) Dwyer, D. J.; Kohanski, M. A.; Collins, J. J. *Current Opinion in Microbiology* **2009**, *12*, 482.
- (15) Norman, A.; Hansen, L. H.; Sørensen, S. J. *Philosophical Transactions of the Royal Society B: Biological Sciences* **2009**, *364*, 2275.
- (16) Zhao, J.; Fan, X.; Wang, S.; Li, S.; Shang, S.; Yang, Y.; Xu, N.; Lü, Y.; Shi, J. *Journal of Natural Products* **2004**, *67*, 1032.
- (17) Li, K.; Li, X.-M.; Gloer, J. B.; Wang, B.-G. *Journal of Agricultural and Food Chemistry* **2011**, *59*, 9916.
- (18) Xu, N.; Fan, X.; Yan, X.; Li, X.; Niu, R.; Tseng, C. K. *Phytochemistry* **2003**, *62*, 1221.
- (19) Zhao, J.; Ma, M.; Wang, S.; Li, S.; Cao, P.; Yang, Y.; Lü, Y.; Shi, J.; Xu, N.; Fan, X.; He, L. *Journal of Natural Products* **2005**, *68*, 691.
- (20) Fan, X.; Xu, N. J.; Shi, J. G. *Journal of Natural Products* **2003**, *66*, 455.
- (21) Kurata, K.; Amiya, T. *Chemistry Letters* **1977**, 1435.
- (22) Kurata, K.; Taniguchii, K.; Takashima, K.; Hayashi, I.; Suzuki, M. *Phytochemistry* **1997**, *45*, 485.
- (23) Oh, K.-B.; Lee, J. H.; Chung, S.-C.; Shin, J.; Shin, H. J.; Kim, H.-K.; Lee, H.-S. *Bioorganic & Medicinal Chemistry Letters* **2008**, *18*, 104.
- (24) Choi, J. S.; Park, H. J.; Jung, H. A.; Chung, H. Y.; Jung, J. H.; Choi, W. C. *Journal of Natural Products* **2000**, *63*, 1705.
- (25) Wang, W.; Okada, Y.; Shi, H.; Wang, Y.; Okuyama, T. *Journal of Natural Products* **2005**, *68*, 620.

-
- (26) Xu, X.; Piggott, A. M.; Yin, L.; Capon, R. J.; Song, F. *Tetrahedron Letters* **2012**, 53, 2103.
- (27) Li, K.; Li, X.-M.; Ji, N.-Y.; Wang, B.-G. *Journal of Natural Products* **2008**, 71, 28.
- (28) Li, K.; Li, X.-M.; Ji, N.-Y.; Wang, B.-G. *Bioorganic & Medicinal Chemistry* **2007**, 15, 6627.
- (29) Li, K.; Li, X.-M.; Ji, N.-Y.; Gloer, J. B.; Wang, B.-G. *Organic Letters* **2008**, 10, 1429.
- (30) Shoeib, N. A.; Bibby, M. C.; Blunden, G.; Linley, P. A.; Swaine, D. J.; Wheelhouse, R. T.; Wright, C. W. *Journal of Natural Products* **2004**, 67, 1445.
- (31) Winter, J. M.; Moore, B. S. *Journal of Biological Chemistry* **2009**, 284, 18577.
- (32) Ron Wever, W. H. *Vanadium haloperoxidases*; John Wiley & Sons, Ltd, Chichester, 2001.
- (33) Pedersén, M.; Collén, J.; Abrahamsson, K.; Ekdahl, A. *Scientia Marina* **1996**, 60, 257.
- (34) Wang, B.-G.; Gloer, J. B.; Ji, N.-Y.; Zhao, J.-C. *Chemical Reviews* **2013**.
- (35) Shi, D.; Li, J.; Jiang, B.; Guo, S.; Su, H.; Wang, T. *Bioorganic & Medicinal Chemistry Letters* **2012**, 22, 2827.
- (36) Lee, H.-S.; Lee, T.-H.; Lee, J. H.; Chae, C.-S.; Chung, S.-C.; Shin, D.-S.; Shin, J.; Oh, K.-B. *Journal of Agricultural and Food Chemistry* **2007**, 55, 6923.
- (37) Kondrashov, F.; Koonin, E.; Morgunov, I.; Finogenova, T.; Kondrashova, M. *Biology Direct* **2006**, 1, 31.
- (38) Oh, K.-B.; Jeon, H. B.; Han, Y.-R.; Lee, Y.-J.; Park, J.; Lee, S.-H.; Yang, D.; Kwon, M.; Shin, J.; Lee, H.-S. *Bioorganic & Medicinal Chemistry Letters* **2010**, 20, 6644.
- (39) Lee, Y.-V.; Wahab, H. A.; Choong, Y. S. *BioMed Research International* **2015**, 2015, 20.
- (40) Muñoz-Elías, E. J.; McKinney, J. D. *Nature Medicine* **2005**, 11, 638.
- (41) Oh, K.-B.; Lee, J. H.; Lee, J. W.; Yoon, K.-M.; Chung, S.-C.; Jeon, H. B.; Shin, J.; Lee, H.-S. *Bioorganic & Medicinal Chemistry Letters* **2009**, 19, 945.
- (42) Storey, K. B. *Functional Metabolism: Regulation and Adaptation*; Wiley, 2005.
- (43) Uttara, B.; Singh, A. V.; Zamboni, P.; Mahajan, R. T. *Current Neuropsychopharmacology* **2009**, 7, 65.
- (44) Ray, P. D.; Huang, B.-W.; Tsuji, Y. *Cellular Signalling* **2012**, 24, 981.
- (45) Alfadda, A. A.; Sallam, R. M. *Journal of Biomedicine and Biotechnology* **2012**, 2012, 14.
- (46) Perera, R. M.; Bardeesy, N. *Nature* **2011**, 475, 43.
- (47) Carocho, M.; Ferreira, I. C. F. R. *Food and Chemical Toxicology* **2013**, 51, 15.
- (48) Liu, Z.-Q. *Chemical Reviews* **2010**, 110, 5675.
- (49) Thanan, R.; Oikawa, S.; Hiraku, Y.; Ohnishi, S.; Ma, N.; Pinlaor, S.; Yongvanit, P.; Kawanishi, S.; Murata, M. *International journal of molecular sciences* **2015**, 16, 193.
- (50) Steel, R.; Cowan, J.; Payerne, E.; O'Connell, M. A.; Searcey, M. *ACS Medicinal Chemistry Letters* **2012**, 3, 407.
- (51) Dinkova-Kostova, A. T.; Holtzclaw, W. D.; Cole, R. N.; Itoh, K.; Wakabayashi, N.; Katoh, Y.; Yamamoto, M.; Talalay, P. *Proceedings of the National Academy of Sciences of the United States of America* **2002**, 99, 11908.
- (52) Trippier, P. C.; Jansen Labby, K.; Hawker, D. D.; Mataka, J. J.; Silverman, R. B. *Journal of Medicinal Chemistry* **2013**, 56, 3121.
- (53) Bhamra, I.; Compagnone-Post, P.; O'Neil, I. A.; Iwanejko, L. A.; Bates, A. D.; Cosstick, R. *Nucleic acids research* **2012**, 40, 11126.
-

-
- (54) Chew, E. Y.; Clemons, T. E.; SanGiovanni, J. P.; Danis, R.; Ferris, F. L.; Elman, M.; Antoszyk, A.; Ruby, A.; Orth, D.; Bressler, S.; Fish, G.; Hubbard, B.; Klein, M.; Chandra, S.; Blodi, B.; Domalpally, A.; Friberg, T.; Wong, W.; Rosenfield, P.; Agron, E.; Toth, C.; Bernstein, P.; Sperduto, R. *JAMA* **2013**, *309*, 2005.
- (55) Klein, E. A.; Thompson, I. M., Jr.; Tangen, C. M.; Crowley, J. J.; Lucia, M. S.; Goodman, P. J.; Minasian, L. M.; Ford, L. G.; Parnes, H. L.; Gaziano, J. M.; Karp, D. D.; Lieber, M. M.; Walther, P. J.; Klotz, L.; Parsons, J. K.; Chin, J. L.; Darke, A. K.; Lippman, S. M.; Goodman, G. E.; Meyskens, F. L., Jr.; Baker, L. H. *JAMA* **2011**, *306*, 1549.
- (56) Kang, J. H.; Cook, N.; Manson, J.; Buring, J. E.; Grodstein, F. *Arch Intern Med* **2006**, *166*, 2462.
- (57) Sano, M.; Ernesto, C.; Thomas, R. G.; Klauber, M. R.; Schafer, K.; Grundman, M.; Woodbury, P.; Growdon, J.; Cotman, C. W.; Pfeiffer, E.; Schneider, L. S.; Thal, L. J. *The New England Journal of Medicine* **1997**, *336*, 1216.
- (58) <http://ods.od.nih.gov/factsheets/VitaminE-HealthProfessional/> Accessed: 2015
- (59) Pietta, P.-G. *Journal of Natural Products* **2000**, *63*, 1035.
- (60) Heim, K. E.; Tagliaferro, A. R.; Bobilya, D. J. *The Journal of Nutritional Biochemistry* **2002**, *13*, 572.
- (61) Richard, T.; Pawlus, A. D.; Iglésias, M.-L.; Pedrot, E.; Waffo-Teguo, P.; Mérillon, J.-M.; Monti, J.-P. *Annals of the New York Academy of Sciences* **2011**, *1215*, 103.
- (62) Aggarwal, B. B.; Harikumar, K. B. *International Journal of Biochemistry and Cell Biology* **2009**, *41*, 40.
- (63) Zhao, R.; Holmgren, A. *Journal of Biological Chemistry* **2002**, *277*, 39456.
- (64) Azad, G.; Tomar, R. *Mol Biol Rep* **2014**, *41*, 4865.
- (65) Armstrong, M. J.; Miyasaki, J. M. *Neurology* **2012**, *79*, 597.
- (66) Ogborne, R. M.; Rushworth, S. A.; O'Connell, M. A. *Biochemical and Biophysical Research Communications* **2008**, *373*, 584.
- (67) Rushworth, S. A.; Ogborne, R. M.; Charalambos, C. A.; O'Connell, M. A. *Biochemical and Biophysical Research Communications* **2006**, *341*, 1007.
- (68) Park, H. J.; Choi, J. S.; Chung, H. Y. *J. Korean Fisheries Soc.* **1998**, *31*, 927.
- (69) Son, S.; Lewis, B. A. *Journal of Agricultural and Food Chemistry* **2002**, *50*, 468.
- (70) Duan, X.-J.; Li, X.-M.; Wang, B.-G. *Journal of Natural Products* **2007**, *70*, 1210.
- (71) Zhao, W.; Feng, X.; Ban, S.; Lin, W.; Li, Q. *Bioorganic & Medicinal Chemistry Letters* **2010**, *20*, 4132.
- (72) Bouthenet, E.; Oh, K.-B.; Park, S.; Nagi, N. K.; Lee, H.-S.; Matthews, S. E. *Bioorganic & Medicinal Chemistry Letters* **2011**, *21*, 7142.
- (73) Rumboldt, G.; Böhmer, V.; Botta, B.; Paulus, E. F. *The Journal of Organic Chemistry* **1998**, *63*, 9618.
- (74) Sandin, R. B.; McKee, R. A. *Organic Syntheses* **1937**, *17*.
- (75) Kiehlmann, E.; Lauener, R. W. *Canadian Journal of Chemistry* **1989**, *67*, 335.
- (76) Bacci, J. P.; Kearney, A. M.; Van Vranken, D. L. *The Journal of Organic Chemistry* **2005**, *70*, 9051.
- (77) Das, B.; Venkateswarlu, K.; Majhi, A.; Siddaiah, V.; Reddy, K. R. *Journal of Molecular Catalysis A: Chemical* **2007**, *267*, 30.
- (78) Tanemura, K.; Suzuki, T.; Nishida, Y.; Satsumabayashi, K.; Horaguchi, T. *Chemical Communications* **2004**, 470.
- (79) Kuhnert, N.; Patel, C.; Jami, F. *Tetrahedron Letters* **2005**, *46*, 7575.
- (80) Michala, K.; Miloš, B.; Jana, H. *Synthetic Communications* **2007**, 161.
-

-
- (81) Santos-Filho, E. F.; Sousa, J. C.; Bezerra, N. M. M.; Menezes, P. H.; Oliveira, R. A. *Tetrahedron Letters* **2011**, 52, 5288.
- (82) Prastaro, A.; Ceci, P.; Chiancone, E.; Boffi, A.; Fabrizi, G.; Cacchi, S. *Tetrahedron Letters* **2010**, 51, 2550.
- (83) http://www.nobelprize.org/nobel_prizes/chemistry/laureates/2010/ Accessed: 24 May 2015
- (84) Lennox, A. J. J.; Lloyd-Jones, G. C. *Chemical Society Reviews* **2014**, 43, 412.
- (85) Miyaura, N.; Yamada, K.; Suzuki, A. *Tetrahedron Letters* **1979**, 20, 3437.
- (86) Miyaura, N.; Suzuki, A. *Chemical Reviews* **1995**, 95, 2457.
- (87) Narasimha, K.; Jayakannan, M. *ACS Applied Materials & Interfaces* **2014**, 6, 19385.
- (88) Kaur, N.; Delcros, J.-G.; Imran, J.; Khaled, A.; Chehtane, M.; Tschammer, N.; Martin, B.; Phanstiel, O. *Journal of Medicinal Chemistry* **2008**, 51, 1393.
- (89) Programs CrysAlisPro, Oxford Diffraction Ltd., Abingdon, UK (2010).
- (90) G. M. Sheldrick, SHELX-97 – Programs for crystal structure determination (SHELXS) and refinement (SHELXL), Acta Cryst. (2008) A64, 112-122.
- (91) 'International Tables for X-ray Crystallography', Kluwer Academic Publishers, Dordrecht (1992). Vol. C, pp. 500, 219 and 193.
- (92) Farrugia, L. J. *Journal of Applied Crystallography* **2012**, 45, 849–854.
- (93) Davis, T. L.; Harrington, V. F. *Journal of the American Chemical Society* **1934**, 56, 129.
- (94) Tabatabai, M.; Vogt, W.; Böhmer, V. *Tetrahedron Letters* **1990**, 31, 3295.
- (95) Sunshine, N. B.; Woods, G. F. *The Journal of Organic Chemistry* **1963**, 28, 2517.
- (96) Talotta, C.; Gaeta, C.; Neri, P. *Organic Letters* **2012**, 14, 3104.
- (97) Dimick, S. M.; Powell, S. C.; McMahon, S. A.; Moothoo, D. N.; Naismith, J. H.; Toone, E. J. *Journal of the American Chemical Society* **1999**, 121, 10286.
- (98) Hu, X.; Xiao, Y.; Wu, J.; Ma, L. *Archiv der Pharmazie* **2011**, 344, 71.
- (99) Kurduker, R.; Subba Rao, N. V. *Proceedings of the Indian Academy of Sciences, Section A* **1963**, 57, 280.
- (100) Shi, J.; Zhang, X.; Neckers, D. C. *The Journal of Organic Chemistry* **1992**, 57, 4418.
- (101) Azuma, E.; Kuramochi, K.; Tsubaki, K. *Tetrahedron* **2013**, 69, 1694.
- (102) Eaton, P. E.; Carlson, G. R.; Lee, J. T. *The Journal of Organic Chemistry* **1973**, 38, 4071.
- (103) Genoux-Bastide, E.; Lorendeau, D.; Nicolle, E.; Yahiaoui, S.; Magnard, S.; Di Pietro, A.; Baubichon-Cortay, H.; Boumendjel, A. *ChemMedChem* **2011**, 6, 1478.
- (104) Liu, Y.; Zou, L.; Ma, L.; Chen, W.-H.; Wang, B.; Xu, Z.-L. *Bioorganic & Medicinal Chemistry* **2006**, 14, 5683.
- (105) Lin, C.-N.; Chung, M.-I.; Liou, S.-J.; Lee, T.-H.; Wang, J.-P. *Journal of Pharmacy and Pharmacology* **1996**, 48, 532.
- (106) Shi, J.; Zhang, X.-P.; Neckers, D. C. *Tetrahedron Letters* **1993**, 34, 6013.
- (107) Olah, G. A.; Wang, Q.; Surya Prakash, G. K. *Synlett* **1992**, 647.
- (108) Olah, G. A.; Arvanaghi, M.; Ohannesian, L. *Synthesis* **1986**, 1986, 770.
- (109) Zarei, A.; Hajipour, A. R.; Khazdooz, L. *Tetrahedron Letters* **2008**, 49, 6715.
- (110) Tamaddon, F.; Khoobi, M.; Keshavarz, E. *Tetrahedron Letters* **2007**, 48, 3643.
- (111) Eshghi, H.; Shafieyoon, P. *Journal of the Chinese Chemical Society* **2005**, 155.
- (112) Mohammadizadeh, M. R.; Hasaninejad, A.; Bahramzadeh, M.; Khanjarlou, Z. S. *Synthetic Communications* **2009**, 39, 1152.
- (113) Ahmad, R. M.; Somayeh, B. *Iranian Journal of Catalysis* **2012**, 2, 31.
- (114) Hosseini Sarvari, M.; Sharghi, H. *Synthesis* **2004**, 2165.
- (115) Kasbekar, A. B.; Hosangadi, B. D. *Indian Journal of Chemistry* **1970**, 8, 1059.
-

-
- (116) Hosangadi, B. D.; Kasbekar, A. B.; Nabar, M. J.; Desai, R. C. *Indian Journal of Chemistry* **1973**, *11*, 711.
- (117) Mauthner, F. J. *Prakt. Chem. (Leipzig)* **1913**, *87*, 403.
- (118) Pettit, G. R.; Grealish, M. P.; Jung, M. K.; Hamel, E.; Pettit, R. K.; Chapuis, J. C.; Schmidt, J. M. *Journal of Medicinal Chemistry* **2002**, *45*, 2534.
- (119) McOmie, J. F. W.; Watts, M. L.; West, D. E. *Tetrahedron* **1968**, *24*, 2289.
- (120) Benton, F. L.; Dillon, T. E. *Journal of the American Chemical Society* **1942**, *64*, 1128.
- (121) Pomerantz, I. H.; Miller, L. J.; Barron, R.; Hansen, E.; Mastbrook, D.; Egry, L. *Tetrahedron* **1972**, *28*, 2183.
- (122) Grover, P. K.; Shah, G. D.; Shah, R. C. *Journal of the Chemical Society (Resumed)* **1955**, 3982.
- (123) Zhang, X.; Li, X.; Ye, S.; Zhang, Y.; Tao, L.; Gao, Y.; Gong, D.; Xi, M.; Meng, H.; Zhang, M.; Gao, W.; Xu, X.; Guo, Q.; You, Q. *Medicinal Chemistry* **2012**, *8*, 1012.
- (124) AbuSalim, D. I.; Merfeld, M. L.; Lash, T. D. *The Journal of Organic Chemistry* **2013**, *78*, 10360.
- (125) Harden, W. C.; Reid, E. E. *Journal of the American Chemical Society* **1932**, *54*, 4325.
- (126) Jansen, J. F. G. A.; de Brabander-van den Berg, E. M. M.; Meijer, E. W. *Science* **1994**, *266*, 1226.
- (127) Hawker, C. J.; Frechet, J. M. J. *Journal of the American Chemical Society* **1990**, *112*, 7638.
- (128) Dalgarno, S. J.; Thallapally, P. K.; Barbour, L. J.; Atwood, J. L. *Chemical Society Reviews* **2007**, *36*, 236.
- (129) Dalgarno, S. J.; Power, N. P.; Atwood, J. L. *Coordination Chemistry Reviews* **2008**, *252*, 825.
- (130) Jin, P.; Dalgarno, S. J.; Atwood, J. L. *Coordination Chemistry Reviews* **2010**, *254*, 1760.
- (131) Lalor, R.; DiGesso, J. L.; Mueller, A.; Matthews, S. E. *Chemical Communications* **2007**, 4907.
- (132) Lalor, R.; Gunning, A. P.; Morris, V. J.; Matthews, S. E. *Chemical Communications* **2010**, *46*, 8665.
- (133) Gutsche, C. D. *Calixarenes By C. David Gutsche*; Royal Society of Chemistry: Cambridge, 1989.
- (134) Lalor, R. *Novel multi-calixarenes and their applications in molecular pharmaceuticals*, University of East Anglia, **2007**.
- (135) Atzori, S. *Synthesis of novel calix[4]arene based dendrimers and their biological applications*, University Of East Anglia, **2013**.
- (136) Hussain, Z. *Design, synthesis and characterization of p-octiphenyloctacalix[4]arene a supramolecular multifunctional pore having practical applications in medicine and mechanics*, University of Karachi, University of East Anglia, **2009**.
- (137) Kolb, H. C.; Sharpless, K. B. *Drug Discovery Today* **2003**, *8*, 1128.
- (138) Kolb, H. C.; Finn, M. G.; Sharpless, K. B. *Angewandte Chemie International Edition* **2001**, *40*, 2004.
- (139) Evans, R. A. *Australian Journal of Chemistry* **2007**, *60*, 384.
- (140) Rostovtsev, V. V.; Green, L. G.; Fokin, V. V.; Sharpless, K. B. *Angewandte Chemie International Edition* **2002**, *41*, 2596.
- (141) Tornøe, C. W.; Christensen, C.; Meldal, M. *The Journal of Organic Chemistry* **2002**, *67*, 3057.
- (142) McNulty, J.; Keskar, K.; Vemula, R. *Chemistry – A European Journal* **2011**, *17*, 14727.
-

-
- (143) Boren, B. C.; Narayan, S.; Rasmussen, L. K.; Zhang, L.; Zhao, H.; Lin, Z.; Jia, G.; Fokin, V. V. *Journal of the American Chemical Society* **2008**, *130*, 8923.
- (144) Worrell, B. T.; Malik, J. A.; Fokin, V. V. *Science* **2013**, *340*, 457.
- (145) Regayeg, M.; Fort, A.; Cregut, O.; Coleman, A.; Shahgaldian, P.; Mugnier, J.; Lamartine, R.; Vocanson, F. *Journal of Materials Chemistry* **2002**, *12*, 2231.
- (146) Verboom, W.; Durie, A.; Egberink, R. J. M.; Asfari, Z.; Reinhoudt, D. N. *The Journal of Organic Chemistry* **1992**, *57*, 1313.
- (147) Budka, J.; Lhoták, P.; Michlová, V.; Stibor, I. *Tetrahedron Letters* **2001**, *42*, 1583.
- (148) Saadioui, M.; Shivanyuk, A.; Böhmer, V.; Vogt, W. *The Journal of Organic Chemistry* **1999**, *64*, 3774.
- (149) Tachon, S.; Michelon, D.; Chambellon, E.; Cantonnet, M.; Mezange, C.; Henno, L.; Cachon, R.; Yvon, M. *Microbiology* **2009**, *155*, 2941.
- (150) Berridge, M. V.; Herst, P. M.; Tan, A. S. In *Biotechnology Annual Review*; El-Gewely, M. R., Ed.; Elsevier: 2005; Vol. Volume 11, p 127.
- (151) Wolf, D.; Rotter, V. *Proceedings of the National Academy of Sciences of the United States of America* **1985**, *82*, 790.
- (152) Alkhalaf, M.; El-Mowafy, A. *Journal of Endocrinology* **2003**, *179*, 55.
- (153) Howell, L. A.; Bowater, R. A.; O'Connell, M. A.; Reszka, A. P.; Neidle, S.; Searcey, M. *ChemMedChem* **2012**, *7*, 792.
- (154) Pryor, W. A.; Cornicelli, J. A.; Devall, L. J.; Tait, B.; Trivedi, B. K.; Witiak, D. T.; Wu, M. *The Journal of Organic Chemistry* **1993**, *58*, 3521.
- (155) Huang, D.; Ou, B.; Prior, R. L. *Journal of Agricultural and Food Chemistry* **2005**, *53*, 1841.
- (156) Naguib, Y. M. A. *Analytical Biochemistry* **2000**, *284*, 93.
- (157) Güçlü, K.; Kıbrıshoğlu, G.; Özyürek, M.; Apak, R. *Journal of Agricultural and Food Chemistry* **2014**, *62*, 1839.
- (158) Benzie, I. F. F.; Strain, J. J. *Analytical Biochemistry* **1996**, *239*, 70.
- (159) Özyürek, M.; Güçlü, K.; Tütem, E.; Başkan, K. S.; Erçağ, E.; Esin Çelik, S.; Baki, S.; Yldz, L.; Karaman, Ş.; Apak, R. *Analytical Methods* **2011**, *3*, 2439.
- (160) Sánchez-Rangel, J. C.; Benavides, J.; Heredia, J. B.; Cisneros-Zevallos, L.; Jacobo-Velázquez, D. A. *Analytical Methods* **2013**, *5*, 5990.
- (161) Singleton, V. L.; Orthofer, R.; Lamuela-Raventós, R. M. In *Methods in Enzymology*; Lester, P., Ed.; Academic Press: 1999; Vol. Volume 299, p 152.
- (162) Sánchez-Moreno, C.; Larrauri, J. A.; Saura-Calixto, F. *Journal of the Science of Food and Agriculture* **1998**, *76*, 270.
- (163) Sanna, D.; Delogu, G.; Mulas, M.; Schirra, M.; Fadda, A. *Food Anal. Methods* **2012**, *5*, 759.
- (164) Milardovic, S.; Iveković, D.; Rumenjak, V.; Grabarić, B. S. *Electroanalysis* **2005**, *17*, 1847.
- (165) Milardović, S.; Iveković, D.; Grabarić, B. S. *Bioelectrochemistry* **2006**, *68*, 175.
- (166) Apak, R.; Gorinstein, S.; Böhm, V.; Schaich, K. M.; Özyürek, M.; Güçlü, K. *Pure and Applied Chemistry* **2013**, *85*, 957.
- (167) Re, R.; Pellegrini, N.; Proteggente, A.; Pannala, A.; Yang, M.; Rice-Evans, C. *Free Radical Biology and Medicine* **1999**, *26*, 1231.
- (168) Kedare, S. B.; Singh, R. P. *Journal of Food Science and Technology* **2011**, *48*, 412.
- (169) Proll, P. J.; Sutcliffe, L. H. *Transactions of the Faraday Society* **1963**, *59*, 2090.
- (170) Ozcelik, B.; Lee, J. H.; Min, D. B. *Journal of Food Science* **2003**, *68*, 487.
- (171) Litwinienko, G.; Ingold, K. U. *The Journal of Organic Chemistry* **2003**, *68*, 3433.
-

-
- (172) Foti, M. C.; Daquino, C.; Geraci, C. *The Journal of Organic Chemistry* **2004**, 69, 2309.
- (173) Sharma, O. P.; Bhat, T. K. *Food Chemistry* **2009**, 113, 1202.
- (174) Bondet, V.; Brand-Williams, W.; Berset, C. *LWT - Food Science and Technology* **1997**, 30, 609.
- (175) Sang, S.; Pan, M.-H.; Cheng, X.; Bai, N.; Stark, R. E.; Rosen, R. T.; Lin-Shiau, S.-Y.; Lin, J.-K.; Ho, C.-T. *Tetrahedron* **2001**, 57, 9931.
- (176) Kawabata, J.; Okamoto, Y.; Kodama, A.; Makimoto, T.; Kasai, T. *Journal of Agricultural and Food Chemistry* **2002**, 50, 5468.
- (177) Hristea, E. N.; Covaci-Cîmpeanu, I. C.; Ioniță, G.; Ioniță, P.; Draghici, C.; Caăproiu, M. T.; Hillebrand, M.; Constantinescu, T.; Balaban, A. T. *European Journal of Organic Chemistry* **2009**, 2009, 626.
- (178) <http://www.acs.org/content/acs/en/education/whatischemistry/landmarks/freeradicals.html> Accessed: 2015
- (179) Liu, H.; Talalay, P. *Proceedings of the National Academy of Sciences* **2013**, 110, 19065.
- (180) Kawada, M.; Kashiwagi, M.; Koito, K., **1991**, JP 1991-91604
- (181) Balaydin, H. T.; Gülçin, İ.; Menzek, A.; Göksu, S.; Şahin, E. *Journal Of Enzyme Inhibition And Medicinal Chemistry* **2010**, 25, 685.